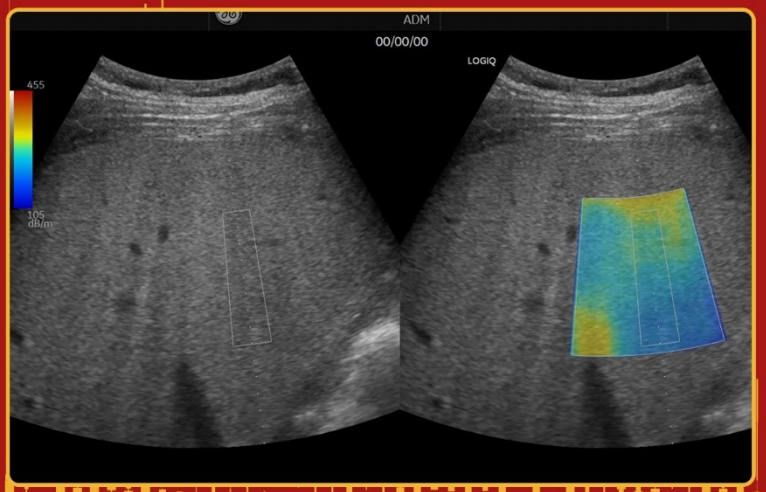

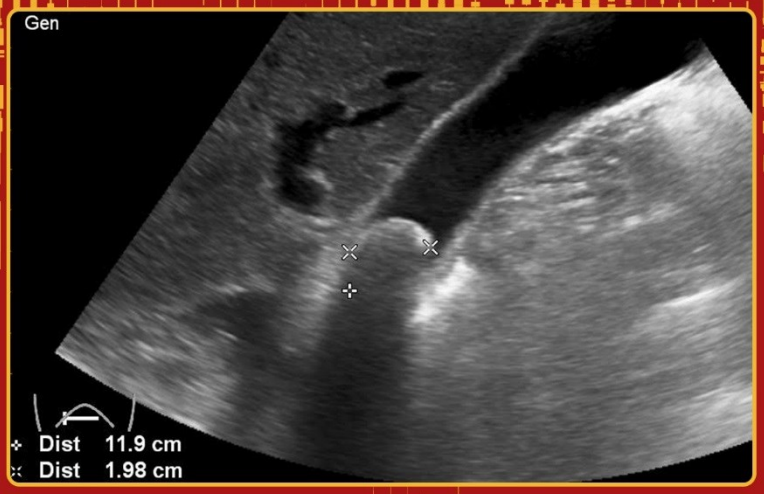

Integrating Ultrasound into Clinical Practice

A collective book of European WFUMB Centers of Education

EDITORS:
Ioan Sporea, Alina Popescu, Sergiu Puiu, Durim Cela, Blerina Saraci, Ivica Grgurevic, Boris Brkljacic, Dieter Nürnberg

"Victor Babeş" Publishing House
Timișoara, 2025

„Victor Babeş" Publishing House
Eftimie Murgu Square 2, room 316, 300041 Timişoara
Tel./ Fax 0256 495 210
e-mail: evb@umft.ro
www.umft.ro/ro/organizare-evb/

General Director: Prof. dr. Sorin Ursoniu

HIPPOCRATE Collection

Collection Coordinator: Prof. dr. Andrei Motoc

Scientific Referent: Prof. dr. Gheorghe Mihalaș

CNCSIS number: 324

ISBN 978-606-786-461-8

CONTENT

LIST OF AUTHORS

- **Ioan Sporea, MD, PhD, FEBGH** – Professor of Gastroenterology, "Victor Babeș" University of Medicine and Pharmacy Timișoara, Romania, The Regional Research Center in Advanced Hepatology of the Romanian Academy of Medical Sciences; World Federation of Ultrasound in Medicine and Biology (WFUMB) Vice-President; Director WFUMB Center of Education, Timișoara, Romania
- **Alina Popescu, MD, PhD** – Professor of Gastroenterology, Department of Gastroenterology and Hepatology, Center for Advanced Research in Gastroenterology and Hepatology, "Victor Babeș" University of Medicine and Pharmacy, Timișoara, Romania, "Pius Brînzeu" Clinical Emergency County Hospital Timișoara, Romania; European Federation of Ultrasound in Medicine and Biology (EFSUMB) Honorary Treasurer; WFUMB Center of Education, Timișoara, Romania
- **Roxana Șirli, MD, PhD** – Professor of Gastroenterology, Department of Gastroenterology and Hepatology, Center for Advanced Research in Gastroenterology and Hepatology, "Victor Babeș" University of Medicine and Pharmacy, Timișoara, Romania, "Pius Brînzeu" Clinical Emergency County Hospital Timișoara, Romania; WFUMB Center of Education, Timișoara, Romania
- **Mirela Dănilă, MD, PhD** – Professor of Gastroenterology, Department of Gastroenterology and Hepatology, Center for Advanced Research in Gastroenterology and Hepatology, "Victor Babeș" University of Medicine and Pharmacy, Timișoara, Romania, "Pius Brînzeu" Clinical Emergency County Hospital Timișoara, Romania; WFUMB Center of Education, Timișoara, Romania
- **Bogdan Miuțescu, MD, PhD** – Department of Gastroenterology and Hepatology, Center for Advanced Research in Gastroenterology and Hepatology, "Victor Babeș" University of Medicine and Pharmacy, Timișoara, Romania, "Pius Brînzeu" Clinical Emergency County Hospital Timișoara, Romania; WFUMB Center of Education, Timișoara, Romania
- **Felix Bende, MD, PhD** – Department of Gastroenterology and Hepatology, Center for Advanced Research in Gastroenterology and Hepatology, "Victor Babeș" University of Medicine and Pharmacy, Timișoara, Romania, "Pius Brînzeu" Clinical Emergency County Hospital Timișoara, Romania; WFUMB Center of Education, Timișoara, Romania
- **Tudor Moga, MD, PhD** – Department of Gastroenterology and Hepatology, Center for Advanced Research in Gastroenterology and Hepatology, "Victor Babeș" University of Medicine and Pharmacy, Timișoara, Romania, "Pius Brînzeu" Clinical Emergency County Hospital Timișoara, Romania; WFUMB Center of Education, Timișoara, Romania
- **Anamaria Ghiuchici, MD, PhD** – Department of Gastroenterology and Hepatology, Center for Advanced Research in Gastroenterology and Hepatology, "Victor Babeș" University of Medicine and Pharmacy, Timișoara, Romania, "Pius Brînzeu" Clinical Emergency County Hospital Timișoara, Romania; WFUMB Center of Education, Timișoara, Romania
- **Alexandru Popa, MD, PhD** – Department of Gastroenterology and Hepatology, Center for Advanced Research in Gastroenterology and Hepatology, "Victor Babeș" University of Medicine and Pharmacy, Timișoara, Romania, "Pius Brînzeu" Clinical Emergency County Hospital Timișoara, Romania; WFUMB Center of Education, Timișoara, Romania

- **Camelia Nica, MD, PhD** – Department of Gastroenterology and Hepatology, Center for Advanced Research in Gastroenterology and Hepatology, "Victor Babeș" University of Medicine and Pharmacy, Timișoara, Romania, "Pius Brînzeu" Clinical Emergency County Hospital Timișoara, Romania; WFUMB Center of Education, Timișoara, Romania
- **Ruxandra Mare, MD, PhD** – Department of Gastroenterology and Hepatology, Center for Advanced Research in Gastroenterology and Hepatology, "Victor Babeș" University of Medicine and Pharmacy, Timișoara, Romania, "Pius Brînzeu" Clinical Emergency County Hospital Timișoara, Romania; WFUMB Center of Education, Timișoara, Romania
- **Flaviu Bob, MD, PhD** – Professor of Nephrology, Nephrology University Clinic, University of Medicine and Pharmacy Timișoara; County University Hospital Timișoara; WFUMB Center of Education, Timișoara, Romania
- **Dana Stoian, MD, PhD, CCD, FECSM** – Professor of Endocrinology, senior consultant endocrinology, Endocrinology Outpatient Unit, County Emergency Hospital Timisoara, Discipline of Endocrinology,"Victor Babeș" University of Medicine Timișoara, WFUMB Center of Education, Timișoara, Romania
- **Iulia Grosu, MD, PhD** – University of Medicine and Pharmacy Timișoara; Nephrology University Clinic, County University Hospital Timișoara; WFUMB Center of Education, Timișoara, Romania
- **Andreea Bena, MD, PhD** – Consultant endocrinology, Endocrinology Outpatient Unit, County Emergency Hospital Timisoara, Discipline of Endocrinology, "Victor Babeș" University of Medicine Timișoara, Romania
- **Adrian Săftoiu, MD, PhD, MSc, FASGE, AGAF** – Professor of Gastroenterology and Hepatology, Elias Emergency University Hospital Bucharest; Carol Davila University of Medicine and Pharmacy, Bucharest, Romania
- **Sergiu Puiu, MD, PhD** – Nicolae Testemițanu State University of Medicine and Pharmacy, Chișinău, Republic of Moldova; Director, WFUMB Center of Education, Chișinău, Republic of Moldova
- **Blerina Saraci Qirinxhi, MD, PhD Candidate** – University of Medicine and UHC Mother Teresa, Tirana, Albania; Co-Director, WFUMB Center of Education, Tirana, Albania
- **Durim Cela, MD, PhD** – Associate Professor of Radiology, University of Medicine, Tirana, Albania; Director, WFUMB Center of Education, Tirana, Albania
- **Erinda Frroku** – Clinical Imaging Unit in the Imaging and Nuclear Medicine Service of the Integrated Administration Division of the Polyvalent Hospital at the " Mother Teresa" University Hospital Center, Tirana, WFUMB Center of Education, Tirana, Albania
- **Denis Qirinxhi, MD, PhD candidate** – Radiologist, University of Medicine and UHC Mother Teresa, Tirana, Albania, WFUMB Center of Education, Tirana, Albania
- **Ivica Grgurević, MD, PhD, FEBGH, FRCP (London)** – Professor of Gastroenterology; Consultant Gastroenterologist and Hepatologist, Department of Gastroenterology, Hepatology and Clinical Nutrition, University of Zagreb School of Medicine; Faculty of Pharmacy and Biochemistry; University Hospital Dubrava; Director, WFUMB Center of Education, Zagreb, Croatia
- **Boris Brkljačić, MD, PhD, MAE, FACR** – Professor of Radiology, University of Zagreb School of Medicine; Department of Diagnostic and Interventional Radiology, University Hospital Dubrava, Zagreb, Croatia
- **Dieter Nürnberg, MD, PhD** – Professor of Internal Medicine and Gastroenterology, Medical School Brandenburg "Theodor Fontane"; Institute for Clinical Ultrasound (BICUS), Neuruppin, Germany

1. INTRODUCTION

Ioan Sporea

WFUMB Center of Education Timișoara, Romania

Many years ago, the World Federation of Ultrasound in Medicine and Biology (WFUMB) decided to develop and support Centers of Excellence in Ultrasound. The aim of these centers was to provide education in ultrasound in geographical areas where such training was most needed. Later on, WFUMB decided to change the name of these centers to Centers of Education (COE). These COEs offer regular ultrasound education for doctors and medical personnel. For this purpose, WFUMB appoints "a dedicated and responsible person as Director, who is in charge of the COE". Currently, at a global level, there are 21 COEs, and this number is continuously increasing.

At the European level, the first COE was established in 2007 in Timișoara, Romania. Over time, many educational activities were organized, the most important being Euroson 2008 and WFUMB 2022. The annual COE Romania workshop has attracted significant participation, and numerous Euroson Ultrasound Schools have been organized, almost every year. After 10 years of experience as a COE, and in collaboration with colleagues and friends from Moldova, the next European COE was opened in Chișinău in 2017. This new center was very active from the very beginning, organizing many well-appreciated ultrasound meetings with large attendance.

The next European COE was opened in Tirana, Albania, in 2019. Despite the fact that the Albanian Society of Ultrasound is relatively small, it is highly enthusiastic and has initiated educational activities in ultrasound. The most recent European Center of Education was established in Zagreb, Croatia, in 2023. With extensive experience in both ultrasound and education in this field, Zagreb quickly became an outstanding COE.

As of now, there are four European Centers of Education: Timișoara, Chișinău, Tirana, and Zagreb. Since the directors of these COEs are good friends and have strong teams behind them, many joint activities have been planned and developed. Some collaborative webinars (2021, 2024) have been highly appreciated.

Later on, we decided that it would be a challenging yet rewarding endeavor to write a book together, focusing on Point-of-Care Ultrasound in different fields. The best specialists from these COEs were invited to contribute chapters, ultimately creating a book that integrates the collective experience of each center for training and teaching purposes.

Behind the development of many European COEs, one name has always stood out: Prof. Dieter Nuerenberg, MD, PhD. A fellow of EFSUMB (European Federation of Ultrasound in Medicine and Biology) and an enthusiastic teacher and mentor in the field of ultrasound, he has

been instrumental in this journey. With over 20 years of experience teaching ultrasound at the European level, his expertise has been invaluable to all European COEs.

We hope that this joint ultrasound book will be highly beneficial for ultrasound practitioners, COE participants (students, fellows, and other professionals interested in learning ultrasound), and beyond. The book aims to cover multiple fields of ultrasound, making it useful for various medical specialties. Highly experienced teachers have contributed their knowledge, ensuring that this book is both educational and practical. Each chapter begins with the question: "How can I use ultrasound for...?", aiming to provide answers to different pathologies and their ultrasound applications.

We hope that this book will be useful in clinical practice and that readers will enjoy and benefit from its content.

2. HOW CAN I USE ULTRASOUND IN CHRONIC DIFFUSE LIVER DISEASES?

Ioan Sporea, Alexandru Popa
WFUMB Center of Education Timișoara, Romania

Ultrasound is increasingly recognized as a clinical specialty and is routinely employed in the daily practice of gastroenterologists and hepatologists. In some countries, such as Romania, ultrasound training is integrated into fellowship programs for these two specialties. In this context, ultrasound can be used as a point-of-care modality within these fields.

When performing abdominal ultrasonography, we recommend a systematic evaluation of the entire abdomen, focusing particularly on the region(s) of clinical interest. According to the recommendations of the "WFUMB Ultrasound Book," a systematic "6+ protocol" for abdominal ultrasound examination can be used. This protocol begins with a transverse epigastric section, followed by a longitudinal epigastric section. Position three is the right oblique subcostal view, followed by the right intercostal view (position four). Position five is the left intercostal view, and lastly, the hypogastric region (both transverse and longitudinal views) is examined. The "6+ protocol" also involves evaluating the right and left iliac fossae for bowel assessment, specifically the sigmoid region on the left and the terminal ileum and appendix on the right.

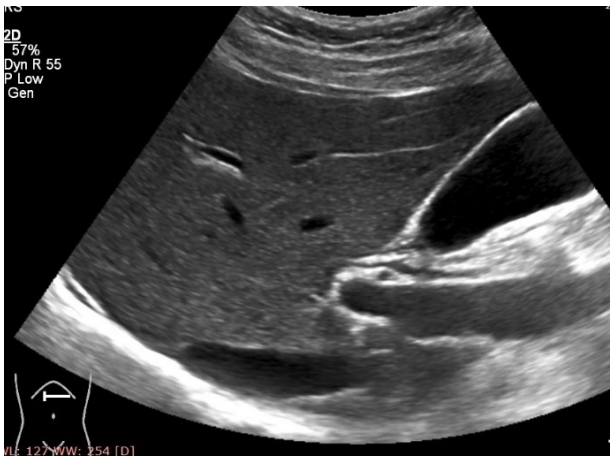

Figure 2.1. Ultrasound image of the normal liver, highlighting the hepatic hilum with the portal vein, common bile duct, and hepatic artery adjacent to the gallbladder

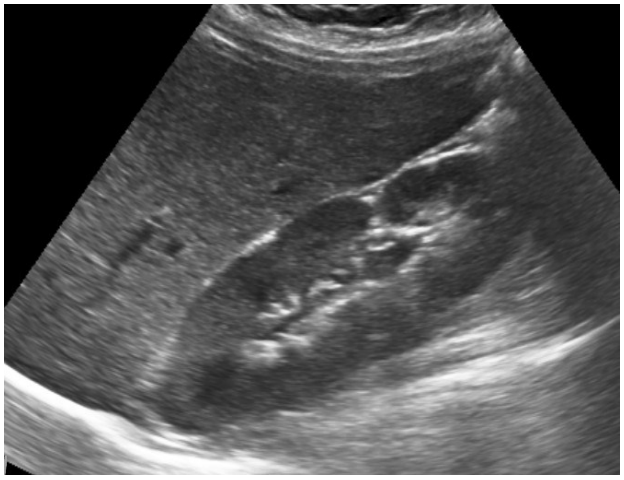

Figure 2.2. Ultrasound image comparing the echogenicity of normal liver parenchyma with that of the renal cortex, illustrating their typical similarity in echotexture.

Under normal conditions, liver examination reveals a homogeneous hepatic structure, with clearly visible hepatic veins, and a portal vein that can be traced to the hepatic hilum. The posterior aspect of the diaphragm should also be well visualized. When examining the spleen, the entire organ must be displayed, and its length measured from one pole to the other. The normal spleen size is typically less than 12 cm in length, although some authors use a cutoff of less than 13 cm.

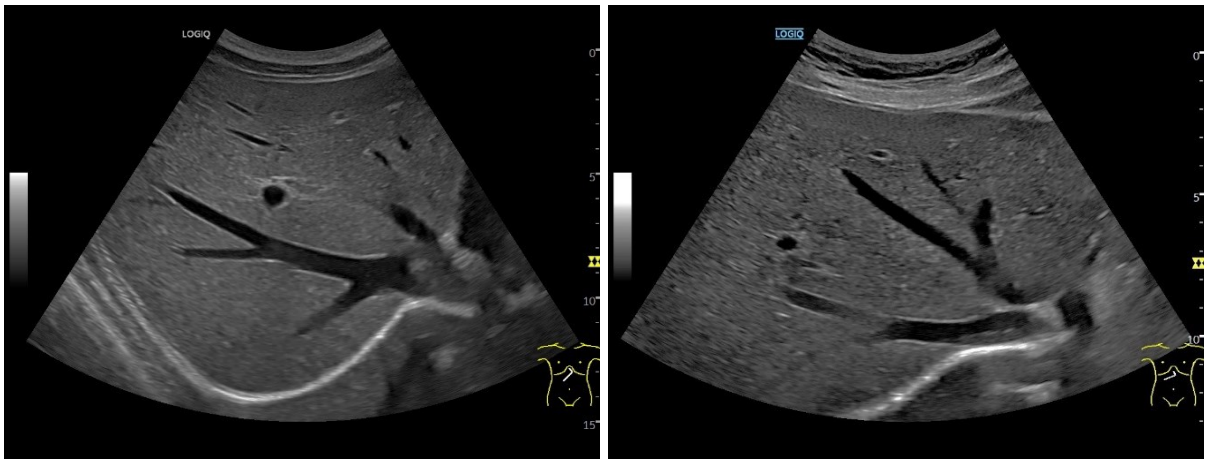

Figure 2.3A-B. Oblique subcostal ultrasound view of the hepatic veins, demonstrating their normal branching pattern and anechoic appearance

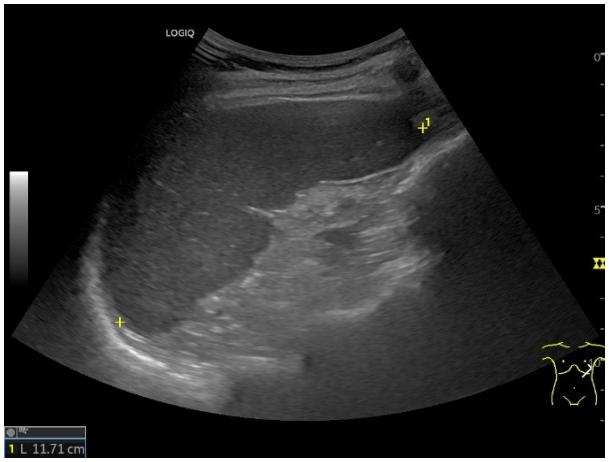

Figure 2.4. Ultrasound image of a normal spleen, demonstrating homogeneous echotexture and a length measurement within the normal range (<12 cm).

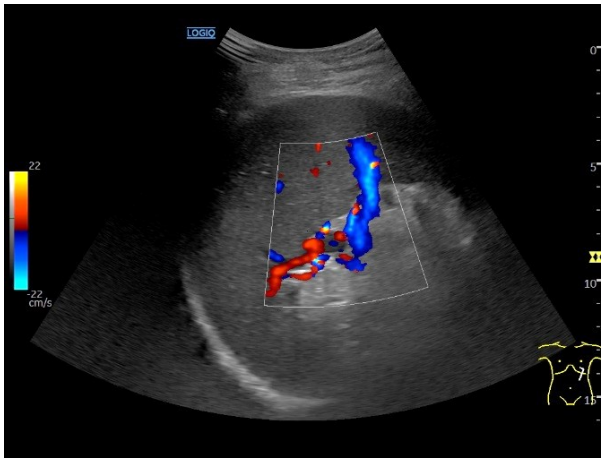

Figure 2.5. Color Doppler ultrasound of the spleen hilum, showing normal splenic vasculature with appropriate arterial and venous flow dynamics.

When evaluating the liver, several key elements must be assessed: the homogeneity (or heterogeneity) of the parenchyma, the surface contour of the liver, patency of the hepatic and portal veins, evidence of fatty infiltration, the diameter of the common bile duct (CBD) and intrahepatic biliary tree (whether normal or dilated), and the presence of any focal liver lesions (FLL).

In terms of clinical context, there are two main scenarios. The first arises when a routine abdominal ultrasound examination incidentally reveals hepatic abnormalities, such as a dysmorphic liver, splenomegaly, ascites, signs of portal hypertension, or focal liver lesions. The second scenario occurs when patients present with specific hepatological issues—for instance, elevated aminotransferases or bilirubin, jaundice, or increased gamma-glutamyl transpeptidase (GGT)—where an ultrasound examination can be especially useful.

This chapter focuses on the role of ultrasound in chronic diffuse liver diseases. In these patients, standard ultrasound should systematically evaluate the structure of the liver parenchyma, spleen size, signs of portal hypertension, and the presence of ascites. Doppler assessment of the portal, hepatic, and splenic veins is also useful, although this topic is covered in the dedicated Doppler chapter. Over the past two decades, ultrasound-based elastography has undergone significant development and is now routinely employed for evaluating both the liver and spleen.

In cases of chronic viral hepatitis, standard ultrasound findings are often normal. However, when structural changes are detected, these findings may suggest more advanced disease (i.e., extensive fibrosis). Mild splenomegaly (>12 cm) can be found in chronic viral hepatitis, underscoring the need for precise measurement of the spleen. In chronic hepatitis B and C, as well as in autoimmune hepatitis or primary biliary cholangitis, one or more ovoid, hypoechoic lymph nodes measuring approximately 2–4 cm by 1–1.5 cm may be visualized in the hepatic hilum (Figure 2.6). Conversely, when a lymph node in the liver hilum is identified during an abdominal ultrasound, further investigation for chronic hepatitis through appropriate laboratory tests is warranted.

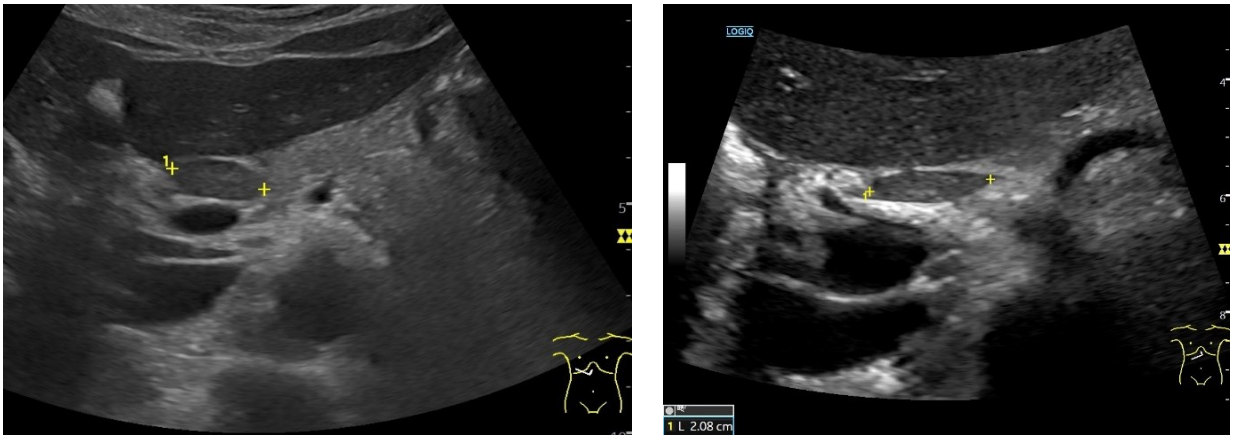

Figure 2.6 A-B. Ultrasound Imaging of a Hepatic Hilum Lymph Node:
Ovoid, Hypoechoic Structure, Suggestive of Reactive or Pathological Lymphadenopathy.

Standard ultrasound plays a critical role in diagnosing fatty liver disease, a condition that has become increasingly common, particularly in developed countries, where it affects approximately 30% of the population. The term “non-alcoholic fatty liver disease” (NAFLD) has now been replaced by “metabolic dysfunction–associated steatotic liver disease” (MASLD).

In the assessment of fatty liver, standard ultrasound demonstrates good accuracy—especially for moderate and severe steatosis (i.e., clinically significant)—and high specificity. The hallmark ultrasound signs include a “bright” liver with “posterior attenuation” of the ultrasound beam (Figure 2.7A). By examining the degree of increased echogenicity (the so-called “bright”

liver) and the extent of beam attenuation, a subjective grading of steatosis severity (mild, moderate, or severe) can be made.

An important indicator of liver steatosis is the hepatorenal index (Figure 2.7B). Under normal conditions, the echogenicity of the renal cortex is similar to that of the adjacent liver parenchyma. However, in steatosis, the liver appears hyperechoic relative to the kidney cortex, leading to an increased difference in echogenicity between the two organs. Studies have shown that the hepatorenal index is a highly relevant ultrasound sign in diagnosing liver steatosis—potentially more reliable than the "bright" liver with "posterior attenuation"—when validated against liver biopsy as the gold standard.

In clinical practice, we recommend routinely comparing the echogenicities of the liver and right kidney during ultrasound, to aid in diagnosing steatosis. However, this comparison may not be valid in patients with chronic kidney disease, who often exhibit increased renal cortical echogenicity, thereby diminishing the reliability of this sign.

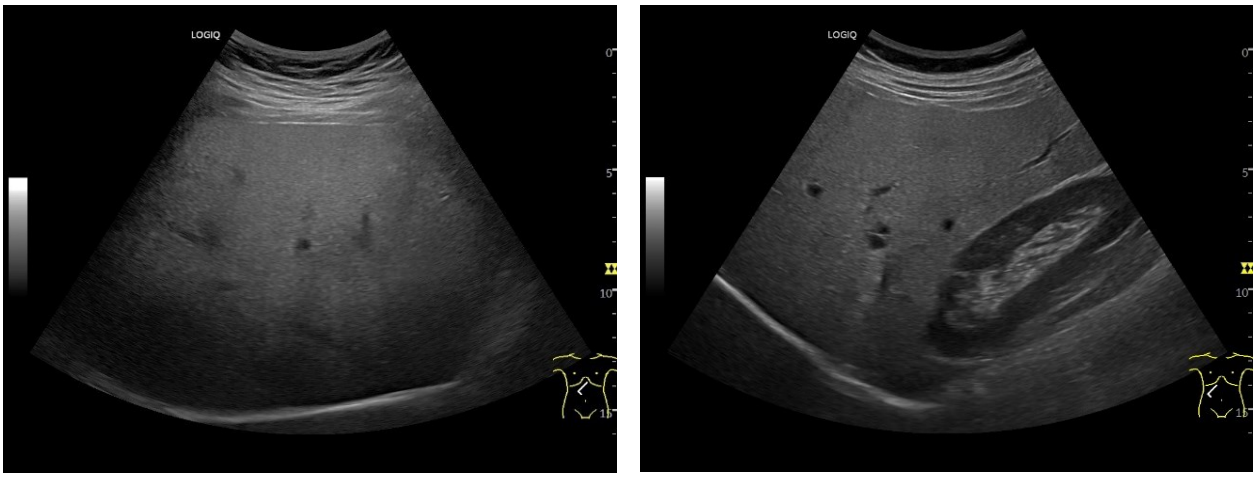

Figure 2.7 A-B. Ultrasound Assessment of Hepatic Steatosis: A. Increased Liver Echogenicity with Posterior Attenuation and B. Increased Hepatorenal Index, Suggestive of Fatty Liver Infiltration.

Because the assessment of liver steatosis is inherently subjective, various scoring systems, such as the Hamaguchi score, have been developed. This particular score assesses four ultrasound findings: liver brightness, posterior attenuation, the hepatorenal index, and vessel blurring (i.e., the clarity of vascular borders and any luminal narrowing). Although the Hamaguchi score appears to provide a more objective evaluation of fatty liver, it is not commonly used in routine practice.

Nonetheless, several critical considerations remain with these subjective methods, including variability in interpretation, differences in ultrasound machine quality, and challenges in monitoring steatosis progression or regression over time.

Over the past decade, the Controlled Attenuation Parameter (CAP) has been introduced as a module within the FibroScan® (Echosens) device, offering a more objective assessment of hepatic fat infiltration. A key advantage of FibroScan is that it can rapidly evaluate both liver steatosis and liver stiffness via vibration-controlled transient elastography (VCTE). Proposed cutoff values for mild, moderate, and severe steatosis have been shown to be consistent for both the M and XL probes (the latter used for obese patients). In MASLD, these cutoffs are approximately 290 dB/m for mild steatosis, 310 dB/m for moderate steatosis, and 330 dB/m for severe steatosis. Meta-analyses suggest that CAP accuracy ranges between 80% and 90% when compared with liver biopsy.

More recently, quantitative ultrasound (QUS) techniques for steatosis assessment have been developed, and most high-end—and some mid-range—ultrasound systems now include these modules. The underlying principles involve measuring attenuation, backscattering, speed of sound, or combinations of these parameters. Different manufacturers have introduced their own commercial names for these modules, such as UGAP (General Electric), UDFF (Siemens), and USSF (Samsung), among others.

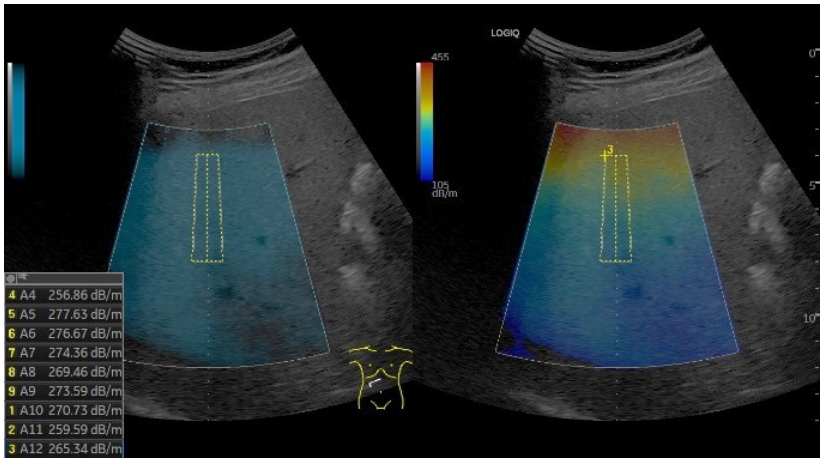

Figure 2.8. Quantitative Ultrasound for Liver Steatosis Assessment (UGAP)

Studies in patients with MASLD, comparing these QUS techniques against liver biopsy or MRI-PDFF, have demonstrated very good accuracy, exceeding 90% in some systems. The main advantage of QUS is its integration into standard ultrasound machines, which allows for objective and reproducible measurements that facilitate patient follow-up. The primary limitation remains the cost of ultrasound devices equipped with these modules; however, several manufacturers now offer these features in mid-range systems, making them more accessible.

Classical ultrasound has limited utility in ***assessing liver fibrosis***, as it typically detects only the signs of advanced disease. Key ultrasound findings suggestive of fibrosis include parenchymal heterogeneity, an irregular liver surface, enlargement of the caudate lobe, splenomegaly, signs of

portal hypertension, and gallbladder wall thickening (attributable to hypoalbuminemia and portal hypertension). In a comparative study using liver biopsy as the gold standard for chronic hepatitis B patients, combining these parameters yielded 80% accuracy for diagnosing compensated cirrhosis. Visualization of the liver surface is facilitated by the presence of perihepatic ascites, which allows better delineation—particularly when employing a high-frequency linear transducer. However, for detecting fibrosis in patients with chronic hepatitis, a study comparing standard ultrasound to biopsy reported a sensitivity of only 25%, although specificity reached 80%.

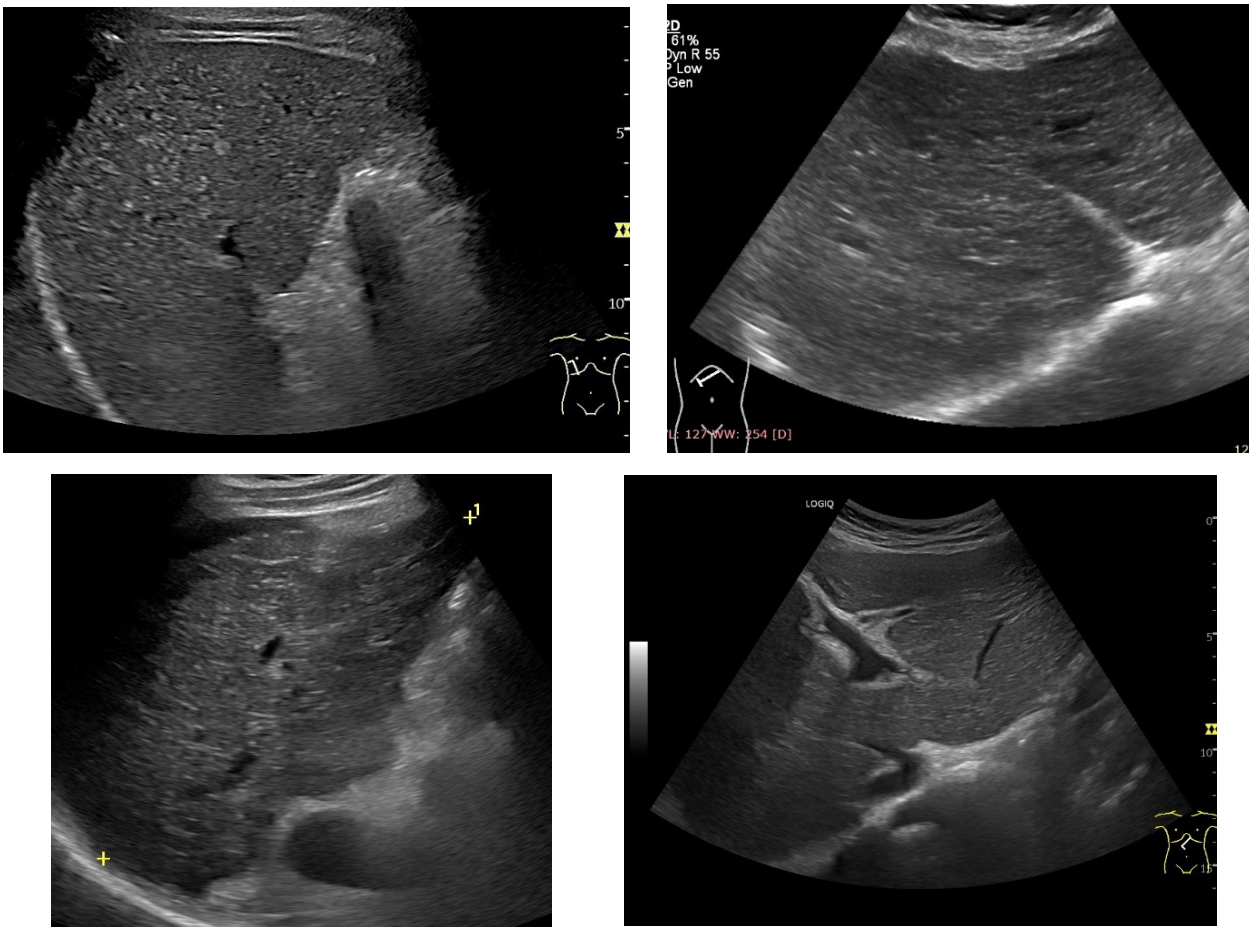

Figure 2.9 A-D. These B-mode ultrasound images show a heterogeneous (inhomogeneous) hepatic parenchyma and an irregular, nodular liver surface, both classic features of cirrhosis reflecting advanced fibrotic changes.

Enlargement of the caudate lobe (segment I of the liver) can also indicate cirrhosis. This lobe is measured in the anteroposterior dimension (from the posterior surface of the lobe to the ligamentum venosum), and normal values are typically below 35 mm. In cirrhotic livers, this dimension can exceed 35 mm - occasionally reaching 50–60 mm - resulting in a characteristic appearance of this segment.

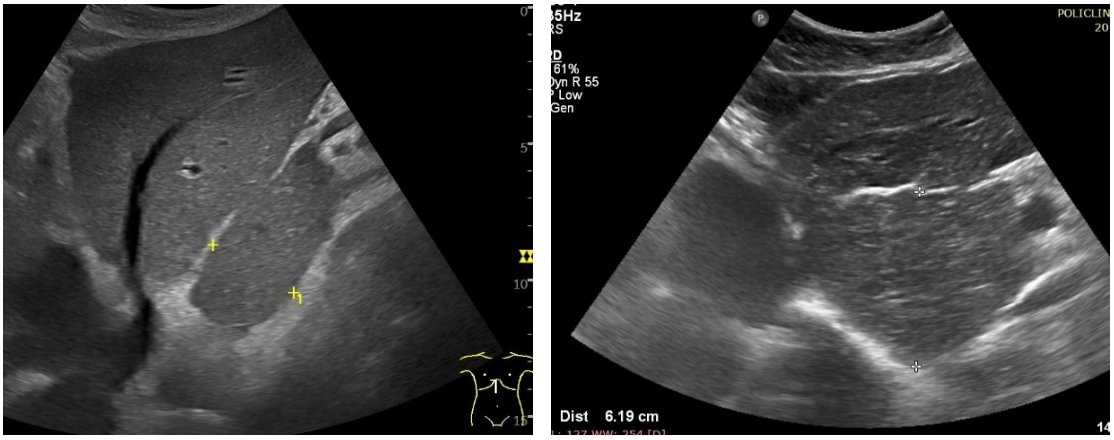

Figure 2.10 A-B. Ultrasound Findings of Normal (A) and Enlarged Caudate Lobe (61 mm) (B)

Evaluation of the portal vein (PV) may reveal signs of portal hypertension (PH). These findings include a PV diameter greater than 14 mm at the hepatic hilum, dilation of the intrahepatic portal branches, enlargement of the splenic vein, and, in some instances, splenic varices. Additionally, the left portal vein may display recanalization of the umbilical vein, forming a vascular channel between the left portal vein and the umbilicus.

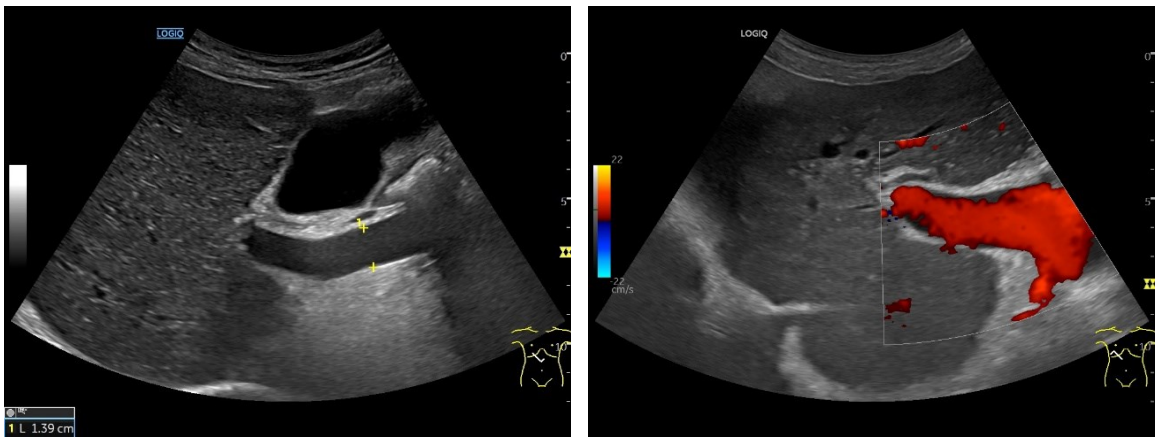

Figure 2.11 A-B. Evaluation of the Portal Vein (A) B-mode ultrasound demonstrating a portal vein diameter of approximately 14 mm at the hepatic hilum, suggestive of mild dilation.
(B) Color Doppler ultrasound confirming an enlarged portal vein lumen,
consistent with early signs of portal hypertension.

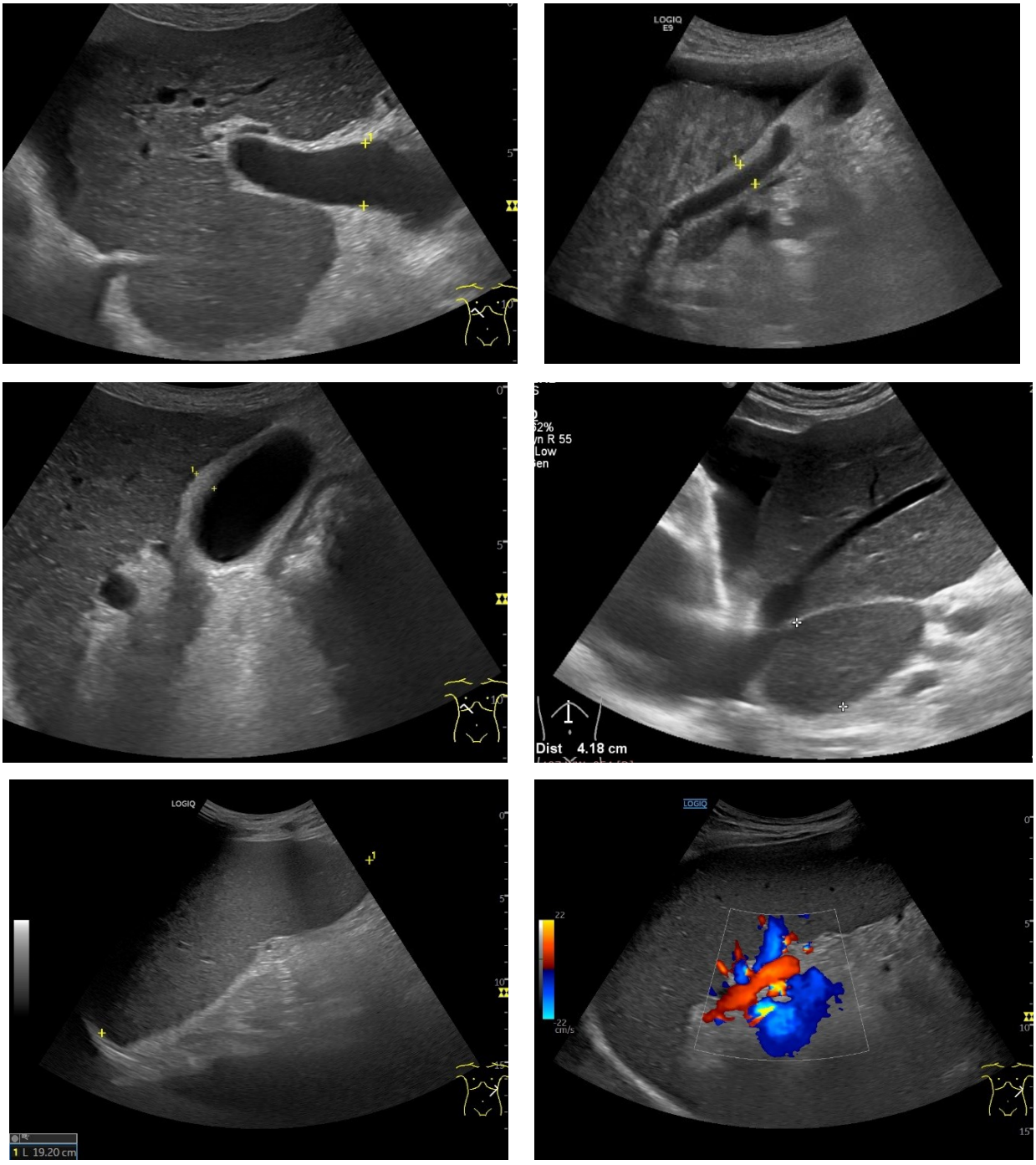

Figure 2.12 A-F. Ultrasound Findings Indicative of Portal Hypertension and Liver Cirrhosis

(A) A dilated portal vein is visible, reflecting increased portal pressure. (B) Recanalization of the paraumbilical (umbilical) vein is evident, forming an abnormal vascular channel in the ligamentum teres. (C) The gallbladder demonstrates a "double-layered" thickened wall, often associated with hypoalbuminemia and portal hypertension. (D) Hypertrophy of the caudate lobe is observed, a common feature in cirrhotic livers. (E) Splenomegaly is clearly depicted, a frequent finding in portal hypertension. (F) Color Doppler imaging reveals splenic varices, confirming collateral circulation due to increased portal pressure.

Ultrasound is highly sensitive for detecting ascites, even in small quantities. Fluid collections can be identified in the pelvic region (in the vesical-rectal pouch), around the liver (perihepatic), or surrounding the spleen. A subjective estimation of ascitic fluid volume can guide appropriate therapy, and serial ultrasound examinations can be used to adjust diuretic dosages accordingly. If paracentesis is required, ultrasound guidance is recommended to minimize the risk of bowel injury.

Evaluating alterations in liver echotexture remains challenging and largely subjective. In advanced cirrhosis, the liver often exhibits marked heterogeneity; however, this sign may be absent in earlier stages. In primary biliary cholangitis, abnormal liver texture is frequently observed.

Because standard ultrasound has limited accuracy for detecting early or moderate fibrosis, more advanced modalities are necessary. Over the past two decades, ***ultrasound-based elastography*** has become a standard tool for evaluating liver stiffness in patients with suspected fibrosis. The first widely adopted technique, vibration-controlled transient elastography (VCTE), is incorporated into the FibroScan device (Echosens). VCTE is a relatively simple method - often performed by technicians in some countries - painless, and capable of providing an objective assessment of liver stiffness/fibrosis in under five minutes. FibroScan offers two main probes: an M probe for non-obese patients and an XL probe for obese patients. Ten valid measurements with an interquartile range (IQR) to median (M) ratio below 30% are required. Proposed cutoff values include <8.5 kPa for no significant fibrosis, >8.5 kPa for significant fibrosis, and >12–15 kPa for compensated advanced chronic liver disease (cACLD). Examinations must be conducted after a 3–4 hour fast, as factors such as elevated aminotransferases (>100 U/L), obstructive jaundice, right-sided heart failure, or a non-fasting state can spuriously increase stiffness measurements.

In the past 15 years, Acoustic Radiation Force Impulse (ARFI) technology has been integrated into ultrasound probes to enable Shear Wave Elastography (SWE). Both point SWE (pSWE) and 2D-SWE are now available on many high-end and some mid-range ultrasound systems, allowing liver stiffness assessment within minutes. Typically, 3–10 measurements are performed, with the median value expressed in kilopascals (kPa) or meters per second (m/s).

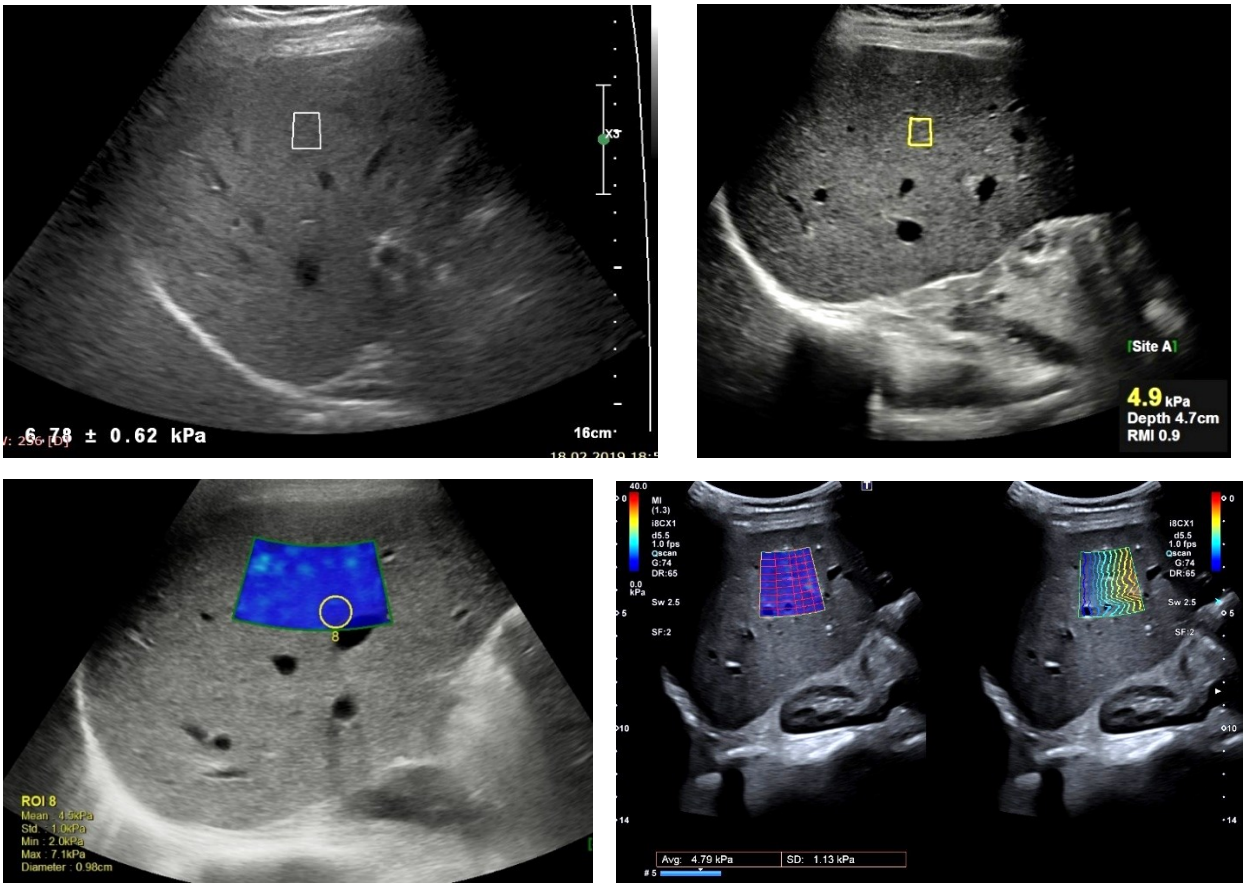

Figure 2.13 A-D. Ultrasound-Based Elastography for Liver Stiffness Assessment.
(A-B) Point Shear Wave Elastography (pSWE), with a focused region of interest for single-point measurements of liver stiffness. (C-D) Two-Dimensional Shear Wave Elastography (2D-SWE), featuring a color-coded elastogram overlay that provides real-time mapping of stiffness across a broader region of the liver parenchyma.

In general, feasibility of ultrasound-based elastography exceeds 90–95%, and measured liver stiffness correlates with fibrosis severity. Accuracy for diagnosing cACLD ranges from 90–95%, whereas for significant fibrosis it is approximately 80–90%. Previously, individual manufacturers proposed their own cutoff values, but in 2020, the Society of Radiologists in Ultrasound (SRU) introduced the "Rule of 4," which applies to any ARFI-based system. According to this rule:

- <5 kPa indicates a normal liver,
- 5–9 kPa rules out cACLD,
- 9–13 kPa suggests a high suspicion of cACLD,
- 13–17 kPa confirms cACLD,
- and >17 kPa corresponds to a high likelihood of portal hypertension.

Liver and spleen elastography can also be used in evaluating portal hypertension (PH). Initially, VCTE was used, with a liver stiffness cut-off of 20 kPa, combined with a platelet count

below 150,000/µL, indicating a high suspicion of PH. More recently, a cut-off of 25 kPa has been proposed as indicative of significant PH. Spleen stiffness measurement is a newer approach for PH assessment, and a single cut-off value of 40 kPa has been suggested for detecting significant PH. Some studies indicate that using both liver and spleen stiffness measurements, along with platelet counts, can enhance the accuracy of noninvasive PH assessment; in many patients with compensated cACLD, this approach may reduce the need for endoscopic evaluation (eso-gastroscopy).

Studies using Acoustic Radiation Force Impulse (ARFI) technologies—namely point SWE (pSWE) and 2D-SWE—have also been published, proposing a 17 kPa cutoff for diagnosing significant portal hypertension. When liver and spleen elastography are combined with a decreased platelet count (<150,000/µL), endoscopy can be avoided in a considerable number of cACLD patients.

In recent years, advanced ultrasound systems have acquired the capability to evaluate the viscoelastic properties of liver tissue. This feature appears particularly promising for MASLD by facilitating the distinction between simple steatosis (in the absence of inflammation) and metabolic dysfunction–associated steatohepatitis (MASH). Some studies have demonstrated that high-end ultrasound devices can achieve approximately 80% accuracy in noninvasively diagnosing MASH. Consequently, when ultrasound systems can quantify fatty infiltration, measure stiffness/fibrosis, and assess inflammation, a truly multiparametric ultrasound (MPUS) approach becomes feasible for evaluating chronic liver diseases.

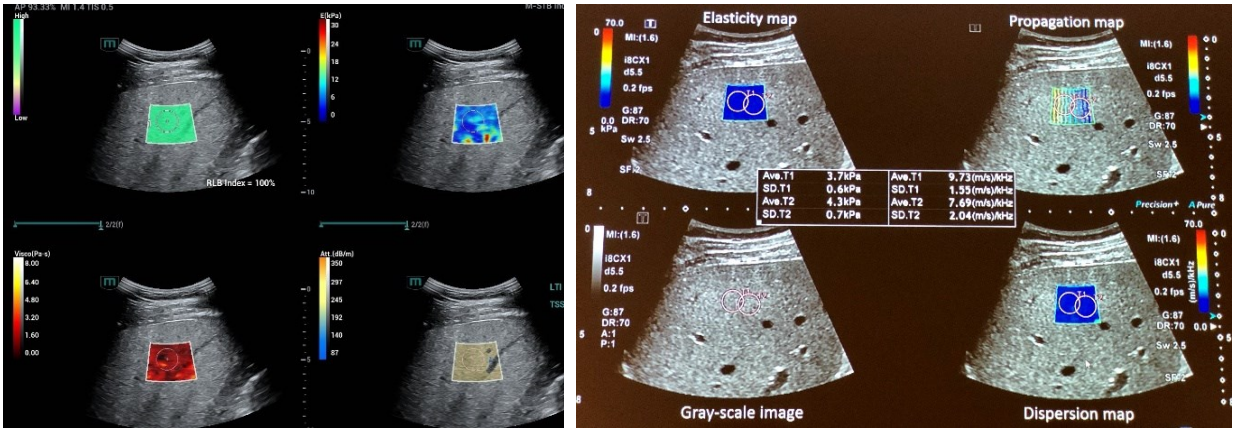

Figure 2.14 A-B. Multiparametric Ultrasound (MPUS) for Liver Evaluation. These images demonstrate an integrated approach that combines shear wave elastography, attenuation measurement, backscatter analysis, and dispersion mapping to provide a comprehensive assessment of the liver parenchyma.

Ultrasound is highly useful in patients presenting with ***jaundice***. In acute hepatitis, significant ultrasound findings are typically absent, although an enlarged, "sandwich-like" gallbladder wall may occasionally be observed due to hypoalbuminemia. In general, the primary clinical question is whether jaundice is obstructive or caused by parenchymal liver disease. With

obstructive jaundice, ultrasound usually reveals biliary tree dilation, including both intrahepatic ductal dilation (producing a “spider-like” appearance) and enlargement of the main biliary duct (MBD). Normally, the MBD measures less than 7 mm in diameter, though it may be slightly larger in post-cholecystectomy patients. In obstructive jaundice, the MBD can measure 15–20 mm. Examination of the dilated duct may detect stones (with roughly 70% accuracy, especially for smaller stones) or a mass in the pancreatic head. If the obstruction is located at the hepatic hilum (e.g., cholangiocarcinoma), the intrahepatic ducts will be dilated, but the MBD will remain normal.

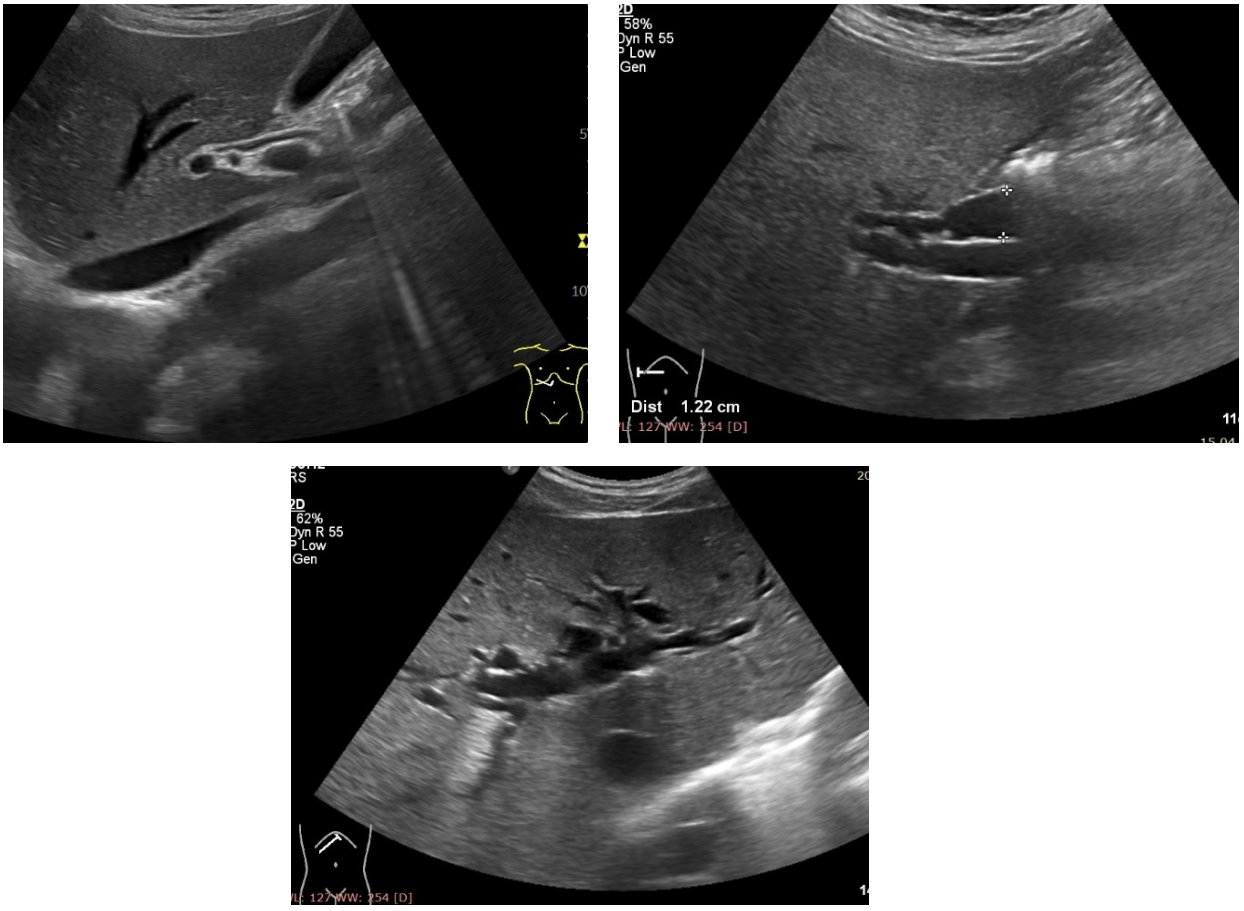

Figure 2.15 A Normal MBD; B-C. Ultrasound Findings in Obstructive Jaundice: Dilated Intrahepatic (C) and Extrahepatic Bile Ducts, Including a Prominent Common Bile Duct (>12 mm) (B)

When jaundice is related to decompensated cirrhosis, ultrasound typically shows cirrhotic changes, such as parenchymal heterogeneity, caudate lobe enlargement, splenomegaly, and ascites, while the biliary tree appears normal. Ultrasound is also valuable for investigating vascular liver disorders like Budd–Chiari syndrome and portal vein thrombosis. In Budd–Chiari syndrome, one or more hepatic veins may be absent or significantly narrowed. Doppler ultrasound and Contrast-EnhancedUultrasound (CEUS) are particularly helpful in these cases.

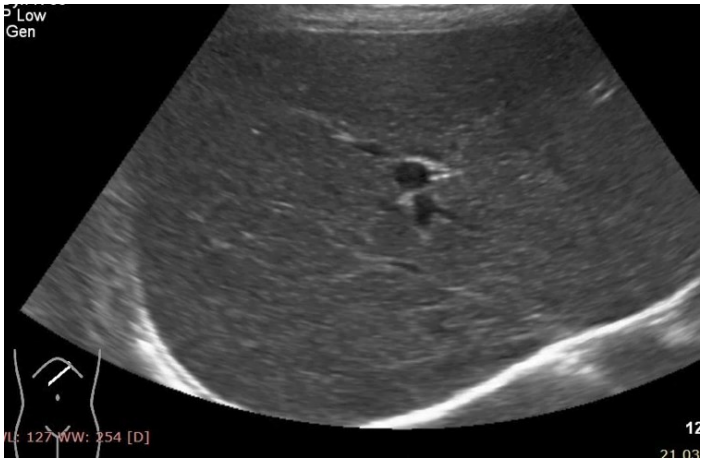

Figure 2.16. Ultrasound findings suggestive of Budd-Chiari syndrome: In this image, the expected hepatic veins are not clearly visualized. The hepatic veins appear absent.

Assessment of the portal vein may reveal either partial or complete thrombosis, appearing as a "solid structure" within the lumen. CEUS can differentiate benign from malignant thrombi with high accuracy. In patients with cirrhosis or hepatic malignancies, evaluating the entire portal system is essential, as the detection of a thrombus can substantially alter the therapeutic plan.

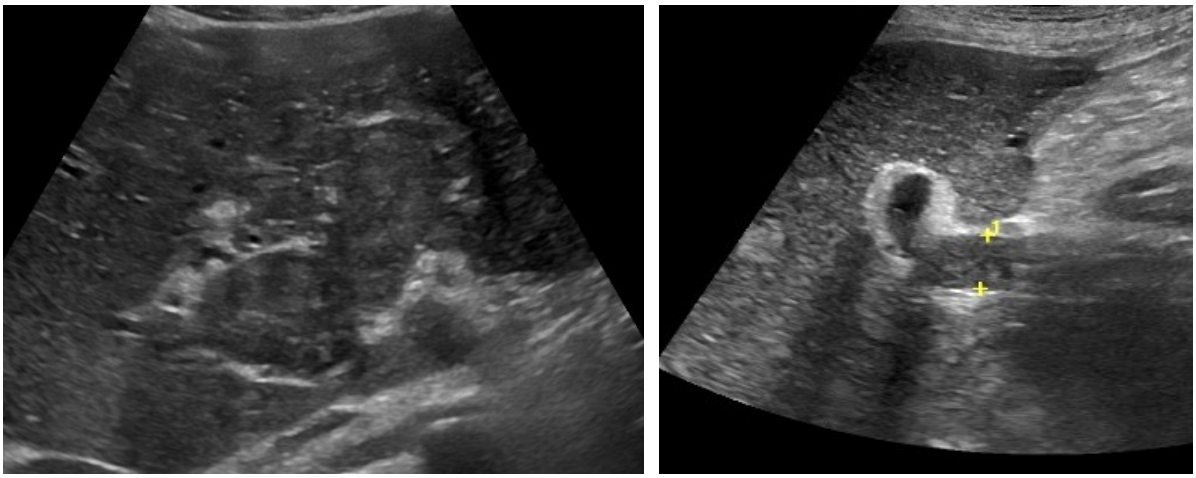

Figure 2.17 A-B. Two B-mode ultrasound images illustrating echogenic material within the lumen of the portal vein, consistent with portal thrombosis. The normally anechoic vascular channel appears partially or completely filled.

In individuals with cACLD or advanced fibrosis, ultrasound is essential for hepatocellular carcinoma (HCC) surveillance. These patients have a 1%–5% annual risk of developing HCC, depending on factors such as etiology, sex, and age. Current guidelines recommend bi-annual ultrasound screening alongside alpha-fetoprotein (AFP) testing for early detection. To optimize

sensitivity, the ultrasound must be performed by experienced operators—particularly for patients with markedly heterogeneous livers—and must include thorough scanning of the entire hepatic parenchyma. Adequate patient cooperation and a high-quality ultrasound machine are also crucial. In cases where certain liver regions cannot be visualized or the liver is extremely heterogeneous, additional imaging (e.g., contrast-enhanced CT or contrast-enhanced MRI) is indicated. The concept of abbreviated MRI for HCC screening has gained attention in recent years, but the large number of cACLD patients requiring lifelong surveillance poses substantial cost and logistical challenges. Importantly, individuals with cirrhosis who achieve a virological cure from HCV infection must continue lifelong HCC surveillance.

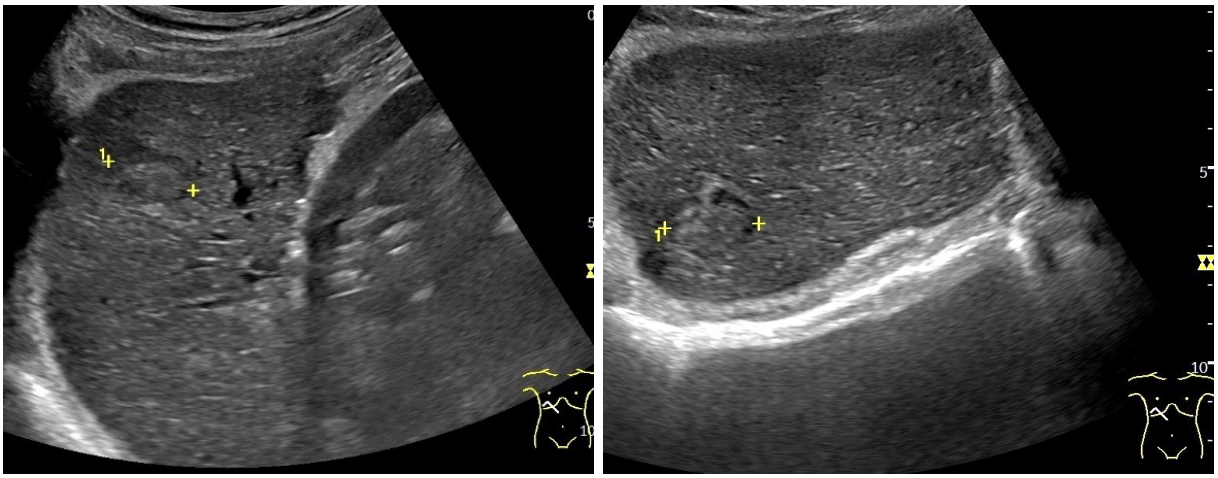

Figure 2.18 A-B. B-mode ultrasound images showing a predominantly heterogenous focal lesion in the right hepatic lobe, with a hypoechoic halo, findings that raise suspicion for hepatocellular carcinoma in the context of liver cirrhosis.

In ***conclusion***, ultrasound remains a cornerstone in the evaluation of chronic liver disease due to its safety, cost-effectiveness, and real-time imaging capabilities. While intrinsic limitations such as operator dependency and challenges with image quality—especially in patients with obesity or excessive bowel gas—are acknowledged, these issues can be mitigated by strict adherence to standardized protocols and proper training. Recent advancements, including Shear Wave Elasto-graphy, Contrast Enhanced Ultrasound have further enhanced the reproducibility and precision of this modality, allowing for earlier detection of fibrosis and other diffuse hepatic changes.

Although sectional imaging techniques like CT and MRI may offer superior sensitivity in identifying subtle parenchymal alterations, ultrasound's evolving technology continues to narrow that gap, while maintaining its unique advantages as a point-of-care tool. Its ability to rapidly deliver diagnostic and therapeutic insights makes it indispensable for a range of clinicians - from hepatologists to radiologists, internists and general practitioners - ultimately reinforcing its pivotal role in the daily management of chronic liver disease.

Selective references

1. Ferraioli G, Wong VW, Castera L, Berzigotti A, Sporea I, Dietrich CF, et al. Liver ultrasound elastography: An update to the World Federation for Ultrasound in Medicine and Biology guidelines and recommendations. Ultrasound Med Biol. 2018;44(12):2419-2440.

2. Ferraioli G, Barr RG, Berzigotti A, Sporea I, Wong VWS, Reiberger T, et al. WFUMB Guideline/Guidance on Liver Multiparametric Ultrasound: Part 1. Update to 2018 Guidelines on Liver Ultrasound Elastography. Ultrasound Med Biol. 2024;50(8):1071-1087. doi:10.1016/j.ultrasmedbio.2024.03.013.

3. Barr RG, Wilson SR, Rubens D, Garcia-Tsao G, Ferraioli G. Update to the Society of Radiologists in Ultrasound Liver Elastography Consensus Statement. Radiology. 2020;296(2):263-274. doi:10.1148/radiol.2020192437.

4. Sporea I, Șirli R, Popescu A, Stoian D. Textbook of Elastography. E-book: https://www.umft.ro/wp-content/upload/2024/10/TEXTBOOK-OF-ELASTOGRAPHY-21-oct.pdf

5. Sporea I, Badea R, Popescu A, Spârchez Z, Sirli RL, Dănilă M, et al. Contrast-enhanced ultrasound (CEUS) for the evaluation of focal liver lesions - a prospective multicenter study of its usefulness in clinical practice. Ultraschall Med. 2014;35(3):259-266. doi:10.1055/s-0033-1355728. Epub 2014 Feb 21. PMID:24563420.

6. Sidhu PS, Brabrand K, Cantisani V, Correas JM, Cui XW, D'Onofrio M, et al. EFSUMB Guidelines on Interventional Ultrasound (INVUS), Part II. Diagnostic Ultrasound-Guided Interventional Procedures (Long Version). Ultraschall Med. 2015;36(6):E15-35. doi:10.1055/s-0035-1554036. Epub 2015 Dec 15. PMID:26669871.

7. Sporea I, Friedrich-Rust M, Gilja OH, Bota S, Șirli R. Liver elastography. In: Dietrich CF, editor. EFSUMB Course Book on Ultrasound. 2nd ed. London: European Federation of Societies for Ultrasound in Medicine and Biology (EFSUMB); 2019. p. 123-145.

8. Nürnberg D, Chammas MC, Gilja OH, Sporea I, Șirli R, editors. WFUMB Course Book. 1st ed.: World Federation for Ultrasound in Medicine and Biology (WFUMB); 2021. ISBN: 978-1-8384990-0-6.

9. Ferraioli G, Barr RG, Berzigotti A, **S**porea I, Wong VW, et al. WFUMB Guideline/Guidance on Liver Multiparametric Ultrasound. Part 2: Guidance on Liver Fat Quantification. Ultrasound Med. Biol. 2024 Aug.;50(8):1088-1098

10. Dietrich CF, Nolsøe CP, Barr RG, Berzigotti A, Burns PN, et al. Guidelines and Good Clinical Practice Recommendations for Contrast-Enhanced Ultrasound (CEUS) in the Liver-Update 2020 WFUMB in Cooperation with EFSUMB, AFSUMB, AIUM, and FLAUS. Ultrasound Med Biol. 2020 Oct;46(10):2579-2604.

3. ULTRASOUND IN THE EVALUATION OF PORTAL HYPERTENSION; ULTRASOUND IN SPLEEN PATHOLOGY

Ivica Grgurević
WFUMB Centre of Education Croatia

3.a. ULTRASOUND IN THE EVALUATION OF PORTAL HYPERTENSION

1. Introduction

Portal hypertension (PH) is an increase in pressure within the portal vein system, leading to the opening of porto-systemic collaterals, which allow blood to bypass the high-pressure portal system and flow into the systemic circulation, where venous pressure is lower. The most common cause of portal hypertension is liver cirrhosis, characterized by increased vascular resistance at the level of hepatic sinusoids due to the accumulation of fibrous tissue in the liver and sinusoidal contraction. Other causes of portal hypertension can be classified as posthepatic, intrahepatic postsinusoidal, intrahepatic presinusoidal, and prehepatic (explained in more details in the paragraph 3 of this chapter).

The gold standard for quantifying the severity of portal hypertension in cirrhosis is the hepatic venous pressure gradient (HVPG), with the value of>5 mmHg indicating the presence of portal hypertension, and >10 mmHg clinically significant portal hypertension (CSPH), the later associated with the risk of developing complications such as esophageal varices and liver decompensation and death. HVPG is measured by invasive procedure of catheterisation of hepatic veins and represents difference between wedged pressure (when the lumen of hepatic vein is occluded by small balloon at the tip of the catheter) and free pressure when the balloon has been deflated. In fact, this is surrogate but most approximate measure of the portal pressure. To date, no imaging method has been demonstrated to accurately replace HVPG measurement. Since this method is invasive and requires skilled and dedicated personnel it has not become available in many centres. Therefore, in clinical practice diagnosis of PH relies still on the imaging methods and/or endoscopy. Moreover, the numerical value of HVPG is not a reliable measure for assessing the severity of portal hypertension in cases of postsinusoidal and presinusoidal causes. In these situations, we must rely on morphological indicators of portal hypertension, including imaging and endoscopic findings. Both of these are capable to detect complications, but not initial stages of PH, nor they can numerically quantify the severity of PH. Complications of PH including oesophageal varices (EV), portosystemic shunts and ascites start to develop when HVPG exceeds 10 mmHg, and from this threshold PH is considered as clinically significant (CSPH). The presence of these complications may be assessed by imaging methods including US. Therefore, ultrasound (US) can be used to confirm the presence of clinically significant portal hypertension (CSPH) if typical morphological signs are present. However, the absence of these morphological signs does not exclude the presence of portal hypertension.

Apart from detecting morphological signs of PH, US may be used to search for the cause (-es) of PH, i.e. to define the pathophysiological substrate responsible for the development of PH including the anatomical level at which this substrate exists. In a significant number of cases achievements of these goals can be facilitated by using Doppler in addition to grey-scale US. Nowdays elastography has become inevitable tool for assessment of CLD including PH, and by combining all these modalities US has indeed become multiparametric and powerfull diagnostic method. In the text that follows we discuss the use of grayscale ultrasound, Doppler, and elastography in diagnosing portal hypertension.

2. Ultrasound signs of PH

2.1. Morphological signs of portal hypertension by grey-scale ultrasound

The presence of certain morphological signs may vary depending on the cause of PH, i.e. the anatomical level at which the causative substrate has been localised. Since the most prevalent cause of PH is liver cirrhosis, US findings typical for PH as described in the following text refer mostly to this aetiology of PH. Some distinctive US findings typical for other causes of PH will be highlighted.

Most common US signs of PH include dilated portal vein (PV), splenic vein (SV), superior mesenteric vein (SMV) with reduced respiratory variation, the presence of porto-systemic venous collaterals, as well as the signs of visceral congestion such as splenomegaly, gallbladder and stomach/bowel wall edema, and ascites (Figures 3.a.1 and 3.a.2).

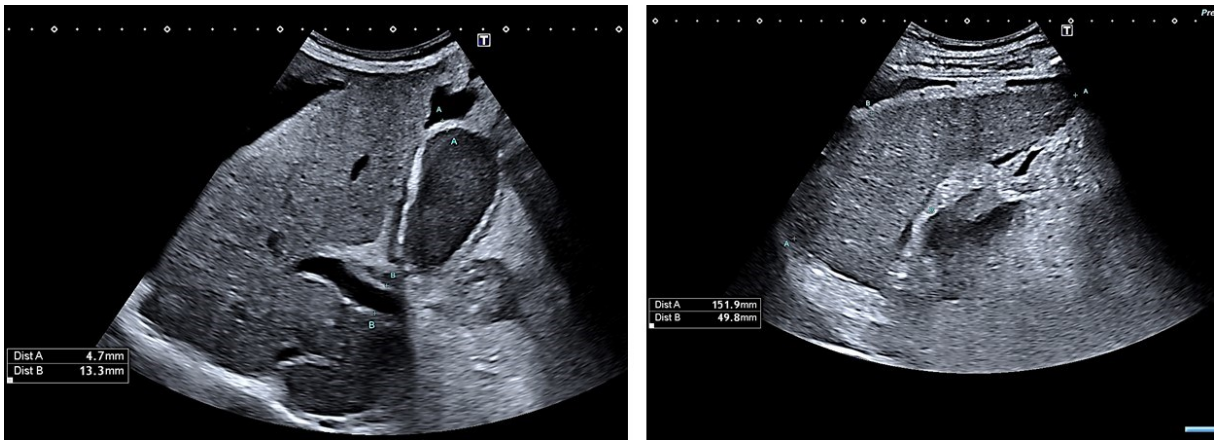

Figure 3.a.1. Morphological signs of portal hypertension by grey-scale (B-mode) ultrasound. Cirrhotic liver surrounded by ascites, dilated portal vein (>13 mm), galbladder wall edema (>3 mm) (left panel). Splenomegaly (>13 cm) (right panel).

Splenomegaly is defined by the bipolar (cranio-caudal) diameter exceeding 12 cm in average person (or >13 cm in very tall individuals). However, it might be absent in about 20-30% of cases, especially in alcoholic cirrhosis. Ascites is typical, but only if accompanied by other signs

of PH in patients with the history of chronic liver disease (CLD), as it can be caused by other conditions such as heart failure, severe hypoalbuminemia or peritoneal carcinomatosis. When the causative substrate is localized downstream to the main trunk of PV (intrahepatic and post-hepatic causes of PH) it becomes dilated (>12.5-13 mm for PV and >11 mm for SV) and loses the respiratory variation (<40%) in diameter due to high portal pressure.

Porto-systemic collaterals are highly specific for the presence of portal hypertension on imaging studies including the US. The most common porto-systemic collaterals include the recanalized umbilical vein and collaterals in the splenic hilum (Figure 3.a.2). The umbilical vein typically originates from the left branch of the portal vein, passing through the ligamentum teres to reach the anterior abdominal wall, where it travels beneath the rectus muscle and terminates in the umbilical region. Splenic collaterals appear as serpentine anechoic tubular structures filled with colour on Doppler imaging, located in the splenic hilum or on the splenic surface. Among these collaterals, veins forming a splenorenal shunt can be observed, where blood flow is directed from the spleen to the renal vein.

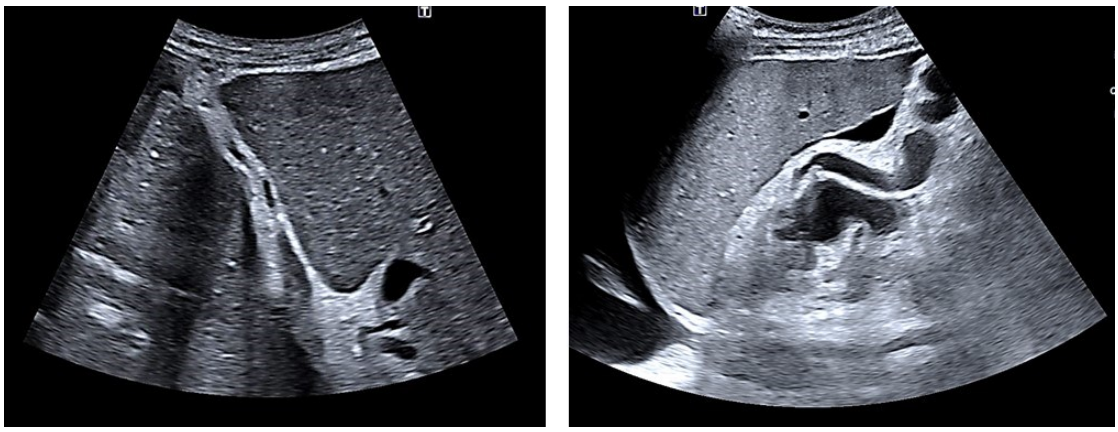

Figure 3.a.2. Portosystemic collaterals: recanalized umbilical vein arizing from the left liver lobe (left panel), serpiginous collateral veins in the splenic hilus (right panel).

Additionally, collaterals from the upper pole of the spleen drain blood into the paraesophageal veins, leading to the development of esophageal varices. The left gastric vein (LGV), also known as the coronary vein, arises from the portal vein trunk and runs along the lesser curvature of the stomach. It can be visualized between the stomach and the left liver lobe. In cases of portal hypertension, the LGV becomes dilated, and its blood flow direction becomes hepatofugal, meaning blood is redirected from the portal vein into the paraesophageal veins, leading to the formation of esophageal varices. Less commonly, retroperitoneal and pelvic collaterals can also be observed, as well as ectopic collaterals within the duodenal and small bowel walls. In some cases, careful scanning through the epigastrium or left intercostal spaces—using the spleen as an acoustic window—can reveal gastric fundal varices, particularly if the stomach is filled with liquid, which can be achieved by having the patient drink two glasses of water.

2.2. Haemodynamic changes in portal hypertension by Doppler ultrasound

2.2.1. Doppler in healthy liver

Blood is supplied to the liver through the portal vein (approximately 75% of the volume) and the hepatic artery (the remaining 25%), while it is drained into the inferior vena cava via the hepatic veins. The portal vein branches into left and right divisions, which further divide into smaller branches for each of the eight hepatic segments, and the same pattern applies to the hepatic artery. There are three main hepatic veins, with the left and middle veins most commonly sharing a common trunk.

Blood flow in the liver's blood vessels can be analyzed using Doppler ultrasound. Color Doppler is used to assess the presence of blood flow and its direction within the vessel, while pulsed Doppler performs spectral analysis, evaluating the morphology of the Doppler spectrum and blood flow velocity. By applying specific mathematical ratios to blood flow velocities, Doppler indices have been developed. These indices provide not only velocity measurements but also additional numerical information about the resistance to blood flow in the liver or spleen.

In the portal vein, the direction of blood flow is hepatopetal, meaning it is directed toward the liver, and it is coded in red if the ultrasound probe is placed in the intercostal space above the right liver lobe. Pulsed Doppler imaging reveals a linear appearance of the Doppler spectrum in the portal vein, with slight oscillations in peak velocities due to respiration and cardiac pulsations. The average peak velocity (Time Averaged Maximum Velocity, TAMax) ranges between 20 and 40 cm/s, while the average mean velocity (Time Averaged Mean Velocity, TAMV) ranges between 15 and 30 cm/s.

The Doppler spectrum in the hepatic artery has a typical shape seen in parenchymal organs of the abdomen (liver, spleen, and kidneys). It consists of a systolic component and a continuously antegrade diastolic component, meaning that velocities remain above the baseline throughout the cardiac cycle. This indicates that blood flow is continuously directed toward the liver during both systole and diastole, without the initial negative diastolic deflection observed in muscular or visceral arteries. This type of spectrum is referred to as a low-resistance spectrum. The normal systolic peak velocity ranges between 30 and 75 cm/s, while the end-diastolic velocity ranges between 15 and 25 cm/s (Figure 3.a.3, right panel).

One of the most commonly used Doppler indices is the resistance index (RI), which is calculated by dividing the difference between the systolic peak velocity and the end-diastolic velocity by the systolic peak velocity. A similar index is the pulsatility index (PI), which is obtained by dividing the difference between the systolic peak velocity and the end-diastolic velocity by the time-averaged maximum velocity (TAMax) measured by the device's software over one full cardiac cycle (systole and diastole). Normal RI values range between 0.55 and 0.7, while normal PI values are up to 0.9.

In cases of increased resistance to blood flow, such as cirrhosis, the systolic peak velocity increases while the end-diastolic velocity decreases, leading to a rise in RI and PI. Conversely, in

cases of reduced resistance (e.g., the presence of an arteriovenous shunt), the end-diastolic velocity increases, resulting in a lower RI.

The most complex Doppler spectrum is observed in the hepatic veins, which exhibit a triphasic waveform. When the ultrasound probe is placed below the right costal margin and directed cranially, toward the junction of the hepatic veins and the inferior vena cava (IVC), a triphasic spectrum is obtained. This consists of one positive deflection (above the baseline) and two negative deflections (below the baseline) (Figure 3.a.3, left panel).

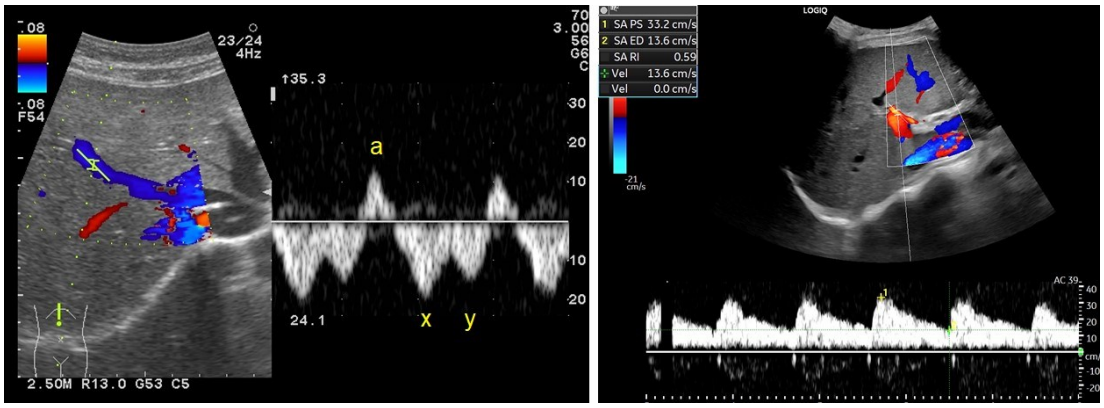

Figure 3.a.3. Spectral Doppler imaging of the hepatic vein (left panel) and hepatic artery (right panel) in a healthy person. Note triphasic waveform from the hepatic vein, and low resistance arterial waveform from the hepatic artery (normal peak systolic, end diastolic velocities and resistive index).

The positive deflection represents the "a" wave of atrial contraction, during which a portion of the blood from the atrium is directed toward the liver—toward the ultrasound probe—resulting in a positive Doppler shift. The two negative waves correspond to ventricular systole and diastole. During these phases, blood flows from the liver into the right heart and from the atrium into the right ventricle, moving away from the ultrasound probe, which is why these deflections appear below the baseline in the spectral Doppler display. This waveform can undergo changes depending on the structure of the surrounding liver tissue, hemodynamic conditions in the right heart, and potential pathological connections, such as direct blood shunting from the portal vein or hepatic artery into the hepatic veins.

The spleen is a very important organ that should be analyzed in the context of portal hypertension (PH), as it undergoes not only morphological but also hemodynamic changes. In a healthy spleen, blood enters through the splenic artery and drains via the splenic vein, which contributes to the portal vein flow. Doppler waiveform of the splenic artery is also of the low-resistance type. In addition to the resistance index (RI), the pulsatility index (PI) is also analyzed. In the absence of portal hypertension, these values should be <0.63 and <1, respectively. The average mean blood flow velocity in the splenic vein at the splenic hilum in individuals without portal hypertension is <15 cm/s.

2.2.2. Doppler in portal hypertension

With the onset of PH significant changes take place in the portal circulation and these can be assessed by Doppler US. In turn, these findings may help to establish the diagnosis and reveal the cause of PH. As in previous paragraph, most of the findings discussed here refer to PH caused by liver cirrhosis. Abundance of the accumulated fibrous tissue accompanied by its biochemical changes lead to the distortion of liver architecture and shrinkage of the liver with the resultant compression of the intrahepatic branches of hepatic veins, portal vein and hepatic artery. Together with the narrowing of hepatic sinusoids due to accumulation of extracellular matrix in the sapce of Disse, these changes result in the increased resistance to blood flow through the liver. In turn, phasicity of the Doppler waveform (or less correctly used term „blood flow pulsatility“) from the HV becomes reduced: usually it loses its triphasic form and becomes flattened and linear, and this might be additionally influenced by the presence of the shunt between intrahepatic branches of portal vein and HV. Reversal of the portal blood flowfrom hepatopetal into hepatofugal is highly specific sign of severe PH, usually resulting from the advanced liver cirrhosis, and less frequently from other intrahepatic causes (Figure 4, right panel). However, hepatofugal flow is not frequently present, as the direction of portal vein blood flow remains hepatopetal in majority of patients with cirrhosis (Figure 3.a.4, left panel).

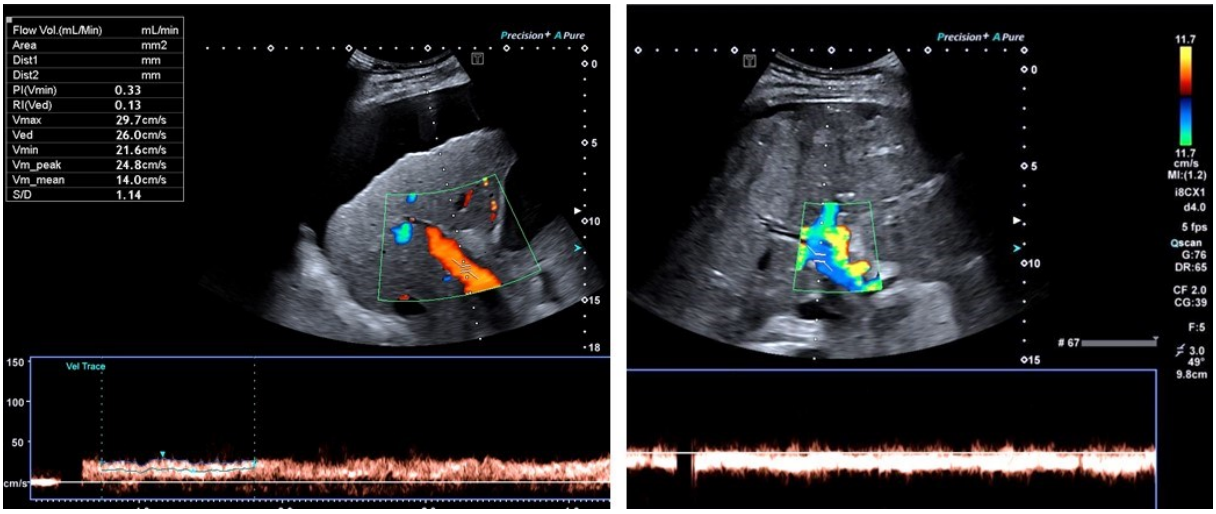

Figure 3.a.4. Spectral Doppler imaging of the portal vein in patients with cirrhosis: hepatopetal flow with diminished velocities (left panel), and hepatofugal flow (coded in blue colour, on the right panel)

Therefore, even if highly specific, this finding lacks sensitivity to detect PH. Nevertheless, with the progression of cirrhosis and PH portal velocity becomes diminished (<15 cm/s for the time averaged mean velocity (TAMV)), whereas in cases with very high intrahepatic resistance and abundant portal blood inflow more sinusoidal shape of the PV waveform can be observed, which is due to helical motion of the blood in PV. Similar reasons lead to the increase of peak systolic

velocity (PSV >60 cm/s) and diminished end-diastolic velocity in HA, resulting in the increased HA resistive index (RI >0.7). However, in cases where the shunt between HA and HV has been formed, HA RI becomes diminished due to drop in the peripheral resistance to arterial blood flow, and the resultant waveform in HA becomes changed with very high both PSV and EDV. Portal hypertension leads to the congestion of the spleen, which is accompanied by the splenic tissue hyperplasia, both leading to the increased splenic resistance to arterial blood flow. Consequently, the spectral recording from the intraparenchymal branches of the splenic artery shows an elongated spectral shape with high peak systolic and low end-diastolic velocities, ultimately resulting in high splenic RI and PI. One of the most well-studied Doppler indicators of portal hypertension is the splenic artery pulsatility index, with a threshold value of >1, where increasing index values are more likely to indicate the presence of portal hypertension. This index is automatically calculated after marking the peak velocities over the area of one cardiac cycle, i.e., the arterial spectrum (manually or automatically). In individuals with esophageal varices, the blood flow velocity in the splenic vein increases and exceeds 15 cm/s. The splenoportal index (SPI>3), calculated as the product of the longer and shorter diameter of the spleen divided by the average mean blood flow velocity in the portal vein, has a high specificity and sensitivity (both >90%) for detecting esophageal varices in patients with cirrhosis. Splanchnic vasodilatation as the typical finding in portal hypertension might be assessed by Doppler by demonstrating decreased superior mesenteric artery (SMA) impedance indices, particularly PI<2.7, whereas RI is less reliable in this context (normal value around 0.87). Conversely, splanchnic and systemic vasodilation lead to impaired arterial perfusion of the kidneys, resulting in increased resistance in the intrarenal arterial branches, with their RI becoming elevated (>0.7), indicating the risk of developing hepatorenal syndrome. Among more complex Doppler indices, one of the most frequently used is congestive index (CI), representing the ratio between cross sectional area and mean velocity of the PV, being pathological over the cut-off value of around 0.1 cm/s.

In conclusion, the presence of portosystemic collaterals and hepatofugal flow in the portal vein are highly specific signs for PH, but lack sensitivity. The abundance of other Doppler features and indices as described above highlights the fact that none of them has proven to be a sufficiently reliable tool for diagnosing and stratifying the severity of portal hypertension. Additionally, numerous other factors affecting hemodynamics—such as cardiac function, metabolic status, the presence of atherosclerosis, and the use of certain medications—must be taken into account. Therefore, the presence of some of these hemodynamic changes or Doppler findings increases the likelihood of a diagnosis of portal hypertension in the appropriate clinical context. However, it would be incorrect to establish this diagnosis based solely on a single finding in the absence of other elements of the clinical picture. Similar to the morphological signs of portal hypertension, Doppler changes have also been shown to lack sensitivity, and therefore the absence of a certain hemodynamic feature on Doppler analysis does not exclude portal hypertension. In this regard, elastographic assessment of liver and spleen stiffness is now considered a more reliable method, and will be described in the next paragraph.

2.3. Elastography for the assessment of portal hypertension

In patients with chronic liver diseases suspected of developing PH, but without typical ultrasound or hemodynamic changes described in previous sections, liver and/or spleen elastography is recommended as an additional non-invasive method for assessing PH. Elastography can help determine or exclude CSPH and rule out high-risk esophageal varices (HRV), thereby avoiding the need for invasive methods such as hepatic vein catheterization and HVPG measurements or endoscopy. In cirrhotic patients, the early stages of PH are primarily due to increased resistance to portal blood flow caused by the accumulation of fibrous tissue, making the liver stiffer—something that can be measured with elastography. As liver disease progresses PH increasingly becomes influenced by hemodynamic factors, particularly increased blood flow volume through the portal vein. This, combined with hepatic resistance, exacerbates PH. While LSM cannot assess this hemodynamic factor, spleen stiffness measurement can, as rising portal pressure leads to increased spleen congestion, making it stiffer. Therefore, LSM can be used to determine the presence or absence of CSPH and HRV, but not for further numerical quantification of portal hypertension severity.

Spleen stiffness measurement can also be used to determine or exclude the presence of CSPH and high-risk esophageal varices. Among all elastographic methods, transient elastography has been the most extensively validated, which is why the Baveno guidelines provide recommendations specifically for this technique. According to the Baveno VII guidelines, the following non-invasive criteria can be used for the diagnosis of PH and HRV:

- Presence of CSPH (HVPG≥10 mmHg): LSM≥25 kPa (in all etiologies except for obese NAFLD patients), or SSM>50 kPa
- CSPH ruled-out: LSM≤15 kPa + Plt≥150, or SSM≤21 kPa
- HRV ruled-out: LSM<20 kPa + Plt≥150, or SSM≤40 kPa

Other elastographic methods based on acoustic radiation force impulse (ARFI) imaging, including point-shear wave elastography (pSWE) and two-dimensional shear wave elastography (2DSWE), have also been investigated with similar results. However, since these methods have been tested on significantly fewer subjects, additional studies are recommended for this indication. For illustration, the pSWE method using Philips technology has proven reliable in ruling out high-risk esophageal varices with a cutoff LSM <12 kPa and platelet count >150 (sensitivity 0.95, specificity 0.42). Meanwhile, a meta-analysis of studies using 2DSWE (Supersonic Imagine) identified cutoff LSM values of 14 kPa and 32 kPa for excluding and confirming CSPH, respectively, as well as 14 kPa and 50 kPa for excluding and confirming high-risk esophageal varices.

3. Detecting the cause of portal hypertension

Causes of PH can be classified according to anatomical level at which they express their pathogenic actions as to: 1. Post-hepatic causes (congestive heart failure (CHF) leading to congestive liver disease and cirrhosis, Budd-Chiari syndrome BCS); 2. Hepatic causes (2a-postsinusoidal (sinusoidal obstructive syndrome (SOS)), 2b-sinusoidal (cirrhosis)), and 2c—pre-sinusoidal (idiopathic non-cirrhotic portal hypertension (INCPH) or porto-sinusoidal vascular disease, including the nodular regenerative hyperplasia (NRH), primary biliary cholangitis (PBC), shistosomiasis); 3. Pre-hepatic causes (portal vein thrombosis (PVT) and portal vein stenosis (PVS), just to mention the most common conditions (1).

3.1. Post-hepatic causes of PH

Patients with CHF have increased filling pressures of the right-sided heart cavities, and this pressure transmits to the inferior vena cava (IVC) and hepatic veins leading to the deranged blood outflow from the liver, that becomes congested and therefore enlarged. Hepatic veins become dilated (>8 mm as measured at least 2 cm from their inflow into IVC. Due to congestion the gallbladder wall becomes thickened (>3 mm), usually with clear delineation between the histological layers. Inferior vena cava is dilated (>2 cm) with the loss of inspiratory collapse (<50%). Doppler studies reveal typical changes in addition to the described morphological features. Since in majority of patients right-sided heart failure is accompanied by dilation of tricuspid valve with resulting regurgitation in systole, spectral analysis of the HV waveform reveals reverted systolic wave fussed with „a“ wave of atrial contraction. Together they make a single positive deflection (above the zero line at pulse Doppler spectral analysis) followed by the negative deflection representing the diastolic wave of right-ventricular filling. High pressures from HVs transmit through the liver sinusoids into PV. Therefore blood flow in PV becomes pulsatile as well, acquiring the sinusoidal shape at spectral analysis. In patients with severe congestion and very high right-sided pressures the flow in PV becomes biphasic (to and fro, on the both sides of the zero line) resembling the shape of Doppler spectrum from HV.

In Budd-Chiari syndrome obstructive substrate causes deranged venous drainage of the liver and can be localised at any level from the smallest tributaries of the HV to the entrance in the right atrium. Sometimes it can be found in the IVC as well. In the western hemisphere it is most frequently caused by the thrombosis of the respective veins. Therefore, echogenic material in the lumen of one or more HVs can be detected by grey-scale US, with lack of blood flow on Doppler studies. As the result intrahepatic venous collaterals develop directing blood to the patent HV. These collaterals may have typical shape known as „hockey-stick sign (Figure 3.a.5).

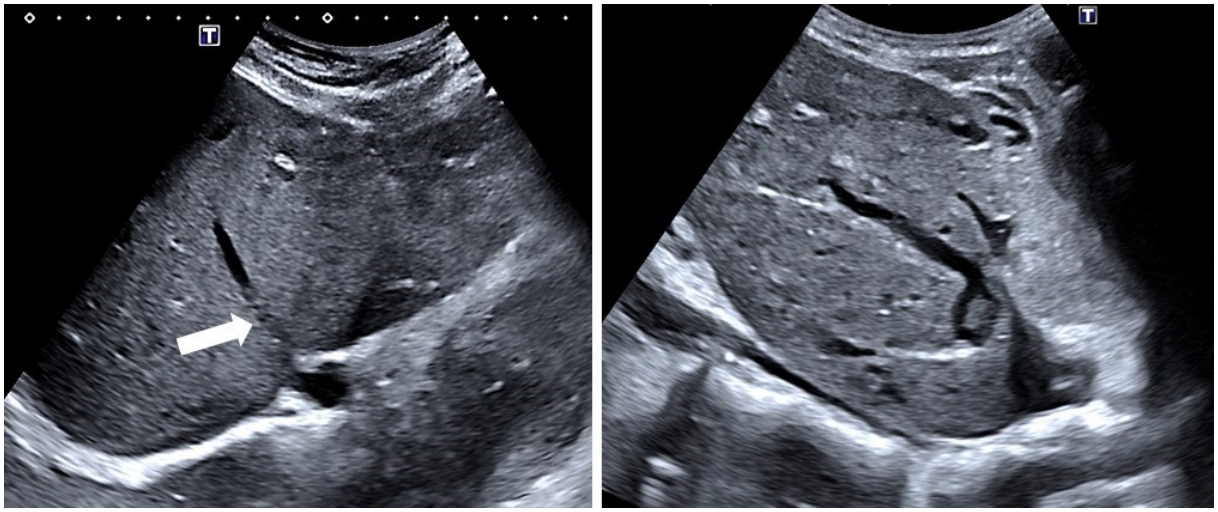

Figure 3.a.5. B-mode and Doppler images of Budd-Chiari syndrome. Segmental obstruction of the middle hepatic vein (white arrow, left panel); intrahepatic venous collateral resembling hockey-stick (right panel).

Peri-caval segments of the liver might drain directly to the IVC through short hepatic veins, which are not that functionally important under physiological conditions, but in cases of BCS might acquire a decisive role to preserve liver perfusion. These veins become dilated and clearly visible at US examination, especially those draining the caudate lobe or right inferior liver segments.

3.2. Hepatic causes of PH

These can be divided into post-sinusoidal, sinusoidal and pre-sinusoidal causes. Typical representative of post-sinusoidal intrahepatic causes of PH is SOS. This condition takes place usually after very toxic chemotherapeutic regimens (such as those used for myeloablative therapy in acute leukemias). This therapy causes endothelitis and peeling of endothelial cells in central veins and microscopic tributaries of HV leading to the obstruction of their lumen. This in turn causes increased upstream pressure (in sinusoids and PV) leading to accumulation of ascites and oedema to the gallbladder wall. Blood flow direction in PV is typically hepatofugal, but this Doppler finding should be considered pathognomonic only if physiological (hepatopedal) flow was documented before the initiation of the mentioned therapy.

As already pointed-out, the most common cause of PH is liver cirrhosis where the pathological substrate typically occurs in the perisinusoidal space of Disse, the place where hepatic stelate cells as the main source of extracellular matrix reside within the liver. In cirrhosis liver texture is coarse, surface nodular and the edges blunted. In early stage of cirrhosis, especially micronodular one, nodularity of the liver surface might not be readily detected by US. In these cases some authors advice to analyse interface of the hepatic veins which becomes irregular as well, and usually is free of the artefacts which are common when analysing outer liver contours. Caudate lobe becomes enlarged (>3 cm in antero-posterior diameter), HVs narrowed with irregular contours, whereas PV becomes dilated, and umbilical vein reanalysed. Again, gallbladder wall

oedema can be easily detected. Other signs are common to other causes of PH as described in the paragraph 2.1.

Idiopathic non-cirrhotic portal hypertension (INCPH, or porto-sinusoidal liver disease, PSVD, according to the new nomenclature) develops as the result of phlebitis of terminal branches of PV producing ischaemia of the irrigated hepatocytes that undergo regeneration in nodular fashion but without excessive accumulation of fibrosis. Therefore, in these patients liver resemble cirrhosis, but lacks increased amount of fibrosis and the prognosis is much better. By grey-scale US and even Doppler studies it is often not possible to reliably differentiate PSVD from cirrhosis, and the best way to do so by non-invasive means is to perform liver elastography. In cirrhosis liver stiffness is high (usually >15 kPa by transient elastography) and in PSVD only slightly increased (usually below 10 kPa), whereas the spleen stiffness is increased if portal hypertension exists.

In PBC pathological substrate initially takes place at the portal tracts. However, in the later course of the disease fibrosis progresses and finally encompasses liver lobules, so the morphological features do not differ significantly from other causes of PH caused by other types of cirrhosis.

3.3 Pre-hepatic causes of PH

Most common cause of pre-hepatic PH is portal vein thrombosis (PVT) which may have different extension encountering only intrahepatic branches, or main portal trunk with or without extending into other visceral veins such as SMV, SV and IMV. In acute phase PVT might be missed by grey-scale US as in this phase thrombus has hypo- to anechoic appearance (Figure 3.a.6).

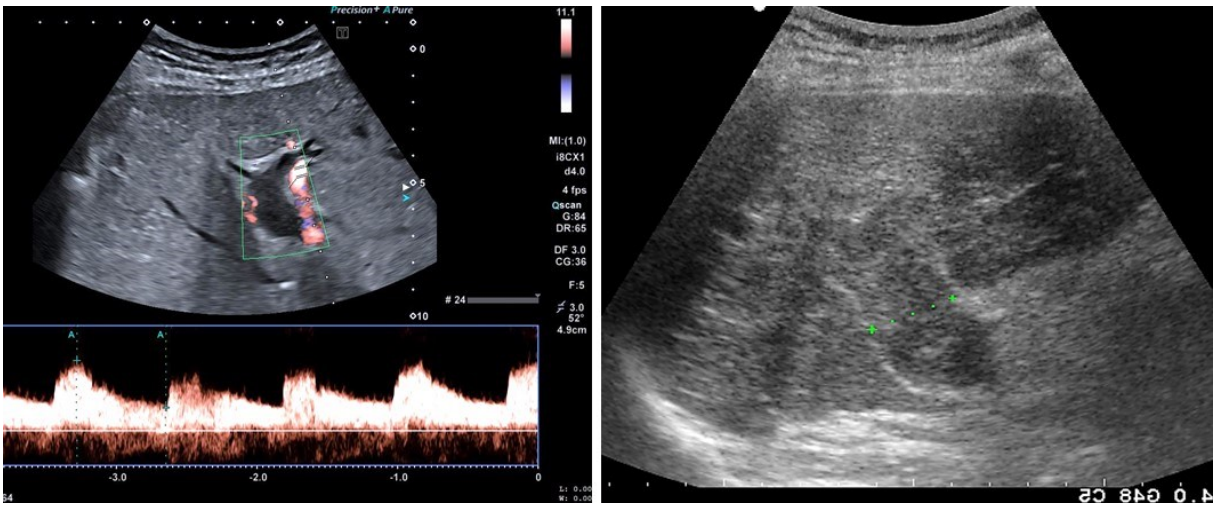

Figure 3.a.6. Portal vein thrombosis. Acute thrombosis with almost anechoic thrombus occupying the intrahepatic segment of the portal vein, with patent hepatic artery (left panel). Neoplastic infiltration of the portal vein, filled with echogenic material; portal vein is dilated and no patent lumen is seen (right panel).

However, by using Doppler no flow in the affected vein can be detected provided correct angle of insonation (beware: if Doppler beam enters the longer axis of the investigated blood vessel under 90° no flow will be detected eventhough it is present and normal, this is due to physical reasons of Doppler formula used to calculate the flow). With time thrombus becomes more echogenic and may be readily detected by grey-scale US. In long-standing thrombosis collateral veins develop to by-pass the obstructed segment of the PV forming so called cavernoma (cavernous transformation of the PV). This cavernoma is usually composed of the small veins running alongside or even within the wall of the the extrahepatic biliary ducts. In the latter cases common bile duct (CBD) wall becomes thickened which might be a source of potentially dangerous misinterpretation, as it might be wrongly considered as extrahepatic cholangiocarcinoma. This dilemma may be easily resolved by Doppler revealing abundant venous type flow within such a changed CBD wall.

Portal vein stenosis most frequently develops as the result of iatrogenic interventions with surgical resection of pancreatic head or other local structures including the liver transplantation. In these cases PV acquire the shape of the sandglass. By using Doppler very high velocities might be observed at the level of stenosis, with turbulent flow downstream to stenosis.

4. Monitoring the Patency of the Transjugular Intrahepatic Portosystemic Shunt

The transjugular intrahepatic portosystemic shunt (TIPS) is placed in patients with severe portal hypertension and serves as a connection between the hepatic vein and the portal vein. The patency of the TIPS can be monitored using Doppler ultrasound. After TIPS placement, blood flow in the branches of the portal vein becomes hepatofugal, meaning it is directed toward the TIPS, while the flow velocity in the main portal vein accelerates (over 30 cm/s). The normal range of blood flow velocity in the TIPS is between 90 and 190 cm/s, with velocities outside this range indicating TIPS stenosis (Figure 3.a.7).

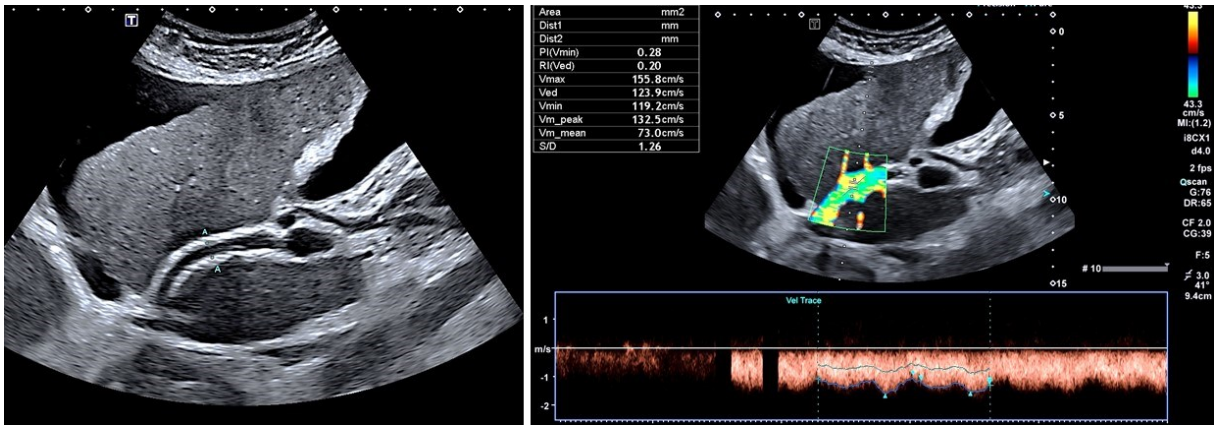

Figure 3.a.7. Ultrasound imaging of the transjugular intrahepatic porto-systemic stent shunt (TIPS). On B-mode imaging TIPS looks as the curvilinear tubular structure with echogenic walls, and patent lumen, inserted between the right hepatic vein and portal vein (left panel). On Doppler studies there is flow through the TIPS directed towards the right hepatic vein, with mean peak velocity of 132 cm/s, which is considered normal (right panel).

Stenosis can also be visualized using grayscale ultrasound and color Doppler, with optimized scan settings to avoid artifacts. Additionally, an increase or decrease in velocity of more than 50 cm/s at the site of stenosis compared to previous measurements is considered an indicator of significant stenosis. In cases of TIPS stenosis intrahepatic portal flow that was hepatofugal on the prior examination changes to hepatopetal again. Measurement of SSM is also a useful parameter in monitoring TIPS functionality, as SSM decreases immediately after its placement, while an increase in spleen stiffness may indicate TIPS stenosis.

5. Conclusion

Ultrasound is an indispensable method in the diagnosis of patients with portal hypertension, allowing the detection of typical morphological changes such as the development of portosystemic collaterals, splenomegaly, and ascites. Doppler ultrasound can analyze hemodynamic changes in the hepatic and portal circulation that are characteristic of portal hypertension. If certain morphological signs or hemodynamic changes are observed, the presence of clinically significant portal hypertension (CSPH) can be determined with high probability. However, the absence of these signs in an appropriate clinical context does not reliably exclude CSPH. Ultrasound and Doppler are reliable methods for determining the cause of portal hypertension, including the diagnosis of vascular liver diseases. In patients with compensated cirrhosis who do not exhibit clear signs of clinically significant portal hypertension (CSPH), liver and spleen elastography can be used non-invasively to determine or exclude its presence and to rule out high-risk esophageal varices. Summary of the most typical mophological and haemodynamic features of portal hypertension is present in Table 3.a.1. Proposed algorithm of using ultrasound methods to assess for the presence of PH is depicted in Figure 3.a.8.

Table 3.a.1. Morphological and haemodynamic (on Doppler ultrasound examination) features of portal hypertension. PH-portal hypertension; PI-pulsatility index, RI-resistive index, SMA-superior mesenteric artery.

Morphological signs of portal hypertension	**Description**	**Comment**
Dilated portal vein	>12.5-13 mm	Not highly specific, as it may be dilated in cases of non-cirrhotic splenomegaly such as systemic diseases and haematological malignancies
Porto-systemic collaterals	Recanalized umbilical vein, splenic collaterals (hilum, surface, spleno-renal shunt), ectopic collaterals	Highly specific, low sensitivity
Splenomegaly	Cranio-caudal diameter >12 cm (>13 cm in tall individuals)	Not universally present (20-30% of patients with PH do not have splenomegaly)
Ascites	Anechoic fluid in the abdominal cavity	Specific for PH only in the appropriate clinical context (i.e. presence of cirrhosis); otherwise consider other causes (peritoneal carcinomatosis!)

Doppler features of portal hypertension	Description	Comment
Hepatofugal direction in the portal vein	Flow in the portal vein coded by the blue colour	Highly specific, low sensitivity
Decreased portal velocity	<15 cm/s (Time averaged mean velocity, or <20-25 cm/s of Time averaged maximum velocity; conversion factor 0.57)	Sometimes „helical“ shape of the waveform on the spectral analysis may be observed due to the high resistance to portal flow in the liver
Flattened waveform in the hepatic veins	Normal waiveform is triphasic	Might be flattened in the absence of cirrhosis and PH (fatty liver, other infiltrative diseases)
Increased hepatic artery RI	RI>0.7	Specific for CSPH if >0.78, but low sensitivity
Increased splenic artery PI (parenchymal branches)	PI>1	Portal hypertension more likely with the higher range of PI value
Diminished SMA PI	<2.7	Due to splanchnic vasodilatation

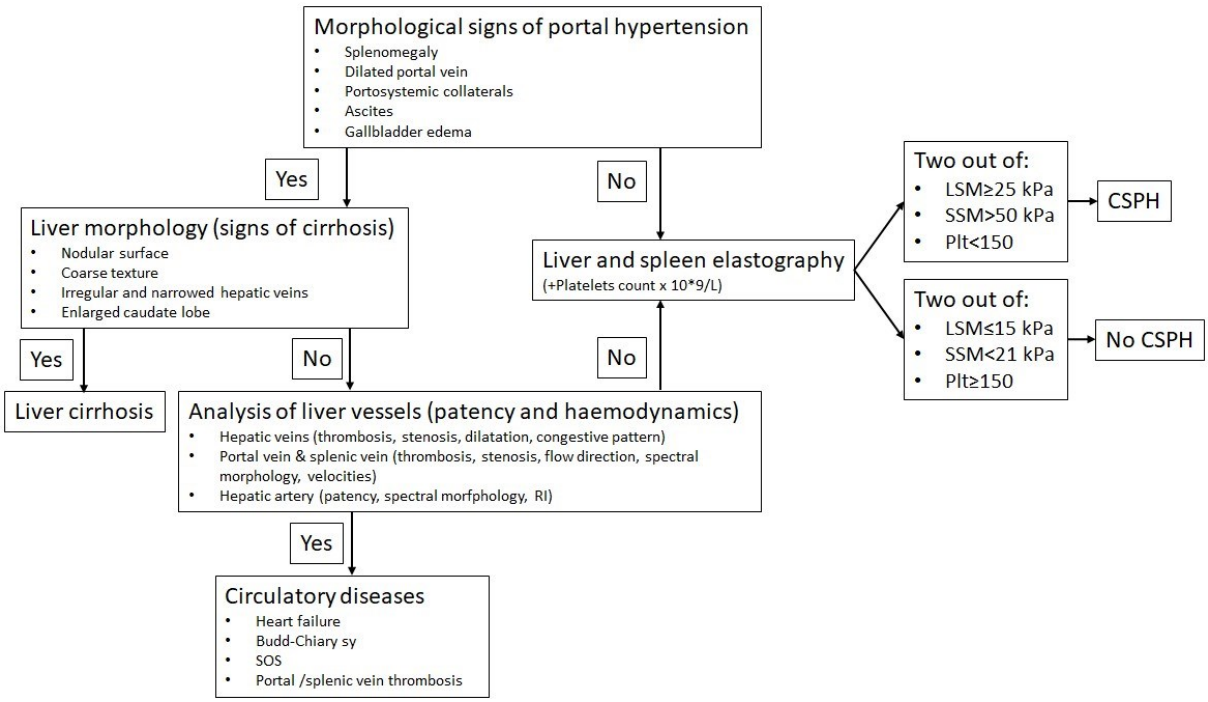

Figure 3.a.8. Ultrasound algorithm in clinical suspicion on portal hypertension (PH). LSM-liver stiffness measurement, SSM-spleen stiffness measurement, Plt-Platelets count, CSPH-Clinically signifficant portal hypertension, SOS-sinusoidal obstructive syndrome. LSM and SSM values refer to transient elastography (Fibroscan) by 50Hz probe. When using 100Hz probe SSM cut-offs for ruling-in/-out CSPH should be 55/25 kPa according to NICER algorithm.

Selected references

1. Berzigotti A, Piscaglia F. Ultrasound in Portal Hypertension – Part 1. Ultraschall in Med 2011; 32: 548–571.
2. Berzigotti A, Piscaglia F. Ultrasound in Portal Hypertension – Part 2 – and EFSUMB Recommendations for the Performance and Reporting of Ultrasound Examinations in Portal Hypertension. Ultraschall in Med 2012; 33: 8–32
3. Grgurevic I, Tjesic Drinkovic I, Pinzani M. Multiparametric ultrasound in liver diseases: an overview for the practising clinician. Postgrad Med J. 2019;95(1126):425-432
4. Piscaglia F, Donati G, Serra C et al. Value of splanchnic Doppler ultrasound in the diagnosis of portal hypertension. Ultrasound Med Biol 2001; 27: 893–899
5. McNaughton DA, Abu-Yousef MM. Doppler US of the Liver Made Simple. RadioGraphics 2011; 31:161–188.
6. de Franchis R, Bosch J, Garcia-Tsao G, Reiberger T, Ripoll C; Baveno VII Faculty. Baveno VII - Renewing consensus in portal hypertension. J Hepatol. 2022 Apr;76(4):959-974.
7. Dajti E, Ravaioli F, Zykus R, Rautou PE, Elkrief L, Grgurevic I, et al; Spleen Stiffness—IPD-MA Study Group. Accuracy of spleen stiffness measurement for the diagnosis of clinically significant portal hypertension in patients with compensated advanced chronic liver disease: a systematic review and individual patient data meta-analysis. Lancet Gastroenterol Hepatol. 2023 Sep;8(9):816-828.
8. Jachs M, Odriozola A, Turon F, Moga L, Téllez L, Fischer P, et al. SSM-100Hz/ACLD Study Group; Baveno Cooperation. Spleen stiffness measurement by vibration-controlled transient elastography at 100 Hz for non-invasive predicted diagnosis of clinically significant portal hypertension in patients with compensated advanced chronic liver disease: a modelling study. Lancet Gastroenterol Hepatol. 2024 Dec;9(12):1111-1120..
9. Garcovich M, Di Stasio E, Zocco MA, Riccardi L, Ainora ME, Annicchiarico BE, Gibiino G, Santopaolo F, Gasbarrini A, Pompili M. Assessing Baveno VI criteria with liver stiffness measured using a new point-shear wave elastography technique (BAVElastPQ study). Liver Int. 2020 Aug;40(8):1952-1960
10. Thiele M, Hugger MB, Kim Y, Rautou PE, Elkrief L, Jansen C, Verlinden W, Allegretti G, Israelsen M, Stefanescu H, Piscaglia F, García-Pagán JC, Franque S, Berzigotti A, Castera L, Jeong WK, Trebicka J, Krag A. 2D shear wave liver elastography by Aixplorer to detect portal hypertension in cirrhosis: An individual patient data meta-analysis. Liver Int. 2020 Jun;40(6):1435-1446.

3.b. ULTRASOUND IN SPLEEN PATHOLOGY

Ivica Grgurević
WFUMB Centre of Education Croatia

The spleen is a parenchymal organ located beneath the left rib cage, between the 9th and 11th rib, connected to other anatomical structures through the splenorenal and gastrosplenic ligaments. The normal size of the spleen is up to 13 cm in its longest (craniocaudal) dimension and up to 6 cm in transverse diameter. The spleen receives blood through the splenic artery, a branch of the celiac trunk, while blood is drained from the spleen via the splenic vein, which flows into the portal vein. Ultrasound analysis of the spleen includes morphological assessment using grayscale imaging (B-mode), vascular analysis with Doppler (color and spectral Doppler), microcirculation evaluation using contrast-enhanced ultrasound (CEUS), and stiffness analysis through elastography.

The most common scanning approach involves the patient lying on their back, with the left arm abducted if necessary (placing the arm under the head), and during inspiration, when the spleen moves caudally, making it more accessible for examination. The examination usually begins by placing the ultrasound probe in the mid or posterior left axillary line above the rib cage, directing it medially to obtain a longitudinal view of the spleen. Depending on the patient's body habitus, spleen size, and position, the probe's position may be adjusted, and scanning can be performed using a subcostal approach or different tomographic planes with sub- or intercostal access. In rare cases, when the spleen is small and located high cranially and posteriorly, an attempt can be made to visualize it from a posterior position with the patient lying on their right side or in a prone position.

1. Anatomical Variants

Anatomical variants that do not represent pathological findings include accessory spleen, polysplenia, asplenia, and splenic malrotation.

- **Accessory spleen** (*lat. Splenunculus*) occurs due to the failure of splenic tissue fusion during intrauterine development and is found in 15–30% of individuals, according to studies using computed tomography (CT) and autopsy analyses. An accessory spleen is usually up to 2 cm in size, located at the splenic hilum or near the tail of the pancreas, has the same echotexture as the spleen, and is typically asymptomatic (Figure 3.b.1).
- **Polysplenia** is a rare condition characterized by the presence of multiple small spleens located in the left or right upper quadrant of the abdomen. It is often associated with congenital anomalies affecting the development and positioning of other organs, such as the heart, pancreas, intestinal malrotation, and inferior vena cava abnormalities.
- **Asplenia** is an extremely rare condition in which the spleen is absent. It is frequently associated with other congenital anomalies.

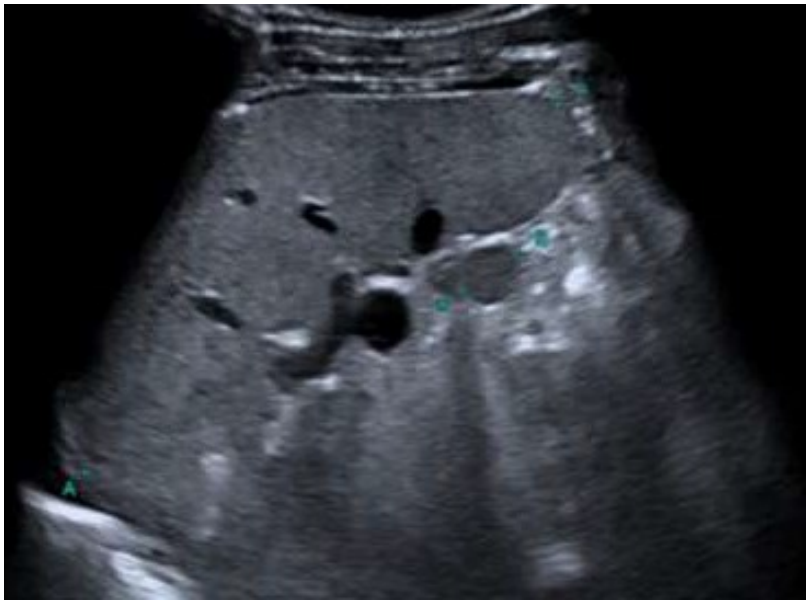

Figure 3.b.1. Accessory spleen, depicted as the small solid lesion of the same echotexture as the spleen, localized in the splenic hilus.

2. Pathological Conditions

Pathological conditions affecting the spleen include trauma, splenosis, focal splenic lesions, vascular diseases, and changes occurring as part of systemic diseases.

2.1. Changes in Spleen Size

The spleen can either be enlarged (**splenomegaly**) or reduced in size.

Splenomegaly is more commonly observed, with primary causes including **portal hypertension**, systemic inflammatory diseases, splenic infiltration due to hematologic disorders (such as extramedullary hematopoiesis, lymphoma, and leukemia), dissemination of malignant diseases, or storage disorders like amyloidosis. The infiltration of the spleen by malignant tumors (metastases) and amyloidosis will be discussed in subsequent sections, while this section focuses on the differential diagnosis of splenomegaly due to portal hypertension versus systemic inflammatory or hematologic diseases.

Regardless of the cause of portal hypertension, the spleen becomes congested, leading to hypertrophy and hyperplasia of its cellular components. This results in increased resistance to blood flow, causing the spleen to become stiffer. Doppler ultrasound can measure this increased resistance, as discussed in the section on portal hypertension. In short, resistance index (RI) and pulsatility index (PI) of intrasplenic arterial branches are elevated (Figure 3.b.2). In some patients with splenomegaly due to PH Gamna-Gandy bodies representing microhaemorrhagic foci within the spleen that tend to produce small calcifications following haemosiderin deposition might be observed. Since cirrhosis is the most common cause of portal hypertension, patients with cirrhosis often present with portal vein dilation and slowed blood flow in the portal vein, accompanied by

splenomegaly. In contrast, patients with splenomegaly due to systemic inflammatory or hematologic diseases do not have cirrhosis, and while the portal vein may also be dilated due to increased blood volume flow, portal vein flow velocity remains normal or is often increased. This distinction can help differentiate between the two causes of splenomegaly. Additionally, splenic artery pulsatility index (SAPI) is typically normal or mildly elevated in hematologic splenomegaly, while in severe cirrhosis-related portal hypertension, it is significantly elevated.

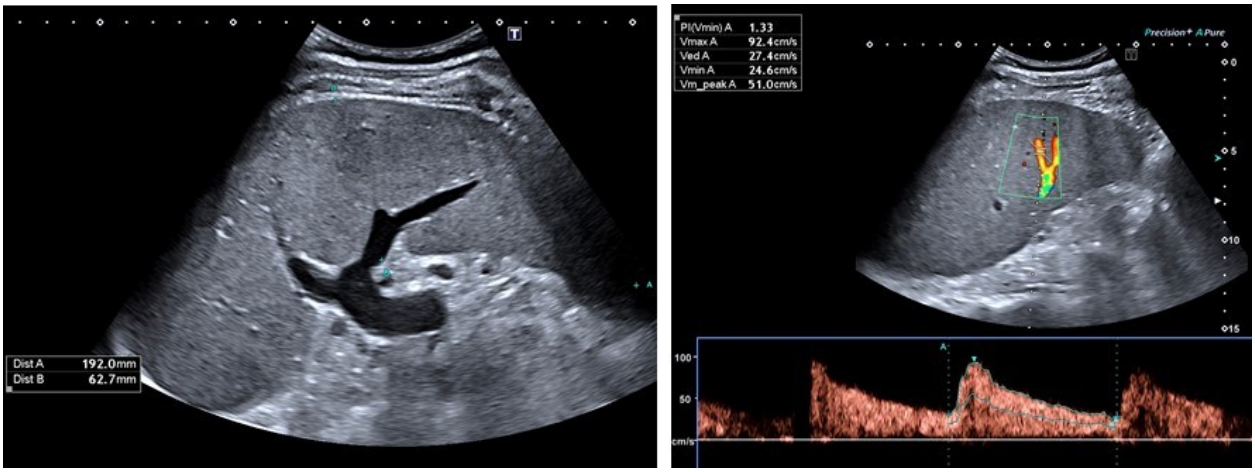

Figure 3.b.2. Splenomegaly in patients with portal hypertension. Enlarged spleen measuring>19 cm in longitudinal diameter (left panel). Increased pulsatility index from intrasplenic branches of splenic artery (SAPI=1.3, right panel).

Elastography is now commonly used in the differential diagnosis of splenomegaly, with transient elastography being the most extensively studied. In cirrhosis, the liver is stiff, typically ≥15 kPa, and in clinically significant portal hypertension (CSPH)—defined as a hepatic venous pressure gradient (HVPG) ≥10 mmHg—liver stiffness measurement (LSM) exceeds 25 kPa for most liver disease etiologies, except in obese MASLD patients, where this threshold is less reliable.

Spleeen stiffness measurement (SSM) can also be used to detect CSPH:

- SSM >50 kPa rules-in CSPH (specificity >90%).
- SSM <21 kPa reliably excludes CSPH (sensitivity >90%)

The aforementioned cut-offs refer to the 50Hz probe of the Fibroscan device, whereas it has recently been suggested that in case of using 100Hz probe respective cut-offs for ruling-in/-out CSPH should be 55 and 25 kPa. In non-cirrhotic portal hypertension (e.g., porto-sinusoidal vascular disease), liver stiffness is almost always below 10 kPa, while spleen stiffness depends on the severity of portal hypertension.

A reduced spleen size or splenic hypoplasia may be congenital or acquired. The most common cause of acquired splenic hypoplasia are thromboembolic events affecting the splenic

arterial circulation. In cases of embolization of a larger branch of the splenic artery, or recurrent embolization of smaller branches, tissue necrosis and fibrotic retraction may lead to spleen shrinkage, often resulting in a lobulated and irregular spleen contours. In some cirrhotic patients, chronic hypoxia of the spleen due to congestion, and malnutrition may also lead to spleen atrophy. Additionally, in sickle cell anemia, repeated microinfarctions cause progressive splenic shrinkage, although in childhood, the spleen is usually enlarged before it eventually becomes smaller.

2.2. Splenic Trauma

The most common cause of splenic trauma is blunt abdominal trauma, often due to motor vehicle accidents or other injuries. It may also result from iatrogenic injury following surgical procedures or spleen biopsy. Splenic trauma can manifest as a splenic hematoma or splenic rupture. **Splenic haematoma** appears as a localized collection of dense fluid, while **splenic rupture** is characterized by a defect in the external contour of the spleen, often accompanied by a layered hematoma in the surrounding area. Splenic rupture presents with symptoms of acute abdomen and signs of internal bleeding, which can progress to shock.

In some cases, detached splenic fragments may implant elsewhere in the abdominal cavity (called „splenosis“) and can be incidentally detected during ultrasound or other imaging studies. These implants vary in size but have the same echotexture as the spleen. The primary differential diagnosis includes lymphadenopathy or solid tumors. A definitive diagnosis can be made using scintigraphy with 99m-labeled heat-denatured red blood cells, as an accessory spleen will demonstrate phagocytic activity. Alternatively, a biopsy of the ectopic spleen can confirm the diagnosis. However, this is usually not necessary as upon ultrasound contrast administration ectopic splenic tissue demonstrates hyperenhancement in the parenchymal phase.

2.3. Focal Lesions of the Spleen

Focal splenic lesions (FSL) are rare pathological changes, detected in approximately 0.2–0.6% of ultrasound examinations. These lesions can be classified into neoplastic and non-neoplastic types.

Non-Neoplastic Lesions

Non-neoplastic focal lesions include cysts, calcifications, hematomas, ischemic lesions, traumatic lesions, infectious lesions, and several other abnormalities.

Neoplastic Lesions

Neoplastic lesions can be further categorized into **benign** and **malignant** tumors:

- **Benign FSL**: Includes hemangiomas, lymphangiomas, hamartomas, and littoral cell angiomas.
- **Malignant FSL**: Includes primary malignant tumors such as hemangiosarcoma, leiomyosarcoma, fibrosarcoma, and primary splenic lymphoma. Secondary malignant lesions include metastases and lymphoma-related changes.

From a morphological perspective, focal splenic lesions are classified into **cystic lesions, solid lesions,** and **calcifications** (Figure 3.b.3).

Focal splenic lesions are more commonly associated with systemic diseases—such as hematological, malignant, or infectious conditions—rather than being primary splenic diseases. Notably, around 50% of patients with FSLs remain asymptomatic, including up to 75% of those with malignant FSLs.

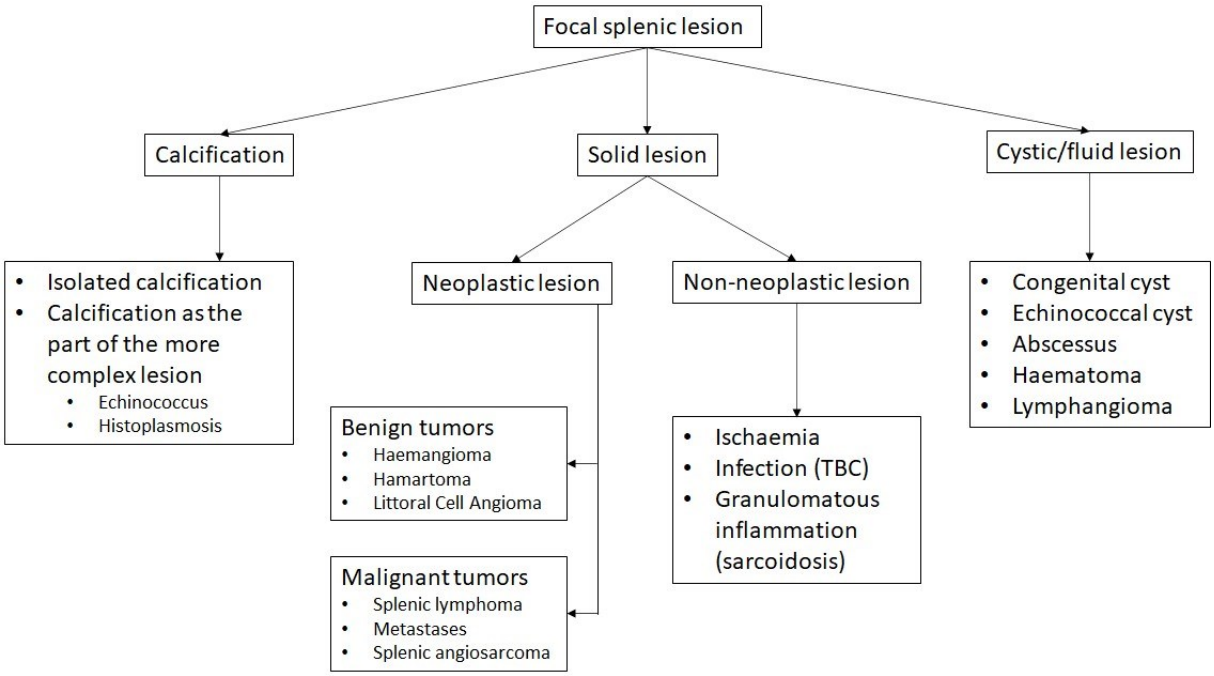

Figure 3.b.3. Simplified Ultrasound classification of focal splenic lesions.

Cystic Lesions of the Spleen

Cystic lesions of the spleen can be classified as **congenital** or **acquired**.

Congenital cysts are typically simple fluid-filled cavities with characteristic ultrasound features, including anechoic structure (appearing completely black on ultrasound), posterior acoustic enhancement (increased brightness behind the cyst), clear, thin walls without solid components or septations, and no enhancement after i.v. contrast administration (Figure 3.b.4).

Acquired cysts usually develop due to resorption of an intrasplenic haematoma (Figure 3.b.4), splenic infarction, resolution of an inflammatory process and Echinococcal (hydatid) infection. These cysts tend to have irregular shapes, thicker walls, and septations. Their contents can be anechoic (fluid-filled) or contain denser debris**.**

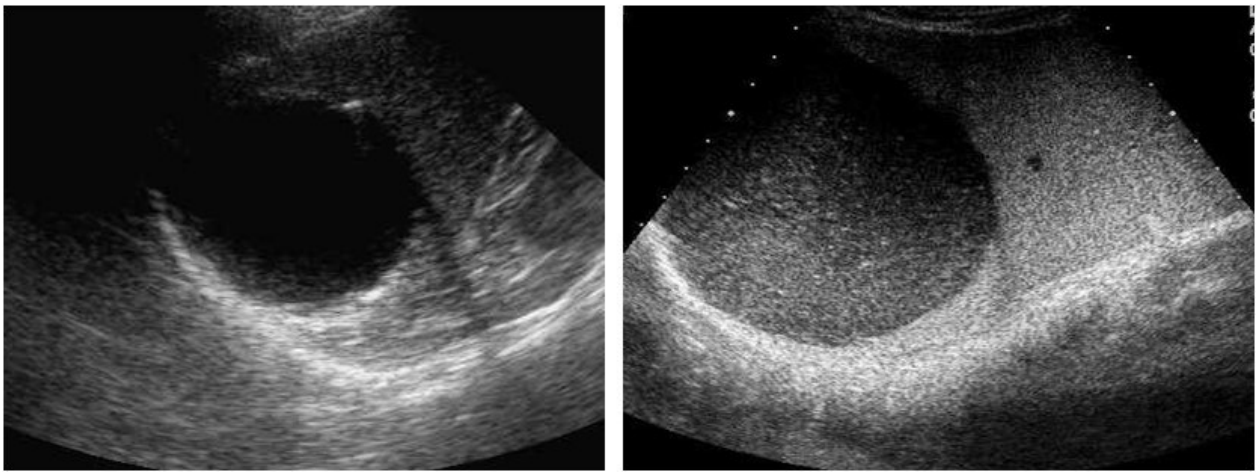

Figure 3.b.4. Splenic cystic lesions. Simple cyst filled with an anechoic fluid (left panel). Haemorrhagic cyst filled with dense hyperechoic fluid containing blood (right panel). Courtesy of Prof. Boris Brkljacic, MD PhD, from his archive.

Echinococcal cysts vary in size and shape depending on the developmental stage of the Echinococcus parasite. They may contain septations and calcifications and do not enhance with contrast**.**

Lymphangiomas are multiloculated (multi-chambered) cystic structures**,** usually found just beneath the splenic capsule**.** They do not enhance with contrast and are typically asymptomatic.

Solid Focal Lesions of the Spleen

Solid focal lesions of the spleen include **calcifications** and **solid tumors**. Splenic calcifications commonly develop after trauma or as part of more complex lesions, such as cysts, echinococcal disease, or certain fungal infections like histoplasmosis. Solid tumors of the spleen can be divided into benign and malignant.

Benign tumors

- **Hemangiomas** are the most common benign tumors of the spleen, resembling hepatic hemangiomas. They appear as hyperechoic, but sometimes even hypoechoic lesions on ultrasound, without a surrounding halo (Figure 3.b.5). After contrast administration, they show early peripheral nodular enhancement**,** some of them demonstrating centripetal filling, without contrast washout in later phases.
- **Hamartomas** are rare, occurring in fewer than 1% of individuals. On ultrasound, they appear as hyperechoic to isoechoic nodules that enhance with contrast, eventually becoming isoechoic to the surrounding pancreatic parenchyma in the venous and delayed phases. They are typically discovered incidentally and occur equally in both sexes across all age groups**.**

- **Littoral Cell Angioma (LCA)** is a rare benign tumor arising from the lining cells of the splenic sinuses. On ultrasound, it appears as one or more solid nodules, showing hyper or in the arterial phase and isoenhancement in the delayed phase after contrast administration.

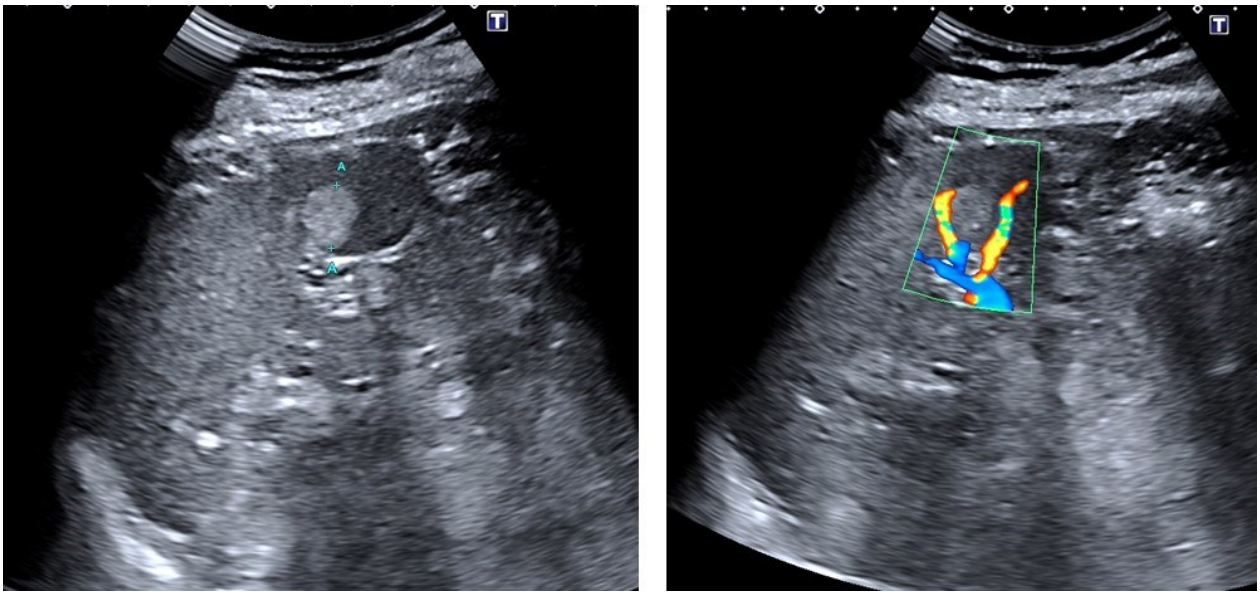

Figure 3.b.5. Splenic haemangioma. Focal round shaped hyperechoic lesion in the spleen, with sharp borders (lef panel), without detactable flow on Doppler examination (right panel)..

Malignant Tumors

- **Splenic Lymphoma** is the most common malignant tumor of the spleen and can be primary or secondary. Primary splenic lymphoma is most often Non-Hodgkin's lymphoma and presents as either diffuse splenomegaly or hypoechoic tumor nodules within the spleen (Figure 3.b.6). After contrast administration, these lesions are hypoenhanced in arterial phase, followed by wash-out in parenchymal phase. Abdominal lymphadenopathy is often present alongside splenic enlargement.
- **Metastases** to the spleen are rare and can appear in various shapes, numbers, and sizes. The most common primary tumors that metastasize to the spleen originate from melanoma, breast cancer, ovarian cancer, lung cancer, and colon cancer. Some metastases might contain areas of central necrosis, as well as calcifications of punctiform or linear shapes (Figure 3.b.6).
- **Splenic angiosarcoma** is an extremely rare tumor, with an incidence of approximately 1 case per 4 million people per year. It occurs more frequently in older men and has a poor prognosis, with a 30% risk of splenic rupture. On ultrasound, it appears as one or more irregular nodules with a heterogeneous structure and areas of necrosis, accompanied by calcifications (Figure 3.b.6). After contrast administration, it shows centripetal filling with heterogeneous enhancement, depending on the extent of necrosis, and washout in the parenchymal phase. This tumor has a high metastatic potential, most commonly spreading to the liver and lungs.

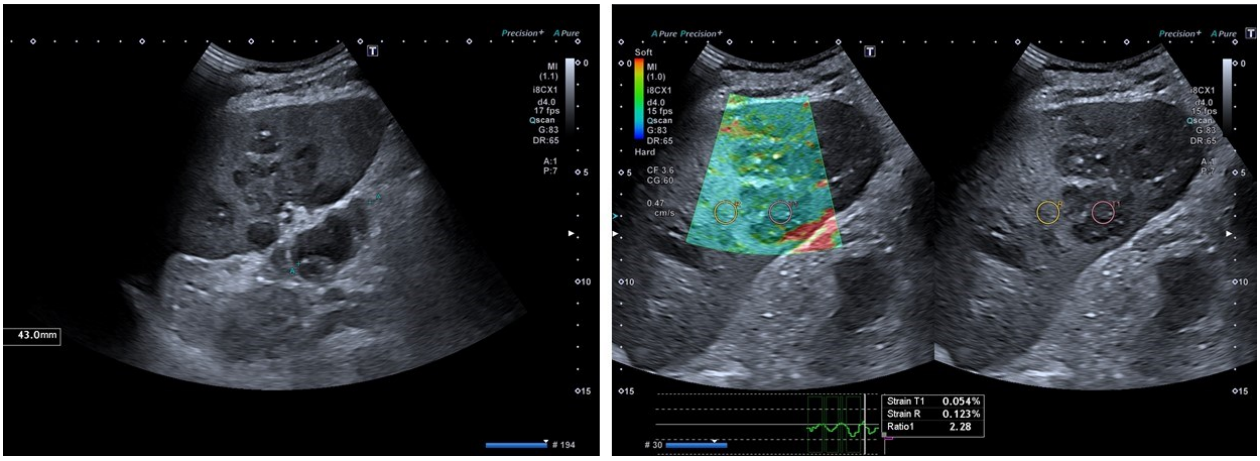

Figure 3.b.6. Malignant splenic lymphoma. B mode ultrasound demonstrates hypoechoic solid foci within the spleen and lymphadenopathy in the splenic hilus (left panel). Real time elastography demonstrates increased stiffness of the lymphoma in comparison to the surrounding splenic parenchyma (Strain ratio 2.28, right panel)

Unfortunately, B-mode ultrasound and Doppler are not sufficiently reliable for distinguishing benign from malignant focal splenic lesions. Generally, it can be stated that hyperechoic lesions are mostly benign, while iso- or hypoechoic lesions are more often malignant. CEUS can be helpful in differentiating between benign and malignant lesions. On CEUS, benign lesions typically show no enhancement or hypoenhancement throughout all imaging phases, and retain contrast in the parenchymal phase. In contrast, malignant lesions show washout in the parenchymal phase. Hyper- or iso-enhancement in the arterial phase is considered a benign feature, provided there is no washout in the parenchymal phase. Therefore, lesions that show weak enhancement in the arterial phase along with washout in the parenchymal phase are suspected to be malignant and require further evaluation, including biopsy for definitive tissue diagnosis.

2.4. Vascular Diseases of the Spleen

Vascular diseases affecting the spleen include splenic infarction, splenic artery aneurysm, and splenic vein thrombosis**.**

Splenic Infarction is most commonly associated with atrial fibrillation or infective endocarditis**.** It presents as sudden-onset pain in the left upper quadrant of the abdomen. On ultrasound, infarction appears as a hypoechoic, wedge-shaped area, with its apex directed towards the splenic hilum (Figure 3.b.7). Doppler imaging shows an absence of arterial blood flow in the affected region. In later stages, necrosis and liquefaction may occur, leading to the formation of fluid collections within the spleen or even splenic rupture. After intravenous contrast administration, the infarcted area remains non-enhancing (hypoechoic) compared to the surrounding splenic parenchyma.

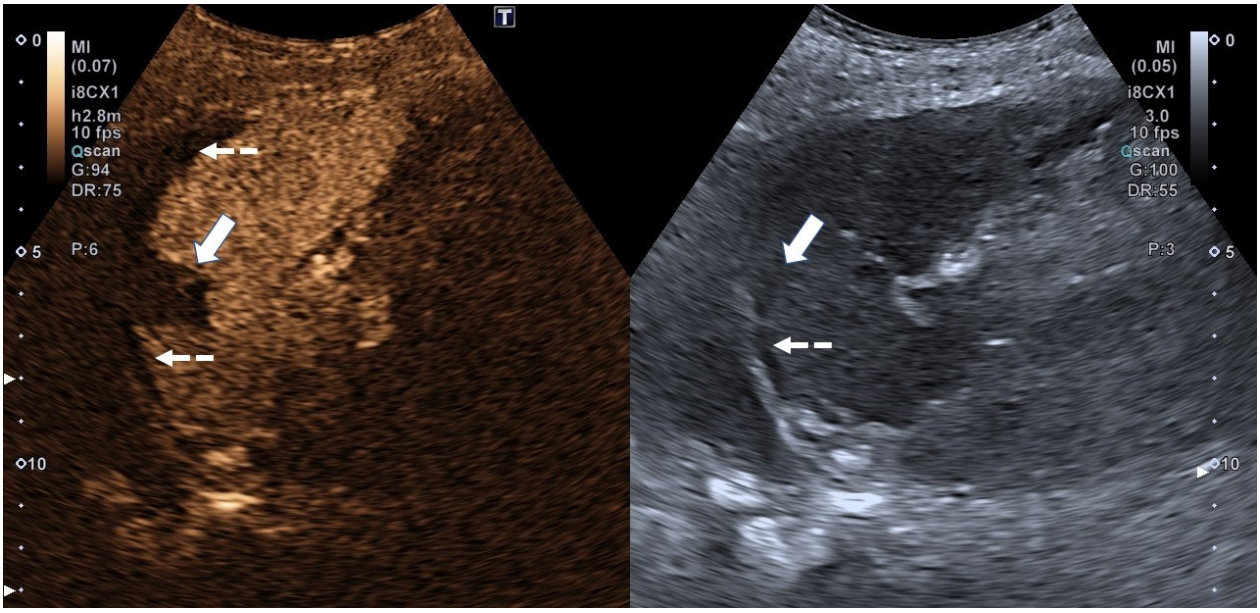

Figure 3.b.7. Splenic infarction. Slightly hypoechoic wedge-shaped area in subcapsular region of the spleen (white full arrow on the right panel), with adjacent haematoma on the surface (dotted arrow). Upon contrast agent administration there is a clear demarcation of the infarcted area that is unenhanced in contrast to the normal spleen (white full arrow, left panel), as well as the unenhanced haematoma on the spleen surface (dotted arrows, left panel).

Splenic Artery Aneurysm can be classified into **true aneurysms**, which involve all three layers of the arterial wall **(**intima, media, and adventitia**),** and **pseudoaneurysms**, which involve only the intima and media**.** These aneurysms are most commonly located in the splenic hilum or distal parts of the splenic artery. They can be isolated or, less commonly, multiple**.** Pseudoaneurysms are more frequently observed and are usually caused by pancreatitis, penetrating gastric ulcers, trauma, or septic emboli. On ultrasound, a splenic artery aneurysm appears as a localized fusiform or saccular dilation of the artery (greater than 50% of the normal diameter). It typically does not involve the entire circumference of the artery. Doppler imaging reveals turbulent blood flow, known as the "to-and-fro" pattern, which appears as alternating red and blue color signals. If the aneurysm ruptures, it can lead to significant hemorrhage or the formation of a contained hematoma. Surrounding anatomical structures may limit hematoma expansion. In cases of rupture, ultrasound may show an artery surrounded by hematoma layers, with a central area of active blood flow within the ruptured aneurysm. The risk of rupture increases when the aneurysm diameter exceeds 2 cm**.**

2.5. Infectious and Inflammatory Diseases of the Spleen

Infectious Diseases of the Spleen include splenic abscesses and tuberculosis**.**

Splenic Abscesses can be either pyogenic (bacterial) or fungal. **Pyogenic abscesses** most commonly arise due to hematogenous spread of infection but can also develop from direct extension of infection from adjacent structures. On ultrasound, they appear as hypoechoic areas of varying size and shape, with hypervascular peripheral margins and central liquefaction. In some

cases, gas bubbles may be visible within the abscess. **Fungal abscesses** share similar imaging characteristics and are more common in immunocompromised individuals. In later stages, these abscesses may develop calcifications**.**

Inflammatory Diseases of the Spleen includes non-infectious inflammatory diseases such as sarcoidosis and amyloidosis**.**

Sarcoidosis is characterized by the formation of non-caseating granulomas, which appear on ultrasound as hypoechoic to isoechoic (and les commonly hyperechoic in cases of fibrous tissue accumulation) hypovascular nodules within the spleen (Fig. 3.b.8). It is usually associated with hepatic sarcoidosis and abdominal lymphadenopathy.

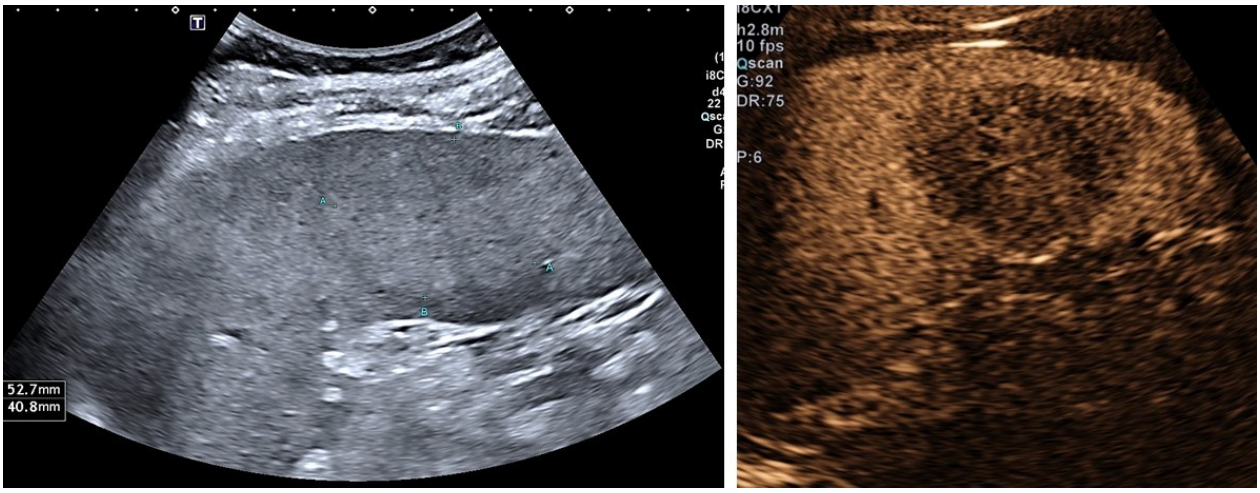

Fig. 3.b.8. Splenic sarcoidosis. An isoechoic, on B-mode barely visible focal nodular lesion of the spleen parenchyma (5.3 cm, left panel). Following ultrasound contrast administration the lesion is hypoenchanced in comparison to the surrounding parenchyma, but retains contrast up to the late phase (right panel, 4 min after contrast administration)

Amyloidosis typically leads to diffuse splenic enlargement (splenomegaly), often accompanied by hepatomegaly. Due to widespread amyloid deposition, resistance indices of the splenic arterial blood flow are increased. Additionally, there is a reduction in peripheral arterial branching within the spleen, reflecting impaired vascular architecture.

Selected references

1. Vancauwenberghe T, Snoeckx A, Vanbeckevoort D, Dymarkowski S, Vanhoenacker FM. Imaging of the spleen: what the clinician needs to know. Singapore Med J 2015; 56:133–144.
2. Lenti MV, Luu S, Carsetti R, et al . Asplenia and spleen hypofunction. Nat Rev Dis Primers 2022; 8:71

3. Makoba IG. Splenic injury following trauma: the role of ultrasonography. Afr Health Sci. 2001 Aug;1(1):23-5. PMID: 12789129; PMCID: PMC2704455.
4. Sidhu PS, Cantisani V, Dietrich CF, Gilja OH, Saftoiu A, Bartels E,et al. The EFSUMB Guidelines and Recommendations for the Clinical Practice of Contrast-Enhanced Ultrasound (CEUS) in Non-Hepatic Applications: Update 2017 (Long Version). Ultraschall Med. 2018 Apr;39(2):e2-e44.
5. Omar A, Freeman S. Contrast-enhanced ultrasound of the spleen. Ultrasound. 2016 Feb;24(1):41-9.
6. Ignee A, Cui X, Hirche T, Demolo C, Barreiros AP, Schuessler G, Dietrich CF. Percutaneous biopsies of splenic lesions--a clinical and contrast enhanced ultrasound based algorithm. Clin Hemorheol Microcirc. 2014;58(4):529-41.
7. Choi G, Kim KA, Lee J, Park YS, Lee J, Choi JW, Lee CH. Ultrasonographic atlas of splenic lesions. Ultrasonography. 2022 Apr;41(2):416-429.
8. Zeng QY, Liao J, Song Y, Zhang DQ, Li H, Wang J. Multimodality imaging findings of splenic littoral cell angioma: a case description and analysis of literature. Quant Imaging Med Surg. 2023 Apr 1;13(4):2740-2743.
9. Hou C, He J, Liao L, Liang J. Contrast-enhanced ultrasonographic features of primary splenic angiosarcoma. Pol Arch Intern Med. 2021 Sep 30;131(9):872-874.
10. Ishida H, Konno K, Hamashima Y, Naganuma H, Komatsuda T, Ohyama Y, Ishida J, Masamune O. Splenic artery aneurysm: value of color Doppler and the limitation of gray-scale ultrasonography. Abdom Imaging. 1998 Nov-Dec;23(6):627-32.

4. HOW CAN I USE US IN FOCAL LIVER LESIONS?

4.a. CYSTIC AND BENIGN LESIONS

Roxana Șirli, Ruxandra Mare,
WFUMB Center of Education Timișoara, Romania

Ultrasound (US) is currently one of the most widely used imaging method, with a significant number of examinations performed daily. This high volume of examinations often leads to the discovery of focal liver lesions (FLL), some expected some not, which can be either cystic (liquid content) or solid.

The clinical presentation of patients with FLLs varies widely, from asymptomatic individuals to those with advanced chronic liver disease or a history of malignancy. It is very important to know the medical history, since most FLLs are benign in low risk patients, defined as asymptomatic subjects, with no history of cancer (especially if under 40), no known metabolic or chronic liver disease, normal liver tests.

The primary question when a FLL is discovered is whether it is benign or malignant. B-mode ultrasound alone often cannot answer this question, except for very typical lesions such as simple cysts, some types of Hydatid cysts, or typically localized focal fat accumulations.

Of course, histology is the most precise diagnostic method, however it is an invasive technique, and its primary use is in the positive diagnosis of malignant liver lesions, especially before chemotherapy, but is contraindicated if curative surgical treatment is possible. Nowadays, liver biopsy is rarely needed due to the advancements in imaging techniques.

For differentiating benign versus malignant ILLs, contrast-enhanced (CE) imaging methods are needed. CE-computer tomography (CE-CT) is the oldest and most widely available technique, however there is radiation exposure involved and potential adverse reactions to contrast agents. CE-magnetic resonance imaging (CE-MRI) is highly accurate and lacks ionizing radiation risks, but it is more expensive and less available. Power and Color Doppler ultrasound rarely provide significant additional information due to their low performance in visualizing small tumor vessels.

In the past 15-20 years, contrast-enhanced ultrasonography (CEUS) has become available, offering a non-irradiating, point-of-care imaging method with practically no adverse events, with more than 90% accuracy in differentiating benign vs. malignant FLLs (similarly to CE-CT and CE-MRI). Ultrasound contrast agents (CA) are microbubbles containing an inert gas, encased by a shell and thus they amplify the US signal. They are strictly intravascular and consequently they allow the characterization of microvasculature as well as of the macrovasculature of FLLs. The examination is performed with low mechanical index, and after 5-6 minutes the microbubbles

begin to break and the CA slowly dissipates, the inert gas being excreted through the lungs, so that they can safely be administered in patients with renal failure. Thus, the most recent WFUMB-EFSUMB guidelines on CEUS recommend that CEUS should be used as a first-line CE imaging method in patients with renal impairment.

Rapidly after the bolus injection, the CA enhances the vascular pool, arriving in the liver and in the FLLs. Due to the dual blood supply in the liver, three enhancement "phases" are described (Table 4.a.1). Based on the enhancement pattern in the arterial, portal and late phases, the type of FLL can be established with similar accuracy to CE-CT and CE-MRI. The most important aspect in differentiating benign vs. malignant lesions is the fact that in the portal and/or late phases, malignant lesions lose the CA and appear hypoenhanced as compared to the surrounding liver (the "wash-out" phenomenon).

A newer CEUS CA, Sonazoid, is retained into the Kupffer cells where it remains for hours, allowing FLL characterization in the post-vascular phase. Malignant FLLs do not have Kupffer cells and will appear as hypoenhanced in the post-vascular phase.

Table 4.a.1. Vascular phases in Contrast Enhanced Ultrasound of the liver

Phase	Start (seconds after bolus injection)	End (seconds after bolus injection)
Arterial phase	10-20	30-45
Portal phase	30-45	120
Late phase	>120	Until the bubbles dissipate

Due to the good performance of CEUS in diagnosing FLLs, the latest WFUMB-EFSUMB guidelines recommend the use of CEUS as a first-line CE imaging method for the differentiation of benign vs. malignant IFLL in non-cirrhotic patients, with or without history or clinical suspicion of malignancy. Furthermore, it is recommended in lesions in which CE-CT or CE-MRI were inconclusive. CEUS can be used for liver metastases detection as part of multimodality imaging approach. Furthermore, CEUS can be used as a first-line CE imaging modality for the characterization of IFLL in patients with a history of malignancy. In patients with cirrhosis, CEUS can be used as first line CE imaging method to establish a diagnosis of malignancy or specifically of hepatocellular carcinoma (HCC), however CT or MR imaging are required for staging. In cirrhotics, CEUS can be used for differential diagnosis if CT and MRI are inconclusive and to select the FLL that require biopsy.

Furthermore, the American College of Radiologists' Appropriateness Criteria® state that CEUS is suitable for diagnosing an indeterminate FLL >1cm found by non-contrast or single-phase CT, or by non-contrast MRI in a normal liver. It is recommended for patients with a history of malignancy and usually appropriate for those with chronic liver disease.

However, one must not forget the disadvantages of CEUS: it is an operator dependent method, it can evaluate only one lesion at a time, deep situated lesions are difficult to evaluate, the examination is impaired if the patient has a poor acoustic window and/or is unable to cooperate with the examiner (for instance unable to hold breathing).

In conclusion, which are the steps when finding an IFLL? First, medical history and clinical examination are important as well as biological tests to detect patients at high risk for malignancy. The high-risk patients include those with a history of chronic liver disease, especially with severe fibrosis and cirrhosis, in which any newly found FLL should be considered as HCC until proven otherwise. Liver elastography is very helpful to diagnose those with severe fibrosis and cirrhosis to further stratify the patients. Another category of high-risk patients includes those with a history of malignancy, in whom any new lesions should be suspected of being a metastasis. The next step is performing CEUS, thus achieving a multiparametric point-of care examination of the patient and reaching a diagnosis in a short time interval.

In the following pages we will present the most frequently encountered FLL and the best way to diagnose them.

a) ***Anechoic (cystic) focal liver lesions*** are frequently found incidentally. A large study on more than 45000 US examinations found a prevalence of cystic lesions of 5.8%, but reported data range from 0.1% and 11.3%.

1. ***Typical liver cysts (biliary cysts)*** are usually round or oval anechoic lesions, with a very thin wall which can be irregular, thin septa can also be present. The wall is so thin because it consists of a single epithelial layer. Additional features are post-cystic enhancement (due to the US speed acceleration when passing from the solid environment of the liver to the liquid environment of the cyst), refraction shadows at the edges as well as a strong posterior wall echo (Fig. 4.a.1 and Fig. 4.a.2). They are unique or multiple and their size can vary from a few millimeters to a few centimeters, rarely larger than 5 cm. The patients are usually asymptomatic, biliary cysts being the typical IFLL. Rarely, in the case of large biliary cysts, discomfort in the right hypocondrium may be present. Their US diagnosis is straightforward and no other imaging methods are needed.

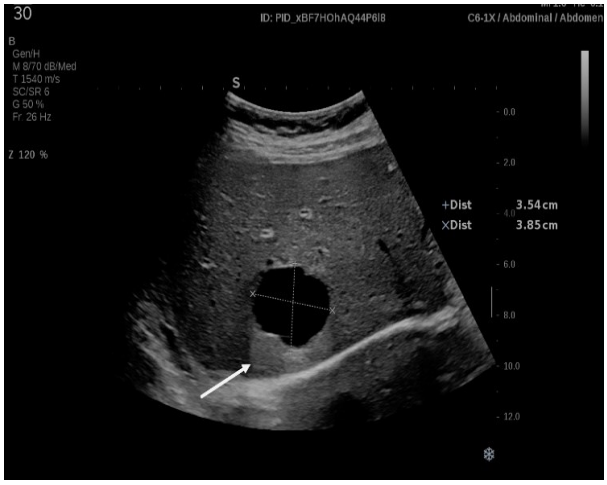

Fig. 4.a.1. Biliary cyst, anechoic lesion with thin, irregular walls and post-cystic enhancement (arrow)

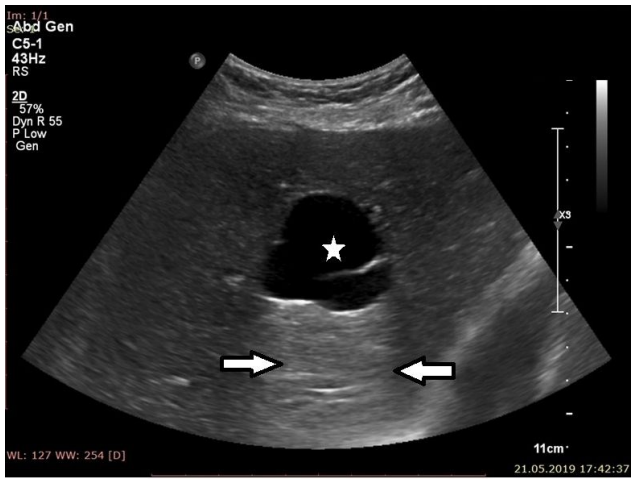

Fig. 4.a.2. Biliary cyst, anechoic lesion with thin, irregular walls and post-cystic enhancement (arrows). A thin septum (star) as well as a strong posterior wall echo are also seen

2. Polycystic liver, frequently associated with polycystic kidney, is a congenital disease. It is often an incidental finding in asymptomatic patients. The US aspect is of multiple cysts in the liver, similar in appearance to the simple biliary cysts (Fig. 4.a.3), with sizes varying from a few millimeters to a few centimeters. When the polycystic kidney is present, the kidney is completely replaced with cysts.

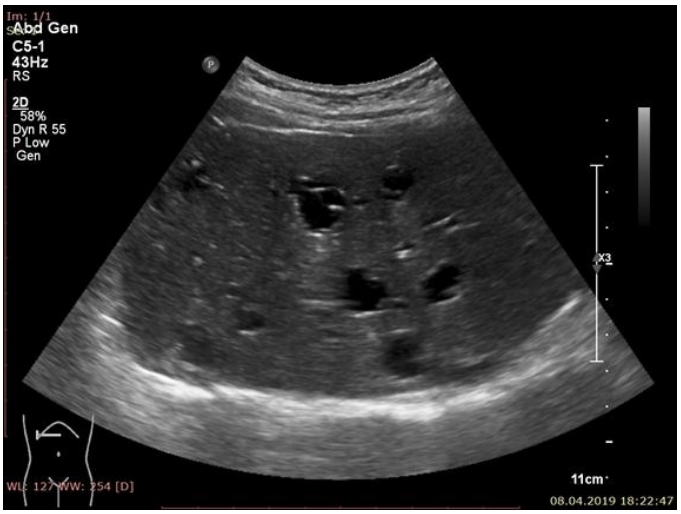

Fig. 4.a.3. Polycystic liver. Numerous anechoic lesions with thin, irregular walls are seen in the liver.

3. Hydatid cysts are parasitic, generated by infection with Echinococcus tapeworm species, being an endemic infection in the Mediterranean area. The US aspect of hydatid cysts vary according to the cysts' age; however, the most characteristic feature is the thick wall formed by the superposition of the proligerous membrane, and the compressed hepatic tissue.

According to the World Health Organization Informal Working Group on Echinococcosis (WHO-IWGE) the US appearance of hydatid cysts can be classified as seen in Table 4.a.2:

Table 4.a.2. US classification of hydatid cysts

Hydatid cyst type		US aspect	Clinical significance
CE 1		unilocular anechoic cyst with thick wall, sometimes with fine internal echoes - "hydatid sand" (fluid and protoscolices), visible after patient repositioning (Fig. 4.a.4)	young hydatid cyst – active stage
CE 2		thick wall cyst with one or multiple internal thick septations which are walls of daughter cysts (Fig. 4.a.5), described as multivesicular, rosette, or honeycomb appearance	mature cyst – active stage
CE 3	CE 3a	anechoic content, detached laminated "floating" membranes (water lily sign) (Fig. 4.a.4, Fig. 4.a.6)	transitional stage, usually seen after successful anthelmintic treatment
	CE 3b	daughter cysts within a solid matrix (Fig. 4.a.7)	mature cyst - transitional stage
CE 4		cyst with heterogeneous hypoechoic and hyperechoic content ("ball of wool", or "onion" sign) (Fig. 4.a.8); absence of daughter cysts	inactive/degenerative stage
CE 5		echoic content, solid and calcified wall (Fig. 4.a.9)	Old cyst - inactive/degenerative stage

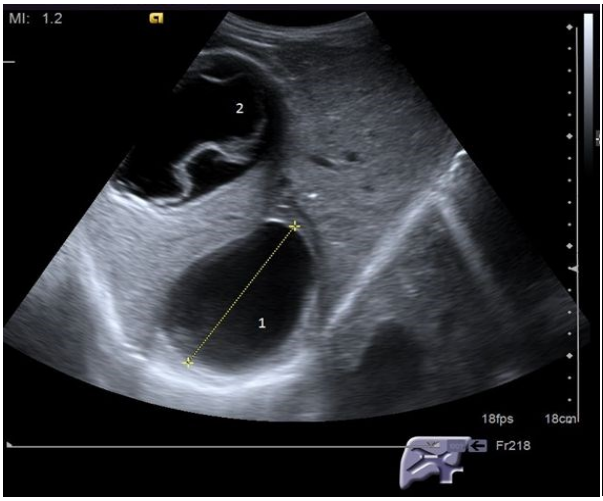

Fig. 4.a.4. CE 1 Hydatid Cyst (1) – anechoic content, thick walls; CE 3a Hydatid Cyst (2) – anechoic content, thick walls, detached endomembrane "water-lily" sign

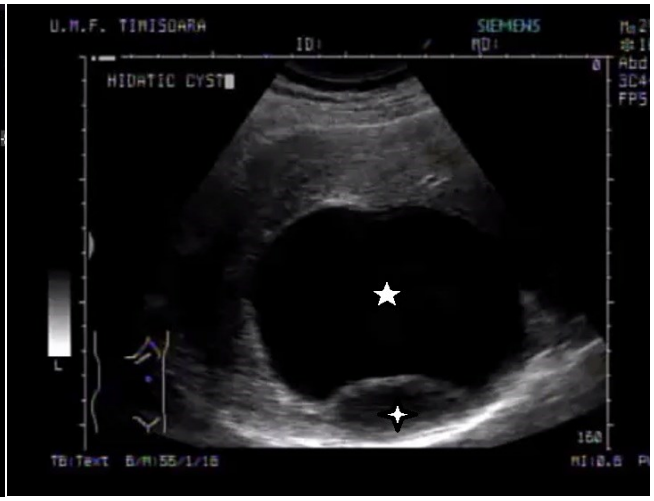

Fig. 4.a.5. Large hydatid cyst (5 pointed star) with anechoic content and thick walls, with one daughter vesicle (4 pointed star), also with thick walls

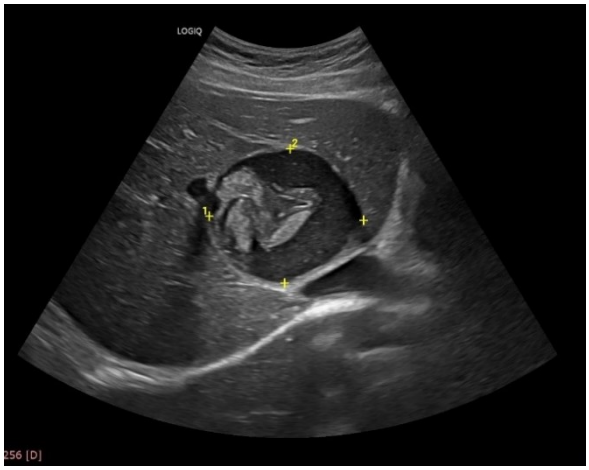

Fig. 4.a.6. CE 3a Hydatid Cyst – an/hypoechoic content, thick walls, detached endomembrane "water-lily" sign

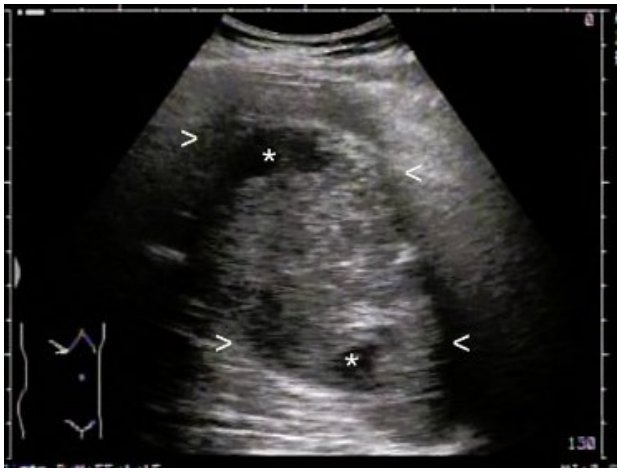

Fig. 4.a.7. CE 3b Hydatid Cyst (between arrows) – daughter cysts (stars) within a solid matrix

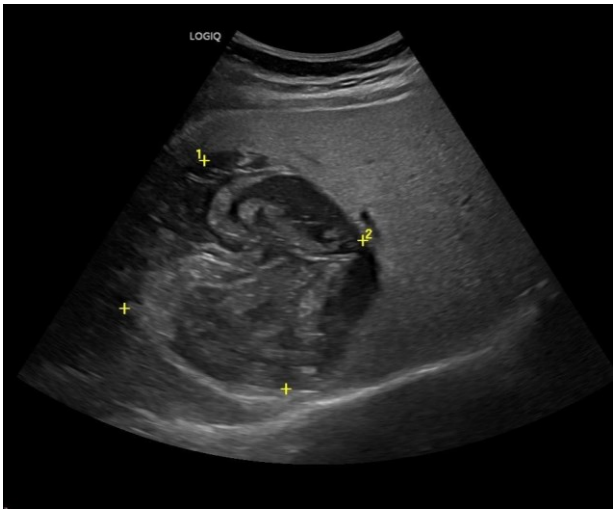

Fig. 4.a.8. CE 4 Hydatid Cyst – cyst with heterogeneous hypo- and hyperechoic content ("ball of wool", or "onion" sign)

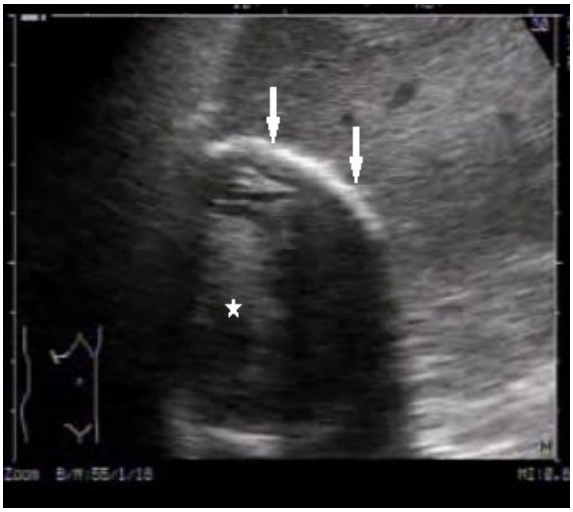

Fig. 4.a.9. CE 5 Hydatid Cyst – echoic content (star), solid and calcified wall (arrows)

The US diagnostic of hydatid cysts CE 1, CE 2, CE 3a is straightforward, no additional imaging is needed. For confirmation anti-Echinococcus antibodies should be evaluated, especially in CE 1, where differential diagnosis problems with simple biliary cysts may arise. However, simple biliary cysts have a very thin wall and sometimes a "geographical" delineation, unlike the CE 1 hydatid cyst, that has a thick wall and an "inside strain" appearance. If still in doubt, ultrasound guided aspiration can be performed. The procedure should be done using a 0.6-0.7 mm needle, passing through normal hepatic parenchyma, under protection with Hydrocortisone Hemisuccinate and Albendazole. In hydatid cysts, the aspirated fluid is crystal-clear and microscopic examination will reveal scolexes.

In gray scale US, CE 3b, CE 4 and CE 5 hydatid cysts are difficult to differentiate from liver tumors. Contrast enhanced imaging is useful in such cases revealing an unenhancing lesion since hydatid cysts are avascular (Fig.4.a.10). Anti Echinococcus antibodies can be negative in CE 5 hydatid cysts since the parasite is long dead when wall calcifications appear.

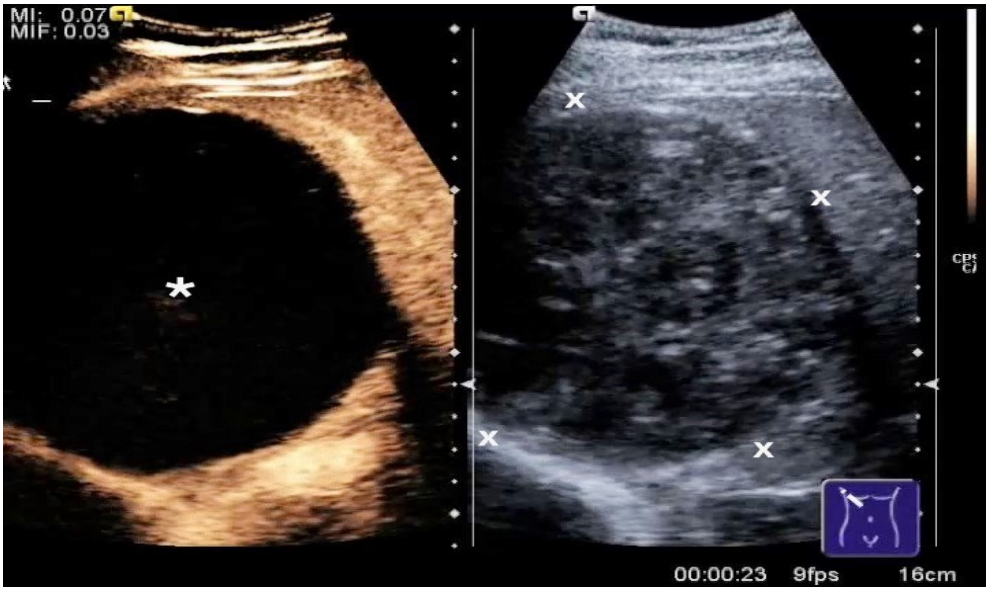

Fig. 4.a.10. CEUS hydatid cyst. Right panel - B-mode US (inhomogeneous, echoic content, thick walls). Left panel – unenhancing lesion (star)

4. Liver abscess is a puss-containing FLL, most often caused by a bacterial infection, but also by fungi. It is found in symptomatic patients (septic state, fever, malaise, night sweats, weight loss, and abdominal pain). Less common are mild symptoms, such as subfever, especially in diabetics and immune compromised patients. Leukocytosis and inflammatory syndrome are present, as well as elevated liver function tests, while patients' history can reveal an infecting moment.

The standard US aspect is of a hypoechoic, poorly delineated lesion, sometimes with anechoic content and thick septa (Fig. 4.a.11, Fig. 4.a.12). Sometimes the lesion can be slightly hyperechoic and/or inhomogeneous (Fig. 4.a.13 left panel). Characteristic for liver abscess is that their appearance changes during time. The anechoic areas correspond to necrotic, avascular liver tissue (puss), while hypoechoic areas correspond to inflamed liver tissue.

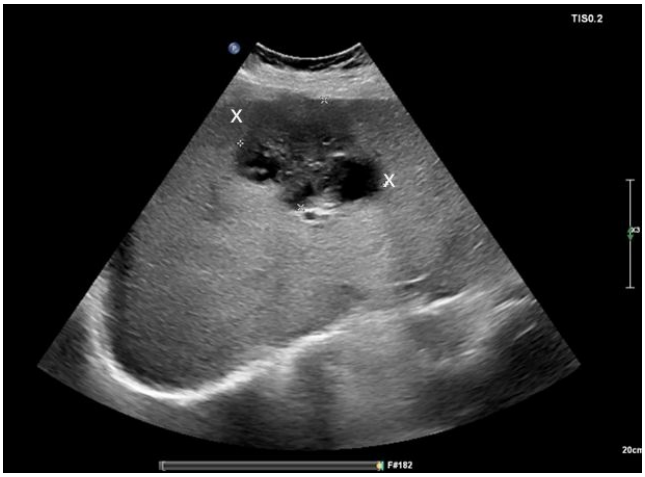

Fig. 4.a.11. Liver abscess - hypoechoic, poorly delineated lesion, with anechoic content

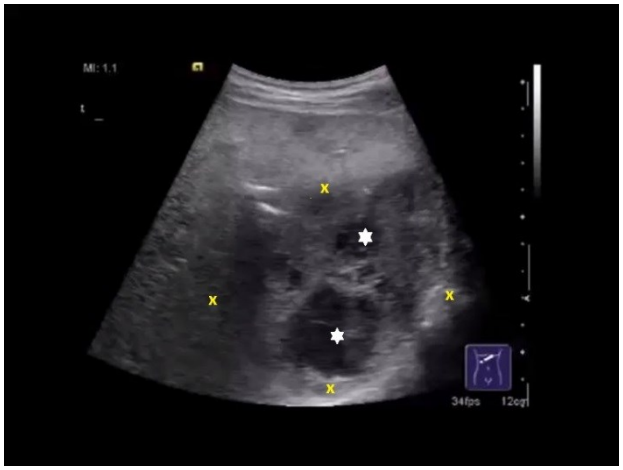

Fig. 4.a.12. Liver abscess - hypoechoic, poorly delineated lesion, with anechoic content (stars)

CEUS is very useful for the differential diagnosis, bringing several typical elements, which corroborated with the clinical presentation lead to a positive diagnosis. The CEUS pattern includes marginal rim enhancement in the arterial phase, with enhancement of the septa (honeycomb appearance), with no enhancement in the liquid areas (Fig. 4.a.13), and venous hypoenhancement (Fig. 4.a.14). The clinical presentation is paramount for the differential diagnosis since cystic metastases can have a similar aspect. US guided aspiration is recommended for the positive diagnosis and to obtain cultures to guide antibiotic therapy.

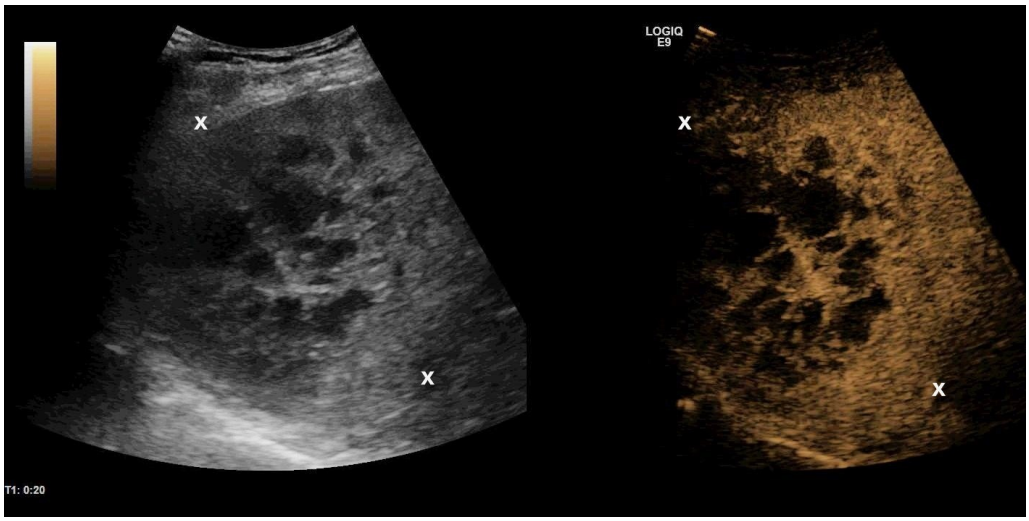

Fig. 4.a.13. Left – B-mode US liver abscess – Hyperechoic, poorly delineated lesion, with thick septa: honeycomb appearance; Right – CEUS arterial phase Hyperenhancing walls and septa, with unenhancing areas.

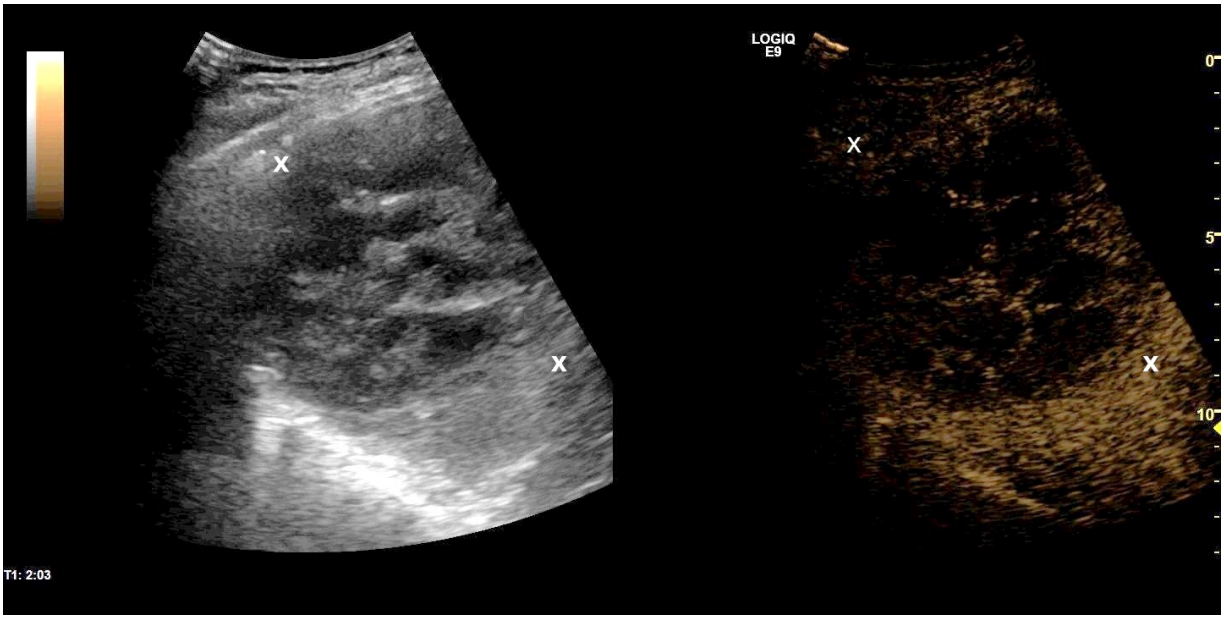

Fig. 4.a.14. Left – B-mode US liver abscess – Right - CEUS liver abscess late phase.
The walls and septa became hypoenhancing

Treatment of liver abscesses include antibiotics and drainage either by US guided aspiration or by US guided percutaneous placement of the drainage tube. CEUS is important also for therapy, since it allows US guided placement of the drainage in the unenhancing areas, corresponding to necrotic tissue.

If CEUS is unavailable or if the patient has a poor acoustic window, CE-CT can be used for diagnosis and for guidance.

5. Liver hematoma is a blood containing lesion inside the liver. It can be found in patients following a blunt abdominal trauma or after an invasive diagnostic or therapeutic procedure and can be associated with signs of anemia or even of hemorrhagic shock, pain in the right hypocondrium, or, more rarely, asymptomatic.

The US aspect is of a hypo/anechoic lesion inside the parenchyma (Fig. 4.a.15), or, in subcapsular disposition, as a crescent shaped hypoechoic area (rarely anechoic or almost anechoic), located between the liver parenchyma and the Glisson's capsule. If Glisson's capsule ruptures, hemoperitoneum develops, sometimes associated with hemorrhagic shock.

CEUS is very useful for delimiting the hematoma extent, as an unenhancing area (Fig. 4.a.16), but also to show if there is, or not, active bleeding. If microbubbles are seen in the liquid surrounding the liver or in the hematoma area, it means that there is active bleeding, and a therapeutic decision should be taken.

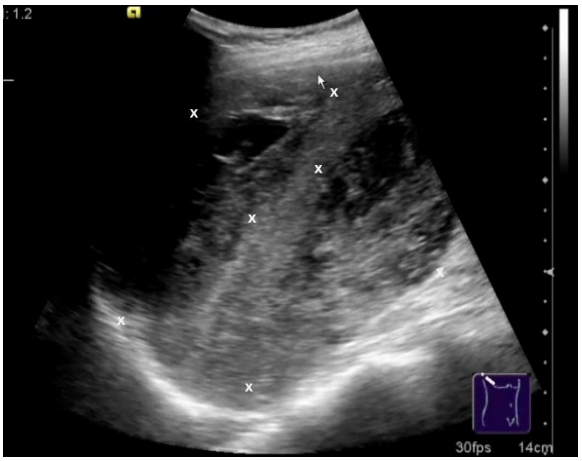

Fig. 4.a.15. Liver hematoma: B-mode US - two hypoechoic inhomogeneous lesions (markers) in a patient who underwent liver biopsy 24 hours prior. Associated – decrease of hemoglobin level by 2 g/l, pain in the upper right quadrant.

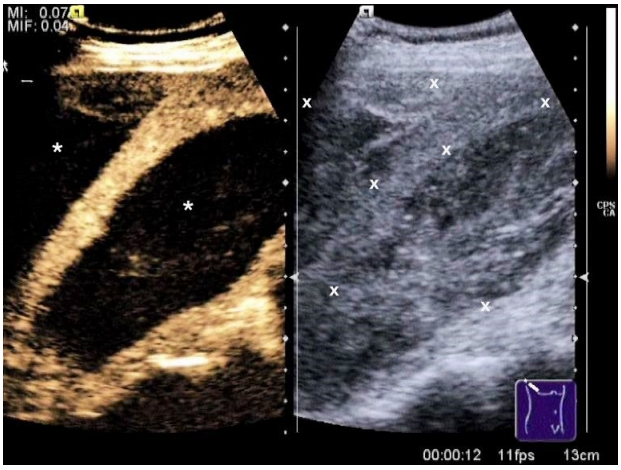

Fig. 4.a.16. Liver hematoma: B-mode US in the right panel; CEUS arterial phase in the left panel – two unenhancing areas (stars).

If a clear acoustic window to visualize the entire liver cannot be obtained in a patient with blunt abdominal trauma, in extensive trauma or if the patient is unstable, CE-CT is the imaging method of choice.

7. Hepatic mucinous cystic neoplasm **(MCN)**, previously referred to as cystadenoma is a rare tumor, more frequent in women, frequently in asymptomatic patients. If large, they can cause discomfort or pain in the right hypocondrium. Biology can be normal or with elevated liver function tests.

The US aspect is of a hypo/anechoic lesion with thick, irregular walls sometimes with wall nodularity (Fig. 4.a.17). They have a 15% risk of malignant transformation, and they should be resected by enucleation or segmental resection any time when it is possible. If the MCN is multiple or large and resection is not feasible, liver transplantation is recommended.

CEUS is a good method for differential diagnosis, revealing arterial hypenhancement of the capsule, protrusions and septa (Fig. 4.a.18), which remain enhancing in the late phase (Fig. 4.a.19). Alternatively, CE-CT or CE-MRI can be used for the differential diagnosis.

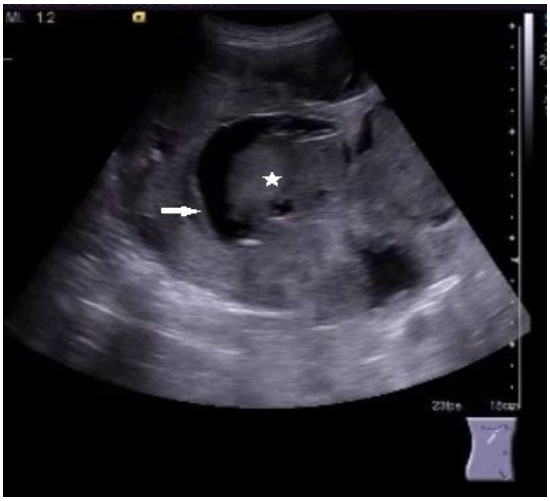

Fig. 4.a.17. MCN: B-mode US - anechoic lesion with thick, irregular walls (arrow) with wall nodularity (star).

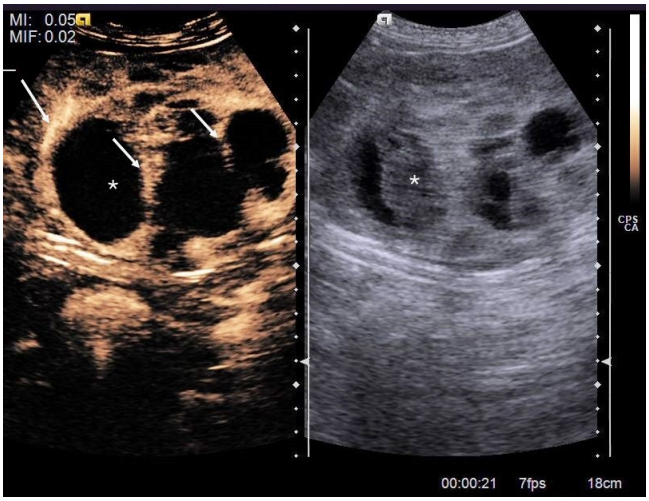

Fig. 4.a.18. MCN: CEUS, arterial phase (left panel) – Hyperenhancing walls and septa (arrows), unenhancing wall nodularity (star) probably mucus.

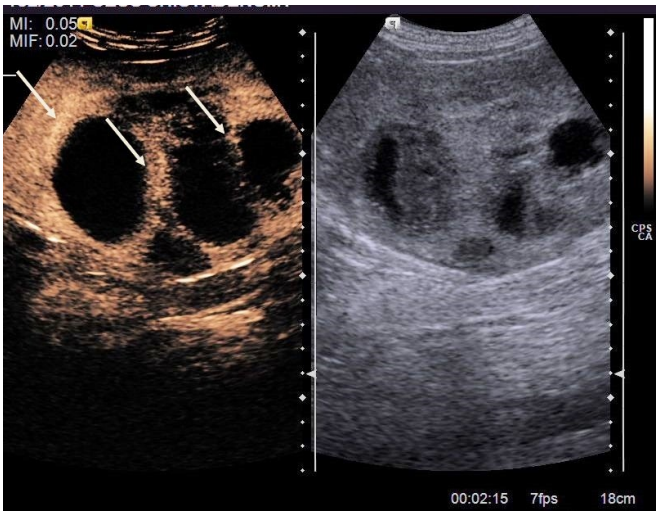

Fig. 4.a.19. MCN: CEUS, late phase (left panel) – The walls and septa are still hyperenhancing (arrows),

b) Benign focal liver lesions

Benign focal liver lesions include hemangioma, focal nodular hyperplasia (FNH), adenoma and focal fatty alterations. As said before, in low-risk individuals, most focal liver lesions are benign. But it is very important to establish if the patient is really low-risk (no oncologic history, no past or present chronic liver disease with severe fibrosis/cirrhosis). Thorough anamnesis, as well as biological tests and liver elastography should be used to stratify the patients. In solid focal liver lesions, B mode ultrasound is not enough for a definitive diagnosis, except for typical hemangioma and focal fatty alteration with typical location. Otherwise, a contrast enhanced imaging method is needed.

1. Hemangiomas are the most frequent benign liver tumors. Hemangioma is considered to be a vascular malformation since it consists of clusters of capillaries and fibrous septa. Its prevalence ranges from 5 to 7% in the general population, more frequent in women than in men (5:1 ratio). Most frequently it is incidentally found in completely asymptomatic patients. They can be single or multiple ranging in size from a few millimeters to a few centimeters, rarely more than 10 cm.

In B-mode US, most hemangiomas, approximately 90%, have a typical ultrasound appearance as a hyperechoic, well delineated, homogeneous lesion, less than 3 centimeters in diameter (Fig. 4.a.20). If such a lesion is found in a low-risk patient, no further imaging is needed for a positive diagnosis.

In 10% of the cases, hemangiomas are atypical. The lesion is larger than 3 centimeters, it can be hyperechoic and/or inhomogeneous (Fig. 4.a.21), or hypoechoic with thin hyperechoic rim, especially in a steatotic liver. Posterior enhancement is sometimes seen (Fig. 4.a.21), as well as the "mirror effect" if the lesion is situated near the diaphragm (Fig. 4.a.22). In these cases, a contrast enhanced imaging method is needed for a positive diagnosis.

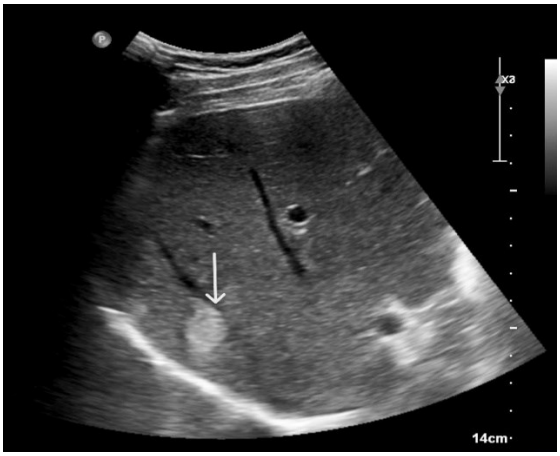

Fig. 4.a.20. Typical hemangioma – B-mode US: hyperechoic, well delineated, homogeneous lesion, < 3 cm in diameter (arrow).

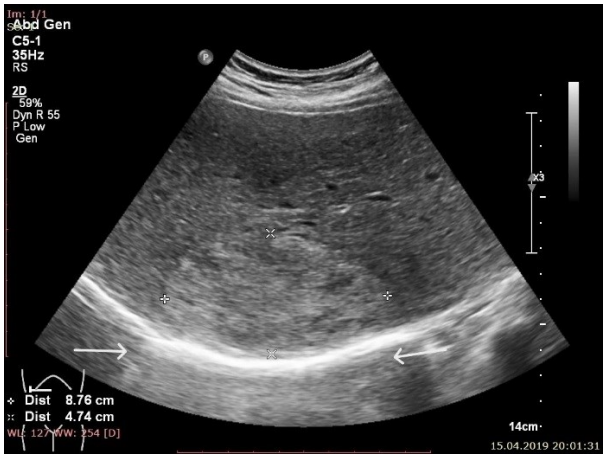

Fig. 4.a.21. Atypical hemangioma – B-mode US: hyperechoic, well delineated, inhomogeneous lesion, > 3 cm in diameter (markers). Posterior enhancement is visible (arrows).

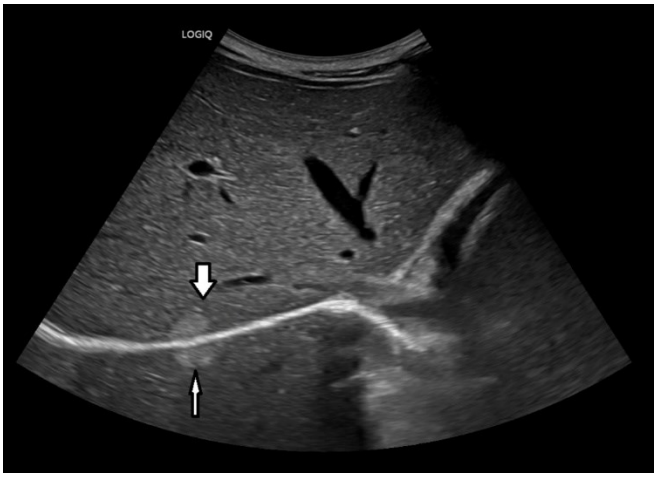

Fig. 4.a.22. Typical hemangioma – B-mode US: small hyperechoic, well delineated, homogeneous subdiaphragmatic lesion, (thick arrow), "mirror effect" (thin arrow)

CEUS has a very good performance for diagnosing hemangiomas, with more than 95% accuracy, and even better specificity (Fig. 4.a.23-4.a.26). On CEUS, hemangiomas show arterial, nodular, peripheral, centripetal hyperenhancement (Fig. 4.a.24), which slowly progresses from the periphery to the center in the portal (Fig. 4.a.25) and late phases, so that in the late phases they appear as hyperenhancing (Fig. 4.a.26). Large hemangiomas do not enhance completely, even in the late phase, due to central necrosis/fibrosis. Small hemangiomas (<15 mm) can exhibit in approximately 10% of cases rapid arterial enhancement due to the presence of arterio-portal shunts ("high-flow" hemangioma), which can lead to difficulties in differentiating them from FNH. They are frequently situated in a fatty sparing area. Another trap is continuous insonation, especially in superficial hemangiomas, which can lead to a premature destruction of the CA microbubbles pooling in the capillaries, and to a false "wash-out", leading to a misdiagnosis of malignant lesion.

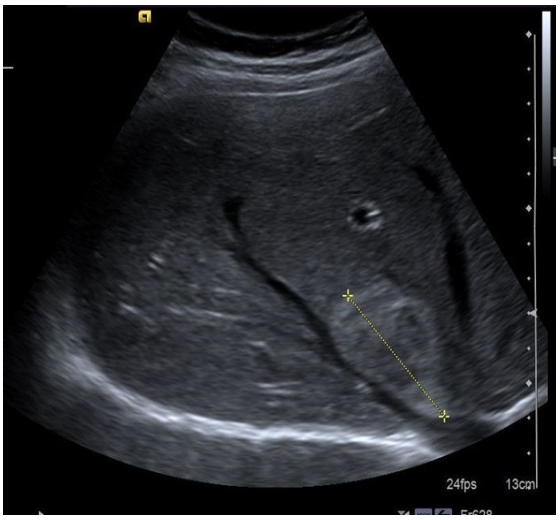

Fig. 4.a.23. Atypical hemangioma – B-mode US: hyperechoic, well delineated, inhomogeneous lesion

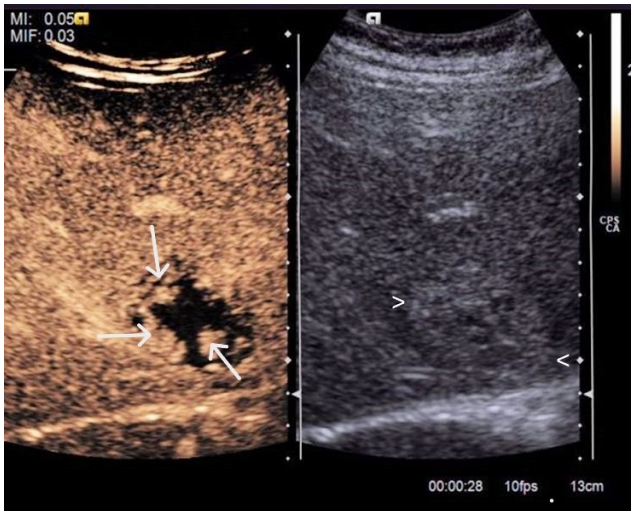

Fig. 4.a.24. Atypical hemangioma – CEUS, arterial phase: nodular, peripheral, centripetal hyperenhancement (arrows)

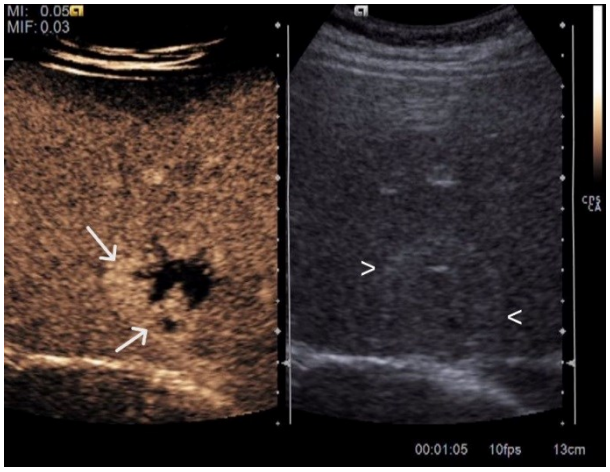

Fig. 4.a.25. Atypical hemangioma – CEUS, portal phase: the nodular, peripheral, centripetal hyperenhancement slowly continues (arrows)

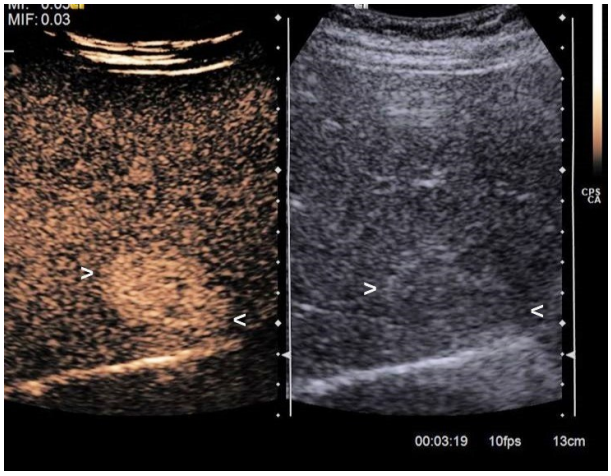

Fig. 4.a.26. Atypical hemangioma – CEUS, late phase: the lesion is completely hyperenhanced (matkers)

In inconclusive cases, the second line imaging method should be CE-MRI, since it is the most specific, revealing a well-defined, homogenous lesion, hypointense on T1-weighted sequences and hyperintense on T2-weighted sequences, with similar enhancement pattern to CEUS, after gadolinium-based contrast.

2. Focal nodular hyperplasia (FNH) is also a frequent benign liver tumor, the second in terms of prevalence, estimated to be 3% in general population, more frequent in women than in men, associated to contraceptives administration. FNH is a hyperplastic hepatocyte response to an abnormal congenital artery. It is most frequently an incidental finding in an asymptomatic patient. Characteristic for FNH in CE-imaging are arterialization and the presence of central scar.

The B-mode US aspect of FNH is not typical, frequently it is isoechoic, or discretely hyperechoic due to mild fatty loading. It can be discretely hypoechoic in patients with diffuse hepatic steatosis. B-mode US delineation is not always very neat and the FNH typical central scar is rarely visible. In isoechoic FNHs the diagnosis is suggested by the "bulge sign" (liver contour deformation) or by vascular impingement (Fig.4.a.27). Power or color Doppler can sometimes reveal a typical vascular pattern (multiple radial vessels with “spoke wheel” pattern) (Fig. 4.a.28). A CE imaging method is needed for a positive diagnosis.

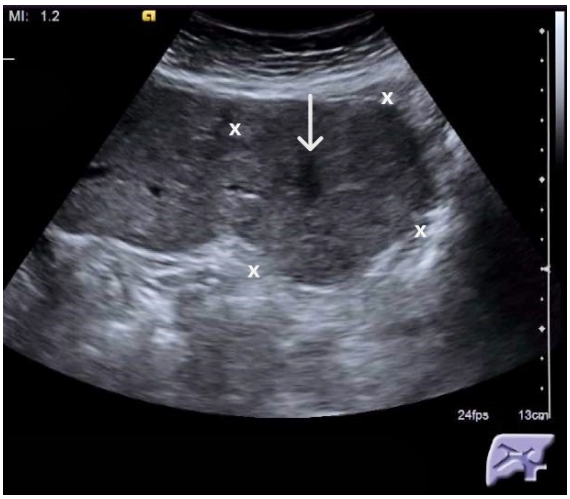

Fig. 4.a.27. Isoechoic FNH – deforming the liver outline (markers). Central scar visible (arrow)

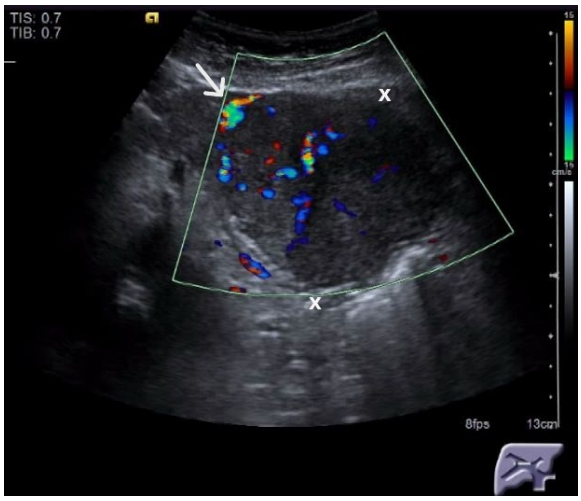

Fig. 4.a.28. Isoechoic FNH – Power Doppler "spoke wheel" pattern. Feeding artery visible (arrow)

CEUS is very useful for diagnosing FNH, with reported accuracy of more than 95% and specificity as high as 100% in some studies. On CEUS (Fig. 4.a.29-4.a.32), FNHs are characterized by hyper-vascularity and exhibit homogeneous hyper-enhancement during the arterial phase, with rapid and centrifugal filling (Fig. 4.a.30 and Fig. 4.a.31). This "spoke-wheel" pattern is crucial for distinguishing FNHs from other arterialized FLLS such as HCCs, adenomas, hyper-vascular metastases, or high-flow hemangiomas. In approximately 30% of cases, an eccentric feeding vessel may be observed shortly before nodule enhancement. Typically, FNHs display hyper-enhancement in the portal phase and either hyper- or iso-enhancement in the late phase (Fig. 4.a.32), while the central scar is hypoenhancing in the late phase. In large FNHs, the accuracy of CEUS is lower. This can be explained by the increased vascular supply and multiple feeding arteries in these cases, which obscure the typical spoke-wheel pattern.

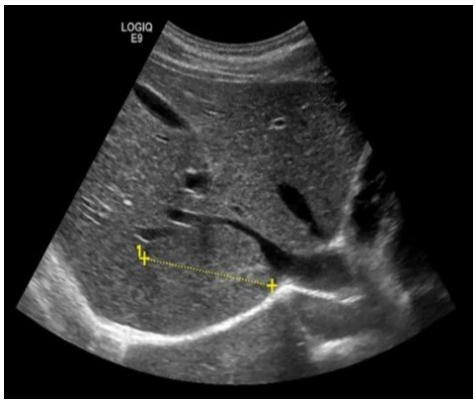

Fig. 4.a.29. Isoechoic FNH – deforming the right hepatic vein (markers).

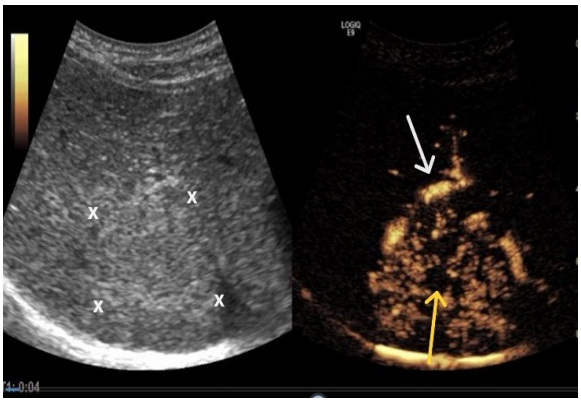

Fig. 4.a.30. FNH CEUS, early arterial phase (5s after bolus), centrifugal hyperenhancement, feeding artery visible (white arrow), central scar (yellow arrow)

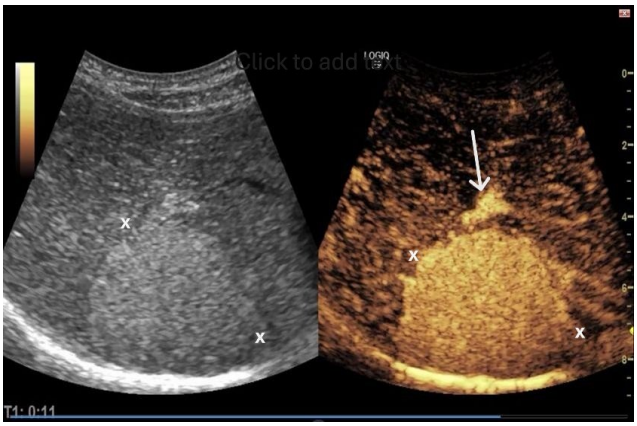

Fig. 4.a.31. FNH CEUS, early arterial phase (11s after bolus), the lesion is completely hyperenhanced, feeding artery visible (white arrow)

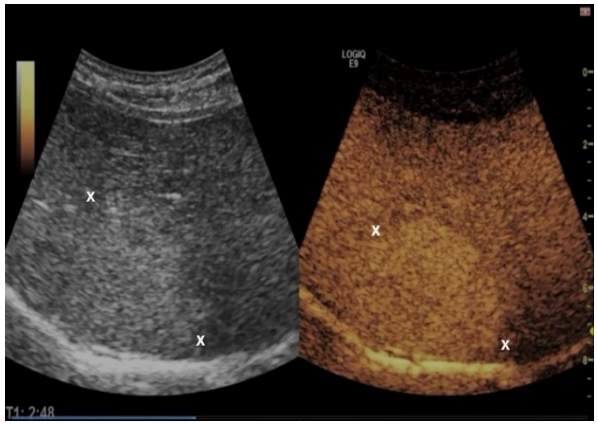

Fig. 4.a.32. FNH CEUS, late phase, the lesion is still hyperenhanced.

On CE-CT, FNH appears hyperdense with isodense aspect in the portal-venous phase. The central scar is hyperdense in the late phase. On unenhanced MRI, FNHs are isointense on T1-weighted images and iso- to slightly hyperintense on T2-weighted images. Following MRI liver-specific contrast the FNHs are hyperintense in the initial phase with an isointense aspect in the delayed phase, the central scar being enhanced in the late phases.

3. Hepatocellular adenoma (HCA) is a relatively rare benign liver tumor, with an estimated prevalence of less than 0.05%, occurring predominantly in women of childbearing age (with a 9:1 gender prevalence). It is believed that hormonal factors influence their growth and the risk of complications. HCAs are more challenging to diagnose but are significant due to their potential for spontaneous rupture (in women) and malignant transformation (in men). Based on genotypic and phenotypic characteristics, HCAs can be classified into three subtypes: HCA with hepatocyte nuclear factor (HNF)-1 alpha mutation (30-35% of all HCAs, occurring almost exclusively in women, carry a low risk of complications if smaller than 5 cm); inflammatory HCA (40-45% of HCAs, mainly in women); and HCA with beta-catenin activation (10-15% of cases, more frequently in males, with high risk of malignant transformation).

HCAs are difficult to diagnose by B-mode US since they do not have a typical appearance. They are usually isoechoic (Fig. 4.a.33) or slightly hyperechoic, often inhomogeneous. In liver steatosis, they can be hypoechoic (Fig. 4.a.34). In isoechoic HCAs the diagnosis is suggested by the "bulge sign" (liver outline deformation) or by vascular impingement. HCAs are difficult diagnoses no matter of the CE imaging method used.

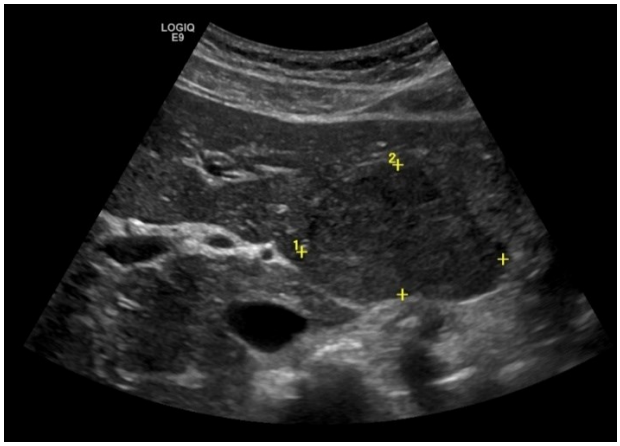

Fig. 4.a.33. Isoehoic lesion in the left liver lobe (markers), deforming the liver outline, CEUS and MRI - HCA

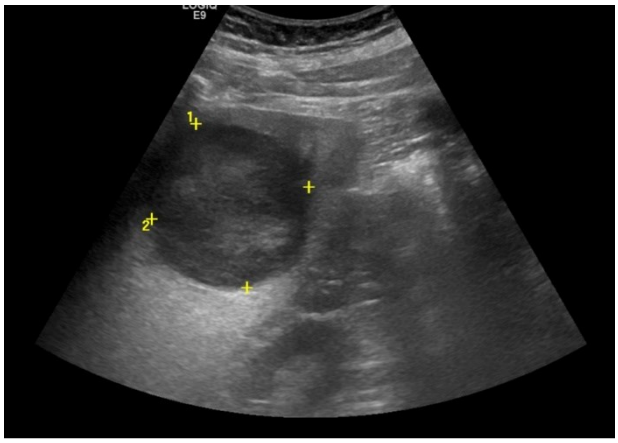

Fig. 4.a.34. Steatotic liver, hypoechoic lesion in segment VI, intercostal approach (markers) - CEUS and MRI - HCA

On CEUS, HCAs exhibit rapid arterial complete enhancement (Fig. 4.a.35) with a centripetal fill-in (very important for differentiating it from FNHs, which exhibit centrifugal fill-in). Since HCAs do not have portal vessels, in the portal and late phase they will appear as iso (Fig. 4.a.36) or slightly hypoenhancing (Fig. 4.a.37). Thus, they are very difficult to differentiate from HCCs, which are also arterialized and, in well differentiated lesions, exhibit very late and mild wash-out. In the pivotal DEGUM study CEUS has only 57.9% accuracy in diagnosing HCAs, with pathological exam as reference.

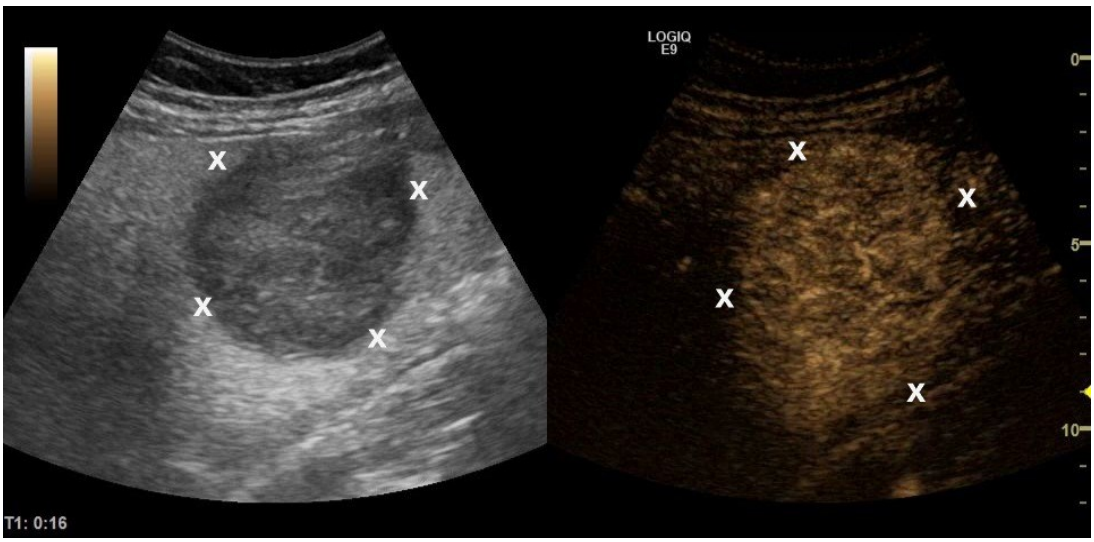

Fig. 4.a.35. CEUS HCA. Left panel B-mode US. Right panel – arterial phase: rapid hyperenhancement (16 s – HCA completely enhanced)

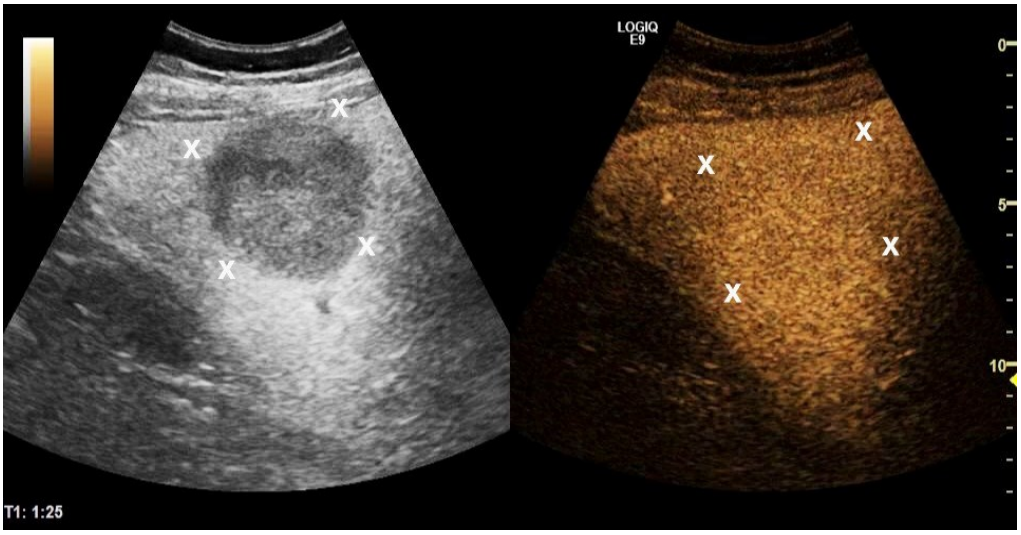

Fig. 4.a.36. CEUS HCA. Left panel B-mode US. Right panel – portal phase: the lesion is isoenhancing

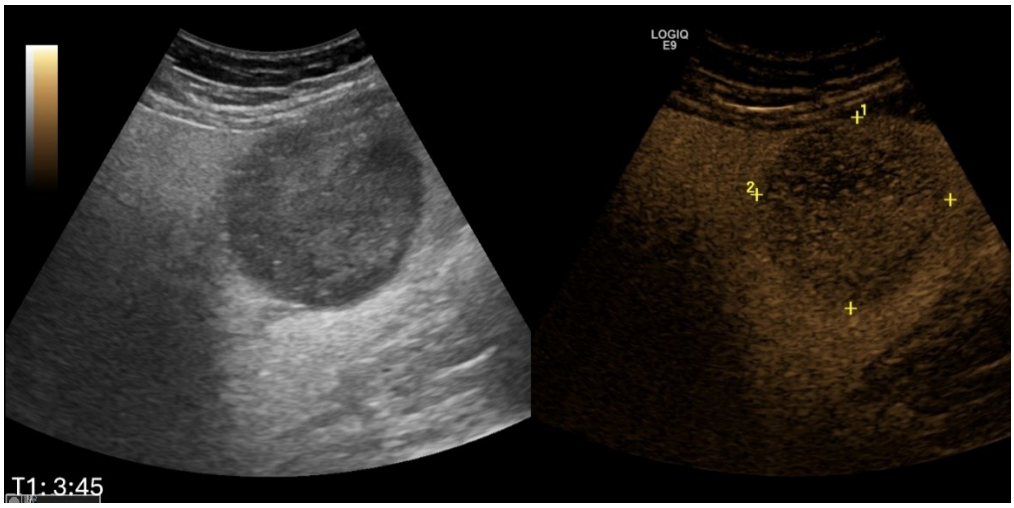

Fig. 4.a 37. CEUS HCA. Left panel B-mode US. Right panel – late phase: the lesion is mildly hypoenhancing.

CE-MRI seems to be the best imaging method to diagnose HCA: HCA with HNF-1 alpha mutation exhibits moderate arterial enhancement that does not extend into the portal venous phase; inflammatory HCA exhibits intense arterial enhancement that persists into the portal venous and delayed phases; while HCA with beta-catenin activation lacks characteristic features on CE-MRI.

***4. Focal fatty alterations* (*focal fatty infiltration and focal fatty sparing*)** are increasingly common in clinical practice due to the rising prevalence of conditions that predispose individuals to steatosis (obesity, diabetes mellitus, dyslipidemia, and alcoholism). Focal fatty sparing can be

observed by US in almost all patients with bright liver, while focal fatty infiltration can be seen in about 40% of patients with inflammatory bowel disease receiving corticosteroids.

In B-mode US, focal fatty alterations appear as juxtaposition of areas of hepatic parenchyma with different ultrasound aspects: hyperechoic as compared to the rest in focal fatty infiltration (Fig. 4.a.38) and hypoechoic as compared to the rest in focal fatty spearing areas (Fig. 4.a.39, and Fig. 4.a.40). They often have a neat, map-like delineation or a triangular aspect and do not show surface changes of the liver or vessel invasion. The most frequent locations include the gallbladder fossa, the medial segment near the falciform ligament, the subcapsular region, and near the porta hepatis. Their actual etiological factor is believed to be a variant venous vasculature. Sometimes, focal fatty alterations can be indirect hints for focal solid lesions (Fig. 4.a.41) which will be only visible after contrast-examination.

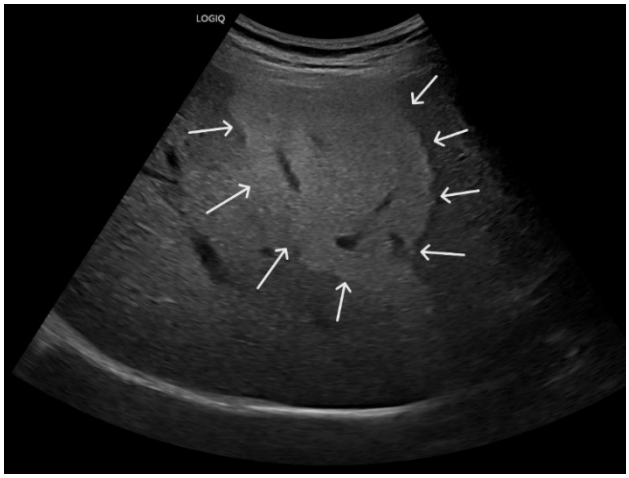

Fig. 4.a.38. Focal fatty infiltration - B-mode US. Hyperechoic area with neat, map-line delineation (arrows)

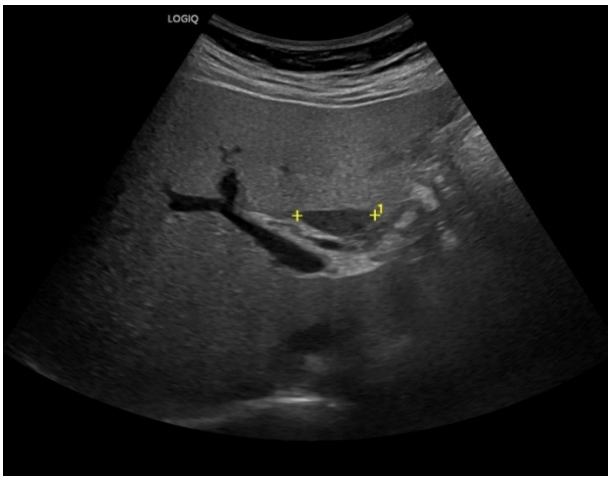

Fig. 4.a.39. Focal fatty sparing - B-mode US. Triangular hypoechoic area with neat, delineation near the portal vein (markers)

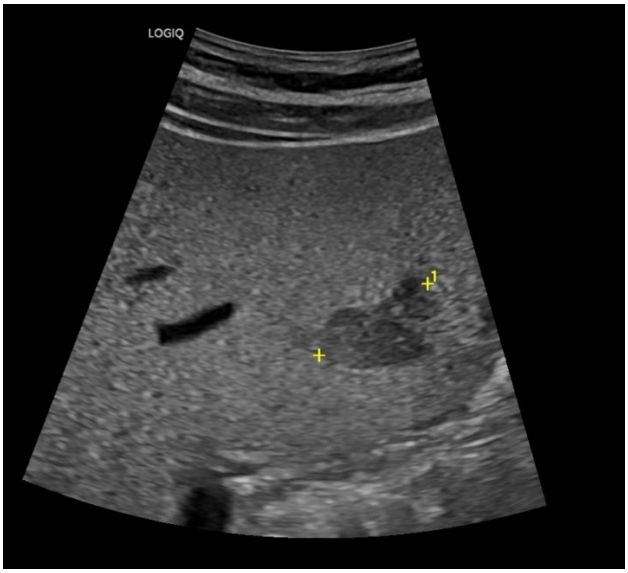

Fig. 4.a.40. Focal fatty sparing - B-mode US. Irregular, hypoechoic area with neat, map-like delineation (markers)

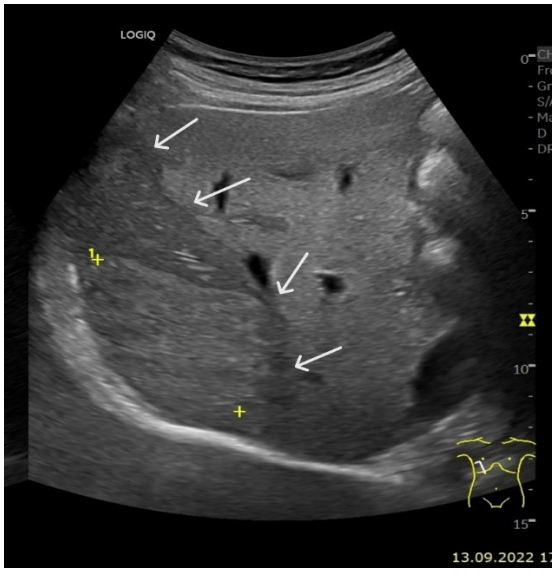

Fig. 4.a.41. Focal fatty sparing - B-mode US. Large hypoechoic area with neat, map-like delineation (arrows). Inside, near the diaphragm, hyperechoic FLL (markers) – CEUS hemangioma

If the focal fatty alteration has a typical appearance (triangular or with geographical delineation) and is situated in a typical location, no further imaging is needed. However, if we deal with a hypoechoic, round lesion (Fig. 4.a.42), a CE imaging method is needed to differentiate a focal fatty sparing area from a malignant lesion. CEUS is a very good method for diagnosing focal fatty alterations. Both focal fatty sparing and focal fatty infiltration are isoenhancing to the adjacent parenchyma in all vascular phases, in CEUS (Fig. 4.a.42 – 4.a.44), as well as in CE-CT and CE-MRI.

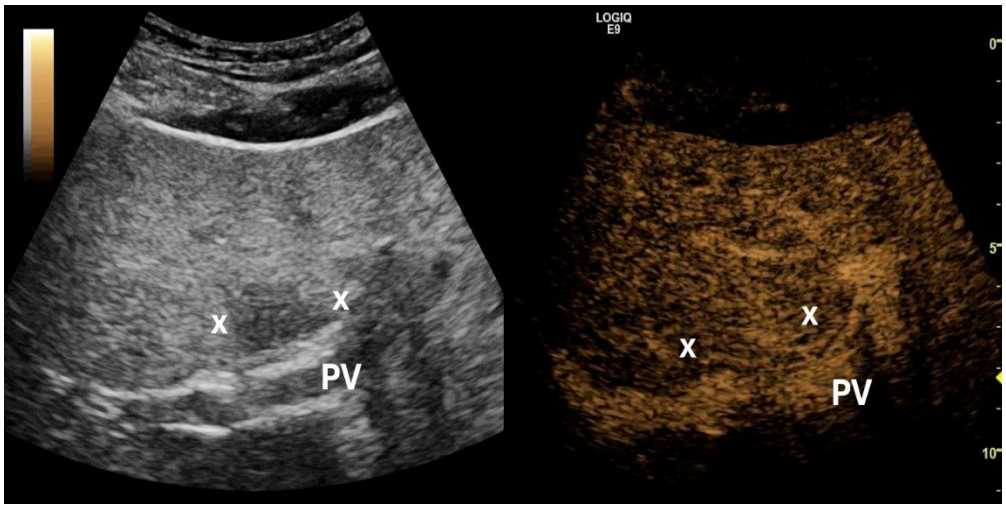

Fig. 4.a.42. Focal fatty sparing - B-mode US (left panel) - Hypoechoic round area near the portal bifurcation. CEUS arterial phase (right panel) – the area is isoenhancing

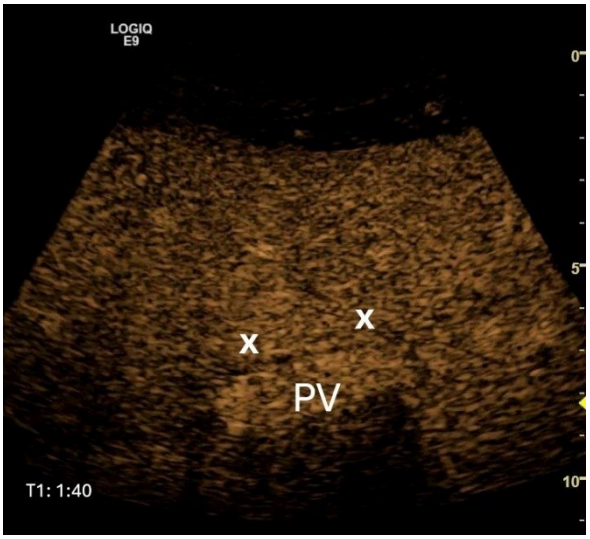

Fig. 4.a.43. Focal fatty sparing. CEUS portal phase – the area is isoenhancing.

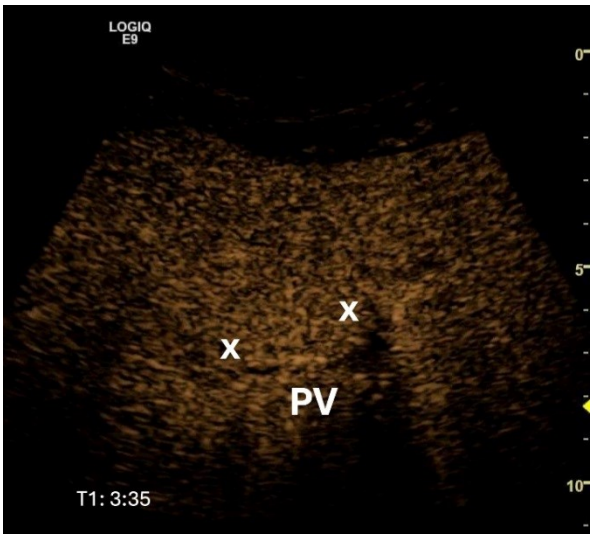

Fig. 4.a.44. Focal fatty sparing. CEUS late phase – the area is isoenhancing.

5. ***Biliary hamartomas*** (von Meyenburg complex) are asymptomatic, uncommon benign solitary or multiple malformations of the intrahepatic bile ducts with a prevalence of 0.6-2.8% in necroptic studies, consisting of cystic dilatations of intrahepatic bile ducts embedded in fibrous tissue. On B-mode US they vary in appearance based on the histopathology, stage, and size, the most characteristic aspect is the "starry sky" liver. Biliary hamartomas can appear as hyperechoic (when mostly solid), with mixed echogenicity with cystic components, or purely anechoic (cystic). In a steatotic liver, they may be hypoechoic. Typically small (<5 mm), hyperechoic, and peripherally located, they may become hypoechoic or microcystic as they grow larger, leading to a coarse echotexture of the liver parenchyma. Bile microcrystals within microcysts can cause "comet tail" artefacts (Fig. 4.a.45). On CEUS they mostly appear unenhancing. However, they can be a difficult differential diagnosis in a patient evaluated for oncologic disease.

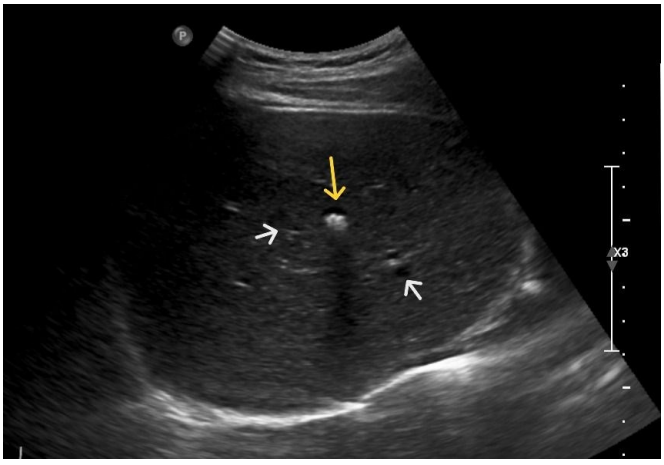

Fig. 4.a.45. von Meyenburg complex. Smal cystic lesions (white arrows). "Comet tail" artefacts (yellow arrow)

Selective references

1. Dietrich CF, Nolsoe CP, Barr RG, Berzigotti A, Burns PN, Cantisani V, et al. Guidelines and Good Clinical Practice Recommendations for Contrast Enhanced Ultrasound (CEUS) in the Liver - Update 2020 - WFUMB in Cooperation with EFSUMB, AFSUMB, AIUM, and FLAUS. Ultraschall Med. 2020;41(5):562-85.
2. Şirli R, Popescu A, Jenssen C, Möller K, Lim A, Dong Y, Sporea I, Nürnberg D, Petry M, Dietrich CF. WFUMB Review Paper. Incidental Findings in Otherwise Healthy Subjects, How to Manage: Liver. Cancers (Basel). 2024 Aug 21;16(16):2908.
3. Sirli R, Sporea I, Popescu A. When to refer patients for liver elastography. Expert Rev Gastroenterol Hepatol. 2024 Dec;18(12):753-755.
4. Strobel D, Seitz K, Blank W, Schuler A, Dietrich C, von Herbay A, et al. Contrast-enhanced ultrasound for the characterization of focal liver lesions--diagnostic accuracy in clinical practice (DEGUM multicenter trial). Ultraschall Med. 2008;29(5):499-505.
5. Trillaud H, Bruel JM, Valette PJ, Vilgrain V, Schmutz G, Oyen R, et al. Characterization of focal liver lesions with SonoVue-enhanced sonography: international multicenter-study in comparison to CT and MRI. World J Gastroenterol. 2009;15(30):3748-56.
6. Sporea I, Sandulescu DL, Sirli R, Popescu A, Danila M, Sparchez Z, et al. Contrast-Enhanced Ultrasound for the Characterization of Malignant versus Benign Focal Liver Lesions in a Prospective Multicenter Experience - The SRUMB Study. J Gastrointestin Liver Dis. 2019;28:191-6.
7. Burrowes DP, Medellin A, Harris AC, Milot L, Lethebe BC, Wilson SR. Characterization of Focal Liver Masses: A Multicenter Comparison of Contrast-Enhanced Ultrasound, Computed Tomography, and Magnetic Resonance Imaging. J Ultrasound Med. 2021.

4.b. MALIGNANT FOCAL LIVER LESIONS

Mirela Dănilă, Ana Maria Ghiuchici
WFUMB Center of Education Timișoara, Romania

Malignant FLL may be incidental US findings in quasi-symptomatic patients or may be detected in patients with a known history of chronic liver disease or neoplastic disease. Therefore, the patient's history, clinical symptoms, and laboratory tests are crucial steps in diagnosing a malignant lesion.

For example, the detection of a liver mass in a patient with a history of cancer suggests possible metastases, while the detection of a liver mass in a patient with known chronic liver disease indicates hepatocellular carcinoma (HCC).

The liver is the site of many malignant tumors, but the most common are HCC and cholangiocarcinoma (CCA) as primary liver tumors, as well as liver metastases, which are secondary liver tumors.

Primary malignant liver tumors

1. Hepatocellular carcinoma

HCC is the most common primary liver cancer, accounting for approximately 90% of primary liver cancers. HCC is the sixth most common malignancy and the fourth leading cause of cancer death worldwide. 80% of adult HCC cases occur in liver cirrhosis. Patients with cirrhosis from any etiology are at risk for developing HCC.

Ultrasound for early detection of HCC

US surveillance for hepatocellular carcinoma (HCC) is recommended for all cirrhotic patients unless they are at a relatively high risk of death from other causes than HCC. US evaluation of the liver every six months is advised for the early detection of HCC to reduce disease-related mortality. The European Association for the Study of the Liver (EASL) guidelines recommend that monitoring should be performed by experienced personnel.

Studies regarding US accuracy as a screening tool for HCC report variable sensitivity but with very good specificity. Any new nodule detected in the setting of cirrhosis should be considered HCC until proven otherwise.

The Ultrasound Liver Imaging Reporting and Data System (LI-RADS) algorithm was introduced as a standardization tool for US interpretation. It categorizes the limitations as follows:

A - no or minimal limitation, B - moderate limitation, and C - severe limitation in the liver with severe heterogeneity and severe beam attenuation, where most of the liver is not visualized. This scoring system could help identify patients who may not be ideal candidates for US HCC screening.

In standard ultrasound, small HCCs 2-3 cm in size are often hypoechoic but sometimes can be also hyperechoic. HCC echogenicity depends on its size and the surrounding liver parenchyma (cirrhotic vs non-cirrhotic). Larges nodules are frequently inhomogeneous in ultrasound examination. A mosaic appearance and "nodule-in-nodule" architecture are other characteristic features of HCC. Examples of HCC appearance in conventional B-mode US are shown in Figures 4.b.46-4.b.49.

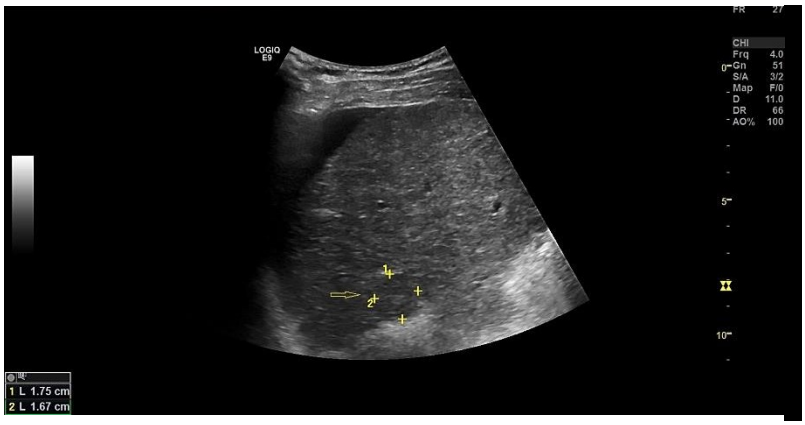

Fig. 4.b.46. Conventional B-mode US: hypoecoic small HCC in a patient with liver cirrhosis and ascites.

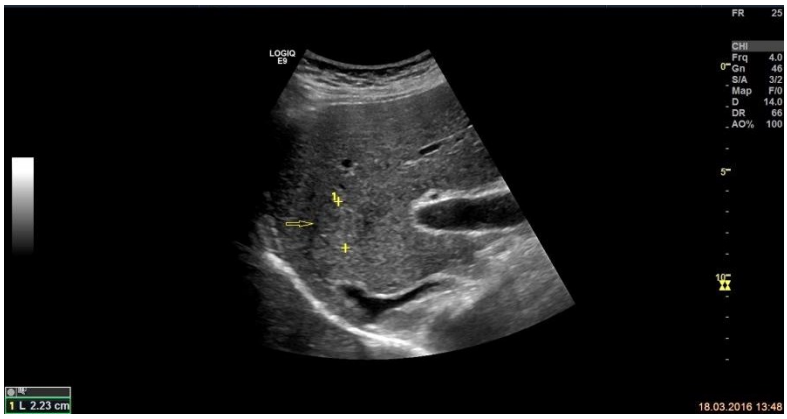

Fig. 4.b.47. Conventional B-mode US: slightly hyperechoic 2.3 cm HCC nodule in a patient with liver cirrhosis.

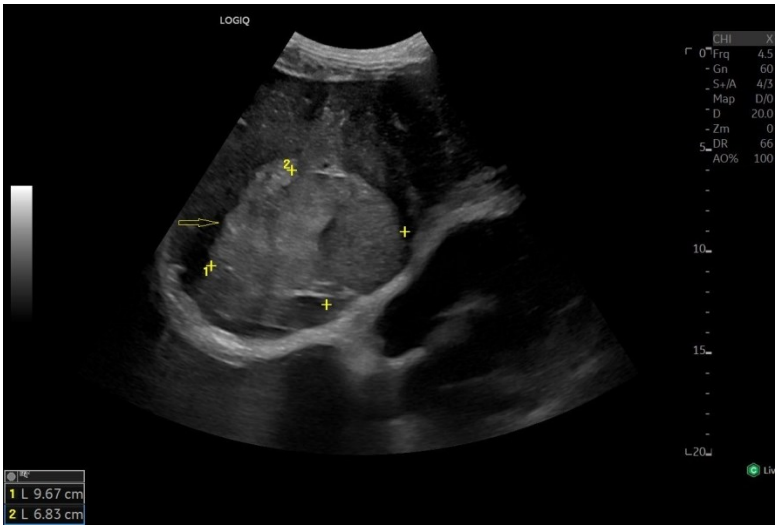

Fig. 4.b.48. Conventional B-mode US: hyperechoic, slightly inhomogeneous large HCC nodule.

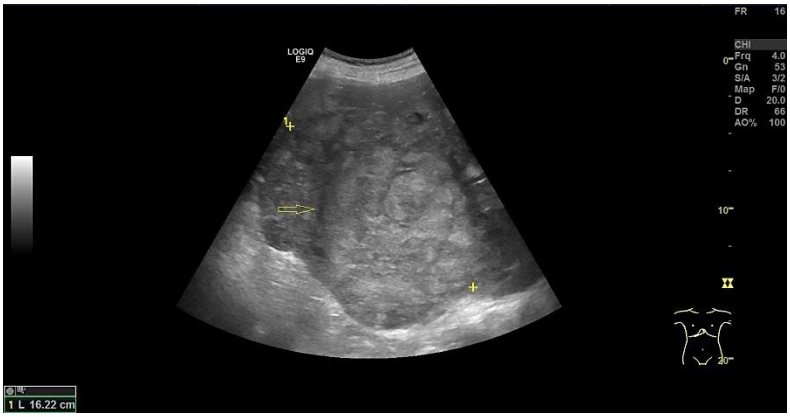

Fig. 4.b.49. Conventional B-mode US: nearly 17 cm large heterogeneous HCC.

In this case, US examination will also reveal other signs suggestive of liver cirrhosis diagnosis: enlarged caudate lobe, irregular liver surface, slightly inhomogeneous appearance of the liver structure, splenomegaly, signs of portal hypertension, etc. (Fig. 4.b.50 – Fig.4.b.51)

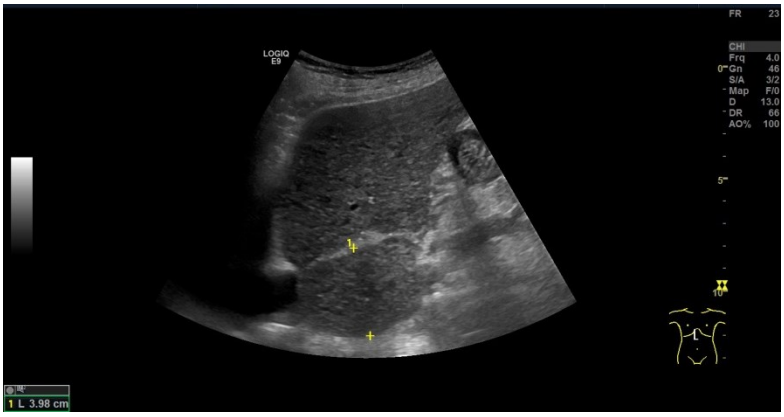

Fig. 4.b.50. Conventional B-mode US: signs of liver cirrhosis – enlarged caudate lobe and slightly inhomogeneous liver structure.

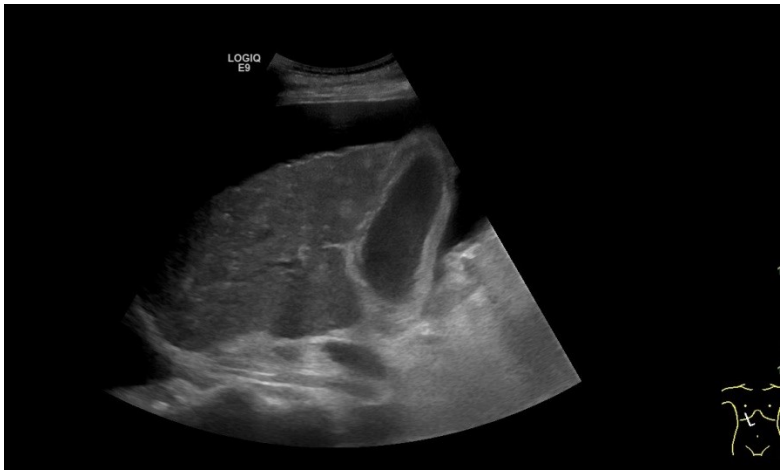

Fig. 4.b.51. Conventional B-mode US: signs of liver cirrhosis – ascites, irregular liver surface, heterogeneous liver structure, thickening of the gallbladder wall due to hypoalbuminemia.

If no increase in size is observed in nodules less than 1 cm detected during the screening program, they will be US monitored at 3-4 month intervals for two years.

The next step in evaluating liver nodules detected in the screening program is characterization with contrast-enhanced imaging techniques.

Contrast-enhanced imaging techniques such as MRI, CT, or contrast-enhanced ultrasound (CEUS) are required to confirm or exclude the diagnosis of HCC: Because CEUS is a fast, reliable, and sensitive examination for characterizing liver nodules detected at screening and uses gas microbubble-based contrast agents with almost no side effects, it is often the first imaging modality used to characterize these nodules in clinical practice. HCC nodules are, in most cases, hypervascularised tumors showing hyperenhancement in the arterial vascular phase at CEUS examination (Fig. 4.b.52- Fig. 4.b.53 a).

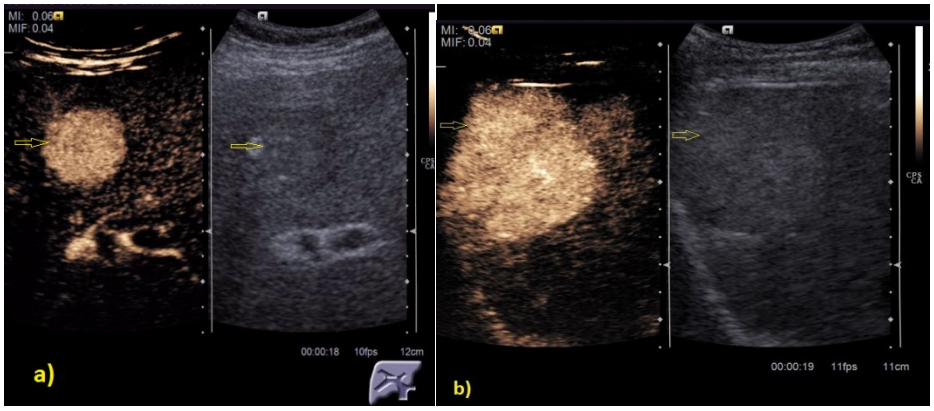

Fig. 4.b.52. HCC nodules with hyperenhancement in the arterial vascular phase (a, b) on CEUS examination.

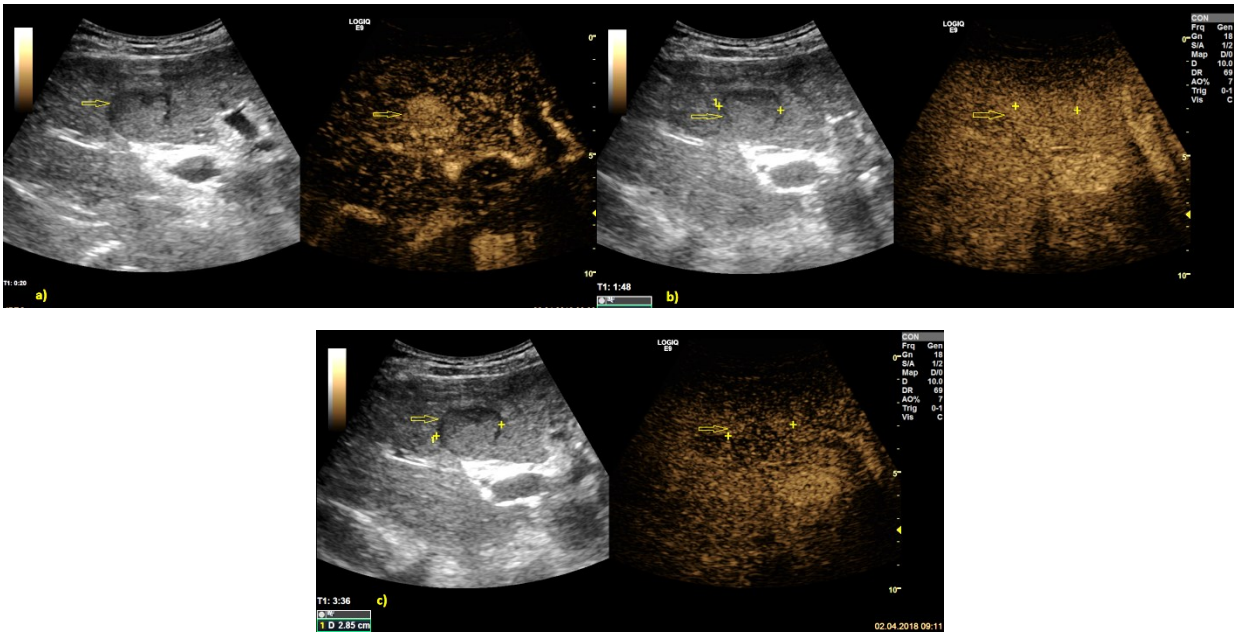

Fig. 4.b.53. CEUS examination: HCC nodule showing hyperenhancement in the arterial phase (a), isoenhancement in the portal venous phase (b) with mild washout in the late vascular phase (c).

Patients with no history of chronic liver disease or not enrolled in a screening program for HCC often present with advanced-stage disease, large tumors, and a poor prognosis. In these situations, the initial step in the multiparametric US evaluation is to assess liver elasticity using shear wave elastography. If the elastographic assessment indicates cirrhosis, HCC becomes the primary suspicion, which can be further characterized using CEUS (Fig. 4.b.54).

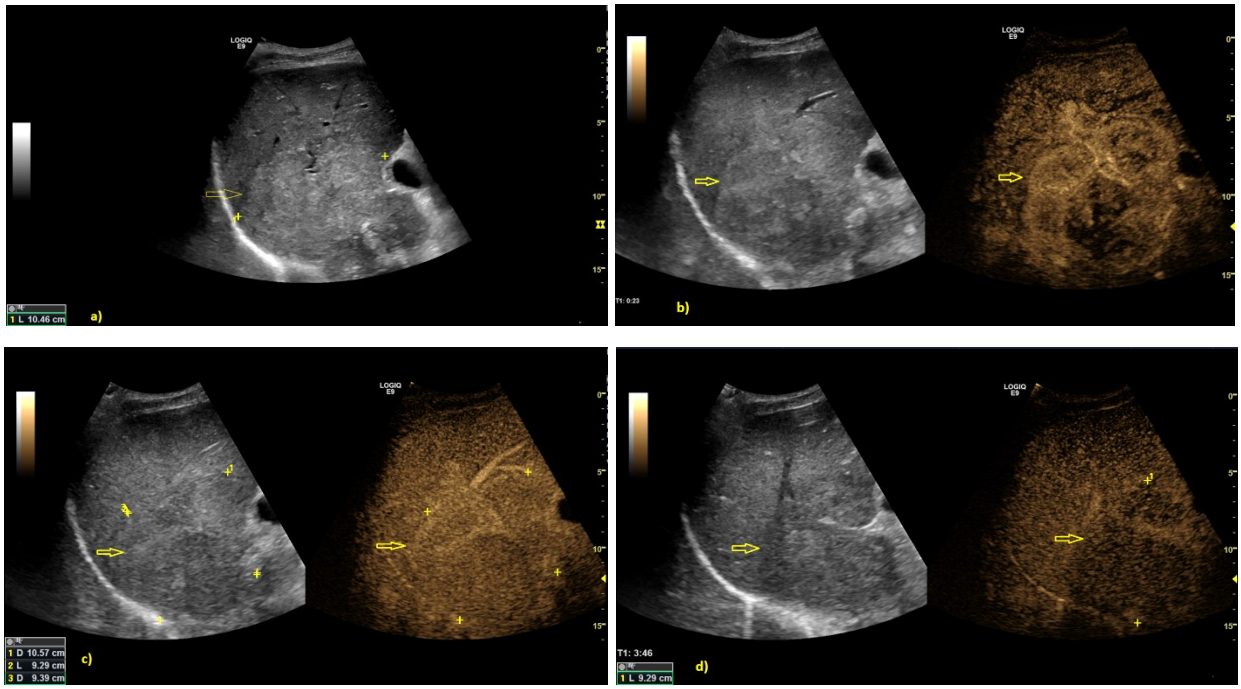

Fig. 4.b.54. Conventional B-mode US (a) large heterogeneous HCC showing inhomogeneous hyperenhancement in the arterial phase (a), isoenhancement in the portal venous phase (b) and mild washout in the late vascular phase (c) on CEUS examination.

Contrast enhanced ultrasound in HCC.

Typical features of HCC on CEUS examination are:

- *Hyperenhancement* in the arterial phase (APHE), usually homogeneous and intense (Fig. 4.b.55) but may be inhomogeneous in larger nodules (Fig. 4.b.56).
- Late (>60 s) and mild washout

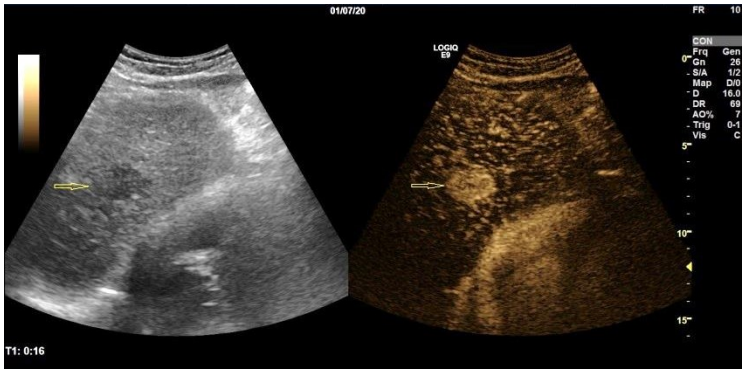

Fig. 4.b.55. CEUS examination: hypoechoic HCC with hyperenhancement in the arterial phase.

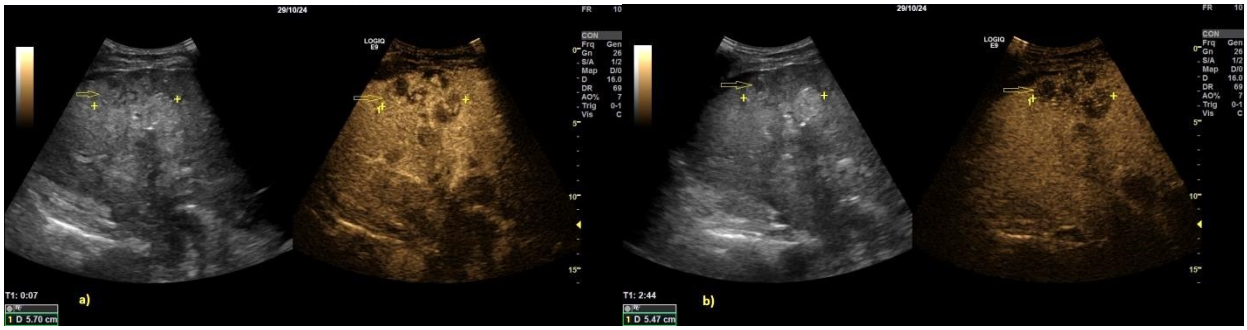

Fig. 4.b.56. CEUS examination: biopsy-proven HCC 5.8 cm in size with inhomogeneous hyperenhancement in the arterial phase (a) and washout in the late vascular phase (b).

The sensitivity of CEUS examination in detecting arterial hypervascularity of nodules in cirrhosis has been reported to be significantly higher than that of CT or MRI. Hyperenhancement is more common in moderately differentiated HCC compared to well-differentiated or poorly differentiated HCC. Washout is observed in about half of the HCC cases overall, but it is less frequently observed in very small nodules.

Numerous studies suggest that tumor size may influence the diagnostic accuracy of CEUS in HCC detection, with lower sensitivity for HCC nodules that are ≤ 2 cm compared to those that are > 2 cm.

CEUS accuracy for HCC diagnosis was evaluated in a comprehensive meta-analysis that included studies from 2001 to 2021. The sensitivity of CEUS for detecting HCC of varying sizes and stages was 77.8% (95% [CI]: 69.4% to 84.4%), while the specificity was 93.8% (95% CI: 89.1% to 96.6%). In cases of resectable HCC, CEUS demonstrated a sensitivity of 77.5% (95% CI: 62.9% to 87.6%) and a specificity of 92.7% (95% CI: 86.8% to 96.1%).

The application of CEUS as a non-invasive diagnostic tool for HCC has been controversial due to the potential risk of misdiagnosing intrahepatic cholangiocarcinoma, which occurs in approximately 2-5% of all new nodules in cirrhotic patients.

CEUS Liver Imaging Reporting and Data System (LI-RADS) algorithm was developed to increase CEUS specificity for HCC diagnosis. This algorithm provides a standardized reporting system for medical imaging data, facilitating the classification of liver lesions found in patients with cirrhosis. Recent EASL guidelines for the management of HCC recommend that the noninvasive diagnosis of HCC should be based on the LIRADS CT/MR v2018 or LI-RADS CEUS v2017 criteria. On CEUS, non-rim arterial hyperenhancement with late-onset (>60 s) and low-intensity washout represent the diagnostic criteria for HCC.

The CEUS LI-RADS algorithm can be used in high-risk patients, but only for lesions visible on pre-contrast ultrasound. It applies to CEUS examinations performed with pure blood pool agents (Lumason® in the US, SonoVue® outside the US; Definity® in the US and Canada, Luminity® outside the US or Canada).

This algorithm classifies liver lesions into eight diagnostic categories ranging from LR-1 (definitely benign) to LR-5 (definitely HCC) and additional categories of LR-M (for malignancies other than HCC), LR-TIV (malignant venous thrombosis), and LR-NC (unclassifiable lesions). A definite HCC (LR-5) is present when a lesion >10 mm shows non-rim and non-peripheral discontinuous globular APHE plus late and mild washout (Fig. 4.b.57). Using the LIRADS criteria, studies reported excellent positive predictive value of the LR5 category for HCC but with decreased sensitivity of CEUS examination in HCC diagnosis.

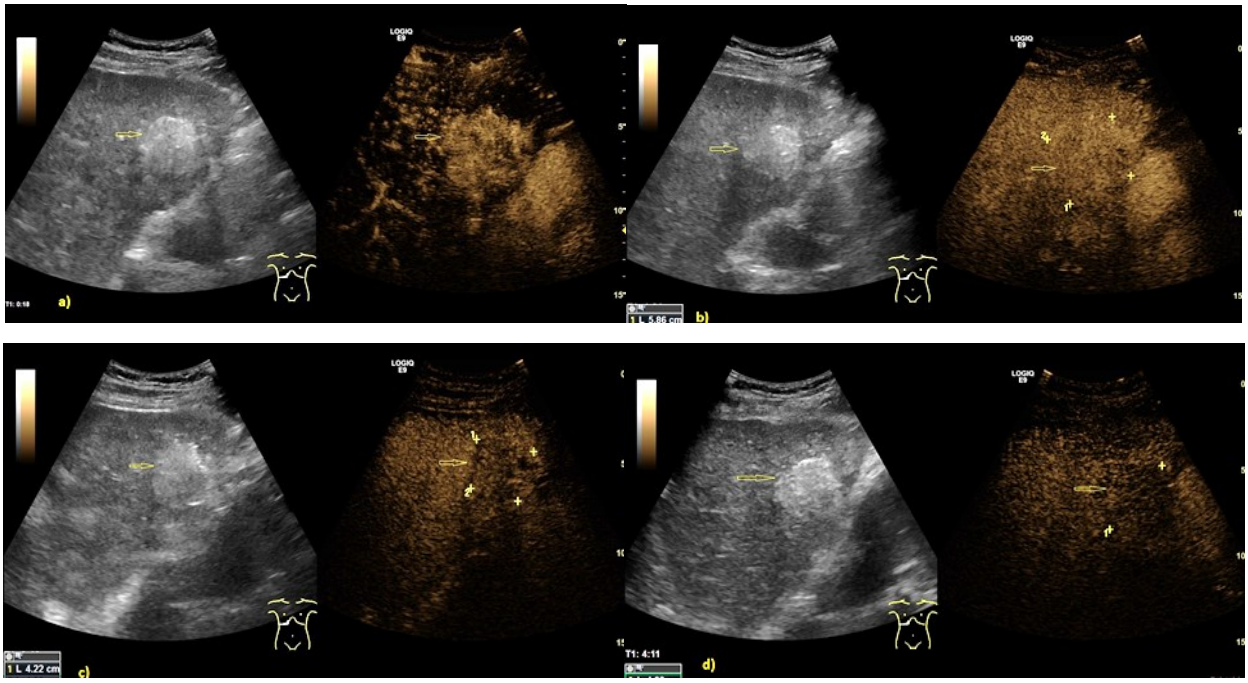

Fig. 4.b.57. CEUS examination: hyperechoic HCC nodule in B-mode showing hyperenhancement in the arterial phase (a), isoenhancement in the portal venous phase (b) with mild and late washout in the late vascular phase (c,d). LR-5 lesion.

Elastography in the diagnosis of HCC

Ultrasound-based elastography is a non-invasive and reproducible method with an established role in assessing liver fibrosis. Elastography can complement a conventional B-mode US examination, with most elastographic methods integrated into modern ultrasonography systems. Point and twodimensional p-SWE and 2D-SWE are the most studied methods for characterizing tumor elasticity. Numerous studies have shown promising results regarding the diagnostic accuracy of elastography in determining the nature and type of tumors. Malignant FLLs are generally stiffer than benign lesions.

In liver cirrhosis, HCC nodules may exhibit lower stiffness compared to the adjacent hepatic parenchyma or other malignant liver tumors such as metastases or iCCA. The p-SWE evaluation

shows variable stiffness in HCC, with values ranging between 2.16 ± 0.75 m/s and 3.07 ± 0.89 m/s, which correlates with the degree of vascularization and histological differentiation. The 2D-SWE evaluation of HCC nodules revealed increased variability in stiffness, ranging from 19.6 kPa to 44.8 kPa.

EFSUMB/WFUMB have not yet validated the use of elastographic methods for FLL differential or HCC diagnosis. Still, elastography can be used as a part of a multiparametric US FLL evaluation in clinical practice.

2. Cholangiocarcinoma (CCA)

CCA is a malignant liver tumor that arises from epithelial cells, cholangiocytes, anywhere along the biliary tree within or outside the liver. CCA is subclassified as intrahepatic CCA (iCCA), arising from the bile ducts proximal to the second-order bile ducts (segmental bile ducts); perihilar CCA (pCCA), arising in the right and/or left hepatic duct and/or at their junction (so-called perihilar bile ducts); and distal CCA (dCCA), arising from the epithelium distal to the cystic duct insertion. Perihilar CCA (or Klatskin's tumor) is the most common type, accounting for 50-60% of CCA, followed by extrahepatic CCA (20-30%) and intrahepatic CCA (10-20%)

Intrahepatic cholangiocarcinoma (iCCA) represents the second most frequent primary liver cancer after HCC, accounting for 10%-15% of all primary liver cancers. The most common imaging modalities used to diagnose and stage intrahepatic cholangiocarcinoma include US, CT, and MRI/MRCP with contrast.

On ultrasound, iCCA appears as a homogeneous mass with moderate to increased echogenicity and a peripheral hypoechoic halo. Typically, tumors larger than 3 cm are hyperechoic, while smaller tumors are iso- to hypoechoic. The shape of the mass may be irregular, but the margins are typically circumscribed, and associated capsular retraction may be sonographically visible.

Contrast enhanced ultrasound (CEUS) in iCCA

The enhancement pattern of intrahepatic iCCA on CEUS has been evaluated in several studies.

In the arterial vascular phase, four types of enhancement patterns were described:

- rim-like hyperenhancement (Fig. 4.b.58 a),
- homogeneous hyperenhancement (Fig. 4.b.59 b),
- heterogeneous hyperenhancement and
- hypoenhancement pattern.

In the portal–venous and late phases, all iCCA present an early (<60s) and marked washout Fig.4.b.58 b – Fig.4.b.59 c). The presence of rapid and intense washout is the main diagnostic difference between iCCA and HCC in patients with a history of cirrhosis, as HCC is typically characterized by mild and late washout.

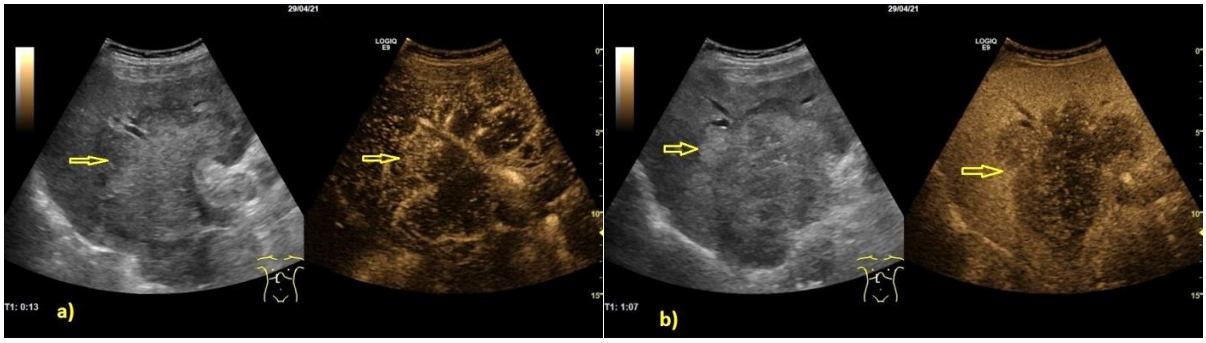

Fig. 4.b.58. Biopsy-proven iCCA, Large liver mass slightly hyperechoic in conventional US B-mode showing rim-like hyperenhancement in the arterial phase (a) and marked, rapid washout in the portal venous phase (b) on CEUS examination.

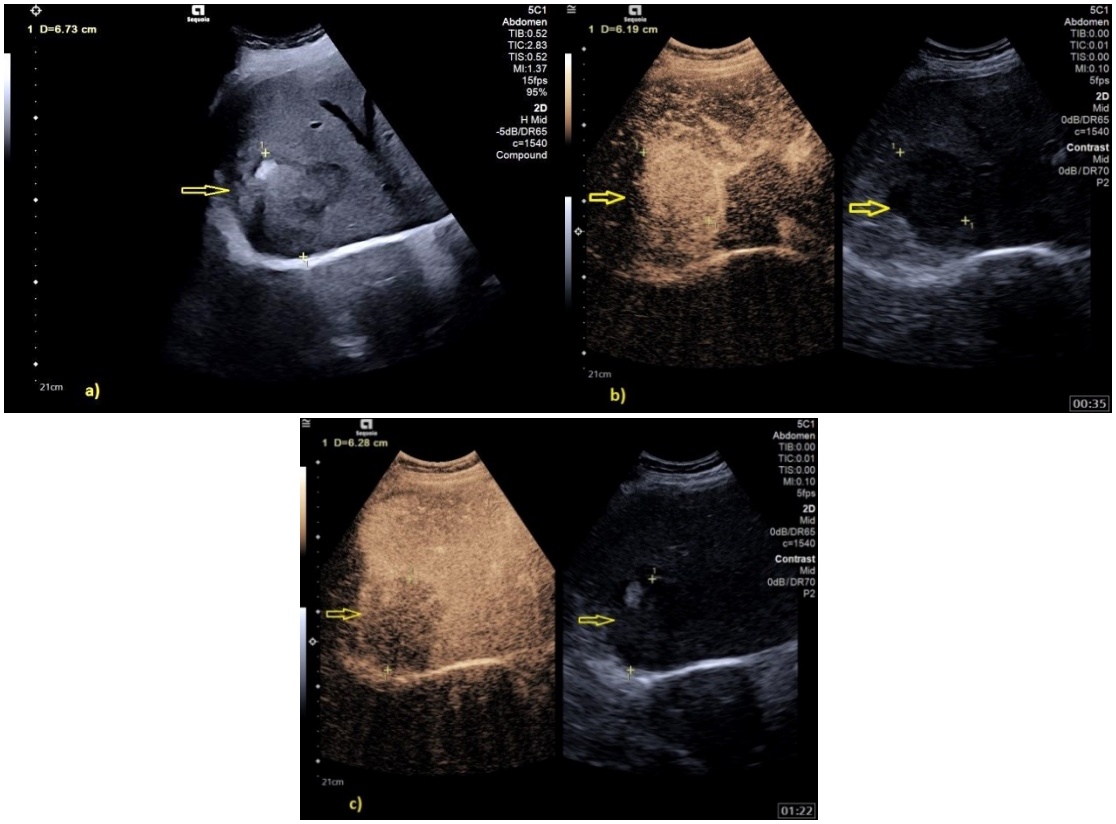

Fig. 4.b.59. Conventional US B-mode (a) – hyperechoic, irregular liver mass with a peripheral hypoechoic halo. CEUS examination: the tumor shows homogeneous hyperenhancement in the arterial phase (b) and marked, rapid washout in the portal venous phase (c).

The role of CEUS in differentiating iCCA from HCC was evaluated in a recent meta-analysis of 8 studies. The authors identified three CEUS features that could discriminate HCC and iCCA (hyperenhancement in the arterial phase, mild and late washout in the portal-venous and late phases for HCC and arterial rim enhancement, marked and early washout in the portal-venous and late phases for iCCA). The pooled diagnostic performance of CEUS in differentiating HCC from iCCA was good, with a specificity of 0.87 (95%CI: 0.79-0.92) and a sensitivity of 0.92 (95%CI: 0.84-0.96). In most cases, the diagnosis of iCCA requires a biopsy for pathologic confirmation.

Patients with hilar and extrahepatic cholangiocarcinoma usually present with symptoms of biliary obstruction, including painless jaundice, pale stools, dark urine, and pruritus. Initial workup for biliary obstruction or suspected liver disease includes abdominal US examination that shows dilatation of the intrahepatic bile ducts, usually without an identifiable mass; papillary tumors may be observed as polypoid masses within the biliary tract.

US can demonstrate larger hilar lesions in addition to biliary dilatation, but small lesions and distal cholangiocarcinomas are difficult to visualize.

Endoscopic ultrasonography (EUS) allows both biliary visualization and tumor evaluation. This technique also allows aspiration for cytologic examination and anatomopathologic diagnosis.

3. Other rare primary liver malignancies

Fibrolamellar carcinoma is a rare subtype of cancer that occurs in the absence of liver cirrhosis, especially in young patients, and is often found in late stages. The US appearance is uncharacteristic, biopsy and histopathologic exam are needed for a final diagnosis.

Biliary cystadenocarcinoma

Cystadenocarcinoma of the liver is a rare malignant tumor derived from the hepatobiliary epithelium. Most often unilocular but also multiloculated can be observed. Imaging techniques cannot reliably differentiate malignant cystadenocarcinoma from other benign lesions such as cystadenoma.

On standard US examination, cystadenocarcinoma appears as a well-demarcated anechoic mass with multiple internal septations (Fig. 4.b.60). The tumor is also encapsulated. Mural and septal nodularity (> 1 cm) may also be seen as a hemorrhagic internal fluid. Contrast-enhanced ultrasound demonstrates minimal enhancement.

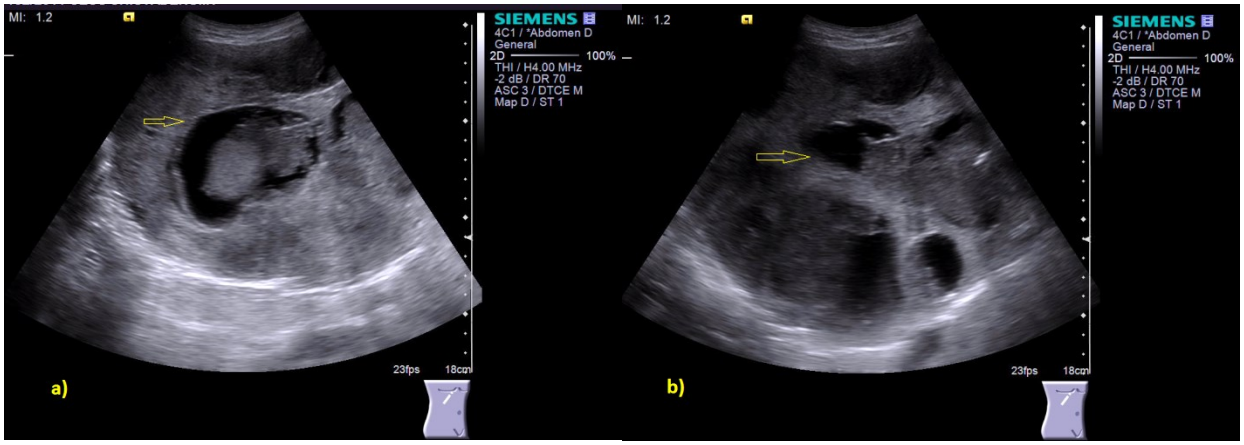

Fig. 4.b.60. Conventional US B-mode (a) well-demarcated unilocular cyst with mass with possible hemorragic fluid; (b) multilocular cyst with mural nodules and papillary projections extended into the cyst lumen.

Malignant vascular tumors of the liver

Hepatic epithelioid hemangioendothelioma (HEH) is a rare vascular tumor of endothelial origin that exhibits variable malignant potential. Diagnosing HEH can be challenging, and many cases are initially misdiagnosed. In US it is usually seen as a predominantly hypoechoic liver lesion with mixed ecostructure and can produce hepatic capsular retraction if the lesion is adjacent to the liver capsule (Fig. 4.b.61). A biopsy is often required to confirm the diagnosis.

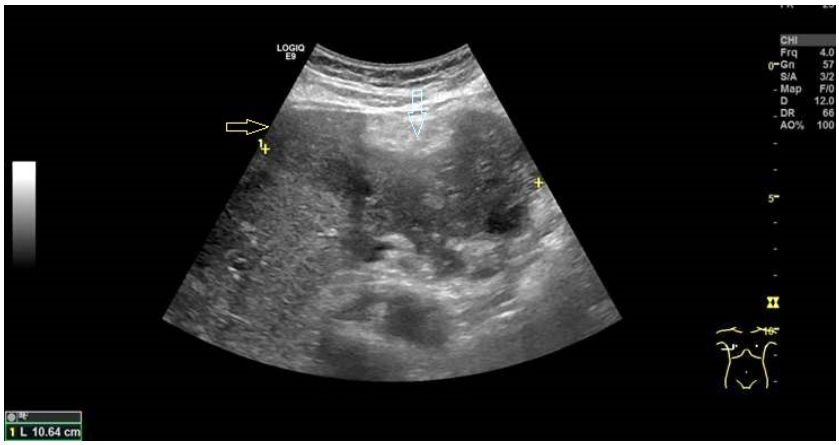

Fig.4.b.61. Biopsy-proven HEH. Conventional US B-mode: large hypoechoic 10 cm in size liver lesion with mixed ecostructure localized in the left hepatic lobe with retraction of the liver capsule at this level.

Secondary malignant liver tumors

Liver metastases

Liver metastases are the most common liver malignancies and occur mainly in gastrointestinal neoplasms, but other malignancies can also cause liver metastases (breast, lung, prostate, neuroendocrine tumors, etc.).

US has an important role in the detection of liver metastases, either as a screening modality in patients with known malignancy or as the first imaging modality in symptomatic patients.

Liver metastases may be single when the differential diagnosis is made with primary liver tumors (Fig. 4.62), but the presence of multiple liver nodules of different sizes in the liver always suggests liver metastases (Fig. 4.b.63, 4.b.64).

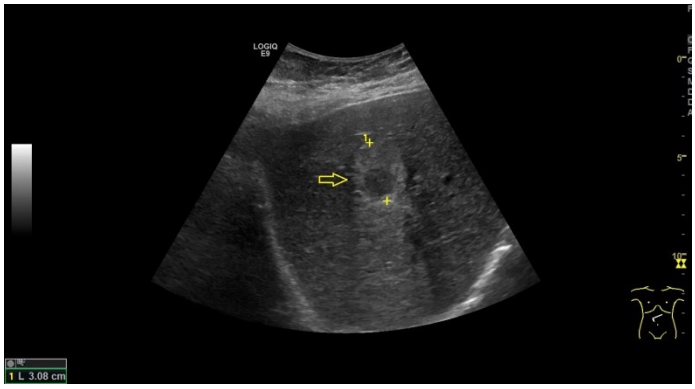

Fig.4.b.62. Biopsy-proven liver metastasis from a neuroendocrine pancreatic tumor. Conventional US B-mode: hypoechoic focal liver lesion with hyperechoic halo in a patient known with oncologic history.

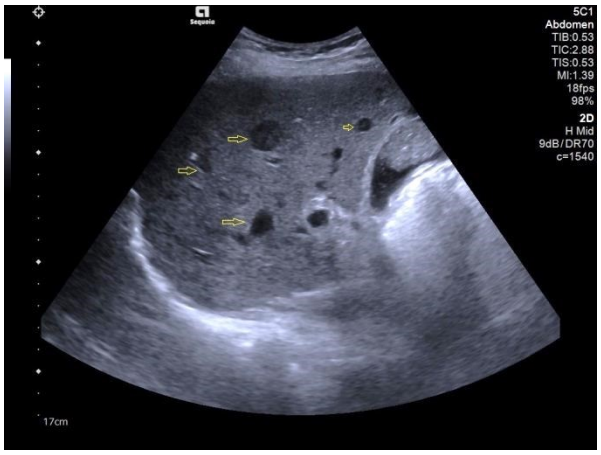

Fig.4.b.63. Conventional US B-mode: multiple hypoechoic focal liver lesions suggestive of liver metastases in a patient with pancreatic cancer. Gallbladder with ball-like organized sludge.

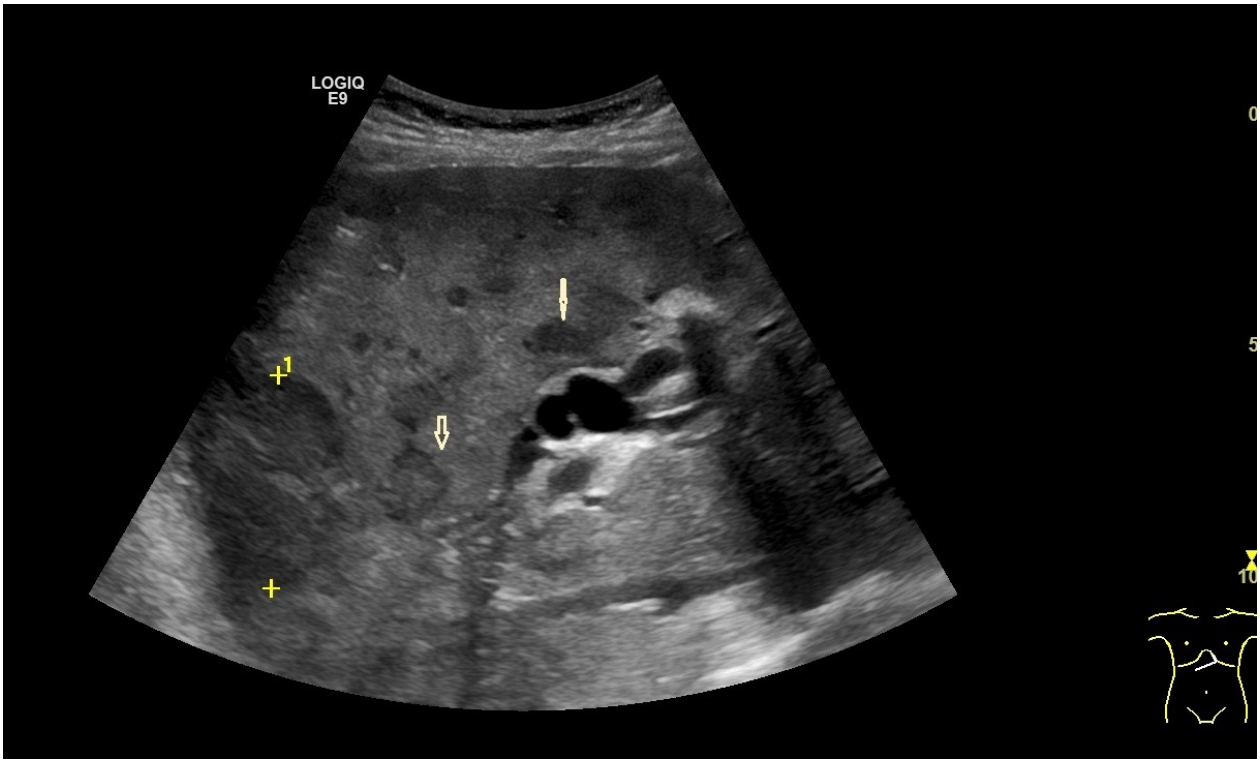

Fig. 4.b.64. Conventional US B-mode: multiple hypoechoic liver metastases.

The ultrasonographic appearance of liver metastases depends on the degree of vascularization of the tumor, the cellular composition, and the presence or absence of necrosis, fibrosis, and fatty changes. Metastases complicated by hemorrhage, necrosis, or infection may have an inhomogeneous appearance with a fluid component.

The US appearance of liver metastases can vary from isoechoic (which can be difficult to detect) to hypo-, hyper-echoic, as well as bull's-eye metastases. In rare cases, they may have a cystic appearance, which can mimic abscesses, hemorrhagic infarcts, hematomas, simple cysts, or hydatid cysts.

The US characteristics of metastases may provide clues about the primary tumor. Hypoechoic metastases are often associated with lung cancer, breast cancer, and pancreatic adenocarcinoma, while hyperechoic metastases are commonly linked to colorectal cancer, renal cell carcinoma, Kaposi sarcoma, and neuroendocrine tumors. The bull's eye or target pattern is the most suggestive lesion for liver metastases and is common in many cancers: gastrointestinal adenocarcinoma, and ovarian adenocarcinoma (Fig. 4.b.65 - Fig. 4.b.66). Cystic metastases occur more often in squamous cell carcinoma, ovarian cancer, pancreatic adenocarcinoma, and colorectal cancer.

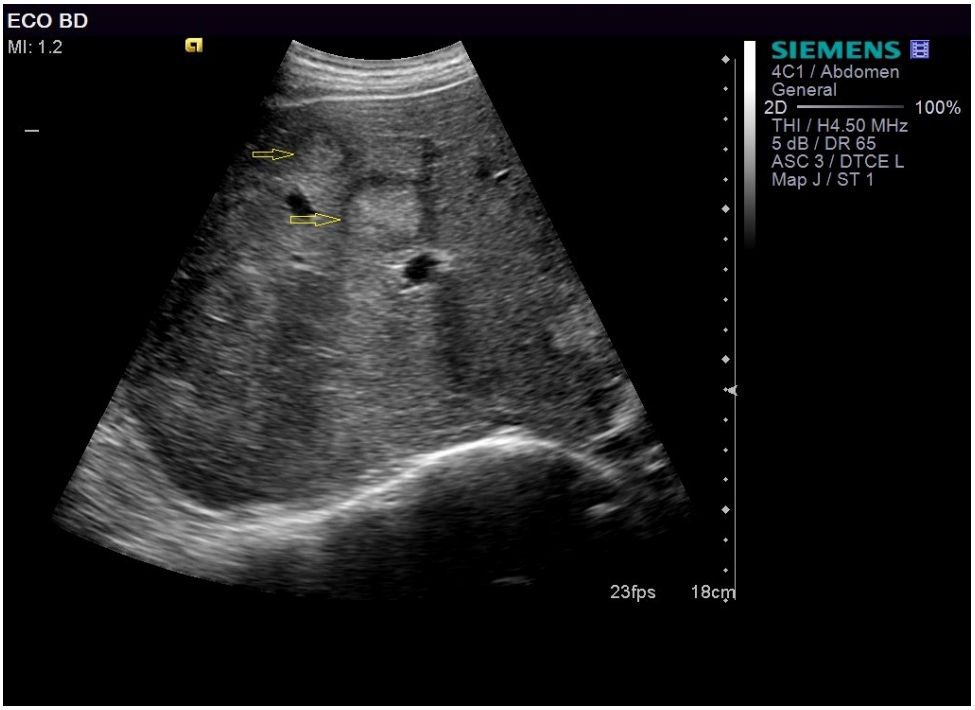

Fig. 4.b.65. Conventional US B-mode: multiple liver metastases with bull`s-eye appearance.

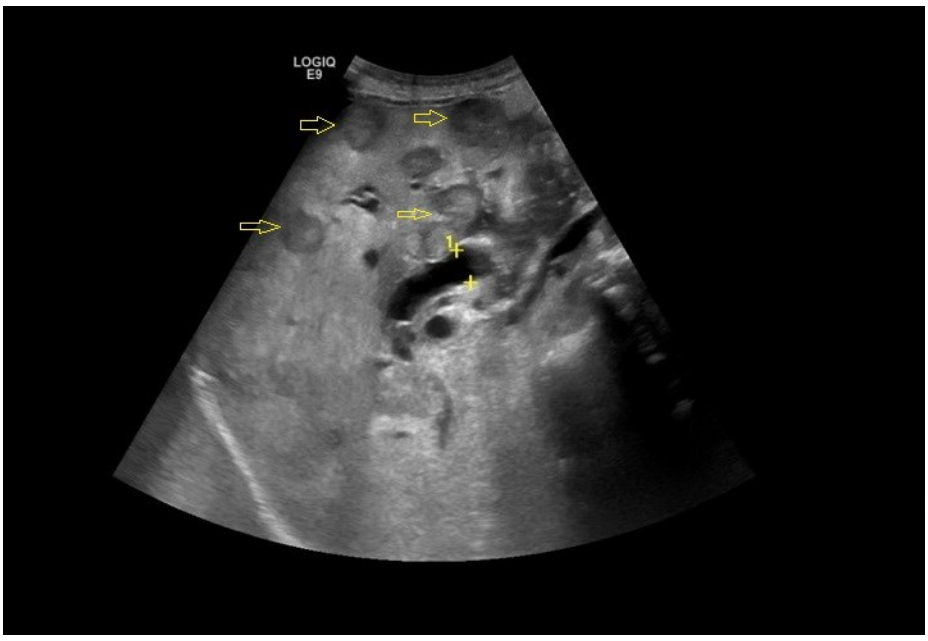

Fig. 4.b. 66. Conventional US B-mode: multiple bull`s-eye liver metastases and biliary obstruction.

The sensitivity of US in detecting liver metastases is influenced by several factors, including the lesion's appearance, its size, and the quality of liver visualization. Reported sensitivity rates for ultrasounds in detecting liver metastases range from 50% to 76%.

Contrast enhanced ultrasound (CEUS) in liver metastases

CEUS examination is effective for characterizing liver metastases and diagnosing malignant lesions. Liver metastases typically exhibit rapid and intense washout during CEUS assessment.

The arterial phase is variable depending on the primary tumor:

- Hypoenhancement especially in gastrointestinal cancer (Fig. 4.b.67), ovarian cancer, pancreatic adenocarcinoma.
- Hyperenhancement in neuroendocrine tumor, melanoma, renal cancer (Fig. 4.b.68).

In the portal and late phases, almost all metastases show rapid and intense washout (Fig. 4.b.69).

Studies in the literature support the role of CEUS in the detection of liver metastases with similar sensitivity compared to CT and MRI. Detection of liver metastases by CEUS is based on their behavior in the portal and late phases, where intense washout is noted.

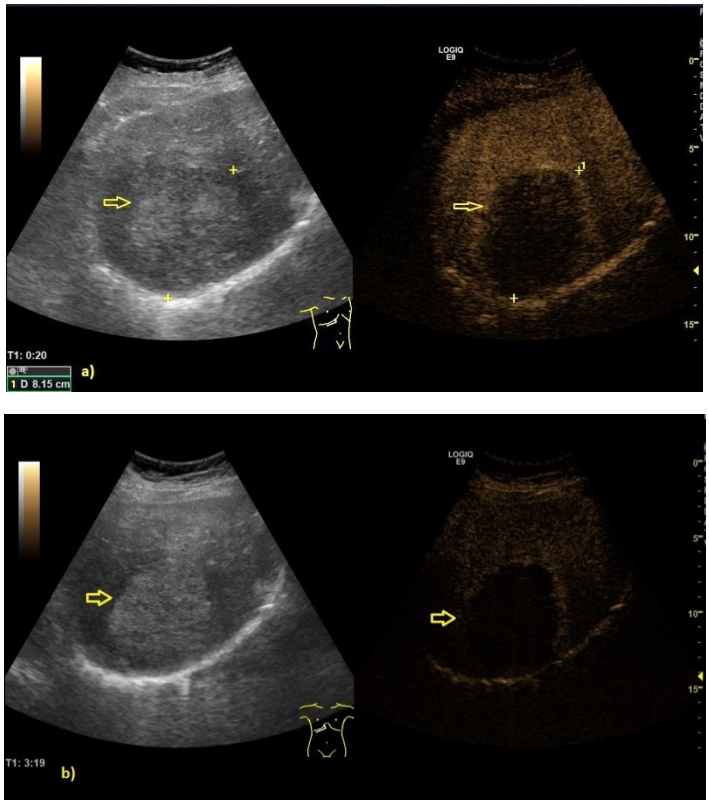

Fig.4. b.67. Large hyperechoic metastasis in a patient with colon cancer. CEUS examination – Hypovascular metastasis: lesion with hypoenhancement in the arterial phase (a) and marked washout in the late phase (b).

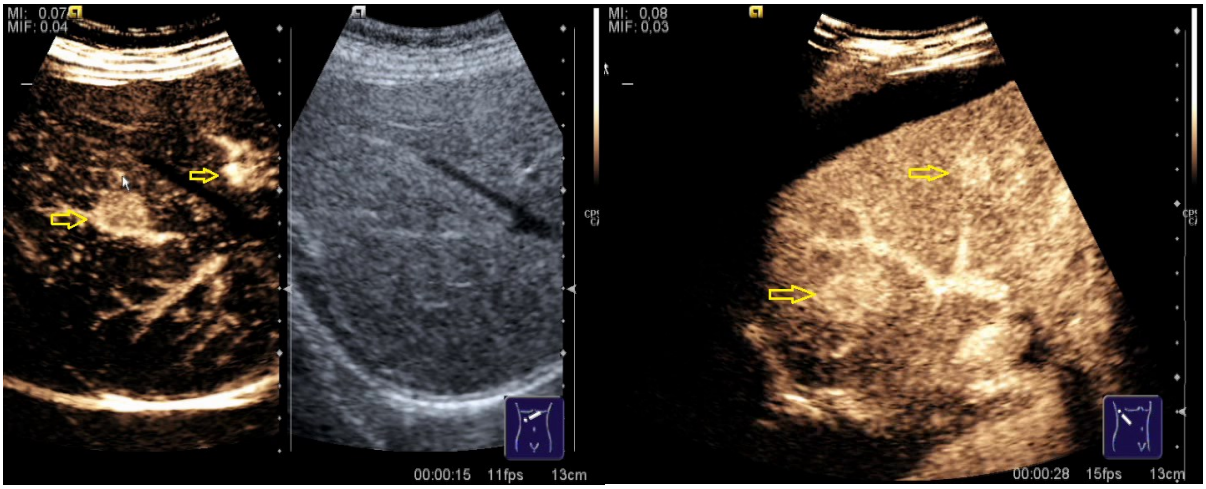

Fig.4.b.68. CEUS examination – Hypervascular metastases: slightly hypoechoic liver lesion with intense hyperenhancement in the arterial phase.

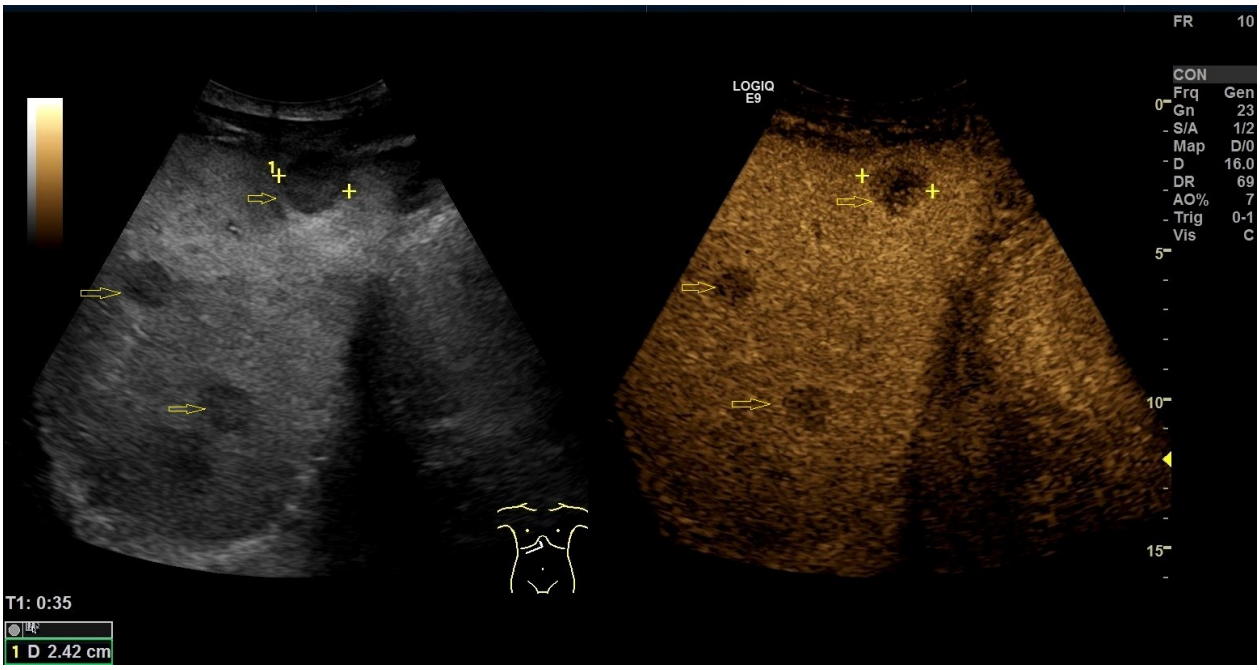

Fig. 4.b.69. CEUS examination - Liver metastases with rapid and intense washout beginning at the end of the arterial phase.

Conclusion

Standard US and CEUS allow the detection and characterization of hepatic masses. Washout in the portal and/or late vascular phases on CEUS examination often suggests malignancy.

Several studies, including meta-analyses, have emphasized the role of CEUS in differentiating between benign and malignant tumors, as well as diagnosing malignant tumors such as HCC and liver metastases.

Given the variety of malignant liver tumors, liver biopsy with histopathologic examination is necessary for diagnosis and targeted oncologic therapy. When liver malignancy is confirmed, additional contrast-enhanced imaging techniques (CT or MRI) are required for staging.

Selective references

1. Bray F, et al. Global cancer statistics 2018: GLOBOCAN estimates of incidence and mortality worldwide for 36 cancers in 185 countries. CA: A Cancer J Clinicians 2018;68(6):394–424.
2. EASL Clinical Practice Guidelines on the management of hepatocellular carcinoma Journal of Hepatology, February 2025. vol. 82 j 315–374.
3. Morgan TA, et al. US li-rads: ultrasound liver imaging reporting and data system for screening and surveillance of hepatocellular carcinoma. Abdom Radiol (NY) 2018;43(1):41–55.
4. Dietrich CF, Nolsøe CP, Barr RG et al. Guidelines and Good Clinical Practice Recommendations for Contrast Enhanced Ultrasound (CEUS) in the Liver – Update 2020 – WFUMB in Cooperation with EFSUMB, AFSUMB, AIUM, and FLAUS. Ultraschall Med 2020;41:562-585.
5. Fraquelli M, Nadarevic T, Colli A, Manzotti C, Giljaca V, Miletic D, Štimac D, Casazza GContrast-enhanced ultrasound for the diagnosis of hepatocellular carcinoma in adults with chronic liver disease. Cochrane Database of Systematic Reviews 2022, Issue 9. Art. No.: CD013483. DOI: 10.1002/14651858.CD013483.pub2.
6. (ACR), A.C.o.R. The liver imaging reporting and data system (LI-rads). 2018.
7. Nakanuma Y, Kakuda Y. Pathologic classification of cholangiocarcinoma: new concepts. Best Pract Res Clin Gastroenterol. 2015;29(2):277-293.
8. Chen, Y.; Zhu, Y.; Chen, K.; Wang, H.; Zhang, W.; Bao, J.; Wang, W. Differentiation between hepatocellular carcinoma and intrahepatic cholangiocarcinoma using contrast-enhanced ultrasound: A systematic review and meta-analysis. Clin. Hemorheol. Microcirc. 2021, 79, 293–309.
9. Riccardo Lencioni, Dania Cioni, Carlo Bartolozzi. Focal Liver Lesions. (2004) ISBN: 9783540644644 - Google Books.
10. Albrecht T, Hohmann J, Oldenburg A, Skrok J, Wolf KJ. Detection and characterisation of liver metastases. Eur Radiol. 2004 Oct;14 Suppl 8:P25-33. doi: 10.1007/s10406-004-0088-z. PMID: 15700330.

5. HOW CAN I USE ULTRASOUND IN BILIARY PATHOLOGY?

Alina Popescu, Camelia Nica
WFUMB Center of Education Timișoara, Romania

Introduction

Ultrasound is an extremely useful diagnostic tool for evaluating biliary and gallbladder normal aspects but also pathology. It is recommended as a first-line imaging approach, when screening for asymptomatic cases and in associated clinical settings. It is an accurate, safe, non-invasive, inexpensive, accessible, repeatable imaging modality, highly sensitive and specific for the detection of gallstones and biliary obstruction, which also frequently demonstrates an alternate diagnosis as the cause of the patient's symptoms, when the biliary system is normal.

The operator must be aware of the limitations of ultrasound in evaluating the gallbladder and hepatobiliary system, the method being an operator-dependent imaging modality, and in which several factors, including obesity, non-fasting, the presence of recent surgical incisions, and a bloated abdomen from gastrointestinal (GI) gas, could also affect the diagnostic effectiveness.

Anatomy

The gallbladder is a saccular structure, functioning as bile storage, with a pear shape aspect, anatomically situated laterally to the second part of the duodenum and anteriorly to the right kidney and transverse colon. Usually, by ultrasound it can be evaluated obliquely, in the right hypochondrium, below the right costal margin. However, different constitutional body types cause variations in its location and orientation.

The gallbladder is divided into a fundus, body, infundibulum and neck. The fundus is the rounded, distal portion of the gallbladder. The body is the largest portion that tapers to the infundibulum and neck. Sometimes, there is a saccular outpouching from the infundibulum/neck known as Hartmann's Pouch, which is a common location for gallstones to become lodged. The bile enters to the main biliary duct through the cystic duct of the gallbladder.

Examination technique:

The examination of the gallbladder and the biliary system is recommended to be performed on fasting, patients should not eat or drink 8 hours before. It is also recommended to avoid smoking.

It is recommended to have a short history of the patient and always to palpate the abdomen before the ultrasound examination.

Routinely, a convex transducer is used for the evaluation of the gallbladder, with a multifrequency of 2-5 MHz. Patients need to be examined in supine position and left lateral recumbent, a mobile content of the gallbladder, such as gallbladder stones or sludge, could be demonstrated by switching the position of the patient. Sometimes, lower frequencies are needed to increase depth of penetration, for example in obese patients or when the gallbladder is deep (e.g. hypersthenic patients). On the other hand, in very slim patients (e.g. asthenic/hyposthenic types), we can switch to linear transducer (e.g. 4-12 MHz) or a convex one with higher frequencies.

The examination can begin with a right subcostal oblique view, positioning the probe along the ribs and angling it superiorly to avoid bowel interference, while instructing the patient to hold a deep breath. Longitudinal views in the same area, as well as intercostal views, may also be employed depending on the gallbladder's location. Key landmarks for assessing the gallbladder include the inferior edge of the right hepatic lobe and the liver hilum. In the right subcostal oblique view, the primary reference point is the interlobar fissure. The gallbladder can be identified by aligning the probe with the fissure and tilting it; the gallbladder typically lies inferior or lateral to this fissure, between liver segments IV and V. Next step is to try to evaluate the cystic duct. It is easiest in deep inspiration with the patient in supine or left lateral recumbent. It is visualized beginning from the infundibulum of the gallbladder.

The evaluation should focus on gallbladder size, wall thickness, and content. A normal gallbladder appears anechoic, with thin echogenic walls measuring 1–3 mm (Fig. 5.1). When performing a measurement, the gallbladder must be positioned to ensure its long axis is almost horizontal on the screen, with the walls perpendicular to the ultrasound beam. After scanning the gallbladder in long axis, the transducer should be rotated over the gallbladder, through 90 degrees towards the practitioner, to image the gallbladder in its true short axis section.

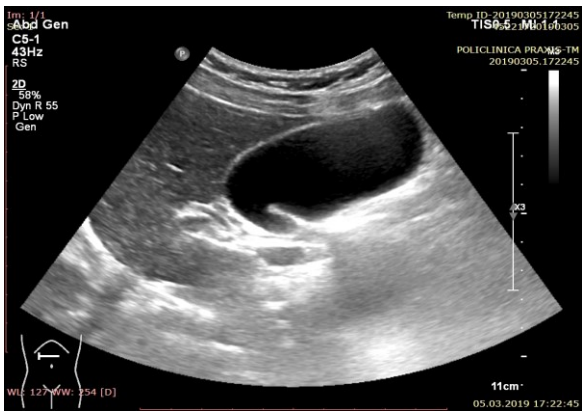

Fig. 5.1. Longitudinal section of the gallbladder, in long axis, using a subcostal approach. The gallbladder appears as an anechoic, fluid-filled structure with well-defined walls, consistent with its normal ultrasonographic appearance.

Inadequate fasting can lead to partial or complete contraction of the gallbladder, resulting in an apparent thickening of its walls, with a double layer aspect on ultrasound imaging (Fig. 5.2). This phenomenon may mimic pathological gallbladder wall thickening, potentially leading to a misdiagnosis.

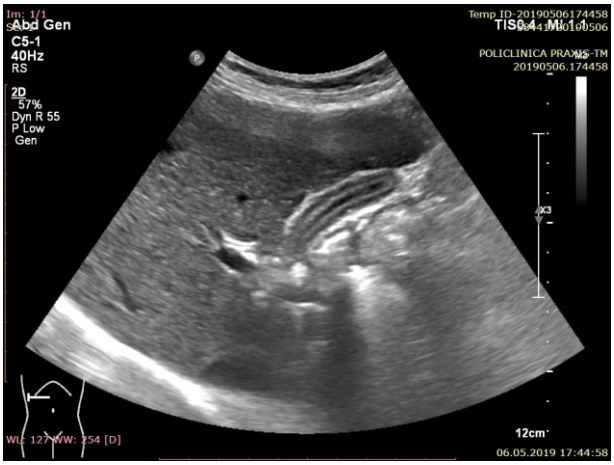

Fig. 5.2. The images depict a small, contracted gallbladder, long-axis section, with a markedly narrow lumen and distinct layers of the thickened wall visible.

The following step in assessing the biliary system involves the imaging of the main biliary duct (MBD), with the common hepatic duct (CHD, region of the liver hilum) and the common bile duct (CBD, choledochal duct). With the patient in supine or lateral decubitus, a perpendicular section on the ribs in the right hypochondrium is recommended for the visualization of hepatic hilum, where MBD, portal vein and hepatic artery can be evaluated. Located in front of the portal vein, the main biliary duct resembles a tube (Fig. 5.3). Color Doppler imaging is used to verify that the bile duct is measured (no flow) and not inadvertently another vessel, such as the hepatic artery/portal vein. Sometimes, if there is a good acoustic window, the MBD can be also followed into the retro-pancreatic area.

We must evaluate the MBD regarding the size (normal up to 6 mm), wall thickness and content. The main bile duct is often measured at the hepatic hilum, from inner wall to inner wall, by the axial resolution of the ultrasound beam. It is recommended that the bile duct is imaged along its entire length and measured at multiple points, including close to the pancreatic head, as a single measurement at this level may be false because the bile duct may be normal at this point and enlarged lower down in early biliary obstruction. Size, form variations, wall thickness, and lumen contents should all be considered while evaluating the duct.

Because bile is expelled from the gallbladder to the duodenum after eating, the main biliary duct's width usually widens. Additionally, individuals with a juxta papillary duodenal diverticulum may exhibit a little dilation of the MBD. Furthermore, the duct usually enlarges by 1 mm every ten

years after cholecystectomy and after the age of 60 years. It is crucial for the operator to evaluate the origin of the distension and ascertain if it is pathological or merely a result of aging or a cholecystectomy. The left lateral decubitus posture should be used consistently for all patients in order to provide sufficient visualization of the hepatic hilum.

The intrahepatic biliary ducts are normally invisible, but as they dilate, in different pathological situations, they become visible. Alongside the portal branches, they can occasionally be seen in the left liver lobe of healthy individuals.

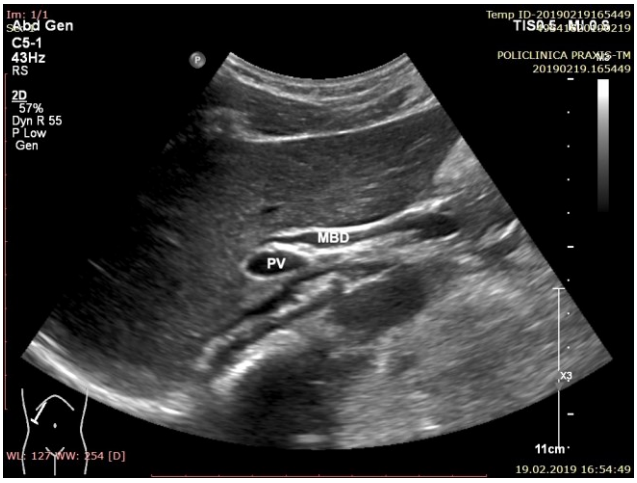

Fig. 5.3. Ultrasound view in the right subcostal position, the transducer positioned perpendicular to the ribs, displaying the hepatic hilum along with the main biliary duct (MBD) and the portal vein (PV).

Abnormalities of gallbladder or biliary system

1. *Abnormal position and variations of the gallbladder*

It is uncommon for the gallbladder to be positioned abnormally. Other sites that have been described are left-sided (with or without situs inversus), intrahepatic (<5%), suprahepatic, lesser sac or abdominal wall, and retroperitoneal. It is important to keep in mind, that the body variations of asthenic, hyposthenic or hypherstenic may lead to natural variations.

Gallbladder shape variations, such as the "Phrygian cap", are more common but rarely have any clinical significance. The distal fundus inverts into the body, forming a phryngian cap, to which it may cling. Up to 5% of sonograms have it, and it can be either an acquired anomaly or an anatomical variety.

2. *Congenital anomalies of the gallbladder and hepato-biliary system*

A micro gallbladder, which is smaller than 2 to 3 cm long and 0.5 to 1.5 cm wide, is thought to be a common sign of cystic fibrosis, but it is also linked to alpha-1-antitrypsin illness and

idiopathic newborn hepatitis. Gallbladder agenesis, or absence, is uncommon and typically has little clinical relevance. Hypoplasia, meaning incomplete development of the gallbladder can be seen and can be associated with extrahepatic biliary atresia.

A multiseptated gallbladder can be either congenital or acquired and is characterized by the presence of three or more interconnected compartments. Solitary congenital diverticula vary significantly in size, ranging from 5 mm to 10 cm. Although these anatomical variations are rarely observed during routine ultrasound examinations, they are essential considerations in differential diagnosis.

3. *Aerobilia*

The presence of gas in the biliary ducts is known as aerobilia and is not always a sign of disease, though. It is typically discovered after ERCP with endoscopic sphincterotomy, when the existence of aerobilia is evidence of the biliary ducts' or biliary stent's patency or following surgical anastomosis between the biliary ducts and the digestive tract.

Without the usual posterior shadowing caused by stones, the ultrasonography examination will reveal intraductal gas bubbles as linear hyperechoic chains of bubbles following the intrahepatic biliary channels.

In some cases, a biliary-digestive fistula resulting from a stone perforation may potentially be the reason for aerobilia. Patients with suspected aerobilia may be at risk for Bouveret's syndrome.

Pathology

Ultrasound is the primary imaging modality for assessing the gallbladder and hepatobiliary system due to its high sensitivity and specificity for detecting biliary pathology. The evaluation is warranted in various clinical circumstances, where a biliary pathology is suspected. Several clinical scenarios can be encountered more frequently. Thus:

1. The patient presents with different symptoms, such as upper abdominal discomfort, mostly in the right upper abdomen, bloating, nausea, stool changes (frequency and/or consistency), that are suggestive for a functional disorder. Ultrasound should be the first imaging investigation that will exclude a biliary pathology and suggest the next investigations needed to confirm the functional disorder diagnosis.
2. Suspected Cholelithiasis or Cholecystitis: the patient presents with

- Right upper quadrant (RUQ) pain, particularly postprandial or colicky in nature, accompanied or not by nausea, vomiting - suspicion of biliary colic.
- Right upper quadrant (RUQ) pain accompanied by fever, with positive Murphy's sign on physical examination – suspicion of acute cholecystitis.

In these situations, ultrasound should also be first line imaging investigation since it is very accurate for the diagnosis of both gallstones and acute cholecystitis.

3. Jaundice, Hyperbilirubinemia or Abnormal Liver Function Tests: the patient can present with

- Unexplained elevation in liver enzymes, particularly cholestatic patterns, with or without hyperbilirubinemia.
- Jaundice with or without pain.
- Suspected biliary obstruction due to gallstones, tumors, or strictures, investigation of dilated intrahepatic or extrahepatic bile ducts on other imaging studies.

  In these situations, ultrasound should also be the first line imaging investigation since it can diagnose biliary obstruction with high sensitivity and specificity, and can differentiate between a hepatological disorder vs. a biliary problem

4. Asymptomatic patients with or without family history of biliary pathology, where screening for biliary pathology is desired.

Thus, ultrasound should be the first-line, non-invasive modality for detecting and characterizing hepatobiliary pathology. However, in cases where ultrasound findings are inconclusive or further anatomical detail is required, additional imaging modalities such as magnetic resonance cholangiopancreatography (MRCP), endoscopic ultrasound or computed tomography (CT) may be indicated.

The following subchapters will describe the ultrasound aspects in the most frequently encountered biliary pathologies.

1. Gallbladder pathology

1.1 Biliary sludge

A range of precipitates, most frequently calcium salts or cholesterol crystals, are produced from bile and are referred to as biliary sludge. Pregnancy, complete parenteral feeding, extrahepatic bile duct stenosis, patients in intensive care units (25–47%), fasting, rapid weight loss, post-solid organ transplantation, and situations have all been linked to it.

Sludge is usually an incidental ultrasonography finding that is asymptomatic in the majority of patients. Patients may occasionally arrive with nausea, vomiting, and discomfort. Gallstones can occasionally be preceded by sludge. With no distal acoustic shadowing, the ultrasound image shows uniform echogenic material in the gallbladder lumen.

Because of its bulk and gravity, the sludge usually collects on the gallbladder's "inferior" wall, forming a straight horizontal line; the "black" anechoic bile without sludge sits above (Fig. 5.4).

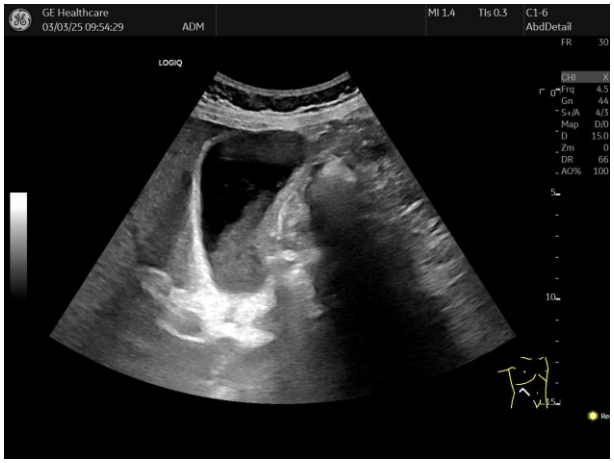

Fig. 5.4. Abdominal ultrasound image displaying a longitudinal section of the gallbladder. The image demonstrates echogenic material without posterior acoustic shadowing in the gallbladder indicative of sludge.

It is advised to move the patient during the scan to illustrate how the sludge travels slowly in response to changes in patient posture. It might be challenging to differentiate the gallbladder from the nearby liver parenchyma if the sludge covers it entirely. The sludge is sometimes referred to as “ball like” or “tumor like” sludge because it is hypoechoic, round-shaped, and lacks acoustic shadowing (Fig. 5.5). To distinguish between gallbladder neoplasia and localized, "tumor-like" sludge, performing contrast-enhanced ultrasound is a useful investigation.

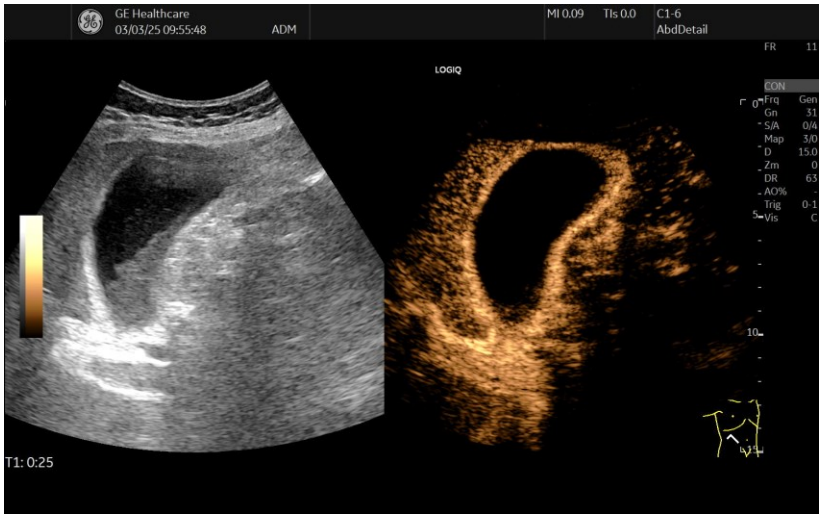

Fig. 5.5. This image presents a dual-panel ultrasound examination of the gallbladder, with a conventional B-mode image on the left and a contrast-enhanced ultrasound (CEUS) image on the right. The uniform enhancement of the gallbladder wall suggests an intact vascular supply. Additionally, the anechoic lumen of the gallbladder remains non-enhancing, confirming the presence of bile and sludge.

1.2 Gallbladder stones

The presence of stones in the biliary tract is commonly referred to as cholelithiasis. The difference between cholecystolithiasis (stones in the gallbladder) and choledocholithiasis (stones in the bile duct) can be observed based on the location of the concrement. When evaluating, 5–15% of people will have both diseases.

The most frequent biliary system condition is **cholecystolithiasis**. Age, female gender, obesity, ethnicity, family history, and genetic susceptibility, pregnancy and hormones are among the several risk factors for gallbladder stones and reports show that it occurs in more than 30% of females over 70 years old. 70 % of gallbladder stones will be asymptomatic, while only 5% of the symptomatic will develop complications. Gallstones are predicted to become more common in the future due to the rising rates of adult and pediatric obesity, which will put more financial strain on the delivery of healthcare.

Typically, gallbladder stones appear on ultrasound as hyperechoic structures within the gallbladder lumen, accompanied by distal acoustic shadowing (Fig 5.6, 5.7, 5.8, 5.9, 5.10). A comprehensive analysis and documentation of gallbladder stones should include if they are single or multiple, dimensions, echo texture, presence of acoustic shadowing, and mobility. Both the number and size of gallbladder stones have clinical significance. Multiple tiny stones in women were linked to a greater prevalence of complications, primarily choledocholithiasis and biliary pancreatitis, than single bigger stones in males, which were mostly linked to acute cholecystitis. On the other hand, patients with a long history of big gallbladder stones (> 30 mm) have a higher risk of developing gallbladder cancer.

To more clearly observe acoustic shadows and small stones, insonate the gallbladder's "inferior" wall at a 90-degree angle and use different patient positions. The "rolling stones sign" develops when a patient shifts positions, causing tiny stones to move with the gallbladder which makes it easier to differentiate it from gallbladder polyps.

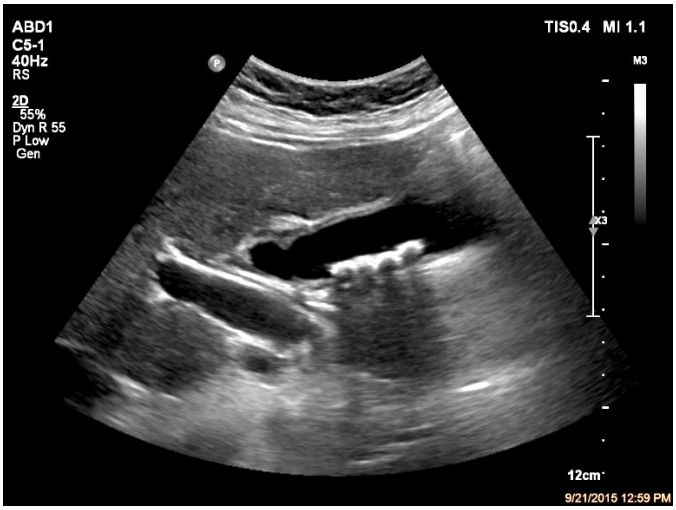

Fig. 5.6. The ultrasound image shows small and multiple gallbladder stones, hyperechoic (bright), posterior acoustic shadowing.

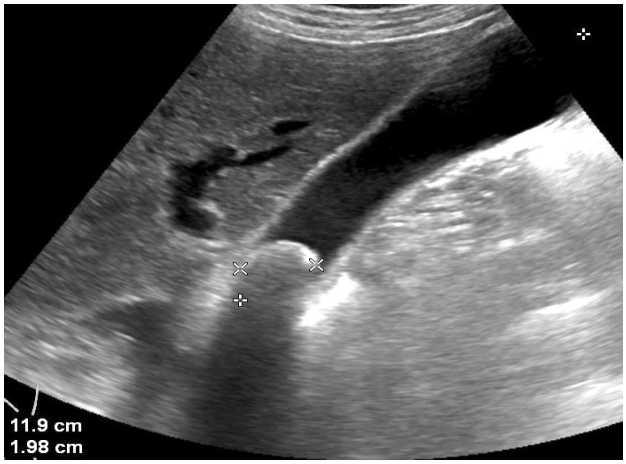

Fig. 5.7. The ultrasound image shows a gallbladder stone, hyperechoic (bright), posterior acoustic shadowing, situated in the infundibulum of the gallbladder. The measured stone size is approximately 2 cm.

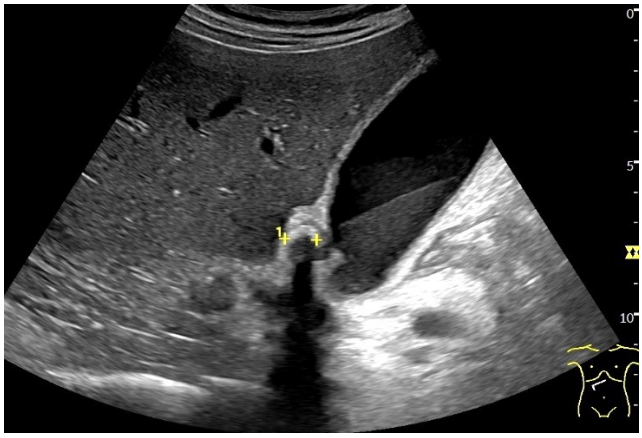

Fig. 5.8 The ultrasound image shows a gallbladder stone, hyperechoic (bright), posterior acoustic shadowing, situated in the infundibulum of the gallbladder, and also sludge (echoic material with no posterior shadow, and horizontal level).

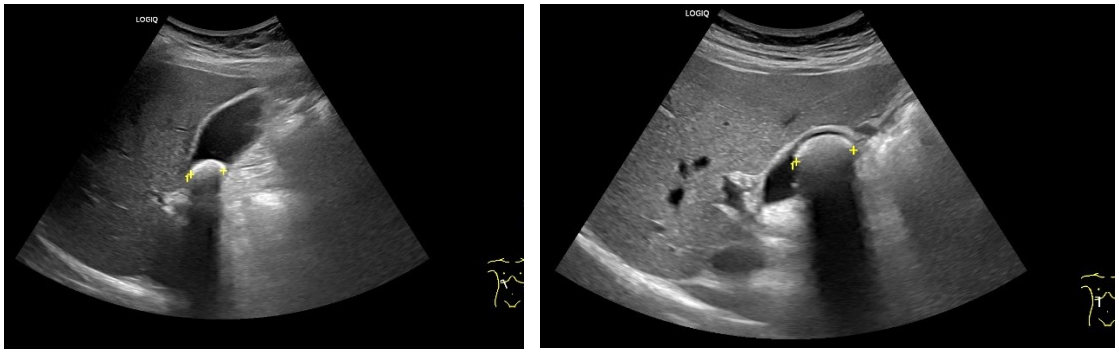

Fig. 5.9, 5.10. The ultrasound images show large gallbladder stones, hyperechoic (bright), with posterior acoustic shadowing.

Mobile calculi generally settle on the "inferior" wall of the gallbladder due to gravity; however, this is influenced by the density of bile and the composition of the stones. To enhance the visibility of acoustic shadowing and detect small stones, it is crucial to utilize different patient positions. Many very small stones may produce a "sum shadow" (Fig. 5.11). A gallbladder filled with stones (“shell sign”) can be easily confused with gas from the gastrointestinal tract (Fig. 5.12).

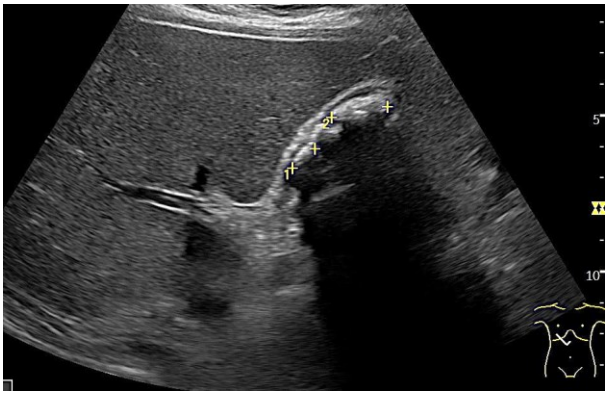

Fig. 5.11. The ultrasound view of multiple gallbladder stones, hyperechoic images with posterior acoustic shadowing "sum shadow".

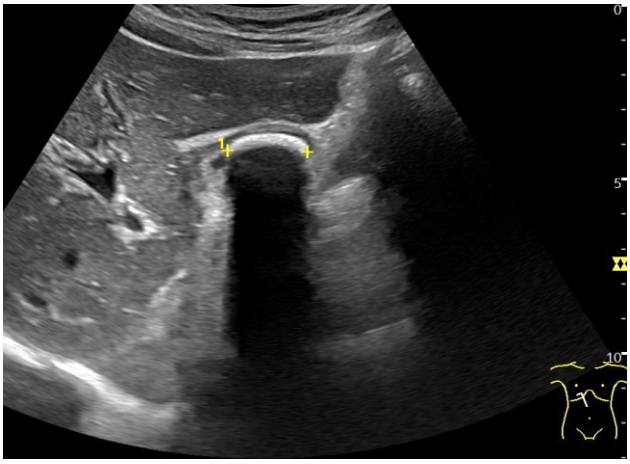

Fig. 5.12. “Shell sign” of the gallbladder showing highly echogenic (bright) area with posterior acoustic shadowing

1.3 Complications of cholecystolithiasis

Acute cholecystitis

The most frequent complication of cholecystolithiasis is acute cholecystitis, almost a third of individuals developing this complication and is a common cause of emergency hospitalization. Gallstone-associated (acute calculous cholecystitis), 95% of the cases, and non-gallstone-associated (acute acalculous cholecystitis) are the two categories of acute cholecystitis. Rare and potentially life-threatening, acute acalculous cholecystitis is typically associated with individuals who are severely impaired as a result of infections, burns, trauma, shock, etc.

In acute cholecystitis ultrasound shows a dilated gallbladder with a thicker multi-layered wall and possibly inflammatory fluid near the gallbladder wall, “eye-brow” appearance (Fig. 5.13). The presence of gallstones on ultrasound combined with pain when pressure is applied using the

transducer - called positive ultrasound Murphy's sign, has a positive predictive value of more than 90% for the diagnosis of acute cholecystitis.

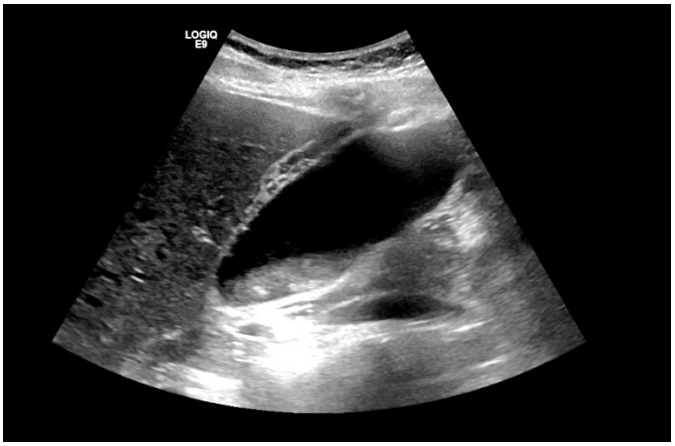

Fig. 5.13. Enlarged gallbladder with a thicker multi-layered wall, with sludge and small stones in the inferior part and also an enlarged wall with oedema inside

To be noticed that gallbladder wall thickening (>3–4 mm) is commonly found, in other conditions like liver cirrhosis, hypoalbuminemia, and acute hepatitis. In these circumstances, the lack of sludge or stones, a small non-dilated gallbladder, and the absence of positive Murphy's sign are characteristic ultrasonographic indicators.

15% of acute cholecystitis with mural infarction can develop gangrenous cholecystitis, and over 25% have perforation. Gas can be easily seen in the gallbladder lumen and for the assessment of the wall's integrity and identifying perforations and necrotic regions, contrast enhanced ultrasound is helpful.

To be noted that in the suspicion of acute cholecystitis, ultrasound should be the first imaging technique used for the diagnosis due to its high accuracy.

Bouveret's syndrome

Gastric outlet blockage due to duodenal impaction of a big gallstone that enters the duodenal bulb through a cholecystoduodenal or cholecystogastric fistula is the syndrome's definition. This is a rare complication of cholecystolithiasis. Although duodenal stones may be difficult to identify by ultrasound imaging, the presence of gas in the biliary system (aerobilia) should warn the examiner, particularly if there is impaired stomach emptying.

Mirizzi syndrome

Common biliary duct obstruction caused by extrinsic compression from an impacted stone in the gallbladder's cystic duct or infundibulum is known as Mirizzi syndrome. Jaundice and pain

in the right upper quadrant are some of the symptoms that patients with Mirizzi syndrome may exhibit. Ultrasound will reveal a large gallbladder, usually with a large stone in the infundibulum, associated with a high level of biliary obstruction.

1.4 Gallbladder polyps

Gallbladder polyps are benign tumors that are discovered by accident on ultrasonography and are entirely asymptomatic. Classification of gallbladder polyps consists of pseudopolyps: cholesterol polyps and inflammatory polyps and true polyps: adenoma. The most common polyps found are *cholesterol polyps or adenomas*.

The adenoma of the gallbladder has an ultrasound aspect of echoic structure fixed to the wall, has the same echogenicity as the wall, is immobile, and does not have posterior shadowing (Fig. 5.14a, 5.14b, 5.15). To distinguish it from gallbladder stone, CEUS is helpful in demonstrating vascularity. Adenomas are considered premalignant. Risk factors for malignancy are size ≥ 10 mm, sessile and solitary polyp, simultaneous gallbladder stones, age > 50 years, and quick size growth. Lesions larger than 6–10 mm need serial follow-up at least once a year. Due to the possibility of malignant transformation, gallbladder polyps bigger than 10 mm or those increasing on repeated scans should be surgically removed.

Cholesterol polyps appear on ultrasound as small, hyperechoic lesions that are attached to the gallbladder wall and extend into the lumen. They also have a particular posterior artefact that resembles a "comet tail".

Cholesterolosis is a benign condition characterized by the accumulation of cholesterol esters and triglycerides in the mucosa of the gallbladder wall. It is either diffuse or polypoid. The term cholesterolosis refers to the diffuse type. Cholesterol polyps are the polypoid form of cholesterolosis.

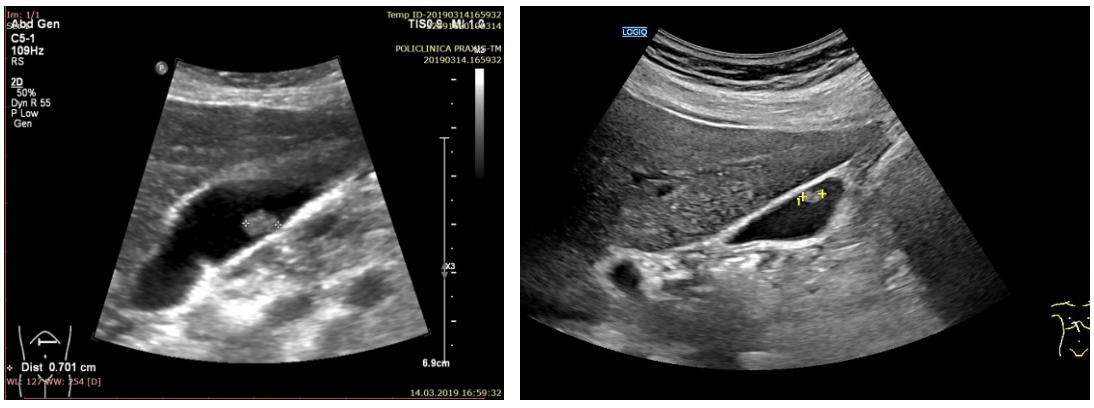

Fig. 5.14 a, b. Ultrasound evaluation of the gallbladder showing a benign adenoma of approximately 7 mm

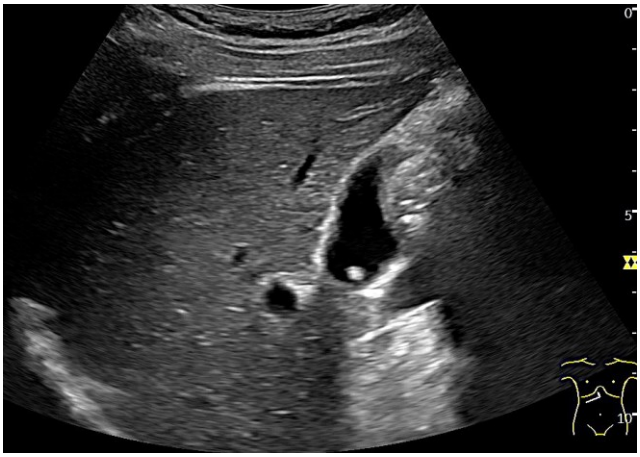

Fig. 5.15 Ultrasound evaluation of the gallbladder showing an adenomatous polyp, small, homogeneous and echogenic with smooth borders

1.5 Adenomyomatosis

Adenomyomatosis is an abnormality of the gallbladder characterized by overgrowth of the mucosa, thickening of the muscle wall and epithelial infolding within the underlying muscular layer - intramural diverticula, called Rokitansky-Aschoff sinuses. It can be segmental, localized or diffuse.

Adenomyomatosis in ultrasonography appears as hypoechoic areas, typically accompanied by hyperechoic cholesterol crystals or calcifications, which provide a reverberation effect resulting in comet-tail distortions. Usually, CEUS or CT, MRI with contrast substance is required, because it can be difficult to distinguish between gallbladder carcinoma and adenomyomatosis.

1.6 Gallbladder carcinoma

Gallbladder carcinoma is a rare tumor that is more often found in people over the age of 65 years, it is nearly always linked to cholecystolithiasis and typically associated with bigger stones (>3 cm). Early detection of the illness is unfortunately uncommon due to the lack of symptoms in early stages. Even if carcinomas of the gallbladder can be easily recognized using standard abdominal ultrasound, the correct staging requires complimentary imaging such as CT or MRI.

Gallbladder tumors can be described in 3 types by means of ultrasound:

1. Focal – disorganized, thick wall or a poorly defined extending mass in the gallbladder lumen
2. Diffuse – asymmetrical thickening of the gallbladder wall
3. Complete replacement of gallbladder lumen with tumor - a solid, often hypoechoic mass has replaced the gallbladder lumen and now occupies the gallbladder entirely, usually with a solitary trapped stone inside the tumor tissue (Fig. 5.16)

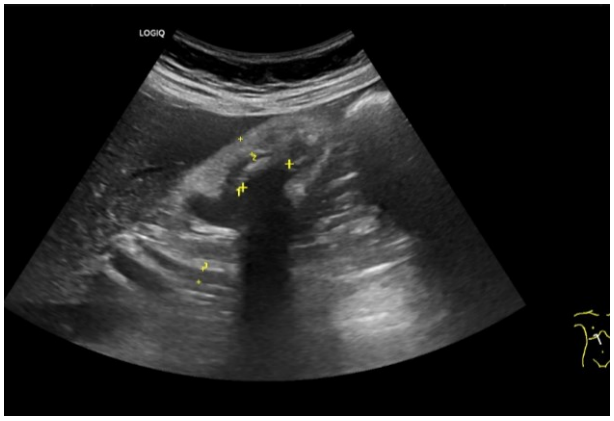

Fig. 5.16. Ultrasound aspect of diffuse gallbladder carcinoma and gallbladder stones

2. Biliary obstruction

As mentioned above, ultrasound is the primary imaging method when evaluating a patient with clinical aspects of jaundice, or abnormal liver test, for the differentiation between intrahepatic and extrahepatic cholestasis. If intrahepatic cholestasis is excluded, extrahepatic cholestasis is mainly due to biliary obstruction given by gallstones, tumors, or strictures.

As an algorithm of evaluating the patients with jaundice, we need to have three questions in mind: Is it due to biliary obstruction? If Yes, Which is the level of obstruction and Which is the cause?

Biliary obstruction is diagnosed in ultrasonography by detecting the dilated intrahepatic biliary ducts (when normal not seen on ultrasonography) that accompany the portal branches. The so-called "shotgun" sign is caused by the dilated intrahepatic bile ducts, which give the liver a "spider" look in the center and a characteristic "double duct" on the perimeter. Furthermore, the gallbladder can be modified according to the level of obstruction, it may appear normal, small, or enlarged (Fig. 5.17, 5.18).

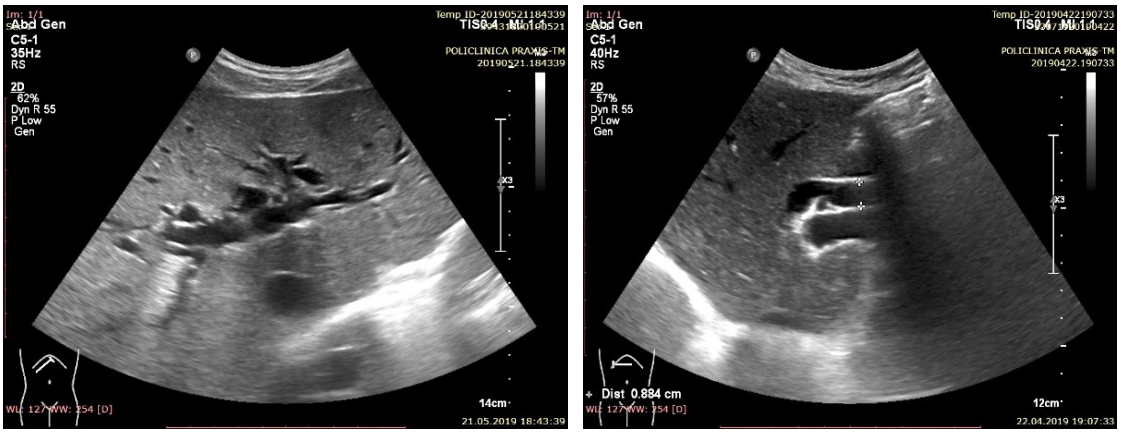

Fig. 5.17. Ultrasound aspect of biliary obstruction: The "spider" aspect in the center of the liver (left), and Fig. 5.18. Enlarged main biliary duct (right)

Regarding obstruction level, we can have 3 types of obstruction with different signs in ultrasound for each of it:

- *intrahepatic level* – characterized by
    - Segmental or one-sided dilatation of intrahepatic bile ducts
    - Normal diameter of the extrahepatic bile duct
    - Normal in size gallbladder
- *Hilar level* – characterized by
    - Bilateral or unilateral dilatation of intrahepatic bile ducts
    - Normal diameter of extrahepatic bile duct
    - Small or normal in size gallbladder
- *Subhilar level* – characterized by
    - Bilateral dilatation of intrahepatic bile ducts
    - Normal diameter of CBD
    - Small or normal in size gallbladder
- *Distal level* (CBD, papilla) – characterized by
    - Bilateral dilatation of intrahepatic bile ducts
    - Dilatation of the MBD
    - Distended gallbladder (Curvoisier's sign)

Depending on the level of the obstruction, several diagnoses may be suspected. Thus, facing an intrahepatic cause of obstruction the most frequent causes that need to be differentiated are central cholangiocarcinoma or Klatskin tumor, hepatocellular carcinoma, or liver metastases, while in an extrahepatic cause of obstruction choledocholithiasis, tumor of the head of the pancreas, chronic pancreatitis, ampuloma, compression of the main biliary duct are the most frequent causes encountered.

Ultrasound is a very sensitive method to detect the presence of the biliary obstruction and also establish the level of the obstruction. It is also a good method for diagnosing the cause of obstruction, for example detecting a hypoechoic mass in the liver hilum in case of a hepatocellular carcinoma, or a bull's eye in liver metastasis, or a hypoechoic mass in the head of the pancreas, or calcifications in the pancreatic parenchyma in chronic pancreatitis. If there is an obstruction of the main biliary duct that stops abruptly in or just below the hepatic hilum, without identifying a mass or a calculus, a cholangiocarcinoma may be present. However, ultrasound is less sensitive in assessing the etiology of the obstruction compared to detection of biliary obstruction and level of the obstruction. It is still the first imaging method recommended for assessing these patients.

Choledocholithiasis

Choledocholithiasis is the most frequent cause of biliary obstruction. It is usually suspected in patients that present the typical biliary pain usually accompanied by elevated liver enzymes (cytolysis and cholestasis). Transabdominal ultrasound is less sensitive in detecting choledocholithiasis as compared to gallbladder stones due to the difficulties in assessing the distal part of the main biliary duct, which is challenging due to the gas-filled duodenum nearby. The examiner's skill and experience are therefore important as well as the ability to see by ultrasound the periampullary area of the main biliary duct.

On ultrasound, whenever visible, choledocholithiasis will have the same aspect as the stones in the gallbladder, hyperechoic images with posterior shadowing but located in the main biliary duct (Fig. 5.19, 5.20, 5.21). The stones may lack posterior shadowing, especially when they are small, which makes the diagnosis more challenging. Endoscopic ultrasound and MRCP have higher sensitivity for this diagnosis and should follow ultrasound when the diagnosis is suspected and not confirmed by transabdominal ultrasound.

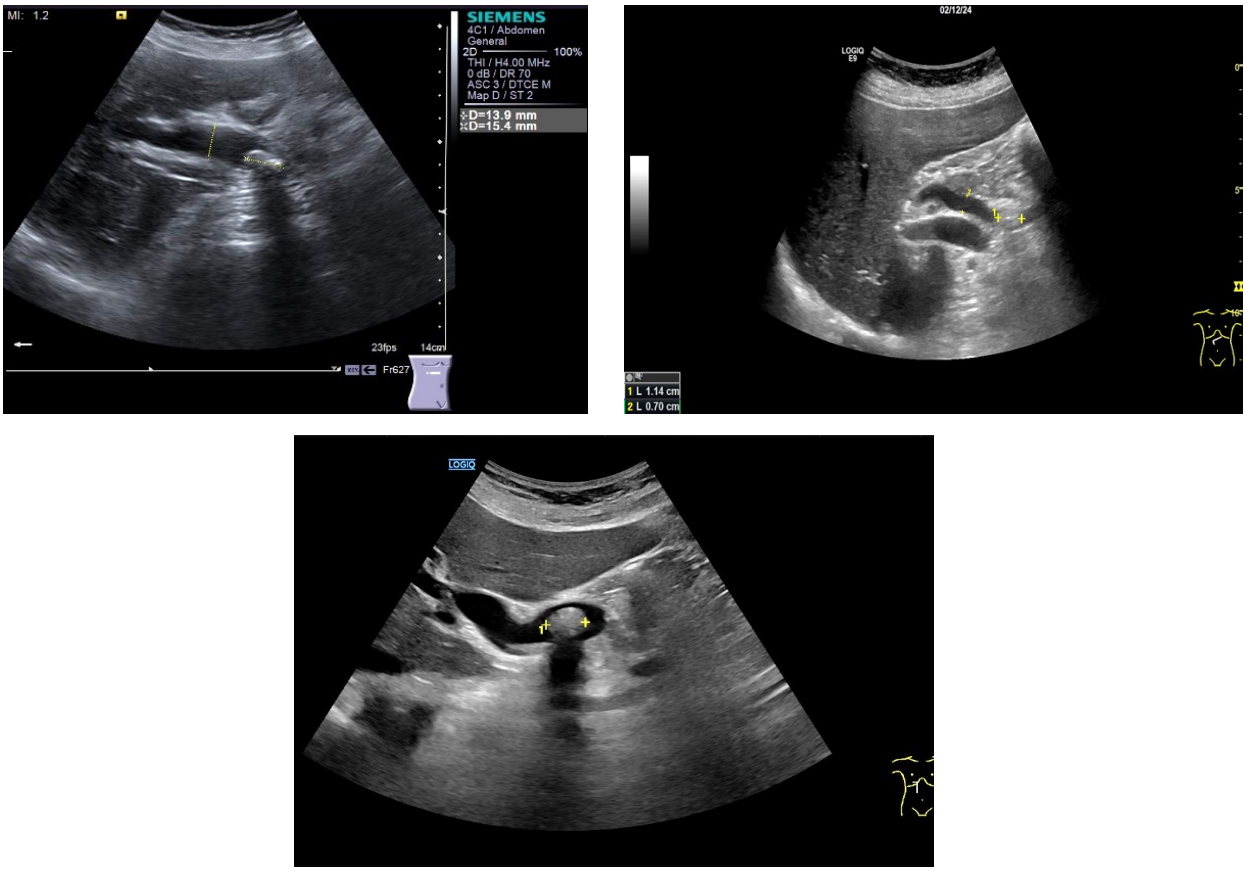

Fig. 5.19, 5.20, 5.21. Ultrasound aspect of dilated main biliary duct with the presence of hyperechoic images with posterior shadowing located inside

Intrahepatic lithiasis may also occur, in rarer cases, with the same ultrasound characteristics, causing an intrahepatic biliary obstruction.

In conclusion, whenever biliary pathology is suspected ultrasound should be the first imaging investigation due to its high sensitivity and specificity for the most frequent diagnosis related to the biliary system.

Selective references

1. Barreiros AP, Popescu A, Walton J, Dietrich CF. Ultrasound of the biliary system. In: EFSUMB course book on ultrasound. Dietrich CF (Ed). 2012.
2. Popescu A, Sporea I. Ultrasound examination of normal gallbladder and biliary system. Medical ultrasonography 2010, 12(2), 150-2 .
3. Nuernberg D, Ignee A, Dietrich CF. (Ultrasound in gastroenterology. Biliopancreatic system). Med Klin (Munich) 2007; 102(2):112-126
4. Sporea I, Cijevschi Prelipcean C. The gallbladder in: Abdominal ultrasound in clinical practice. Victor Babeş Publishing 2017, 70-91
5. Badea R, Zaro R, Opincariu I, Chiorean L. Ultrasound in the examination of the gallbladder - a holistic approach: grey scale, Doppler, CEUS, elastography, and 3D. Med Ultrason. 2014 Dec;16(4):345-55.
6. Cooperberg PL, Burhenne HJ. Real-time ultrasonography. Diagnostic technique of choice in calculous gallbladder disease. N Engl J Med 1980; 302(23):1277-1279.
7. Freitas ML, Bell RL, Duffy AJ. Choledocholithiasis: evolving standards for diagnosis and management. World J Gastroenterol 2006; 12(20):3162-3167
8. Jenssen C, Lorentzen T, Dietrich CF, Lee JY, Chaubal N, Choi BI, Rosenberg J, Gutt C, Nolsøe CP. Incidental Findings of Gallbladder and Bile Ducts-Management Strategies: General Aspects, Gallbladder Polyps and Gallbladder Wall Thickening-A World Federation of Ultrasound in Medicine and Biology (WFUMB) Position Paper. Ultrasound Med Biol. 2022 Dec;48(12):2355-2378.
9. Okaniwa S. Advanced ultrasound diagnosis of extrahepatic bile duct lesions. J Med Ultrason (2001). 2025 Jan;52(1):69-83.
10. Yu MH, Kim YJ, Park HS, Jung SI. Benign gallbladder diseases: Imaging techniques and tips for differentiating with malignant gallbladder diseases. World J Gastroenterol. 2020 Jun 14;26(22):2967-2986.

6. HOW CAN I USE US IN PANCREATIC PATHOLOGY?

Bogdan Miuțescu, Adrian Săftoiu

WFUMB Center of Education Timișoara, Romania, Bucharest, Romania

6.1 Introduction

Pancreatic ultrasound, a fundamental aspect of ultrasonographic imaging, can be particularly challenging for those new to the technique. However, with the transformative experience gained from countless examinations, the ability to identify pancreatic structures and elusive lesions becomes a rewarding journey. Mastering pancreatic ultrasound requires time and practice, but with persistence, assessing the pancreas will no longer be a troublesome component of ultrasonography.

Pancreatic ultrasound examination is crucial in identifying abnormalities and providing objective evidence that complements subjective impressions. Using typical reference values to identify deviations makes these measurements useful in various clinical contexts. Upper abdominal discomfort, hyperlipidemia, new-onset diabetes mellitus or exacerbation, acute or chronic pancreatitis, exocrine pancreatic in_adequacy, obstructive jaundice, and potential tumors routinely indicate ultrasound evaluation of the pancreas. These measurements are instrumental in assessing the pancreas's focal or diffuse swelling and can be a reference for follow-up examinations.

Pancreatic tumor assessment requires a comprehensive approach involving multiple imaging modalities, including ultrasound, contrast-enhanced ultrasound (CEUS), endoscopic ultrasound (EUS), computed tomography (CT), and magnetic resonance imaging (MRI). Each modality offers unique advantages, with ultrasound as the first-line approach due to its accessibility. CEUS provides additional benefits by enhancing lesion characterization and improving diagnostic accuracy. For solid pancreatic lesions, ultrasound findings often require confirmation with CT. If CT is inconclusive, MRI or EUS with fine-needle aspiration (FNA) is recommended. EUS, with its superior sensitivity for small malignancies, is crucial for confirming malignancy, especially before neoadjuvant chemoradiotherapy, providing a secure foundation for further treatment decisions.

Ultrasound remains a widely used imaging modality for pancreatic evaluation due to its non-invasive nature, real-time imaging capabilities, and accessibility. It serves as a first-line diagnostic tool, particularly in patients with abdominal symptoms, allowing dynamic assessment of pancreatic structures and vascularization. Introducing CEUS has significantly improved lesion characterization, distinguishing between solid and cystic formations and enhancing diagnostic accuracy. Moreover, ultrasound's avoidance of ionizing radiation makes it safer for repeated evaluations than CT. EUS offers even greater detail and enables guided FNA or biopsy (FNB) for cytological and histological confirmation, playing a crucial role in diagnosing pancreatic

malignancies. Furthermore, ultrasound's cost-effectiveness compared to MRI and CT makes it a practical choice in many clinical settings.

However, ultrasound also has several limitations. Its effectiveness is highly operator-dependent, meaning that image quality relies on the skill and experience of the examiner. Certain patient factors, such as obesity and bowel gas, can significantly interfere with pancreatic visualization. Moreover, ultrasound is less sensitive to detecting small pancreatic tumors, particularly those under 2 cm, than CT and MRI. Limited penetration depth reduces its ability to evaluate deeper structures, especially lesions in the pancreatic tail. Additionally, ultrasound provides valuable initial findings but cannot replace histological confirmation, often requiring complementary imaging techniques for a definitive diagnosis.

6.2 Examination technique

For accurate ultrasound measurements, selecting the appropriate transducer type, frequency, and proper patient positioning is crucial. Ideally, the examination should be performed on an empty stomach, as gastric contents may create artifacts that interfere with pancreatic visualization. However, one of the benefits of ultrasound is its ability to be conducted at any time, especially in urgent situations. For optimal imaging, a fasting period of 4 to 6 hours is recommended, though fasting may extend up to 8 hours in research settings. Additionally, drinking 500–700 ml of water 10–15 minutes before the procedure may enhance image quality.

The standard patient position for ultrasound measurements is supine. However, adjusting the patient's position is often necessary to better visualize the pancreas. A left lateral oblique position (15–30°) can improve imaging of the pancreatic head, while a right lateral oblique position may be more suitable for assessing the tail. Other advantageous positions include right or left decubitus and seated or standing postures.

A 2–7 MHz multifrequency curvilinear probe is typically used for abdominal ultrasound. The initial transducer placement should be in the epigastric region, just below the sternum, with subcostal and subxiphoid approaches providing views of the pancreatic head, body, and part of the tail. An intercostal approach, positioning the probe between the 10th and 11th intercostal spaces, is recommended for imaging the lateral portion of the pancreatic tail.

6.3 Normal Pancreatic Ultrasound Examination and Dimensions

6.3.1 Normal Pancreatic Ultrasound

To identify the pancreas, we first locate key landmarks: posteriorly, the porto-splenic axis, and anteriorly, the gastric antrum or the left liver lobe. The pancreas is a parenchymal structure between these elements (Fig. 6.1). The splenic vein runs along its dorsal border, extending from the splenic hilum to its confluence with the superior mesenteric vein at the pancreatic neck. The

pancreatic head and uncinate process encircle the venous confluence, forming the portal vein with anterior and posterior pancreatic tissue.

The superior mesenteric vessels serve as markers distinguishing the head from the body. The pancreatic head is positioned within the duodenal curve, while the tail extends toward the splenic hilum. The celiac trunk, emerging from the aorta at the gland's superior border, is another key landmark.

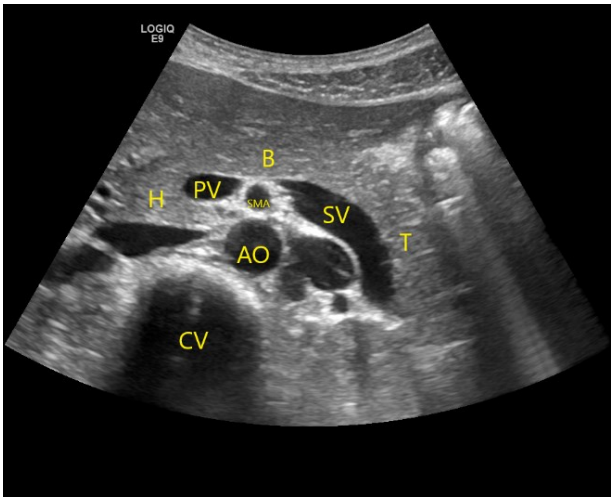

Fig. 6.1. The normal aspect of the pancreas: PV - portal vein; SV - splenic vein;
AO - Aorta; H - head of the pancreas; B - the body of the pancreas; T-tail of the pancreas;
CV - vertebra; SMA - superior mesenteric artery.

A transverse scan provides a broad view of the pancreas, but due to its slightly upward trajectory, the entire gland is rarely visible in one section. This approach is particularly useful for the pancreatic body and tail, while sagittal sections are preferred for the head. The tail, especially if elongated or bulbous, requires a thorough assessment to avoid missing distal tumors.

Evaluation of the pancreatic head concludes with assessing the main biliary duct (MBD). Right oblique sections help visualize the MBD at the hepatic hilum and within the pancreas. For better imaging, the patient may need to be positioned in left lateral decubitus

6.3.2 Pancreatic dimensions

The pancreas is measured in transverse and longitudinal sections, with the head assessed at its largest dimensions, the body at the level of the superior mesenteric artery, and the tail using an intercostal approach. Pancreatic size correlated with body height, weight, and BMI, while age significantly influenced the head and body size. Although patients with chronic pancreatitis

exhibited slightly larger pancreatic measurements, values remained within normal percentiles, making size differentiation clinically uncertain.

Pancreatic dimensions vary with aging, inflammation, and disease. Chronic conditions such as pancreatitis and diabetes impact size differently; type 2 diabetes correlates with increased pancreatic size, while type 1 diabetes and prolonged disease duration are associated with pancreatic atrophy. Inflammatory diseases, neoplasms, and cystic fibrosis can also alter pancreatic size. Most studies indicate that pancreatic size is more significant in men and decreases with age, although no significant sex-related difference was observed in diabetics.

Reference values for pancreatic dimensions include a craniocaudal head diameter of 49 ± 10 mm, a right-left diameter of 34 ± 8 mm, and an anteroposterior diameter of 23 ± 5 mm. The body measures 10–20 mm, while the tail ranges from 20–35 mm. At least two dimensions of the pancreatic head should be documented, with all three preferred for better diagnostic accuracy. However, the clinical relevance of absolute size measurements remains uncertain.

6.3.3 Pancreatic duct

The pancreatic duct should be measured in all mobile patients, with additional assessments in different positions. The maximum diameter, measured from the inner to the inner layer of the pancreatic body, should be under 2 mm, though values in the neck region may be slightly larger. Age-related dilation has been documented, with about 50% of healthy individuals showing increased duct size when moving from a supine to an upright position and during inspiration and secretin stimulation. However, pharmaceutical secretin is no longer available for clinical use.

Reference values suggest a pancreatic body duct diameter of <2 mm, increasing to 2.5 mm in those over 50 years. The head and neck regions may have upper limits of 3 mm. If the pancreatic duct is not visualized, this should be documented. A consensus review reinforced the 3–2–1 mm head, body, and tail standard. While slight duct dilation can be age-related, a diameter exceeding 2 mm in the body may indicate an underlying pathology such as pancreatic ductal adenocarcinoma. In elderly, palliative, or non-mobile patients, clinical priorities may shift toward complications of pancreatitis and other conditions rather than precise duct measurements. Position changes influence measurements, with the duct appearing wider in an upright posture than in a supine.

6.4 Ultrasound of Common Benign Pancreatic Lesions

6.4.1 Acute Pancreatitis

Transabdominal ultrasound is often the first imaging method for acute abdomen due to its accessibility. However, in acute pancreatitis, its effectiveness may be limited by abdominal pain, which hinders probe compression, and by overlying gas from paralytic ileus, leading to incomplete visualization of the pancreas in the early stages. Despite this, ultrasound plays a key role in ruling out other causes of acute abdominal pain and detecting indirect signs of pancreatitis, such as

effusions in typical locations. CT remains essential for initial assessment, while ultrasound monitors complications and guides interventions.

Ultrasound findings may be expected in interstitial edematous acute pancreatitis. However, edema often enlarges the pancreas, with reduced echogenicity. Typically, its echogenicity is lower than the liver's, and the parenchyma may appear heterogeneous.

In acute necrotizing pancreatitis, portions of the pancreas may be destroyed and liquefied, appearing as hypo-anechoic areas on ultrasound. Conventional B-mode ultrasound's limitation is its inability to detect non-liquefied parenchymal necrosis, as it does not assess vascularity.

Acute peri-pancreatic fluid collections appear anechoic (Fig. 6.2). In contrast, acute necrotic collections are more heterogeneous due to echogenic debris within the fluid. These collections typically form around the pancreas. They can extend into the lesser sac, anterior para-renal space, and peri-colic region.

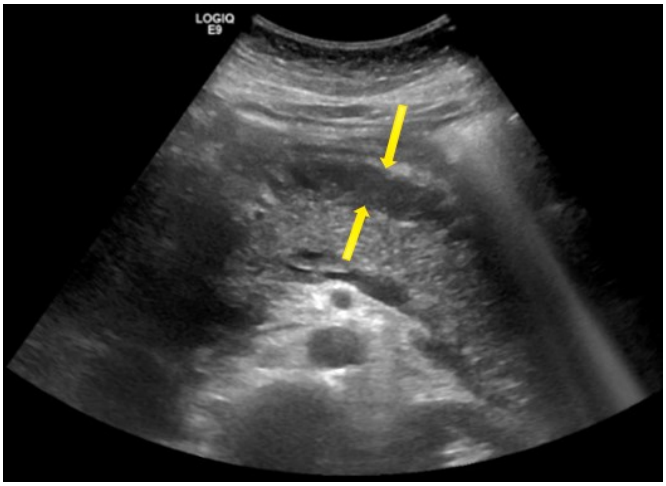

Fig. 6.2 Acute pancreatitis: pancreatic parenchyma is heterogeneous with focal hypoechoic areas and a small effusion within the lesser sac (arrows)

Transabdominal ultrasound is essential for detecting gallstones as a potential cause of acute pancreatitis and assessing complications such as intestinal paralysis, pancreatic ascites, necrotic collections, and splanchnic vein thrombosis.

Inflammation in acute pancreatitis softens the pancreatic parenchyma, which can be evaluated using strain or shear wave elastography, including **acoustic radiation force impulse (**ARFI). Necrotic areas appear as soft regions with distinct color patterns.

CEUS highlights hyperemic pancreatic segments in interstitial edematous pancreatitis, while fluid collections (Fig. 6.3) and necrotic areas appear avascular, improving their identification. Pseudocysts appear well-defined, anechoic lesions with distal acoustic enhancement, typically

round or oval. Walled-off necrosis, in contrast, consists of fluid collections containing echogenic debris. Both exhibit an enhancing wall on CEUS, with avascular fluid and debris inside (Fig. 6.4).

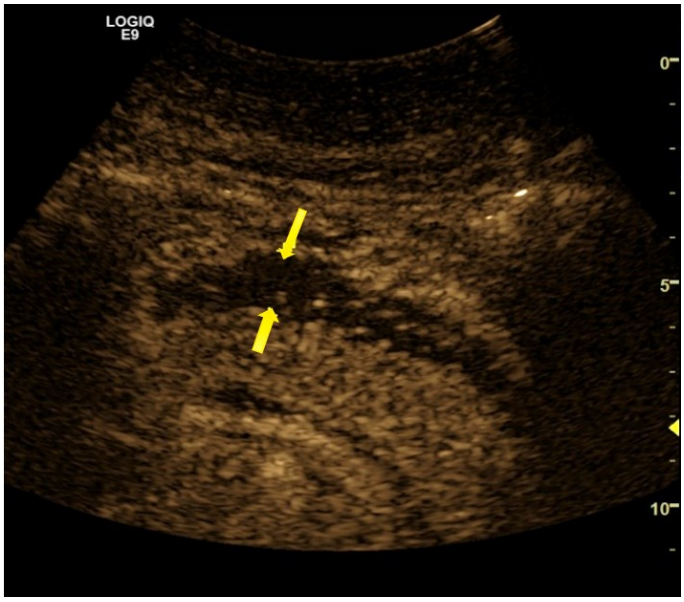

Fig. 6.3. Acute pancreatitis: Avascular fluid collections in CEUS (arrows)

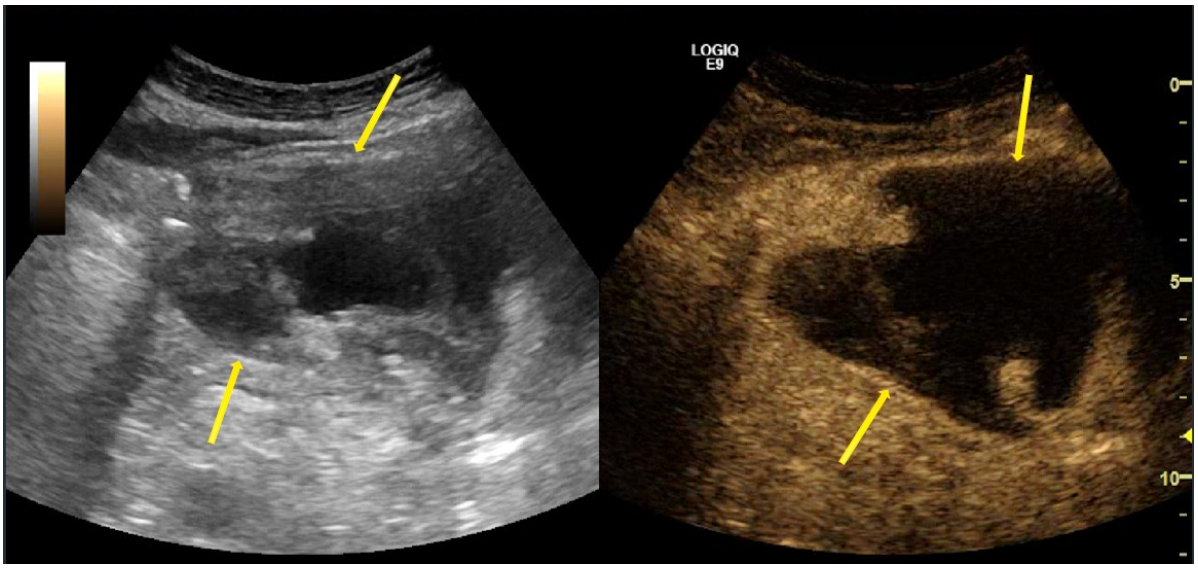

Fig. 6.4. Acute pancreatitis: Pseudocysts in B-mode and CEUS (arrows)

6.4.2 Chronic Pancreatitis

The diagnosis of chronic pancreatitis is based on clinical symptoms, laboratory tests, and imaging findings. While early changes are challenging to detect, advanced disease is more evident,

with pancreatic atrophy and focal size reduction being key indicators. Due to chronic inflammation, the glandular contours become irregular and sometimes nodular, decreasing gland volume.

Pancreatic echogenicity is often increased due to fat infiltration and fibrosis, but this is not a specific marker, especially in elderly or obese patients. A more relevant sign is the alteration of the parenchymal echo pattern, which appears heterogeneous and coarse due to the mix of hyperechoic and hypoechoic areas, fibrosis, and inflammation. These features are present in 50–70% of cases, while in early disease, the echo pattern may still appear normal.

High-frequency ultrasound can detect acceptable glandular texture changes (honeycombing) in the early stages. The most specific diagnostic marker is pancreatic calcifications (Fig. 6.5), which appear hyperechoic spots with posterior shadowing. Small calcifications may be challenging to detect, but Doppler twinkling artifacts and high-resolution ultrasound can improve visualization.

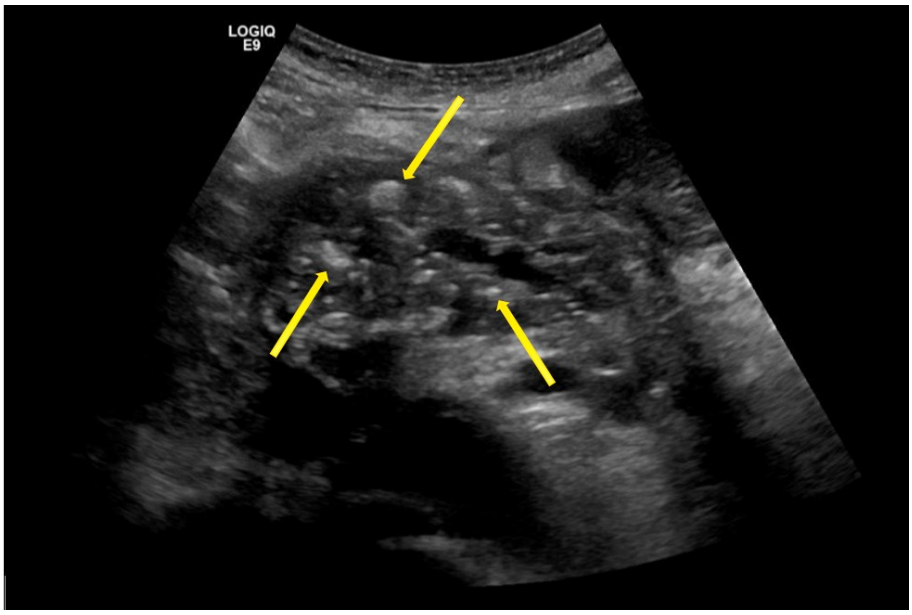

Fig. 6.5. Chronic pancreatitis: Calcifications as bright spots (arrows)

Chronic pancreatitis is also associated with pancreatic duct dilation (Fig. 6.6), a diameter exceeding 3 mm, with a sensitivity of approximately 60–70% and a specificity of about 80–90%. The moderate sensitivity is due to the infrequent ductal dilation in early or mild cases of chronic pancreatitis. In the initial stages, the main pancreatic duct may still appear within normal limits.

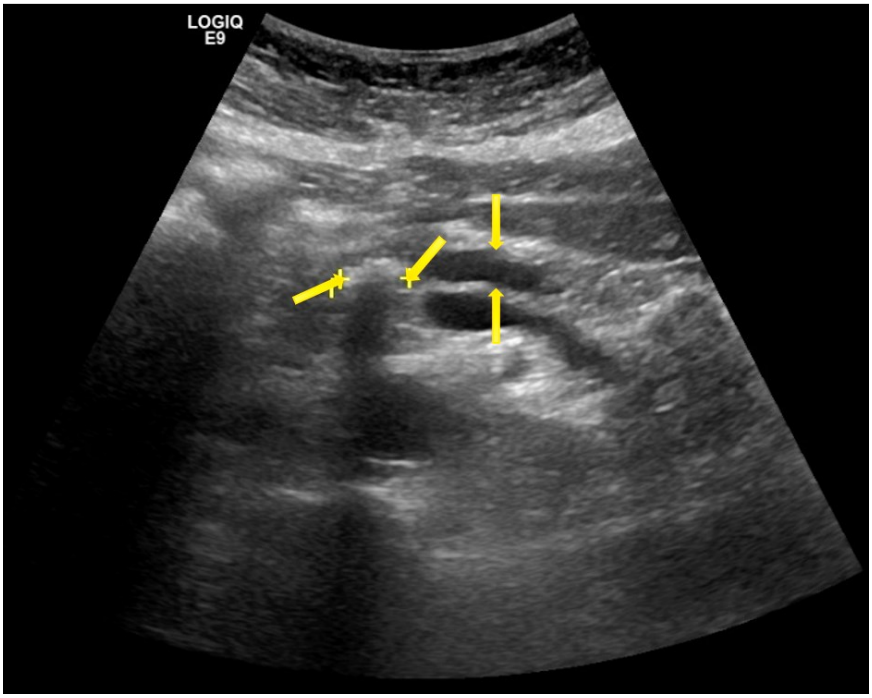

Fig. 6.6. Chronic pancreatitis: Main pancreatic duct dilation and a pancreatic stone (arrows).

Obstructing the main pancreatic duct can result in secondary obstructive chronic pancreatitis upstream of the blockage, following the exact pathogenic mechanism. Both solid and cystic lesions adjacent to the duct can lead to either compression (benign) or infiltration (malignant), progressively causing obstructive chronic pancreatitis. This process complicates the accurate detection and characterization of such lesions. Therefore, in all cases of chronic pancreatitis, interruptions in a dilated pancreatic duct should be carefully assessed to determine the underlying cause of ductal stricture.

6.4.3 Autoimune Pancreatitis

Autoimmune pancreatitis is a rare form characterized by periductal inflammation driven primarily by lymphocytic infiltration, leading to fibrosis. It is classified into two morphological subtypes: focal and diffuse. Unlike other forms of chronic pancreatitis, autoimmune pancreatitis typically results in pancreatic enlargement, often involving the entire gland and creating a distinctive "sausage-like" appearance. In diffuse autoimmune pancreatitis, the main pancreatic duct appears compressed or string-like.

Ultrasound findings include decreased pancreatic echogenicity, diffuse or localized glandular enlargement, and the absence of fluid collections or calcifications. The diagnostic sensitivity of ultrasound varies between 60% and 70% across studies. Focal autoimmune pancreatitis can closely mimic mass-forming pancreatitis or pancreatic cancer, particularly when localized in the pancreatic head, where it may lead to isolated dilation of the common bile duct.

CEUS typically reveals moderate and diffuse enhancement in the early phase, though it may appear inhomogeneous. Contrast agent washout is generally slow but progressive, making CEUS particularly valuable in differentiating focal autoimmune pancreatitis from pancreatic ductal adenocarcinoma, which typically exhibits hypoenhancement.

A hallmark of autoimmune pancreatitis is its dramatic response to corticosteroid therapy. Additionally, elastography may aid in assessment, as focal autoimmune pancreatitis exhibits a characteristic stiff elastographic pattern in the lesion and the surrounding pancreatic parenchyma.

6.4.4 Other benign pancreatic lesions

6.4.4.1 Mass forming

Mass-forming pancreatitis typically occurs in patients with a history of chronic pancreatitis and can be challenging to distinguish from pancreatic ductal adenocarcinoma due to their similar ultrasound characteristics. Both conditions often appear as hypoechoic masses and may present with overlapping clinical symptoms.

During an ultrasound examination, detecting small calcifications within the lesion may indicate an inflammatory origin, although this sign has limited specificity. CEUS is crucial in improving the differentiation between these two entities, particularly in cases with an autoimmune etiology. Mass-forming pancreatitis typically exhibits a “parenchymographic” enhancement pattern, where the enhancement is comparable to that of the surrounding pancreatic parenchyma, contrasting with the pronounced hypervascularity seen in pancreatic ductal adenocarcinoma.

Additionally, while pancreatic ductal adenocarcinoma remains hypoechoic throughout all contrast phases due to its intense desmoplastic reaction and low vascular density, mass-forming pancreatitis displays enhancement similar to the adjacent pancreatic tissue. The duration of the underlying inflammatory process influences the intensity of this enhancement. In long-standing chronic pancreatitis, heterogeneous hypovascularization and reduced intralesional enhancement may be observed, likely due to extensive fibrosis, making differentiation more difficult. In contrast, more recent-onset mass-forming pancreatitis shows a more intense and prolonged enhancement pattern.

For an accurate diagnosis, biopsy or FNA, guided by either transabdominal or endoscopic ultrasound, is often necessary.

*6.4.4.2 **Pancreatic Pseudocysts and Walled-Off Necrosis***

Pseudocysts are a potential complication that may arise at least four weeks after acute pancreatitis or in the context of chronic pancreatitis. These fluid-filled structures are characterized by a well-defined fibrous wall lacking an epithelial lining. On ultrasound, pseudocysts appear as anechoic lesions with clear margins and posterior acoustic enhancement.

Distinguishing pseudocysts from pancreatic cystic tumors, particularly mucinous cystadenomas, is crucial since their management differs significantly. A history of acute or chronic pancreatitis is key to accurate diagnosis. CEUS is essential in differentiating between pseudocysts and cystic tumors by providing a more detailed assessment of vascularization within the lesion walls and any intralesional components. Typically, pseudocyst walls exhibit low vascularity on CEUS, while the internal fluid and debris remain entirely avascular.

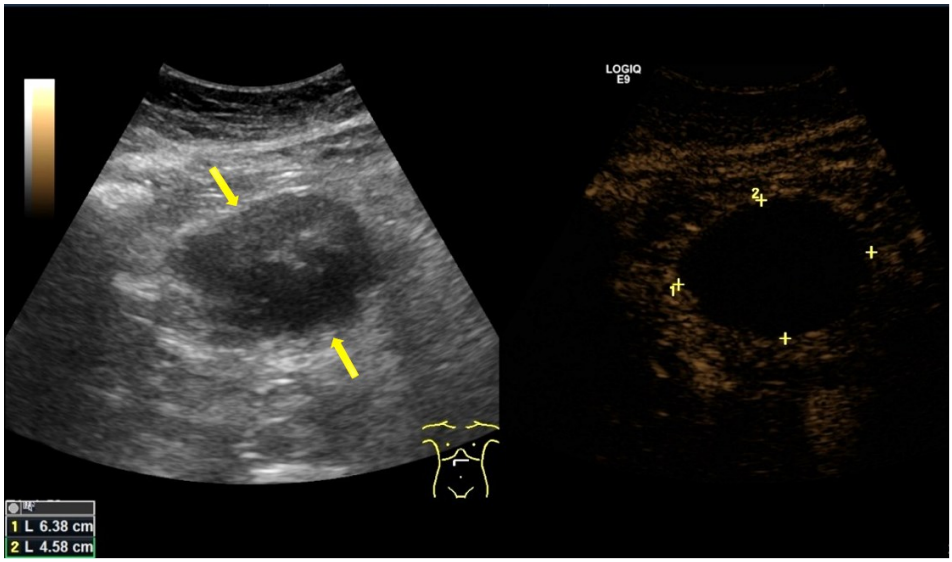

Fig. 6.7. Pseudocyst: A rounded cystic lesion after severe acute pancreatitis in B-mode and CEUS (arrows)

Another potential complication of acute pancreatitis is walled-off necrosis (WON), which, like pseudocysts, develops approximately four weeks after symptom onset. WON consists of chronic fluid collections containing necrotic material and debris, which appear as echogenic particles within an anechoic background on ultrasound. Following contrast administration, CEUS demonstrates an enhancing wall while the internal contents remain avascular, confirming the presence of nonviable tissue.

6.5 Pancreatic Tumors

6.5.1 Pancreatic solid malign tumors

6.5.1.1 Adenocarcinoma

Pancreatic ductal adenocarcinoma is the most common solid pancreatic malignancy, accounting for approximately 90% of pancreatic tumors. It comprises infiltrating epithelial cells that resemble ductal structures and is most frequently found in the head of the pancreas. It causes ductal obstruction and subsequent dilation of the common bile duct and the main pancreatic duct,

leading to the characteristic "double-duct sign." Although this sign is also present in chronic pancreatitis, it is a crucial indicator for early tumor detection.

On ultrasound, pancreatic ductal adenocarcinoma typically appears as a solid, hypoechoic mass with poorly defined margins due to its infiltrative nature (Fig. 6.8). The central pancreatic duct is often dilated with an abrupt cutoff, which should prompt further imaging studies. Additionally, Doppler ultrasound usually reveals poor or absent vascularity within the lesion. Evaluation of adjacent vascular structures is essential to differentiate resectable from non-resectable tumors by assessing the echogenic fatty interface between the tumor and nearby vessels and their blood flow characteristics.

CEUS significantly enhances diagnostic accuracy by better-visualizing tumor margins and vascular characteristics. In CEUS, pancreatic ductal adenocarcinoma generally presents as a hypoenhancing lesion in all contrast-enhanced phases, a pattern observed in approximately 90% of cases (Fig. 6.9). This feature helps distinguish adenocarcinoma from other pancreatic masses, making CEUS a valuable tool for early diagnosis. Furthermore, CEUS is essential for detecting liver metastases, which are best visualized during the late phase of contrast administration. Any focal hypoechoic lesion detected in the liver during this phase should be considered metastatic until proven otherwise.

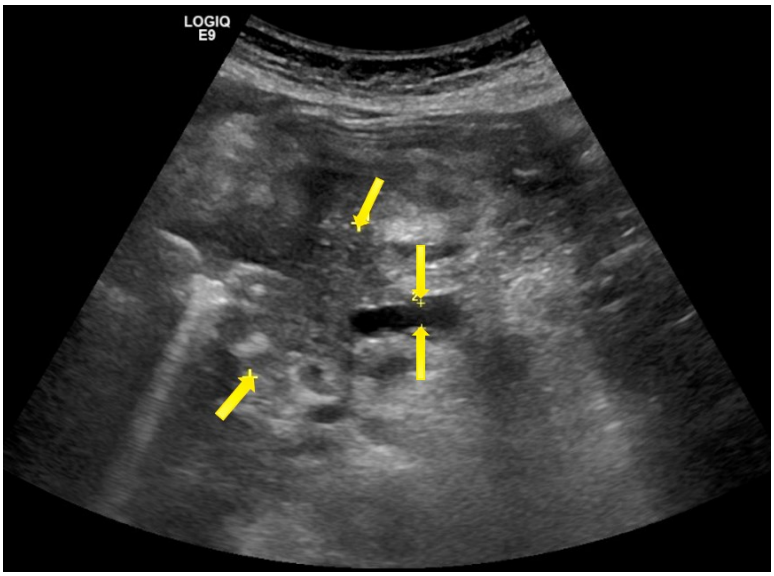

Fig. 6.8. Adenocarcinoma: Hypoechoic mass and upstream main pancreatic duct dilation (arrows).

Elastography is another proper imaging technique, as pancreatic ductal adenocarcinoma is typically a complex, hypovascular mass with increased stiffness compared to the surrounding pancreatic parenchyma. Malignant pancreatic neoplasms generally exhibit greater stiffness than benign lesions, although differentiating between them solely based on elastography may not always be straightforward.

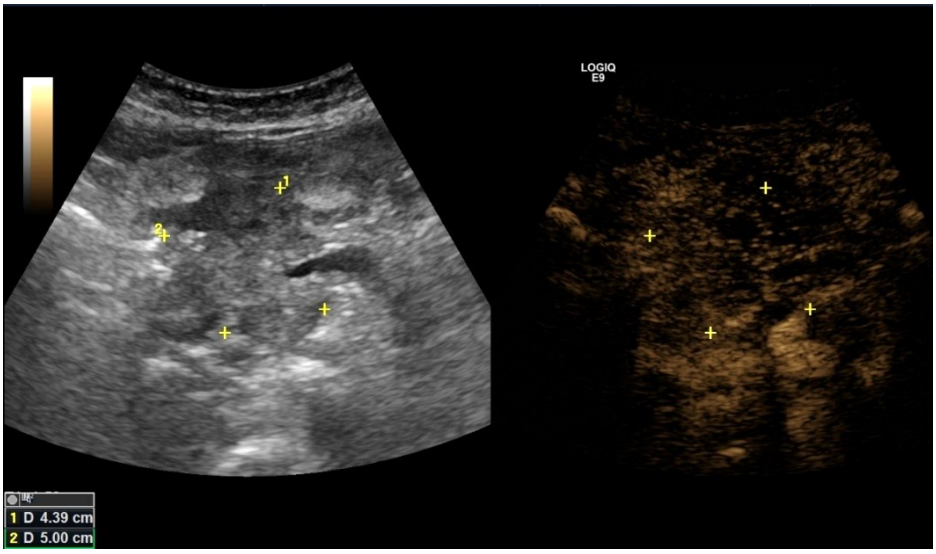

Fig. 6.9. Adenocarcinoma: CEUS showing a hypoechoic pancreatic mass with irregular borders

Since ultrasound is often the first imaging modality used for pancreatic evaluation, integrating CEUS and elastography into the diagnostic workflow can significantly improve the identification and characterization of pancreatic ductal adenocarcinoma, facilitating earlier detection and appropriate clinical management.

6.5.1.2 Neuroendocrine Tumors

Pancreatic neuroendocrine tumors (PNETs), also known as islet cell tumors, originate from neuroendocrine cells within the pancreas. These tumors are classified as either functioning or non-functioning based on their ability to produce hormones and cause clinical symptoms. Functioning PNETs, such as insulinomas and gastrinomas, are typically smaller at diagnosis, whereas other functioning tumors like VIPomas, glucagonomas, and somatostatinomas are rarer, larger, and generally more malignant. Non-functioning tumors, which do not produce symptoms related to hormone secretion, tend to be larger at diagnosis and frequently exhibit malignant behavior.

Insulinomas, the most common PNETs, account for approximately 60% of cases. They are generally benign, solitary, and small, with diameters ranging between 0.5 and 2 cm. However, in multiple endocrine neoplasia type 1 (MEN1) syndrome, they can be multifocal. Malignant insulinomas are typically larger than 3 cm and may present with metastases at diagnosis.

On ultrasound, insulinomas appear as well-defined, hypoechoic, and encapsulated nodules that exhibit hyperenhancement during CEUS. Gastrinomas, the second most common functioning PNETs, are often found within the gastrinoma triangle and are usually larger than insulinomas, making their detection easier. These tumors are frequently multifocal, especially in MEN1 syndrome, and metastasize to the liver in approximately 60% of cases. On ultrasound, they appear as homogeneous hypoechoic masses.

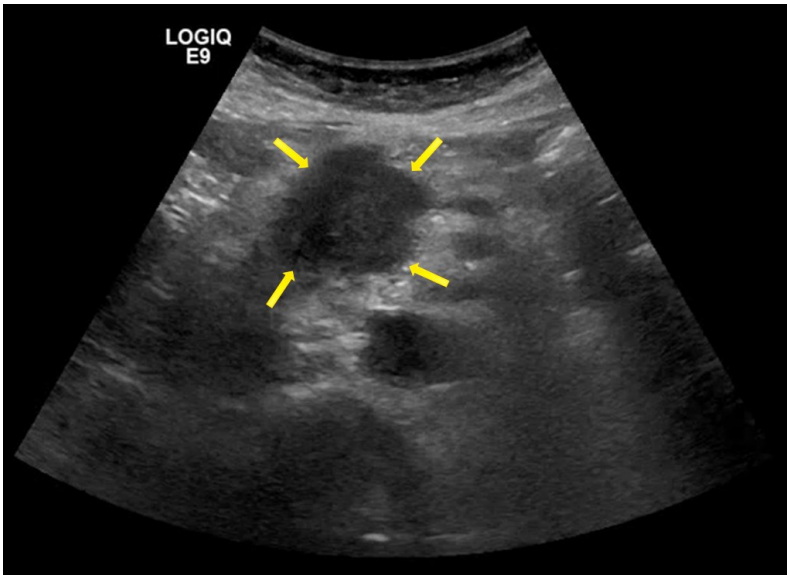

Fig. 6.10. Pancreatic neuroendocrine tumor: Well-defined, hypoechoic, and encapsulated nodule.

Less common functioning PNETs, including glucagonomas, VIPomas, and somatostatinomas, tend to be larger, more aggressive, and prone to early metastasis. Non-functioning PNETs, which constitute up to one-third of all PNETs, can range in size from 1 to 20 cm and have a malignancy rate of up to 90%. Despite their malignant potential, they tend to be less aggressive than pancreatic ductal adenocarcinomas, and distinguishing between these two entities is crucial due to their different treatment approaches. Non-functioning PNETs often remain asymptomatic until they grow large enough to affect adjacent structures. On ultrasound, they appear as well-circumscribed, easily detectable masses due to their size. Larger tumors may develop necrotic or cystic areas, leading to an inhomogeneous appearance with small calcifications.

Doppler ultrasound typically reveals multiple intratumoral vascular spots, producing a characteristic "spotted" pattern in both small and large PNETs. However, in some cases, hypervascular tumors may not show vascularity on Doppler due to their fine vascular network. CEUS plays a crucial role in characterizing PNETs, as these tumors generally demonstrate rapid and intense enhancement during the early contrast phase, except for necrotic areas. Small to moderate-sized PNETs may exhibit a capillary blush pattern in the early contrast phase and appear hypoechoic in the late phase. Non-functioning PNETs may be hypovascular depending on the stromal content, which is often dense and hyalinized.

The high resolution of CEUS enables precise visualization of tumor vascularity, making it a valuable tool in differentiating PNETs from pancreatic ductal adenocarcinomas. Elastography studies indicate that PNETs are typically stiffer than normal pancreatic parenchyma but generally less stiff than ductal adenocarcinomas. This additional imaging modality contributes to the improved characterization and differentiation of pancreatic tumors, aiding in accurate diagnosis and treatment planning.

6.5.2 Cystic Neoplasms

6.5.2.1 Serous cystadenoma

Serous cystadenoma (SCA) is a benign pancreatic lesion, most commonly found in middle-aged women (50–60 years old), with a female-to-male ratio of 2:1. These cystic tumors are usually solitary, but in the context of von Hippel–Lindau disease, they can be multifocal. The most common type of serous pancreatic neoplasm is serous cystadenoma, which is frequently located in the head of the pancreas.

Morphologically, SCA typically presents as a multilocular microcystic lesion with a honeycomb architecture characterized by multiple microcysts (<20 mm), thin walls, and fine septa oriented toward the center without communication with the pancreatic ductal system. A central scar is present in approximately 15% of cases, which may calcify.

The microcystic type, found in 70% of cases, has a cloud-like morphology and is well visualized on ultrasound. It displays lobulated contours and anechoic microcysts separated by thin internal septa arranged radially. SCA may appear solid on ultrasound and CT in extremely microcystic cases, resembling a neuroendocrine pancreatic tumor due to the homogeneous hyperenhancement of the densely packed internal septa after contrast administration. However, MRI typically reveals its characteristic cystic appearance.

Other subtypes of serous cystadenoma include the macrocystic and oligocystic types, which pose a diagnostic challenge in differentiating them from other macrocystic pancreatic tumors, particularly mucinous cystic neoplasms. The cystic content is glycogen-rich and serous, appearing anechoic on ultrasound. Importantly, SCAs do not communicate with the main pancreatic duct, although they may cause compression and upstream dilation. The absence of ductal communication is a key feature in distinguishing SCA from branch-duct intraductal papillary mucinous neoplasms (IPMN), though this can be challenging to confirm via ultrasound.

CEUS plays a crucial role in identifying SCA's microcystic features by enhancing the visualization of intralesional septa. When present, the central scar shows homogeneous enhancement. Elastographic studies indicate that the serous content of SCA produces a mosaic pattern and non-numerical values in quantitative ultrasound elastographic assessment, mainly using ARFI imaging.

6.5.2.2 Mucinous cystadenoma

Mucinous cystic neoplasms (MCNs) represent a spectrum of pancreatic cystic tumors, ranging from benign mucinous cystadenoma (MCA) to invasive and potentially metastasizing mucinous cystadenocarcinoma. These neoplasms, which occur predominantly in women (F: M = 9:1) and are most commonly found in the body and tail of the pancreas, can potentially metastasize. Given this grave possibility, surgical resection is always indicated.

MCA typically appears as a unilocular or oligolocular (≤6 cysts) cystic lesion with a thick wall and a rounded, ball-like morphology without communication with the main pancreatic duct. On ultrasound, it presents as a round or ovoid lesion with thick walls, internal septa, and sometimes peripheral calcifications. The mucinous content is highly viscous, often producing fine internal echoes, resulting in a heterogeneously hypoechoic ultrasound appearance. Additionally, MCA may contain internal septa or solid papillary projections. Detecting vascularized mural nodules is crucial for differentiating MCNs from pseudocysts, as enhanced mural nodules are closely associated with an increased risk of malignancy and potential transformation into mucinous cystadenocarcinoma. However, the number and thickness of intralesional septa and nodules do not always correlate with malignancy grade.

CEUS significantly improves the identification of parietal nodules and septa, primarily by detecting their vascularization. Using a hyperechoic beam and a blood pool contrast agent, CEUS assesses dynamic perfusion, often demonstrating septal and nodule enhancement more effectively than other imaging modalities. By suppressing background tissue and echogenic intra-cystic content (such as mucin, clots, or debris), CEUS plays a pivotal role in enhancing the visualization of septa and nodules compared to conventional B-mode ultrasound. This makes it a superior and precise tool for characterizing cystic tumors and distinguishing MCA from pseudocyst

All mucin-producing tumors contain complex fluid, which impacts their elastographic properties. At quantitative elastographic imaging, such as ARFI, MCNs exhibit higher shear wave velocity values than serous neoplasms, reflecting their mucinous content's dense, viscous nature.

6.5.2.3 Mucinous cystadenocarcinoma

Mucinous cystadenocarcinoma, a result of the malignant transformation of a mucinous cystadenoma, is starkly contrasted to its benign counterpart. It exhibits thicker walls and septa, heterogeneous internal content, and mural nodules (Fig. 6.11). These nodules undergo significant cellular proliferation, contributing to wall infiltration and eventual invasion of surrounding structures, which may result in lymph node involvement and liver metastases.

As mentioned earlier, CEUS effectively highlights the enhancement of neoplastic growths within the tumor, aiding in distinguishing between viable neoplastic tissue and echogenic intra-cystic components, such as mucin, clots, or debris, which consist of non-viable material. However, the real intrigue lies in the quantitative perfusion analysis of CEUS enhancement. This analysis can reveal increased perfusion values in areas undergoing neoplastic transformation, providing a deeper understanding of the tumor's behavior and aiding in treatment planning.

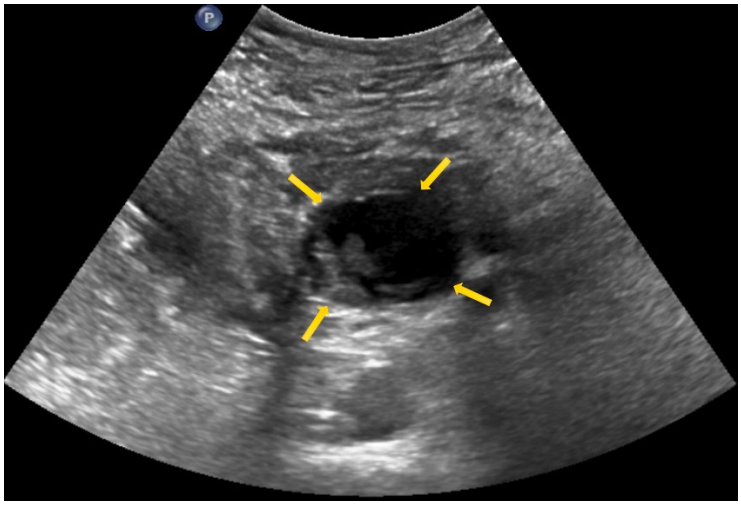

Fig. 6.11. Mucinous cystadenocarcinoma B-Mode

6.5.2.4 Intraductal papillary mucinous neoplasm

IPMN is a mucin-producing exocrine pancreatic tumor frequently diagnosed in men around 60. With advancements in imaging techniques, the detection of these neoplasms has significantly increased in recent years. IPMN is characterized by cystic dilation of the main pancreatic duct and/or its branches, accompanied by epithelial proliferation and excessive mucin production. Depending on its anatomical involvement, IPMN is classified into three types: the main duct type, which manifests as segmental or diffuse dilation without abrupt cut-off; the branch duct type, appearing as unilocular or multilocular cystic lesions with grape-like clusters; and the mixed type, which affects both the main duct and its branches.

The main duct variant carries the highest risk of malignancy and is typically associated with inhomogeneous intraductal masses and upstream ductal dilation. In contrast, the branch duct type consists of cystic ectasia of pancreatic side branches, forming mass-like structures. Establishing communication with the main pancreatic duct is crucial for an accurate diagnosis, as segmental or diffuse ductal involvement significantly raises the risk of malignancy. A pancreatic duct diameter exceeding 10 mm strongly suggests malignant transformation. At the same time, additional features such as mural nodules, thickened septa, ductal wall enhancement, solid intralesional components, and peripheral or septal calcifications further support the suspicion of malignancy.

On ultrasound, IPMN often appears as a complex hypoechoic mass with main duct dilation if the primary duct is involved. In the branch duct type, the connection to the pancreatic duct is often not visible on transabdominal ultrasound, and these lesions typically present as multilocular, grape-like cystic formations. Mucinous content may be difficult to distinguish from solid tumor portions, sometimes leading to misclassification. Harmonic imaging, with its improved contrast resolution, enhances the ability to differentiate between solid and cystic components. However, ultrasound alone frequently fails to confirm communication with the main pancreatic duct and may

underestimate the number of lesions, a critical factor in treatment planning; up to two-thirds of branch-duct IPMNs present as multifocal lesions, further complicating assessment.

CEUS is vital in improving lesion characterization by allowing better visualization of vascularized tumor components such as mural nodules and septa. With real-time, high-resolution imaging capabilities, CEUS enables the identification of intraductal papillary tumor tissue by assessing its vascularization. This is essential for distinguishing malignant from benign lesions, as enhanced mural nodules are closely associated with a higher risk of malignancy. Moreover, CEUS facilitates non-invasive monitoring of borderline lesions by tracking changes in size and vascularization over time, offering a safe and cost-effective surveillance method for pancreatic cystic neoplasms.

From a clinical management perspective, malignant potential is suggested by local invasion, vascular encasement, peri-pancreatic lymph node enlargement, and distant metastases. The International Consensus Guidelines recommend surgical resection for all main-duct IPMNs and branch-duct IPMNs exhibiting high-risk stigmata of malignancy, which include mural nodules, main pancreatic duct dilation exceeding 10 mm, or an associated solid mass. In contrast, asymptomatic branch-duct IPMNs measuring less than 3 cm without solid components or significant main duct dilation should be managed with careful surveillance rather than immediate surgical intervention.

Given the increasing recognition of IPMNs and their variable malignant potential, accurate imaging evaluation is essential for risk stratification and treatment planning. Early detection, coupled with precise characterization through advanced imaging modalities, ensures timely intervention in cases with malignant potential while preventing unnecessary surgical procedures in benign lesions.

6.5.2.5 Rare pancreatic tumors

Primary pancreatic lymphoma is an exceptionally rare pancreatic tumor, a stark contrast to the more frequent secondary pancreatic involvement by non-Hodgkin's B-cell lymphoma, which occurs in 30–40% of patients with extranodal disease.

Various radiological patterns have been described for primary pancreatic lymphoma, including a well-defined nodular form with a solitary pancreatic mass (the most common presentation), a diffuse form characterized by pancreatic enlargement, peripheral lymphomatous involvement that may resemble autoimmune pancreatitis and a multinodular form. When presenting as a solitary mass, it is crucial to distinguish primary pancreatic lymphoma from ductal adenocarcinoma, as it often appears large, heterogeneous, and capable of extending beyond the gland while encasing major peri-pancreatic vessels. However, despite potential ductal invasion, the degree of pancreatic duct dilation remains minimal, making this a key distinguishing feature suggestive of pancreatic lymphoma.

A diffuse pattern of pancreatic infiltration and enlargement should raise suspicion of pancreatic lymphoma, but only when accompanied by clinical signs of acute pancreatitis and systemic symptoms, not in isolation. Ultrasound imaging typically reveals focal or diffuse pancreatic enlargement, which is hypoechoic compared to normal pancreatic parenchyma.

Metastatic involvement of the pancreas is uncommon. The most frequent primary tumors that spread to the pancreas originate from the lung, breast, kidney, and melanoma. Pancreatic metastases may present as solitary or multiple nodules or diffusely infiltrate the pancreatic parenchyma. When appearing as nodular lesions, they are typically well-defined and occur in patients with a known primary malignancy.

It is essential to consider pancreatic metastases in the differential diagnosis of primary pancreatic tumors, such as ductal adenocarcinoma and neuroendocrine tumors. Metastases from renal cell carcinoma and melanoma are often hypervascular and show characteristic enhancement on CEUS. Due to their similar enhancement patterns, they must be distinguished from neuroendocrine tumors based on clinical history, symptoms, and cytological evaluation. In contrast, hypovascular pancreatic metastases should be differentiated from pancreatic ductal adenocarcinoma.

Solid pseudopapillary tumors (SPTs) are rare epithelial neoplasms with low malignant potential. They primarily affect young women (85-90%) between the second and fourth decades of life. Their appearance varies widely, ranging from entirely solid tumors to predominantly cystic masses. Smaller lesions are typically solid or mostly solid. In contrast, larger ones tend to present as well-encapsulated masses with a mix of solid and cystic areas, often resulting from hemorrhagic degeneration.

On ultrasound, SPTs usually appear as well-encapsulated lesions containing solid and cystic components. However, the tumor may be entirely solid in some cases, presenting as a hypoechoic mass with well-defined borders, particularly in smaller lesions. Internal septations or calcifications may also be observed. A distinguishing feature is the absence of upstream ductal dilatation.

CEUS typically reveals rim enhancement in SPTs, with non-enhancing regions within the tumor corresponding to areas of necrosis or hemorrhage. This peripheral enhancement is attributed to a pseudocapsule formed by compressed normal pancreatic tissue. Throughout all phases of CEUS, these tumors generally appear iso- or hypoenhancing relative to the surrounding pancreatic parenchyma.

6.6 Role of Interventional Ultrasound

For solid pancreatic lesions, preoperative biopsy is generally avoided in resectable ductal adenocarcinoma to prevent false-negative results, with direct surgical referral being the preferred

approach. However, histopathological confirmation is necessary for inoperable cases or when neoadjuvant therapy is planned. A biopsy may also be required to distinguish between rare entities like lymphoma or metastases, mainly if imaging is inconclusive. FNA or core needle biopsy (CNB) can help determine the Ki-67 index in neuroendocrine neoplasms, which is essential for prognosis. Multiple FNA passes are more effective than a single core biopsy.

Percutaneous sampling is less reliable for cystic pancreatic lesions and EUS-guided FNA is preferred. EUS-FNA cytology has higher accuracy than fluid analysis alone in differentiating benign from malignant cystic lesions. It is beneficial when prior imaging is inconclusive, especially in distinguishing mucinous from non-mucinous lesions or when chemotherapy is considered for advanced malignancies. However, typical cystic neoplasms requiring surgery do not necessarily need preoperative EUS-FNA.

Focal pancreatic lesions are first detected via transabdominal ultrasound, with elastography helping assess tissue stiffness. Contrast-enhanced CT remains the primary imaging modality for solid lesions, with MRI and EUS used as second-line tools. Magnetic resonance cholangiopancreatography is the gold standard for cystic lesions, while EUS further aids in characterization. A biopsy is necessary for borderline resectable solid lesions before neoadjuvant therapy but is not required for clearly resectable cases. Percutaneous US-FNA is the preferred sampling method due to its minimal invasiveness, lower cost, and rapid diagnosis, with an overall accuracy exceeding 90%. The diagnostic yield varies by lesion location and is higher for body-tail lesions than head lesions.

Indications for biopsy include characterization of unresectable solid masses, differentiation between neoplasms and inflammatory conditions, evaluation of suspected metastases or lymphoma, and Ki-67 assessment in neuroendocrine tumors. Cystic lesions of uncertain malignant potential may also require sampling, preferably via EUS. Absolute contraindications include coagulation disorders and patient refusal of treatment.

US-guided biopsy involves B-mode and Doppler imaging to identify the optimal access route, with CEUS assisting in targeting viable areas. Fine-needle aspiration is performed with 20–25 gauge needles, while core biopsies use larger ones. A cytologist can provide immediate sample assessment during the procedure. Complications are rare, with percutaneous US-guided FNA having lower complication rates than CT-guided procedures. Tumor seeding risk is minimal and comparable between percutaneous and endoscopic approaches.

Post-procedure ultrasound is recommended for follow-up to detect immediate complications, with CT performed if clinically indicated. Biopsy of the pancreatic parenchyma is generally unnecessary for diffuse pancreatic diseases, except in autoimmune pancreatitis, where histological confirmation is crucial. In pancreatitis-associated fluid collections, FNA for microbial culture is applicable only when infection is suspected, though it is not routinely indicated due to a high false-negative rate. In pseudocysts, biopsy is warranted when differentiation from mucinous or serous cystic neoplasms remains unclear on imaging.

6.7 The utility of other imagistic methods

The characterization of solid and cystic pancreatic tumors can be enhanced through the combined use of various imaging modalities, including B-mode ultrasound, CEUS, EUS, CT, and MRI. In clinical practice, particularly in Europe, ultrasound is often the initial imaging modality for patients with abdominal symptoms. Therefore, a thorough understanding of ultrasound features in different pancreatic diseases and appropriate diagnostic and therapeutic management is essential for clinicians.

When a focal pancreatic lesion is identified via ultrasound, the immediate administration of ultrasound contrast agents represents a relatively new, safe, and effective technique for improved lesion characterization and staging within the same examination. CEUS enhances the differentiation of solid versus cystic lesions and helps classify them as hyper-enhancing, hypo-enhancing, or non-enhancing, thereby guiding further diagnostic steps and expediting the diagnostic process.

Elastography is a valuable tool for assessing tissue stiffness, and there is growing interest in its use in pancreatic pathology. However, the pancreas's deep location makes precise measurements challenging, making biopsy correlation difficult. Two main techniques are used: **strain elastography**, which estimates stiffness by analyzing tissue deformation from internal (e.g., aortic pulsations) or external forces, and **shear-wave elastography (SWE)**, which measures shear-wave velocity for a more objective assessment.

Real-Time Elastography (RTE) initially provided qualitative evaluations, improving pancreatic tumor detection from **70–80%** (ultrasound alone) to over **90%**. However, subjectivity led to the **strain-ratio** method, which remains inconsistent due to a lack of consensus on the reference tissue. **SWE**, using **ARFI** technology, offers a more reliable quantitative approach. **Virtual Touch Quantification (VTQ)** by Siemens, one of the first SWE techniques, provides objective stiffness measurements, making it a preferred method for pancreatic evaluation.

CT is typically the next step for further characterization and staging for solid pancreatic lesions detected on ultrasound. However, up to 30% of ductal adenocarcinomas smaller than 2 cm may appear isodense during the arterial phase of CT, making detection challenging. Suppose CT results are inconclusive despite a clear ultrasound finding of a solid lesion. In that case, MRI and EUS (preferably with fine-needle aspiration or biopsy) are recommended due to their superior sensitivity in detecting small pancreatic tumors. In such cases, MRI is preferable to CT for evaluating pancreatic nodules smaller than 2 cm. EUS with fine-needle sampling is valuable for cytological or histological confirmation, particularly in cases requiring neoadjuvant chemoradiotherapy, as it maintains high diagnostic accuracy even for small lesions.

MRI remains the preferred imaging modality for cystic pancreatic lesions due to its superior ability to visualize fluid components within cysts. Magnetic resonance cholangiopancreatography is particularly effective in assessing ductal communication in pancreatic cystic neoplasms. CT may be used in cases where MRI is contraindicated, although it has lower accuracy in evaluating cystic

lesion characteristics. Current guidelines suggest using EUS, with optional FNA, for further assessment of cystic pancreatic neoplasms that present concerning features on imaging. However, FNA is only recommended in cases with ambiguous imaging findings. There is no evidence supporting the efficacy of percutaneous image-guided sampling for pancreatic cystic neoplasms; instead, FNA should be performed under EUS guidance. Moreover, EUS provides additional morphological information, improving the identification of malignancy-suspect features, although it cannot definitively distinguish between mucinous and non-mucinous cystic neoplasms.

Combining multiple imaging techniques improves diagnostic accuracy, allowing for earlier and more precise detection of pancreatic tumors. The integration of ultrasound, CEUS, MRI, CT, and EUS—along with targeted sampling techniques—enhances diagnostic confidence, aids in therapeutic decision-making, and ultimately improves patient outcomes.

Selective references

1. D'Onofrio M, Ciaravino V, Valek V, Belei A, Jenssen C, De Robertis R. *Ultrasound of the pancreas.* In: Dietrich CF, editor. *EFSUMB – European Course Book.* Published in 2020.
2. D'Onofrio M, Săftoiu A. *Pancreas.* In: Nürnberg D, Chammas MC, Gilja OH, Sporea I, Șirli R, editors. *WFUMB Course Book.* 1st ed. World Federation for Ultrasound in Medicine and Biology; 2021.
3. Dietrich CF, Braden B. Sonographic assessments of gastrointestinal and biliary functions. Best Pract Res Clin Gastroenterol. 2009;23:353-367.
4. Schmidt G. Thieme Clinical Companions: Ultrasound. Thieme; 2007:293-300.
5. Meier J, Lucius C, Möller K, et al. Pancreatic ultrasound: An update of measurements, reference values, and variations of the pancreas. Ultrasound Int Open. 2024;10:a23899085. Published 2024 Oct 14. doi:10.1055/a-2389-9085.
6. Miuțescu B, Popa A, Săftoiu A. The role of elastography in pancreatic pathology. In: Popescu A, Șirli R, Moga T, editors. Textbook of Elastography. Timișoara, Romania: Editura „Victor Babeș"; 2024:192.
7. Piscaglia F, Nolsøe C, Dietrich CF, et al. The EFSUMB Guidelines and Recommendations on the Clinical Practice of Contrast-Enhanced Ultrasound (CEUS): Update 2011 on non-hepatic applications. Ultraschall Med. 2012;33(1):33-59.
8. Sidhu PS, Brabrand K, Cantisani V, et al. *EFSUMB Guidelines on Interventional Ultrasound (INVUS), Part II. Diagnostic Ultrasound-Guided Interventional Procedures (Long Version). Ultraschall Med.* 2015;36(6):E15-E35. doi:10.1055/s-0035-1554036.
9. Sienz M, Ignee A, Dietrich CF. *Reference values in abdominal ultrasound – biliopancreatic system and spleen. Z Gastroenterol* 2011; 49: 845–870.
10. Sirli R, Sporea I. *Ultrasound examination of the normal pancreas. Med Ultrason. 2*010;12(1):62-65.

7. HOW CAN I USE US IN DIGESTIVE TRACT PATHOLOGY?

Dieter Nürnberg
Past Chair of Task Force Group European COEs

Introduction

The role of ultrasound (US) in the diagnosis of the GIT (gastrointestinal tract) is partly primary, but partly complementary and supplementary. This is mainly due to the fact that not all parts of the GIT can be reached sonographically and that we sometimes find gas inside, which makes assessment difficult. The special value of US in the field of the GIT also lies in its ubiquitous availability and the speed of implementation, the methodology that can be used at any time and largely independently of equipment resource planning. In the following, we want to discuss the prerequisites, examination technique, important indications and areas of application, as well as typical findings. Gastrointestinal Ultrasound (GIUS) is able to depict the wall, lumen and surroundings of the GIT (especially the intestine) and to assess peristalsis!

Basics

In principle, it is beneficial if the GIT contains little air and is filled with fluid. From personal experience, an examination without any special preparation is best. For stomach examination, liquid intake (while avoiding air intake) is sometimes beneficial. For the small intestine in particular, it is advisable to drink plenty of fluids beforehand.

Special preparation techniques such as filling the small intestine with fluid and retrograde filling the colon with fluid have been described, but this method is not suitable for everyday use. I think that flatulent medication is superfluous. So, in summary, drink plenty beforehand, otherwise no special preparation is required.

GIUS most often is a symptom-oriented examination. It should begin with the convex probe (abdomen) to get an overview of the position of the GIT and its filling. Major changes, such as larger wall thickenings, can also be easily visualized with the convex probe. After this preliminary examination, it is usually necessary to switch to the high-frequency probe (linear probe with 7-12 MHz).

The examiner usually finds a suitable preset for intestinal sonography, which can be individually optimized depending on the device. Colour Doppler is often used, especially in cases of wall thickening, where hypervascularization indicates acute inflammatory changes.

The special feature of the intestinal sonography technique is that the intestine is increasingly compressed during the examination. The method has been described as particularly successful in appendix diagnostics. The compression pushes away disruptive intestinal gas and surrounding structures.

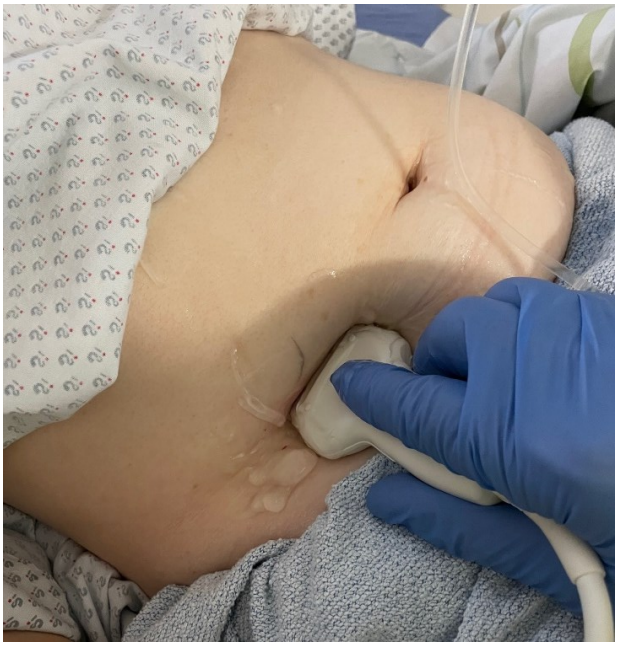

Fig. 7.1. Compression technique in diagnostics of Appendicitis

Unlike with parenchymatous organs, the focus is not on scanning/swinging the probe, but on keeping it in one position and observing the movement of the intestine (peristalsis). Consideration of this functional aspect is important in classifying a clinical picture.

Overall we differentiate between a structured examination and a symptom-focused examination. The latter is recommended, for example, if appendicitis or diverticulitis is suspected and is discussed in more detail there. The systematic examination of GIT begins with the colon. Usually, we start at the cecum and scan via the ascendancy and transverse to the descent and finally the sigmoid colon.

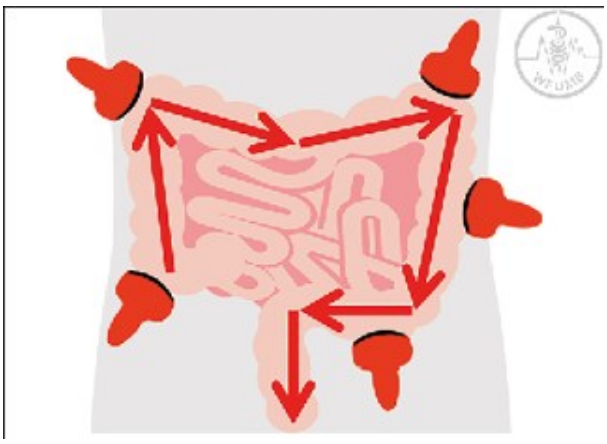

Fig. 7.2. Structured examination of colon

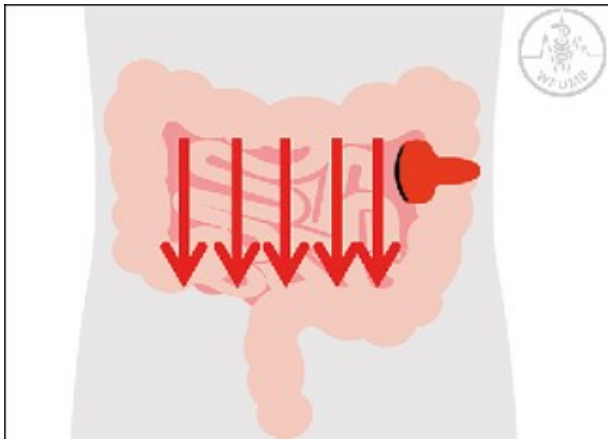

Fig. 7.3. Structured examination of small bowel

(according to Gilja OHG in WFUMB Book)

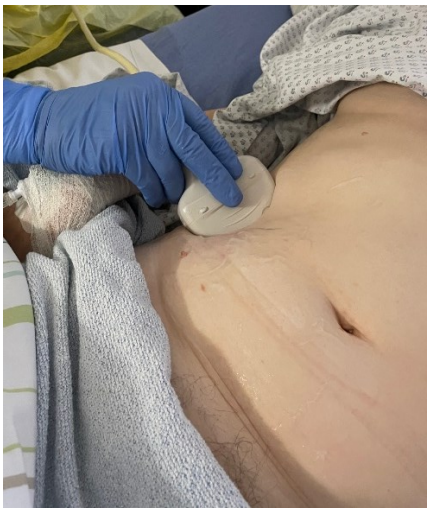

Fig. 7.4. Examination scheme colon start at coecum

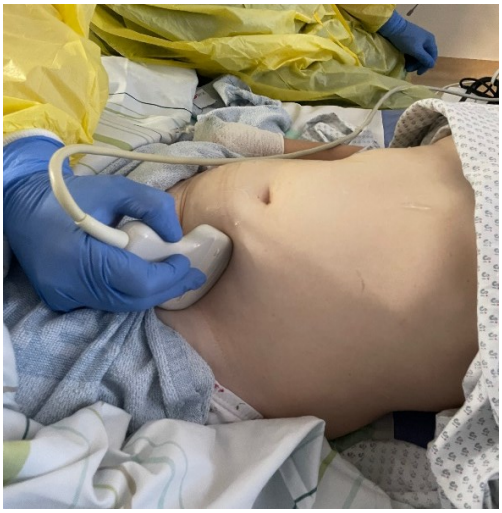

Fig. 7.5. Examination of colon, finish at sigma

Because of the regular gas filling, mainly the ventral wall of the colon can be assessed. Only the sigmoid colon can be extensively compressed, so that the posterior wall and surrounding area can also be clearly seen.

To assess the small intestine, the region within the colon frame is systematically scanned. This also happens while applying pressure, without causing additional discomfort to the patient. The examiner and patient remain in constant contact, so that the pressure can be well tolerated.

The wall structure of the GIT is relevant and typical. While the convex transducer can usually only distinguish 3 layers, we typically resolve 5 layers with the HF transducer. Although these layers are strictly speaking physical interface phenomena, they largely correspond to the anatomical conditions and are equated with them in everyday clinical practice. We encounter this layering again in EUS and it is particularly relevant here for T-staging and inflammatory changes. The table below explains the layering.

Tab. 7.1. Layers of GIT wall

No of layer	Sonographic layer	Histological layer
1	Entrance echo-innermost hyperechoic layer	Mucosal surface
2	Innermost hypoechoic layer	Mucosa
3	Central hyperechoic layer	Submucosa
4	Outermost hypoechoic layer	Muscularis propria
5	Outermost hyperchoic layer-entrance/exit echo	Serosal surface

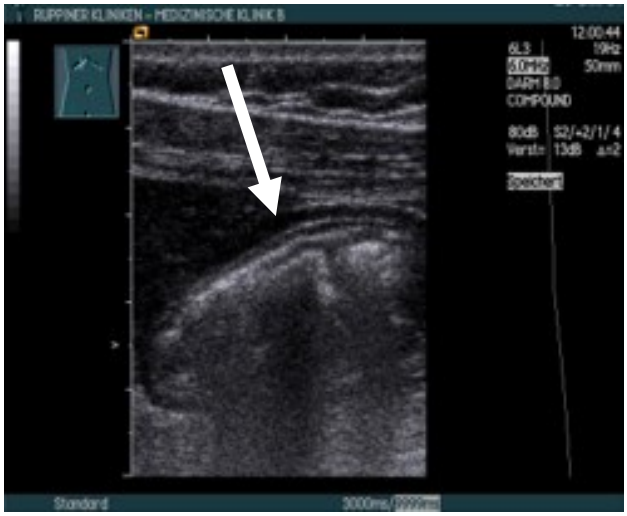

Fig. 7.6. Layers of GIT wall

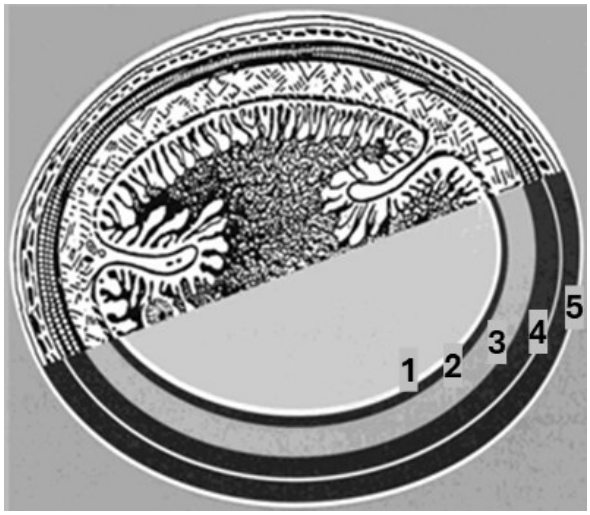

Fig. 7.7. Scheme of GIT layers

(Schmidt, Greiner, Nürnberg. Differential Diagnosis in Ultrasound Imaging. Thieme 2014)

The layering, preservation or removal of the wall, as well as the wall thickness, play an important role in the assessment. The following wall thicknesses are given as normal in the literature:

Tab. 7.2. Normal wall thickness

GIT section	Normal wall thickness
stomach	3 mm
jejunum	1-2 mm
ileum	1-2 mm
colon	3 mm

Orientation in the intestinal area is sometimes not easy. The question could be "Where am I?" In addition to the topographical position and type of wall, the gas content and particularly the peristalsis can be used to distinguish between the intestinal sections.

The colon is heavily filled with gas, shows little or practically no peristalsis and is easily identified by haustration. The small intestine usually shows liquid or thin stool in the lumen, impresses with its active peristalsis and has a thinner wall of approx. 1-2 mm. The jejunum has the typical Kerkring folds, while the ileum has smooth walls. The latter is better examined from the ileocoecal region, while the jejunum is found more in the left upper and middle abdomen.

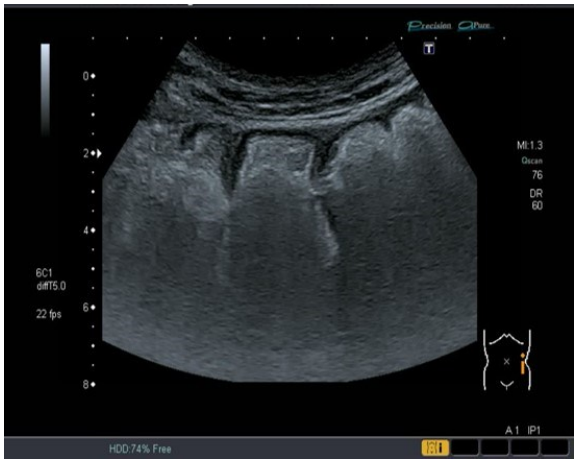

Fig. 7.8. Typical gas filled colon (haustration)

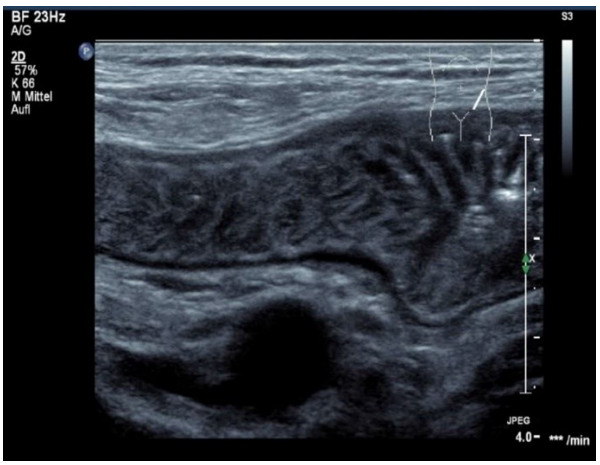

Fig. 7.9. Jejunum in left upper abdomen

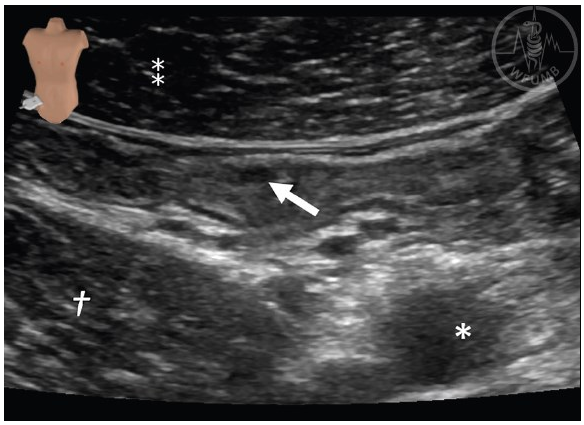

Fig. 7.10. Ileum in ileocoecal region (©OHG)

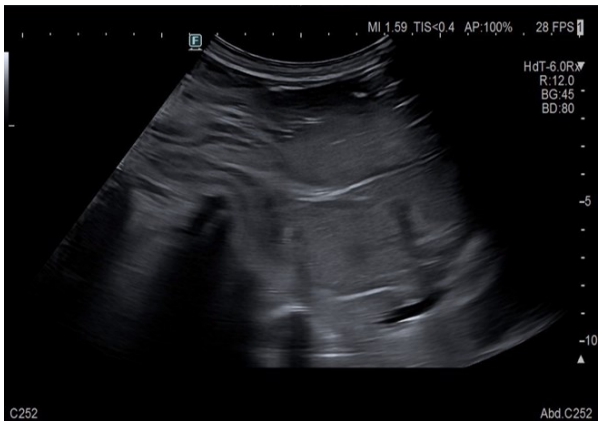

Fig. 7.11. Ileum, partially filled with thin stool

In addition to the small bowel and large bowel, other GIT sections can be at least partially visualized, these are the esophagus, the stomach and the rectum.

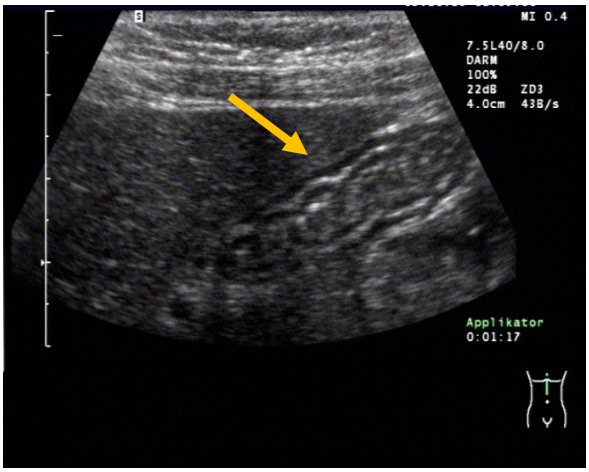

Fig. 7.12. Stomach

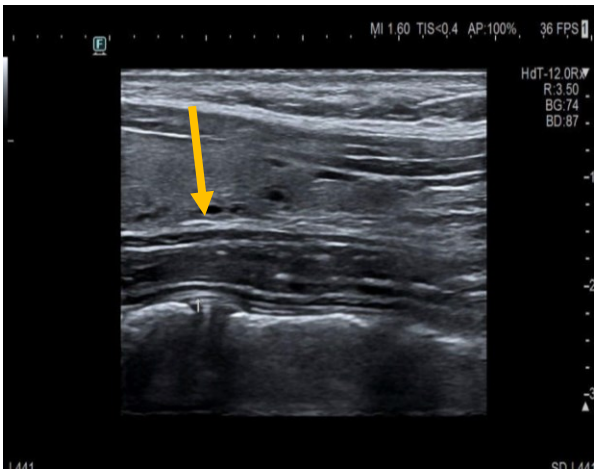

Fig. 7.13. Esophagus neck region

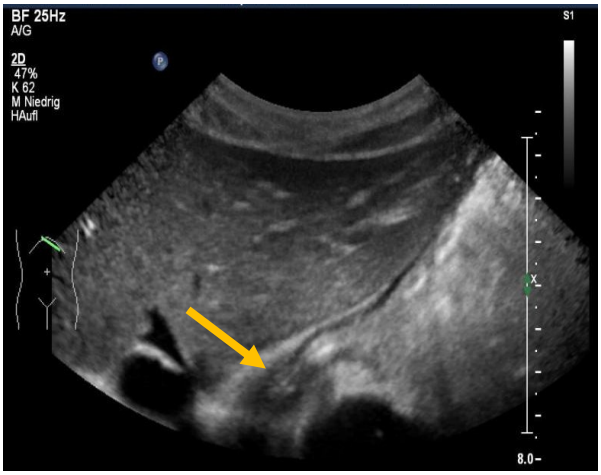

Fig. 7.14. Esophagus, distal part

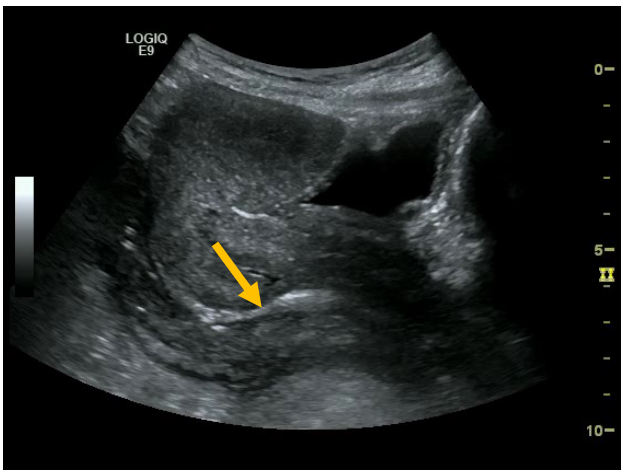

Fig. 7.15. Rectum (transvesical scan)

Inflammatory diseases

The two forms of IBD, Crohn's disease (CD) and ulcerative colitis (UC), shows different sonographic pictures.

a) Crohn's disease (CD)

In CD, changes in the wall, the surroundings and changes in peristalsis can be seen. The wall is thickened by more than 5 mm and can even reach wall thicknesses of up to 15-18 mm. Abolition or destruction of the wall can be typical, which occurs particularly in the case of local or pseudo-tumor involvement. If the layering is preserved, we also speak of an "accentuated" wall. A discontinuous pattern of involvement is usually found and peristalsis is reduced or eliminated in affected sections.

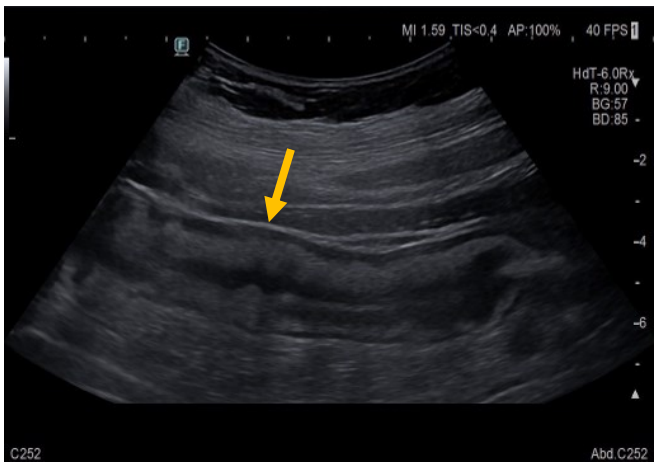

Fig. 7.16. CD of terminal Ileum. Accentuated wall

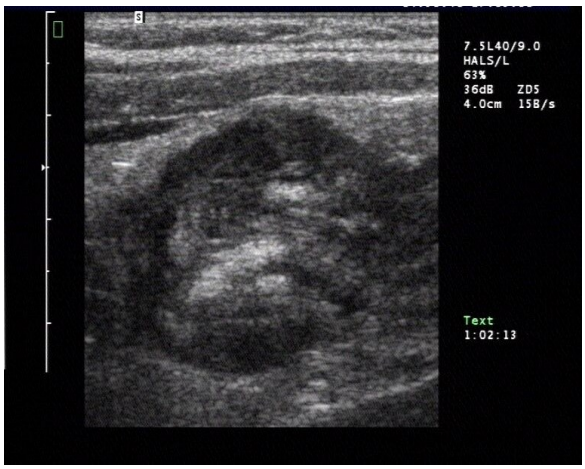

Fig. 7.17. CD of terminal Ileum with destroyed layers an pseudotumor

Crohn's disease as a transmural inflammation is also characterized by complications. These include fistulas, abscesses and stenoses. Fistulas are characterized sonographically by hypoechoic fluid pathways extraintestinal and contrasting effects due to gas contained in them. The fistulas often lead to the formation of abscesses. Abscesses are extraintestinal, are hypoechoic to hypoechoic and may contain gas inclusions.

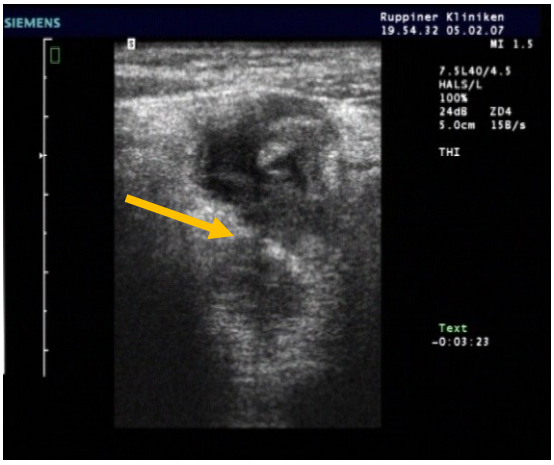

Fig. 7.18. Fistula in CD

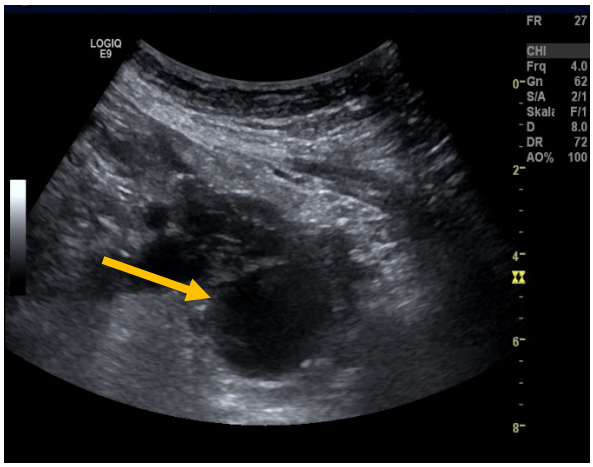

Fig. 7.19. Abscess in CD

Another complication is CD stenosis. Here, US can help to show the extent of the obstruction and to verify the type and length of the stenosis. US can be helpful in differentiating between an acute inflammatory stenosis and a chronic fibrous one and thus also determine the therapy (conservative or surgical/interventional).

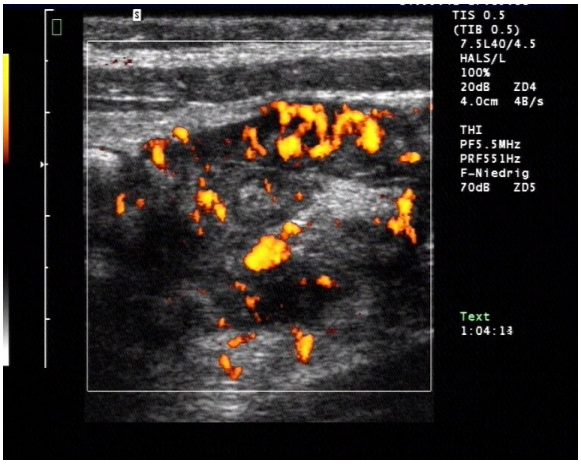

Fig. 7.20. Stenosis in acute situation (hypervascularized)

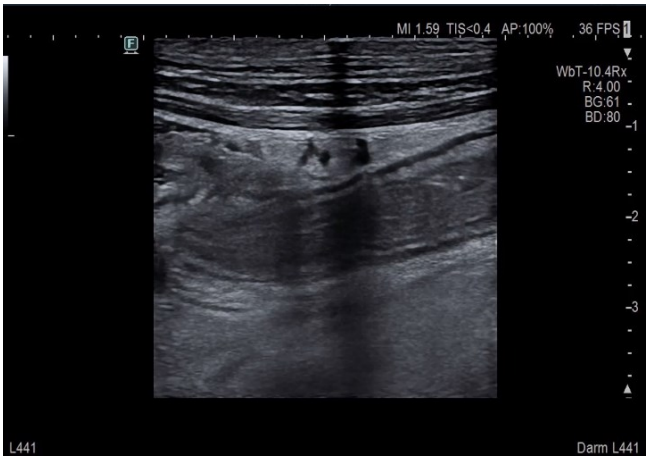

Fig.7. 21. Chronic stenosis

b) Ulcerative colitis

Ulcerative colitis also shows wall thickening, but usually only up to 8-10 mm while maintaining the layering. The extent is continuous, and the inflammation or layer thickening is limited to mucosa and submucosa in most cases. Only in very severe cases can the deep ulcers or crypt abscesses be seen, and the surrounding area also shows inflammatory changes such as mesenteritis (inflammatory mesenteric edema), lymphadenitis and small amounts of ascites. These extraintestinal accompanying phenomena are common in CD.

US can provide information on activity in addition to laboratory assessment and endoscopic/histological assessment. Colour Doppler is particularly helpful here, as is the extent of the paraintestinal reactions.

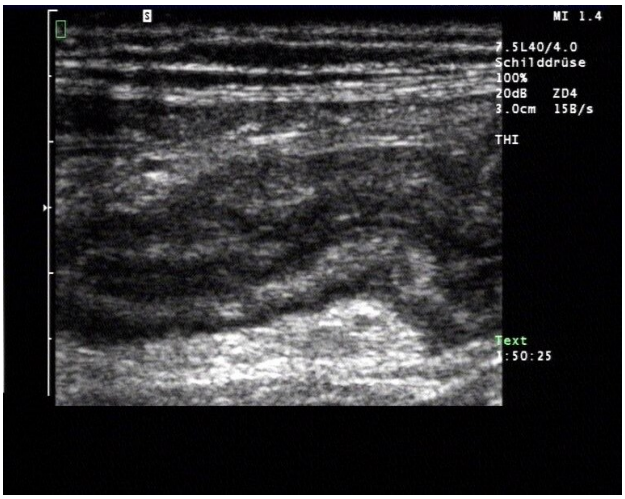

Fig. 7.22. Typical image of ulcerative colitis

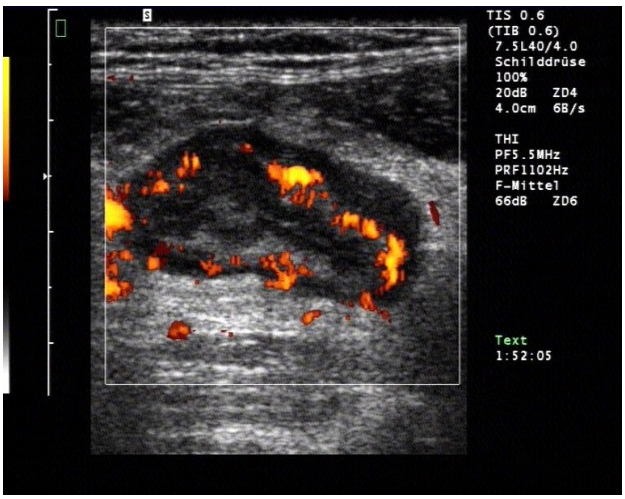

Fig. 7.23. UC activity in Colour Doppler

Appendicitis

To locate the appendix in the right lower abdomen, guiding structures should be used: cecum pole, iliac vessels, psoas muscle.

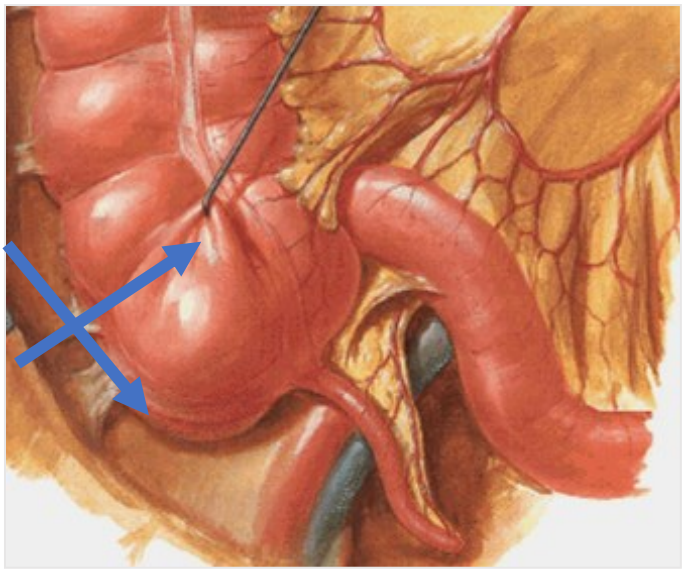

Fig. 7.24. Anatomical guiding structures to find appendix

The search for the normal appendix should be practiced regularly. Those who are experienced will succeed in more than 50% of cases. Then the pathologically altered appendix can also be identified with certainty.

Signs of appendicitis are:

- diameter of appendix > 8 mm
- rigid wall
- fecal stone
- surrounding mesenteritis
- accompanying lymph adenitis
- local fluid accumulation

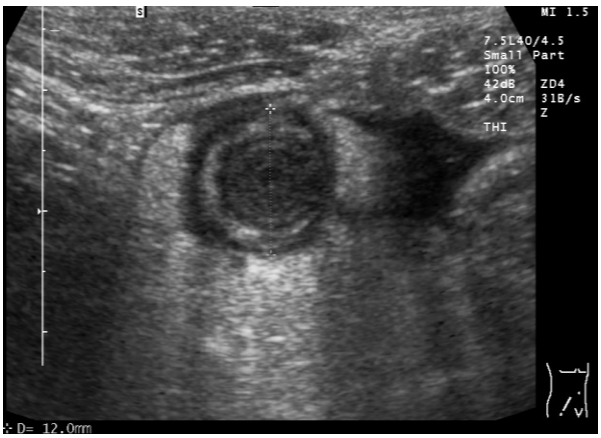

Fig. 7.25. Acute appendicitis (transversal)

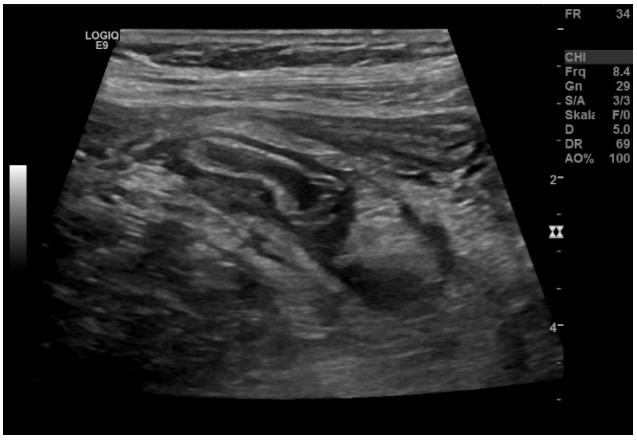

Fig, 7.26. Acute appendicitis

The use of US in acute diagnostics increases accuracy (reduces false positive findings), saves time compared to radiological imaging and improves diagnostics, particularly in children, geriatric patients and in atypical positions. Training by the surgeons themselves has significantly improved the methodology and acceptance. It is possible to differentiate the disease from other acute diseases of the right lower abdomen (increased specificity) and to identify complications such as abscess formation and perforation.

Diverticulitis (diverticula diseases – DD)

The formation of diverticula is primarily found in the sigmoid colon. This part of the colon can be examined well by US. Gas-filled, non-inflamed larger diverticula can be easily visualized. Pain in the left lower abdomen determines the direction of the ultrasound probe when diverticulitis is suspected. Typical signs of inflammation in addition to clinical signs (pain and inflammation laboratory results) are shown below and assigned to the stages.

Tab. 7.3. Complications and stadium (classification of DD)

Stage	Designation	US signs
Typ 0	asymptomatic DD	diverticula with gas „outside“ of bowel
Typ 1	uncomplicated DD	
Typ 1a	no phlegmon	inflammatory diverticula, thicker wall
Typ 1b	with phlegmon	more mesenteritis, liquids
Typ 2	complicated DD	
Typ 2 a	microabscess	abcess < 3 cm, < extra-GIT gas
Typ 2 b	macroabscess	abscess > 3cm, free perforation, liquids
Typ 2 c	perforation	free perforation and peritonitis
Typ 3	chronic DD	relapses
Typ 4	bleeding of diverticula	

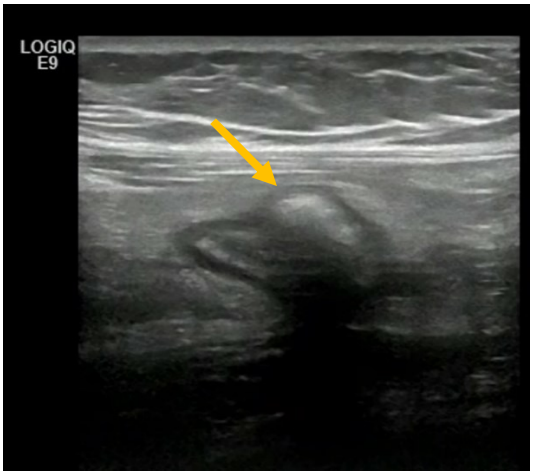

Fig. 7.27. Diverticulosis

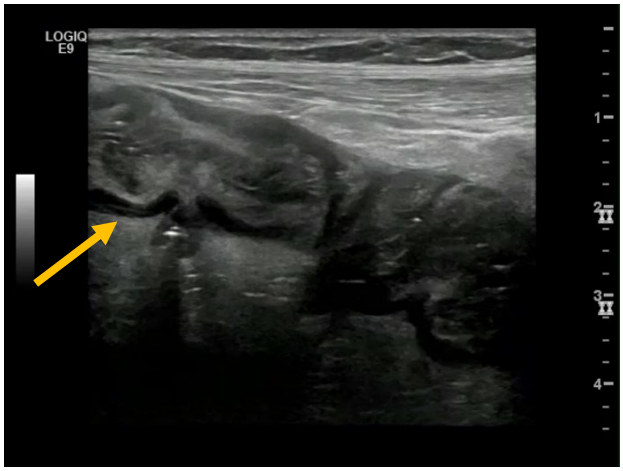

Fig. 7.28. Diverticulitis Typ 1 b

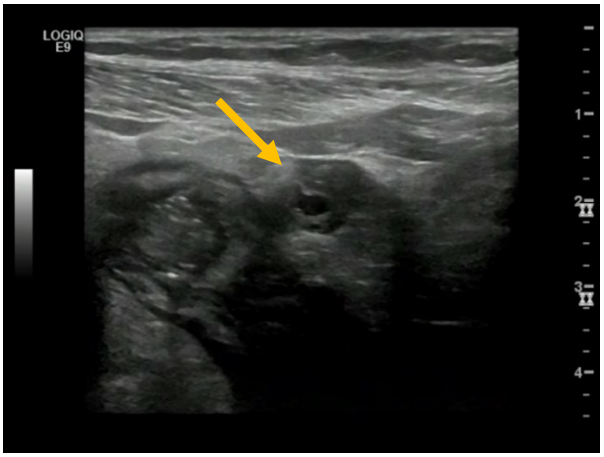

Fig. 7.29. Diverticulitis Type 2 a

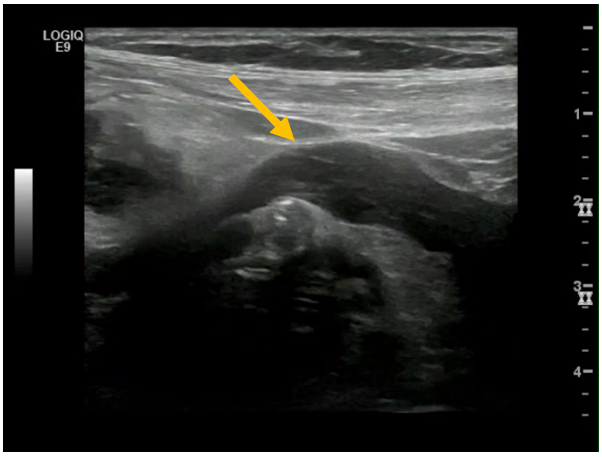

Fig. 7.30. Diverticulitis Type 2 b

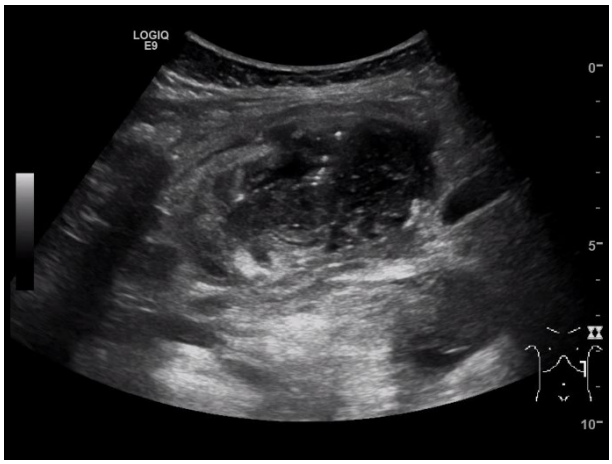

Fig. 7.31. Diverticulitis Type 2 b

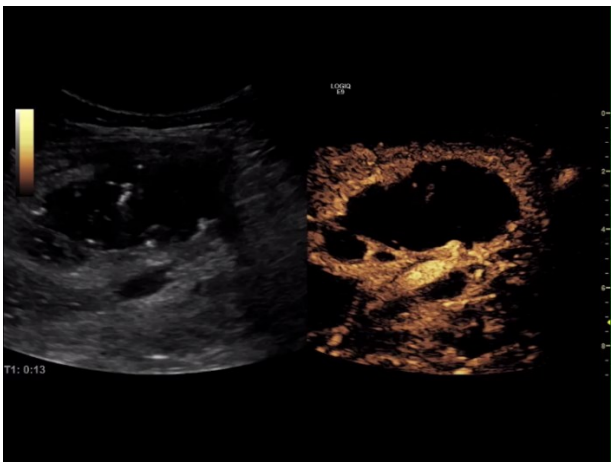

Fig. 7.32. CEUS in differentiation of abscess

US should be the first examination for known reasons. If complications are suspected (stage 2) and the image is inadequate, it is recommended to complete the examination with a computer tomography (CT). Contrast-enhanced ultrasound (CEUS) helps us to plan interventional or surgical treatment.

Intestinal emergencies

Emergencies threaten the patient and require quick decisions. US can set the course in a time-saving manner. The emergencies in the field of the GIT include bowel obstruction (ileus), perforation and ischemia.

Bowel obstruction (ileus)

If the passage is obstructed, particularly in the small intestine, there is an increase in fluid in the lumen and thus distension. In the case of ileus, this reaches more than 3 cm. And the peristalsis changes. It can be increased in the initial phase as the intestine tries to overcome the resistance. However, unlike other forms of hypermotile intestine, it no longer constricts completely. The liquid contents of the small intestine move back and forth; it swings (pendulum peristalsis). The US can determine the height of the obstruction very well. It is recommended to systematically examine the stomach transspleenally, then the small intestine in the left upper abdomen (jejunum) and finally the intestine in the right lower abdomen (terminal ileum). This 3-step sonography according to Hollerweger is helpful in daily practice. The causes of an obstruction are varied.

The most common are adhesions after previous operations and hernias. Stenoses in Crohn's disease, intussusceptions or tumors are less common. US shows the distension and the disturbed peristalsis much earlier than, for example, an X-ray overview. The ileus or obstruction can be detected around 6 hours earlier.

Tab. 7.4. Causes of obstruction (adapted to Hollerweger)

Detectable on US	Difficult to detect on US	
Small bowel		
hernia, incarcerated	**adhesion**	
intussusception	anatomical stenosis	
tumor (prim, peritonealcarc)	bezoar	
inflammatory stenosis (CD)	volvulus	
gallstone ileus	internal hernia	
Large bowel		
tumor	post-inflammatory stenosis - diverticulitis	
inflammatory stenosis (CD)	anatomical stenosis	
	volvulus	
	post-ischemic stenosis	

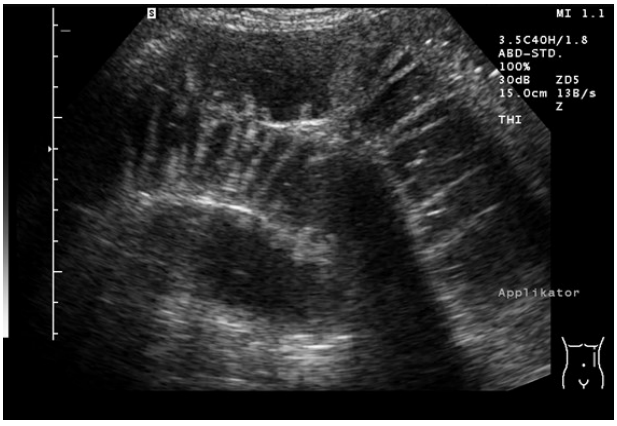

Fig. 7.33. Typical signs of small bowel ileus

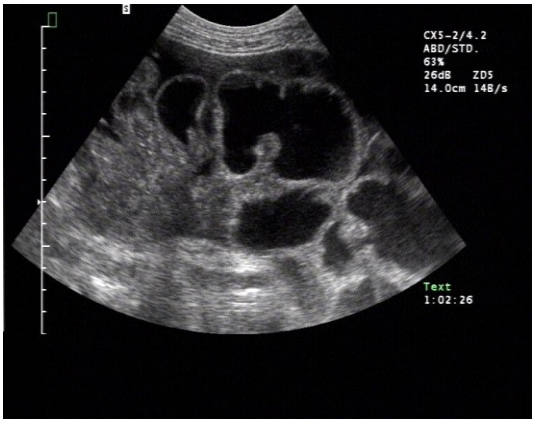

Fig. 7.34. Large bowel ileus

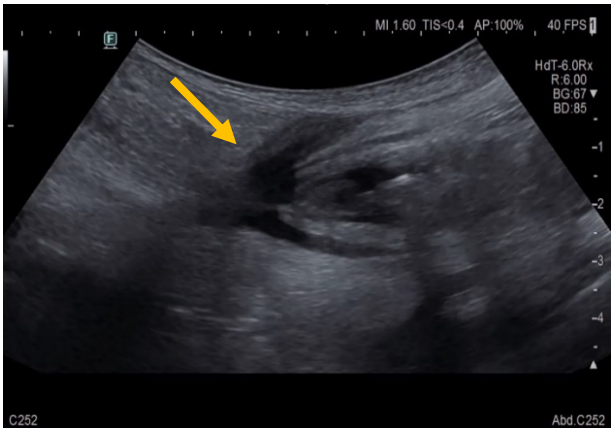

Fig. 7.35. Hernia with incarcerated SB loop

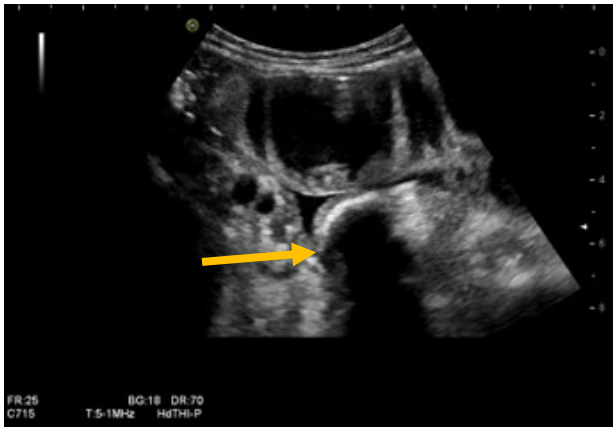

Fig. 7.36. Gallstone ileus

Perforation

Gas detection is a domain of US. However, it is sometimes difficult to differentiate between gas within the GIT lumen and free gas in the peritoneal room. The most reliable way to differentiate is when gas can be visualized in "forbidden" places. This is the case, for example, between the liver and the lateral abdominal wall. The gas also moves more during inspiration and expiration if it is located in the lumen of GIT. The causes of perforation can be varied.

Causes of Perforation:

- gastric / duodenal ulcer
- inflammatory bowel disease
- (diverticulitis, appendicitis, IBD)
- postoperative, suture insufficiency
- iatrogenic (endoscopy)
- injury, foreign body
- tumor

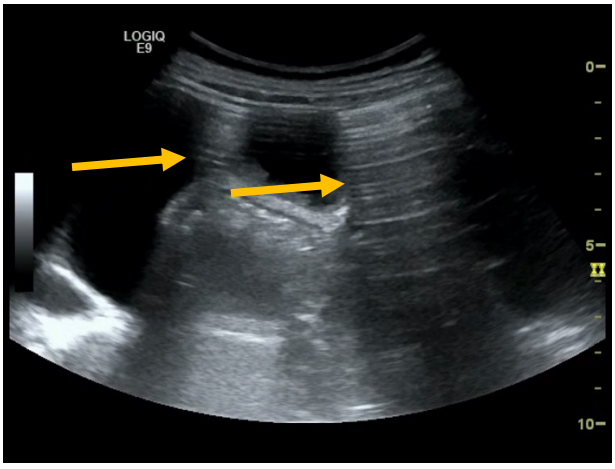

Fig. 7.37. Free gas and dilatated bowel loops

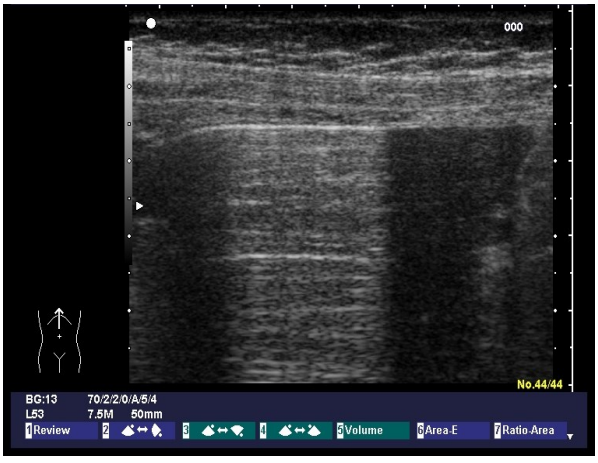

Fig. 7.38. Free gas between liver and abdominal wall

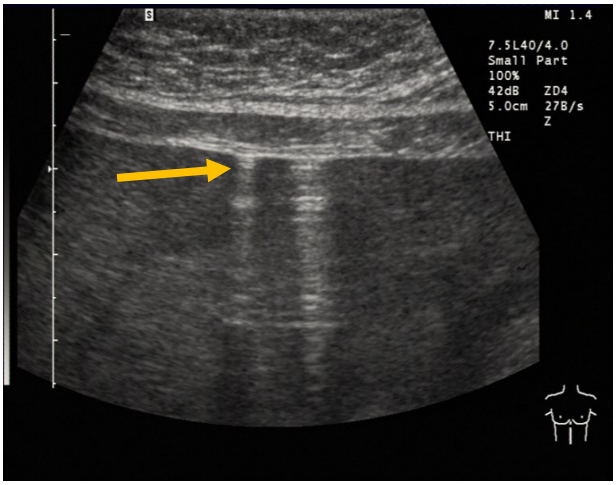

Fig. 7.39. Small amounts of free gas ventral of liver

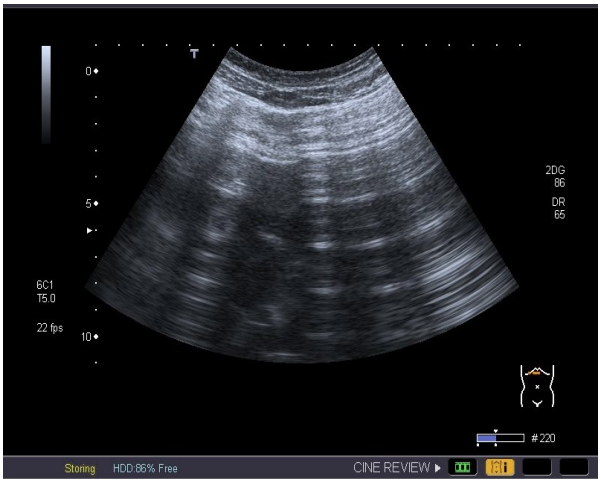

Fig. 7.40. Massive gas collection, no organ visible

US can also show smallest amounts of free gas (macro bubbles). However, determining the amount is difficult and must be left to CT if relevant. The advantage of imaging (including US) is that it can show even local gas accumulations. Unusual gas accumulations, e.g. in the retroperitoneum, can also be shown.

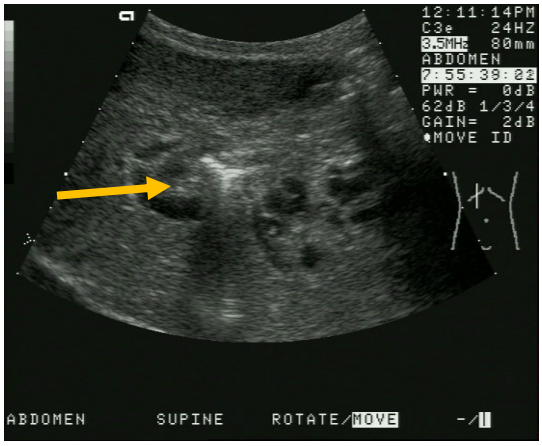

Fig. 7.41. Local perforation with gas collection liver collection

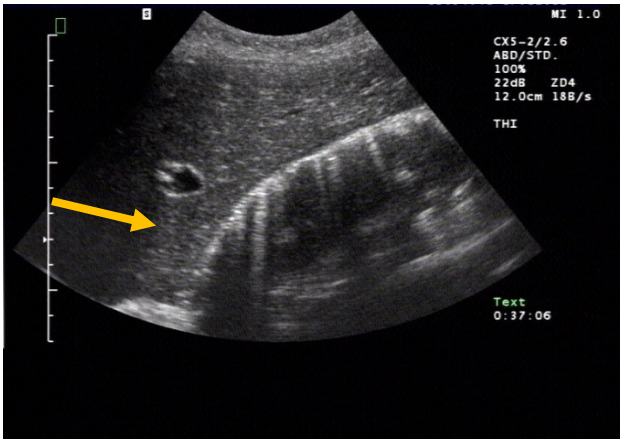

Fig. 7.42. Retroperitoneal perforation with gas in the surrounding the kidney

Ischemia

Ischemia can be highly acute (arterial) or chronic (arterial and venous thrombotic). Ischemic colitis typically shows a hypoechoic thickened wall up to 1 cm with raised layers. In the repair phase, the intestine in the colour doppler can already appear hypervascularized. The acutely ischemic small intestine is also hypoechoic, hypovascularized and aperistaltic.

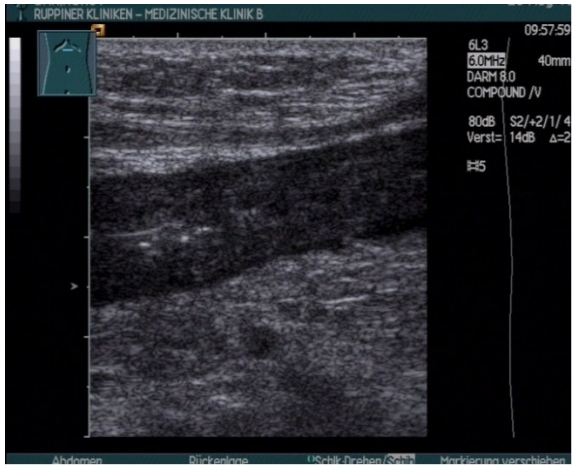

Fig. 7.43. Echopoor wall in ischemic colitis

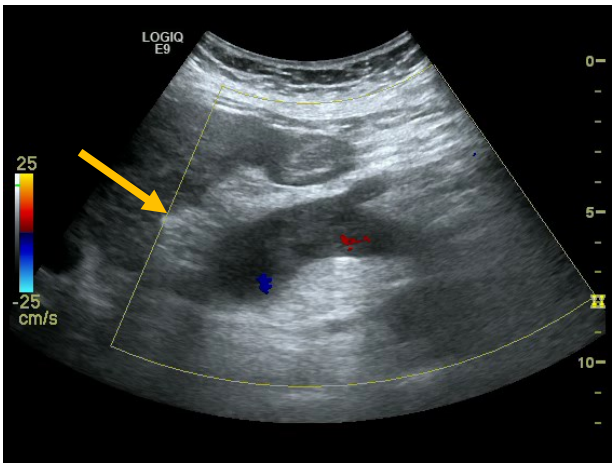

Fig. 7.44. Acute thrombosis of mesenteric vein

Miscelleaneous

Intusseption

An intusseption or intussusception is painful and is usually accompanied by an obstruction of passage. It can be temporary, for example, in the case of hypermotile bowel (e.g. sprue). Tumors or enlarged lymph nodes promote the invagination of a section of small intestine into the preceding section. A common location is the ileocoecal region. In children, repositioning can be carried out under sonographic vision.

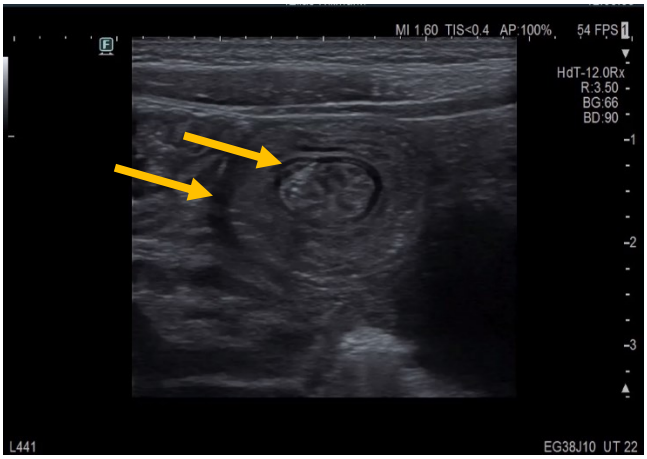

Fig. 7.45. Invagination in a child

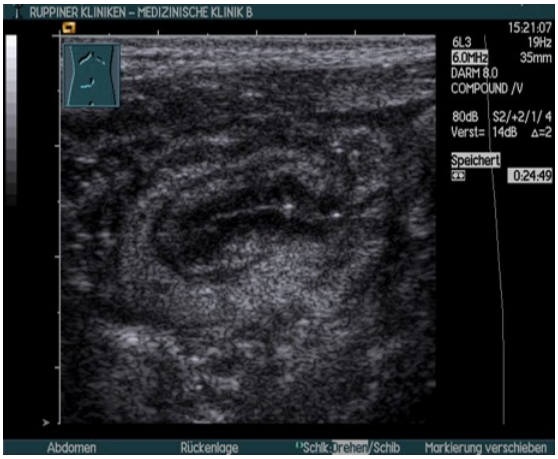

Fig. 7.46. Invagination in CD

Tumours

The detection of tumours is generally not a primary domain of US. In the colon in particular, only the larger tumours (T3+4) are clearly visible. Smaller tumours are usually missed by US due to the incomplete intestinal wall imaging. In the small intestine, the results with US are better

because there is more fluid filling and less disruptive gas. In this respect, it is worth looking for a small intestine tumour if NET is suspected or secondary examination with colour doppler and CEUS in the case of suspicion NET or GIST. Tumours from 1.5 to 2 cm can certainly be found sonographically. In the colon, US is not a method for polyp detection or tumour screening. The assignment of an abdominal tumour is possible through the connection to the intestinal wall or the intraluminal gas accumulation. The colour doppler can be helpful in the differential diagnosis of a malignant lymphoma (hypervascularized).

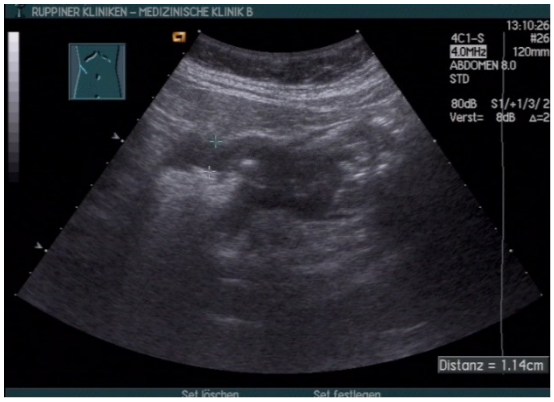

Fig. 7.47. Echopoor tumour of large bowel, colon carcinoma

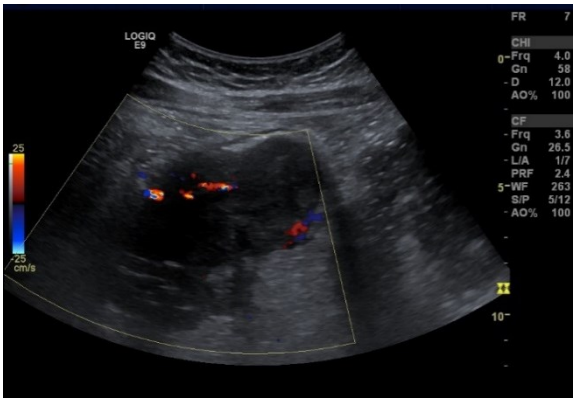

Fig. 7.48. Echopoor hypervascularized tumour of colon, malignant lymphoma

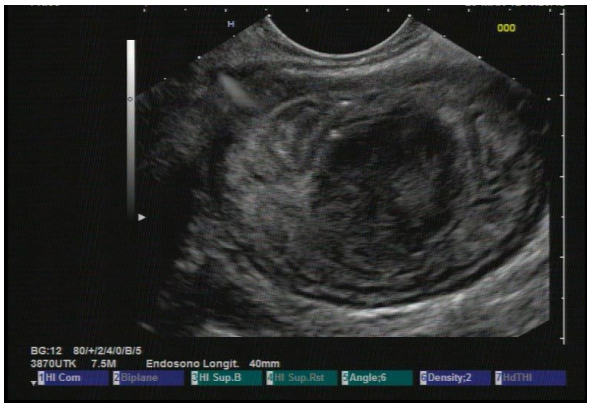

Fig. 7.49. Small bowel (jejunum) tumour, NET

Special techniques (CEUS, elastography, INVUS, PNUS, EUS)

When is the use of contrast enhanced ultrasound (CEUS) helpful? In any case, contrast media helps with the exact differentiation and size determination and thus also with the decision on treatment for abscesses (CD, diverticulitis). In abscesses, the pus-filled abscess cavity remains without enhancement, while the inflammatory surrounding infiltrate enriches contrast media. Acute ischemia can only be detected with contrast media in the highly acute phase. Contrast media has also been used to assess activity in IBD, but has not been established in everyday practice.

The use of elastography is being discussed in the differentiation of fibrous and acute inflammatory stenoses in CD, but has not yet been relevant in everyday practice.

US guided interventions (drainages) are indicated for proven abscesses and are the method of choice here. Diagnostic punctures of GIT tumours can play a role if endoscopic access is difficult or impossible.

Perineal ultrasound (PNUS) is an uncomplicated method for detecting distal intestinal fistulas or abscesses. It is also used to assess anal tumours. It can be performed using the normal transducer technique (convex probe and linear probe) and can narrow down the indication for rectal endoscopic US (rEUS) or MRI.

Endosonography is a specialized US application in addition to percutaneous diagnostics and is indicated for the following indications in the GIT: diagnosis of submucosal processes (esophagus, stomach, rectum), staging of GIT tumours.

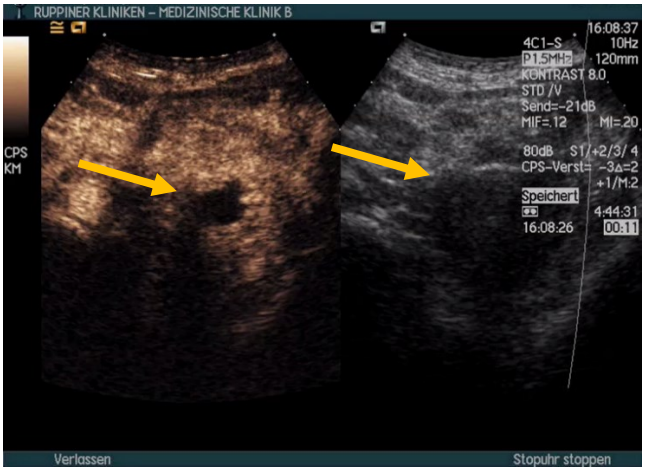

Fig. 7.50. CEUS in diagnostics of CD abscess

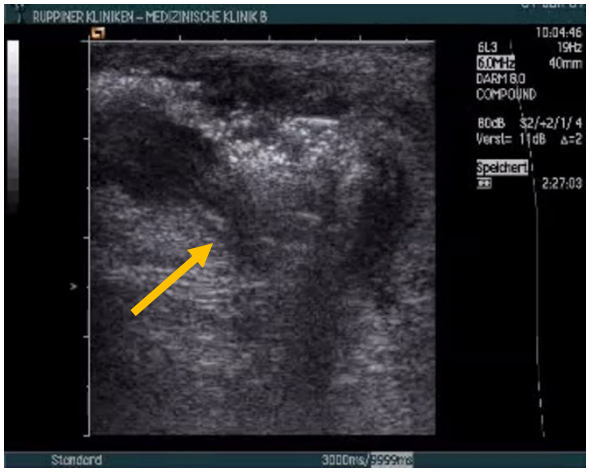

Fig. 7.51. PNUS shows perineal fistula and abscess

Tab. 7.5.Summary Importance of GIUS for diseases and BG

Indication	Importance of US	Remark
Ileus	Emergency diagnostics	1st method
Perforation	Emergency diagnostics	1st method
Appendicitis	Acute diagnostics	1st method (?)
Diverticulitis	Acute diagnostics	1st method
IBD		
CU	extent, activity	in primary diagnostics and follow up
CD	staging, activity, complication	in primary diagnostics and follow up, in complications
Enteritis	Differential diagnosis	
Tumour	Complementary method, TNM staging	Large colon tumours DD of tumours (?)
Polyps	No significance	Endoscopy 1st method

Selective references

1. EFSUMB GIUS Guidelines. Edit by Gilja OH:
    - Nylund K at al. EFSUMB Recommendations and Guidelines for Gastrointestinal Ultrasound. Part 1: Examination Techniques and Normal Findings. Ultraschall Med. 2017 Jun;38(3):e1-e15. doi: 10.1055/s-0042-115853.
    - Maconi G at al. EFSUMB Recommendations and Clinical Guidelines for Intestinal Ultrasound (GIUS, Part 2) in Inflammatory Bowel Diseases. Ultraschall Med. 2018;39(3):304-17.
    - Nuernberg D at al. EFSUMB Recommendations for Gastrointestinal Ultrasound Part 3: Endorectal, Endoanal and Perineal Ultrasound. Ultrasound Int Open 2018; 4: 1–18.
    - Dirks K at al. EFSUMB Position Paper: Recommendations for Gastrointestinal Ultrasound (GIUS Part 4) in Acute Appendicitis and Diverticulitis. Ultraschall in Med. 2021 DOI https://doi.org/10.1055/a-0824-6952.
    - Dietrich CF at al. EFSUMB Gastrointestinal Ultrasound (GIUS Part 5) Task Force Group: Celiac sprue and other rare gastrointestinal diseases ultrasound. Features. Med Ultrason 2019, Vol. 21, no. 3, 1-17
    - Hollerweger A at al. Gastrointestinaler Ultraschall (GIUS) bei intestinalen Notfällen Ein EFSUMB-Positionspapier. / Gastrointestinal Ultrasound (GIUS Part 6) in Intestinal Emergencies - An EFSUMB Position Paper. Ultraschall Med ; 41(6): 646-657, 2020 Dec
    - Maconi G at al. Gastrointestinal Ultrasound in Functional Disorders of the Gastrointestinal Tract - EFSUMB Consensus Statement. GIUS Part 7. Ultrasound Int Open 2021; 7: E14–E15.
2. WFUMB Book Chapter 12, 19, WFUMB ULTRASOUND BOOK
3. EFSUMB Course Book, 2nd Edition 2019. Editor: Christoph F. Dietrich. www.efsumb.ECB
4. Schmidt G, Greiner L, Nürnberg D. Differential diagnosis of sonography. Thieme Stuttgart 2017. 4th edition
5. Hollerweger A et al. Bowel Obstruction: Sonographic Evaluation. UIM/EJU. 2015; 36.
6. Atkinson NS, Bryant RV, Dong Y, et al. WFUMB Position Paper. Learning Gastrointestinal Ultrasound: Theory and Practice. Ultrasound Med Biol 2016;42:2732-2742
7. Petersen F et al. Why is ultrasound needed in inflammatory bowel disease? *Med* Ultrason 2025:0, 1-10 Online first. DOI: 10.11152/mu

8. US IN INTERVENTIONAL PROCEDURES

Tudor Moga, Felix Bende
WFUMB Center of Education Timișoara, Romania

1. Introduction

Ultrasound has been used for procedural guidance almost since its debut as an imaging modality. Its ability to provide real-time images without exposure to ionizing radiation presents significant advantages over alternative techniques. Advances in ultrasound technology and methodology have further expanded its applications and improved the accuracy of ultrasound-guided interventions. Ultrasound is increasingly recognized as the preferred guidance tool for a wide range of interventional procedures.

What makes ultrasound the preferred choice for many procedures? The reasons are both technological and economic:

Advantages of Ultrasound as an Image Guidance Tool:

- Real-time imaging
- Enhanced accuracy, leading to reduced procedure time and cost
- Direct vessel visualization in real time
- Multiplanar imaging capability for better spatial assessment
- Portable and widely available, ensuring accessibility
- Radiation-free, eliminating exposure to ionizing radiation

Unique Advantages of Ultrasound Guidance:

- Biopsy of small lesions that are not detectable on non-contrast CT or are only briefly visible with contrast-enhanced CT (CECT).
- Biopsy or aspiration of lesions that are difficult to access using CT guidance.
- Utilization of transvaginal, transrectal, or trans-perineal approaches for biopsy, aspiration, and drainage of deep pelvic masses and fluid collections.
- Direct probe compression can be utilized to shift bowel loops away from biopsy targets, helping to control intra-procedural bleeding and reducing the risk of post-procedure bleeding complications.
- Pre-procedure ultrasound lesion characterization can act as a diagnostic aid, offering greater confidence in diagnosis and potentially preventing unnecessary or high-risk procedures.

2. Principles of Ultrasound Guidance

2.1. Image Acquisition and Optimization

The key point of a successful ultrasound-guided procedure relies on obtaining high-quality images. This involves:

- Transducer Selection: The choice of transducer depends on the target depth and the anatomical region. Linear probes (high frequency, 7–15 MHz) are ideal for superficial structures, while curvilinear probes (low frequency, 2–5 MHz) are preferred for deeper structures.
- Image Orientation: Understanding the orientation of the ultrasound image is crucial. Typically, the left side of the screen represents the probe marker side however the examiner should have a good spatial orientation before proceeding to the intervention.
- Gain and Depth Adjustment: Proper gain settings and depth selection enhance image clarity and ensure visualization of the target structure and needle path.

2.2. Needle Visualization Techniques

Precise needle placement is fundamental to successful ultrasound-guided interventions. In the most commonly used approach, the "freehand technique," two primary methods are utilized to visualize the needle the “in-plane” and “out-of-plane” sections however, there are many others factors influencing needle visibility:

- Large-bore needles are more visible and easier to maneuver under ultrasound guidance, however, their use is associated with greater tissue trauma and increased patient discomfort. In contrast, small-bore needles are more challenging to visualize but tend to produce fewer artifacts, making them the preferred option for superficial structures. Needles for most interventional procedures typically range from 24G to 16G (0.5–1.2 mm), with size selection based on clinical indication, target characteristics, and proximity to high-risk structures.

Needle visibility in ultrasound depends on the needle-beam angle, with optimal visibility occurring near 90° due to increased echo reflection from the needle’s smooth metallic surface (Figure 8.1).

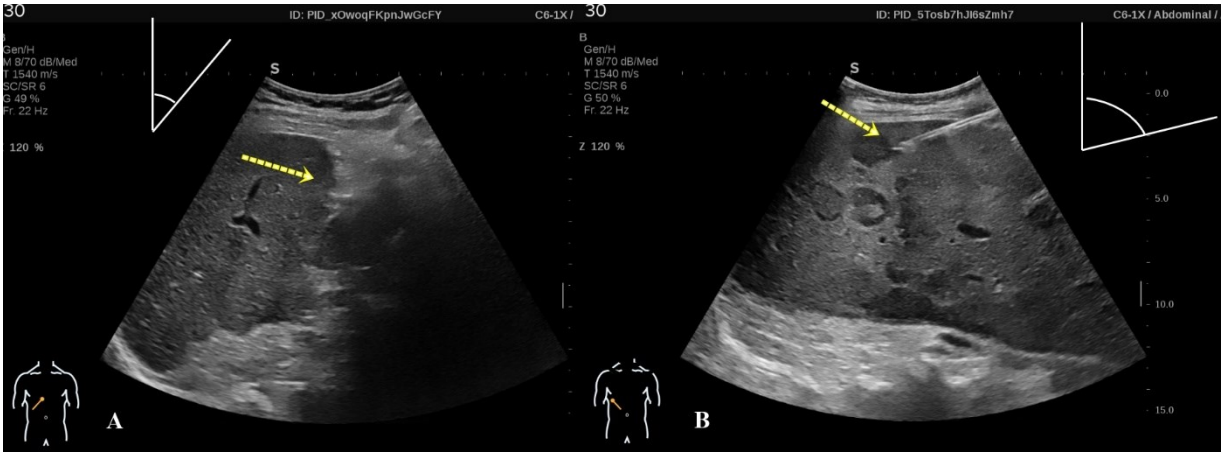

Fig. 8.1. (A) Ultrasound-guided liver tumor biopsy with a narrow needle angle, resulting in poor needle visibility (yellow arrow). (B) A wider needle angle, significantly enhancing needle shaft visualization, demonstrating the direct relationship between needle angle and visibility under ultrasound.

- Guidewires are crucial in ultrasound-guided procedures (Seldinger technique), usually bridging Chiba needles and specific catheters. The preferred ones are hydrophilic, that have stiff or flexible tips, come in straight, angled, or curved shapes, and typically measure 0.018 or 0.035 inches in diameter. Inserting a guidewire enhances needle shaft visibility, but this effect is lost with tightly fitting guidewires due to the absence of an acoustic interface; similarly, stylet and hollow needles have comparable visibility, though transiently improved echogenicity can be achieved by repeatedly pumping the stylet, a maneuver that generates microbubbles around the needle tip and shaft (Figure 8.2).

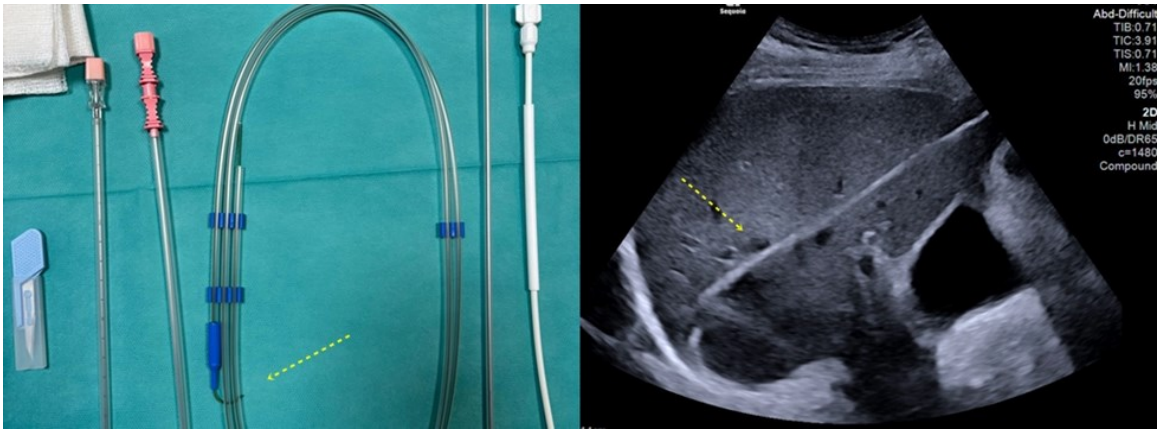

Fig. 8.2. Chiba needle, guidewire (yellow arrow), and drainage tube in a procedural setting.
In the right side, An US guided drainage on a liber abscess with an increased visibility once the guide-wire is introduced thru the Chiba needle.

- In-Plane Technique: The needle is aligned parallel to the ultrasound beam, allowing full visualization along its length. This technique provides better control but requires precise alignment (Figure 8.3-B).

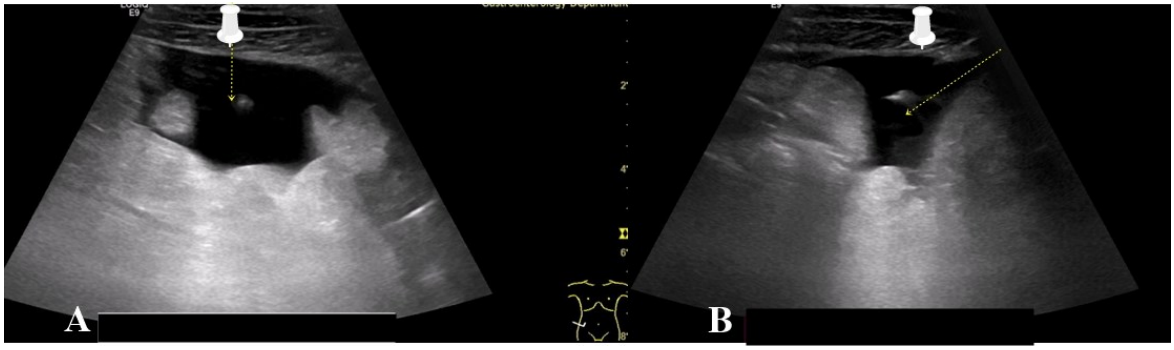

Fig. 8.3. (A) Ultrasound-guided aspiration, showing only the needle tip due to the "out-of-plane" approach (dotted arrow indicating the direction of the needle). (B) "In-plane" approach, allowing full visualization of the needle trajectory, enabling better control and accuracy.

- Out-of-Plane Technique: The needle crosses the ultrasound beam perpendicularly, making only a cross-section of the needle visible. This method is often used when space constraints prevent an in-plane approach but requires careful angulation to avoid missing the needle tip (Figure 8.3-A).
- To enhance accuracy, needle steering devices have been developed to improve needle visibility and trajectory control. Some applications employ mechanized stabilization or electromagnetic tracking to maximize needle-sample alignment within the ultrasound beam, especially in deeper or more complicated procedures.

2.3 Patient Positioning and Preparation

Proper patient preparation enhances procedural efficiency and comfort. Considerations include:

- Patients should receive clear and concise information regarding the procedure, its risks, and alternatives. Informed consent is required for procedures with significant risks or potential side effects.
- Patients should dress appropriately, remain fasting, and have their blood tests, including coagulation status and anticoagulant use, reviewed beforehand. INR should be corrected to <2.0 for low-risk procedures and <1.5 for moderate to high-risk procedures. For patients with <70,000 platelets, a platelet transfusion is required before high bleeding risk procedures.

- Ergonomics: Both the patient and the operator should be positioned to allow easy probe and needle manipulation while ensuring a stable hand position. Environmental distractions, such as light, noise, and movement, should be minimized as much as possible.
- Sterile setting: Procedures requiring sterile technique (e.g., vascular access, biliary access, drainages, biopsies) should follow strict aseptic protocols, including sterile probe covers and gel. Special probe and machine cover allow image guidance and adjustments while minimizing infection risk.
- Local anesthesia, with or without sedation, is standard for INVUS procedures. Some physicians, to ensure effective pain control along the puncture tract, prefer using US guidance for local anesthesia administration, while vasoconstrictors like epinephrine can be used to limit systemic absorption of the anesthetic.

2.5. Safety and Complication Prevention

Avoiding Critical Structures: Careful scanning before needle insertion helps identify nerves, vessels, and other sensitive structures.

- A check-lists to confirm patient readiness and equipment availability is recommend for a standardize work flow. While fine-needle procedures are often outpatient, others require hospitalization.
- A successful ultrasound-guided intervention relies on selecting the optimal path, preferably the shortest, unless a safer alternative is needed to avoid risky structures. Fine needles can safely pass through the stomach and small bowel, but colon punctures should be avoided due to infection risk, except in rare cases for abscess drainage.
- Real-Time Monitoring: Continuous visualization of the needle trajectory, including both the visible and obscured segments during its passage, along with key anatomical landmarks, helps minimize complications such as vessel perforation, organ injury, or unintended drug deposition (Figure 8.4).

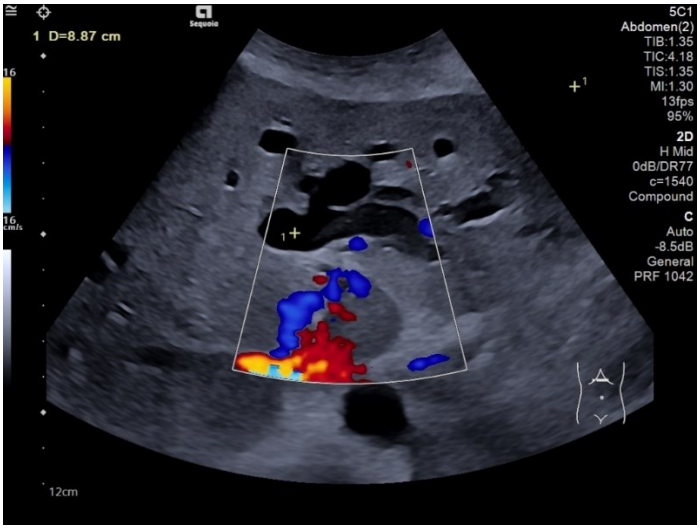

Fig. 8.4. Color Doppler image of a patient with dilated bile ducts during pre-procedural evaluation. Yellow markers indicate the intended needle direction.

- Color Doppler and power Doppler imaging aid in identifying blood vessels and differentiating vascular from non-vascular structures while in select cases, CEUS improves delineation of lesions and vascular structures for more precise interventions.
- Patients should be monitored for at least two to four hours, as most complications occur during this period.
- According to a large multicentric study made on 8172 US-guided intraabdominal interventions, clinically significant bleeding occurred in 0.4% (requiring transfusion), 0.1% (surgical control), and 0.05% (radiological coiling), with fatal bleeding in 0.05% (4 patients); major bleeding risk was significantly higher in patients with INR > 1.5 ($p < 0.001$) or those on anticoagulant or antiplatelet medication ($p < 0.0333$).

3. Common Interventional Procedures Using Ultrasound

Ultrasound-guided interventional procedures are diverse and continually evolving, the most common being vascular procedures, biopsies, drainages, sclerotherapy and ablations.

3.1 Vascular Procedures

US guidance for vascular access requires a high-frequency probe (≥7MHz) for better resolution of superficial vessels. Sterile technique is essential, including probe covers, antiseptic preparation, and proper attire to minimize infection risk. Proper probe orientation is critical, most operators orient the probe for needle insertion from the right side of the screen, and consistency in orientation helps avoid confusion.

Real-time US guidance is the preferred method for vascular access, offering better outcomes than static imaging. Pre-procedure scanning of both sides of the neck helps identify the best cannulation site, assessing vessel size, patency, and proximity to surrounding structures (Figure 8.5). Hand-eye coordination is key to successful cannulation. The non-dominant hand holds the probe, while the dominant hand controls the needle. The needle tip should be tracked in real-time, with aspiration applied until blood return is confirmed, after which the guidewire or catheter is advanced under US verification.

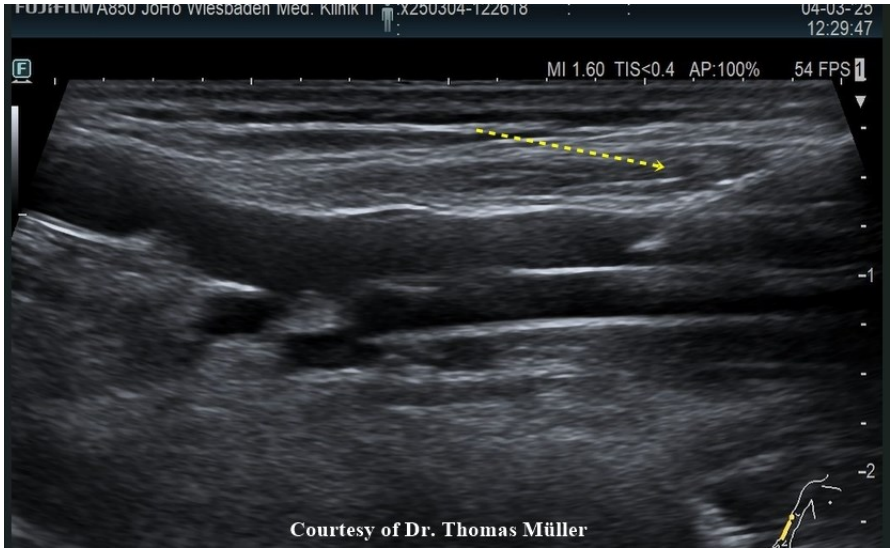

Fig. 8.5. Ultrasound-guided cannulation of the right cubital vein with a high-frequency probe. The needle is visualized in the long axis using the in-plane technique (yellow arrow).

US vessel identification is crucial to prevent accidental arterial cannulation. Veins are thin-walled, compressible, and change with respiration, while arteries are thicker, non-compressible, and pulsatile under normal conditions. Placing the patient in a head-down position helps enlarge veins and reduce air embolism risk. Color Doppler and spectral Doppler imaging aid in distinguishing vessels, as arterial flow is pulsatile (mainly during systole) and venous flow is continuous during systole and diastole. Color alone cannot differentiate veins from arteries, as it depends on flow direction relative to the probe.

Despite ultrasound (US) guidance, immediate complications occur in about 20% of internal jugular vein (IJV) central line insertions, with catheter misplacement in the right atrium (6–14%) posing a risk of cardiac perforation and tamponade. Pneumothorax and hemothorax are rare when real-time US is used (Figure 8.6).

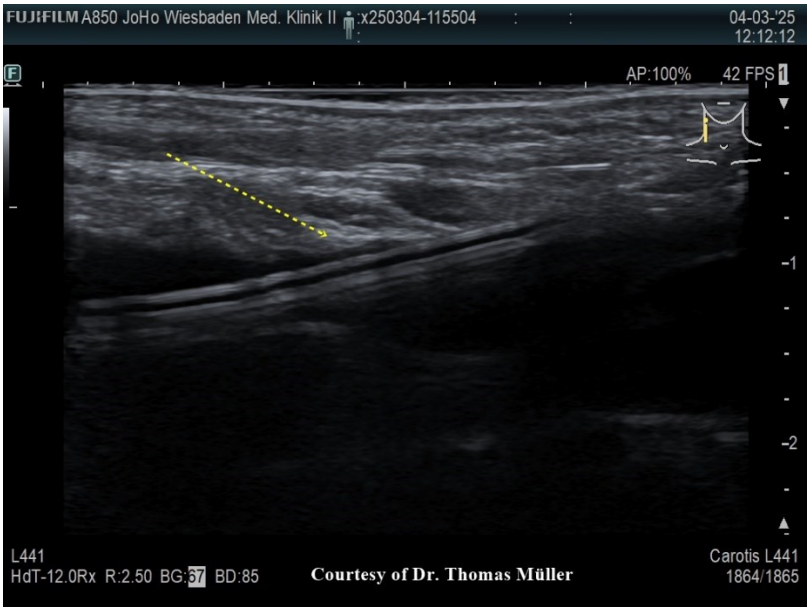

Fig. 8.6. Ultrasound-guided cannulation of the jugular vein with a high-frequency probe. The cannula is visualized in the long axis using the in-plane technique (yellow arrow).

3.2 Percutaneous Biopsies

Percutaneous biopsy is one of the most common ultrasound-guided procedures, involving tissue sampling for pathologic analysis. Except for lung, bone, and brain biopsies, ultrasound is the preferred imaging modality when feasible. Indications include masses in the breast, thyroid, liver, kidney, or enlarged lymph nodes. When the target contains liquid or viscous material, aspiration is performed using a small-caliber Chiba needle under ultrasound guidance for cytology, by means of fine needle aspiration (FNA).

Performing a percutaneous biopsy involves several steps, starting with selecting the shortest possible path while avoiding large vessels, the spleen, pancreas, and the gastrointestinal lumen whenever feasible. For liquid lesions, a Chiba needle (with or without inner needle) is advanced to suitable position in the fluid, the stylet (if any) is removed and the liquid is aspired. For solid lesions, core biopsy (CB) is preferred, as it provides histological samples for a more comprehensive pathological assessment. The two main techniques for liver biopsies are the Menghini and Tru-Cut methods.

- Menghini technique: This suction-cutting method uses a semi-automatic needle, allowing a single-pass biopsy with minimal trauma. The needle is introduced under a previous US assisted track or ultrasound guidance, and a vacuum-assisted aspiration is applied while the cutting mechanism collects the tissue sample. It is fast, efficient, and often used for diffuse liver disease, offering high tissue yield with minimal complications (Figure 8.7-A).

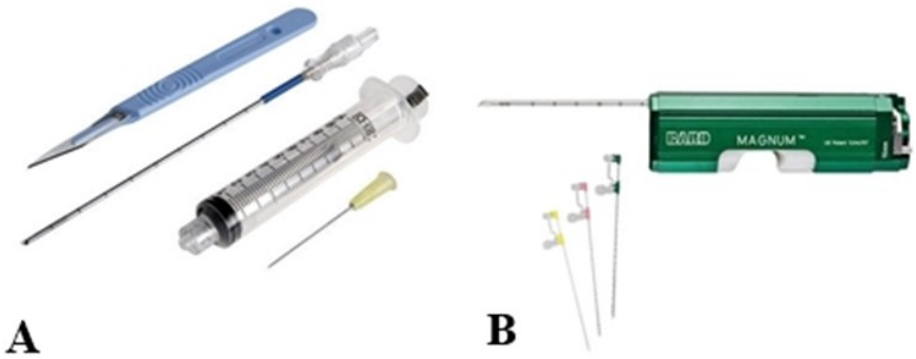

Fig. 8.7. (A) Menghini set, including a scalpel, dedicated vacuum syringe, and needle. (B) Tru-Cut needle with an automatic biopsy gun (Bard Magnum gun).

- Tru-Cut technique, mainly used in CB: A spring-loaded, semi-automatic, or automatic biopsy gun is used to obtain core tissue samples with a cutting needle. The lesion is biopsied under US guidance, always passing through healthy tissue first, to avoid bleeding (Figure 8). This technique is widely used for breast, liver, kidney, and soft tissue lesions, offering high diagnostic accuracy. Ensure the needle tip does not pass beyond the lesion into critical structures after firing. Maintain a safe margin to prevent unintended puncture of adjacent vital areas (Figure 8.7-B).

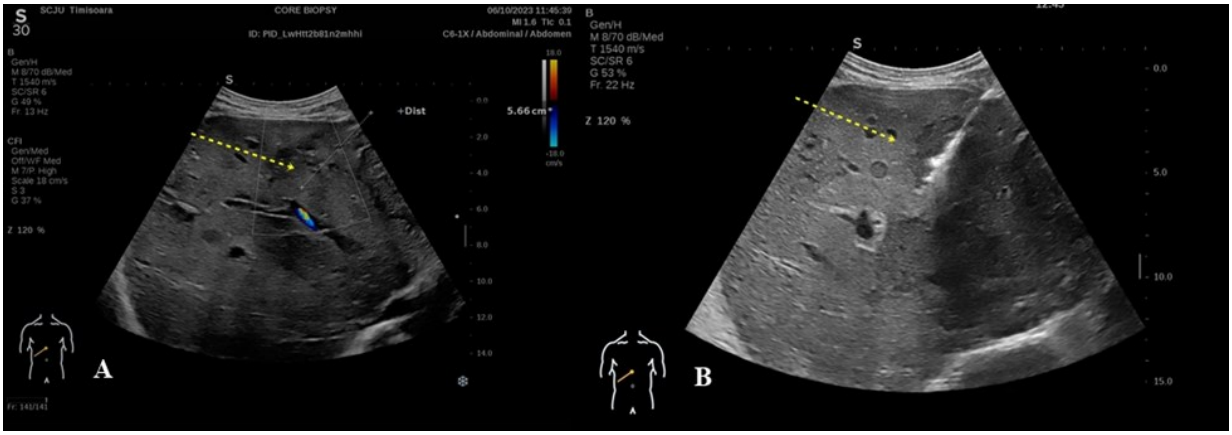

Fig. 8.8. (A) Pre-procedural evaluation of the lesion, trajectory planning, and Color Doppler assessment of nearby vascular structures. (B) Ultrasound-guided Tru-Cut needle biopsy using an automatic biopsy gun, targeting a focal liver lesion. Small air traces (hyperechoic inclusions) are visible after the needle pierces the parenchyma (yellow arrow).

The choice between FNA, Menghini, or Tru-Cut techniques depends on lesion type, location, and required tissue quality, ensuring the most accurate and minimally invasive diagnostic approach.

3.3 Drainages of fluid collections

Drainages rely on catheters to connect the skin to a target cavity, varying in stiffness, shape (pigtail, straight, star), and size. Their selection depends on clinical indication, target structure, fluid density, and patient comfort. Fluid collections have diverse causes, including inflammatory, infectious, postoperative, post-interventional, and post-traumatic conditions, and can be classified by type, location, and composition.

The use of US-guided drainage continues to expand, offering a safe and effective approach for both solitary and multiloculated fluid collections, including those connected to the gastrointestinal tract. This minimally invasive technique helps facilitate recovery while reducing the risks and morbidity associated with surgery and general anesthesia. In elderly or high-risk patients, particularly those with sepsis, drainage can serve as a temporary stabilization measure until surgery becomes feasible, though in some cases, it may be the definitive treatment.

3.3.1 Abscess Treatment

Ultrasound is the first-line imaging modality for abscess detection and drainage, providing dynamic evaluation and real-time guidance. CEUS aids in distinguishing vascularized from avascular areas, while CT imaging offers superior anatomical detail, including precise location, size, shape, and organ relationships. Ultrasound-guided abscess drainage follows a structured approach to ensure safe and effective fluid evacuation.

From large studies we know that catheter drainage is more effective than repeated needle aspiration for liver abscesses, with higher success rates and faster recovery. For abdominal abscesses, needle aspiration works well for simple abscesses <5 cm, while larger abscesses respond better to catheter drainage. In needle aspiration, a 0.9–1.2 mm Chiba needle is used under ultrasound guidance to puncture the abscess, evacuate the pus, and perform saline lavage (3–5 times) until clear fluid is obtained. This technique can be repeated if recurrence occurs and is the preferred treatment for small abscesses (≤5 cm). Catheter drainage is advised for large abscesses or suspected GIT/biliary communication. Small catheters (6–8F) suit thin pus or difficult sites, while larger ones (12–18F) handle thick pus or complex abscesses (Figure 8.9).

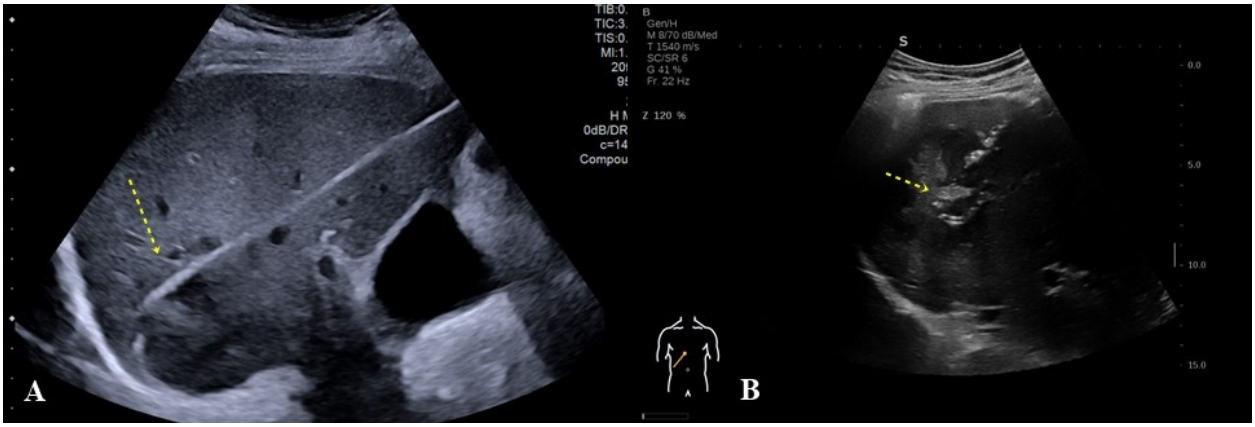

Fig. 8.9. (A) Challenging location of a liver abscess, drained using an 8 Fr catheter via the Seldinger technique (yellow arrow indicating the guidewire). (B) Large liver abscess, drained using a 10 Fr catheter via direct puncture -Trocar technique (see the deployment of the drain-yellow arrow).

There are two methods for drainage catheter insertion: the trocar (one-step) technique and the Seldinger (two-step) technique. Each has its own advantages and limitations and can be performed using a free-hand or needle-guided approach, based on the operator's preference and experience (Figure 8.10).

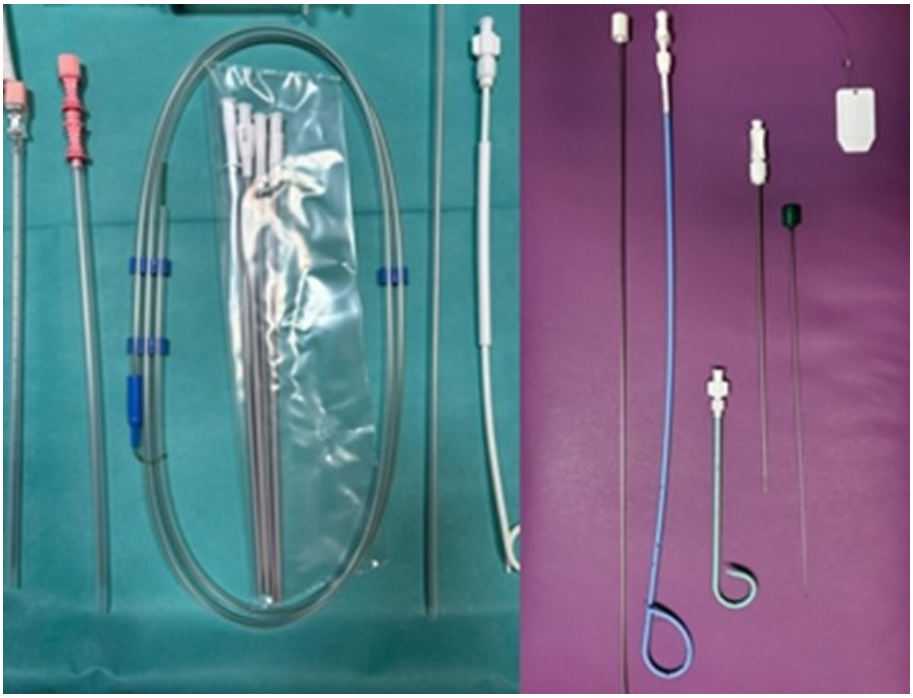

Fig. 8.10. Left: Setup for the Seldinger technique, including a Chiba needle, guidewire, dilators, and drainage tube. Right: Two drainage tubes, each consisting of a trocar and a stylet.

Treatment planning involves US-assessing the size, shape, content, and extent of the abscess, including fistula identification. Direct CEUS injection through a needle or catheter helps confirm placement and detect cavity communication at the bedside.

3.3.2 Drainage of Biliary or Urinary Obstruction

Catheter drainage treats biliary or urinary obstructions, either as definitive, temporary, or preparatory for stent placement. Access is via the biliary/urinary ducts, gallbladder, or bladder, using 7–10F catheters with locking systems.

The Seldinger technique is preferred for external biliary drainage and minimally dilated urinary calyces, while the trocar technique is used for gallbladder, bladder drainage, or severe hydronephrosis. In critically ill patients, drainage provides lifesaving relief. Percutaneous cholecystostomy is an alternative for acute or acalculous cholecystitis, serving as definitive treatment for acalculous cases or temporary relief in stone-related cases until improvement (Figure 8.11).

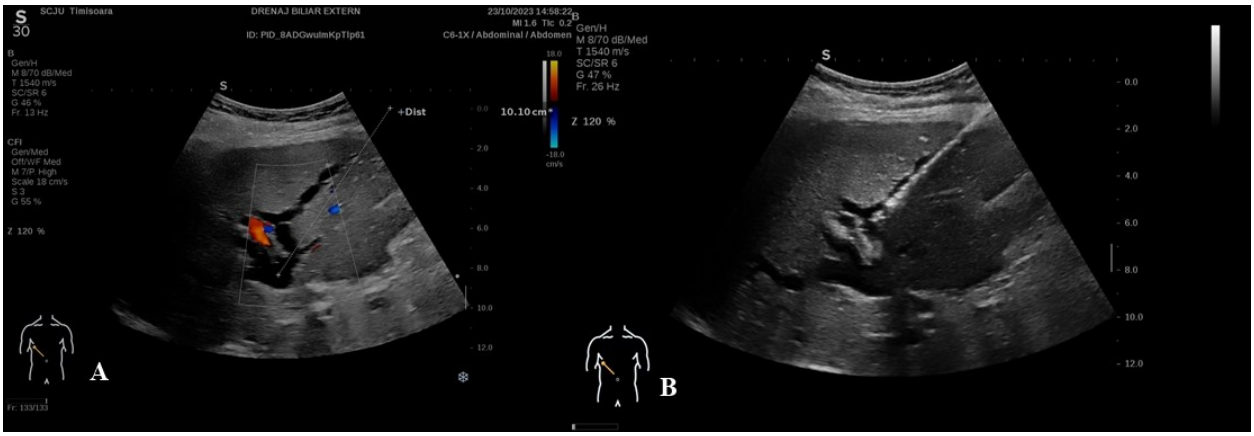

Fig. 8.11. (A) Pre-procedural evaluation of the dilated bile ducts, including precise measurements and Color Doppler assessment of adjacent vascular structures. (B) US-guided external biliary drainage with guidewire insertion through the Chiba needle.

3.3.3 Ultrasound-guided paracentesis

Paracentesis is performed for diagnostic or therapeutic purposes in cases of ascites or suspected bacterial peritonitis, with therapeutic paracentesis providing rapid symptom relief and being well tolerated. The procedure is safely performed using a 14–18G needle or a small-bore (5F–7F) catheter under US guidance, which enhances safety by providing real-time visualization of the needle tip and surrounding structures. In many cases, US assistance (pre-procedure localization) is as safe as full US guidance. Paracentesis is generally low-risk with a 1% complication rate, including fluid leakage, infection, hematoma, hemorrhage, and intestinal perforation. Strict antiseptic measures and US guidance further reduce complication risks.

Malignant ascites, occurring in ~10% of cases, is associated with various cancers and can cause pain, dyspnea, nausea, appetite loss, and mobility issues due to increased abdominal pressure. Long-term paracentesis is recommended for symptomatic patients with recurrent ascites despite repeated drainage.

3.3.4 Sclerotherapy of Non-Parasitic Hepatic Cysts

Percutaneous sclerotherapy is a minimally invasive treatment for large or symptomatic hepatic cysts (>6–10 cm), involving fluid aspiration followed by sclerosing agent injection under ultrasound guidance. It is preferred over surgery due to lower complication rates, but laparoscopic fenestration is considered for refractory cases. Multidisciplinary evaluation is essential, as treatment options include sclerotherapy, laparoscopic deroofing, or open surgery.

Ethanol (95–98%) is the most commonly used sclerosing agent, often requiring multiple sessions with catheter drainage (6–8F) or Chiba needles (18–20G), achieving up to 80–100% cyst volume reduction. Complications include pain, ethanol-induced fever, intoxication, and intra-cystic bleeding, but the procedure is generally well tolerated. Sclerotherapy is less effective in polycystic liver disease, where recurrence rates are high (77–100%).

3.4 Tumor Ablation

Percutaneous tumor ablation is a rapidly advancing field in interventional ultrasound, utilizing thermal, chemical, and electric ablation techniques with ultrasound guidance for precise probe placement, real-time monitoring, and complication detection.

Ablation methods include:

- Cryoablation: Uses helium-argon gas to induce extreme hypothermia and freeze tumors.
- Microwave and radiofrequency ablation: Convert electromagnetic radiation into heat, causing tumor necrosis.
- Ethanol ablation: Involves US-guided injection of 98% ethanol to destroy targeted lesions.
- Irreversible electroporation: Applies electric currents to trigger apoptosis in cancer cells.

Percutaneous tumor ablation is a minimally invasive treatment for primary and secondary liver tumors, renal tumors, and (para)thyroid tumors. It induces necrosis through chemical (ethanol injection, PEI) or physical (heat, cold, or electric current) methods. The goal of thermal ablation is to heat tumor tissue above 60°C, covering the tumor plus a 5–10 mm safety margin while preserving surrounding structures. Microwave ablation (MWA) (Figure 8.12) has become the preferred method in many centers due to faster ablation times, higher intra-tumoral temperatures (>150°C), and better energy penetration. Unlike RFA, MWA is less affected by the heat-sink effect, making it suitable for tumors near large vessels.

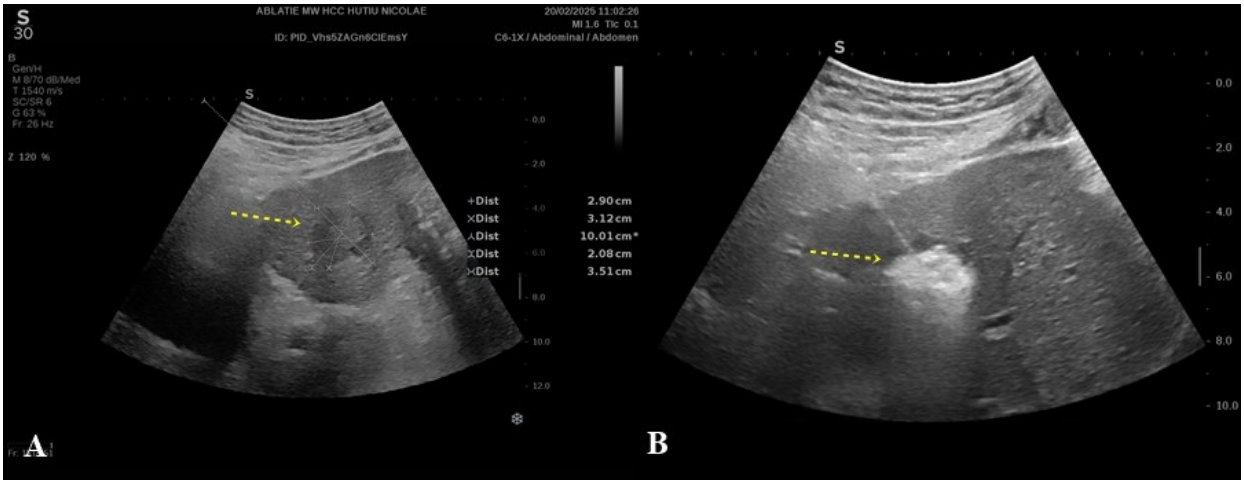

Fig. 8.12. (A) Hepatocellular carcinoma in the left liver lobe, with proper measurements. (B) Typical appearance of microwave ablation during thermal treatment, showing the characteristic echogenic cloud.

Ablation probes are placed under image guidance, with ultrasound (US) being the most commonly used modality. The procedure can be percutaneous, intraoperative, or laparoscopic. In metastatic liver tumors, ablation is a key alternative for non-surgical candidates, improving survival and quality of life. In small HCC, it is considered a first-line treatment option.

4. Technical Challenges and Limitations

Despite its many advantages, ultrasound-guided interventions have several technical limitations. Addressing these limitations requires continuous training, optimized equipment settings, and adherence to sterile protocols for safe and effective ultrasound-guided procedures.

- Operator dependency remains a key challenge, as image interpretation and needle guidance require experience and skill, leading to a learning curve that may affect procedural success.
- Image artifacts from factors like acoustic shadowing, reverberation, and refraction can obscure visualization, making it difficult to identify small lesions or needle tips, particularly in complex anatomical regions.
- Additionally, patient-specific factors, such as obesity, bowel gas interference, or deep target structures, can reduce image clarity and penetration, limiting procedural accuracy.
- Maintaining a sterile environment is another concern, as ultrasound requires contact with the patient's skin, necessitating strict infection control measures to prevent contamination, particularly in vascular access, drainages, and biopsies.

5. Innovations and Future Directions

US technology continues to evolve, expanding its role in interventional procedures through automation, enhanced imaging, and Artificial intelligence (AI) integration. These advancements aim to improve precision, reduce operator dependency, and enhance patient safety.

- AI Integration and Automation- AI and deep learning algorithms are being developed to assist with real-time image interpretation, needle tracking, and automated lesion detection. These tools can help less experienced operators improve procedural accuracy and efficiency. AI-powered systems may also predict procedural success based on pre-procedure imaging, aiding decision-making.
- Robotic-Assisted Ultrasound Interventions- Robotics and haptic feedback systems are being integrated into US-guided interventions, particularly for biopsies and ablations. These systems provide stabilization, precise movement control, and better ergonomics, reducing fatigue and human error.
- Microbubble Contrast-Enhanced Ultrasound (CEUS) for Targeted Interventions- CEUS improves lesion characterization and vascular assessment, making it particularly useful in liver tumor biopsies and ablations
- Targeted microbubble agents are being investigated for image-guided drug delivery, allowing site-specific therapy, particularly in oncology.
- Portable and Handheld Ultrasound for Point-of-Care Interventions- Advancements in miniaturized ultrasound technology have led to the development of portable and handheld US devices, expanding access to interventional ultrasound in emergency settings, rural areas, and resource-limited environments.

Selective references

1. Raja, J., Latich, I., & Mathur, M. (2021). Ultrasound-guided interventions. In J. Li, R. M. D. Chow, N. Vadivelu, & A. D. Kaye (Eds.), Ultrasound Fundamentals. Springer, Cham. https://doi.org/10.1007/978-3-030-46839-2_29
2. Miller, D. L., & Abu-Yousef, M. M. (2018). Safety of ultrasound-guided interventions: What are the risks? Radiology, 287(3), 664-673.
3. Müller, T., Martiny, H., Merz, E., Döffert, J., Wüstner, M., Lessel, W., Heynemann, H., Enzmann, T., Dudwiesus, H., Nuernberg, D., Tesch, C., Weber, M. A., Krishnabhakdi, S., Heil, J., Wree, A., & Jenssen, C. (2018). DEGUM recommendations on infection prevention in ultrasound and endoscopic ultrasound. Ultraschall in der Medizin, 39(3), 284-303. https://doi.org/10.1055/s-0044-102006
4. Moore, C. L., Copel, J. A., & Nelson, B. P. (2019). Ultrasound-guided needle placement: Principles and techniques. Ultrasound in Medicine & Biology, 45(4), 789-804.

5. Lorentzen, T., Nolsøe, C. P., Ewertsen, C., et al. (2015). EFSUMB guidelines on interventional ultrasound (INVUS), Part I. General aspects (Short version). Ultraschall in der Medizin, 36(5), 464-472. https://doi.org/10.1055/s-0035-1553601
6. Strobel, D., Bernatik, T., Blank, W., et al. (2015). Incidence of bleeding in 8172 percutaneous ultrasound-guided intraabdominal diagnostic and therapeutic interventions – results of the prospective multicenter DEGUM interventional ultrasound study (PIUS study). Ultraschall in der Medizin, 36(2), 122-131. https://doi.org/10.1055/s-0034-1399282
7. Sidhu, P. S., Brabrand, K., Cantisani, V., et al. (2015). EFSUMB guidelines on interventional ultrasound (INVUS), Part II. Diagnostic ultrasound-guided interventional procedures (Short version). Ultraschall in der Medizin, 36(6), 566-580. https://doi.org/10.1055/s-0035-1566760
8. Dietrich, C. F., Lorentzen, T., Appelbaum, L., Buscarini, E., Cantisani, V., Correas, J. M., Cui, X. W., D'Onofrio, M., Gilja, O. H., Hocke, M., Ignee, A., Jenssen, C., Kabaalioğlu, A., Leen, E., Nicolau, C., Nolsøe, C. P., Radzina, M., Serra, C., Sidhu, P. S., Sparchez, Z., & Piscaglia, F. (2016). EFSUMB guidelines on interventional ultrasound (INVUS), Part III - Abdominal treatment procedures (Short Version). Ultraschall in der Medizin, 37(1), 27-45. https://doi.org/10.1055/s-0035-1553965
9. Sparchez, Z., Brugerra, C., & Nolsoe, C. (2021). Interventional ultrasound. In D. Nürnberg, M. C. Chammas, O. H. Gilja, I. Sporea, & R. Șirli (Eds.), WFUMB Ultrasound Book (Chapter 31, pp. 1-18). World Federation for Ultrasound in Medicine and Biology. https://indd.adobe.com/view/75771e38-af00-4e25-8762-2c0213ebaf12
10. Cui, X. W., Goudie, A., Blaivas, M., et al. (2025). WFUMB commentary paper on artificial intelligence in medical ultrasound imaging. Ultrasound in Medicine & Biology, 51(3), 428-438. https://doi.org/10.1016/j.ultrasmedbio.2024.10.016

9. HOW CAN I USE US IN NEPHROLOGY?

Flaviu Bob, Iulia Grosu
WFUMB Center of Education Timișoara, Romania

For the activity of the nephrologists, urologists and other connected specialities, ultrasound is of great importance, and it should belong to their daily clinical activity. It could be considered to be the fifth pillar of the physical exam, after the traditional inspection, palpation, percussion and auscultation. On the other hand, it is known that diagnosis in nephrology is mainly based on biochemical and sometimes histological features, and therefore, apparently, ultrasound is not considered by nephrologists to be indispensable. Also, conventional US does not offer a lot of useful quantifiable results, to be used in the diagnosis of chronic kidney disease (CKD), for example.

Despite these aspects there are a lot of advantages of the ultrasound examination (accessible, real- time examination, safety etc.), that makes it not just attractive, but also an inseparable component of the nephrological assessment, as it will be shown in this chapter[1]. Ultrasound is an essential tool in the management of the nephrological patient allowing besides diagnosis, also the performance of invasive procedures (such as renal biopsy)[2]. Moreover, the activity of the nephrologist leads to the use of ultrasound, even beyond the assessment of the kidneys, with a special attention towards the assessment of vessels.

9.1 *Normal kidney US*

The US examination of the kidneys should be part of the general abdominal ultrasound, and there is no special preparation required for the patient. The usually recommended four hours fasting is not improving renal imaging. In order to examine the kidneys, the patient should take a deep breath, thus even the upper pole is visible (it could be otherwise covered by a posterior shadow from the rib). The patient should be in dorsal, lateral or ventral decubitus, the position that enables the best acoustic window should be chosen.

The kidney is a paired organ, normally located in the lumbar region, with the left kidney being 1-2 cm more cranial compared to the right one. The normal size is 10-12 cm length and 5-6 cm width, the right kidney being usually slightly smaller compared to the left one. Normally both kidneys move with respiration. The shape in a sagittal plane is beam like, while in a transverse plane it is round or oval, and the contour is regular. The normal sonographic aspect of the kidney is:

- Hyperechoic renal pelvis
- Hypoechoic renal parenchyma (it is difficult to differentiate between cortex and medulla)

- The echogenicity of the kidney is decreased compared to liver and spleen
- The renal capsule is fibrotic, thus hyperechoic
- The kidney may be surrounded by perirenal fat

In order to best describe the potential sonographic findings, that we can encounter during ultrasound of the kidneys and the urinary tract, we can start by mentioning the reason for performing this assessment. As stated above, being a part of the standard abdominal ultrasound, it is possible that during renal US, different findings are made, with or without clinical implications. On the other hand, sometimes renal ultrasound is performed due to symptoms or signs (pain, hematuria, proteinuria or impaired renal function).

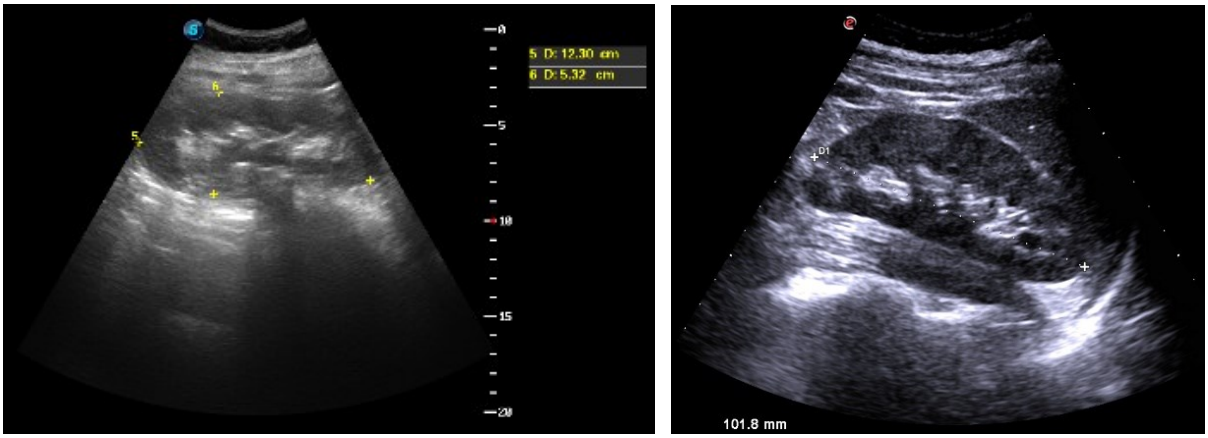

Figure 9.1. US of the kidney

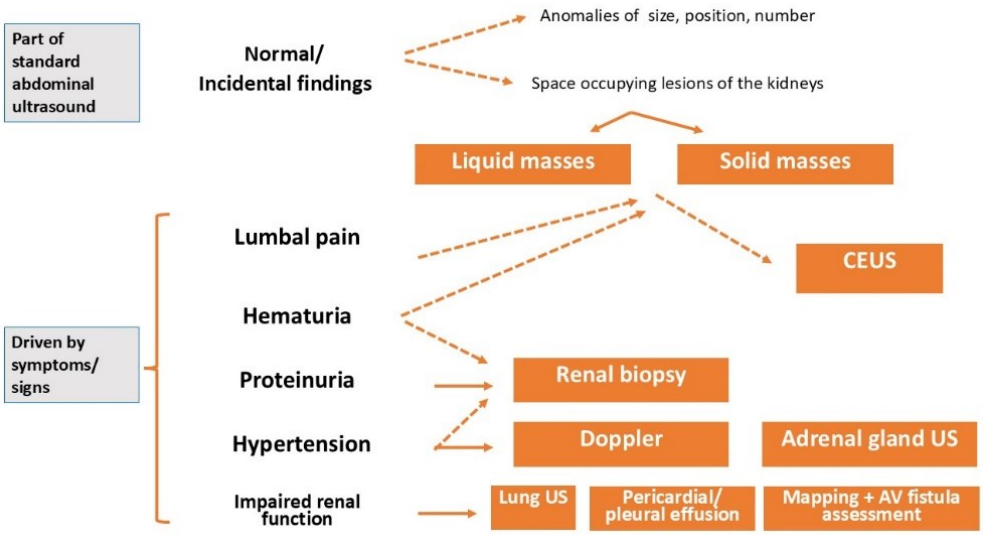

Figure 9.2. US, a helpful tool for the nephrologist- reasons and findings

9.2. Incidental findings during renal US

9.2.1. Abnormalities of the kidneys

Size abnormalities

From the three measurable items of the kidney (length, width and thickness), renal length is more adequate to be used in the examination of adults. The unilateral small kidney (**unilateral renal hypoplasia**) is congenital, or can be due to acquired causes. It is sometimes an incidental finding. It is usually asymptomatic, renal function is usually normal, and the contralateral kidney shows a compensatory hypertrophy. The contributing pathological conditions involved can be congenital hypoplasia, chronic pyelonephritis, renovascular hypertension/ ischemic nephropathy or post- surgery.

Position abnormalities

Due to a failure to ascend during embryologic development, the kidney can be situated in the pelvic region. The **pelvic kidney** can be smaller in size. Most cases are asymptomatic, although they are generally associated with higher risks for traumatic injury, urinary tract infections, renal calculi, and other urological problems. It is very important to search for the kidney in the pelvic region, when it is not found in the renal fossae.

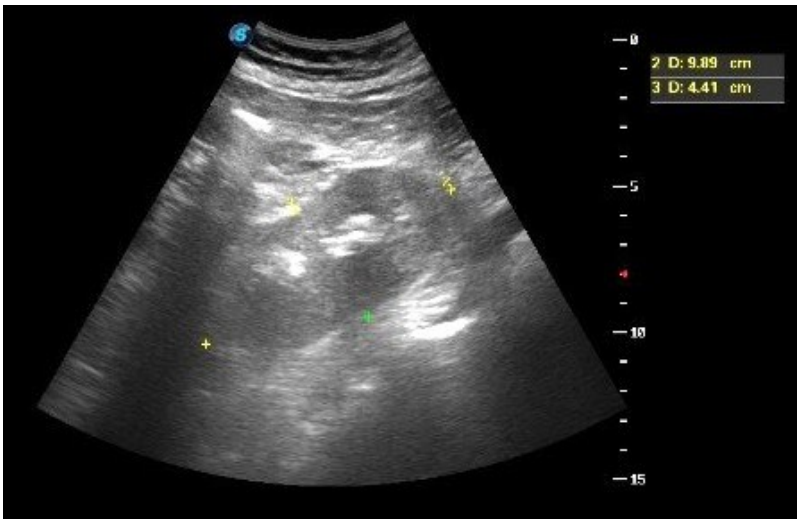

Figure 9.3. Right pelvic ectopic kidney

If the poles of the kidneys are fused, it is called **horseshoe kidney.** Usually**,** the fusion is at the level of the lower poles, resulting a "U" shape. At ultrasound, horseshoe kidneys are usually lower than normal and a transverse imaging of the retroperitoneum will demonstrate the renal isthmus crossing the midline anterior to abdominal great vessels.

Number abnormalities

Solitary kidney is represented by the condition when only one kidney is present, either congenital or after nephrectomy. The contralateral kidney is usually hypertrophied compensatory, and the renal function is normal, however there is an increased risk of progression towards advanced stages of CKD.

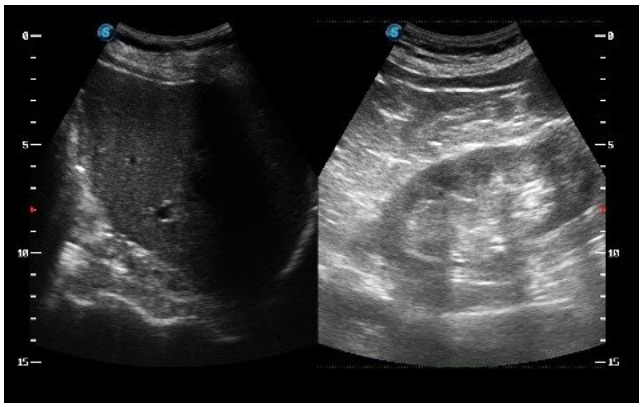

Figure 9.4. Left single kidney, kidney absent in the right renal fossa

Sometimes a **supranumerary kidney** can be found, but it is smaller in size, and situated near to the normal kidney.

A more common congenital anomaly is represented by the **duplex collecting system**, that in ultrasound appears as two central echogenic renal sinuses with intervening, bridging renal parenchyma.[3]

9.2.2. Space occupying lesions of the kidneys

These anomalies, represented by superimposed images on the ultrasound image of the kidney can be found incidentally quite often, but some of these conditions can lead to symptoms such as pain or hematuria. The space occupying lesions can be divided into liquid and solid masses.

9.2.2.1. Liquid masses- Cystic lesions

Simple renal cyst

The simple renal cysts are quite frequent findings in renal ultrasound. They are benign lesions, mostly asymptomatic, with an incidence increasing with age. Being fluid structures, the sonographic appearance is that of an anechoic round or ovoidal zone that has a clear margin, and shows enhancement of echogenicity, distal from the cyst. Sometimes there are multiple simple cysts in one or both kidneys. The simple cyst does not require any treatment.

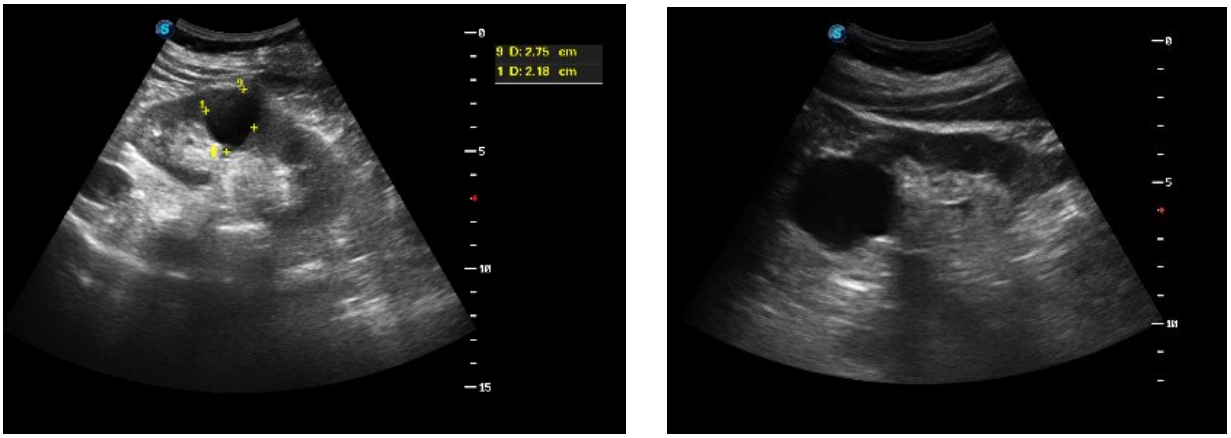

Figure 9.5. Simple renal cyst (left and right figure)

Sometimes the location of the cyst can lead to diagnosis problems, such as in the case of **parapelvic cysts**. These are a subset of simple cysts that arise within the renal parenchyma, adjacent to the renal sinus, characterized by being generally single, larger, and incompletely surrounded by renal parenchyma. The differential diagnosis of parapelvic cysts is sometimes necessary with hydronephrosis, but also with rare diseases such as Fabry disease, autosomal dominant polycystic kidney disease, polycystic liver disease and tuberous sclerosis complex disease.

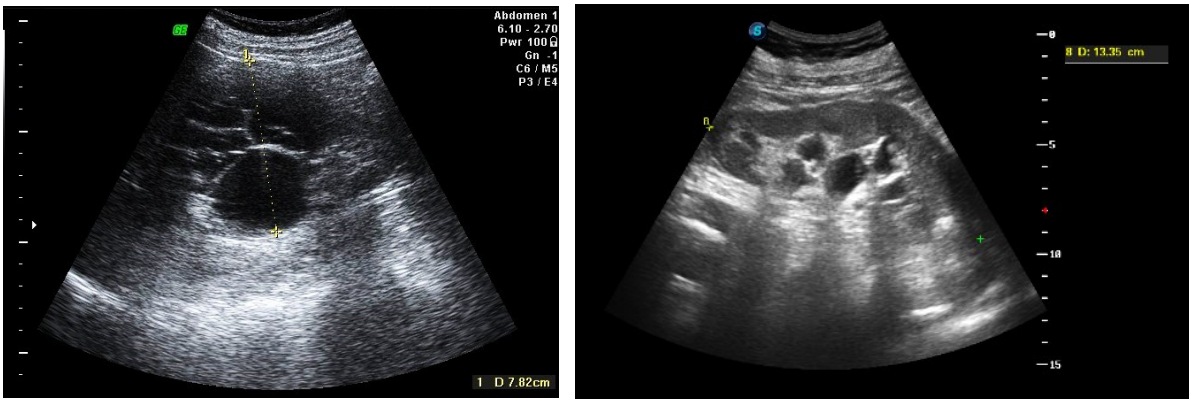

Figure 9.6. Parapelvic anechoic zones- simple renal cyst (left) and multiple renal parapelvic cysts (right)

Complex renal cyst

If a renal cyst does not fulfill the criteria above, and contains calcifications, septae or if the walls are nodular, the cyst is considered a complex cyst, and requires further imaging. The most important issue is the aim to differentiate between benign and malignant lesions. CEUS can be used in order to classify complex cysts using the Bosniak criteria, that have been initially established for CT and MRI. According to this classification cysts can be divided into 5 categories.

Simple renal cysts, that fulfill the criteria mentioned above are considered Bosniak category I. If the cyst has 1-3 thin (<2mm) septa it is considered category II, but if there multiple septa, with uptake of contrast, the cyst is considered Bosniak IIF, which means it requires follow-up, because there is a chance of 5-10% of malignancy [3].

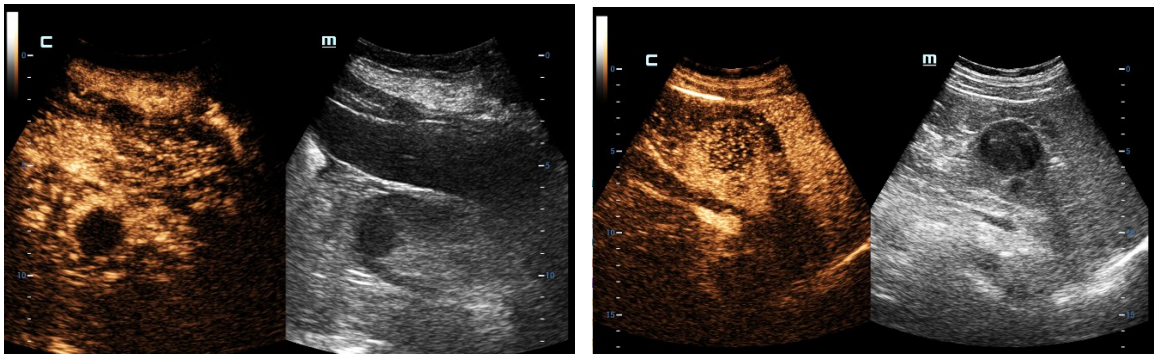

Figure 9.7. Renal CEUS showing a Bosniak category I cyst (left) and Bosniak IV cyst (right)

Cysts with irregular septa (with uptake of contrast), with thick walls (>3mm), with calcifications are considered Bosniak III cysts, with a 54% risk of malignancy. The presence in addition of nodular or soft tissue lesions, with contrast enhancement, means a Bosniak IV cyst (91% risk of malignancy). Both Bosniak III and IV cysts must be solved surgically [4].

Autosomal dominant polycystic kidney disease (ADPKD)

ADPKD is considered to be the most frequent genetic disorder of the kidneys. Despite the increased knowledge regarding genetic changes of the disease, imagistic criteria, especially ultrasound, are mostly used. In young subjects (15–39 years) at-risk because of an affected first-degree relative, three cysts in both kidneys, are sufficient for the diagnosis, whereas in older subjects where the finding of simple cysts is common, 2 or more cysts in each kidney is required for the definite diagnosis of ADPKD.

The sonographic appearance of ADPKD is characteristic, with bilateral enlarged kidneys, with bilateral multiple anechoic masses. Sometimes multiple hepatic cysts are associated.

The differential diagnosis is important and sometimes difficult and the following aspects should be ruled out:

- Multiple benign renal cysts
- Acquired renal cystic disease- is characterized usually by the presence of cysts in small kidneys with chronic kidney disease

- Medullary sponge kidneys- is due to malformation of the distal collecting tubules with nephrolithiasis (haematuria), renal function impairment, tubular acidosis, recurrent urinary tract infections.
- Autosomal recessive polycystic kidney disease- is diagnosed at an early stage, is characterized by the presence of multiple cysts, but however no macrocysts present, and no liver cysts present, in contrast to ADPKD
- Tuberous sclerosis complex- is an autosomal dominant disease characterized by the presence of renal angiomyolipomas, but also with extrarenal manifestations (facial angiofibromas, cerebral pathology, benign neurocutaneous tumours)

Ultrasound is also useful in the assessment of complications of ADPKD, such as intracystic haemorrhage or infection, in both of them with an inhomogenous appearance of the involved cysts.

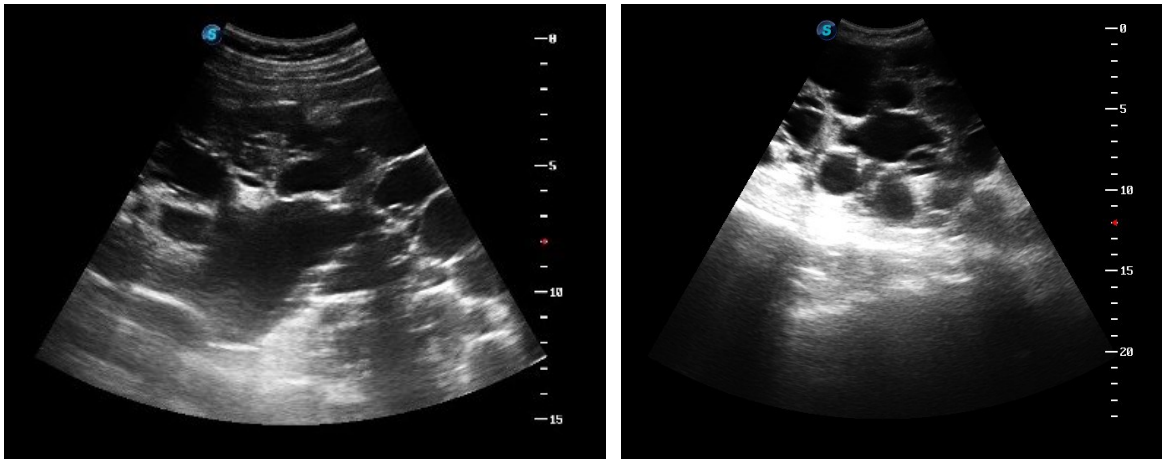

Figure 9.8. Multiple anechoic zones, characteristic for ADPKD

9.2.2.2. Solid renal masses

Hypertrophied column of Bertin, is a normal variant but may mimic renal masses and is the result of persistent polar parenchyma, which should be resorbed normally. There are some ultrasound criteria to diagnose this entity:

- It leads to an indentation of the renal sinus
- It is continuous with adjacent renal cortex
- It has similar color flow to surrounding parenchyma
- It is less than 3 cm in size

For the differential diagnosis with a solid renal mass CEUS can be used. The hypertrophied column shows similar uptake of contrast compared to the surrounding parenchyma

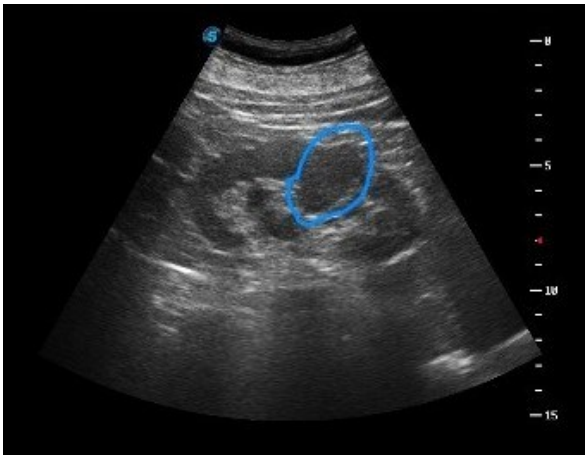

Figure 9.9. Hypertrophied column of Bertin

Angiomyolipomas

Angiomyolipomas are benign tumours composed of adipose tissue, smooth muscle cells, and blood vessels, and they can occur sporadically or may be found in patients with tuberous sclerosis. The ultrasound classical aspect of angiomyolipomas is a hyperechoic mass with shadowing, but however, if vascular structures predominate, then the aspect will be hypoechoic.[3]

Renal tumours

The most frequent form is represented by transitional cell carcinoma, that can be located at the level of the kidney, ureters or bladder. They are associated sometimes with hematuria, sometimes with flank pain, but can be also incidental findings.

Regarding ultrasound of renal tumours, the diagnosis is sometimes difficult. If they are located in the renal sinus, they will appear as a hypoechoic mass, hard to distinguish from the presence of fat in the renal sinus. Renal tumours can appear with increased echogenicity, some carcinomas present with calcifications or with areas of necrosis inside. Tumors 25 mm and bigger can be detected reliably, whereas tumors of size 20-25 mm will be detected in only 80% of cases. Smaller tumors cannot be reliably detected. Large tumours may show central necrosis and should be differentiated from abscesses or cysts and the necrotic part can be super infected.

Color Doppler US can show hypervascularization of malignant tumors with decreased resistive index values. CEUS can be used to differentiate between pseudotumours (ex. hypertrophied column of Bertin) and solid renal masses, showing in the latter a different, usually inhomogenous, uptake of contrast compared to adjacent parenchyma.

Squamous cell carcinoma is rare and can be produced by chronic infection, irritation or stones. It destroys the normal echostructure of the renal tissue, and is often associated to the presence of a stone. It is difficult to differentiate from xanthogranulomatous pyelonephritis.

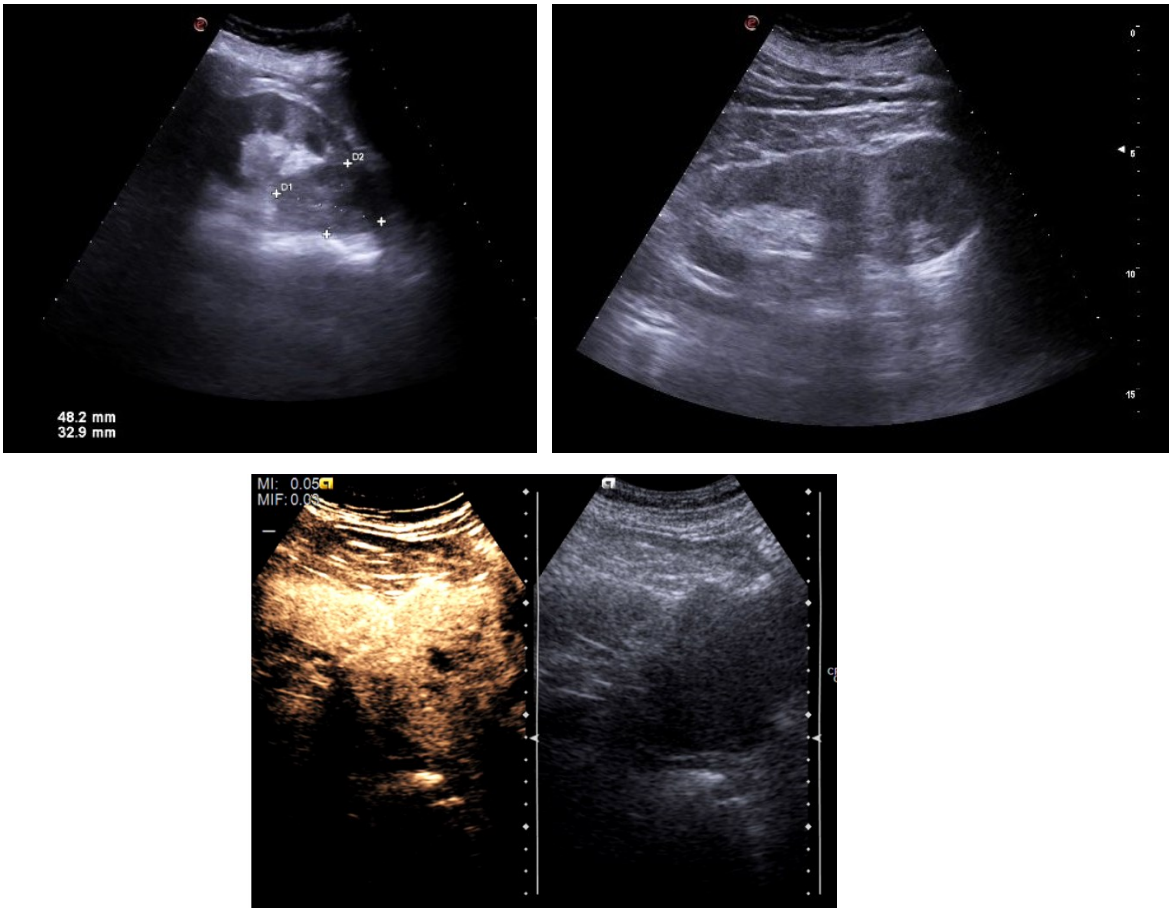

Figure 9.10. Images of inhomogenous masses (above). CEUS showing uptake of contrast in a renal tumour (below)

9.3. Renal US- Reason "Pain"

The reason for performing renal ultrasound is sometimes because of symptoms or some biological changes. Very often lumbar pain is leading to the necessity of an ultrasound examination, that is very helpful in establishing the diagnosis.

9.3.1. Hydronephrosis

Hydronephrosis is represented by the dilation of the collecting system. If the dilation of the renal pelvis is associated with the dilation of the ureters, it is called uretero-hydronephrosis. The cause is usually, but not always, obstruction. Initially the kidney with hydronephrosis is enlarged, however if the obstruction is chronic, the kidney will become fibrotic and thus smaller in size.

In the presence of hydronephrosis, the relationship with voiding should be assessed, because if dilation diminishes after emptying the bladder, it could be because of a vesicoureteral reflux, and hydronephrosis is considered non-obstructive.

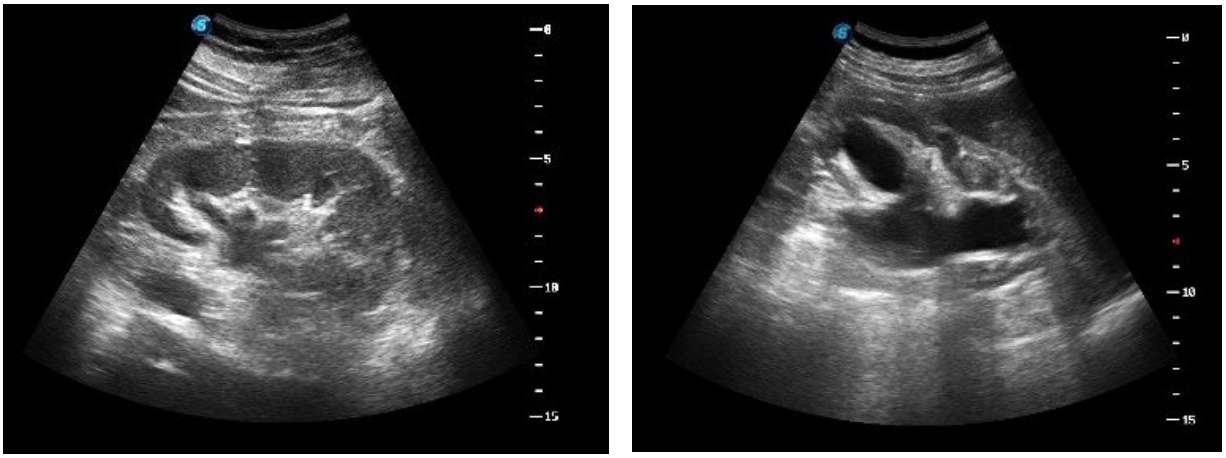

Figure 9.11. Image of hydronephrosis (left and right figure)

In case of obstruction the assessment of the pelvis should be performed, in order to find the obstructive lesion- prostate hypertrophy, genital tumors, bladder tumor. After excluding the pelvic site of obstruction, the ureter should be assessed, a procedure that is, however, more difficult.

In order to perform differential diagnosis of obstructive hydronephrosis there are some specific features that have to be looked upon:

- Lithiasis- the presence of the hyperechoic stone with posterior shadow is most frequently at the level of the pelvic-ureteral junction or uretero-vesical junction
- Ureteropelvic junction obstruction- there is no dilation of the ureter, extrarenal pelvis may be dilated
- Ureteral stricture- history of infection, surgery or radiation may be helpful
- Neurogenic bladder- there is an important postvoid residual
- Urothelial tumour (transitional cell carcinoma)- associated to hematuria
- Pelvic tumour or lymphadenopathy- sonographic abnormal mass in the pelvis
- Retroperitoneal fibrosis- unilateral, but also bilateral hydronephrosis, however CT is needed for the diagnosis
- Prostata hypertrophy- enlarged prostate in ultrasound examination
- Extrinsic obstruction due to aneurysma, pregnancy or endometriosis- diagnosis is done using ultrasound

In case of non-obstructive hydronephrosis, the use of ultrasound is also helpful:

- Vesicoureteral reflux- can lead to chronic pyelonephritis, with the presence of cortical scars, especially at the level of the upper poles
- Congenital megaureter and congenital megacalices- may be unilateral or bilateral

- Infection- can lead to mild dilation, even in the absence of obstruction
- Post- obstruction- after removal of the obstruction a severe dilation may not return to normal

9.3.2. Acute pyelonephritis

Acute pyelonephritis is an upper urinary tract infection, characterized by the tubulo-interstitial inflammation of the kidney. The ultrasound appearance of the kidney with acute pyelonephritis is normal in most of the cases. Despite this fact, ultrasound examination of the kidneys is important, especially in severe cases, that do not respond to the initial treatment in order to diagnose obstruction, abscesses, or favorizing factors such as lithiasis.

The ultrasound findings that can be present in acute pyelonephritis are: enlarged kidneys, decreased echogenicity due to edema, loss of the corticomedullary differentiation. It is important to assess mobility of the kidney, that can be reduced due to perinephritis. Sometimes hypoechoic, echogenic or inhomogeneous masses, without a clear margin can be found. In this case pyelonephritis is focal.

An important complication of acute pyelonephritis is represented by renal or perinephric abscesses. The suspicion of diagnosis can be made using ultrasound. The ultrasound appearance of the abscess is a hypoechoic mass, often inhomogenous because of internal debris. It is important to make the differential diagnosis with complicated cysts (infected or hemorrhagic), neoplastic or parasitic cysts. Very useful in the diagnosis of renal abscesses is CEUS, that shows an area without contrast uptake, surrounded by peripheral contrast uptake. The use of CEUS is also important in the follow-up of patients with renal abscess, that are treated conservatively.

The presence of purulent material in the obstructed collecting system is called pyonephrosis, and the diagnosis can be established using ultrasound. The presence of debris or gas in the dilated collecting system is suggestive of pyonephrosis.

Xanthogranulomatous pyelonephritis is a chronic suppurative pyelonephritis, that leads to a non-functioning kidney, that is enlarged, with multiple hypoechoic areas and without corticomedullary differentiation. If xanthogranulomatous pyelonephritis is focal, and not diffuse as described, it cannot be distinguished sonographically from a tumour or from an abscess.

Papillary necrosis, a complication of analgesic nephropathy, but also of infection or renal vein thrombosis, has the ultrasonographic appearance of a transonic, cystic area in the medullary pyramids associated with the presence of the papilla in the collecting system, that appears as an echogenic mass without shadowing. A calcification of the papilla can occur and then it is seen sonographically, as a hyperechoic area with posterior shadow, similar to the appearance in nephrocalcinosis.

Renal tuberculosis, occurs due to hematogenous dissemination of Mycobacterium tuberculosis from a primary focus, such as lung. The sonographical appearance of urinary tract tuberculosis is usually represented by focal lesions, tuberculomas. These are small masses that

appear either echogenic or hypoechogenic, with echogenic margins. Tuberculomas can enlarge and communicate with the collecting system, leading to the spread of the infection to the ureters and the bladder. The ureteral inflammation can cause hydronephrosis, while at the level of the bladder, thickening of the bladder wall can occur. In time the chronic changes in urinary tract tuberculosis are represented by fibrosis that leads to strictures, extensive cavitation, dilation of the collecting duct, associated to calcifications or perinephric abscesses.

9.3.3. Renal infarction

Renal infarction is a rare ischemic event caused by the complete or partial occlusion of the main renal artery or its segmental branches, which may ultimately lead to renal ischemia. The diagnosis is established using CT-scan. Regarding ultrasound, Doppler examination of the renal artery can be used, however it cannot assess nonstenotic lesions and determine the etiology. CEUS however, clearly outperformed color Doppler, with a significantly higher detection rate of renal infarction, being able to differentiate between renal infarctions and cortical ischemia.

9.4. Renal US- Reason "Hypertension"

For the assessment of hypertension the potential secondary causes should be ruled out, such as renal hypertension (renovascular or reno-parenchymal), but also causes related to the suprarenal gland (feocromocytoma). Because the ultrasound evaluation in reno-parenchymal hypertension (glomerulopathies, ADPKD) will be discussed in other sections of this chapter, we will now refer to renovascular hypertension and ultrasound of the adrenal glands.

9.4.1. Renal artery stenosis (renovascular hypertension)

Ultrasound is an important screening tool for patients with suspicion of renal artery stenosis. The evaluation of the main renal artery using Doppler ultrasound is, in most cases, not possible and therefore the assessment of intrarenal vasculature should be performed. Normally, there is a steep upstroke in systole with a second small peak in early systole. A tardus-parvus waveform downstream from a stenosis refers to a slowed systolic acceleration with low amplitude. For the assessment two measurements are needed, the acceleration time (from the start of systole to peak systole) and the acceleration index (slope of the systolic upstroke) [3].

9.4.2. Adrenal gland adenoma

The ultrasound assessment of the adrenal glands is important in patients with hypertension, and besides the different analyses required, it should be part of the work-up in these patients. Functional adrenal adenomas appear in pheocromocytoma, hyperaldosteronism or Cushing syndrome, all of these associated with hypertension [5].

In pheocromocytoma the adenoma is more frequent in the right adrenal gland, the ultrasound aspect is homogenous, but sometimes inhomogenous because of bleeding or necrosis. When using CEUS the adenoma has a better uptake compared to liver parenchyma.

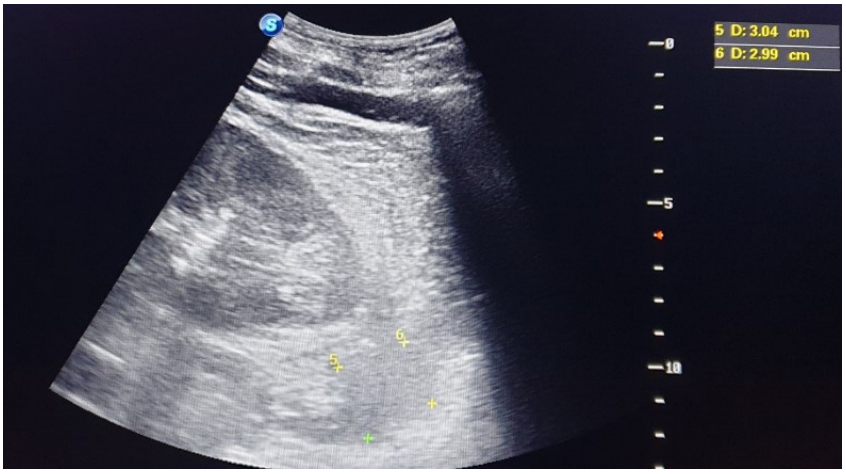

Figure 9.12. Adrenal gland adenoma

9.5. Renal US- Reason "Hematuria"

9.5.1. Lithiasis

Renal calculi are a frequent finding when performing renal ultrasound, and can be a cause for macroscopic or microscopic hematuria, or sometimes pain, but can be found even in the absence of symptoms. Ultrasound is considered the primary diagnostic tool for renal stones. The sonographic appearance of a renal stone is an echogenic zone with sharp distal acoustic shadow. The use of color Doppler US may improve the detection of stones, because of the appearance in some cases of the twinkling artifact. Despite the typical sonographical aspect of a renal stone, there are some differential diagnoses that have to be performed: calcifications (papillary necrosis, vessels, tumours) or intrarenal gas. In the case of staghorn lithiasis, that are calculi that occupy the entire renal pelvis, and one or more calyces, the ultrasound appearance is of multiple echoic zones with posterior shadow.

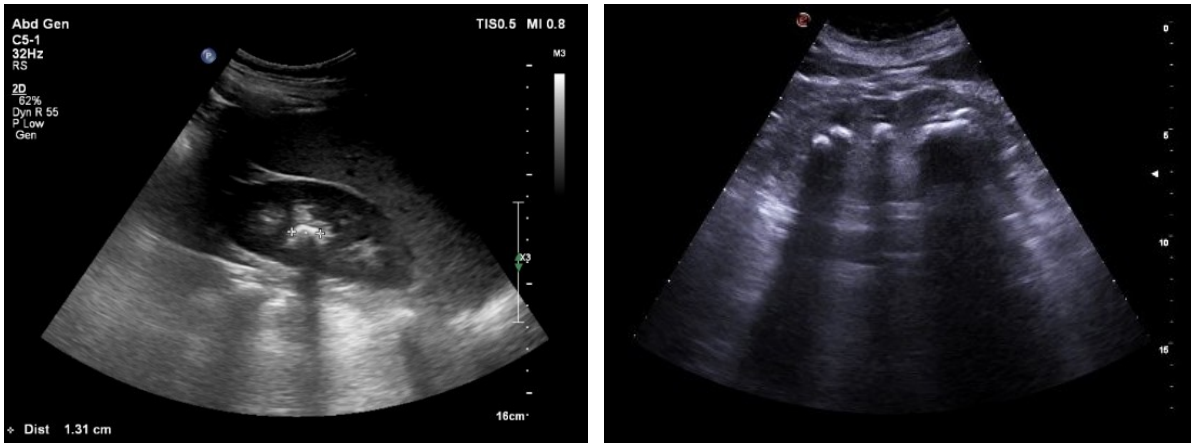

Figure 9.13. Renal lithiasis (left) and renal staghorn lithiasis (right)

The calculi can be present in the ureter or in the bladder, having the same hyperechoic appearance with posterior shadow.

9.5.2. Nephrocalcinosis

Nephrocalcinosis is represented by renal parenchymal calcifications in ischemic or necrotic tissues. The sonographical aspect is represented by medullary calcifications that surround the medullary pyramids and are first without posterior shadow, but after progression of disease, they will develop acoustic shadowing.

9.5.3. Bladder tumour

Another cause for macroscopic hematuria is represented by bladder tumours, that can be diagnosed using ultrasound. The aspect is a focal mass or urothelial thickening. A focal mass in the bladder should be differentiated from a blood clot, while the thickening of the bladder wall can occur in cystitis or post-radiation as well.

9.6. Renal US- Reason "Proteinuria"

9.6.1. Glomerulopathies

The presence of clinically significant proteinuria, sometimes associated to hematuria and hypertension, indicates the diagnosis of glomerulopathy, that can be acute, chronic or rapidly progressive. The disease can be limited to the kidneys, but it can also be part of a systemic disease, such as diabetes mellitus, systemic lupus erythematosus, vasculitis. The ultrasound aspect of the kidneys in this disease is not specific, despite the fact that both kidneys are affected. The size of the kidneys can be normal, or the kidneys could be enlarged in acute glomerulonephritis, while in chronic glomerulonephritis, with the progression of the disease, the size of the kidneys decreases. The changes, if present occur mainly at the level of the cortex, that can be either normal, echoic or hypoechogenic.

In diabetic kidney disease, because of the initial hyperfiltration that occurs, the kidneys appear enlarged, with an increase of cortical echogenicity and with preserved cortico-medullary junctions. With the progression of disease, the kidneys become smaller and hyperechoic, such as in other renal diseases.

Another renal disease that is associated to large bilateral kidneys is represented by amyloidosis, when also spleen and liver may be enlarged. Such as in most other glomerulopathies, in amyloidosis the diagnosis is made after renal biopsy, and during this procedure the role of ultrasound is indispensable.

9.6.2. The use of ultrasound for invasive procedures- renal biopsy

In the assessment of some diffuse renal diseases, such as glomerulopathies, but also sometimes in acute kidney injury, there is a need for histological assessment of the renal tissue

obtained through renal biopsy. In order to perform a renal biopsy ultrasound is indispensable before, during and after the procedure.

Firstly, after establishing the indication for performing the renal biopsy, the patient has to be assessed sonographically in the same position as the procedure to evaluate the location of the kidney, its excursion during breathing, the cortical thickness, and the distance of the kidney from the skin surface. This examination permits to rule out potential (relative) contraindications, such as: obstructive uropathy, ADPKD, single kidney.

The procedure itself is echoguided, with the patient positioned in prone position (for native kidneys), or supine position (for transplanted kidneys). The procedure can be performed either free-hand or using a needle-guide attached to the transducer. The lower pole of the kidney should be targeted, because it is poorly vascularized. The trajectory of the needle (16 or 18 gauge) is visualized on the monitor. During the procedure the collaboration of the patient is important, in order to maintain apnea during the execution of the biopsy [6].

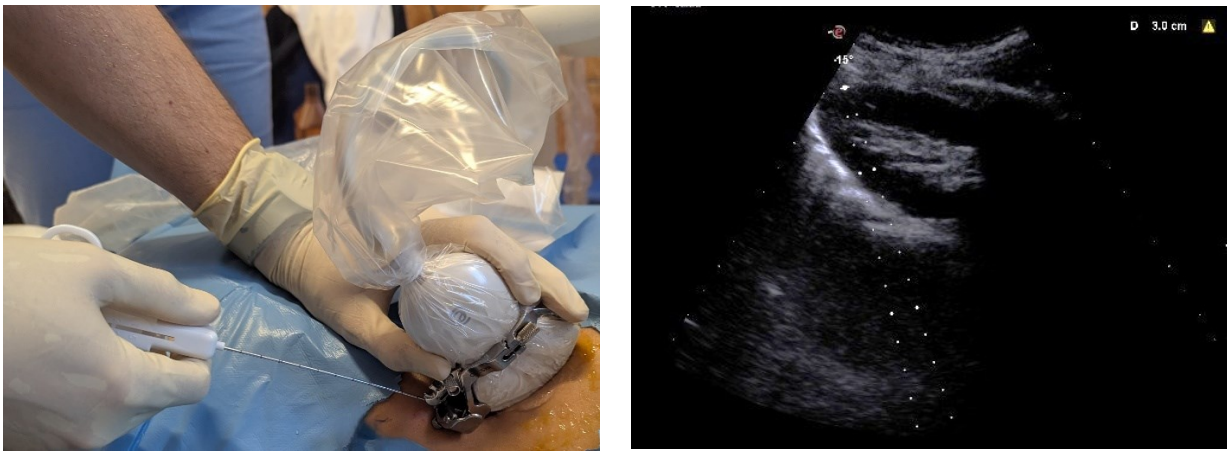

Figure 9.14. Echoguided renal biopsy

In order to diagnose potential complications an ultrasound assessment after procedure should be performed, usually 24 hours post-biopsy, but in case of hematuria or intense pain, whenever needed. The most common complication is bleeding and ultrasound can help diagnose the presence of hematoma (subcapsular or retroperitoneal), or of blood clots inside the bladder.

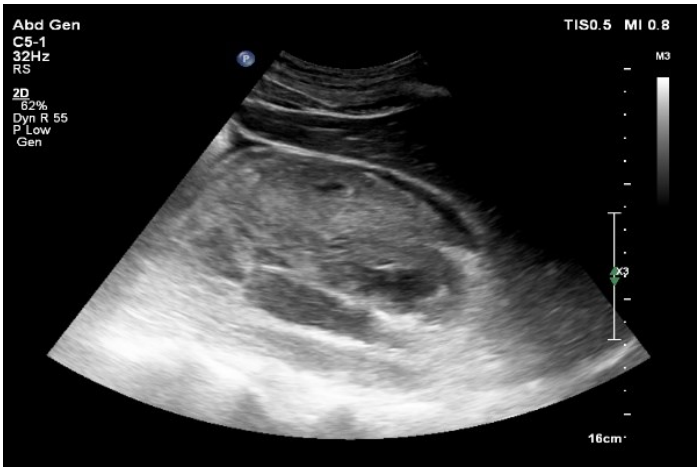

Figure 9.15. Perirenal hematoma, post renal biopsy

9.7. Renal US- Reason "Impaired renal function"

9.7.1. Acute kidney injury

Acute kidney injury (AKI) is characterized by a rapid loss of renal function, and is characterized by three different group of causes in: pre-renal AKI, intrinsic renal AKI and post-renal AKI. For the differential diagnosis between these three settings, anamnestic and complex clinical data are required, but ultrasound plays an important additional role. Regarding imaging, ultrasound should be a preferred method, in these patients with impaired renal function. The use of other tools is associated to risks, such as contrast enhanced CT scan because of the increased risk of contrast nephropathy, and MRI with gadolinium because of the risk of systemic nephrogenic fibrosis.

First of all, ultrasound can help in differentiate AKI from chronic kidney disease. Especially longitudinal lengths of the kidneys is helpful for the diagnosis. Usually in AKI the kidneys are bilaterally enlarged. Also, cortical thickness can be helpful in differentiating AKI from chronic kidney disease. In AKI the cortex is thick, suggesting the presence of edema or infiltration. In AKI the pyramids appear usually hypoechoic.

The most important role of ultrasound in the assessment of AKI, is to rule out post-renal AKI, by diagnosing urinary tract obstruction (bilateral or unilateral in single functioning kidney).

Regarding the role of color Doppler in the assessment of AKI, many studies demonstrate that renal resistive indexes (RI) vary depending on the primary disease, but several studies assessed that higher RI values are predictive of persistent AKI.

Regarding CEUS, it is safe to be used even in patients with impaired renal function, and the usefulness of the method is related to the quantification of the uptake of contrast at the level of the renal tissue. The use of dynamic contrast enhanced ultrasound leads to an estimation of renal blood flow. This is important in patients with AKI, that have reduced microcirculatory perfusion,

prolonged perfusion time and a reduced rising slope of the contrast in the renal cortex. These changes seem to appear before changes in serum creatinine, and therefore it could be potentially helpful in diagnosing AKI.

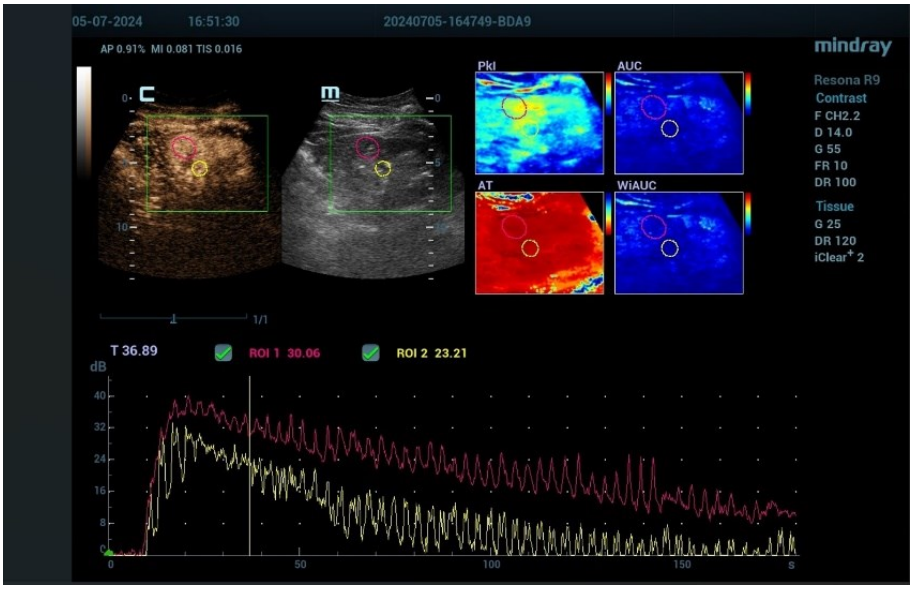

Figure 9.16. Dynamic contrast enhanced ultrasound of the kidney

9.7.2. Chronic kidney disease

Chronic kidney disease means a chronic, at least 3 months, injury of the renal tissue. In chronic kidney disease, especially in more advanced stages, the kidneys are bilaterally reduced in size, with a thinner cortex, that has increased echogenicity. Also, there is a disappearing of the corticomedullary differentiation. However, this increase of echogenicity, observed by the investigator, is not quantifiable using conventional ultrasound, being therefore a subjective observation. Elastography could represent an ultrasound- based method to be used in the assessment of chronic kidney disease, and several attempts have been made in this direction. It seems that elastography, similar cu dynamic contrast enhanced ultrasound, is influenced by renal blood flow.

Besides the assessment of the kidneys and of the uro-genital tract, especially in patients with chronic kidney disease, the nephrologist needs to perform ultrasound of other organs as well. Thus, in nephrology, multi-organ ultrasound is increasingly being integrated into routine practice.

Figure 9.17. Small and hyperechoic kidney in a patient with advanced CKD (left) and 2D-SWE elastography measuring renal stiffness

9.8. *US beyond Kidneys*

9.8.1. Multi-organ Ultrasound

Lung ultrasound is a technique used for assessing and quantifying extravascular lung water, using sonographic artifacts that show fluid accumulation in lung interstitium and alveoli. Due to the thickening of interlobular septa B-lines appear. The B-lines are vertical and hyperechoic, starting from the pleural line. Thus, lung ultrasound can be used in order to assess fluid overload in patients with end-stage renal disease, and to guide treatment in these patients.[7]

Inferior vena cava ultrasound which measures its diameter and respiratory collapse is an important parameter for estimating right atrial pressure.

The prevalence of ***pericardial or pleural effusion*** is of great importance in patients with end stage kidney disease, and should be assessed using ultrasound.

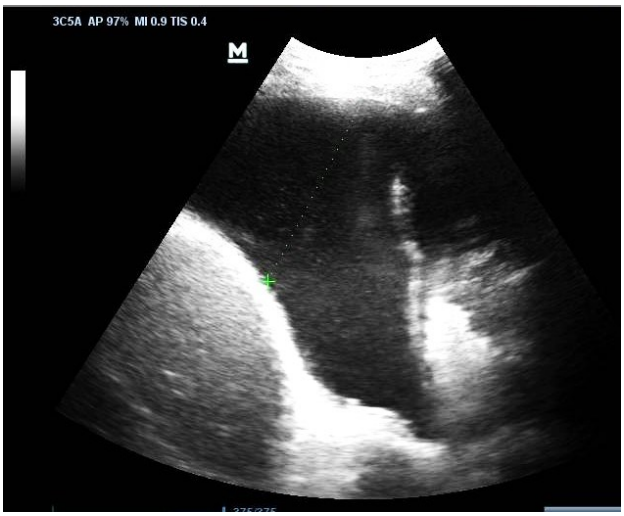

Figure 9.18. Pleural effusion in a hyperhydrated CKD patient

9.8.2. Ultrasound of arteriovenous fistula

9.8.2.1. Preoperative Ultrasound Mapping of the Arm

Arteriovenous fistulas (AVF) are considered the gold standard vascular access (VA) for chronic hemodialysis (HD) patients, as recommended by current guidelines [8], which makes their surveillance of utmost importance in clinical practice. Nowadays, the most widespread renal replacement modality is in-center hemodialysis, with increasing 5-year survival rates of around 40%, therefore VA formation and patency is a clinically relevant topic.

The referral to AVF creation should ideally be performed before the initiation of HD therapy, when the patient reaches chronic kidney disease (CKD) stage G5 (eGFR drops below 15 ml/min/1.73m2). In the preoperative setting, in order to decide which type of AVF is most suitable for the patient, both a clinical and ultrasound (US) examination should be performed.

The three major types of autogenous AVFs created on the upper limbs are: radio-cephalic, brachio-cephalic, and brachio-basilic. The current approach, according to KDOQI guidelines [9] with regards to the surgical decision should include the ultrasound mapping criteria and the patient's End Stage Kidney Disease (ESKD) Life Plan. Ideally, AVF formation should start on the non-dominant arm from a distal to a proximal position, using and end-to-side anastomosis.

The clinical examination performed by the nephrologist or vascular surgeon prior to the ultrasound mapping of the arteries and veins should include: the *arterial tree patency assessment* – presence of pulses and Allen's maneuver; the *venous tree assessment*- distensibility, trajectory and tortuosity. Even though the clinical examination holds its importance, it may be misleading and subjective. Hence, the ultrasound examination should follow the clinical assessment, mainly when complications are suspected.

The protocol for performing ultrasound mapping should include the following protocol. Patients should be positioned supine with their arms relaxed in a warm environment. A high-frequency ultrasound probe, operating at 7-12 MHz (or 5 MHz or higher for Doppler), should be utilized. The examination incorporates several modes: B-mode for morphological details, spectral Doppler for assessing flow, and Color-Doppler for detecting flow and its direction. For accurate results, the following considerations are essential:

- Position the transducer longitudinally and set the sample volume ("gate" size) to two-thirds of the vessel's width.
- Maintain an insonation angle of less than 60 degrees, typically aligning it parallel to the vessel's long axis.
- Adjust the gain setting to ensure clear visibility of Doppler flow in the area of interest.
- Modify the Pulse Repetition Frequency (PRF) based on velocity ranges; higher PRF levels facilitate the detection of faster velocities.
- If available, set the wall filter to eliminate low-velocity frequency shifts.

After performing these adjustments, record the following variables:

- For the arterial system, starting distally and moving proximally: the *internal diameter and depth of the radial and brachial arteries, peak systolic velocities (PSV) and end-diastolic velocities (EDV), resistive index (RI)* using Doppler examination and the *hyperemic response* of the radial artery. This last test involves recording the changes in the spectral waveform after a 2-minute fist clenching, which induces distal ischemia. (Fig. 9.19., Fig. 9.20)

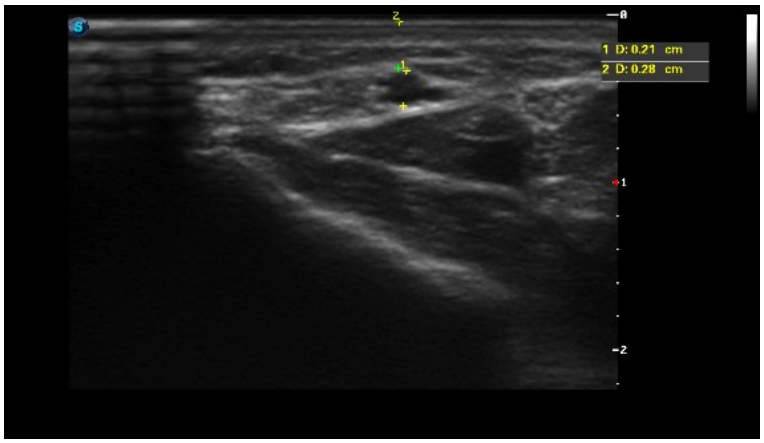

Figure 9.19. B-mode assessment of the diameter and depth of a radial artery.

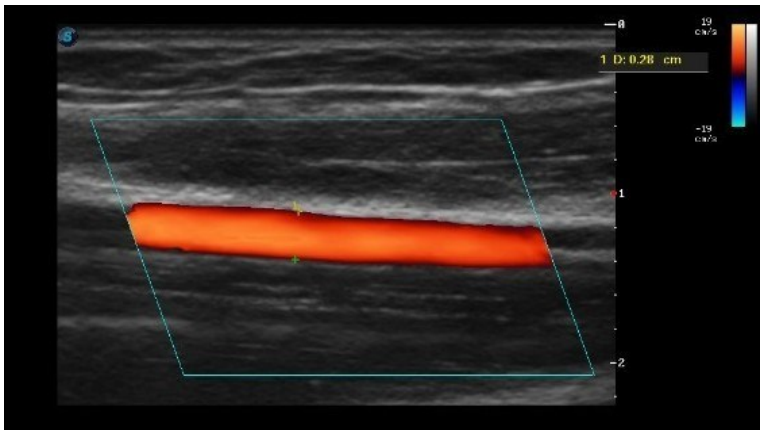

Figure 9.20. Color mode assessment of the diameter and depth of a radial artery.

- For the venous system: the *internal diameter and depth of the cephalic vein (in the forearm and arm), and of the basilic vein; the trajectory*- which should be straight (Fig. 9.21), *the compressibility*- the vein should be fully compressible if there are no ongoing thromboses, and *the distensibility* after tourniquet application (at least 40% increase in diameter)

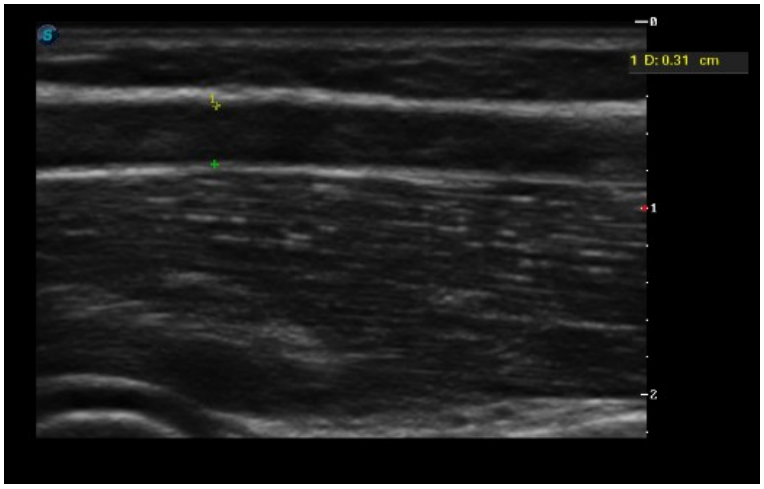

Fig. 9.21. B-mode assessment of a brachial vein, in longitudinal section.

Current guidelines and research papers [8,9] recommend the following thresholds:

Arterial system	PSV radial artery > 50 cm/s RI < 0,7 during hyperemic response maneuver Diameter radial artery > 0,2 cm Lack of diffuse calcifications
Venous system	Diameter cephalic vein (forearm) > 0,2 cm

Arteriovenous Fistula Ultrasound Assessment Protocol

After AVF creation, postoperative US surveillance is not routinely recommended as per current VA guidelines [8,9], with the first scan typically occurring 4-6 weeks later to assess maturation. Cannulating immature AVFs can lead to failure or thrombosis. An ideal AVF should meet the following criteria: minimum 600 ml/min flow, minimum 6 mm diameter, and maximum 6 mm depth. While routine, scheduled US surveillance is not generally recommended, guidelines [8] suggest US as the first investigation for suspected complications. Clinical signs indicating the need for US evaluation include:

- Distal edema and cyanosis of the hand/arm
- Hand pain, cold fingers
- Low blood flow alerts during the dialysis session and inadequate toxin removal
- Local hematomas or suspected collections and infections
- No thrill or bruit upon auscultation.

- AVF with high pulsatility, low perceptible thrill - AVF stenosis.
- Aneurysms, dilatations - may suggest high flow AVFs.
- Blood clots removed upon cannulation - segmental or total AVF thrombosis.

The examination should be performed using a 7-12 MHz linear transducer. Although there is no current available consensus regarding a systematic protocol, the available literature suggests a methodological approach for VA Duplex US examination, by using B-mode as well as color and spectral Doppler modes.

- Inflow artery – measure *diameter and caliber change*, proximal to the brachial artery bifurcation using B-mode transverse section; measure *blood flow* either using the US machine software, or the following formula:

  AVF flow (ml/min) = 3,14 x brachial artery radius 2 x Time Averaged Mean Velocity mean x 60.

  Finally, calculate the RI, either using the US machine software, or by using the following formula:

  RI = PSV-EDV/PSV.

  Values should be below 0,6, otherwise a stenosis either in the anastomosis or in the outflow vein should be suspected.

- Anastomosis – using B-mode in two planes, the anastomosis diameter should be measured
- Outflow vein – using B- mode follow the trajectory of the vein in a distal-to-proximal way, measure the largest and smallest diameters, depth, and needling sites.

B-mode and Doppler are useful for identifying possible AVF complications, which are detailed below.

9.8.2.2. AVF Complications

AVF Stenosis

Stenoses are characterized by the AVF narrowing which results in hemodynamic and functional repercussions. The hemodynamic changes caused by a stenosis include a turbulent flow at the stenotic site and reduced blood flow in the segment following the stenosis.

Various factors contribute to AVF stenosis, including atherosclerotic calcified plaques (commonly found in longstanding AVFs), partial thrombosis, external compression from hematomas or edema, and intimal hyperplasia. AVF stenosis typically develops in the juxta-anastomotic segment but can also appear in the middle segment or central veins.

Radiocontrast angiography has a better sensitivity for AVF stenosis detection; however, US is frequently employed as a first-line tool because it also allows the visualization of the surrounding tissues as well as the impact of the stenosis on hemodynamics.

Therefore – in B-mode the diameter of the AVF should decrease significantly and suddenly. The stenosis percentage should be measured in a longitudinal section, implying the following formula:

% stenosis= (original lumen- residual lumen)/original residual lumen x 100

B-mode evaluation is not sufficient for this suspected complication, it should always be completed by color and spectral Doppler- mainly PSV evaluation. A pre-stenosis/stenosis ration of over 3 signifies a stenosis of over 75%.

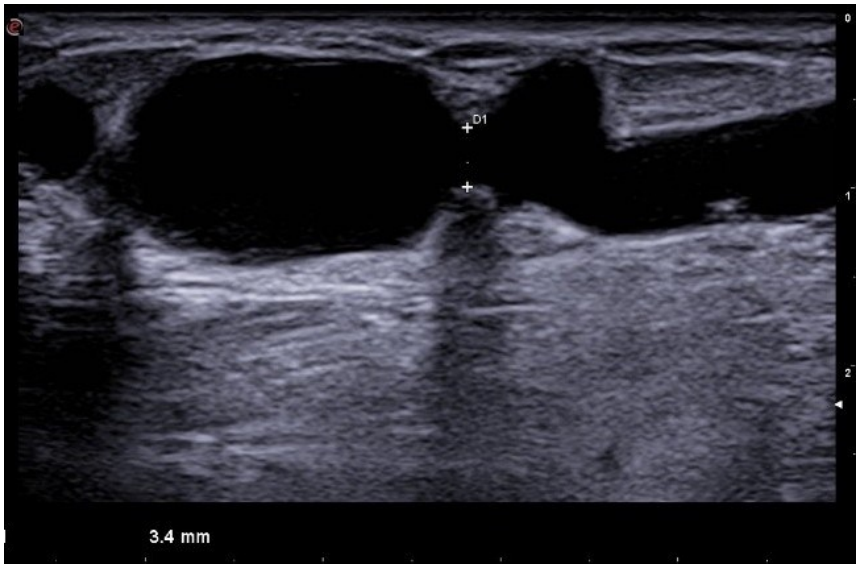

Figure 9.22. AVF stenosis

AVF thrombosis

Complete AVF thrombosis is the most feared AVF complication as it renders the VA non-functional, and thus the patient is unable to undergo HD treatment. AVF thrombosis may occur due to hypotension, poor cannulation technique, or extrinsic compression. Partial thromboses may represent an emergency, because if recanalization techniques are not employed quickly, most of them progress to complete thrombosis.

The following US aspects indicate complete or partial thrombosis.

- B-mode should show a partially or completely incompressible vein, with the presence of hyperechoic material inside the AVF lumen
- Color and spectral Doppler demonstrate the reduction of AVF flow at the site of thrombosis

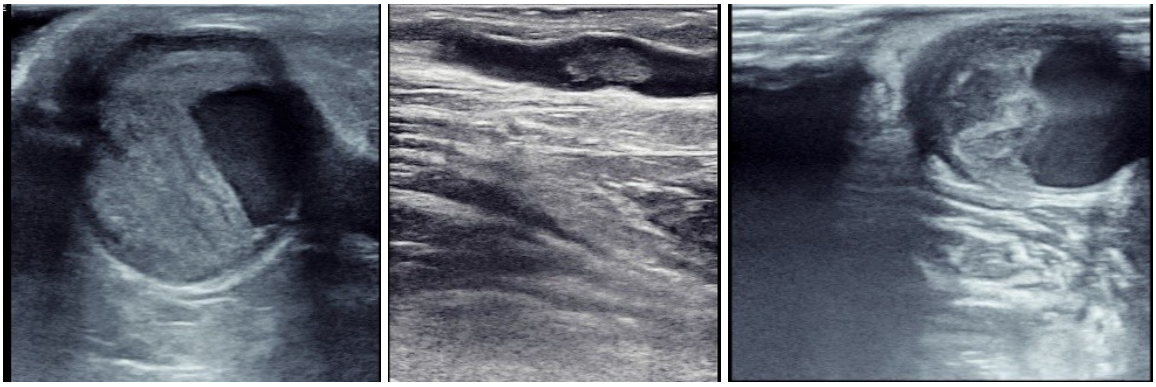

Figure 9.23. Images of AVF thrombosis

AVF pseudoaneurysms

The diagnosis of an AVF aneurysm is clinical and there is no required US examination. It represents an abnormally dilated vessel, usually secondary to repeated cannulations in the same place (the "area" cannulation technique). These are usually stable lesions, with a small rate of VA patency complications.

On the other hand, pseudoaneurysms represent a communication with the surrounding structures, due to a tear in either the anterior or posterior AVF walls. Therefore, the lesion may appear as a pulsating are, sometimes painful, with blood flowing into a false saccular structure. Pseudoaneurysms represent an emergency due to their high risk of AVF rupture and massive hemorrhage.

From the US point of view, pseudoaneurysms will appear in B-mode as an additional structure anterior or posterior to the AVF, while the vessel wall will present a rupture. It is important to employ the color and spectral Doppler because they will objectify the presence of blood flow in the adjacent structure. Usually, the color pattern will be "to-and-fro" (red and blue colors alternating), while the spectral curve will show both positive and negative waveforms.

AVF hematomas

AVF hematomas usually occur due to cannulation incidents, or coagulation defects in the setting of improper local hemostasis. They do not result in an actual tear of the vessel wall, as in the case of pseudoaneurysms, but generate an extravasation of blood in the surrounding tissues, self-limitative. Hence, the US B-mode will show a vaguely delimitated collection, while the color and spectral Doppler will show no flow inside the lesion.

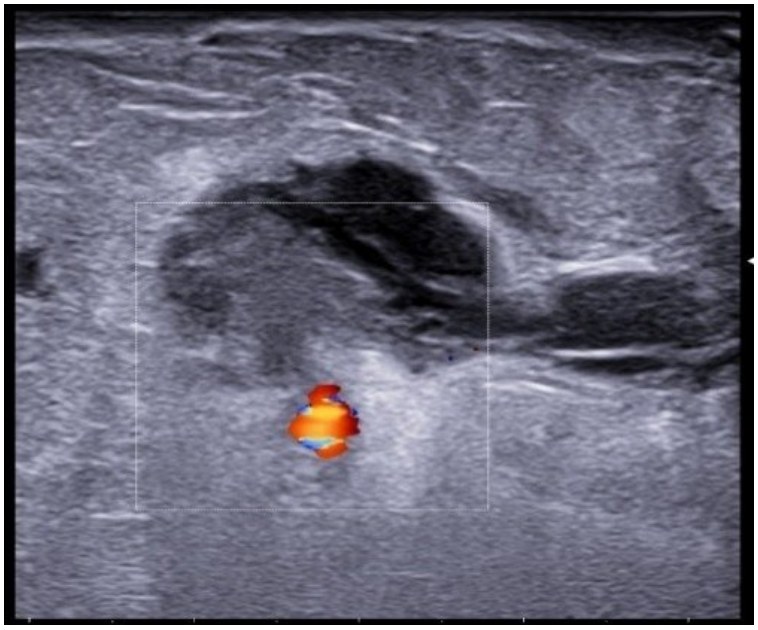

Figure 9.24. AVF hematoma

High Flow AVF and Steal Syndrome

High flow AVFs usually imply that the outflow vein is extremely dilated, usually throughout its entire trajectory, and may hold a blood flow of over 1500 ml/min. Clinically, the patient complains of dyspnea and palpitations, and presents with signs of right heart decompensation. Once this complication in suspected due to the cardiac symptoms, it will be confirmed by identifying blood flows in the brachial artery of over 1500 ml/min, and a ratio between AVF blood flow and cardiac output of over 40% [10].

High flow AVFs may result in Steal syndrome, which represents ischemia induced in the structures situated distally from the AVF. However, high flow AVFs are not the only cause for Steal syndrome. Other situations such as low arterial inflow due to arterial stenosis or increased distal arterial resistance may be underlying pathogenic mechanisms. The US examination in color and spectral Doppler will show an inverse flow pattern in the distal artery, typically exhibiting antegrade flow during systole and retrograde flow during diastole, as well as reduced PSV in the radial or ulnar territories.

AVF US- guided cannulations

Lastly, US is an extremely important instrument that assists nephrologists and HD nurses in the cannulation process. Using a handheld, portable transducer, it may help avoid needling incidents, by the direct visualization of the tip of the needle on the US screen. This is easily achieved using a B-mod longitudinal scan, with the needle directed at around 45 degrees, and inserted below the US probe.

9.9. Conclusions

The use of ultrasound has become a daily tool for nephrologists, with an important development in the last years. The importance of using ultrasound in every day clinical practice goes beyond conventional B-mode ultrasound of the kidneys, towards the use of Doppler, CEUS and elastography, associated with the assessment, not only of the urinary tract, but also of lungs, heart or peripheral vessels. In nephrology ultrasound is not just a diagnostic tool, but also an essential help for guiding renal biopsy. Therefore, ultrasound should be a part of the educational curriculum for nephrologists, and the efforts of the nephrological community should be oriented towards the extensive use of multi-organ and multi-parametric ultrasound.

Selective references

1. O'Neill WC, Ross DW. Retooling Nephrology with Ultrasound. Clin J Am Soc Nephrol. 2019 May 7;14(5):771-773. doi: 10.2215/CJN.10430818. Epub 2019 Mar 27. PMID: 30917993; PMCID: PMC6500941.
2. Rivera Gorrín M, Sosa Barrios RH, Ruiz-Zorrilla López C, Fernández JM, Marrero Robayna S, Ibeas López J, Salgueira Lazo M, Moyano Franco MJ, Narváez Mejía C, Ceballos Guerrero M, Calabia Martínez J, García Herrera AL, Roca Tey R, Paraíso Cuevas V, Merino Rivas JL, Abuward Abu-Sharkh I, Betriu Bars À; en representación del Grupo de Trabajo en Nefrología Diagnóstica e Intervencionista (GNDI) de la Sociedad Española de Nefrología (SEN). Consensus document for ultrasound training in the specialty of Nephrology. Nefrologia (Engl Ed). 2020 Nov-Dec;40(6):623-633. English, Spanish. doi: 10.1016/j.nefro.2020.05.008. Epub 2020 Aug 6. PMID: 32773327.
3. Rumack CM, Wilson SR, Charboneau JW, Levine D. Diagnostic Ultrasound. Elsevier/Mosby, 2011
4. Spiesecke P, Thiemann J, Conen P, Clevert DA. Contrast enhanced ultrasound of cystic renal lesions, from diagnosis up to treatment. Clin Hemorheol Microcirc. 2024;88(s1):S21-S33. doi: 10.3233/CH-248102. PMID: 39365320; PMCID: PMC11612966.
5. Kim KW, Kim JK, Choi HJ, Kim MH, Lee J, Cho KS. Sonography of the adrenal glands in the adult. J Clin Ultrasound. 2012 Jul-Aug;40(6):357-63. doi: 10.1002/jcu.21947. Epub 2012 May 15. PMID: 22585678.
6. Granata A, Distefano G, Pesce F, Battaglia Y, Suavo Bulzis P, Venturini M, Palmucci S, Cantisani V, Basile A, Gesualdo L. Performing an Ultrasound-Guided Percutaneous Needle Kidney Biopsy: An Up-To-Date Procedural Review. Diagnostics (Basel). 2021 Nov 24;11(12):2186.
7. Gómez-Johnson VH, López-Gil S, Argaiz ER, Koratala A. Point-of-Care Ultrasound in Nephrology: Beyond Kidney Ultrasound. Diagnostics (Basel). 2025 Jan 27;15(3):297. doi: 10.3390/diagnostics15030297. PMID: 39941227; PMCID: PMC11817333.
8. Schmidli J, Widmer MK, Basile C, de Donato G, Gallieni M, Gibbons CP, Haage P, Hamilton G, Hedin U, Kamper L, Lazarides MK, Lindsey B, Mestres G, Pegoraro M, Roy J, Setacci C, Shemesh D, Tordoir JHM, van Loon M, Esvs Guidelines Committee, Kolh P, de Borst GJ,

Chakfe N, Debus S, Hinchliffe R, Kakkos S, Koncar I, Lindholt J, Naylor R, Vega de Ceniga M, Vermassen F, Verzini F, Esvs Guidelines Reviewers, Mohaupt M, Ricco JB, Roca-Tey R. Editor's Choice - Vascular Access: 2018 Clinical Practice Guidelines of the European Society for Vascular Surgery (ESVS). Eur J Vasc Endovasc Surg. 2018 Jun;55(6):757-818. doi: 10.1016/j.ejvs.2018.02.001. Epub 2018 May 2. PMID: 29730128.

9. Lok CE, Huber TS, Lee T, Shenoy S, Yevzlin AS, Abreo K, Allon M, Asif A, Astor BC, Glickman MH, Graham J, Moist LM, Rajan DK, Roberts C, Vachharajani TJ, Valentini RP; National Kidney Foundation. KDOQI Clinical Practice Guideline for Vascular Access: 2019 Update. Am J Kidney Dis. 2020 Apr;75(4 Suppl 2):S1-S164. doi: 10.1053/j.ajkd.2019.12.001. Epub 2020 Mar 12. Erratum in: Am J Kidney Dis. 2021 Apr;77(4):551. PMID: 32778223.
10. MacRae JM, Pandeya S, Humen DP, Krivitski N, Lindsay RM. Arteriovenous fistula-associated high-output cardiac failure: a review of mechanisms. Am J Kidney Dis, 43 (2004), pp. e17-e22

10. IMAGING THE ABDOMEN: ULTRASOUND, CT AND MRI, WHEN AND HOW?

Durim Cela, Blerina Saraci, Erinda Kola
WFUMB Center of Education Tirana, Albania

10.1 Introduction: the role of imaging in abdominal diagnostics

Imaging plays a crucial role in abdominal health and diagnostics, offering detailed insights into the complex anatomy and function of abdominal organs. When diseases or abnormalities arise, the intricate anatomy and overlapping systems often make clinical assessment alone insufficient. Here, imaging emerges as an indispensable tool for accurate and timely diagnosis. Advanced imaging technologies, such as ultrasound, computed tomography (CT), and magnetic resonance imaging (MRI), allow healthcare providers to visualize and assess these organs non-invasively. This enables early detection of abnormalities, guides accurate diagnoses, and informs treatment plans. For example, imaging is essential for diagnosing conditions like appendicitis, gallstones, liver diseases, tumors, and inflammatory conditions. Moreover, imaging plays a critical role in assessing abdominal trauma, identifying internal bleeding, and evaluating organ damage. It also guides minimally invasive procedures, such as biopsies or abscess drainage, ensuring precision and reducing the need for more invasive surgeries. In essence, abdominal imaging is indispensable for improving patient outcomes by providing detailed, timely information, supporting accurate diagnoses, and facilitating effective treatments across a wide range of abdominal health concerns.

Modern imaging modalities such as ultrasound (US), computed tomography (CT), and magnetic resonance imaging (MRI) offer unparalleled insights into the abdominal cavity.

Ultrasound is a widely used, non-invasive imaging technique that utilizes high-frequency sound waves to create real-time images of the body's internal structures. It is particularly valuable in abdominal imaging, offering a safe and cost-effective way to evaluate organs such as the liver, gallbladder, kidneys, and pancreas. With no exposure to ionizing radiation, ultrasound is often the first-line modality for diagnosing conditions like gallstones, kidney stones, or fluid collections. It is also instrumental in guiding procedures such as biopsies or drain placements. Portable and versatile, ultrasound continues to be an essential tool in both routine diagnostics and emergency care.

Computed Tomography scanner is a powerful imaging tool that uses X-rays and advanced computer technology to produce detailed cross-sectional images of the body. In abdominal imaging, CT scans are invaluable for diagnosing a wide range of conditions, including trauma,

tumors, infections, and vascular abnormalities. With its ability to provide high-resolution images quickly, CT is particularly essential in emergency settings, such as assessing internal bleeding or organ damage. It also plays a critical role in planning surgeries, guiding interventions, and monitoring treatment progress, making it a cornerstone of modern diagnostic medicine.

Magnetic Resonance Imaging (MRI) is a cutting-edge imaging technology that uses strong magnetic fields and radio waves to produce highly detailed images of the body's internal structures. In abdominal imaging, MRI is particularly valuable for its exceptional soft-tissue contrast, making it ideal for evaluating the liver, pancreas, bile ducts, and other complex areas. MRI is often used to diagnose and monitor conditions such as tumors, liver disease, vascular abnormalities, and inflammatory conditions. With its non-invasive approach and lack of ionizing radiation, MRI is a safe and powerful tool for gaining deep insights into abdominal health.

Abdominal imaging is essential in evaluating a wide range of conditions, such as:

- Abdominal pain: Imaging helps identify the underlying causes of acute or chronic abdominal pain, such as appendicitis, cholecystitis, pancreatitis, or bowel obstructions.
- Trauma: In cases of abdominal injury, imaging is vital for detecting internal bleeding, organ rupture, or damage to major blood vessels.
- Tumors and masses: Imaging aids in the detection and characterization of tumors in the liver, pancreas, kidneys, or other abdominal organs, helping guide diagnosis and staging of cancers.
- Infections and abscesses: Conditions like diverticulitis, pelvic inflammatory disease, or hepatic abscesses are often diagnosed and monitored using imaging.
- Gallstones and kidney stones: Ultrasound and CT scans are commonly used to confirm the presence of stones and assess complications like obstruction or infection.
- Liver diseases: Imaging evaluates conditions such as fatty liver disease, cirrhosis, or hepatic tumors, and helps monitor disease progression.
- Bowel conditions: Imaging is crucial in diagnosing inflammatory bowel diseases (Crohn's disease and ulcerative colitis), ischemic bowel, and intestinal perforations.
- Vascular conditions: Abdominal imaging can detect aneurysms, blood clots, or ischemia affecting abdominal vessels.
- Gynecological and obstetrical issues: For women, imaging evaluates pregnancy, ovarian cysts, ectopic pregnancies, uterine fibroids, or pelvic masses.

10.2 Understanding the imaging modalities

US is a non-invasive imaging technique that uses high-frequency sound waves to create real-time images of the inside of the body. It is a safe and widely used method for assessing abdominal organs, such as the liver, kidneys, and gallbladder. It is also commonly used in obstetrics, musculoskeletal evaluations, and guiding certain procedures like biopsies. Ultrasound is portable, quick, and cost-effective, making it an essential tool in both emergency and routine diagnostics. While US is a highly useful and non-invasive imaging tool, it does have some limitations:

1. Limited penetration in obese patients: The effectiveness of ultrasound can be reduced in patients with a high body mass index (BMI), as sound waves may not penetrate deeply enough to provide clear images.
2. Image quality: US images can be affected by factors such as the patient's body type, the skill of the technician, and the location of the organ being imaged. Structures that are deep within the body or obstructed by gas (e.g., bowel gas) may not be well visualized.
3. Operator dependency: The quality of the images and the accuracy of the results can be influenced by the experience and expertise of the operator performing the ultrasound.
4. Limited field of view: US provides a real-time view of a specific area, but it may not always capture a comprehensive view of the entire region, particularly when deeper structures need to be assessed.

CT is a medical imaging technology that uses X-rays combined with advanced computer processing to generate detailed, cross-sectional images of the body. By capturing images from multiple angles, CT scans provide precise visualizations of bones, organs, blood vessels, and soft tissues. CT delivers high-resolution images with exceptional anatomical detail. It is fast imaging, making it ideal for trauma and emergency situations. Although these mentioned above priorities, CT has some limitations: it involves exposure to ionizing radiation, which requires careful consideration, especially in vulnerable populations and use of contrast agents carries a risk of allergic reactions or kidney issues in certain individuals. Despite these limitations, CT remains an essential diagnostic tool, offering unmatched speed and accuracy in critical and complex medical cases.

MRI is a non-invasive imaging technology that uses powerful magnetic fields and radiofrequency pulses to generate detailed images of the body's internal structures. It offers precise, high-quality imaging, with no exposure to ionizing radiation, making it a safer imaging choice for many. Although the advantages it has, mri has some limitations: high cost compared to other imaging techniques, which may limit accessibility; longer imaging times, often requiring patients to remain still for extended periods; contraindications for patients with certain implanted devices (e.g., pacemakers or metal implants) due to potential interference with the magnetic field.

10.3 When to use each modality: indications for abdominal imaging

US is particularly valuable for early detection and routine assessment of conditions affecting the hepatobiliary system, renal system, and pregnancy. Its ability to visualize soft tissues, fluid collections, and blood flow in real time makes it an essential tool for primary diagnosis and follow-up.

- **Hepatobiliary system**: US is the gold standard for assessing gallbladder and liver disease, offering detailed imaging of the hepatobiliary system.
- Gallstones (cholelithiasis): US detects echogenic stones with posterior acoustic shadowing in the gallbladder. It is the preferred modality for diagnosing gallstones and their complications, such as acute cholecystitis.
- Liver disease:
  - Fatty liver disease: Appears as an increased echogenicity of the liver.
  - Cirrhosis: Identified through coarse liver texture, nodular surface, and splenomegaly.
  - Liver masses: Used to differentiate benign (hemangiomas, cysts) from malignant tumors (hepatocellular carcinoma, metastases).
- Biliary obstruction: Detects dilated bile ducts due to stones, strictures, or tumors affecting bile flow.

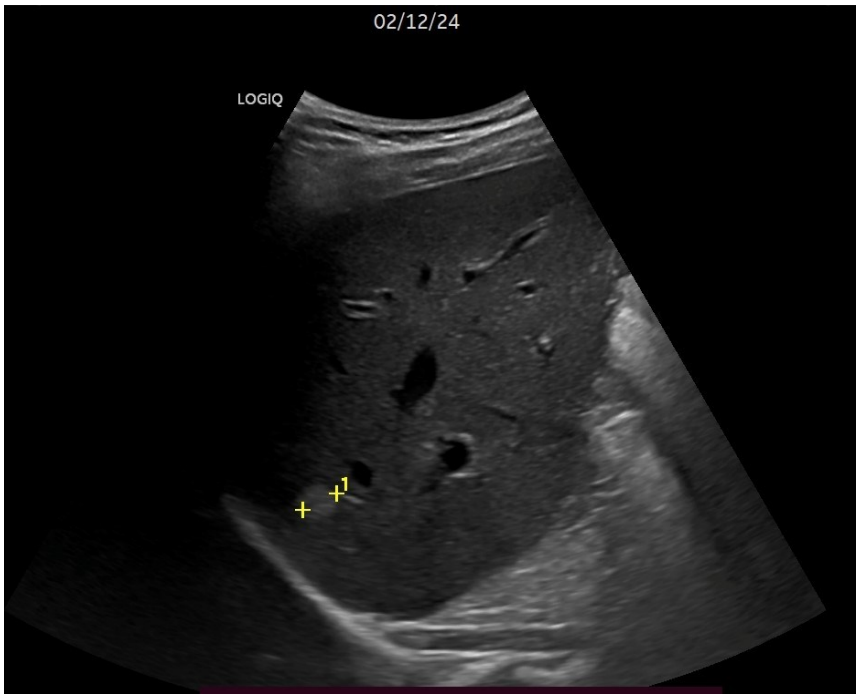

Fig. 10.1. Liver hyperechoic lesion suggestive of hemangioma

◆**Renal system**: US is commonly used for initial kidney evaluation, providing detailed images of renal structure and pathology.

- Kidney stones (nephrolithiasis):
    - Stones appear as echogenic structures with acoustic shadowing.
    - Hydronephrosis (swelling of the kidney due to obstruction) can be visualized, suggesting urinary tract obstruction.
- Renal cysts or masses: Simple cysts appear as anechoic structures with thin walls; complex cysts (with septations or solid components) may suggest malignancy; hyperechogenic masses may suggest renal masses like angiomyolipoma or renal cell carcinoma.
- Chronic kidney disease (CKD): US helps in monitoring cortical thinning, small echogenic kidneys, and loss of corticomedullary differentiation in advanced CKD.

◆**Pregnancy monitoring**: Obstetric ultrasound is essential for assessing fetal health, growth, and structural development. It is used in:

- First trimester: Confirms pregnancy and gestational age; rules out ectopic pregnancy; detects early fetal abnormalities.
- Second and third trimester: Assesses fetal anatomy, growth, and amniotic fluid levels; screens for congenital anomalies (e.g., neural tube defects, cardiac abnormalities); evaluates placenta previa, placental abruption, and fetal distress.

  Ultrasound is also vital in guiding invasive procedures like amniocentesis and chorionic villus sampling (CVS).
- Gynecological issues: For women, imaging evaluates ovarian cysts, ectopic pregnancies, uterine fibroids, or pelvic masses.

CT is a highly valuable imaging modality for trauma assessment, detection of masses, and evaluation of abdominal pain or unexplained symptoms. Due to its high spatial resolution, rapid acquisition, and ability to provide detailed cross-sectional imaging, CT is often the preferred diagnostic tool in acute and complex cases.

➢ **Trauma cases. CT is the** gold standard **for evaluating abdominal trauma due to its ability to quickly identify** internal injuries, hemorrhage, and organ damage**.**

- Blunt trauma: CT helps assess solid organ injuries (e.g., liver lacerations, splenic rupture, renal contusions).
- Penetrating trauma: Used to detect vascular injuries, bowel perforation, or foreign bodies.

- Hemorrhage detection: Contrast-enhanced CT scan localize active bleeding, guiding surgical or interventional management. CT imaging with IV contrast is essential in trauma cases to improve the detection of vascular injuries and internal bleeding.

➢ **Detection of abdominal masses**. **CT plays a critical role in detecting and characterizing** abdominal masses**, differentiating between** benign and malignant lesions**, and staging cancers.**

- Pancreatic cancer: CT can identify pancreatic masses, ductal dilation, and metastatic spread. Triphasic contrast-enhanced CT improves the detection of small pancreatic tumors.
- Colorectal cancer: CT is useful for tumor staging, lymph node involvement, and metastasis evaluation.
- Liver tumors: Differentiates benign lesions (hemangiomas, adenomas) from malignant tumors (hepatocellular carcinoma, metastases). CT with arterial-phase imaging enhances detection of hypervascular liver tumors.
- Renal and adrenal masses: Identifies renal cell carcinoma, adrenal adenomas, and pheochromocytomas.

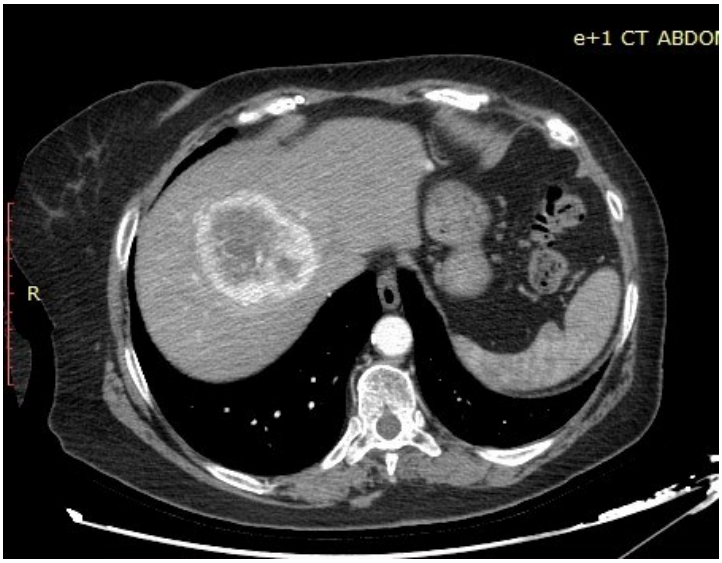

Fig.10.2. Liver mass on CT image proven histologically neuroendocrine tumor.

➢ **Evaluation of abdominal pain and unexplained symptoms.**

CT is frequently used in patients with acute or chronic abdominal pain to rapidly diagnose conditions requiring urgent intervention.

- Appendicitis: CT is the most accurate imaging modality for detecting appendiceal inflammation, perforation, and abscess formation. Findings include enlarged appendix (>6 mm), wall thickening, and peri-appendiceal fat stranding.

- Diverticulitis: CT identifies inflamed diverticula, pericolic fat stranding, and complications such as abscesses or perforation. Differentiates simple from complicated diverticulitis (e.g., presence of fistulas or obstructions).
- Bowel obstruction:CT assesses dilated loops of bowel, transition points, and causes of obstruction (adhesions, tumors, hernias). Can differentiate between mechanical obstruction and paralytic ileus.
- Ischemic bowel disease: Angio- CT detects vascular occlusion, bowel wall thickening, and pneumatosis intestinalis (gas within bowel walls). It helps in early diagnosis to prevent bowel necrosis.
- Unexplained weight loss or fever of unknown origin (FUO): CT can reveal occult malignancies, infections (abscesses, tuberculosis), or inflammatory conditions (Crohn's disease, autoimmune pancreatitis).

MRI is the gold standard for assessing liver lesions and fatty liver disease, particularly when the diagnosis is uncertain after ultrasound or CT. It is particularly valuable in complex cases where precise tissue characterization and functional imaging are essential.

Superior soft tissue differentiation. MRI is the gold standard for assessing soft tissue structures, providing detailed contrast between normal and abnormal tissues.

- Ideal for evaluating lesions with soft tissue components, fibrosis, or inflammation.
- Provides better differentiation between benign and malignant lesions than CT or ultrasound.

Detailed imaging of abdominal organs.

➢ *Liver imaging.* ***MRI is highly sensitive in detecting*** *liver lesions* ***and differentiating between*** *benign and malignant tumors.*

- Hepatic hemangiomas: Bright on T2-weighted images with peripheral nodular enhancement in late arterial phase and progressive centripetal fill-in in venous phase.
- Focal nodular hyperplasia (FNH): Shows arterial enhancement with a characteristic central scar on delayed imaging.
- Hepatocellular carcinoma (HCC): Best evaluated with MRI using hepatobiliary contrast agents for lesion characterization.
- Liver fibrosis and cirrhosis: MRI elastography (MRE) allows for non-invasive liver stiffness measurement, crucial in staging cirrhosis and fibrosis.

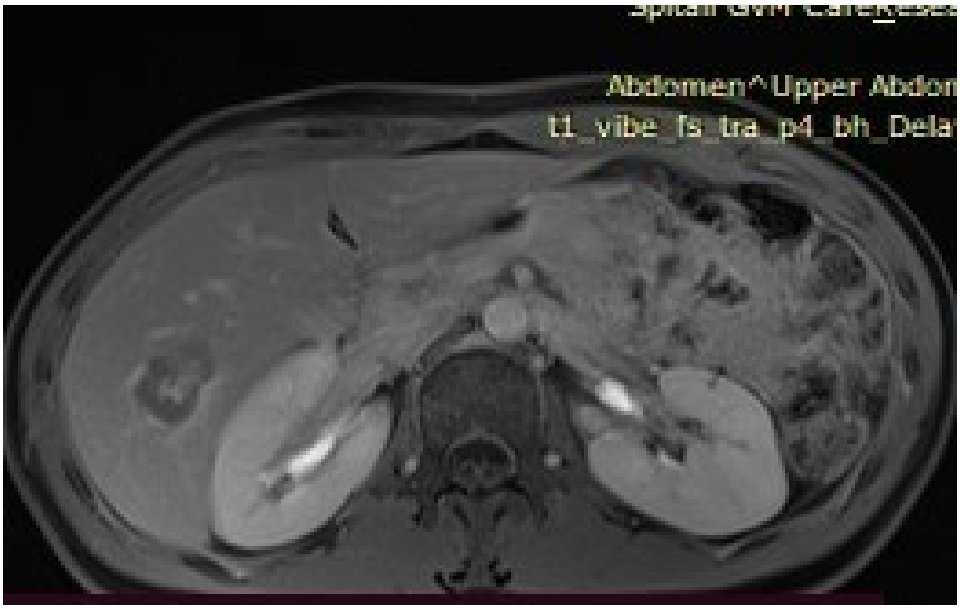

Fig. 10.3. Liver FNH with typically late enhancement of central scar

➢ *Pancreatic imaging.* ***MRI is preferred over CT in cases of*** *pancreatic disease****, especially for detecting*** *early-stage tumors and cystic lesions****.***

- Pancreatic cancer: MRI improves detection of small pancreatic tumors.
- Cystic lesions (IPMNs, pseudocysts): MRI helps classify cysts based on fluid content and wall characteristics.
- Chronic pancreatitis: MR cholangiopancreatography (MRCP) assesses ductal abnormalities, strictures, and calcifications.

➢ *Bowel imaging.* ***MRI is highly effective in assessing*** *inflammatory and neoplastic bowel conditions****.***

- Inflammatory bowel disease (IBD): MRI enterography (MRE) provides detailed imaging of Crohn's disease and ulcerative colitis. Detects bowel wall thickening, strictures, fistulas, and active inflammation.
- Bowel tumors: MRI is superior in characterizing rectal cancers and staging pelvic malignancies.

➢ *Abdominal masses and tumors.* ***MRI is useful for characterizing*** *abdominal masses****, particularly when ultrasound or CT findings are inconclusive.***

- Differentiates solid vs. cystic masses, guides biopsy planning.
- Used in ovarian tumors, adrenal lesions, and retroperitoneal sarcomas.

10.4 How to Use Each Modality: Technique and Procedure

US is a widely used, non-invasive imaging technique that provides real-time visualization of internal structures. With minimal patient discomfort and no radiation exposure, it is a safe and effective diagnostic tool across various medical fields. This is an overview of the technical aspects of sonography, including preparation, procedure, and patient experience. Preparation includes patient and equipment preparation. The patient preparation for an ultrasound exam varies depending on the type of scan being performed:

- Abdominal US: Patients are often required to fast for 6–8 hours to reduce interference from gas and ensure clear imaging of the liver, gallbladder, and pancreas.
- Pelvic US: A full bladder is typically needed for transabdominal pelvic scans to provide a better acoustic window. Patients may be asked to drink water and avoid urinating before the exam.
- Musculoskeletal or vascular US: No specific preparation is needed, though patients may be advised to wear loose clothing for easy access to the area being scanned.
- Transvaginal or transrectal US: Patients may be asked to empty their bladder before the exam.

Equipment preparation includes:

- Ultrasound machine: The machine consists of a transducer (probe), a control panel, and a monitor for image display.
- Transducer selection: Different types of transducers are used depending on the area being examined (e.g., linear, convex or endocavitary probes).
- Gel application: A water-based gel is applied to the skin to facilitate sound wave transmission and eliminate air gaps.

Procedure includes:

1. Patient positioning: The patient is positioned according to the area being examined (e.g., supine, lateral, or seated).
2. Transducer application: The transducer is gently pressed against the skin and moved over the area of interest.
3. Image acquisition: The transducer emits high-frequency sound waves that penetrate the body. These waves reflect off tissues and return to the transducer. The ultrasound machine processes the echoes to generate real-time images.
4. Image interpretation: Sonographers adjust settings such as depth, gain, and focus to optimize image quality.

5. Specialized techniques:
    - 3D/4D Ultrasound: Advanced imaging for obstetric and diagnostic applications.
    - Contrast-Enhanced Ultrasound: Uses microbubble contrast agents to enhance vascular imaging.
    - Elastography: Evaluates tissue stiffness, often used in liver and breast imaging.

*Most ultrasound exams take **15 to 30 minutes**, depending on complexity. T**he procedure is comfort and safe, painless**, with no ionizing radiation exposure, well- tolerated. No recovery time is required, and patients can resume normal activities immediately. Results are interpreted by a radiologist or specialist and reported to the referring physician.*

CT is a powerful diagnostic tool that provides fast, detailed imaging of internal structures. While it involves ionizing radiation, modern dose-reduction techniques ensure patient safety. With minimal discomfort and rapid results, CT remains a critical imaging modality in modern medicine. Preparation for a CT scan varies depending on the type of scan being performed:

- Contrast vs. non-contrast scans: If contrast dye (iodine-based) is required, patients may need to fast for 4–6 hours before the scan. For non-contrast scans, no special preparation is typically needed.
- Specific body region preparation: Abdominal and pelvic CT: Patients may need to drink oral contrast (e.g., gastrografin) to enhance gastrointestinal imaging.
- Metal and clothing[DDC1] restrictions: Patients should remove metal objects (e.g., jewelry, piercings, glasses) as they may interfere with image quality.
- Pre-medication (if required): patients with iodine contrast allergies may need pre-medication; those with kidney disease may need hydration protocols to reduce contrast-induced nephropathy risk.

Procedure.

1. Patient positioning: the patient lies on a motorized examination table, usually supine (face-up).
2. Scanning process. The CT scanner consists of a gantry (large circular structure) that houses X-ray tubes and detectors. The table moves through the gantry while the X-ray beam rotates around the body, capturing multiple cross-sectional images. Data is processed by the computer to reconstruct detailed images of organs, bones, blood vessels, and soft tissues.
3. Use of contrast agents (if needed): Intravenous (IV) contrast, injected into a vein to highlight blood vessels and tissues; oral contrast: iodine-based solution for gastrointestinal imaging; rectal contrast: used for specific bowel studies.

4. Radiation exposure considerations. CT scans use ionizing radiation, but dose-reduction techniques help minimize exposure. Pediatric and pregnant patients require special dose adjustments.
5. Image acquisition and reconstruction. Advanced multi-detector CT (MDCT) allows high-resolution imaging with rapid scan times. Images can be reformatted into 3D reconstructions for surgical planning and intervention.

*The scan itself is **painless**, though the IV contrast injection may cause a warm sensation or metallic taste. The enclosed gantry may cause **claustrophobia** in some patients, though CT scanners are more open than MRI machines. The entire scan typically lasts **5–15 minutes**, with actual imaging taking only seconds. Patients can usually resume normal activities immediately. If contrast was used, drinking plenty of fluids helps flush it from the system. Results are interpreted by a radiologist and sent to the referring physician.*

MRI is a powerful, non-invasive imaging modality that provides detailed images of soft tissues and organs. Below is an overview of the technical aspects of MRI, including preparation, procedure, and patient experience.

Preparation for an MRI scan depends on the body part being examined and whether contrast material is required. Patients must remove metal objects (e.g., jewelry, piercings, watches, eyeglasses, dentures) as they can interfere with the magnetic field. For most MRI scans, no fasting is required. If contrast (gadolinium-based) is used, fasting for 4–6 hours may be recommended to prevent nausea. Patients with implants, pacemakers, cochlear implants, or metal fragments must inform their doctor, as MRI may be contraindicated for them. Pregnant patients should notify their physician, though MRI is generally considered safe without contrast. Contrast administration: In some cases, gadolinium contrast is injected intravenously to enhance tissue visualization. Patients with kidney disease may require screening to assess their ability to safely process the contrast.

Procedure: The patient lies flat on a movable table, usually supine (face-up). Positioning aids like straps, pillows, or cushions help keep the patient still. The table moves into the MRI scanner, a large cylindrical magnet. The machine generates a strong magnetic field, causing hydrogen atoms in the body to align. Radiofrequency (RF) pulses are applied, disrupting the alignment and producing signals that are detected by the system. A computer processes these signals to create high-resolution cross-sectional images of the body. Use of contrast agents (if needed): Gadolinium-based contrast is injected into a vein to enhance visualization of blood vessels, tumors, and inflammation. Unlike CT contrast, gadolinium is not iodine-based and has a lower risk of allergic reaction.

MRI machines produce loud knocking or buzzing noises due to the switching of magnetic gradients. Patients wear earplugs or headphones to reduce noise and may listen to music. A two-way intercom allows communication with the MRI technologist.

Patient experience: *MRI is* ***painless and non-invasive****, with no exposure to ionizing radiation. The* ***narrow bore of the scanner*** *may cause* ***claustrophobia****, but open MRI machines or sedation options are available.* ***Contrast injection*** *may cause* ***mild discomfort****, warmth, or a metallic taste, but reactions are rare. Loud noises can be disorienting.*

Duration: **MRI scans take more often 30-45** minutes**, depending on the area being examined. Some specialized scans may take longer, but breaks can be provided if needed.**

Post-procedure: **Most patients can** resume normal activities immediately **after the scan. If contrast was used, drinking fluids can help flush it out of the body. MRI results are analyzed by a radiologist and reported to the referring physician.**

10.5 Comparison of Ultrasound, CT, and MRI: Strengths and limitations

Table 10.1. Comparison features of imaging modalities

Feature	Ultrasound	CT	MRI
Radiation	None	Yes (X-ray based)	None
Cost	Low	Moderate to High	High
Image Detail	Moderate	High	Very High
Speed	Fast (real-time)	Fast	Slow
Use for Soft Tissue	Limited	Moderate	Excellent
Use for Bone Evaluation	Limited	Excellent	Limited
Common Indications	Gallbladder, Kidney, Pregnancy	Trauma, Cancer, Abdominal Pain	Liver, Pancreas, Soft Tissues
Patient Comfort	High	Moderate (Contrast Injection)	Moderate (Claustrophobia)

Choosing the appropriate imaging modality depends on the clinical scenario, patient condition, and diagnostic goals. Below is a comparative analysis of the most commonly used imaging techniques to guide clinicians in selecting the most suitable option.

Table 10.2. Comparison features of imaging modalities

Feature	Ultrasound	CT	MRI
Primary Use	Obstetrics, soft tissues, vascular imaging	Trauma, cancer staging, internal organ assessment	Neurology, musculoskeletal, soft tissue, tumor characterization
Radiation Exposure	No	Yes (moderate)	No
Contrast Use	No	Often (iodine-based)	Often (gadolinium-based)
Soft Tissue Detail	Moderate	Good	Excellent
Bone Imaging	Limited	Excellent	Limited
Speed	Minutes	Minutes	30- 45 minutes
Portability	Bedside use	Fixed location	Fixed location
Cost	Low	Moderate to high	High
Contraindications	None	Kidney disease (if contrast is needed)	Claustrophobia, metal implants, pacemakers

Modality selection based on clinical indications:

- Trauma and emergency cases. *Best choice:* CT scan. Reasoning: Fast, detailed imaging of fractures, internal bleeding, and organ injuries. *Alternative:* X-ray for fractures; Ultrasound for focused assessments (FAST exam in trauma).
- Abdominal pain (appendicitis, gallbladder and kidney stones). *Best choice:* CT scan. *Reasoning:* Excellent visualization of organs and pathology. *Alternative:* Ultrasound.
- Obstetrics and gynecology (Pregnancy monitoring, gynecological conditions). *Best choice:* Ultrasound. *Reasoning:* No radiation exposure; real-time imaging of fetal development and pelvic structures. *Alternative:* MRI for detailed soft tissue assessment of pelvic organs.
- Vascular disease: arterial disease, aneurysms, thrombosis, ruptures. *Best choice:* CT Angiography. *Reasoning:* High-resolution imaging of blood vessels; non-invasive artery assessment. *Alternative:* Ultrasound/Doppler for peripheral vascular disease.
- Oncology (Tumor detection, staging, treatment monitoring). *Best choice:* MRI for soft tissues; CT for overall staging. *Reasoning:* MRI offers better soft tissue contrast, while CT is preferred for lung, abdominal, and pelvic tumors. *Alternative:* PET-CT for metabolic activity assessment.

Conclusion and decision-making guidelines:

➔ For non-invasive, radiation-free imaging → Ultrasound: pregnancy, soft tissue, vascular.

➔ For detailed, cross-sectional imaging → CT scan: trauma, cancer, abdominal disease.

➔ For highest soft tissue resolution → MRI: liver, pancreas, etc, musculoskeletal, tumors.

Clinicians should consider patient safety, diagnostic accuracy, availability, and cost when selecting the most appropriate imaging modality.

10.6 Challenges and limitations of abdominal imaging

Abdominal imaging plays a crucial role in diagnosing and managing conditions affecting the gastrointestinal (GI) tract, liver, pancreas, kidneys, and vasculature. However, each imaging modality has limitations and challenges that may impact diagnostic accuracy and clinical decision-making. Understanding these limitations helps clinicians recognize when additional testing or alternative approaches are needed.

Ultrasound (US) limitations:

- Body habitus (Obesity).
  - Impact: Excessive subcutaneous fat attenuates sound waves, reducing penetration and degrading image quality.
  - Clinical challenge: Organs like the pancreas, liver, and kidneys may be difficult to visualize in overweight or obese patients.
  - Potential workarounds: using lower-frequency transducers to improve penetration (though at the cost of resolution); adjusting patient positioning to optimize imaging windows; alternative imaging: CT or MRI is often preferred in obese patients for deeper organ assessment.
- Bowel gas interference.
  - Impact: Gas in the intestines scatters ultrasound waves, creating acoustic shadows that obstruct visualization of deeper structures.
  - Clinical challenge: Pancreas, abdominal vasculature, and retroperitoneal structures are often obscured. Conditions like pancreatitis, small tumors, and aneurysms may not be well visualized.
  - Potential workarounds: fasting before the exam (typically 6–8 hours) can reduce bowel gas; using different scanning angles and patient positions to improve visualization; alternative imaging: CT and MRI are often needed for comprehensive evaluation of deep abdominal structures.

- Operator dependence
  - Impact: The quality and accuracy of ultrasound imaging depend heavily on the skill and experience of the sonographer.
  - Clinical challenge: Variability in technique and interpretation can lead to missed diagnoses or false positives/negatives. Subtle pathology (e.g., small tumors, early inflammatory changes) may be overlooked by inexperienced operators.
  - Potential workarounds: Standardized training and certification programs for sonographers; utilization of AI-assisted ultrasound technology to enhance accuracy; alternative imaging: CT and MRI provide more reproducible and standardized results.

- Challenge: Patient cooperation: Movement and inability to hold breath can reduce image clarity. Time -consuming for complex cases: Doppler studies or detailed evaluations require more time and expertise.

- Limited field of view and depth.
  - Impact: Ultrasound has a restricted field of view, limiting its ability to assess large or deep structures. Deep-seated organs such as the pancreas and retroperitoneum may not be well visualized.
  - Clinical Challenge: Large tumors or diffuse disease may be partially visualized, requiring further imaging.
  - Alternative Imaging: CT and MRI provide a more complete anatomical overview.

- Difficulty in evaluating certain pathologies.
  - Challenges in detecting small lesions and tumors: Liver lesions, pancreatic tumors, and small renal masses can be difficult to detect, especially if obscured by bowel gas or in obese patients.
  - Vascular imaging limitations: Doppler ultrasound can assess blood flow but is less effective in obese patients or cases of deep vascular pathology.
  - Alternative imaging: CT or MRI with contrast is often required for precise lesion characterization and vascular assessment.

While ultrasound is an excellent first-line imaging tool, it may not be sufficient in the following cases.

Table 10.3. Clinical scenarios in which US may be not sufficient and alternative imaging.

Clinical scenario	Limitation of Ultrasound	Alternative Imaging
Obese patients	Poor penetration of sound waves	CT
Suspected deep-seated tumors (e.g., pancreatic cancer)	Bowel gas obstruction, limited resolution	CT or MRI
Liver lesion characterization	Limited differentiation of benign vs. malignant masses	CT with contrast
Retroperitoneal pathology (e.g., adrenal tumors, lymphadenopathy)	Poor visualization due to overlying structures	CT
Acute trauma (internal bleeding, solid organ injury)	Incomplete assessment, especially for deep injuries	CT
Bowel obstruction or ischemia	Gas interference limits evaluation	CT with contrast

Computed Tomography (CT). ***Limitations of CT Imaging.***

- Radiation exposure.
  - There is radiation dose compared to MRI and ultrasound.
  - Risk consideration: While the dose is low in a single scan, repeated exposure increases the risk of radiation-induced effects, particularly in pediatric and young patients.
  - Alternative: ultrasound or MRI may be preferred in cases where radiation is a concern.
- Contrast agent risks
  - Iodine-based contrast agents can cause allergic reactions and nephrotoxicity, particularly in patients with pre-existing renal impairment.
  - Workarounds: Use non-contrast CT if possible. Pre-medication and pre-scan hydration in high-risk patients.
- Lower soft tissue contrast compared to MRI
  - CT is less effective in differentiating soft tissue abnormalities compared to MRI.
  - Impact: CT provides excellent anatomical details, but it is less effective in functional or soft tissue assessment compared to MRI.
  - Clinical Challenge: Liver lesion characterization: CT may struggle to differentiate benign vs. malignant tumors compared to MRI with contrast.
  - Alternative Imaging: MRI is preferred for detailed soft tissue and functional imaging. Ultrasound elastography can assess liver fibrosis without radiation.

➢ Cost and availability

- Higher cost than ultrasound, though generally less expensive than MRI.
- Limited access in resource-limited settings or small healthcare facilities.

Challenges in abdominal CT interpretation:

- Motion and breathing artifacts. Impact: Image quality can be degraded by patient movement or poor breath-holding, leading to blurring and difficulty in diagnosis. Clinical challenge: Elderly, pediatric, or critically ill patients may struggle to hold their breath during scanning. Workarounds: Use faster multi-detector CT scanners to minimize motion artifacts; consider sedation in uncooperative patients (e.g., pediatric cases).
- Bowel distension and gas interference. Impact: Overlapping bowel loops and gas can obscure small lesions or vascular abnormalities. Clinical challenge: Small tumors, inflammation, or ischemic changes may be missed in gas-filled regions. Workarounds: Oral contrast can improve differentiation between bowel loops and surrounding structures. MRI may provide better visualization of certain bowel conditions.

When abdominal CT may be insufficient:

- Characterizing small liver lesions (MRI provides better soft tissue contrast).
- Functional assessment of organs, such as detecting biliary motility issues.
- Repeated imaging needs in young patients due to radiation concerns.

Table 10.4. Clinical scenarios in which CT may be not sufficient and alternative imaging.

Clinical Scenario	Limitation of CT	Alternative Imaging
Pediatric patients or frequent follow-ups	High radiation exposure	MRI or ultrasound
Renal failure patients	Risk of contrast-induced nephropathy	MRI (gadolinium-based contrast) or ultrasound
Soft tissue lesion characterization	Limited differentiation of benign vs. malignant tumors	MRI
Functional assessment (e.g., liver fibrosis, bowel motility)	CT provides anatomical, not functional imaging	MRI, ultrasound elastography
Pregnancy	Radiation exposure risk	Ultrasound or MRI
Bowel ischemia vs. inflammation	Functional assessment is difficult	MRI with contrast-enhanced sequences

Magnetic Resonance Imaging (MRI). ***Limitations:***

- High cost. Impact: **MRI is generally more** expensive **compared to other imaging modalities like** CT or ultrasound**, making it less accessible in resource-limited settings.** Clinical challenge:
    - In some cases, cost may limit its use for routine monitoring or when alternative imaging (such as ultrasound) is sufficient.
    - Insurance coverage or reimbursement limitations may also affect its use. Workarounds: Cost-effective alternatives like ultrasound or CT may be considered if MRI is not absolutely necessary. Use MRI for complex cases where it provides significant diagnostic value.
- Limited availability. Impact: **MRI machines are** more specialized **than CT or ultrasound, and not all hospitals or clinics have access to them.** Clinical challenge:
    - Waiting times for an MRI can be long in some regions, especially for non-emergency cases.
    - Lack of availability in smaller facilities or rural areas may necessitate patient referral to larger centers.
    - Workarounds: Timely referral to institutions with MRI capabilities for urgent cases. In cases where MRI is not available, CT or ultrasound may be appropriate alternatives, depending on the clinical scenario.
- Long scanning times. Impact: **MRI exams take** longer to perform **than CT or ultrasound. A typical abdominal MRI can take anywhere from** 30 – 45 minutes**, which may be difficult for certain patients to tolerate. C**linical challenge:
    - Patient discomfort from prolonged immobility, especially in patients with claustrophobia, obesity, or pain.
    - Pediatric patients and elderly patients may struggle to remain still for long periods, affecting image quality.
    - Workarounds: Sedation or anxiolytic medication may be used for patients who have difficulty tolerating the scan. Fast MRI sequences and breath-hold techniques may reduce the scan time, but these may not always be feasible depending on the patient's condition.
- Contraindications for certain implants. Impact: **MRI relies on** magnetic fields **and** radiofrequency waves**, which can be problematic for patients with certain metallic implants, such as: p**acemakers, cochlear implants, metallic stents or aneurysm clips, other implanted medical devices. Clinical Challenge: Contraindicated devices **can pose serious safety risks, such as device malfunction or tissue damage. For patients with incompatible implants, MRI is not an option for evaluating abdominal pathology.**

Workarounds: Pre-scan screening **for implants and devices that may not be MRI-compatible is essential. For patients with contraindications,** alternative imaging modalities **like** CT or ultrasound **may be used.**

Additional challenges with abdominal MRI

- Image artifacts. Impact: **MRI is susceptible to** motion artifacts**, especially when patients cannot hold their breath or remain still during the scan.** Clinical challenge: Bowel motion, respiratory motion, or patient movement **can create artifacts, leading to** suboptimal image quality **and potentially missed diagnoses.** Workarounds: **Techniques like** breath-hold sequences **or** sedation **can help mitigate motion-related issues. If motion artifacts remain significant,** CT or ultrasound **may provide clearer images.**
- Limited assessment of calcifications or bone abnormalities. Impact: **MRI is not ideal for evaluating** calcified lesions **or** bone abnormalities**, as it is less sensitive to these conditions compared to CT.** Clinical challenge: **MRI may miss or poorly visualize** calcified tumors, bone fractures. Alternative imaging: CT **is more effective for assessing** calcifications, bone lesions, and complex fractures**.**

When MRI may be insufficient:

- ◆ Emergent cases where rapid imaging is needed (CT is preferred).
- ◆ Severely ill or uncooperative patients who cannot tolerate the long scan time.
- ◆ Patients with metal implants incompatible with MRI.

When abdominal MRI may be insufficient?

Clinical scenario	Limitation of MRI	Alternative Imaging
Pediatric patients	Long scanning times and potential for patie non-cooperation	Ultrasound, sedation-assisted MRI
Patients with pacemaker or metal implants	Contraindications for MRI	CT or ultrasound
Acute trauma	MRI may be too slow for emergency use, a does not provide good bone detail	CT for quick, comprehensive assessmen
Bone abnormalities	Poor visualization of calcifications and bon structures	CT for better bone detail
Obesity	Difficulty in obtaining high-quality images due to scanner limitations	CT

Each imaging modality has strengths and weaknesses in abdominal imaging. Clinicians should consider patient condition, urgency, safety, and diagnostic accuracy when choosing the best approach. In many cases, a multimodal strategy (e.g., ultrasound followed by CT or MRI) may be required for a definitive diagnosis.

10.7 Recent advances in abdominal imaging

Contrast-Enhanced Ultrasound (CEUS): An emerging tool for liver lesions and tumors

Contrast-Enhanced Ultrasound (CEUS) is gaining recognition as a valuable diagnostic modality in abdominal imaging, particularly for evaluating liver lesions and tumors. Unlike traditional ultrasound, which relies on the reflection of sound waves from tissues, CEUS uses microbubble contrast agents to enhance the quality of the images and improve the visualization of blood flow within tissues.

Clinical applications of CEUS

- Liver tumor evaluation: CEUS allows clinicians to accurately assess lesion morphology and vascularity, which are critical for determining the nature of the lesion and planning treatment.
- Liver transplantation: CEUS can also play a role in pre-transplant assessments by evaluating vascular structures and lesion characteristics, helping in donor liver evaluation.
- Follow-up and monitoring: CEUS is an excellent option for monitoring liver lesions over time, as it can be repeated frequently without the risk of radiation exposure.

Dual-Energy CT (DECT): Dual-Energy CT (DECT) is an advanced imaging technique that uses two different X-ray energy levels to capture images, providing significant improvements in tissue differentiation and radiation dose reduction compared to conventional CT. This technology is increasingly being used in abdominal imaging, particularly for the evaluation of complex cases such as liver lesions, renal stones, and vascular pathologies.

Benefits of Dual-Energy CT:

- Improved tissue differentiation. DECT allows for better differentiation of tissues with similar densities by utilizing two X-ray energy levels. This enables the scanner to differentiate between materials (e.g., iodine contrast, fat, bone, urinary stones, and soft tissues) based on their specific attenuation characteristics at different energy levels. The ability to quantify tissue composition (e.g., fat, water, and muscle) can help in detecting and characterizing liver lesions, tumors, and other abdominal conditions more accurately. For example, DECT is particularly effective in distinguishing iodine-based contrast agents from dense tissues (such as bone) or fat, which can be challenging in standard CT scans.

- Lower radiation dose. Dual-energy CT helps reduce radiation exposure by optimizing the amount of radiation needed to obtain high-quality images. The ability to use lower energy levels for certain scans while still maintaining diagnostic quality reduces the overall radiation dose to the patient. Flash CT scans can also be employed in conjunction with DECT to improve scan speed and reduce the total amount of radiation exposure, especially for abdominal imaging, where large areas of the body need to be scanned. This reduction in radiation is particularly important for pediatric patients or those requiring multiple follow-up scans, helping mitigate the cumulative risks associated with radiation exposure over time.
- Enhanced visualization of vascular structures. DECT is especially beneficial for vascular imaging, as it can improve the visualization of vascular structures such as arteries, veins, and tumors with higher vascularity. The ability to visualize vascular enhancement patterns more accurately allows clinicians to better assess conditions like tumors, aneurysms, and vascular malformations.

Clinical applications of Dual-Energy CT:

- Liver lesions. DECT improves the characterization of liver lesions, including benign lesions like hemangiomas and malignant tumors such as hepatocellular carcinoma (HCC). Better iodine differentiation with DECT helps assess the vascularity of liver tumors, aiding in distinguishing between metastatic tumors and primary liver cancer.
- Renal stone analysis. One of the standout uses of DECT is in the evaluation of renal stones. DECT provides enhanced material differentiation, allowing clinicians to identify different types of stones (e.g., uric acid stones vs. calcium-based stones) based on their unique composition. This capability can influence treatment decisions, such as the need for surgical removal versus conservative management.
- Vascular imaging. Its ability to distinguish contrast material from surrounding tissues allows for clearer delineation of vascular structures, enhancing pre-surgical planning and interventional radiology procedures.
- Abdominal trauma. In cases of abdominal trauma, DECT can assist in identifying and characterizing injuries to solid organs (e.g., liver, spleen, pancreas) and the vascular system (e.g., internal bleeding, aortic injuries) with greater clarity and speed.

Photon-Counting CT (PCCT): A Next-Generation Imaging Technology

PCCT is an advanced CT imaging modality that improves spatial resolution, enhances tissue contrast, and reduces radiation dose by using photon-counting detectors to measure individual X-ray photons.

Key Advantages:

- **Higher resolution:** Detects small lesions and microvascular details.
- **Enhanced tissue contrast:** More precise differentiation of soft tissues.
- **Lower radiation dose:** Efficient photon utilization reduces exposure.
- **Multi-energy imaging:** Provides spectral information in a single scan.

Clinical Applications:

- **Liver lesion characterization:** More accurate differentiation of tumor types.
- **Cardiovascular and vascular imaging:** Superior visualization of arteries and microcirculation.
- **Oncology imaging:** Improved tumor detection and therapy monitoring.

Magnetic Resonance Elastography (MRE). Magnetic Resonance Elastography (MRE) **is an advanced imaging technique that enables** non-invasive assessment **of** liver stiffness**, which is a critical indicator of liver** fibrosis **and** cirrhosis**. By measuring the stiffness of liver tissue, MRE provides valuable insights into the severity of liver disease, making it an essential tool for the diagnosis and monitoring of chronic liver conditions.**

MRE Elastography principles**: MRE uses** magnetic resonance imaging (MRI) **to assess the stiffness of tissues. A mechanical wave is generated and transmitted through the liver, and the MRI scanner detects the propagation of these waves.** Stiffer tissue **(which often corresponds to areas of** fibrosis **or** cirrhosis**) will cause the waves to travel more slowly, while** softer tissue **will allow the waves to propagate faster. By analyzing the wave patterns, MRE can generate a map of liver stiffness.**

Clinical applications of MRE.

- Assessment of liver fibrosis and cirrhosis: Liver stiffness is a key indicator of fibrosis, and in more advanced stages, cirrhosis. MRE provides a quantitative measurement that allows for accurate staging of liver fibrosis, which is crucial for determining disease severity and guiding treatment decisions. MRE is particularly useful in chronic liver diseases such as: Hepatitis B and C, non-alcoholic fatty liver disease (NAFLD), alcoholic liver disease, non-alcoholic steatohepatitis (NASH).
- Monitoring disease progression: MRE is useful for assessing the response to treatment in patients with chronic liver diseases. A reduction in liver stiffness after treatment can indicate improved liver function and a decrease in fibrosis. MRE can help track changes in liver stiffness, which may reflect the progression of fibrosis or cirrhosis, and can guide the timing of interventions such as antiviral therapy or liver transplantation.

Advantages of MRE

- Non-invasive and safe: MRE is a non-invasive procedure with no need for needle insertion or liver tissue removal, making it much safer than a liver biopsy. There is no risk of infection or bleeding, and it does not require sedation.
- Accurate and quantitative: MRE provides quantitative measurements of liver stiffness, which are more objective and reproducible compared to other non-invasive liver tests, such as ultrasound-based elastography.
- High sensitivity and specificity: MRE has been shown to have high sensitivity and specificity in detecting advanced liver fibrosis and cirrhosis, making it a valuable diagnostic tool in clinical practice.
- Reduced need for liver biopsy: Since MRE can provide a reliable measure of liver stiffness, it reduces the need for invasive liver biopsies, particularly in patients with chronic liver diseases who need regular monitoring.

Artificial Intelligence (AI) in radiology: Enhancing diagnosis, accuracy, and reducing human error

Artificial Intelligence (AI) is revolutionizing the field of radiology, assisting radiologists in their efforts to provide accurate and timely diagnoses. By leveraging advanced machine learning (ML) and deep learning (DL) algorithms, AI systems can analyze medical images with exceptional speed and accuracy, improving diagnostic outcomes and minimizing human error.

Role of AI in assisting radiologists:

- Automated image interpretation: AI algorithms are designed to analyze and interpret medical images, such as X-rays, CT scans, MRIs, and ultrasounds. These systems can detect abnormalities such as tumors, fractures, cysts, or other pathologies with high accuracy, sometimes even identifying issues that may be subtle or challenging for human radiologists to detect. Deep learning models, particularly convolutional neural networks (CNNs), are widely used in this domain due to their ability to learn patterns and identify complex features from images.
- Augmenting radiologist decision-making: AI systems are not designed to replace radiologists but to augment their capabilities. By providing secondary assessments, AI tools help radiologists make more informed decisions, thereby improving the efficiency and accuracy of diagnoses. For example, AI can flag potential abnormalities, allowing radiologists to prioritize and focus on complex cases. This collaboration between AI and human expertise leads to more comprehensive and quicker diagnostic evaluations.
- Quantitative analysis: AI is capable of performing quantitative analyses that help in characterizing lesions, measuring tumor volumes, and evaluating changes over time. This

is particularly useful in longitudinal monitoring of cancer treatment, where precise measurement of tumor size and progression is critical. AI can also be employed in evaluating organ sizes and detecting subtle changes in tissue density, which may go unnoticed by human eyes.

- Screening and early detection: AI is particularly valuable in screening programs for conditions like breast, lung, and colorectal cancer. It can help radiologists detect early-stage diseases that may otherwise be missed, improving early intervention and patient outcomes. AI's ability to analyze large datasets quickly and accurately also makes it useful for population health screening and identifying high-risk patients for further diagnostic testing.

Improving diagnostic accuracy with AI.

- Minimizing human error: Radiologists, like any medical professionals, are prone to fatigue, cognitive overload, and subjectivity, especially when interpreting complex imaging data. AI can help minimize these challenges by providing consistent and objective interpretations of images. Error reduction is particularly important in high-stakes diagnoses, such as identifying cancers or acute conditions (e.g., strokes, pulmonary embolism), where missed diagnoses can have serious consequences for patients.
- Consistency across cases: AI systems are trained on vast datasets and can maintain consistency in interpretation across cases. While radiologists may interpret images slightly differently depending on their experience or fatigue levels, AI systems are consistent in their analyses. This can lead to standardized reporting and improved diagnostic confidence across different radiologists and clinical settings.
- High sensitivity and specificity: AI has demonstrated high sensitivity (ability to correctly identify diseased cases) and specificity (ability to correctly identify healthy cases) in several diagnostic tasks. For example, AI models have shown promise in detecting early lung cancer, breast cancer, and brain hemorrhages, sometimes surpassing or matching the performance of experienced radiologists.

Reducing radiologist workload

- Efficiency in routine tasks: AI can significantly reduce the workload of radiologists by automating time-consuming tasks such as image pre-processing, image annotation, and initial analysis. This allows radiologists to focus more on complex cases that require human judgment and expertise. In emergency settings (e.g., trauma imaging or stroke scans), AI can expedite the review process, helping clinicians make faster decisions in critical moments.
- Assisting with overload: Radiologist shortage and increased imaging volumes in many healthcare settings can lead to delays in diagnosis. AI tools can help handle the high volume

of imaging studies by providing preliminary interpretations or highlighting areas of concern, allowing radiologists to focus their attention where it is most needed.

Challenges and considerations

- Data quality and bias: AI models are highly dependent on the quality and diversity of the data they are trained on. If the training data is biased or lacks diversity, AI systems may perform poorly in certain patient populations, leading to misdiagnoses. Ensuring high-quality datasets and eliminating bias in AI models is essential to ensure equitable healthcare.
- Interpretability: Many AI systems, especially deep learning models, function as "black boxes," meaning their decision-making processes are not always transparent to clinicians. This lack of interpretability can be a barrier to widespread adoption, as clinicians need to trust and understand how AI systems arrive at their conclusions.
- Integration into clinical workflow: Integrating AI into existing clinical workflows can be challenging. Radiologists and clinicians need adequate training to use AI tools effectively, and the systems must be designed to complement, not disrupt, clinical practices.
- Regulatory and ethical concerns: AI tools must undergo rigorous regulatory approval (e.g., FDA approval) to ensure their safety and effectiveness. Ethical concerns, such as data privacy and patient consent, also need to be addressed as AI becomes more embedded in clinical practice.

10.8 Conclusion: Choosing the right imaging modality

The choice of an appropriate imaging modality is a critical aspect of modern medical practice, as it directly influences the accuracy of diagnosis, the efficiency of treatment planning, and the overall patient outcome. However, selecting the right imaging technique is not a one-size-fits-all process. It depends on several factors, including clinical questions, patient condition, and available resources. These elements must be carefully considered to make the most informed, effective, and efficient choice.

- The clinical question is the starting point in selecting the right imaging modality. Different imaging techniques are designed to provide varying types of information:

- Structural imaging: If the primary concern is evaluating anatomical details—such as identifying tumors, fractures, or organ abnormalities—modalities like CT and MRI provide high-resolution images of soft tissues and bones.
- Functional imaging: For assessing functional aspects such as tissue perfusion, metabolism, or organ function, techniques like contrast-enhanced ultrasound or nuclear medicine may be more appropriate.

- Acute or emergency situations: In the case of trauma or life-threatening conditions like internal bleeding or stroke, CT offers a fast and detailed examination, helping clinicians quickly assess damage to organs, blood vessels, and bones.

Understanding the clinical question helps clinicians determine whether they need high-resolution anatomical images, functional insights, or a combination of both, and guides them toward the most appropriate modality.

Patient Condition. **Each patient is unique, and their** condition**,** age**, and** medical history **will influence the choice of imaging technique. Considerations include: r**adiation sensitivity, renal function, body habitus, comfort and accessibility. **Considering the** patient's individual characteristics **helps clinicians make a more personalized decision, improving both the accuracy of the diagnosis and the overall patient experience.**

Available resources **play a significant role in imaging modality selection. Not all hospitals or clinics have access to the same imaging technologies, and factors like cost, staff expertise, and equipment availability must be considered**.

Interdisciplinary collaboration: Enhancing diagnostic precision.

Given the complexity of imaging modality selection, interdisciplinary collaboration is key to ensuring the best possible outcome for the patient. This collaborative approach involves radiologists, clinicians, specialists. Radiologists play a central role in guiding the selection of the appropriate imaging modality based on their expertise in interpreting diagnostic images and understanding the strengths and weaknesses of different technologies. Clinicians are vital in providing context for the imaging request. They can help clarify the clinical question by providing detailed patient history, symptoms, and physical findings that influence the imaging decision. In complex or unusual cases, specialists (such as oncologists, cardiologists, or surgeons) can provide insights into the specific diagnostic needs, helping to refine the imaging choice to better suit the clinical scenario. Collaboration among these healthcare professionals ensures a comprehensive, holistic approach to choosing the most appropriate imaging modality, optimizing diagnostic accuracy, reducing unnecessary tests, and improving patient care.

Choosing the right imaging modality requires careful consideration of the clinical question**, the** patient's condition**, and the** available resources**. There is no single imaging modality that is perfect for all scenarios. Each modality has its own set of strengths and weaknesses, making it crucial for healthcare professionals to evaluate all factors and select the most appropriate tool for the task.**

Furthermore, as technology continues to evolve, the integration of new imaging techniques like AI-driven analysis and advanced imaging applications promises to revolutionize how we approach abdominal diagnostics—ushering in an era of even more precise and personalized care.

Selective references

1. Indications for abdominal imaging: When and what to choose? Cosmin Caraiani, Dong Yi, Bianca Petresc, Christoph Dietrich. 2020 Mar 31;20(80):e43–e54. doi:10.15557/JoU.2020.0008

2. Abdominal Pain in the Emergency Department: How to Select the Correct Imaging for Diagnosis. Carmen Wolfe, Maglin Halsey Nichols, Kathryn Ritter, Nicole McCoin. 2022 Jul 20;14:335–345. doi:10.2147/OAEM.S342724.

3. Computer-aided diagnosis of liver lesions using CT images: A systematic review. P Vaidehi Nayantara, Surekha Kamath, Manjunath K.N., Rajagopal K.V. Volume 127, December 2020, 104035.

4. Dual-energy CT kidney stone characterization—can diagnostic accuracy be achieved at low radiation dose? André Euler, Sara Wullschleger , Thomas Sartoretti , Daniel Müller , Etienne Xavier Keller , Dejan Lavrek , Olivio Donati .Eur Radiol. 2023 Mar 29;33(9):6238–6244. doi: 10.1007/s00330-023-09569-1.

5. Contrast enhanced ultrasound: A review of radiology applications. David Erlichman, Amanda Weiss, Mordecai Koenigsberg, Marjorie W. Stein. Volume 60, Issue 2, April 2020, Pages 209-215.

6. MR elastography of liver: current status and future perspectives. Ilkay S Idilman, Jiahui Li, Meng Yin, Sudhakar K Venkatesh. Abdom Radiol (NY). 2020 Jul 23;45(11):3444–3462. doi: 10.1007/s00261-020-02656-7.

7. How Artificial Intelligence Is Shaping Medical Imaging Technology: A Survey of Innovations and Applications. Luís Pinto-Coelho , Bioengineering (Basel). 2023 Dec 18;10(12):1435. doi: 10.3390/bioengineering10121435.

8. MRI of the Acute Abdomen in Adults. W. Brian Hyslop MD, PhD. Volume 55, Issue 4, October 2020, Pages 427-435.

9. Abdominal Imaging in the Coming Decades: Better, Faster, Safer, and Cheaper? Perry J. Pickhardt. Published Online: Mar 14 2023. https://doi.org/10.1148/radiol.223087.

10. Trends in Use of Diagnostic Imaging for Abdominal Pain in U.S. Emergency Department. Ralph C. Wang, MD, MAS, Aaron E. Kornblith, MD, Jacqueline , Grupp-Phelan, MD, MPH, Rebecca, Smith-Bindman, MD, Lillian S. Kao, MS, MD, and Jahan Fahimi, MD, MPH. November 19, 2020.

11. HOW CAN I USE ULTRASOUND IN VASCULAR PATHOLOGY?

Boris Brkljačić
WFUMB Center of Education Zagreb, Croatia

Ultrasound is used extensively in vascular pathology, in large, middle sized and small arteries, in deep and superficial veins and in the evaluation of flow and vascular pathologies in different organs and organ systems.

In order to be able to use ultrasound in vascular pathology we need to understand the basic physics of Doppler, basic hemodynamics and how to acquire and interpret Doppler spectra, and which scanners and transducers to use.

Doppler ultrasound – history and beginning

Christian Doppler (1803–1853), Austrian mathematician and physicist at Czech Technical University in Prague, published in 1842 the paper „On the Coloured Light of the Binary Stars and Some Other Stars of the Heaven“, which was the first statement of a principle that the observed frequency changes if either the observer or the source is moving. This principle valid for optics and acoustics was named in the honour of Christian Doppler the Doppler principle, the Doppler shift, or the Doppler effect. The acoustical Doppler effect was verified experimentally in 1845. The essence of the principle in acoustics is that the emitted and received/reflected frequencies are similar if the source of sound and receptor are static, while if the reflector moves toward the source of the sound the frequency increases, and if the reflector moves away the frequency is decreasing. After more than hundred years Satomura in 1956. realized that red blood cells may reflect ultrasound. This marks the beginning of the use of Doppler principle in ultrasound diagnostics.

Basic physical principles of Doppler ultrasound

Red blood cells, dominant cells in blood by their number and volume, have certain velocity with which they move in the blood stream in certain direction. They are the principal reflectors of ultrasound beam. The difference of frequencies in cases that reflectors (red blood cells) move toward or away from the ultrasound transducer is called Doppler shift and is proportional to the velocity of reflectors / red blood cells, i.e. to the blood flow velocity. This Doppler shift is measured in Herz (Hz) by the ultrasound scanner. For the medical use Doppler effect is most commonly utilized in a fashion that we insonate blood vessels and analyze Doppler shifts of ultrasound beam scattered on red blood cells. To measure the blood flow velocity we need to emit ultrasound beam

into the body using the certain insonating angle in the relation to the vector of the direction of the blood vessel flow. The Doppler equation in this case is:

$$\Delta f = (2f_0 v / c) \times \cos \alpha$$

V = velocity of blood flow (of red blood cells movement), c = speed of ultrasound in tissues, □f = Doppler shift, f_0 = emitted frequency, □ = insonating angle (angle between ultrasound beam and blood vessel, i.e. direction of blood flow)

It is important to notice that Doppler shift for angle of 90° is zero, so that it is not possible to measure velocity at the angle of 90°. The blood flow in the vessel depends also on the diameter of the vessel and the quality of the vessel wall (compliance). If the flow is laminar (when walls are smooth and vessel large enough) the flow profile is parabolic. This means that the highest velocity is in the middle of the vessel and it gradually decreases towards the walls. If there is an obstacle to the flow, like in the case of the atherosclerotic plaque or vessel branching, there is a deviation from parabolic flow, and in the worst case scenario turbulence can occur. The method to quantify Doppler findings is the spectral frequency analysis, by which the ultrasound signal is decomposed in frequency components, that are graphically presented on the time scale, which provided cumulative frequency distribution of the pulse cycle. Comparing these record to normal findings one can quantify the degree of the flow aberration in the analyzed vessel. The computer system in ultrasound scanner (spectral analyzer) is performing the complicated operation, Foust Fourier transformation analysis of data (FFTA), decomposing ultrasound signal in 128 frequency components 160 times per second. FFTA enables that Doppler spectra are shown as the function of time, in "real-time". Graphically we see on the vertical scale Doppler shifts in kilohertz (kHz), proportional to the velocity of blood flow, that scanner automatically converts into velocities in m/s, after the angle correction is performed. On the horizontal scale the time is presented. So the graphical curves on the screen reflect changes of frequencies during cardiac cycles, with time on the horizontal scale (x-axis) and velocities on the vertical scale (y-axis). Figure 11.1.

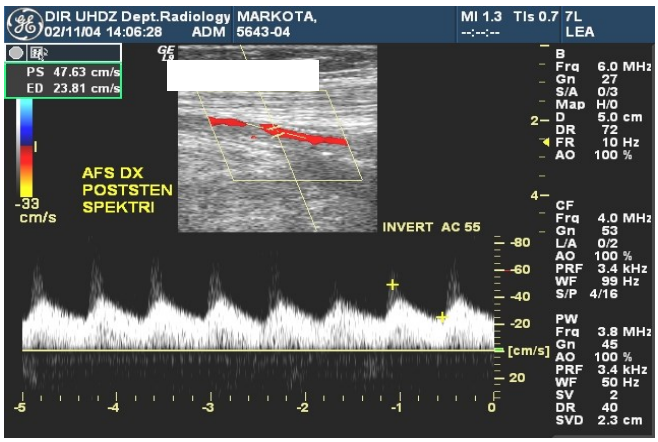

Figure 11.1. Postocclusive biphasic spectrum with low velocities distally from the occlusion in femoral artery. The display with color duplex Doppler, with electronic steering of the beam. Doppler sample volume is positioned in the center of the artery. Graphic display demonstrates changes of velocities in systole and diastole.

The shape of the spectrum depends upon the contractile force of the heart, elasticity and compliance of the arterial wall, viscosity, vessel diameter, and the distance between the heart and the examined vessel. The most important factor influencing the spectrum shape is the peripheral vascular resistance. Depending on the position of the spectrum in relation to the baseline it is possible to determine the direction of the blood flow. The spectrum above the baseline indicates the flow towards the transducer, and below the baseline in the direction away from the transducer.

If the blood flow velocity is measured (v) and the diameter of the vessel is known (d), it is possible to calculate the flow (Q) according to the following formula:

$$\mathbf{Q = v (\pi d^2 / 4)}$$

Apart from the measurements of absolute velocities and volume flow also the relative Doppler indices are defined, which are not dependent upon the angle between the ultrasound beam and the blood vessel. They enable differentiation of low-resistance and high-resistance vascular beds, and the most common index in the routine use is the resistance index (RI, *resistance index*). Elevation of RI is the consequence of the increase of the peripheral resistance distally from the site where the Doppler sample was positioned. All modern machines have embedded software programs for fast and automatic measurement of RI from the spectral recordings. In low resistance vascular beds the RI value is approaching 1.0 when the diastolic velocities are abnormally low, which reflects flow disturbances due to the high peripheral resistance.

The main mode to utilize the Doppler effect in medicine is the pulse-wave Doppler, where ultrasound beam is being transmitted in the form of short impulses, when Doppler shifts are measured after the time needed for the Doppler pulse to reach the certain predestined depth in the body and to reflect backwards. Using pulsed wave Doppler one can measure the velocity of flow in the selected blood vessel, despite of the fact that other vessels are visible in the ultrasound beam/ ultrasound image on the screen of the scanner. The Doppler shifts are registered and demonstrated both visually and audibly, using the fact that Doppler shifts in kHZ are within the audible spectrum of the human ear, so they can be heard in real-time by the scanner speaker. In duplex systems pulsed-wave Doppler is combined with the 2-D display, and if the flow in vessels is coded in different colours (blue and red most commonly) this is colour duplex Doppler. This has enabled the evaluation of previously inaccessible deeply positioned arteries in abdomen and pelvis, including the simultaneous morphological demonstration of the vessel and Doppler analysis of the flow within the artery. Flow directions and velocities are coded with colour, depending on our choice. Most common is coding of the flow towards the transducer in different levels of red colour, while the flow away from the transducer is coded in blue colours. The color coding of the flow direction can be easily changed by pressing the “invert” command on the keyboard. The flow which is insonated under the angle of 90^0 to the vector of the vessel is not demonstrated, as explained earlier (Figure 11.2).

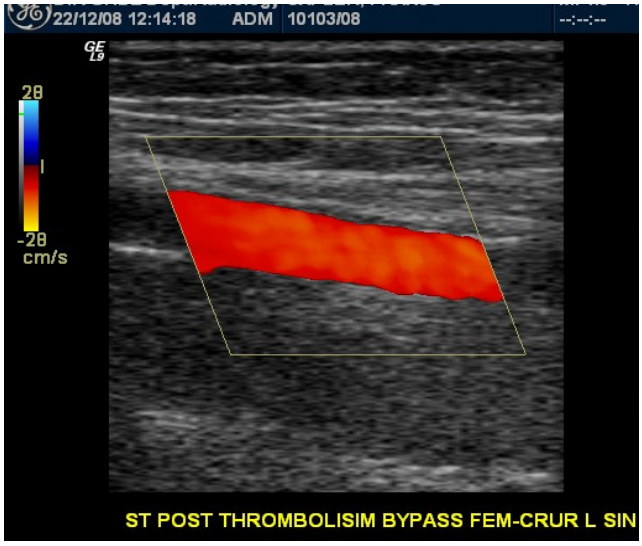

Figure 11.2. Demonstration of flow in the arterial bypass by color Doppler. The flow is coded in red color, directed away from the transducer (from the left to the right side on the image), and the ultrasound beam is electronically steered so that the color box is paralelogram, while the B-mod image is rectangular, since the examination was performed using the linear high-frequency transducer.

The higher velocites are coded in lighter tones of colours, and lower velocities in darker tones. Colour is coding the mean blood flow velocity, so that the part of the spectral information is lost in colour Doppler. In practice, the important information can be obtained even if only colour display is used, e.g. regarding the physiological or pathological direction of flow in many diseases. The examples are the evaluation of flow direction (hepatopetal or hepatofugal) in the portal vein in portal hypertension, evaluation of flow direction in vertebral arteries when suspecting *subclavian steal syndrome*, or in the ophthalmic artery when suspecting stenosis or occlusion of the internal carotid artery. Although semiquantitative, this display has big advantage because it points rapidly where the area is in which the flow should be quantified by using spectral frequency analysis.

Colour Doppler is widely accepted method which is standard in modern ultrasound scanner. During the Doppler examinations several artefacts are encountered which examiner has to know well. The most common artefact is aliasing, that is seen at high velocities due to the arterial stenosis. The highest velocity that can be measured with pulse Doppler equals the half of the pulse repetition frequency. This limitation is known as the Nyquist limit, and transgression of the limit results in aliasing. In Doppler spectrum it is manifested in recording of the too high velocities transferred below the baseline. As mentioned before, when the vector of the blood vessel is perpendicular in the relation to the insonating ultrasound beam the cosinus of the insonating 90 degrees angle is zero, so consequently the Doppler shift is not registered. Thus, the erroneous data are driven that there is no flow at the insonation site, which is an artefact due to the inadequate insonating angle. The other artefacts are mirror image, wrong wall-filter positioning or sample volume mispositioning, and twinkling artefact.

Nowadays color Doppler can be used also in 3D US imaging and in panoramic, extended field-of-view imaging.

State-of-the art high class ultrasound scanners are recommendable for the sonographic evaluation of vascular pathologies, both in large, medium sized and small vessels, as well as to analyse flow in organs. These scanners offer excellent B-mode imaging across a range of depths with good resolution and good sensitivity to high and low flow in both colour flow and spectral Doppler modes. A large range of transducers are ideal but should include: (a) high frequency (around 8–15 MHz) linear array (for tibial/pedal arteries and arm arteries, for evaluation of flow in scrotum, breast, thyroid gland, neck, muscles, etc); high frequency small footprint arrays are also used for imaging of temporal arteries; (b) lower frequency linear array (approximately 4–9 MHz) for subclavian, femoral and popliteal arteries; (c) curvilinear array (1–4 MHz) for iliac arteries, aorta and femoral arteries in larger patients and evaluation of flow in abdominal organs.

The basic hemodynamics and interpretation of Doppler spectra

Arteries and veins are used for the perfusion of tissues with the minimal loss of energy. The purpose is to deliver oxygenated blood needed to preserve normal tissue functions. The quantity of blood that a specific organ or tissue gets depends on the metabolic and functional needs of organs. Some organs, like brain, liver and kidneys need large quantities of blood constantly and have low vascular resistance, because the flow physiologically has to be continuously high. Brain and liver also have excellent collateral flow enabling organ perfusion even if one of important supply arteries is occluded. Some organ systems have variable arterial resistance: small bowel needs lot of blood postprandially, while during fasting the vascular resistance is high, muscles need blood during activities while in inactive stage resistance is high. Depending on physiological changes Doppler spectra change. Venous system has low pressure and venous valves prevent retrograde blood flow and cardiac contractibility and changes of abdominal pressure at respirations have reflection on venous hemodynamics as well. Changes of pressure due to cardiac contractions are directly transmitted into some veins, like into the hepatic veins, while in peripheral veins flow is mostly monophasic, but changes of intraabdominal pressure during respirations are reflected into peripheral veins spectral morphology as well.

Basic terms in description of blood flowing in the body are flow, pressure and resistance and according to the Poiseuille's law two main factors that determine the flow are the pressure and the resistance.

Flow is the quantity of blood delivered to the certain organ/tissues for the exchange of O_2 and CO_2 in the unit of time (e.g. mL of blood in minute per gram of the tissue). If the quantity of blood is too low for the needs of tissues the result is ischemia. If too much blood is delivered the hemorrhage can ensue.

Pressure is the incentive for flow, the form of energy enabling propulsion of the blood through the vessels, and originates from cardiac contractions; pressure is being converted into the

kinetic energy. The factures that reduce pressure gradients, like arterial narrowing (stenosis) result in the decrease of flow in tissues.

Vascular resistance reflects the resistance of the liquid (blood) to move down the tube (blood vessel). Parabolic flow is characterized by the faster flow in the center of the vessel that is lower towards the vessel walls. The resistance is inversely proportional to the fourth potency of vessel diameter, so the smaller the vessel, the higher is the resistance.

Doppler can not accurately measure flow, pressure and resistance, and the only factor that can be measured relatively accurately is the flow velocity. Based on the blood flow velocity and morphology of Doppler spectra most of diagnosis and evaluations of flow disturbances are derived. So regardless of the vessel in the body, color and power duplex Doppler examinations are based on the demonstration of flow in the vessel lumen coded in colour and on the evaluation of Doppler spectra the after spectral waveform analysis was performed. Those three elements – colour demonstration of flow, measurement of velocity and spectral morphology assessment may seem easy to perform, but they depend on numerous factors that one needs to understand in order to establish the accurate diagnosis. In addition to qualitative analysis of colour features, explained when discussing basic physic, more important in evaluation is quantitative analysis of Doppler spectra. It encompasses measuring peak systolic velocity, enddiastolic velocity and mean flow velocity, as well as evaluation of spectral morphology at the site of pathologic changes in the vessel, proximally and distally. One should know well the ranges of normal blood flow velocities in specific vessels, and morphology of normal spectra in specific arteries and veins. There are wide variations in normal ranges.

Figure 11.3 is the example illustrating well the significance of the combination of quantitative demonstration of flow with colour and quantitative analysis of Doppler spectrum in the diagnosis of subclavian steal syndrome.

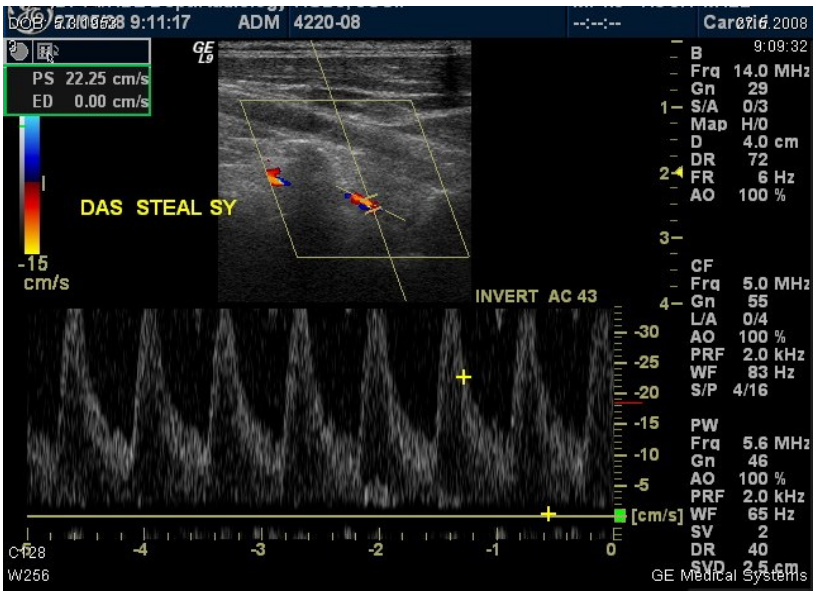

Figure 11.3. Colour duplex Doppler of the flow in vertebral artery

In a patient with blood pressure difference on the right and left arm the colour Doppler of vertebral arteries was performed. Figure 3 demonstrates that the colour coded flow in vertebral artery is red, and looking at colour scale it is visible that it is the retrograde flow (from left to right side, craniocaudal, towards the arm). Colour scale on the left side of the image demonstrates that in this case flow towards the transducer is coded in blue, while flow away from the transducer is coded red. Spectrum is above the baseline, but this is because the spectrum is inverted – see the „invert“ on the image. If the examiner has not pressed command “invert” on the keyboard the spectrum would be presented below the baseline. So the flow in vertebral artery is retrograde, towards the arm and it is the straightforward example of subclavian steal syndrome. This examples demonstrates the importance of observing how the direction of flow is coded every moment during the examination, by looking at the colour scale, and to watch whether the spectrum is inverted or not.

Even by using most modern US scanners small arteries with diameters <1 mm cannot be visualized and Doppler shifts <200 Hz cannot be measured. The largest volume of blood is in arteriolae and capillaries, that are not accessible for ultrasound examination.

The factors influencing Doppler spectrum morphology were already presented. If there is hemodynamically significant stenosis in proximal segment of artery the spectra distally from the stenosis will be altered because of the drop in pressure gradient. The clear example is presented in the Figure 11.1.

Arterial compliance depends on the vessel wall and changes with age, physiological status and atherosclerotic changes. Reduced compliance in atherosclerotic arteries results in rigid vessels. Vascular resistance depends primarily on distal arterial bed and also varies in different physiological states. Arteries that deliver blood to low-resistance organs typically have continuous antegrade diastolic flow and low acceleration time between the beginning of spectrum and systolic peak. The level of antegrade flow is higher if peripheral resistance is lower.

The low-resistance waveform with high diastolic flow in hepatic artery is shown in Figure 11.4. Since the artery is very narrow one can see the spectral broadening and filling of systolic window in the spectrum (spectrum is white in the whole systole), which is physiological finding in such a narrow artery like proper hepatic artery (Figure 11.4).

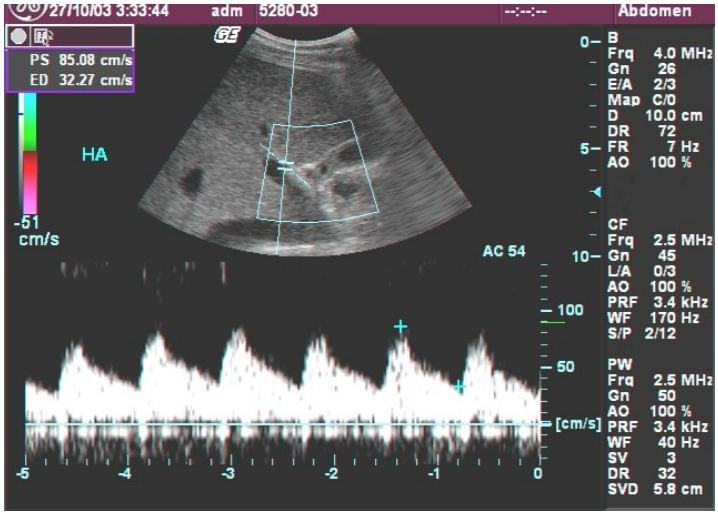

Figure 11.4. Low resistance spectrum in hepatic artery with continuous relatively high diastolic flow and low resistance index. Spectral broadening is visible.

Arteries that supply high-resistance area, like leg muscles, have fast systolic rise and peak, retrograde flow in the initial part of diastole and very slow antegrade diastolic flow in the second part of diastole.

On the Figure 5 the normal high-resistance spectrum in peripheral artery is demonstrated. Since the artery is quite wide, the reflection of the laminar flow (all red blood cells flowing with relatively similar velocities) is a relatively narrow spectrum and the systolic window is empty ("black") as opposed to the spectrum in the Figure 11.4 where spectral broadening is visible.

Figure 11.5. High-resistance spectrum in peripheral artery with triphasic shape, with retrograde flow in early diastole.

Doppler can be used to evaluate physiological state of the supplied vascular bed. As an example, when there is an increased resistance in distal vascular bed, like in the small bowel after longer period of fasting, in the superior mesenteric artery (AMS) physiologically retrograde diastolic flow is observed, reflecting cardiopetal flow in early diastole. After the meal, when the vasodilatation occurs in the bowel wall, a continuous antegrade diastolic flow can be observed in the superior mesenteric artery.

The differences in spectra in superior mesenteric artery at fasting and after the meal in a healthy person are demonstrated in Figures 11.6a and 11.6b.

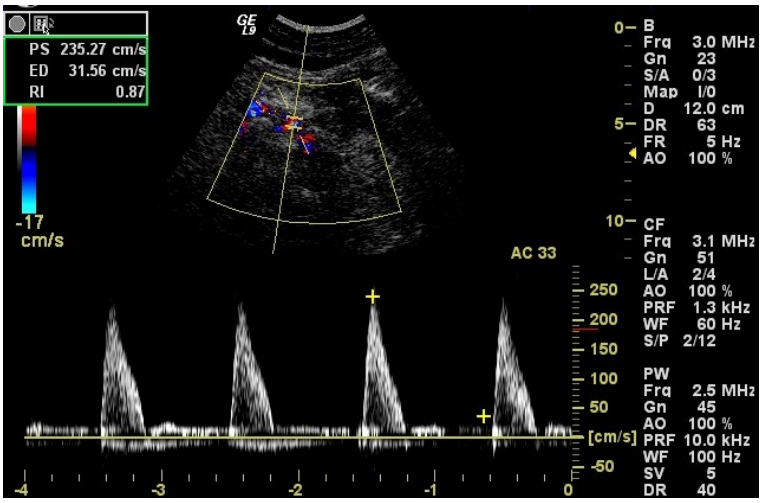

Figure 11.6A. High-resistance Doppler spectrum in superior mesenteric artery after eight-hours fasting period. Early diastolic retrograde flow can be seen.

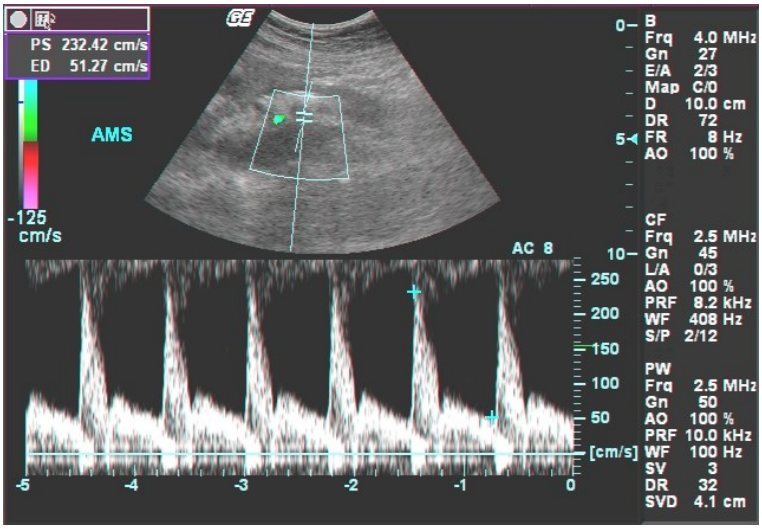

Figure 11.6B. Low-resistance spectrum in superior mesenteric artery of the same individual after the meal; continuous diastolic flow is visible.

Doppler is widely used for functional tests when it is important to evaluate collateral circulation. As the example, radial and ulnar artery supply blood to the arm. When radial artery is harvested for coronary artery bypass grafting it is mandatory to evaluate whether the ulnar artery is sufficient to deliver the blood to the art. On needs to perform radial artery compression test to evaluate whether the blood flow velocity in ulnar artery is increasing or not. Normal elevation of the blood flow velocity in ulnar artery during the compression of radial artery is demonstrated on the figure 11.7.

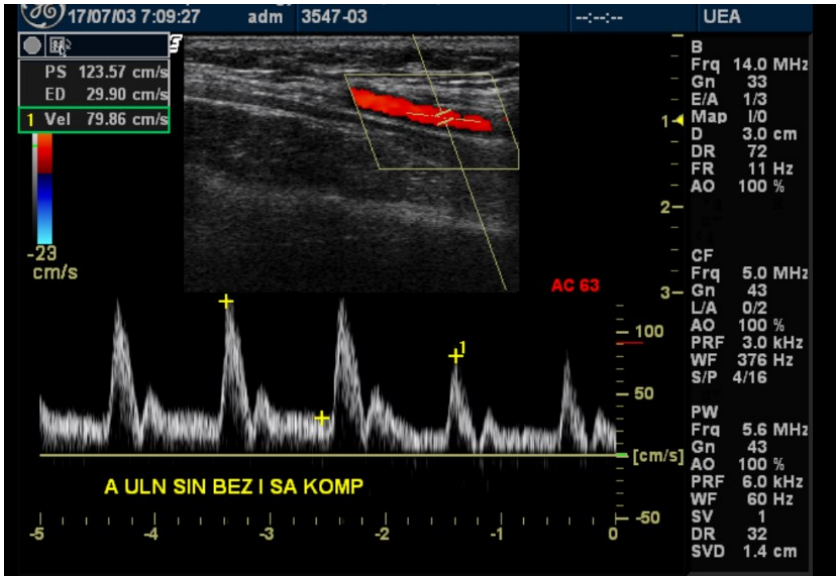

Figure 11.7. Positive test of the compression of radial artery – during the compression of RA the peak systolic velocity in ulnar artery rises from 80 cm/s to 1.23 m/s.

After that it is usual to analyse the flow in the superficial digital branch of radial artey deep on the tenar. During the compression of radial artery physiologically the retrograde flow is visualized, which reflects the normal patency of the palmar arch. This physiological phenomenon is demonstrated at the figure 11.8.

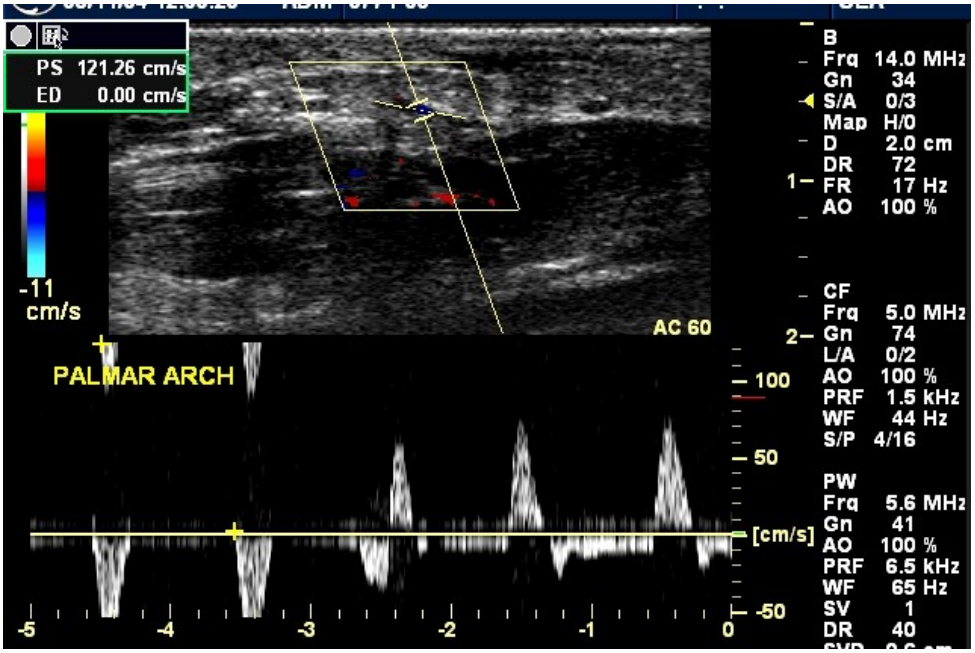

Figure 11.8. Positive functional test when during the compression of radial artery the change of the flow direction is visualised in the digital superficial branch of the radial artery, signifying functionally competent palmar arch.

Functional tests can be performed in different anatomical positions. For the example in the syndrome of upper thoracic aperture one can notice altered Doppler spectra in axillary and brachial artery when the arm is elevated above the head, because subclavian artery is than compressed, while spectra in physiological position of the hand have normal appearance.

When we analyze venous flow the inflow is constant and is not relevant factor in Doppler evaluation. The only significant factor influencing the morphology of Doppler spectra is the outflow, which depends upon the existence of some form of the hindrance or obstruction between the vein and the right cardiac atrium. Venous Doppler spectra are therefore affected by the right atrial pressure and venous obstruction (thrombosis). In normal state the respiratory changes of intraabdominal pressure are transmitted distally into pelvic and peripheral veins, so the spectra are lightly undulated and not completely flat. The normal venous Doppler spectrum is demonstrated in the Figure 11.9.

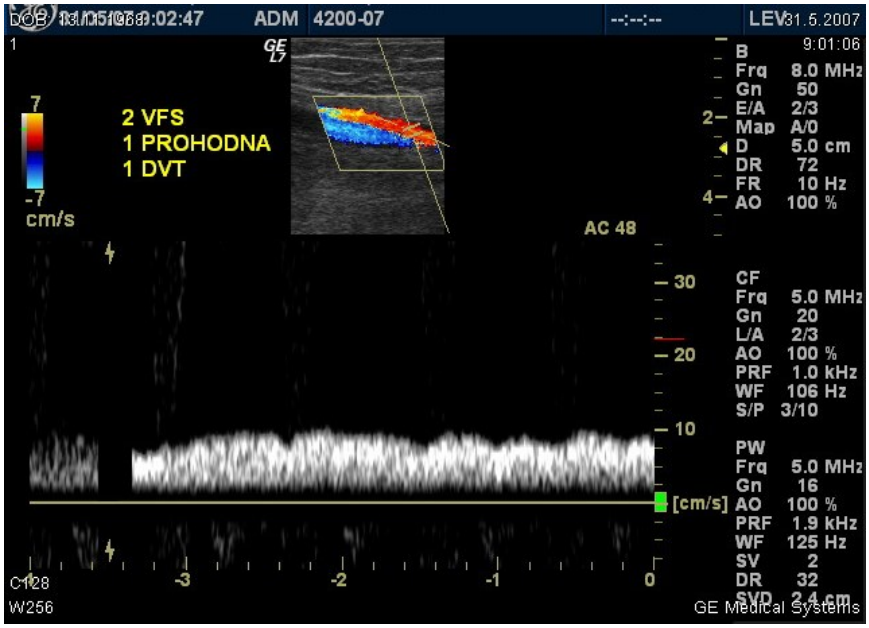

Figure 11.9. Normal, continuous, undulated spectrum in the peripheral vein with mild respiratory phasicity

In veins that are close to the heart the cardiac pulsations are transmitted retrogradely, so that the triphasic spectra are seen. This is the normal finding in hepatic veins that are the last veins entering inferior vena cava before its inflow into the heart. The same finding can be seen in brachiocephalic and jugular veins.

Venous spectra reflecting transmitted cardiac pulsations are demonstrated on Figure 11.10.

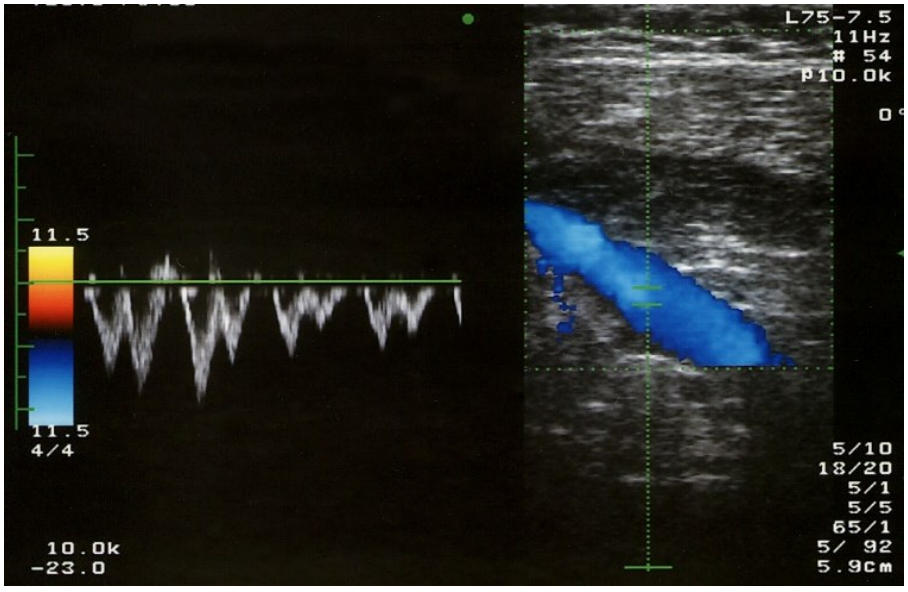

Figure 11.10. Normal triphasic venous spectrum in subclavian vein as a reflection of transmitted cardiac pulsations

Atherosclerosis

Atherosclerosis is the most important disease affection arteries and influencing hemodynamics. Small plaques are common in persons above 50 years of age and are easily seen in carotid arteries. Thickening of intima-media complex on carotid artery implies occult formation of the plaque, and plaques can be directly visualized by ultrasound once they are large enough to protrude into the vessel lumen.

Figure 11.11 demonstrates the thickened intima-media complex in the common carotid artery.

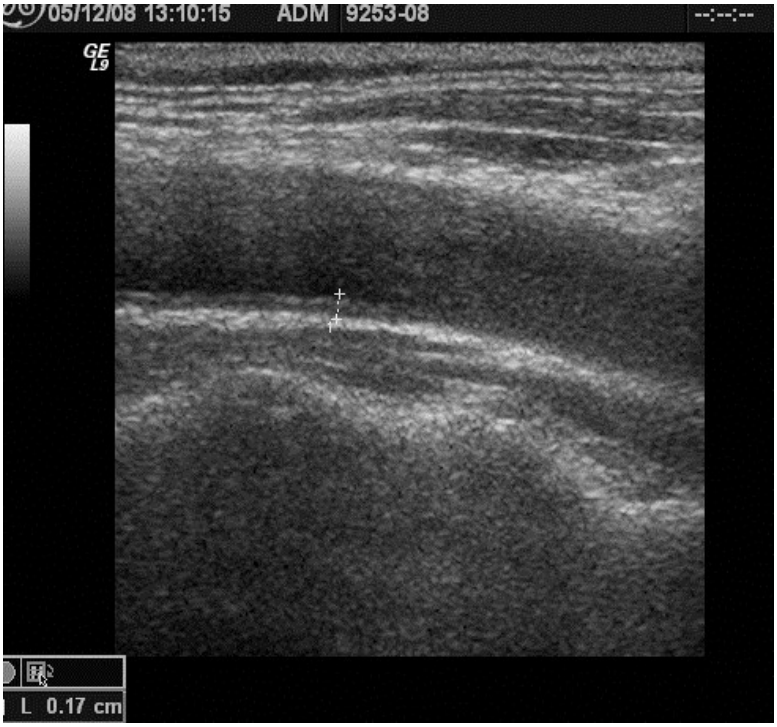

Figure 11.11. Thickened intima-media complex in the common carotid artery

Fibrous plaques usually do not cause symptoms, while clinically significant are complex plaques. Irregular surface of the plaque leads to the loss of normal endothelium. Bleeding into the plaque is serious complication that can be diagnosed by ultrasound. To analyse hemodynamic changes caused by atherosclerosis one should know that those changes develop in certain arterial segments, while the other segments are spared. Usually arteries of the upper arm distally from subclavian artery are spared. Atherosclerosis is the disease of branches and bifurcations: carotid bifurcations, abdominal aortic bifurcation, renal artery origin, celiac trunk and superior mesenteric artery origin, and of common and superficial femoral arteries. Origins and proximal 1-2 cm of arteries are usually affected. Common site of affection is superficial femoral artery in adductor canal. Diabetes affects arteries of the calf**.**

Hemodynamics and Doppler spectra in stenosis

Stenosis is narrowing of the artery most commonly caused by atherosclerotic changes of arterial wall. Different vascular beds of the body have different normal Doppler spectra, but general rules to diagnose stenosis and grade its significance are valid for all. When blood passes through the narrowed segment of the vessel the velocity is increasing in order to preserve the perfusion. The pressure drop through the stenotic segment depends upon the degree of the narrowing. The higher is the degree of stenosis the velocity increases more and more. Distally from hemodynamically significant stenosis so called parvus-tardus poststenotic spectra are observed, because pressure drop is such that laminar flow is not established distally from the high-degree stenosis. When the velocity is extremely increased the pressure drops (pressure dropping lesion) and turbulence results. Turbulence is seen distally from the critical, very narrow stenosis, with chaotic flow on spectral analysis. Measuring velocities and analysing morphology of Doppler spectra we can diagnose presence of the stenosis and evaluate it degree.

At the site of stenosis of high degree the significant elevation of the peak systolic velocity is seen in comparison with the PSV in the prestenotic segment of the artery. Distally spectra are altered in morphology due to the pressure drop. PSV measurement is the most important parameter to establish the diagnosis of stenosis in all arteries in the body. As the stenosis is progressing PSV is being elevated more and more, and after that the elevation of enddiastolic velocity (EDV) occurs. Grading of the level of stenosis is based on PSV measurements and different threshold values are established in literature for different vessels. Absolute values can differ considerably individually and are dependent upon age, cardiac status, vessel compliance, etc. Therefore the most important parameter when assessing the degree of the stenosis is the ration of the PSV at the site of stenosis compared to the PSV in the prestenotic segment. Poststenotic parvus-tardus spectra are characterized by increased acceleration time (AT, *systolic rising time, systolic upstroke*), i.e. the time from the beginning of systole to the maximum systolic speed. Additionally, the diastolic flow is relatively high compared to the systolic flow. *Parvus et tardus* spectra are also seen in arterial collaterals, and are one of typical signs of collateral flow, which is often seen in peripheral arteries in peripheral arterial disease.

Few clinical examples demonstrating elevated velocities at the site of stenosis, increased resistance proximally from stenosis and poststenotic parvus-tardus spectra are demonstrated at Figures 11.12-11.15.

Figure 11.12 demonstrates elevated velocity at the origin of the right renal artery with elevated peak systolic velocity of 4.1 m/s, and increased end-diastolic velocity of 1 m/s. Compared to the PSV in prerenal segment of abdominal aorta the elevation in right renal artery is five times higher.

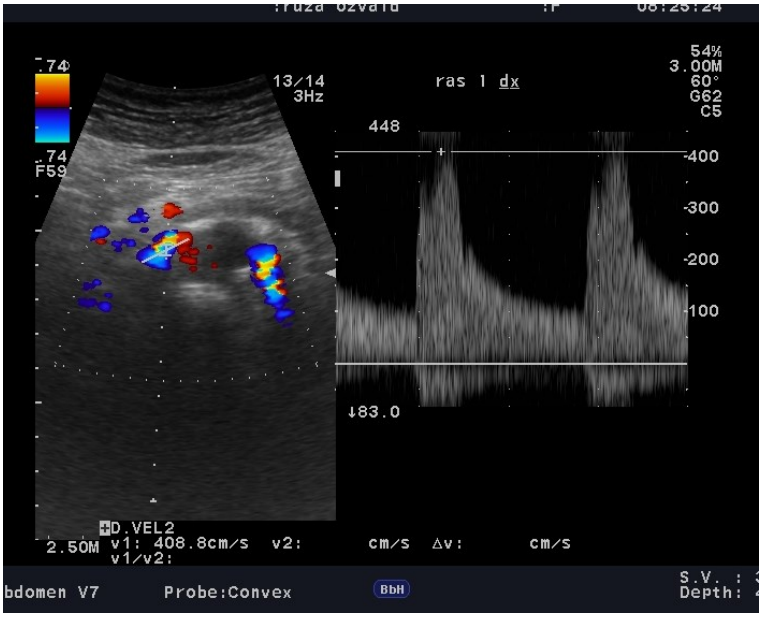

Figure 11.12. Spectrum at the site of high degree stenosis of the right renal artery, PSV 4.1 m/s, EDV 1 m/s

Figure 11.13 demonstrates elevated velocity at the site of the high-degree stenosis (>80%) of the internal carotid artery, with PSV of 3 m/s, and EDV of 1.5 m/s. The ratio of PSV between internal and common carotid artery was 5.

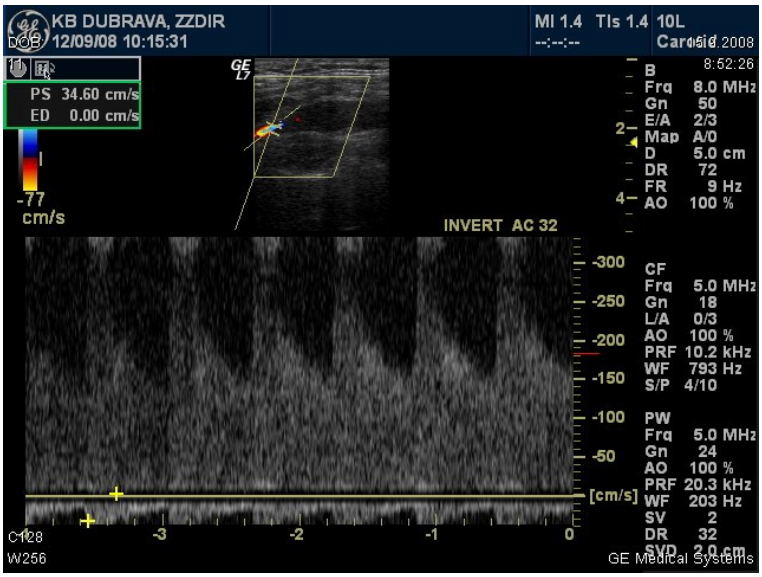

Figure 11.13. Spectrum at the site of the high-degree stenosis (>80%) of internal carotid artery with elevated PSV od 3 m/s and EDV of 1.5 m/s. PSV aci / acc = 5.

Figure 11.14 demonstrates pre-occlusive spectra in common carotid artery with very high resistance and absent diastolic flow, that are visible proximally from the occlusion or high-degree stenosis.

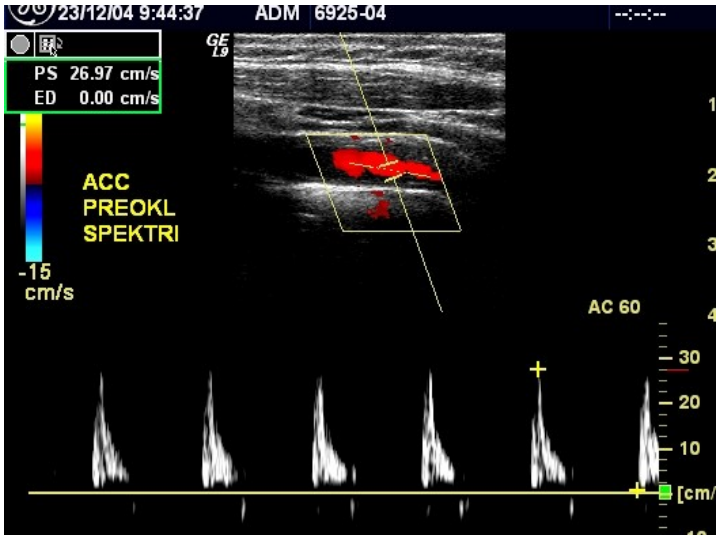

Figure 11.14. Pre-occlusive spectra in CCA, visible proximally from the occlusion

Figure 11.15 demonstrates parvus-tardus spectra. These spectra are typically seen distally from the hemodynamically significant stenosis. In this case this is parvus-tardus spectrum in the posterior tibial artery which is being filled over the profundal collaterals in a patient with the occluded superficial femoral artery.

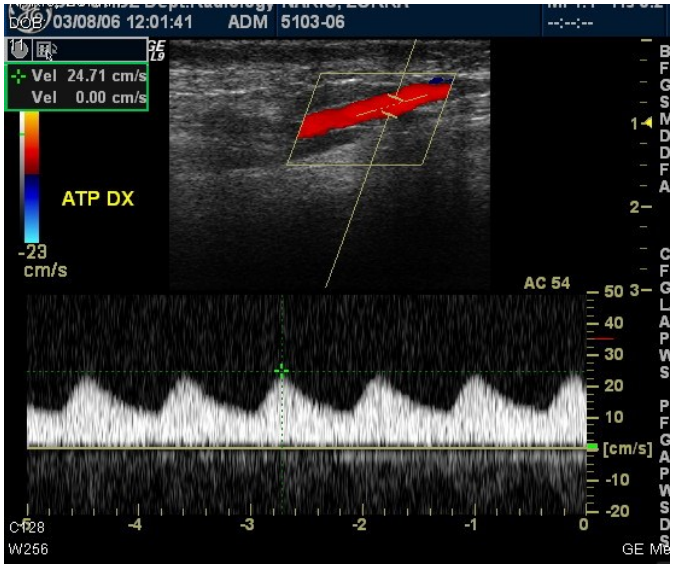

Figure 11.15. Postocclusive parvus-tardus spectra in anterior tibial artery filling through profundal collaterals in patient with occluded superficial femoral artery.

As demonstrated, Doppler US has important role in diagnosing arterial stenosis. When the site of stenosis is easily accessible to direct visualisation, as is the case with internal carotid artery stenosis the diagnosis is easy, based on the demonstration of elevated velocity at the site of stenosis. However, the site of stenosis might not be accessible to visualisation by ultrasound, if covered by bones. If the site of stenosis cannot be demonstrated like in the case of brachiocephalic truncus stenosis or subclavian artery stenosis the easiest way to diagnose stenosis is to demonstrate *parvus-tardus* spectra distally from the stenosis, or to demonstrate reverse flow in vertebral artery in case of subclavian artery origin stenosis or occlusion.

Figure 11.16 demonstrates very altered poststenotic parvus-tardus spectrum in common carotid artery due to the high-degree stenosis at the origin of brachiocephalic truncus that cannot be insonated by ultrasound as it is covered with bones. Blood flow velocities are 5-6 times lower than normally. The diagnosis was confirmed by digital subtraction angiography and CTA.

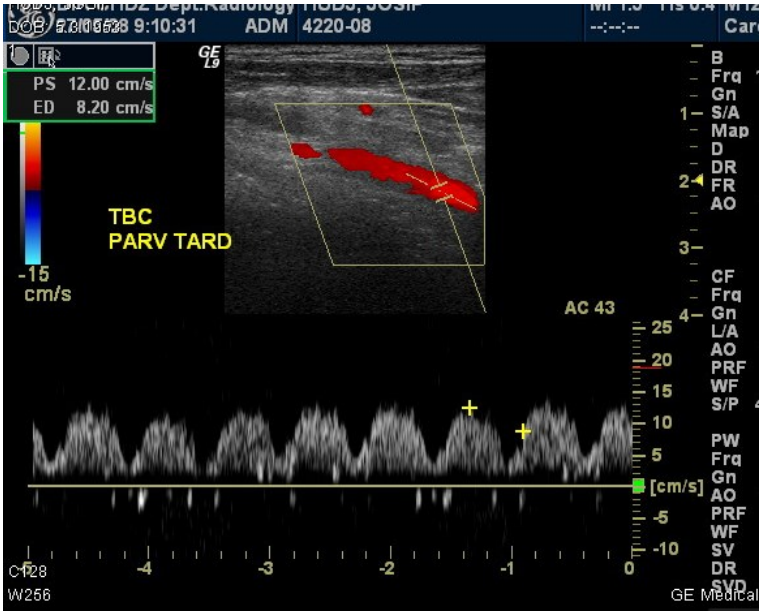

Figure 11.16. Considerably altered, slow flow post-stenotic spectrum in common carotid artery distally from subtotal stenosis of brachiocephalic truncus

Doppler spectra in other pathological conditions

The most important role of Doppler is to detect stenosis and occlusion of arteries and document collateral flow and distal outflow. However colour duplex Doppler ultrasound can be used to establish diagnoses of other arterial and venous pathological conditions that are clinically important, but not so common as arterial stenosis. Several examples will be presented.

Arteriovenous malformation and A-V fistula are characterized by slow acceleration time (AT), increase in systolic and diastolic velocity and high diastolic flow. Iatrogenic AV fistulas can

be found after biopsies in some organs, like kidney. Hemodialysis AV fistulas can be followed by Doppler US and their patency and complications established. AV malformations can be diagnosed and their treatment followed by Doppler US.

AV malformation on the palm of the child is shown on figures 11.17 and 11.18.

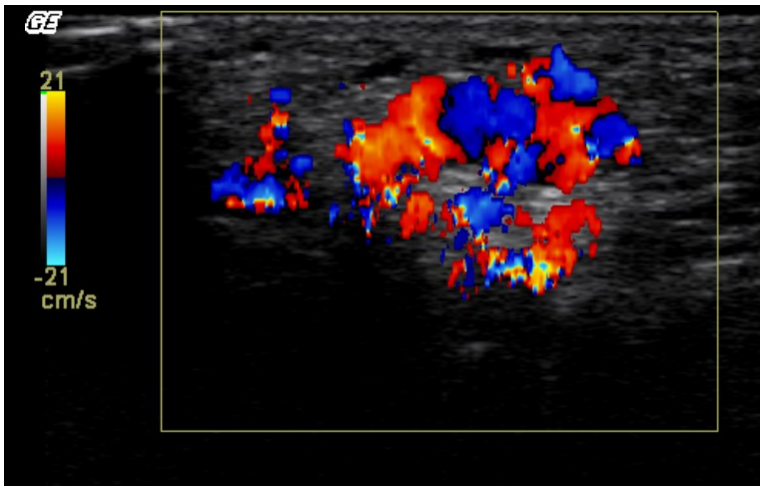

Figure 11.17. Hypotenar of five-years old child: hypervascular mass – colour Doppler image showing high velocity flow with red and blue colours in arterial and venous convolutes

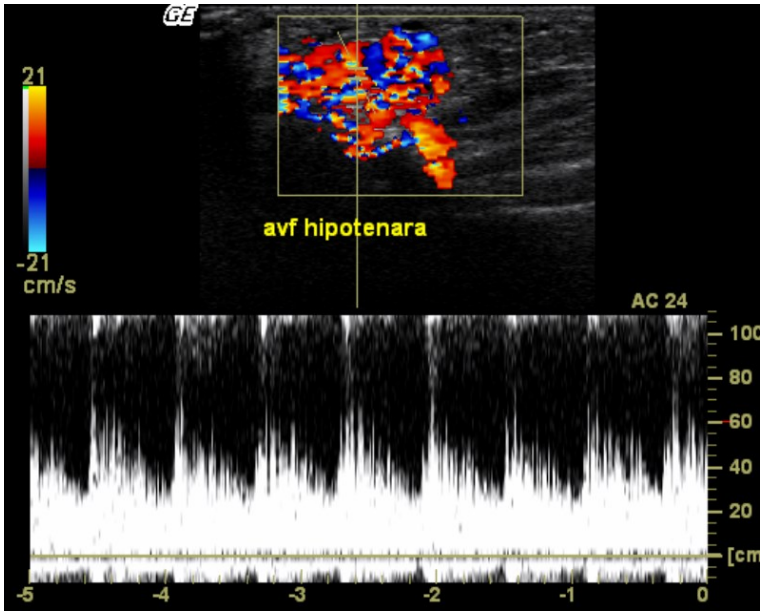

Figure 11.18. Same patient- Doppler spectrum demonstrating high arterial and venous velocities in AVM

Pseudoaneurysm (PSAN) – flow within PSAN has typical spectral waveform with flow in both directions (*to-and-fro pattern*), and colour Doppler demonstrates flow coded with red and blue in the PSAN. Doppler can also demonstrate high flow in the neck of the PSAN. PSAN is demonstrated on figures 11.19 and 11.20.

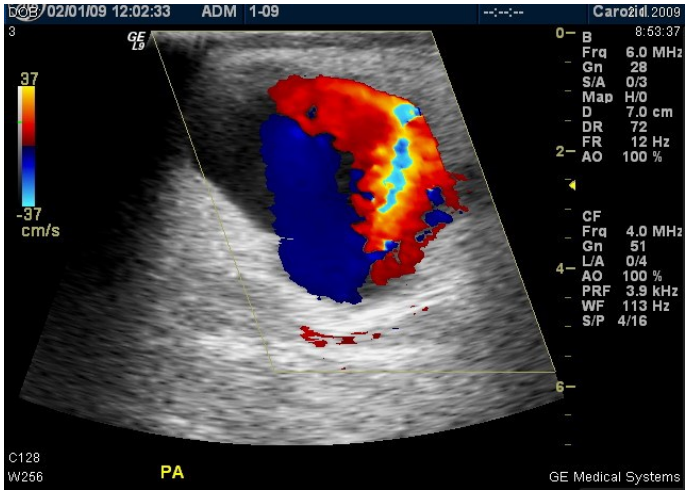

Figure 11.19. Typical image of pseudoaneurysm with colour Doppler with blood flow coded in red and blue reflecting mixing of blood direction within PSAN. This was iatrogenic, posttraumatic PSAN of common femoral artery after catetherization during coronarography

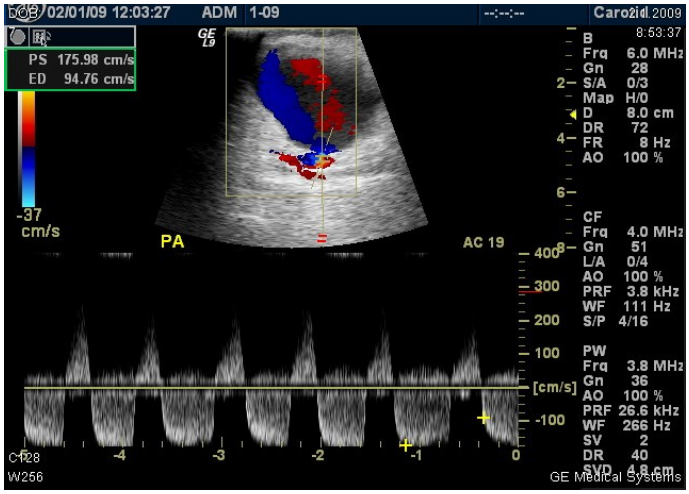

Figure 11.20. Same patent. Typical to-and-fro Doppler spectrum in the neck of the PSAN. Same patient like in the Figure 19.

Demonstration of increased vascular resistance in parenchymal organs is useful to establish several diseases. Most common use is to evaluate renal vascular resistance by measuring resistance index in intararenal interlobar arteries in patients with parenchymal renal disease in which RI is

usually increased. In cases of liver cirrhosis spectral appearance in hepatic arteries demonstrated continuous flow as opposed to normal phasic flow; the same is the case when there is stenosis between hepatic veins and inferior vena cava.

The loss of normal respiratory phasicity in venous spectra in peripheral veins is the consequence of the proximal venous thrombosis, stenosis or venous compression. The example is visible on figure 11.21.

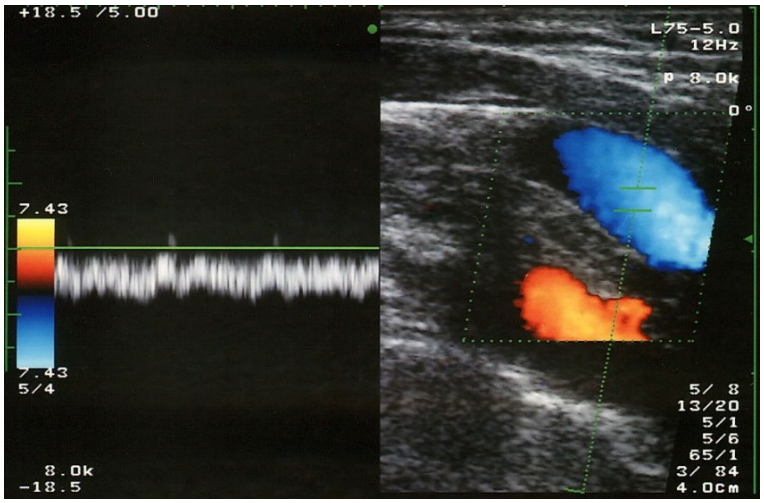

Figure 11.21. Continuous flow in jugular vein (as opposed to normal undulating phasic flow) due to the severe stenosis of superior caval vein

Also the increased venous pulsatility reflects right-sided heart failure, e.g. tricuspidal insufficiency, as demonstrated in figure 11.22.

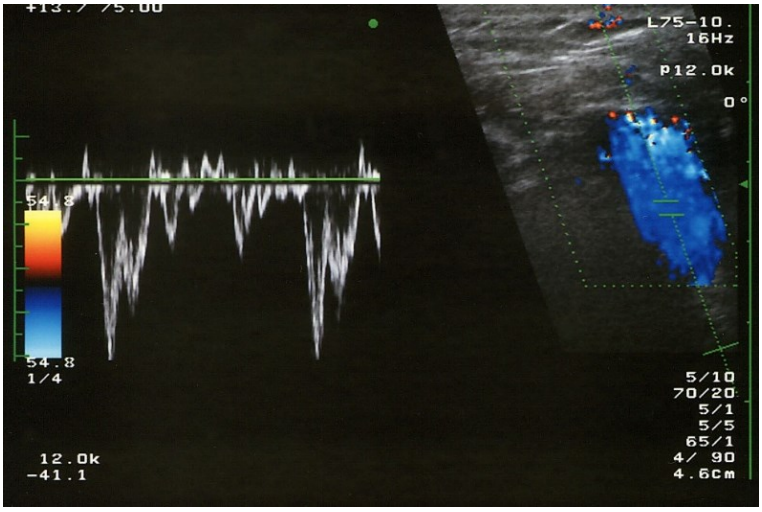

Figure 11.22. Increased pulsatility in jugular vein as the consequence of right-sided heart failure.

In *conclusion*, Doppler ultrasound is used extensively in almost all organs and organ systems and is established vascular imaging method, with some advantages as compared to DSA, CTA, MRA. It is harmless for patients and staff, easily accessible and cheap, can be performed at patient bed-side and enables accurate diagnosis in many pathological conditions. Vascular ultrasound has profoundly changed vascular medicine. To be able to use ultrasound in vascular pathology one needs to thoroughly understand the basic physics of Doppler, hemodynamicis and how to interpret Doppler spectra.

Selective references:

1. Dietrich CF (Ed). EFSUMB Course Book in Ultrasound. 2nd Edition, EFSUMB 2020.
2. Brkljačić B. Vascular Ultrasound. Textboof of University of Zagreb. Medicinska naklada, Zagreb, 2010. 361 pages (in Croatian)
3. Brkljačić B. Ultrasound. In: Brkljačić B, Vidjak V (Eds). Radiology. Textbook of University of Zagreb. Medicinska naklada Zagreb 2022, pp 9-16. (in Croatian)

12. HOW CAN I USE ULTRASOUND IN GYNECOLOGY?

Sergiu Puiu
WFUMB Center of Education Chisinau, Moldova

Rationale

Ultrasound (US) is the first imaging tool performed on all patients presenting to the gynecological emergency department. US can assist to identify the reason for abdominal pain, vaginal bleeding, abdominal distension, pelvic fluid collections or in defining a pelvic mass. Point-of-care-ultrasound (POCUS) enables the clinician to perform the ultrasound scan as an extension of the physical examination. Real-time images can rapidly be correlated with the patient's symptoms and state, particularly in life-threatening conditions. However, a negative finding on POCUS is not a substitute for a detailed diagnostic ultrasound scan.

Scanning technique

Dynamic two-dimensional (2D) pelvic sonography may be performed using abdominal (TAS) and transvaginal approach (TVS). The diagnostic information offered by the two approaches is complementary. TAS gives an initial global overview of the uterus and adnexa using transducer frequencies of 3.5 to 9.0 MHz. For adequate visualization, moderate bladder filling is required to displace the bowel from the field of view. The scanner should be adjusted to operate at the highest clinically appropriate frequency, realizing a compromise between the resolution and beam penetration. Nevertheless, image quality during TAS may be affected by adiposity, scar tissue or uterine retroversion. TVS gives finer details of early gestation and more detailed evaluation of pelvic architecture using higher frequency transducers (up to 12 MHz) at closer proximity to pelvic structures, resulting in improved spatial resolution and diagnostic accuracy. Some gentle pressure applied by the probe may be required to assess uterine and adnexal mobility and to search for site-specific tenderness. Color flow and pulsed Doppler may be added to the examination. However, the higher energy output of Doppler US may have potentially harmful effects on the embryo. Therefore, while performing Doppler US in early pregnancy, the concept of ''as low as reasonably achievable'' (ALARA) is important and the benefits of the Doppler imaging should outweigh the potentially risk.

Ultrasound assessment of the myometrium

Anatomically, the uterus is in the female pelvis immediately posterior to the bladder and anterior to the rectum. The uterus may naturally lie in different positions, such as anteverted/retroverted, anteflexed/retroflexed (fig. 12.1, 12.2), or midline, and it may be rotated (especially during pregnancy). However, the uterus most commonly lies in an anteflexed and anteverted position.

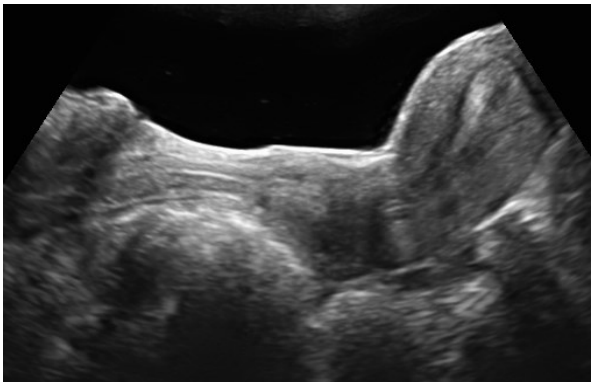

Figure 12.1. Anteverted/anteflexed uterus

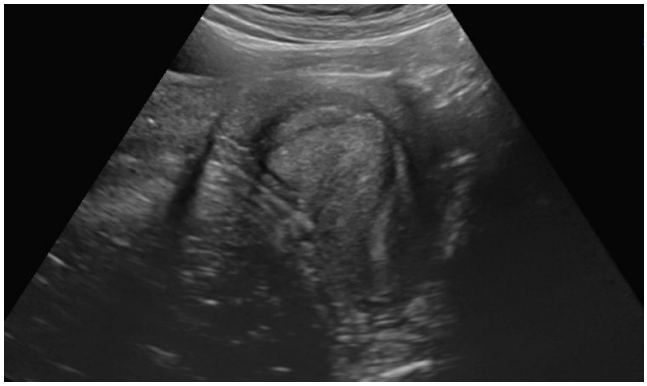

Figure 12.2. Retroverted/retroflexed uterus

The corpus is measured (length, anteroposterior and transverse diameter), the symmetry of the myometrial walls is estimated subjectively, and the overall echogenicity of the myometrium is reported as homogeneous or heterogeneous. If a myometrial lesion is observed, it is noted as well-defined or ill-defined. The extent of an ill-defined lesion can be estimated subjectively as the percentage of the whole myometrial volume that is involved, reported as localized or as diffuse.

The number of well-defined lesions is reported, as well as the location and maximum diameter. The site should be reported using International Federation of Gynecology and Obstetrics (FIGO) classification for myomas: Type 0 – pedunculated, intracavitary (fig. 12.3); Type 1 - submucosal, <50% intramural (fig. 12.4a); Type 2 - submucosal, >50% intramural (fig. 12.4b); Type 3 - 100% intramural, but in contact with the endometrium (fig. 12.5a); Type 4 - intramural (fig. 12.5b); Type 5 - subserosal (fig. 12.6a), ≥50% intramural; Type 6 - subserosal (fig. 12.6b), <50% intramural; Type 7 - subserosal pedunculated (fig. 12.7); Type 8 - other (e.g. cervical).

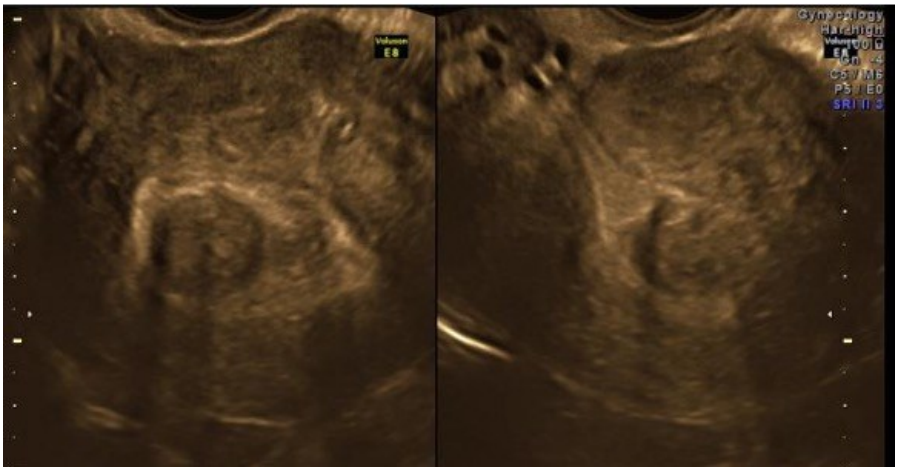

Figure 12.3. Type 0 myoma, intracavitary pedunculated lesion

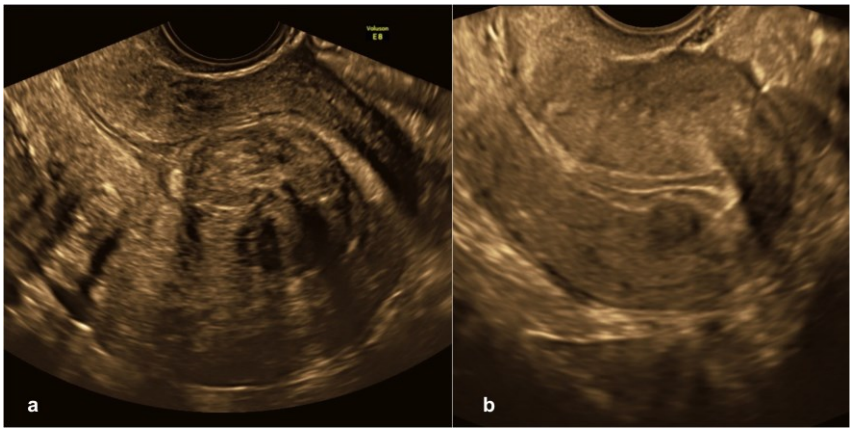

Figure 12.4. a) Type 1 myoma, submucosal, less than 50% intramural;
b) Type 2 myoma submucosal, greater than 50% intramural

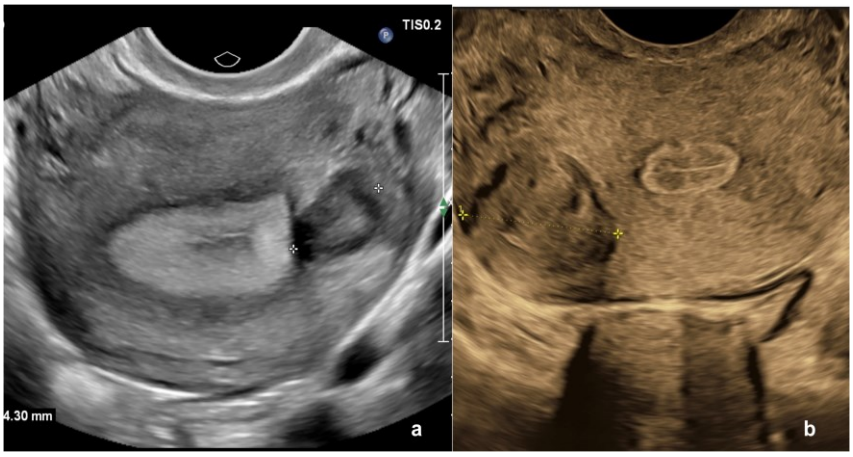

Figure 12.5. a) Type 3 myoma 100% intramural, but in contact with the endometrium;
b) Type 4 myoma, intramural

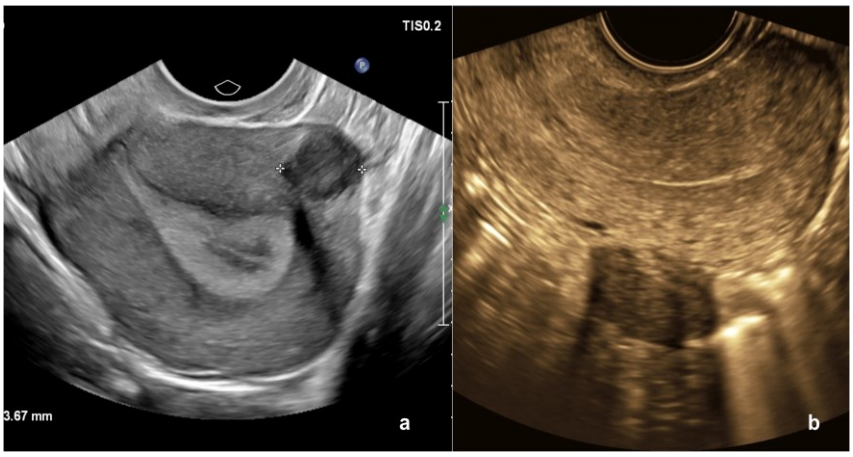

Figure 12.6. a) Type 5 myoma, subserosal, more than 50% intramural;
b) Type 6 myoma, subserosal, less than 50% intramural

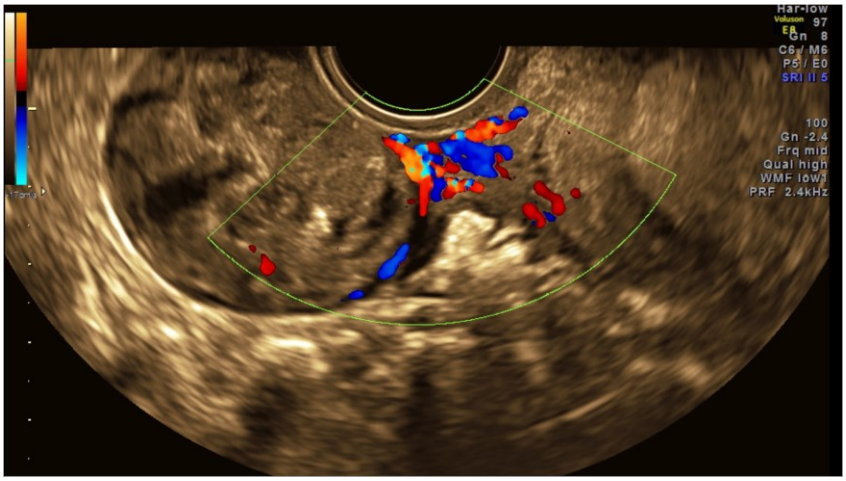

Figure 12.7. Type 7 myoma, subserosal pedunculated

The presence of shadowing (edge shadows, internal shadows or fan-shaped shadowing), myometrial cysts, hyperechogenic islands or subendometrial echogenic lines and buds is reported. The junctional zone (JZ) is reported as regular or poorly defined (if it is irregular, interrupted, poorly defined, not visible or not assessable). The cervical canal appears as an echoic linear stripe. Aspect and thickening do no undergo significant changes during menstrual cycle. Naboth cervical cysts often be seen as anechoic cystic lesions.

Ultrasound assessment of the endometrium

The endometrium is a central line, with varied thickness, echogenicity and appearance, depending on the phase of menstrual cycle. In the menstrual phase the endometrium appears as a thin hyperechoic line due to the interface between the anterior and posterior uterine walls. In the proliferative phase becomes progressively thicker, giving appearance of the three-layer pattern (fig. 12.8). Central hyperechoic stripe due to the interface of the two endometrial surfaces, hypoechoic intermediate layer due to the thickened functional layer and external echoic line, which represents the basal layer. In the secretory phase appears homogeneously hyperechoic, because of vascular changes, glandular hyperplasia and glycogen deposit (fig. 12.9).

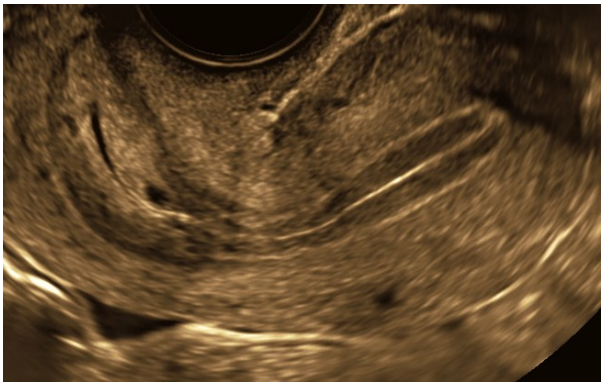

Figure 12.8. Proliferative phase endometrium

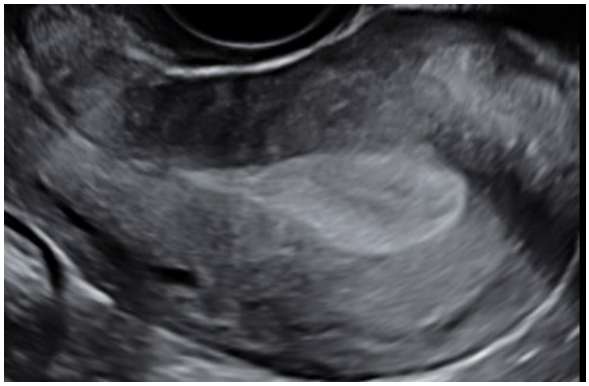

Figure 12.9. Secretory phase endometrium

Endometrial thickness is measured in the sagittal plane including both endometrial layers (fig. 12.10). In the presence of intracavitary fluid, the two layers were measured separately, and then the sum is recorded (fig. 12.11). If the entire endometrium was not clearly visible, it was recorded as "not measurable".

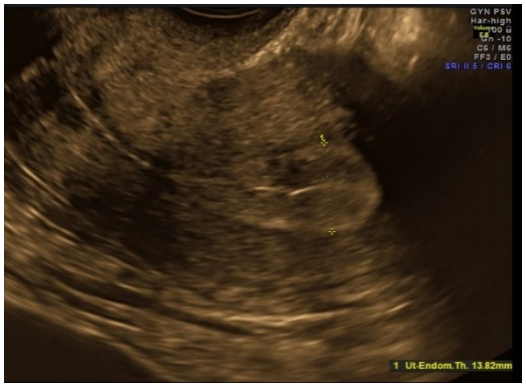

Figure 12.10. Endometrial thickness measurement

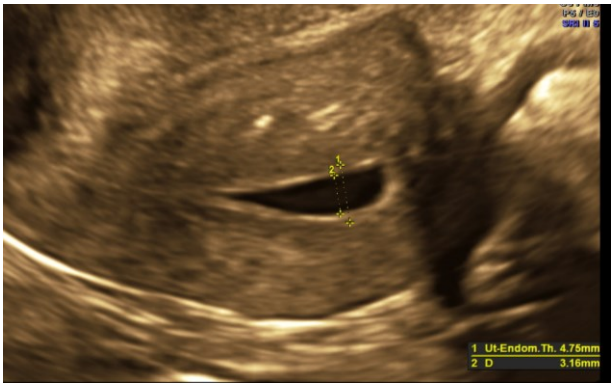

Figure 12.11. Endometrial thickness measurement with intracavitary fluid

Endometrial echogenicity is recorded as uniform or non-uniform. Uniform endometrium may be homogeneous without cysts and hyper-, iso- or hypoechogenic in comparison with the myometrial echogenicity, with symmetric anterior/posterior sides. Non-uniform endometrium may be homogeneous with regular or irregular cysts, or heterogeneous with or without cysts. The endometrial midline may be linear, non-linear, irregular or not defined. The endometrial–myometrial junction (JZ) is recorded as regular, irregular, interrupted or not visible. The color-Doppler score is a subjective assessment, reflecting the vascularity, and is scored as 1 (no color), 2 (minimal color), 3 (moderate color) or 4 (strong color). The vascular pattern may be a single vessel with or without branching, multiple vessels of focal or multifocal origin, scattered flow or circular flow.

Ultrasound assessment of the ovaries

On ultrasound the ovaries appear on ellipsoid shape, with variable location and often asymmetric. Despite numerous connective ligaments, they are very mobile. Usually delimited medial by uterus, lateral by iliac vessels, right by ileocecal junction and left by rectosigmoid. In adult women, the ovary is a dynamic structure and US appearance is according to the phase of the menstrual cycle. The follicles appear as round/oval anechoic structures. In the proliferative phase, some follicles start to growth. The number and dimensions depend on the woman's age and the phase of the menstrual cycle. In menopause, the follicles are no longer identifiable. Commonly, only one dominant follicle will mature. The mean diameter of the dominant follicle at ovulation is 20 mm, with a range of 17–26 mm (fig. 12.12). Follicular diameter is a predictor of ovulation. The follicle bursts and releases the oocyte, forming the corpus luteum, with variable sonographic appearance. Typically, it is a cystic structure, with irregular borders and internal echoes and peripheral color flow (fig. 12.13). In some cases, the follicle collapses and the corpus luteum is no longer identifiable. In other cases, a large hemorrhagic luteal cyst forms but tends to resolve in subsequent cycles.

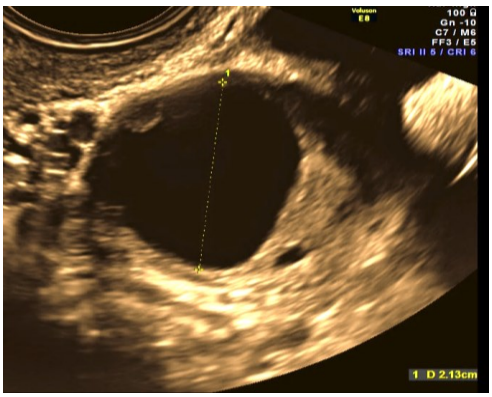

Figure 12.12. Dominant follicle at ovulation

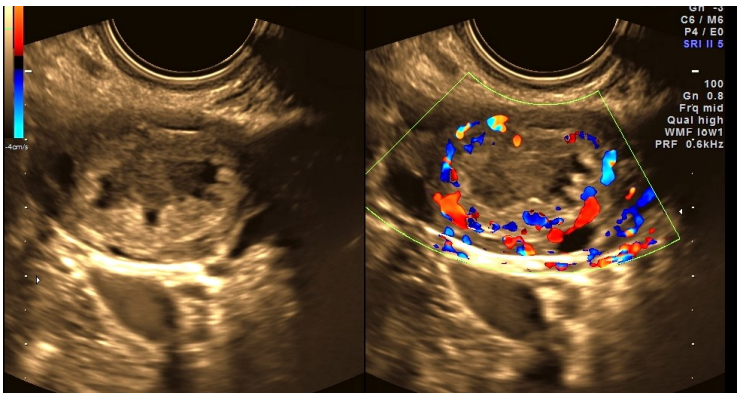

Figure 12.13. Corpus luteum

Gynecological emergencies

Gynecological emergency is a disease condition of the female reproductive system that could threaten the life of the woman, her sexual function and perpetuation of her fertility. Common gynecological emergencies present as: acute abdomen, abnormal vaginal bleeding or combination of both. Pregnancy and gynecological related etiologies are typically the first diagnoses to be considered. Sonography provides high sensitivities across the most critical conditions, some requiring surgical intervention, as: first trimester pregnancy pathologies (early pregnancy failure/miscarriage, threatened or impending miscarriage and ectopic pregnancy), symptomatic ovarian lesions (hemorrhage cyst, cyst rupture, adnexal torsion), pelvic inflammatory disease, uterine myoma necrosis and abnormal uterine bleeding. However, many other causes of pelvic pain can occur. Since the diagnosis can be challenging because many symptoms and signs lack sensitivity and specificity, and laboratory tests can be misleading, US scan should be the initial imaging modality in such cases.

Early pregnancy

Vaginal bleeding in the early pregnancy (up to 10th week of gestation) is a common cause of presentation in emergency care facilities. Clinical assessment of the pregnancy outcome at this stage is less reliable. US examination is important in establishing intrauterine pregnancy (IUP) and early pregnancy failure and to exclude other causes of bleeding, such as ectopic pregnancy (EP) and molar pregnancy/gestational trophoblastic disease. US assessment combined with quantitative beta human chorionic gonadotropin (beta-hCG) is an established diagnostic tool in these patients. The range of the serum beta-hCG level at which an intrauterine gestational sac (GS) is visualized is defined as the discriminatory zone and the widely accepted range is from 1000 to 2000 mIU/mL for TVS and 2400 to 3600 mIU/ml for TAS. The serum beta-hCG level above a discriminatory zone of 1000 mIU/mL and absence of a GS in the uterus on TVS has been found to be highly suspicious for an EP, although not diagnostic.

The earliest positive signs of an IUP such as "intradecidual sac" and "double-decidual ring" define an IUP before the embryo is seen. The ''intradecidual sign'' - on TVS the GS is seen as a well-defined fluid-filled cavity with a surrounding hyperechoic rim, embedded eccentrically in the endometrium (fig. 12.14a). The double decidual sac sign consists of two concentric echogenic rings encasing a central anechoic area that impress on the endometrial stripe (fig. 12.14b). The inner echogenic rim represents the decidua capsularis and chorion laeve, whereas the outer echogenic rim represents the decidua parietalis. Mean Sac Diameter (MSD) should be used when the embryo cannot be assessed. The crown-rump length (CRL) of the embryo is a more accurate indicator of gestational age (GA) than MSD. The yolk sac (YS) within a GS is the first definitive sign of an IUP, followed by embryo visualization at around the 5th week. Cardiac activity should be always seen in an embryo with a CRL>7 mm. Heart rate <100 b/m is suspect for imminent failed pregnancy.

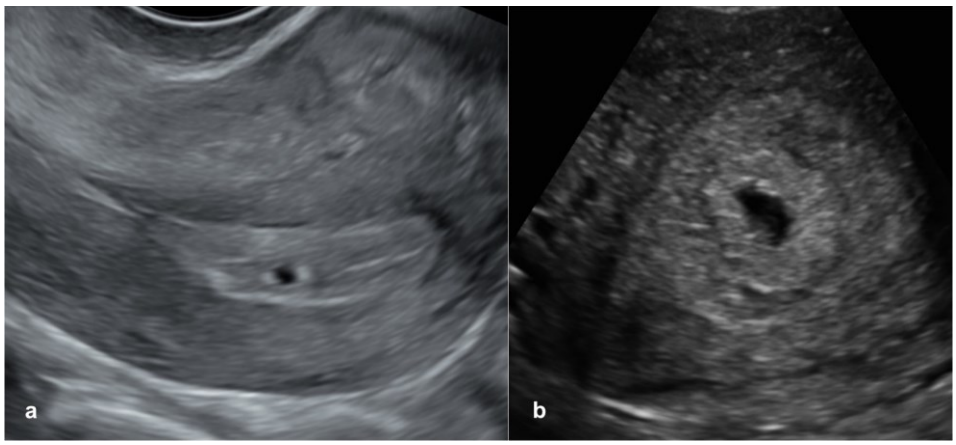

Figure 12.14. a) "Intradecidual sac", well-defined fluid-filled cavity with a surrounding hyperechoic rim, embedded eccentrically in the endometrium b) "Double-decidual ring", two concentric echogenic rings encasing a central anechoic area

The criteria of early pregnancy loss by TVS: IUP with an MSD > 25 mm but without a detectable YS and IUP with a fetal CRL > 7 mm but no detectable fetal cardiac activity. There is no need for follow-up. The term ‘‘miscarriage’’ is the spontaneous termination of a pregnancy before fetal development has reached 20 weeks. Approximately 80% of miscarriages occur in the first trimester and are clinically classified into: threatened abortion, inevitable abortion, complete incomplete abortion and missed abortion. The US findings depend on the developmental stage of the pregnancy at which the patient presents with symptoms. Any one of these conditions might be associated with some degree of vaginal bleeding.

1. Threatened abortion (symptoms indicate a miscarriage is possible). Depending on the GA, sonography may show intrauterine GS with or without an embryo. Up to 20% of women with a threatened abortion have a subchorionic hematoma (fig. 12.15) of which 70% spontaneously regress. Recent hemorrhage may be hyperechoic or isoechoic relative to the chorion, and it becomes isoechoic with the chorionic fluid in 1 to 2 weeks. Size of the hematoma is compared to size of the GS and graded as small when involves less than one third of the GS circumference, moderate when involves one-third to one-half of the GS circumference, large when two-thirds or greater of the GS circumference is involved.
2. Inevitable abortion (the symptoms cannot be stopped, and a miscarriage will happen). Variable US findings, depending on the degree of bleeding and expulsion of the products of conception. Crenated shape, no viable embryo, change in position over time are typical US features. The presence of GS in the lower uterine segment or cervix is usually seen in patients with abortion in progress (fig. 12.16) but can also be seen secondary to low implantation. Vascular flow on color Doppler is useful in differentiating low implantation from abortion.

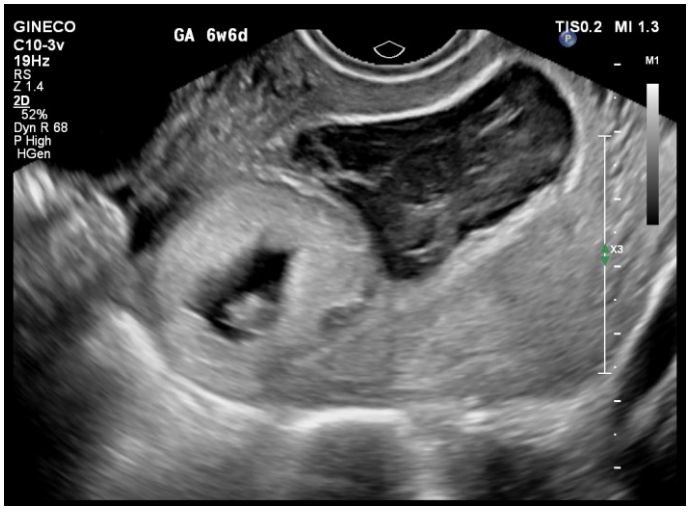

Figure 12.15. Threatened abortion. Uterine GS with an embryo. Hypoechoic subchorionic hematoma

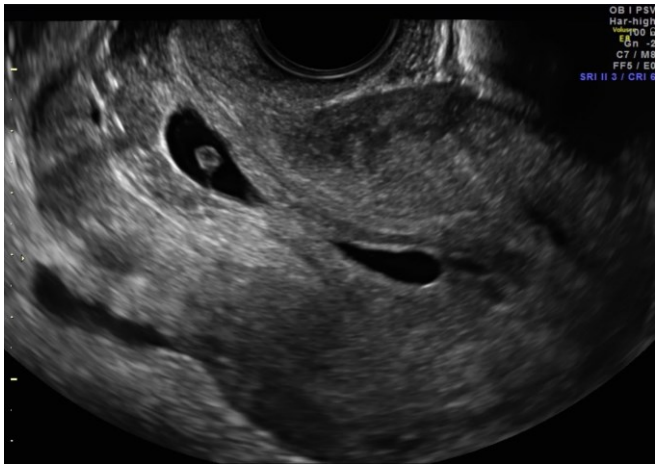

Figure 12.16. Inevitable abortion. Expulsion of the products of conception.

3. Complete abortion (all the products of conception are expelled). Vaginal bleeding and expulsion of all products of conception. US shows an empty uterus (fig. 12.17).
4. Incomplete abortion (not all the products of conception are expelled). Vaginal bleeding with partial expulsion of products of conception, may be associated with significant blood loss. Retained products of conception (RPOC) typically consist of residual trophoblastic tissue. US excludes rather than accurately establishes the diagnosis. The suggestive US findings are thickened irregular endometrium, an echogenic heterogeneous mass in the uterine cavity with blood flow and irregular endometrial–myometrial junction (fig. 12.18). A heterogeneous mass or collection in the cavity may represent a combination of retained placenta, necrotic debris and clot. Color Doppler is useful in differentiating vascularized trophoblastic tissue from clots. However, absence of blood flow does not exclude RPOC.
5. Missed abortion (a pregnancy demise where nothing is expelled).

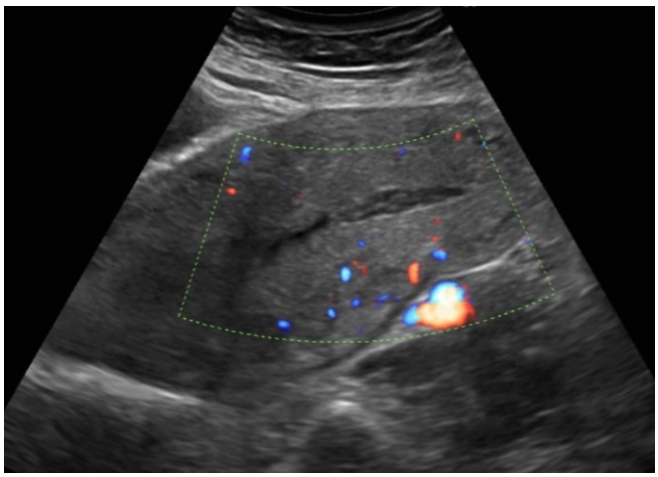

Figure 12.17. Complete abortion. Empty uterus

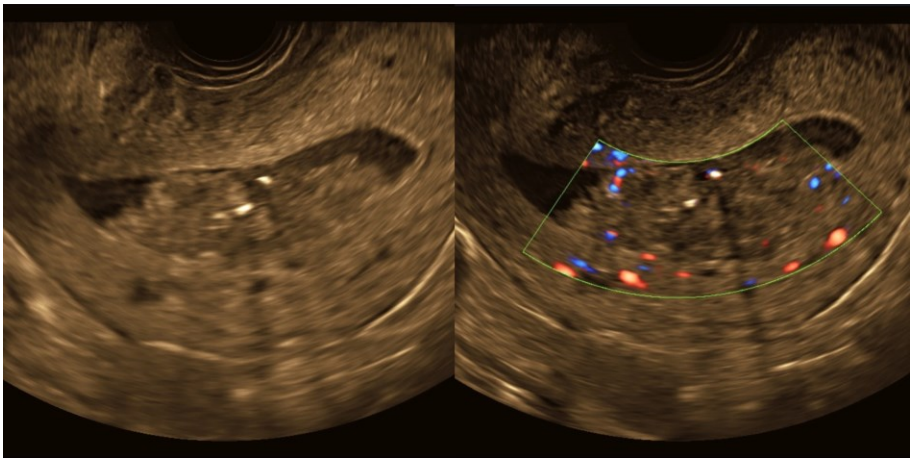

Figure 12.18. Incomplete abortion. Retained products of conception as heterogeneous mass in the uterine cavity with blood flow and irregular endometrial–myometrial junction

Ectopic Pregnancy

Refers to the implantation of a GS outside of the uterine cavity. EP most commonly (95%) occurs in the ampullary or isthmic portions of the fallopian tube (fig. 12.19). Other rare EP sites are cervix, ovary, myometrium, abdominal cavity, interstitial portion of the fallopian tube, cesarean section scar. The prevalence of EP varies between 6 and 16% of all pregnancies. Heterotopic pregnancy refers to the coexistence of an IUP with an EP (fig. 12.20). The incidence of HP is estimated in 1 in 7000 pregnancies in the general population. However, HP are more common in pregnancies of assisted reproduction, occurring in up to 1 in 100 in patients. Ectopic pregnancy remains the leading cause of pregnancy-related death, with maternal mortality overall of 4–10%.

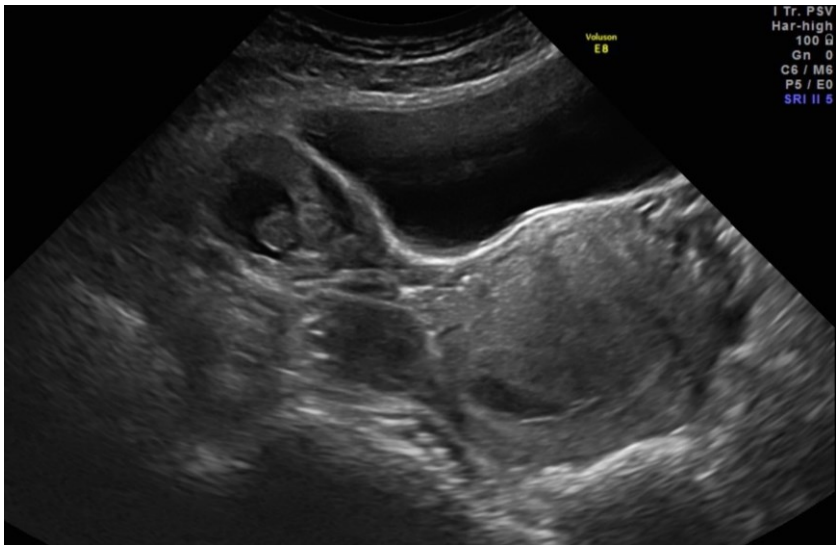

Figure 12.19. Tubal pregnancy. Empty uterine cavity an ectopic (tubal) GS containing a yolk sac with embryo

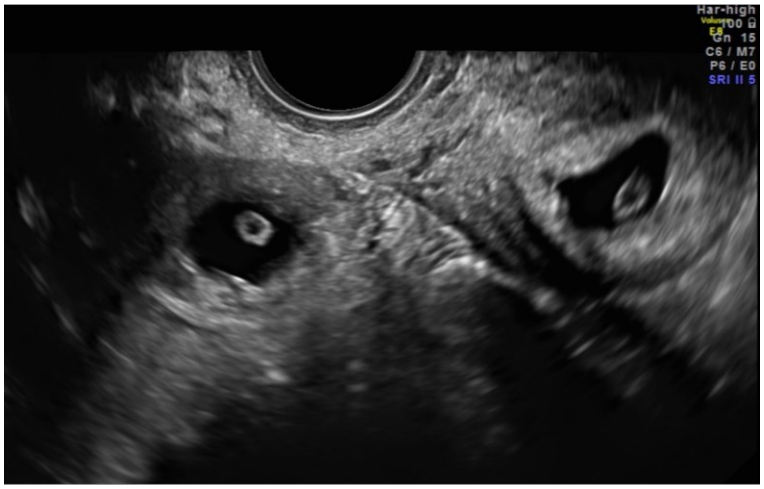

Figure 12.20. Heterotopic pregnancy, uterine GS and the extrauterine GS

EP should be considered in the setting of a positive pregnancy test and absence of a GS in the uterine cavity. The first goal of TVS in a suspected EP is to assess for an IUP. The presence of the intrauterine GS most often excludes the presence of an EP (except heterotopic pregnancy, cornual pregnancy). Sometimes, a gestational pseudosac may be seen in the uterine cavity, as a central intrauterine fluid collection without echogenic rim, with poorly defined margins, no decidual reaction, and shape changing over time (fig. 12.21).

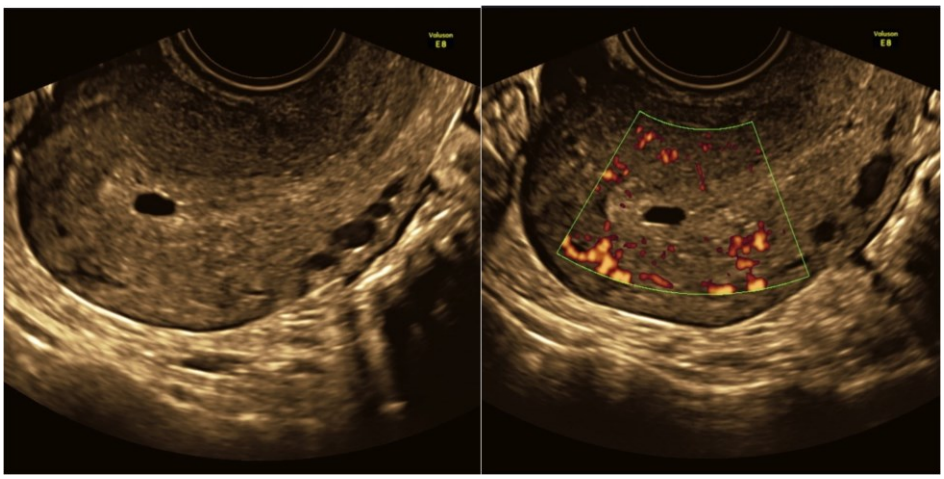

Figure 12.21. Intrauterine gestational pseudosac. A central intrauterine fluid collection without echogenic rim, poorly defined margins and no decidual reaction.

TVS combined with serum beta-hCG dosing are a valuable tool for identifying EP and differentiating from other causes of adnexal mass in the pregnant patient with pelvic pain. Failure to demonstrate intrauterine gestational sac by TVS when the serum beta-hCG more than 1000

mIU/ml is indicative for EP. The most specific finding of tubal pregnancy is the extrauterine GS containing a yolk sac or embryo with or without cardiac activity (fig. 12.19). The most common US appearance of tubal pregnancy is “tubal ring” or “blob sign”. The echogenic vascularized adnexal “tubal or bagel sign”, with a hyperechoic ring around the anechoic center GS and vascular wall (sometimes only focally) is reported in 68% of non-ruptured EP (fig. 12.22a). The “blob sign” - extraovarian inhomogeneous adnexal mass (fig. 12.22b). Both separately moving from the ovary, when gentle pressure is applied with the transducer. Both US signs provide specificity of up to 100% in patients with positive pregnancy test results but no IUP. In one third of cases, the ectopic GS is contralateral to the corpus luteum. When the US is inconclusive for the uterine or ectopic location, the pregnancy is defined as unspecified location and the physician should use the other available criteria.

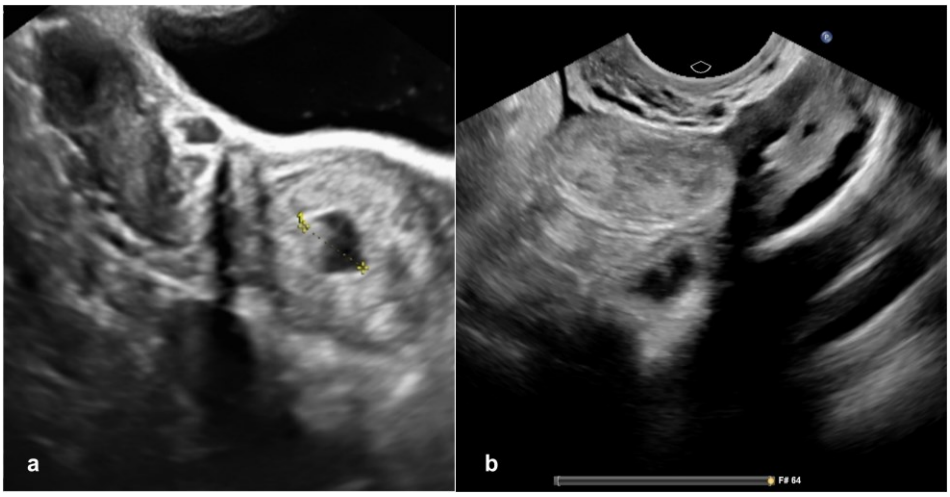

Figure 12.22. a) “Tubal or bagel sign”, a hyperechoic ring around the anechoic center, representing the GS, b) “Blob sign”, echogenic extraovarian inhomogeneous adnexal mass

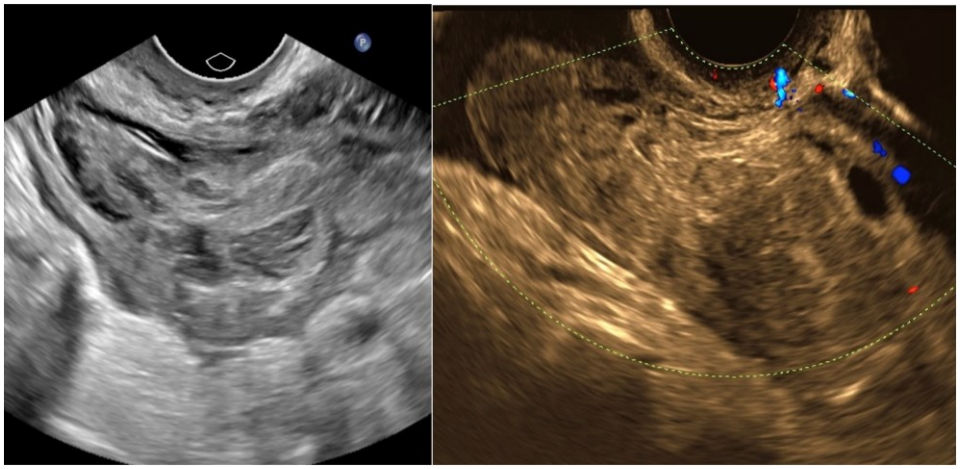

Figure 12.23. Tubal rupture, large tubular adnexal mass with mixed echogenicity and hemoperitoneum

If a patient develops severe pain, it is crucial to evaluate for signs of tubal rupture, such as increase in the size of the adnexal mass or large hemoperitoneum (fig. 12.23). TAS is particularly helpful for evaluation of the peritoneal cavity to detect fluid that could represent blood, which may indicate tubal rupture or tubal abortion. Hemorrhagic collection visualized superior to the uterine fundus or at the level of the ovary (fig. 12.24) indicates significant hemorrhage, while echogenic fluid collection seen in the Morrison (fig. 12.25) space suggests severe hemorrhage.

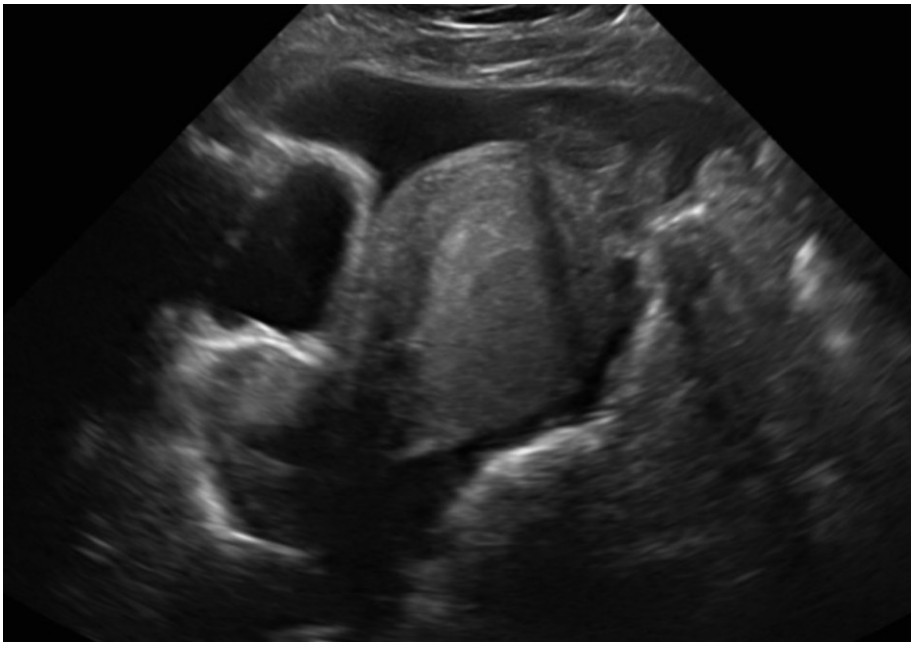

Figure 12.24. Hemorrhagic collection superior to the uterine fundus

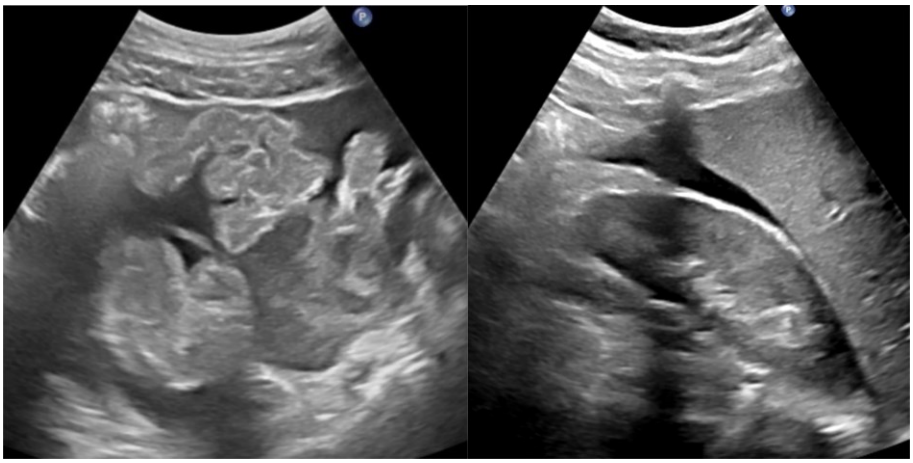

Figure 12.25. Abdominal and Morrison space free fluid

Gestational trophoblastic disease

Gestational trophoblastic disease (GTD) is a spectrum of pregnancy-related trophoblastic proliferative abnormalities that can present with first-trimester bleeding. Classification of GTD is as follows: hydatidiform mole (complete and partial mole), gestational trophoblastic tumors, choriocarcinoma, invasive mole and placental site trophoblastic tumor. Hydatidiform mole constitutes 80% of the cases of GTD. The absence or presence of fetal/embryonic elements classifies the molar pregnancy as complete or partial. Incidence of complete mole is 1:2000 pregnancies, while of partial mole is 1:700 pregnancies. The presence of the maternal genome in partial mole ensures less expressed trophoblast hyperplasia and more advanced fetal development, showing molar changes and fetal/embryonic parts. The embryo/fetus is usually nonviable. Most abort by 10-12 weeks. Uterine bleeding is the most common clinical presentation, and it may vary from spotting to profuse bleeding. Diagnosis is made by markedly elevated serum beta-hCG levels than expected for the GA and by the characteristic sonographic appearance. Half of patients with molar pregnancy have serum beta-hCG values of greater than 100,000 mIU/ml at the time of diagnosis.

Complete mole presents a characteristic vesicular appearance on ultrasound. Appears as thickened endometrial cavity, with multiple cystic areas of different sizes (fig. 12.26), corresponding to hydropic villi [30]. The cystic spaces range from 1 to 30 mm in size and increase in size with GA. Increased vascularity may be observed. Enlarged ovaries with multiple theca-lutein cysts (> 5 cm in diameter), also known as “hyperreactio luteinalis”, are secondary to excess beta-hCG, are seen in 50% of patients with molar pregnancy. In partial mole, an intrauterine embryo is noted along with molar changes (fig. 12.27).

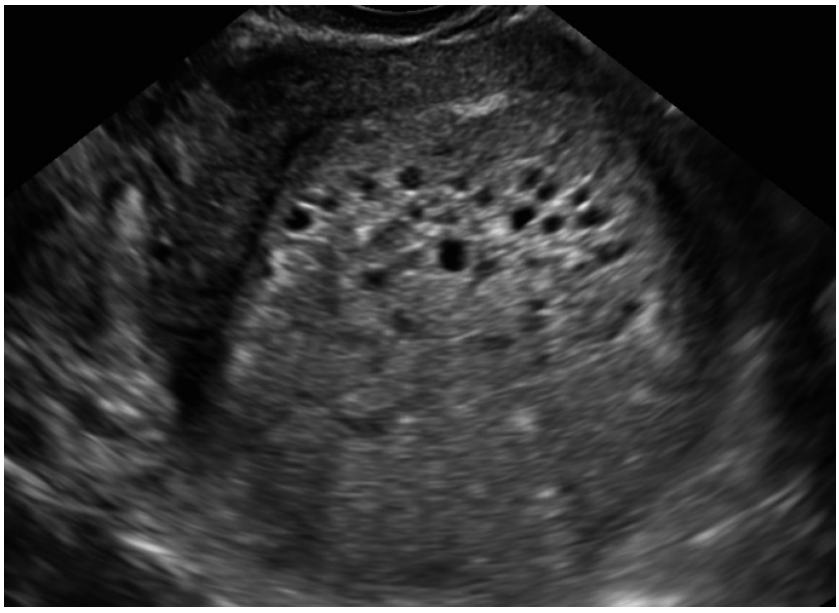

Figure 12.26. Complete mole, thickened endometrial cavity with multiple cystic areas and no embryo

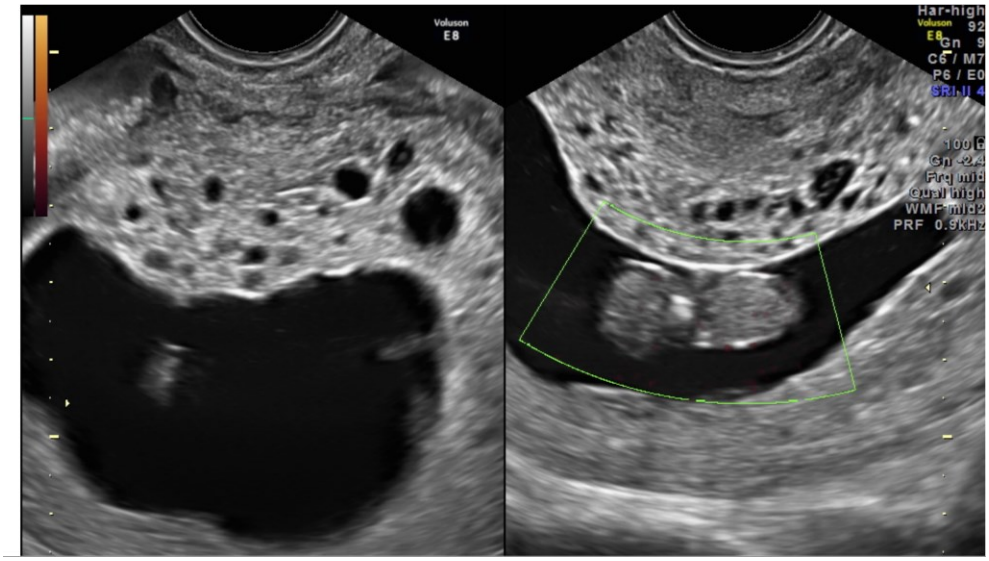

Figure 12.27. Partial mole, an intrauterine nonviable embryo is noted along with molar changes

In missed abortion, impaired trophoblastic vascularity leads to hydropic degeneration of villi and can mimic a partial hydatidiform mole on US. The serum beta-hCG is not elevated, however, and may be normal or at a lower level than for the expected GA. Typical low-resistance and high velocity vascular trophoblastic flow is useful in differentiating the trophoblastic tissue of molar pregnancy from intrauterine blood clots in a patient with abortion.

Uterine rupture. Disruption of uterine wall

Uterine rupture and perforation are rare but potentially devastating event for woman, which are typically diagnosed clinically, based on symptoms such as pelvic pain and vaginal bleeding. Could occur postpartum, after surgery/instrumentation, dilatation and curettage, or blunt trauma. The sonographic findings of uterine rupture include extrauterine blood collection and focal discontinuity/defect of the myometrium/uterine wall (fig. 12.28a). Gas bubbles often seen tracking through the defect. Intrauterine contraceptive device (IUD) outside uterine cavity or eccentric location should raise suspicion of partial perforation (fig. 12.28b).

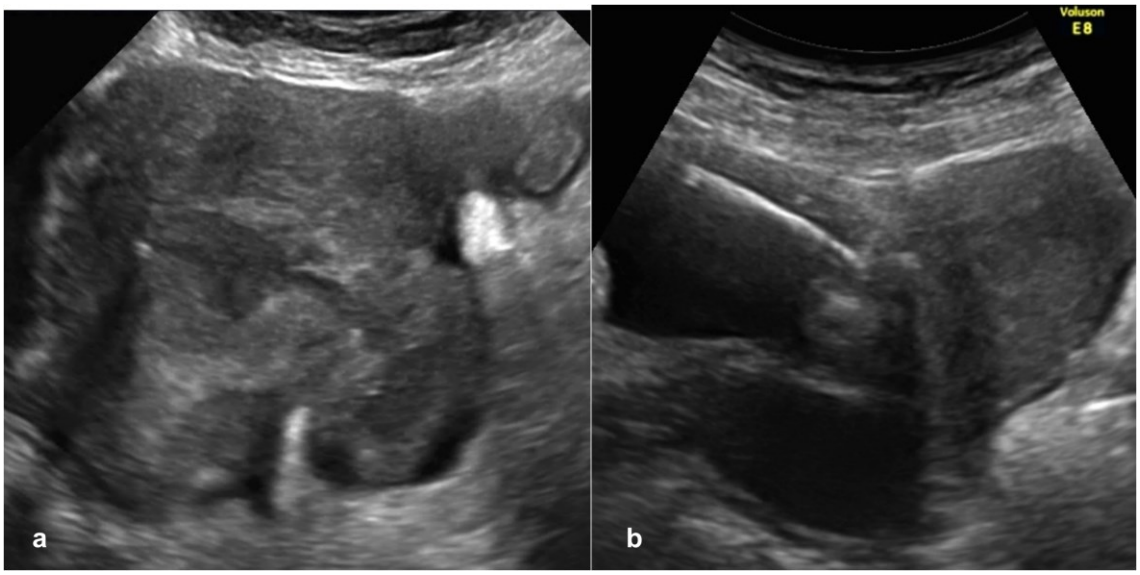

Figure 12.28. a) Uterine rupture, defect of the myometrium/uterine wall
b) Uterine perforation, IUD seen outside uterine cavity

Ovarian Cysts

Most adnexal lesions are non-neoplastic, functional physiologic cysts, including corpus luteal cysts and follicular cysts, that may be simple or hemorrhagic. They could be secondary to failure of a mature follicle to rupture or the collection of blood within the follicle after ovulation occurs. Most of functional cysts resolve within 4 weeks. Acute abdominal pain is most often caused by internal hemorrhage, rupture or leakage, ovarian torsion but may be simply a result of its large size.

The sonographic appearance of a functional cyst is that of a thin-walled unilocular simple cyst, with well-defined wall, increased through transmission. The US appearance of hemorrhagic ovarian cysts varies because the features change over time: clot formation, clot lysis, clot retraction and clot resolution. Initially the hemorrhagic content shows a diffuse hyperechoic or homogeneous pattern of low-level echoes. Over time as the clot forms, a lace-like, reticular pattern (fig. 12.29a) of internal echoes develops because of the presence of fine fibrin strands. The clot may appear as an echogenic mass, lenticular in shape, either mobile or adherent to the cyst wall but without evidence of vascularity, retracting over time (fig. 12.29b). The cyst content shows no color Doppler flow but may demonstrates a circular pattern of vascularity. Reticular and retracting clot patterns allow high diagnostic accuracy of hemorrhagic ovarian cysts since 90% of them will have at least one of these two features.

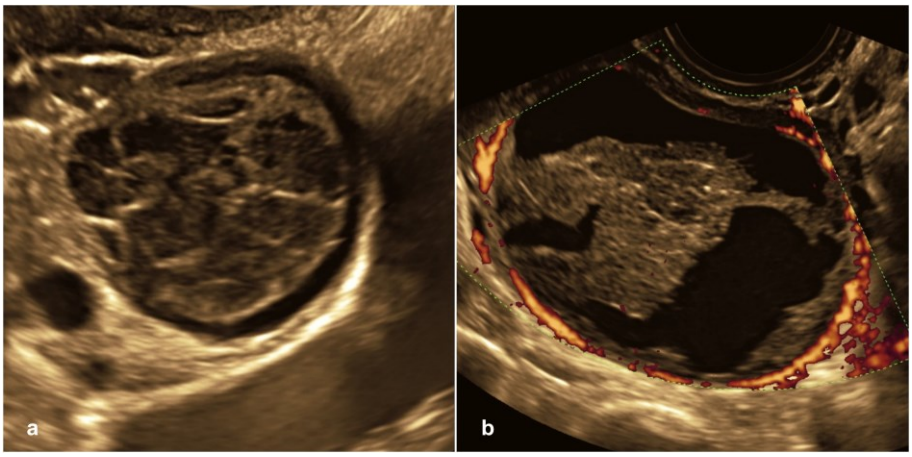

Figure 12.29. Hemorrhagic ovarian cysts. a) Reticular pattern (fine fibrin strands) b) Retracting clot pattern, echogenic mass adherent to the cyst wall and vascularity

Ruptured Ovarian Cyst

All cystic lesions may rupture. Rupture is usually spontaneous, often secondary to trauma or intercourse. Rupture of an ovarian cyst is associated with a sudden onset of unilateral lower abdominal pain and hemorrhage (hemoperitoneum). US findings of an ovarian cyst and blood or a significant amount of pelvic fluid makes the diagnosis highly likely. The ovarian cyst itself may or may not be visualized, since it may partially or totally collapse after rupture. Intracystic pattern may depend on the nature of the cyst. The cyst may have an angular or crenated appearance, and free fluid that contains low-level echoes or clots may be observed in the cul-de-sac, surrounding the ovary or even hemoperitoneum (fig. 12.30). Presence of liquid in the upper abdomen (Morrison pouch) is indicative of an important bleeding (fig. 12.25). As most of ruptured cysts are functional and the hemoperitoneum is low to moderate, conservative treatment is often possible. Non-hemorrhagic abdominal fluid usually reabsorbs within a few days. In rare cases, surgery is necessary to stop bleeding.

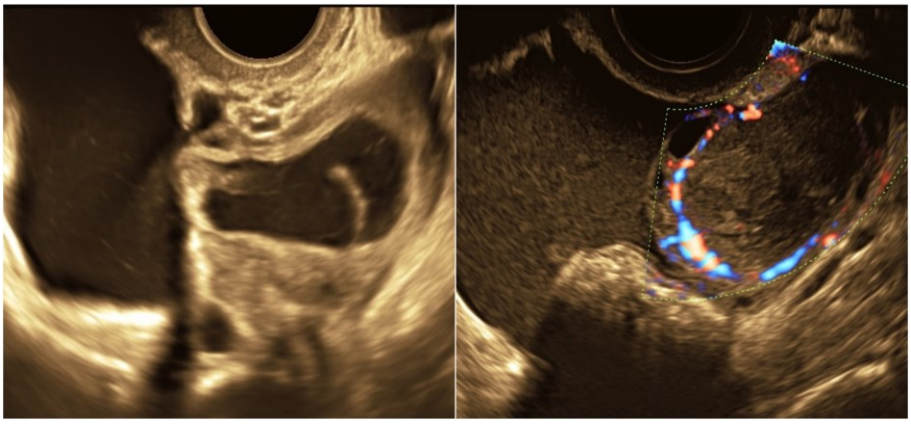

Figure 12.30. Ruptured ovarian cyst. Partially collapsed cyst and free fluid in the cul-de-sac

Assessment of ovarian and adnexal findings discovered on sonography. Malignancy risk stratification of ovarian and adnexal lesions

Correctly discriminating between benign or malignant adnexal lesions is of crucial importance for selecting the optimal management strategy. Since there are currently no approved screening programs for ovarian cancer, unfortunately, most ovarian cancers are detected in advanced stages. The diagnostic accuracy of US in differentiating between benign and malignant adnexal masses has been shown to relate to the expertise of the operator and availability of resources. Subjective assessment appears to be an optimal tool to predict the likelihood of an ovarian malignancy. In fact, subjective assessment by expert ultrasound examiners currently is the most accurate method for sonographic assessment of adnexal lesions. Unfortunately, clinicians with this level of expertise are not universally available. This highlights the need for clinical tools to assist clinicians with different levels of training and expertise in characterizing adnexal pathology and accurately predict which pelvic lesions are likely malignant.

To homogenize and standardize the US assessment, and thereby increase diagnostic accuracy, the International Ovarian Tumor Analysis (IOTA) group first published a consensus paper on terms and definitions to describe adnexal lesions in 2000. According to IOTA definitions there are five lesion types: unilocular (fig. 12.31a), multilocular (fig. 12.31b), unilocular-solid (fig. 12.32a, fig. 12.33), multilocular-solid (fig. 12.32b,) or solid lesion (fig. 12.34). The cyst contents could be anechoic, low level, ground glass, hemorrhagic or mixed. Solid component, papillary projections or wall irregularity (presence and size) should be documented, as well as vascularity, shadows and ascites. In fact, the more complex and more solid component is present, the higher is likelihood of malignancy.

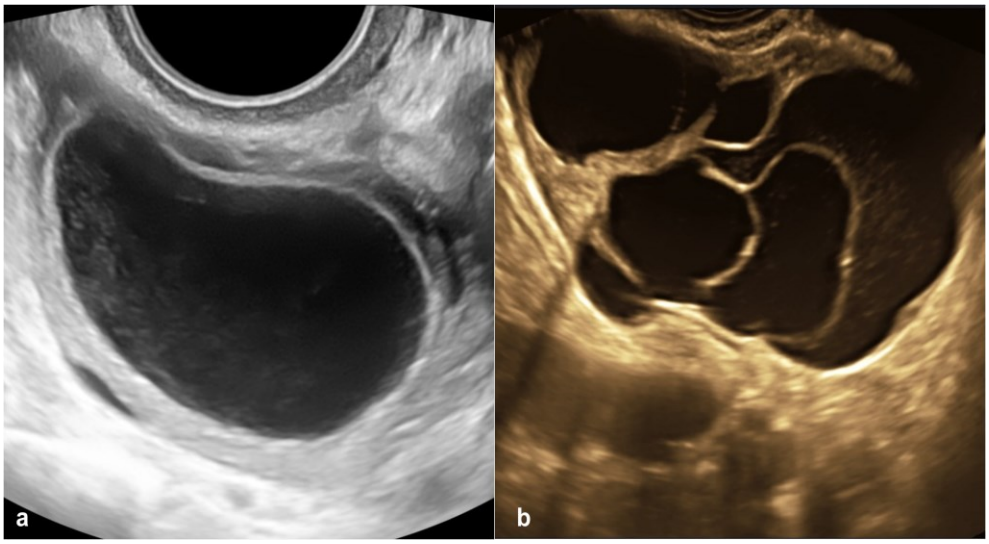

Figure 12.31. a) Unilocular cyst without septa and no papillary projections or solid component
b) Multilocular cyst. Smooth-walled septate cyst and no papillary projections or solid tissue

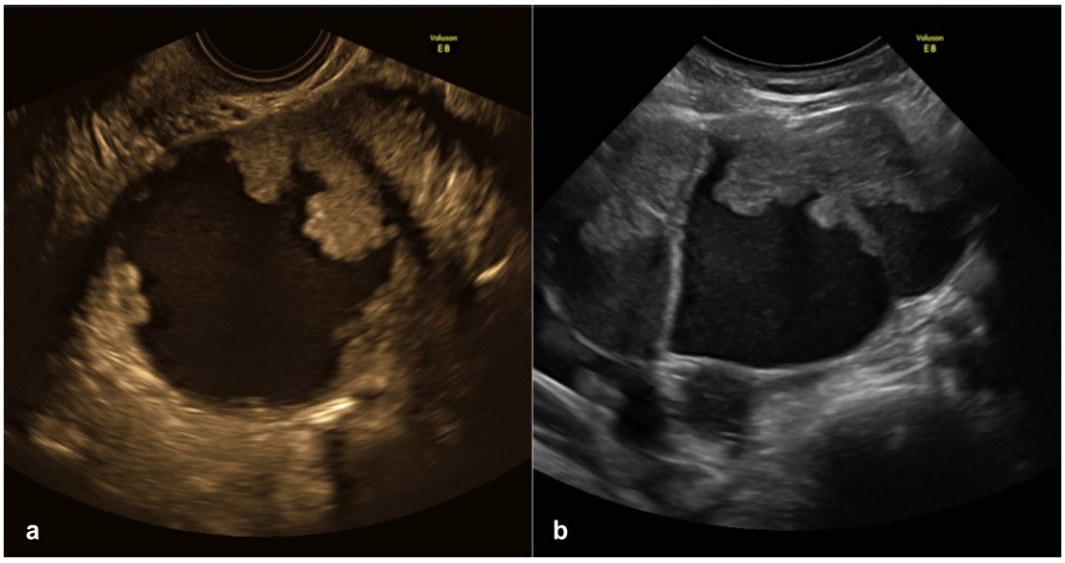

Figure 12.32. a) Unilocular-solid cystic lesion with papillary projections, no septations, b) Multilocular-solid cystic lesion with solid component and papillary projections

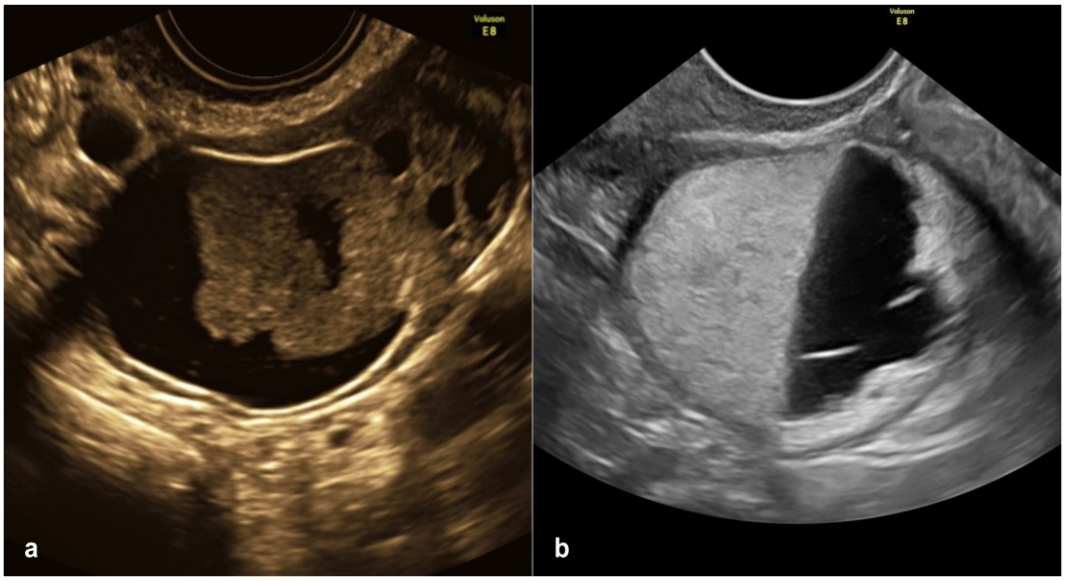

Figure 12.33. a) Unilocular-solid cystic lesion with papillary projection, no septations; b) Unilocular-solid cystic lesion with solid component, no septations

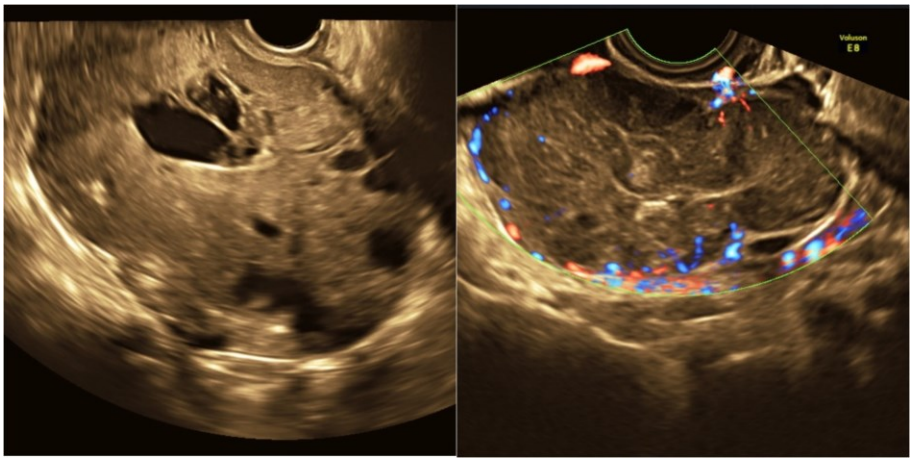

Figure 12.34. Solid tumor (at least 80% of the content).

Some ovarian lesions, such as endometrioma (fig. 12.35), benign cystic teratoma (dermoid) (fig. 12.36), simple cyst or cystadenoma (fig. 12.37), functional hemorrhagic cyst (fig. 12.21) or malignant tumour with ascites (fig. 12.38), exhibit typical features, and are easy to classify using pattern recognition of US features (IOTA Simple Descriptors), providing intuitive/instant diagnosis in approximately half of detected adnexal masses. If the lesion is not instantly recognizable, the IOTA Simple Rules could be applied.

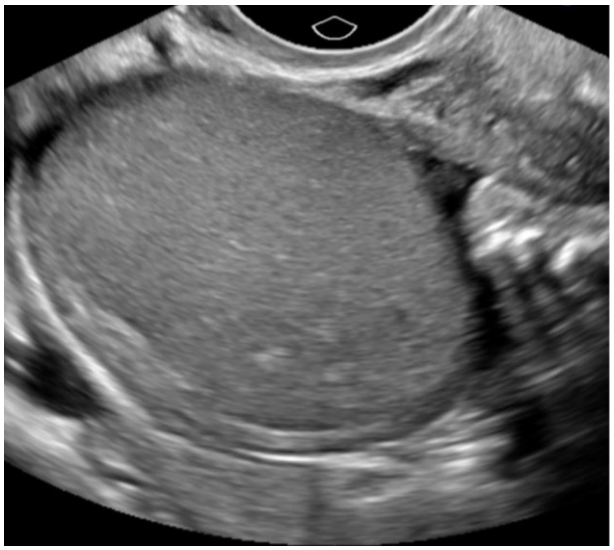

Figure 12.35. Endometrial cyst (endometrioma). Unilocular cyst with ground-glass echogenicity

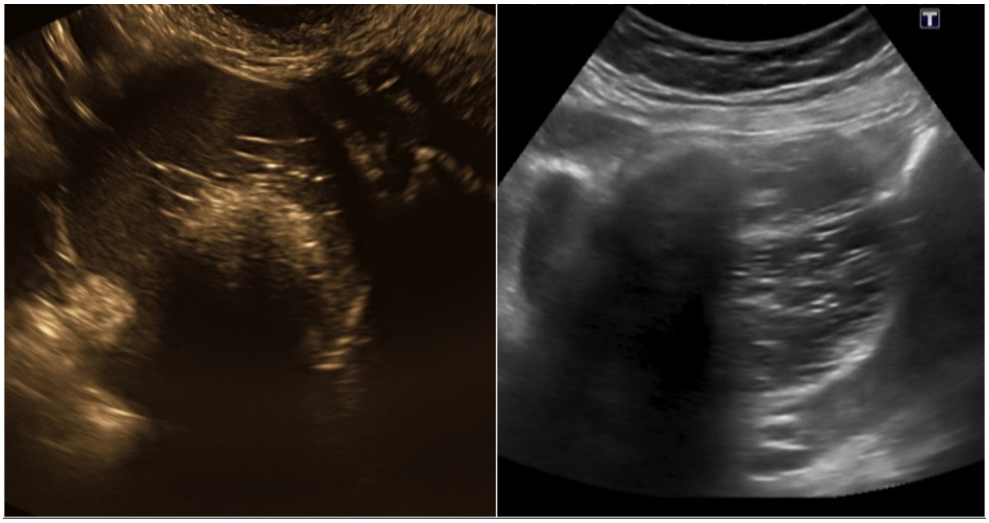

Figure 12.36. Benign cystic teratoma (dermoid). Unilocular cyst with mixed echogenicity, acoustic shadow

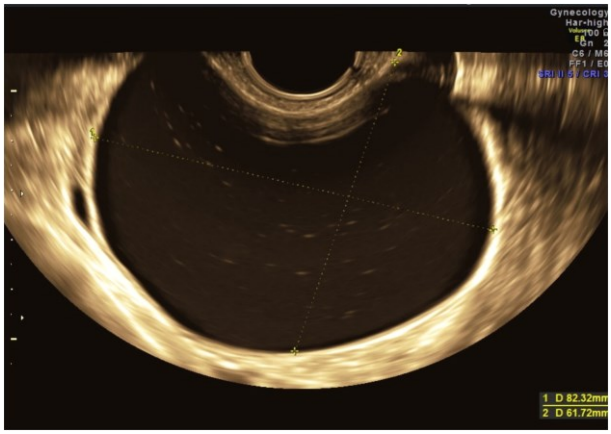

Figure 12.37. Simple cyst or cystadenoma. Unilocular cyst with anechoic/hypoechoic content, smooth internal walls

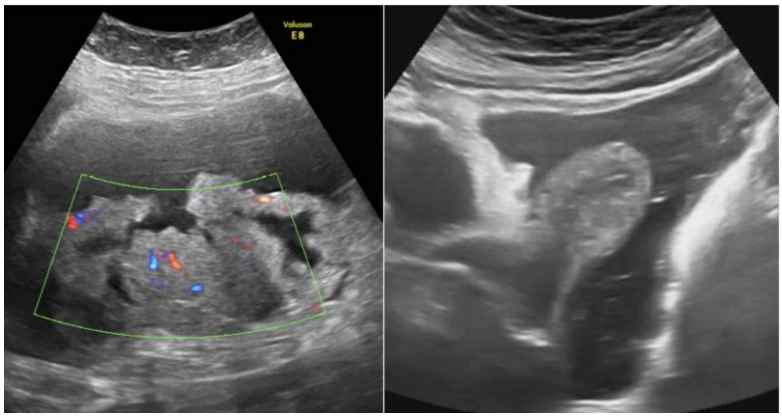

Figure 12.38. Malignant tumour (multilocular solid lesion) with ascites

Simple ultrasound-based rules classify lesions as benign, inconclusive or malignant based on the presence or absence of five benign and five malignant ultrasound features. These rules can be applied to about 80% of adnexal masses, with the rest being classed as inconclusive.

- Benign features: unilocular cyst, smooth multilocular cyst with largest diameter <100 mm, presence of solid areas with largest diameter <7 mm, acoustic shadows, no vascularization on color Doppler
- Malignant features: irregular solid tumor, irregular multilocular solid tumor with largest diameter

≥100 mm, presence of ascites, ≥4 papillary projections, very strong vascularization on color Doppler

No risk estimates. Easy to use without computer. Available as smartphone application

Rule 1: If one or more M features are present in absence of B feature(s), the lesion is classified as malignant.

Rule 2: If one or more B features are present in absence of M feature(s), the lesion is classified as benign.

Rule 3: If both M features and B features are present, or if no B or M features are present, the result is inconclusive, and a second stage test is recommended.

The IOTA group have also developed some logistic regression models, the Assessment of Different NEoplasias in the adneXa (ADNEX) model being recognized as the most accurate. ADNEX uses three clinical and six ultrasound predictors: type of center (oncology centers versus other hospitals), patient age, CA125 level, but can also be used without CA125. The ultrasound predictors are the maximal diameter of the lesion (mm), largest solid component (mm), number of papillary projections (0, 1, 2, 3, > 3), presence of more than 10 cyst locules (yes/no), acoustic shadows (yes/no), and presence of ascites (yes/no). This multiclass prediction model is designed to differentiate between benign and malignant tumors, whilst also offering subclassification (calculates the probability) of any malignancy into borderline tumors, stage-I and stage-II–IV primary invasive cancers and secondary metastatic tumors (e.g. breast cancer or colon cancer).

As the large proportion of adnexal lesions can be easily classified as benign, the two-step strategy was proposed. In clinical practice, as a first step, the modified Benign Descriptors (largest lesion diameter < 10 cm, in a premenopausal woman) are used. If one of these applies, the mass could be classified as certainly benign (risk of malignancy <1%), while if none applies, for the remaining masses, the mathematical ADNEX model can be used to estimate the risk of malignancy. The two-step strategy is convenient and has excellent discriminative performance and is reasonably well calibrated. The malignant simple descriptors are not used in the two-step strategy.

Ovarian hyperstimulation syndrome

Ovarian hyperstimulation syndrome (OHSS) is a potentially dangerous iatrogenic complication of pharmacologic ovulation induction (gonadotropin use) for the treatment of infertility. It occurs in the setting of abnormally high levels of beta-HCG and less frequently has been reported in spontaneous singleton and multiple pregnancies, sex hormone–producing tumors, hydatidiform mole and choriocarcinoma. Although the precise pathophysiology remains unknown, beta-hCG seems to trigger an increase in vascular permeability that results in ovarian enlargement, cyst formation, and third spacing of fluid. It is estimated that mild OHSS may occur in as many as 65% of women who undergo ovulation induction. The incidence of clinically important OHSS ranges up to 10%, but only 5% of these cases are severe, particularly in patients who subsequently became pregnant after ovulation induction, with massively enlarged ovaries. The spectrum of clinical presentation ranges from nausea, vomiting, and abdominal pain to massive ascites, acute respiratory distress syndrome, and hypotension. Ultrasound findings are bilateral ovarian enlargement, diameter > 5 cm is a criterion for mild OHSS. Multiple large, thin-walled cysts are identified (fig. 12.39). Rarely, ascites or pleural fluid effusion could be present. The cysts resolve spontaneously after treatment of gestational trophoblastic disease or cessation of fertility therapy.

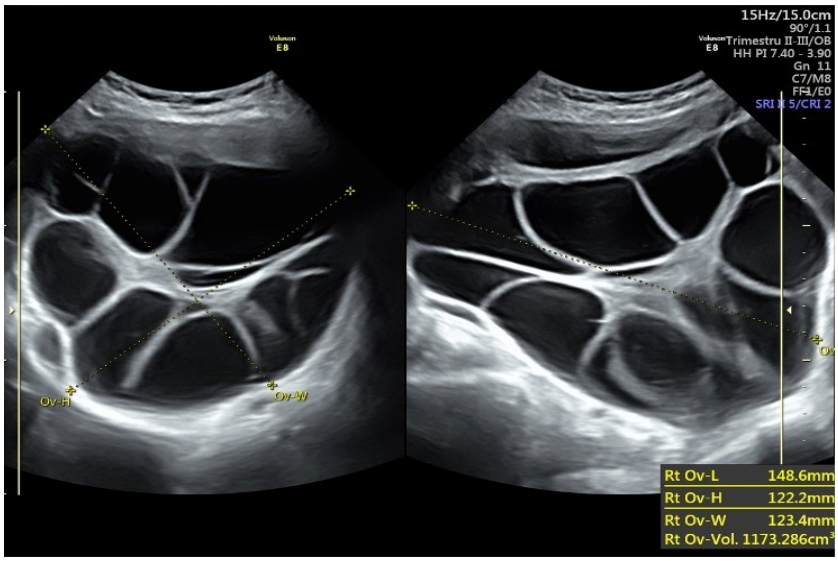

Figure 12.39. Ovarian hyperstimulation syndrome.
Bilateral enlarged ovaries with multiple large, thin-walled cysts

Ovarian/Adnexal Torsion

Ovarian/Adnexal torsion is the result of partial or complete rotation (twist) of the adnexal pedicle on its axis, which results initially in impaired lymphatic and venous drainage and eventual loss of arterial perfusion. The risk of torsion is higher in women of reproductive age and may involve the ovary, the tube or more commonly both. May involve normal adnexa but usually is secondary to a preexisting ovarian mass, particularly a large mass. There is increased risk during

pregnancy, approximately 25% of adnexal torsions occur in pregnant patients. Also, women undergoing ovulation induction (theca lutein cysts and OHSS, which can massively enlarge the ovaries) increase the risk of torsion.

Clinical presentation is characterized by the acute onset of moderate to severe pelvic pain, often with nausea and vomiting, in a woman with an adnexal mass. Torsion can be difficult to diagnose clinically because the presenting symptoms are nonspecific and like many causes of acute abdomen. The most common sonographic finding of ovarian torsion is an enlarged ovary or ovarian mass complex, although the ovarian architecture is variable and depends on the degree of ischemia and time of torsion.

During the early phase, venous compression and edema of the ovarian stroma occurs. At this stage, the adnexa are viable. Typical US findings are rounded and enlarged ovary with heterogeneous central stroma (due to edema and vascular and lymph engorgement). Multiple small peripherally displaced follicles caused by edema (fig. 12.40). If involved, dilated twisted fallopian tube and thickened edematous tubal wall. In a late phase findings of edema are gradually replaced by those of hemorrhagic necrosis, complete or partial. Cystic areas with varying degrees of echogenicity may be observed.

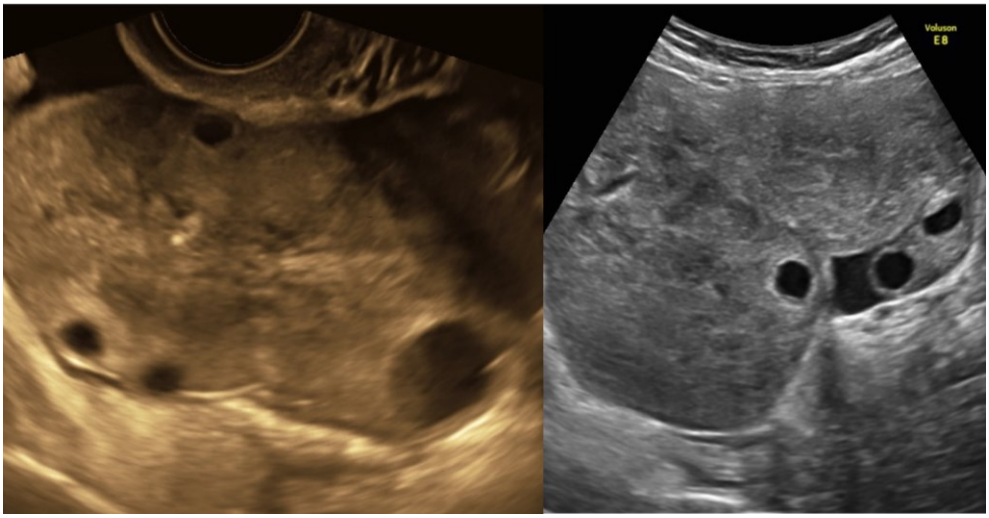

Figure 12.40. Ovarian torsion, early phase. Enlarged ovary with heterogeneous central stroma. Small peripherally displaced follicles caused by edema.

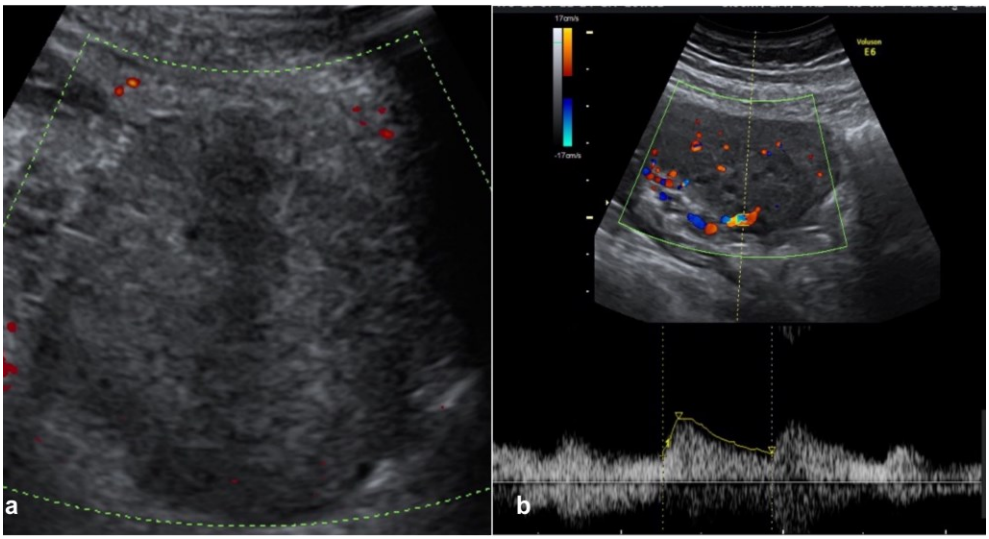

Figure 12.41. a) Ovarian torsion, late phase. Hemorrhagic necrosis. Hypoechoic mass with absent arterial Doppler flow; b) Partial arterial perfusion on early phase of the ovarian torsion

Doppler flow patterns in torsion are variable, depending on the degree of torsion and time. Classically, absent arterial Doppler flow within the ovary (fig.41a). However, early there may be obstruction of lymphatic and venous flow with preservation of arterial perfusion (fig. 12.41b). Because the ovary has dual arterial supply, in early torsion only one may be occluded. In a patient with acute pain and an ovary providing US findings consistent with ovarian torsion, the diagnosis should be considered even present arterial flow. Conversely, an ovarian color Doppler flow has been reported in cases of surgically proven torsion. The "whirlpool sign" on color Doppler and grayscale, which represents the twisted vascular pedicle, is the most definitive finding of ovarian torsion (fig. 12.42).

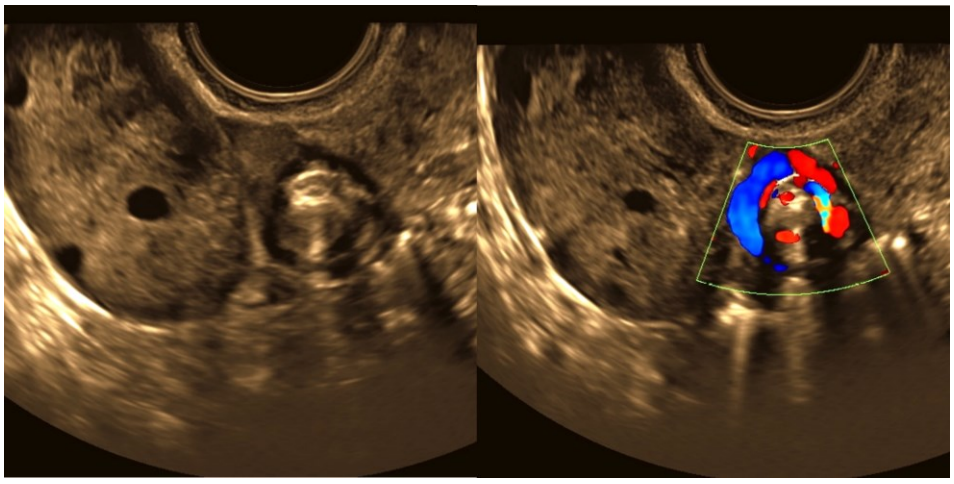

Figure 12.42. The "whirlpool sign" on color Doppler and grayscale.
Twisted vascular pedicle seen in ovarian torsion

Acute Pelvic Inflammatory Disease

Pelvic Inflammatory Disease (PID) refers to a spectrum of inflammation involving the female upper genital tract. It is typically an ascending infection that begins as a cervicitis, progresses to endometritis, and ultimately involves fallopian (salpingitis) tubes and/or ovaries (oophoritis), and the pelvic peritoneum, often simultaneously both realizing. Complications such as tubo-ovarian complex or abscess and/or pelvic peritonitis occur only approximately 5% of patients with PID. Clinical findings have shown some predictive value, although not specific, include pelvic pain, adnexal tenderness, purulent vaginal discharge, dyspareunia, abnormal uterine bleeding, pollakiuria, dysuria or associations and fever. However, it can often start in asymptomatic form. There is no sensitive and specific anamnestic note, instrumental exam, or lab test for the diagnosis of acute PID.

Pelvic US is frequently normal in the early stages of PID. As disease worsens several sonographic features can be identified. In early stage, a thickened edematous hyperemic (increased Color Doppler flow) tube can be visualized, even without intraluminal fluid. With progressive inflammation and distal occlusion of the lumen, the tube fills with either anechoic or low-level echoes purulent content, debris or hemorrhage (fig. 12.43a). Thickened wall, incomplete septa and thickening of endo-salpingeal folds giving the "cog wheel" appearance (fig. 12.43b).

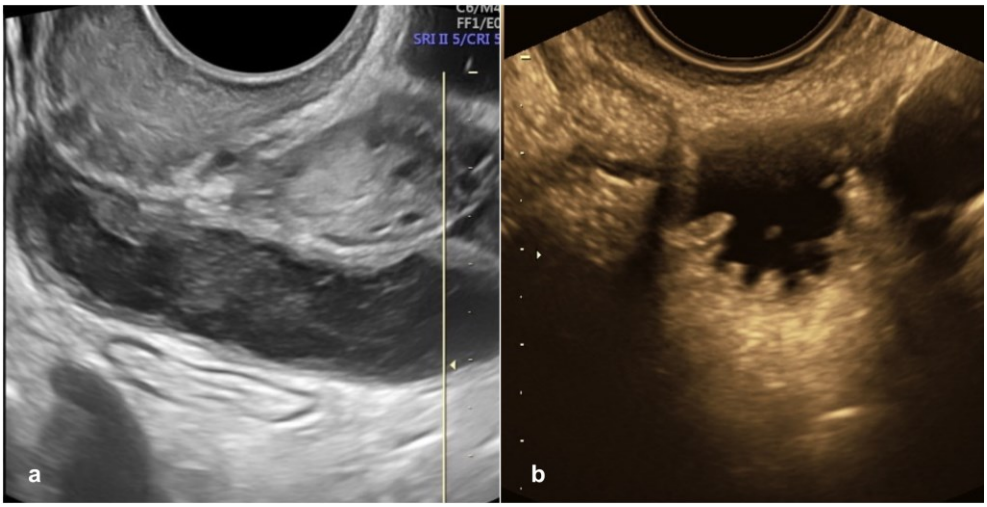

Figure 12.43. a) Pyosalpinx. The Fallopian tube filled with low-level echoes purulent content; b) The "cog wheel" appearance due to thickened wall and thickening of endo-salpingeal folds

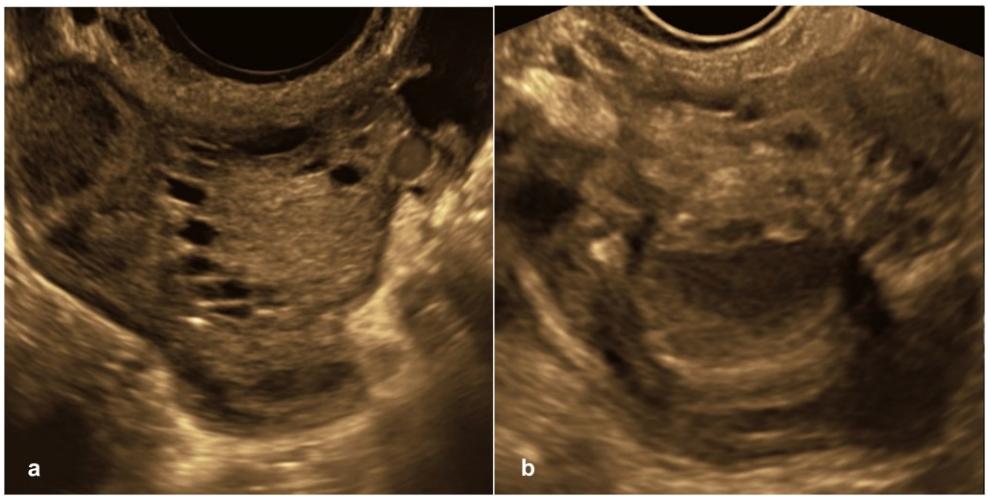

Figure 12.44. a) Tubo-ovarian complex. The ovary and tube are recognized but the ovaries cannot be separated from tube; b) Tubo-ovarian abscess, complete breakdown of the tubal and ovarian architecture, both are no longer identified

With progression of disease, a complex inflammatory adnexal mass including the tube and adjacent ovary is formed. Thick walled, multilocular/unilocular, complex cystic adnexal mass, ill-defined borders. Extent of ovarian involvement is defined as: tubo-ovarian complex, when ovary and tube are recognized, but cannot be separated (fig. 12.44a), and tubo-ovarian abscess, resulting in complete breakdown of the tubal and ovarian architecture so that separate structures are no longer identified (fig. 12.44b).

Pelvic Endometriosis

Endometriosis is a common cause of abdominal pain. Endometriosis can be defined as the presence of endometrial glands and stroma outside the uterus in ectopic locations, primarily the uterus and ovaries, pelvic peritoneum, fallopian tubes, vagina, cervix, uterosacral ligaments, rectosigmoid and rectovaginal septum, bladder, but also in extrapelvic sites. Ectopic tissues respond to normal cyclic hormonal stimulation, resulting in microscopic internal bleeding, with subsequent inflammatory response, neovascularization, and fibrosis formation. Endometriosis affects 6–10% of women of childbearing age, with a prevalence of 38% in infertile women and 71–87% of women with chronic pelvic pain. In women with acute pelvic pain is reported to be greater than 33%.

Superficial endometriosis is defined when limited to the peritoneum; deep endometriosis - defined as peritoneal invasion greater than 5 mm and infiltrating the retroperitoneal space or viscera (rectum, vagina, uterus, bladder, ureter, small intestine, etc.) and ovarian endometrioma (endometrial cyst). The presentation of endometriosis is highly variable and ranges from debilitating pelvic pain and infertility to no symptoms: pain can include dysmenorrhea,

dyspareunia, and dyschezia, depending on the site involved. There is an overlap of symptoms with many conditions, both gynecological and not.

The US appearance is defined by disease site. Classically ovarian endometriomas appear on US as thin-walled unilocular cystic masses that contain diffuse, low-level echoes ("ground glass" appearance) (fig. 12.35). No Doppler flow. Rarely could be multilocular. Echogenic intracystic nodules (show no flow) representing adherent blood clot/hemosiderin. Cysts are commonly covered by fibrous adhesions, which can result in fixation to adjacent structures. This is the reason why the shape is not rounded and has reduced mobility. Can be solitary/multiple lesions in the same ovary or bilateral 1/3 to 1/2 cases.

When endometriotic lesions are located in tissues containing smooth muscle or connective tissue, the predominant pattern is that of a hypovascular hypoechoic nodules or thickening of the wall of the uterosacral ligaments (fig. 12.45a), rectosigmoid (fig. 12.45b), vaginal fornix, rectovaginal septum and bladder (fig. 12.46), with invasion into the intestinal serosa and muscularis, and in the case of the urinary bladder also into the submucosa and bladder mucosa. Due to fibrous adhesions, the mobility of the affected structures is reduced, with a negative "sliding sign" in the vesico-uterine recess or Douglas and defined as obliterated. Also, ureter dilatation due to stricture (extrinsic compression/intrinsic infiltration) caused by endometriosis can be detected. Lesions may be isolated or may be part of a larger nodule that extends from neighboring structures and tissues. Rectosigmoid endometriotic nodule may be associated with a second intestinal lesion in half of cases, multifocal (multiple lesions affecting the same segment) or multicentric (multiple lesions affecting several intestinal segments) involvement.

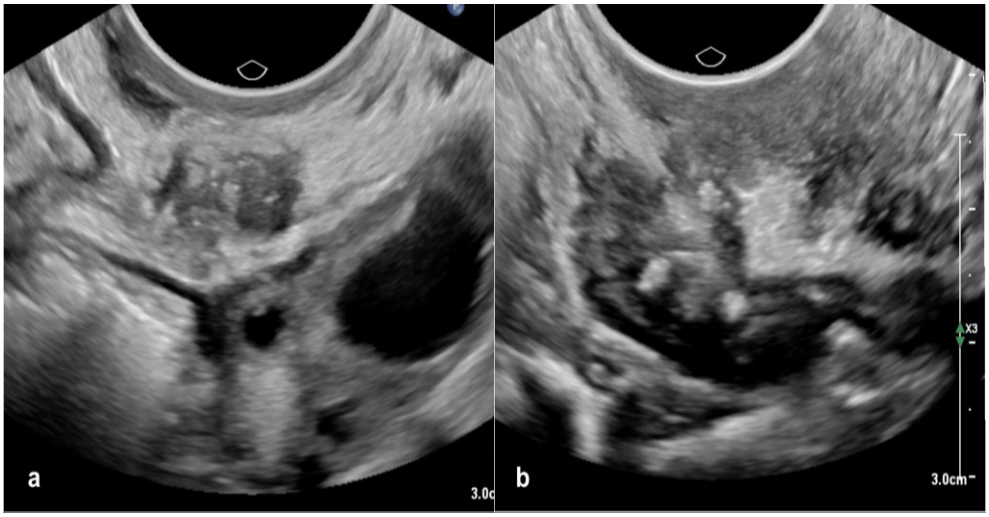

Figure 12.45. a) Hypoechoic endometriotic nodule of the uterosacral ligament;
b) Hypoechoic endometriotic nodule in the rectosigmoid serosa and muscularis

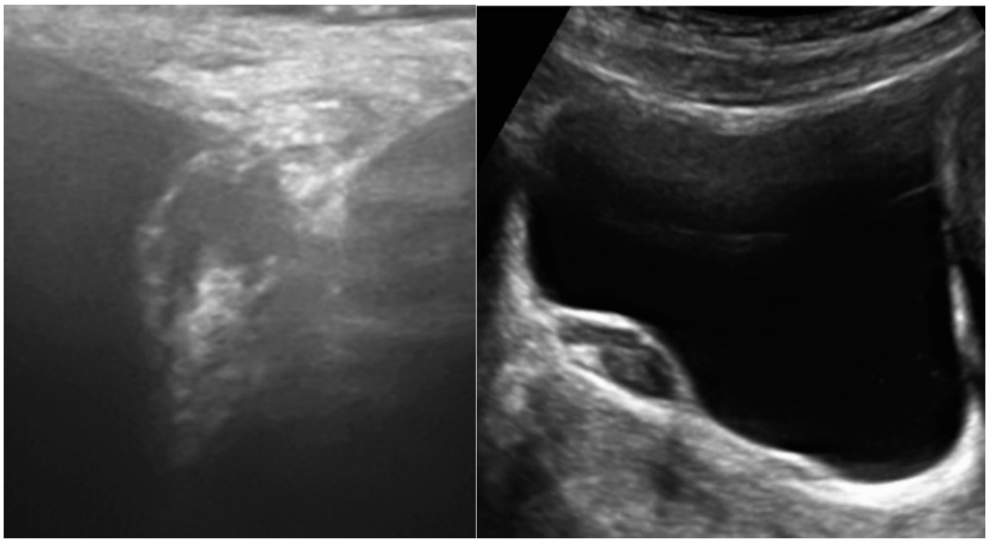

Figure 12.46. Hypoechoic endometriotic nodule in the bladder muscularis, submucosa and mucosa

Uterine leiomyomas

Fibroids (leiomyomas) are composed of smooth muscle cells and connective tissue in densely packed whorls. They are the most common benign gynecological pathology, with an incidence of between 20 and 77% in reproductive age women, but the real incidence is not known as most tumors are asymptomatic. Size and location could lead to complications. Submucosal leiomyoma sometimes associated with abnormal uterine bleeding, others with pelvic pain, feeling of compression, and urinary symptoms. Leiomyoma with infarction commonly occurs with impaired blood supply.

A uterine myoma is seen typically on US as a well-defined round lesion within the myometrium or attached to it, often showing shadows at the edge of the lesion and/or internal fan-shaped shadowing. The echogenicity varies and some hyperechogenicity may be present internally. On color/power Doppler imaging circular pattern is often visible. Submucosal leiomyoma is usually of identical or lower echogenicity than the myometrium, has broad base and elevates the endometrium depending on the degree of protrusion, extends into the myometrium, often shadowing (fig. 12.3-12.7).

Myomas may undergo degeneration, which may be spontaneous (post-abortum, may occur in pregnancy, postpartum, trauma, uterine infection, postmenopausal atrophy) or iatrogenic, because of induced infarction following uterine artery embolization. Colliquative necrosis occurs more frequently during pregnancy due to the rapid growth of the fibroid (hormonally dependent), which makes the blood supply insufficient. The diagnosis becomes suspected based on clinical and US findings. Hemorrhage and edema in these fibroids may give rise to tumors of heterogeneous pattern, having irregular non-vascularized hypoechoic or anechoic cystic areas, along with peripheral vascularization (pseudo-capsule) and pain, especially in lesions larger than 5 cm. There is usually no internal vascularity, or a few disparate vessels are observed (fig. 12.47). Serosal

pedunculated leiomyomas may undergo torsion and necrosis, which results in acute pelvic pain. Color Doppler may help to identify a vascular pedicle (the site of myometrial attachment). For differential, both ovaries should be identifiable separate from the mass.

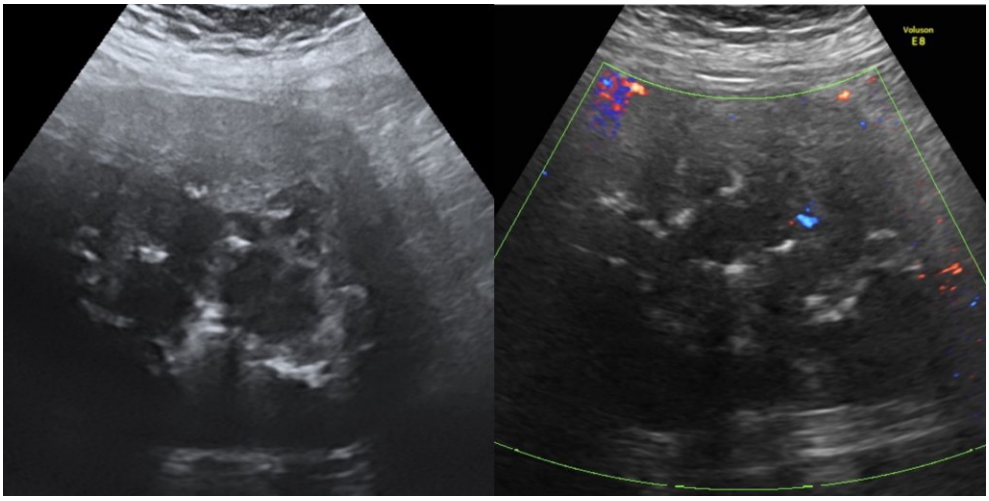

Figure 12.47. Uterine myoma necrosis, heterogeneous mass with hypoechoic/anechoic cystic areas secondary to necrosis and no color Doppler flow

Adenomyosis

Defined by the presence of ectopic endometrial glands and stroma within the myometrium with hypertrophic and hyperplastic reaction in the surrounding myometrial tissue. Common etiological factors are uterine trauma from childbirth, surgery/instrumentation, dilatation and curettage, chronic endometritis, hyperestrogenic state. Occurs in about 30% of the general female population and in up to 70% of hysterectomy specimens. Clinical findings are essential for the diagnosis. Symptoms related to adenomyosis include, pelvic pain, dysmenorrhea, menorrhagia, metrorrhagia, dyspareunia, infertility. There are two main types of adenomyosis. The most common one is diffuse adenomyosis. Less common are focal/circumscribed patterns.

Ultrasound features considered typical of diffuse adenomyosis: globular uterine enlargement without well-defined mass, asymmetrical uterine wall thickening, most frequent the posterior wall, small cysts and anechoic spaces in the myometrium, hyperechoic islands, fan-shaped shadowing, linear striations of attenuation throughout lesion (rain shower appearance), echogenic subendometrial lines and buds, translesional vascularity, irregular JZ and interrupted JZ (fig. 12.48). Adenomyosis is defined as focal if >25% of circumference of lesion is surrounded by normal myometrium, provided that <25% of myometrium of corpus uteri is involved.

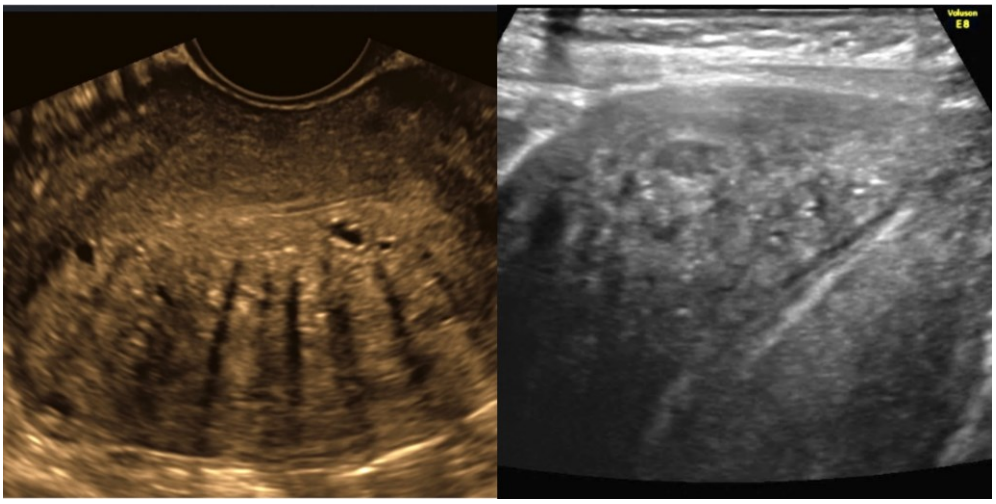

Figure 12.48. Uterine adenomyosis. Asymmetrical uterine wall thickening, small myometrial cysts, hyperechoic islands, fan-shaped shadows/linear translesional striations, irregular and interrupted endo-myometrial junction

Vaginal Bleeding

Abnormal uterine bleeding (AUB) includes non-gestational bleeding in women of reproductive age, defined as bleeding from the uterine corpus that is abnormal in duration, volume, frequency and/or regularity, as well as postmenopausal bleeding, defined as any bleeding after menopause in women not on hormonal therapy, and as unscheduled or heavy bleeding in women on hormonal therapy. Vaginal bleeding is a condition that may be related to many etiologies, both functional and structural. It can take place during menstrual flow, as an increased blood loss, or between two menstrual flows. These situations are, respectively, called menorrhagia and metrorrhagia. Munro in 2011, then updated in 2018, proposed a classification system for AUB in non-gravid women of reproductive age that was officially approved by FIGO. This system is called "PALM-COEIN," as an acronym of the nine categories of causes of vaginal bleeding: Polyp, Adenomyosis, Leiomyoma, Malignancy and hyperplasia, Coagulopathy, Ovulatory dysfunction, Endometrial, Iatrogenic, Not yet classified.

In women with AUB the main goal is endometrial thickness measurements for the exclusion of malignancy and other pathologies, as thin endometrium being associated with a low risk of malignancy and a thick endometrium increasing the risk. However, the value of endometrial-thickness measurements is limited mainly to postmenopausal women. In women of reproductive age, the normal endometrium grows rapidly after menstruation, hence endometrial-thickness measurements are associated with a low specificity for endometrial pathology. Moreover, irrespective of age, a thick endometrium is associated not only with cancer but also, and more frequently, with benign pathology such as endometrial polyps or hyperplasia without atypia.

Polyps: both endometrial and endocervical. Benign proliferation of endometrial glands and stroma lined with epithelium. Prevalence 24% general population, frequently after 40 years,

showing slow growth. Usually are asymptomatic but can also bleed. Polyps are usually benign, only a small minority may have atypical or malignant features. On US appear as echogenic (superior to myometrium) ovoid lesion in the endometrial cavity, without extension into the myometrium (fig. 12.49). Commonly having a bright edge - echogenic halo (interface between lesion and endometrium). May contain cystic areas. On color-Doppler imaging, when detectable, the common vessel pattern is a single vessel with or without branching (fig. 12.50).

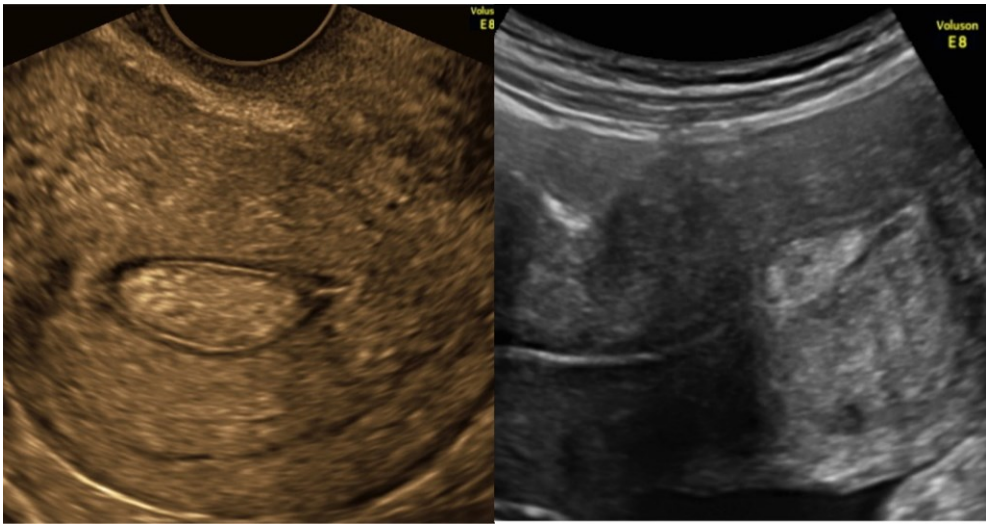

Figure 12.49. Endometrial polyp. Echogenic ovoid lesion in the endometrial cavity having a bright edge

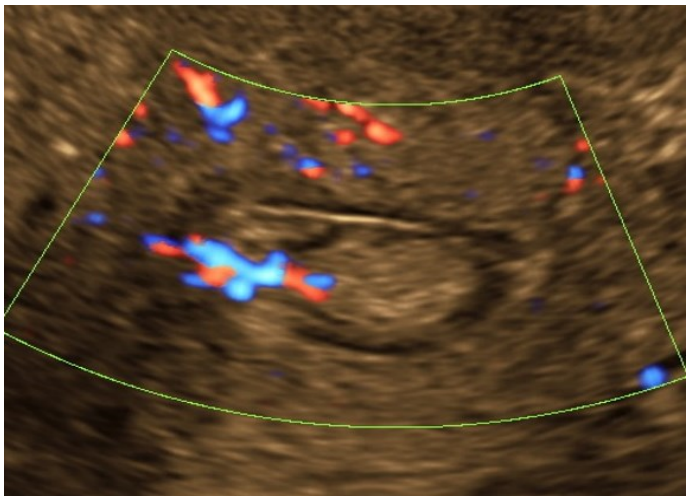

Figure 12.50. Endometrial polyp. Single vessel without branching

Endometrial hyperplasia. Excessive proliferation of endometrial glands with an increased glandular/stromal ratio and cystic glandular dilation due to hyperestrogenia. Moderate, rarely severe or even absent bleeding. US appearance - diffuse (rarely segmental) thickening of the

median echo. In menopause: without hormone replacement therapy greater than 5.0 mm and with hormone replacement therapy greater than 8.0 mm. During the reproductive period the endometrial thickness - low specificity for endometrial pathology. The endometrial hyperplasia usually on US appears as uniform hyperechogenic, non-uniform heterogeneous echogenicity with or without regular cysts. The midline was usually undefined, particularly after menopause, and the endometrial–myometrial junction was usually regular. When color-Doppler signals were present, the most common vessel morphology was multiple vessels with multifocal origin or a scattered pattern (fig. 12.51).

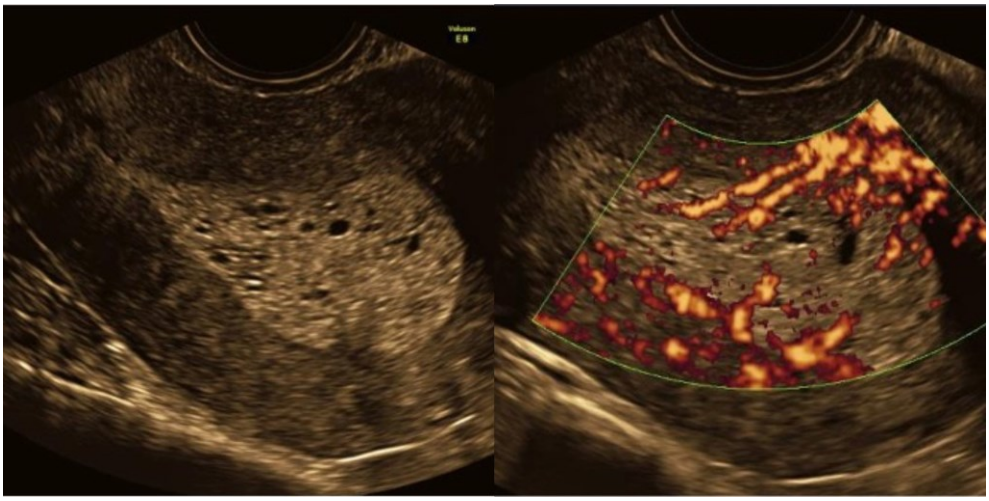

Figure 12.51. Endometrial hyperplasia. Multiple anechoic regular cysts, undefined midline, regular endometrial-myometrial junction. Multiple vessels with multifocal origin

Malignancy and hyperplasia: atypical hyperplasia and malignancy are quite uncommon but are a significant cause of vaginal bleeding that requires further investigation. The thicker endometrium, the higher risk. A median echo $\leq$ 4.0 mm in postmenopausal bleeding virtually excludes endometrial cancer. The risk also depends on endometrial US morphology and color/power Doppler vascularity. In endometrial cancer the endometrium usually is thickened. However, endometrial thickness could not be always measured reliably. In the vast majority the endometrial midline could not be defined and the endometrial–myometrial junction could be interrupted due to invasion into the myometrium. Echogenicity is non-uniform heterogeneous without cysts or heterogeneous with irregular cysts or has the appearance of a pseudosolid mass. Strong vascularity, with high color score of 3 or 4 is common, if color-Doppler detectable and the most common vessel pattern is multiple vessels of focal or multifocal origin (fig. 12.52).

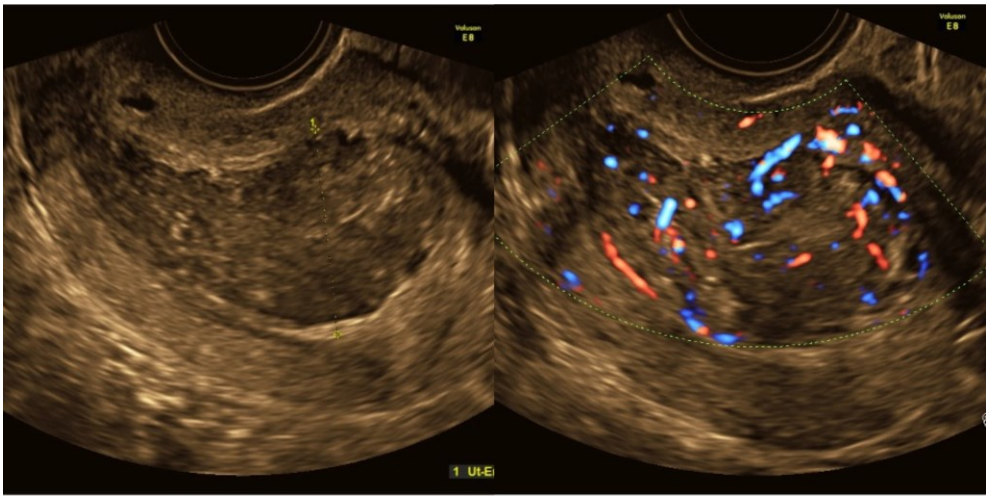

Figure 12.52. Endometrial cancer. Appearance of a pseudosolid mass.
Multiple vessels of focal or multifocal origin pattern

Pelvic ultrasound finding in extra-gynecologic etiologies

The value of TVS in gynecologic assessment is well known. However, pelvic sonography should be not limited only to evaluation of reproductive organs. The examiner must look beyond the expected gynecologic causes of pain to those related to adjacent structures imaged during the scan. Other diagnoses can be missed if only gynecologic etiologies are considered. TVS allows excellent visualization of the ureters, bladder, urethra, rectosigmoid, in some cases the appendix and small bowel, pelvic vessels and other adnexal structures. Familiarity with the normal appearance of imaged pelvic structures, as well as with the appearance of the common causes of acute pelvic pain may prove critical in the emergent setting.

Selective references

1. Amirbekian S, Hooley RJ. Ultrasound evaluation of pelvic pain. Radiol Clin North Am 2014; 52:1215–1235.
2. Van Den Bosch T, Dueholm M, Leone F, Valentin L, Rasmussen C, Votino A, Van Choubroeck D, Landolfo L, A. Installe A, Guerriero S, Exacoustos C, Gordts S, Benacerraf B, D'Hooghe T, de Moor B, Brolmann H, Goldstein S, Epstein E, Bourne T and Timmerman D. Terms, definitions and measurements to describe sonographic features of myometrium and uterine masses: a consensus opinion from the Morphological Uterus Sonographic Assessment (MUSA) group. Ultrasound Obstet Gynecol 2015; 46: 284–298, DOI: 10.1002/uog.14806
3. Munro MG, Critchley HOD, Broder MS, Fraser IS. FIGO classification system (PALM-COEIN) for causes of abnormal uterine bleeding in nongravid women of reproductive age. Int J Gynecol Obstet. 2011;113(1):3–13.

4. Van Den Bosch T, Verbakel J, Valentin L, Wynants L, de Cock B, Pascual M, Leone F, Sladkevicius P, Alcazar J, Votino A, Fruscio R, Lanzani C, van Holsbeke C, Rossi A, Jokubkiene L, Kulda M, Jakab A, Domali E, Epstein E, van Pachterbeke C, Bourne T, van Calster B and Timmerman D. Typical ultrasound features of various endometrial pathologies described using International Endometrial Tumor Analysis (IETA) terminology in women with abnormal uterine bleeding. Ultrasound Obstet Gynecol 2021; 57: 164–172, DOI: 10.1002/uog.22109
5. Rochelle F. Andreotti, Sara M. Harvey. Sonographic Evaluation of Acute Pelvic Pain. J Ultrasound Med 2012; 31:1713–1718
6. Diagnosis and management of ectopic pregnancy. Green□top guideline no. 21. 2016;123(13):e15–55. https://doi.org/10.1111/1471-0528.14189. First published: 3 Nov 2016
7. Timmerman D, Valentin L, Bourne T, Collins W, Verrelst H, Vergote I. Terms, definitions and measurements to describe the sonographic features of adnexal tumors: a consensus opinion from the International Ovarian Tumor Analysis (IOTA) Group. Ultrasound Obstet Gynecol. 2000 Oct;16(5):500-5. doi: 10.1046/j.1469-0705.2000.00287.x.
8. Timmerman D, Planchamp F, Bourne T, Landolfo C, du Bois A, Chiva L, Cibula D, Concin N, Fischerova D, Froyman W, Gallardo G, Lemley B, Loft A, Mereu L, Morice P, Querleu D, Testa AC, Vergote I, Vandecaveye V, Scambia G, Fotopoulou C. ESGO/ISUOG/IOTA/ESGE Consensus Statement on preoperative diagnosis of ovarian tumors. Ultrasound Obstet Gynecol 2021. DOI:10.1002/uog.23635
9. Guerriero S, Condous G, van den Bosch T, Valentin L, Leone FPG, Van Schoubroeck D, et al. Systematic approach to sonographic evaluation of the pelvis in women with suspected endometriosis, including terms, definitions and measurements: a consensus opinion from the International Deep Endometriosis Analysis (IDEA) group. Ultrasound Obstet Gynecol 2016; 48(3): 318–32.
10. Van Den Bosh T, de Bbruijn A, DE Leeuw R, Dueholm M, Exacoustos C, Valentin L, Bourne T, Timmerman D and Huirne J. Sonographic classification and reporting system for diagnosing adenomyosis. Ultrasound Obstet Gynecol 2019; 53: 576–582, DOI: 10.1002/uog.19096

13. HOW TO USE ULTRASOUND IN BREAST PATHOLOGY?

Boris Brkljačić, Dana Stoian
WFUMB Centers of Education Zagreb, Croatia and Timișoara, Romania

Introduction

For many years, mammography has been the only imaging modality used to evaluate the breast. However, ultrasound has been for decades well established in breast imaging, as well as MRI. Thus, modern breast imaging is multimodal and relies on the use of mammography (including digital tomosynthesis and contrast-enhanced mammography), high-resolution ultrasound and contrast-enhanced MRI of the breast. In order to establish an accurate diagnosis a combination of mammography and ultrasound is usually needed, with the addition of MRI in a growing number of cases. The selection of the imaging method depends on the clinical presentation, age, breast density and risk assessment.

State-of-the art ultrasound technology and high-frequency linear transducers offer high resolution and excellent evaluation of acoustic features of breast lesions, but in most clinical scenarios ultrasound still needs to be combined with other imaging modalities. Therefore, breast imagers need to be familiar with the advantages and the shortcomings of each imaging modality and to use established imaging referral guidelines to select the appropriate modality in a specific clinical setting.

Ultrasound is harmless for the patient and staff, relatively cheap and quite accessible, It is a user-friendly technique, well tolerated by patients, noninvasive, independent of menstrual cycle status or timing, much better than mammography which requires often painful compression of the breast. Ultrasound does not expose patients to ionizing radiation and can be used at any age and repeated often, whenever indicated. As a real time modality, it provides superb guidance for aspirations, core and vacuum-assisted biopsies, clip placements into lesions prior to the neoadjuvant chemotherapy, preoperative wire-markings, as well as for the minimally invasive therapeutic procedures like various types of ablations. Visualization of needles and accurate positioning is possible using the real-time features of ultrasound, and it is a major advantage of the modality. As the primary imaging modality, ultrasound is used in young women, under the age of 40, while in women over 40 mammography is performed first, followed by ultrasound for the work-up of mammographic lesions or secondary assessment of dense breasts. Ultrasound is also often used for second-look targeted examinations of alterations observed at contrast-enhanced MRI, either of masses, or in cases of the non-mass enhancement. Ultrasound is also the modality of choice to assess axillary lymph nodes and obtain tissue specimens from such nodes. B-mode or gray-scale ultrasound imaging is the most important sonographic tool for evaluating breast changes. However, US is inefficient in large breasts and in those with significant percentage of adipose tissue, and US does not allow the morphological characterization of calcifications.

Advanced software like compound and harmonic imaging are routinely used in breast ultrasound, as well as color Doppler and sonoelastography. A combination of grayscale, color/power Doppler and strain and/or shear-wave elastography is a comprising multiparametric ultrasound evaluation of the breast which has become standard for the modern breast sonography. Automated whole- breast ultrasound (ABUS) has been on the market for a decade, the examination is performed by radiographers/sonographers and images are interpreted on the workstations, just as in CT and MRI investigations.

A breast imager has to be able to select and use the appropriate ultrasound equipment and transducer for the evaluation of the breast, understanding sonographic anatomy and the features of various breast pathologies. We should never forget the dangers of "satisfaction of search", that is, if benign lesions like cysts and fibroadenomas are found in the breast, it does not necessarily mean that cancer is not present in other parts of the breast.

Ultrasound scanners and techniques of sonographic examination of the breast

Ultrasound is a modality that is significantly operator-dependent, more so than mammography and MRI, resulting in considerable inter-observer variability. The correct execution of examinations using hand-held ultrasonography is essential and needs education and substantial expertise, as the sonographic characteristics of benign and malignant tumors frequently overlap. All regions of the breast must be thoroughly inspected to ensure that no alterations are overlooked. The quality of the ultrasound scanner is the essential aspect of performing a proper sonographic examination of the breast. Ideally, premium ultrasonic scanners and high-frequency linear transducers, typically operating within a frequency range of up to 18 MHz, should be employed for breast imaging. It is widely recognized that a high frequency yields superior resolution, yet a diminished penetration of the ultrasonic beam. Consequently, in cases of enormous breasts, one should reduce the frequency or employ lower-frequency linear transducers to effectively photograph the posterior regions of the breast. Imaging of the prepectoral regions is crucial, as this area is frequently excluded from the mammographic field of view. The apertures of hand-held transducers typically measure between 4.5 and 6.5 cm in width, equal to their field of view, but ABUS use far longer transducers. Gray scale or brightness (B)-mode should consistently employ compound imaging, previously referred to as sono-CT upon its market introduction in 1998. Compound ultrasound employs numerous picture slices acquired from various insonation angles inside the imaging plane to generate the final image, hence offering a superior evaluation of the interior echotexture of the lesion. Harmonic imaging employs harmonic frequencies to produce images, while suppressing the original basic tissue echo frequencies through phase inversion between successive transmitted pulses, resulting in enhanced resolution and the potential elimination of extraneous echoes and noise. The determination regarding the management of the breast lesion observable on ultrasonography is predominantly contingent upon gray-scale characteristics. Nonetheless, the assessment of stiffness using sonoelastography has been established over the past fifteen years. Color Doppler

has been utilized in clinical practice to assess blood flow in both big and small arteries and veins, as well as within different organs. Nowadays, sophisticated scanners with high color sensitivity for slow flow are effective in evaluating internal vessels in breast lesions; thus, the incorporation of color Doppler is beneficial for determining the vascularization of the lesion and identifying the types of vessels present. Nonetheless, we cannot depend on the assessment of resistance indices or other color Doppler characteristics to accurately distinguish between benign and malignant tumors.

The sonographic examination of the breast is initially conducted with the patient in the supine position, followed by the left lateral oblique position for the outer aspect of the right breast and the right lateral oblique position for the outer aspect of the left breast. We urge that both arms of the patient be extended above the head to flatten the breast tissue against the thoracic wall. In unusual circumstances, patients may be assessed in a sitting position, as some individuals are unable to recline. To assess the entire breast, we recommend employing a radial scanning approach, followed by scanning in parallel parasagittal planes, from lateral to medial and top to bottom and vice versa. The radial approach involves positioning the transducer at the nipple and subsequently extending it outwards to illustrate the breast lobes. Subsequently, both axillae must be assessed for diseased lymph nodes and other atypical alterations. Proper method necessitates meticulous focusing on breast lesions, utilization of time-gain compensation, appropriate adjustment of gain, and adequate compression of the breast tissue. The real-time capability of ultrasound is optimal for tracking the needle trajectory in the breast parenchyma to guarantee accurate positioning during biopsies, ablations, and clip placements.

Indication for breast ultrasound

Currently, breast ultrasound are recommended for the following conditions: the evaluation and characterization of palpable masses and other breast related tissues, the additional evaluation of abnormalities detected on mammography, MRI or other imagining modalities, the initial evaluation of palpable masses in patients under 30 years of age, not at high risk for breast cancer, the evaluation of symptoms in lactating and pregnant women, or breast implant patients.

Additional US offers guidance for biopsy, or other interventional procedures, (5) in breasts or in axillae. US also enables supplemental screening in occult cancers, especially in heterogenous breasts, or in high-risk categories patients, where MRI cannot be performed.

In the presence of significant edema or pain, mammography is not possible, as seen in mastitis cases and shown in Fig. 13.1.

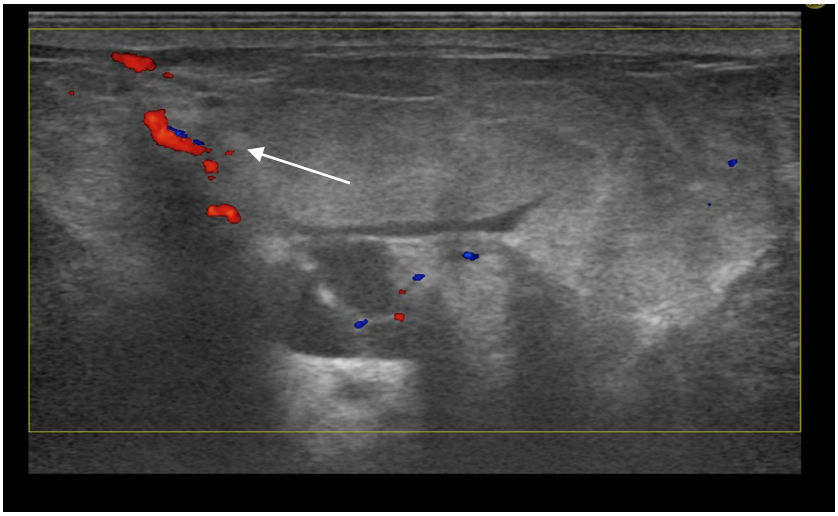

Fig. 13.1: Acute mastitis image

Palpable masses in cases with high density breast on mammography (Fig. 13.2a.) can be distinguished on US (Fig. 13.2.b), as well as fatty palpable masses (Fig. 13.3b) seen in fatty breasts (Fig. 13.3a).

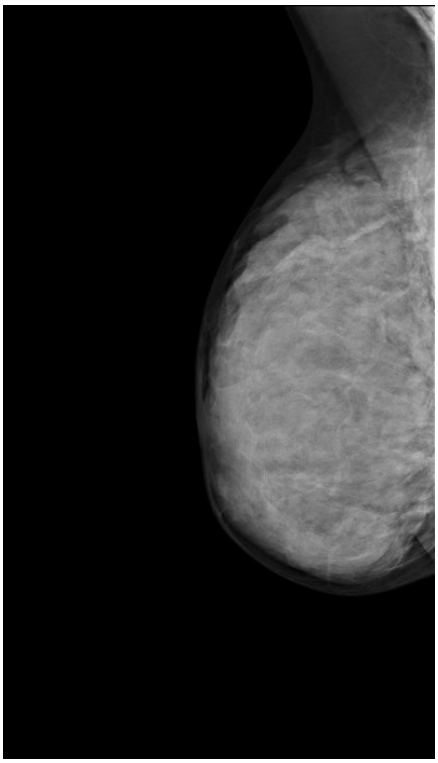

Fig. 13.2a: Mammography MLO view right breast – ACR density D (palpable mass not visible on mammography because of high density)

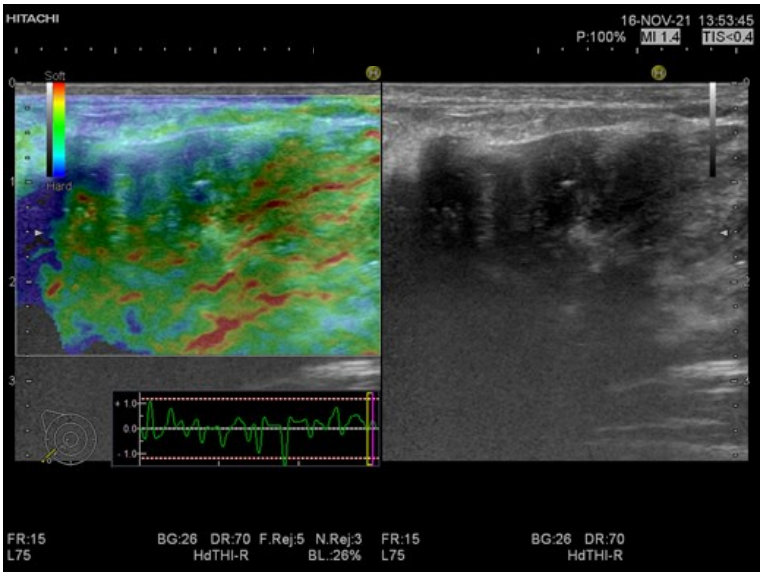

Fig. 13.2b: Palpable mass not visible on mammography because of high density but visible on US - confirmed sclerosant mastosis

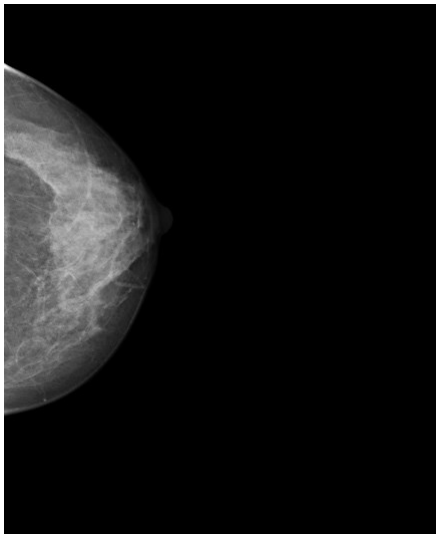

Fig. 13.3a. Mammography CC view inhomogeneous fatty breast

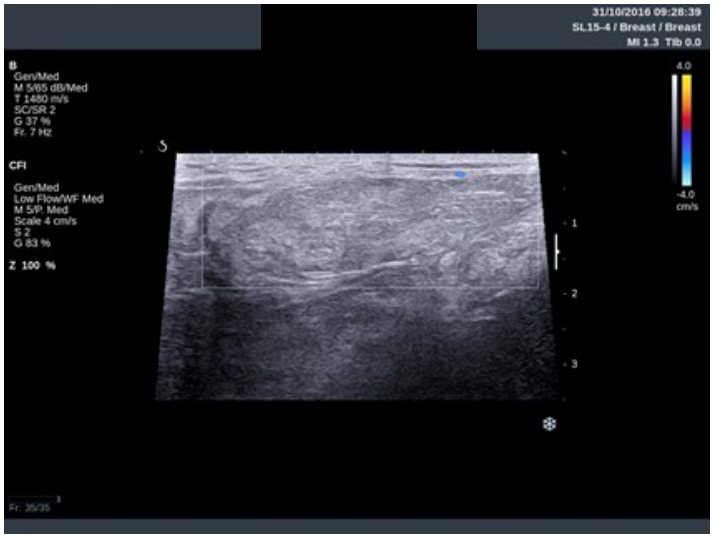

Fig. 13.3b. US evaluation – lipoma present in the preglandular fatty tissue layer.

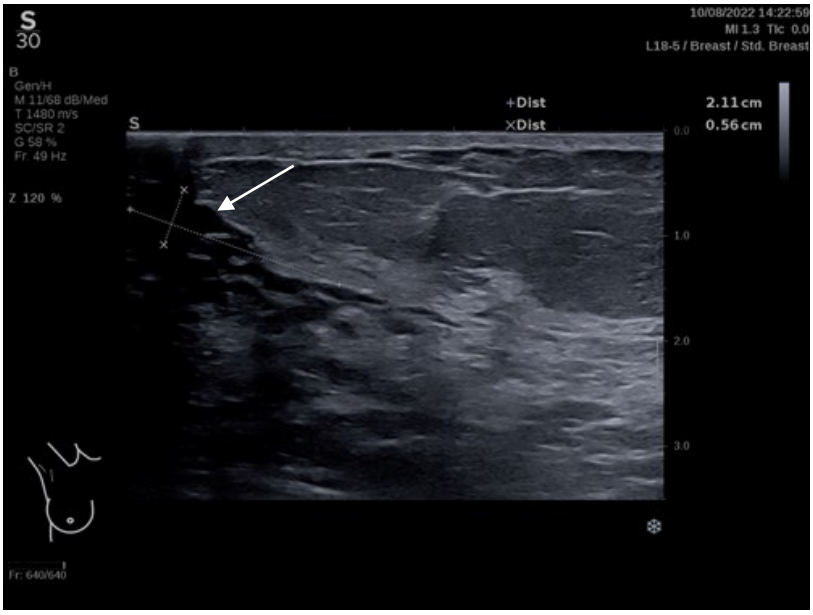

Fig. 13.4: Nipple discharge due to small lobar intraductal changes

Implant complications, both early such as hematoma (Fig. 13.5), infections (Fig. 13.6), or late complications: implant ruptures (Fig. 13.7), siliconomas (Fig. 13.8) or intracapsular seroma (Fig. 13.9) are better evaluated by ultrasound.

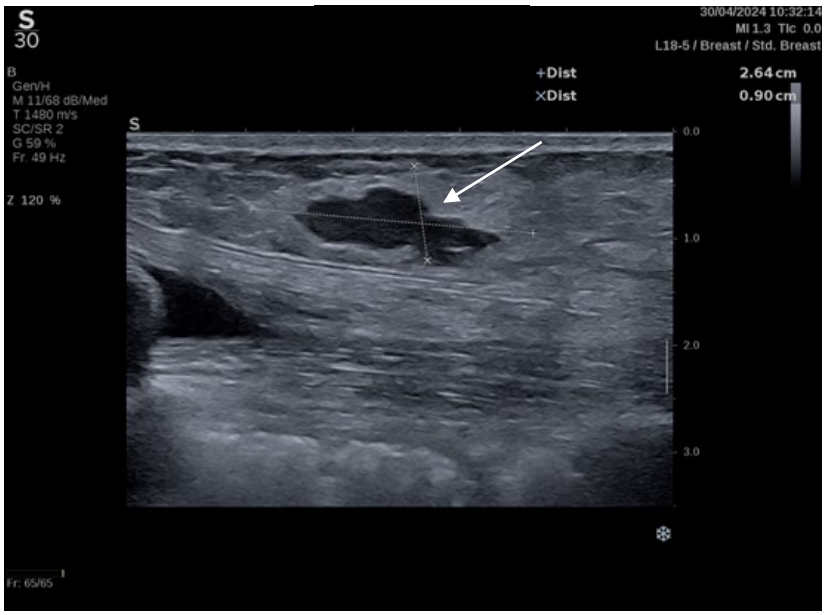

Fig. 13.5: Hematoma

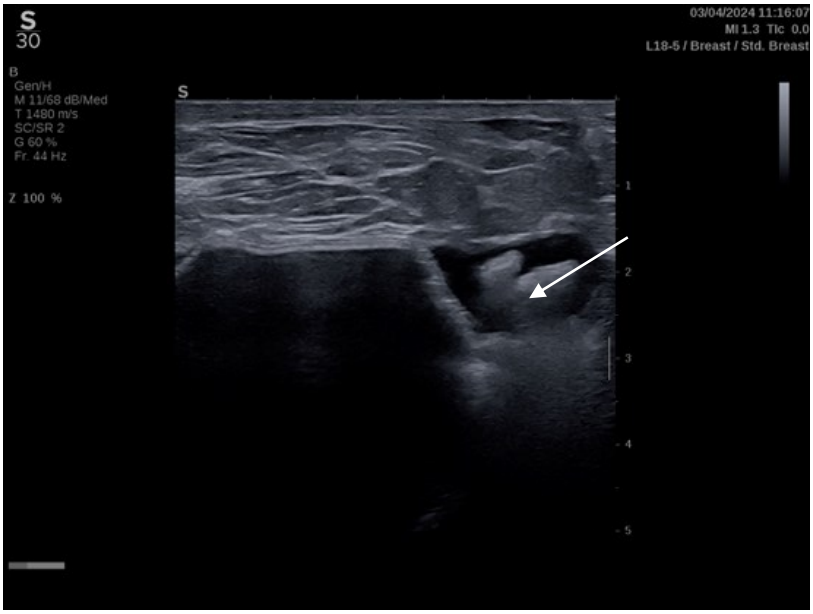

Fig. 13.6: Infection pathology report proven with exclusion of anaplastic large cell lymphoma

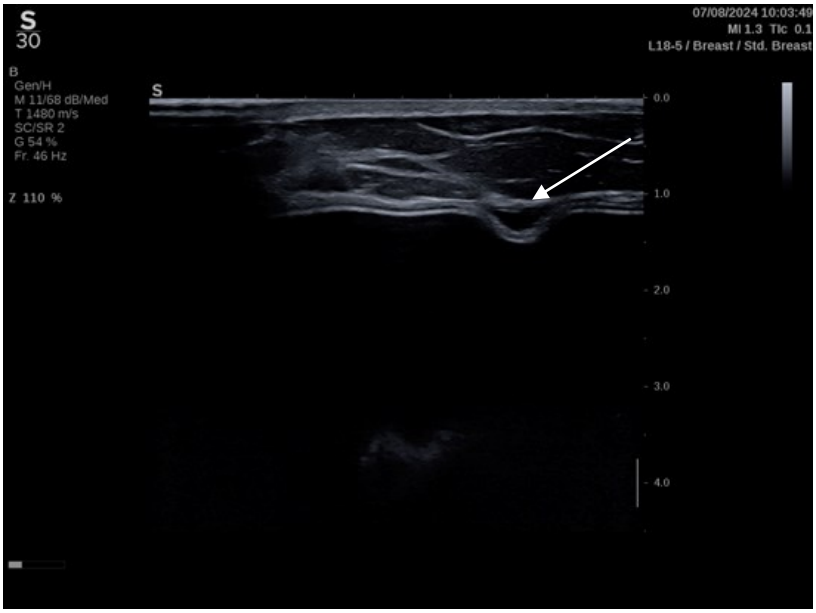

Fig. 13.7: Intracapsular seroma - thin fluid layer between implant and capsule

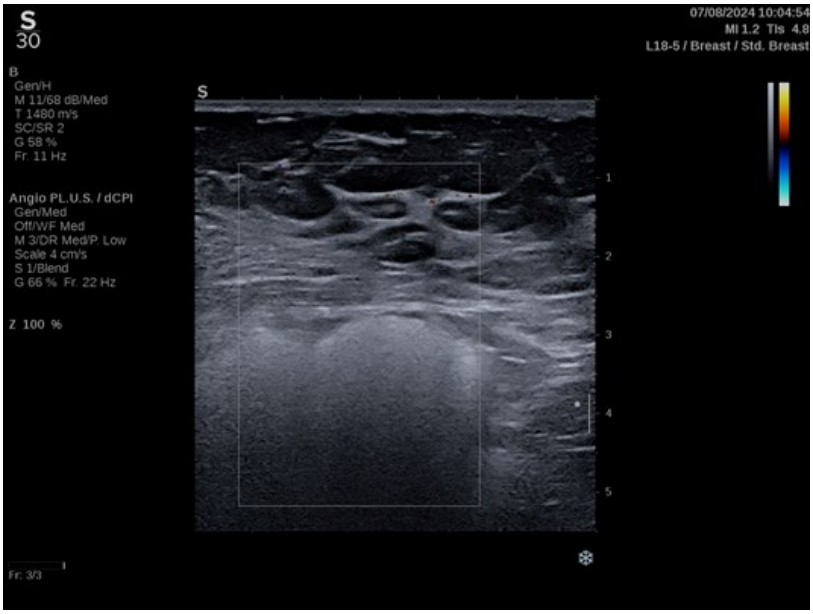

Fig. 13.8: Siliconomas hyperechoic inert masses with posterior attenuation

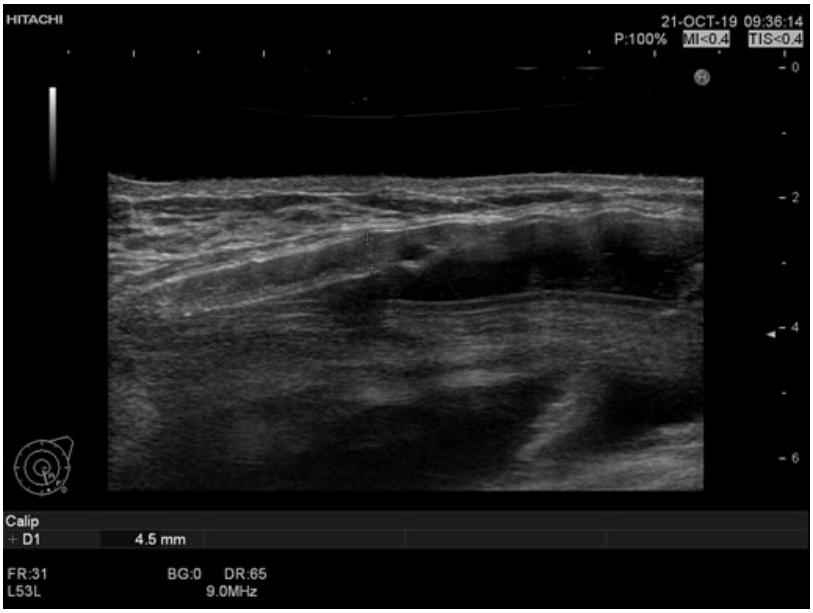

Fig. 13.9: Implant rupture with leakage of the implant content between the layers of the implant

Sonographic anatomy of the normal breast

The adult female breast comprises parenchyma, milk ducts, adipose tissue, and connective tissue, with the quantity of parenchyma varying significantly among individuals based on age, parity, and genetic factors. Ultrasound assessment of breast morphology indicates histological makeup, and pathological structures need to be differentiated from normal tissue.

Malignant tumors predominantly arise from the ducts and ductal epithelium (ductal malignancies). Approximately 10-12% of invasive malignancies arise from lobules (lobular tumors). Malignancies may arise anywhere within the breast parenchyma; however, they are more frequently identified in the upper outer quadrants, where glandular tissue is prevalent. Parenchyma exhibits hyperecogenicity relative to the adjacent adipose tissue, which appears dark. Cooper ligaments appear as slender echogenic linear structures and constitute the connective tissue that attaches to the skin and prepectoral fascia. It is advisable to assess the breast lobe by lobe, as ultrasonography is a superior modality compared to mammography and MRI for illustrating the lobar architecture of the breast. The breast comprises 15-20 lobes, organized centripetally around the nipple. Employing a radial technique of sonographic scanning facilitates a clear visualization of the lobar anatomy and the dissemination of cancer within a lobe. According to the sick-lobe theory, cancers predominantly spread within a single "sick" lobe in a multicentric manner before potentially extending to adjacent lobes. Ultrasound imaging reveals the skin as a thin, hyperechoic, luminous, double-contoured superficial line, measuring less than 3 mm in thickness. The retro areolar region is typically obscured due to acoustic shadowing from the areolar tissue.

Lymphatic fluid from the breast primarily drains into the axillary lymph nodes, whereas lymph from the lower inner quadrants is directed to the internal mammary lymph nodes. It is

common to observe reactive lymph nodes in the axillae, distinguished by a horizontal orientation, a thin cortex, and a regular, somewhat large echogenic sinus.

When breasts are mostly composed of fatty tissue, nearly all lesions are readily discernible on mammographic evaluation, which is commonly observed in elderly women whose breast parenchyma has undergone involution. Nevertheless, increased breast density correlates with diminished accuracy of mammography in identifying and imaging breast lesions due to the superimposition of lesions over dense fibro glandular tissue. Digital tomosynthesis enhances the accuracy of mammography; nonetheless, supplementary tests remain necessary for dense breast tissue. Ultrasound is widely employed as a supplementary modality for the assessment of mammographically dense breasts, as numerous lesions obscured on mammography are distinctly visualized via ultrasound due to the disparate acoustic impedance between lesions and adjacent parenchyma, leading to varying echogenicity; lesions typically appear hypoechoic, while parenchyma is generally hyperechoic.

The breast undergoes significant alterations throughout pregnancy and lactation; the echogenicity of the tissue diminishes due to edema, fluid retention, lobular hyperplasia, and hyperemia, while the ducts become dilated, particularly during breastfeeding. Postmenopausal women undergoing hormone replacement therapy exhibit a hyperechoic appearance on ultrasound, attributable to the proliferation of breast parenchyma induced by hormonal stimulation.

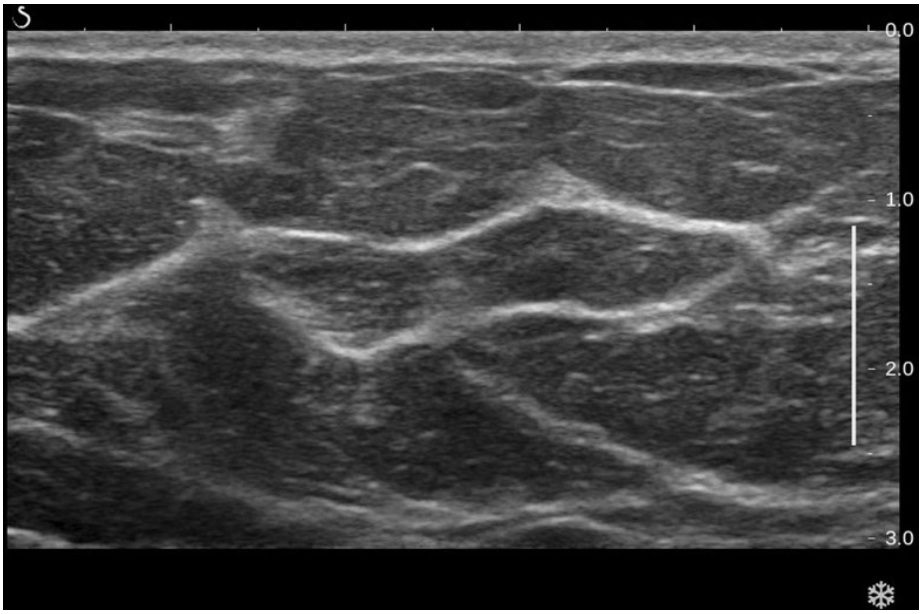

Fig. 13.10: Sonographic image of the fatty breast, with dominantly hypoechoic fat lobules and Cooper ligaments visible as hyperechoic linear bands that traverse the fat.

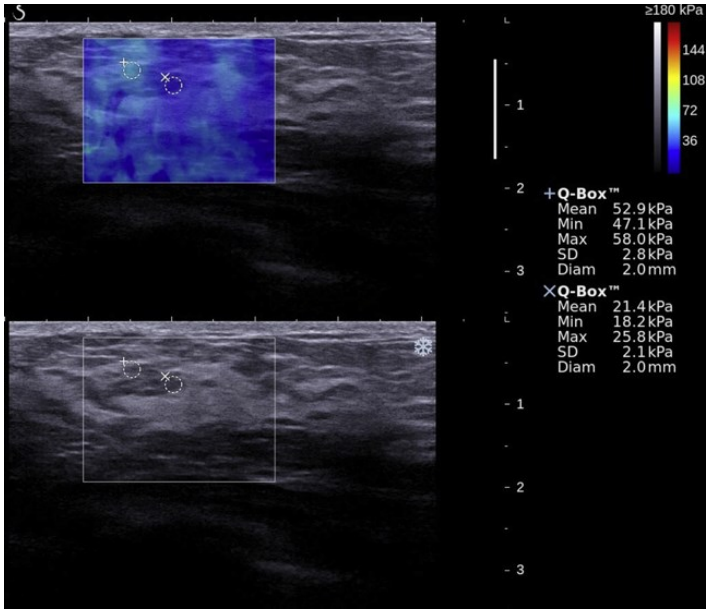

Fig. 13.11: Sonographic images of dense breast, with predominantly hyperechoic glandular parenchyma, with Emax of 58 kPa on shear-wave sonoelastography

Types of breast lesions and structured reporting of breast ultrasound findings

The breast consists of primary lactiferous ducts, minor and terminal ducts, lobes and lobules, fibrous stroma, and adipose tissue. Pathological lesions in the breast arise from those structures. Ductal carcinoma in situ and ductal malignancies arise from ducts, as do papillomas. Ductal enlargement (ductectasia) is relatively prevalent and can be observed using ultrasound. Cysts, fibroadenomas, phyllodes tumors, and lobular tumors arise from lobules. Very rare sarcomas may originate from stroma. Ultrasound is used as a primary imaging modality in women under the age of 40, while in older women mammography is usually performed first. Ultrasound is used to evaluate palpable abnormalities, either after mammography or as the first modality depending on the age, as well as for the evaluation of implants, nipple discharges, to evaluate axillary lymph nodes, and very often as a second-look modality after MRI (8), and as a supplemental screening modality after mammography is performed. Since ultrasound is completely harmless for patients and staff and is a real-time modality, it is the preferred modality for the guidance of fine-needle aspirations, biopsies and other interventional procedures (9), and such procedures are much simpler and faster when performed under US guidance as compared to mammography guided or MR-guided procedures.

The American College of Radiology (ACR) Breast Imaging and Reporting Data System (BIRADS) Lexicon should be used for reporting and classifying breast ultrasound findings. Currently the new edition of BIRADS Lexicon is being published with some changes in sonographic terminology. Structured reporting in radiology was first introduced in the field of breast imaging, first for mammography, then for ultrasound, and finally also for the breast MRI (10). The use of standard vocabulary and organized evaluation categorization significantly

enhances communication among various experts engaged in the diagnosis and treatment of breast illnesses. The utilization of BIRADS is legally mandated in North America and is extensively employed globally. The ACR BIRADS advises radiologists to initially ascertain tissue composition, followed by the characterization of masses, calcifications, and related characteristics. Color Doppler and sonoelastographic assessments constitute components of routine sonographic evaluation. Special cases are also addressed. Following the comprehensive assessment, the BIRADS classification from 0-6 should be allocated to all observations.

The tissue composition categories are similar and analogous to the variability seen on mammographic images: homogeneous fatty background echotexture, scattered fibroglandular echotexture, heterogeneously dense echotexture, and extremely dense echotexture.

Mass is a space occupying lesion that should be demonstrated in two orthogonal projections. The size, shape, orientation, margins, echo pattern and posterior acoustic features of masses should be evaluated, as well as interval changes and associated features like skin thickening or retraction, and axillary lymphadenopathy. Vascularity of the mass should be assessed by color Doppler, and stiffness by sonoelastography. The level of suspicion should be based on the most worrisome feature. In terms of their shape, masses can be oval, round, irregular and lobular. The term “lobular” will be reintroduced in the new edition of BIRADS, as it was omitted in the previous one. Oval and round lesions are usually benign, while invasive cancers are irregular, but some cancers may be round and oval in shape, including very aggressive triple-negative breast cancers. Orientation of the lesion in reference to skin is unique for US examination, as well as the ability of ultrasound to assess the lobar anatomy and lobar localization of breast lesions. Parallel lesions (“wider than taller”) are more likely benign, and vertical (“taller than wider”), in which A-P diameter is larger than latero-lateral diameter, are more likely malignant. Margins of a lesion can be circumscribed (well-defined), or non-circumscribed. Non-circumscribed margins are indistinct, angular, or spiculated, and they raise higher level of suspicion for malignancy. The term “microlobulated” that used to be present in previous editions of BIRADS lexicon will be omitted in the new edition. Echo pattern is compared in reference to fat and glandular tissue. Simple cysts are anechoic, darker than fat, and demonstrate distal acoustic enhancement. Hyperechoic lesions have the same or higher echogenicity as fibro glandular tissue and higher echogenicity than fat; hypoechoic lesions are less echogenic than fat; isoechoic lesions have approximate echogenicity of the surrounding fat and complex lesions contain anechoic (cystic) and echoic (solid) component. A mixture of echogenic patterns within a solid mass is called heterogeneous echo-pattern. Distal acoustic phenomena should be observed: posterior shadowing, posterior enhancement, no changes in the posterior echogenicity, or combined patterns. Posterior enhancement suggests a benign lesion and is typical for cystic lesions, but some carcinomas may also show enhancement, although very rarely. Posterior shadowing of different intensity suggests fibrosis, with or without an underlying malignancy. Areas of acoustic shadowing or enhancement that don't originate from focal lesions commonly appear in dense fibrous breasts; by changing the transducer position we may eliminate shadowing originating from benign fibrous tissue or Cooper ligaments.

Calcifications, including microcalcifications can be seen on ultrasound, if carefully looked for and especially when targeted. Second-look ultrasound exam is performed after mammography, so that the examiner knows where to look for microcalcifications. Calcifications in BIRADS are usually described on mammography and only noted on ultrasound. Only calcifications larger than 0.5 mm show with dorsal acoustic shadowing on sonography, while microcalcifications are too small to cause posterior shadowing, however, using high-frequency and high-resolution transducers, they too become visible as echogenic foci, particularly when in a mass. Microcalcifications cluster show as multiple hyperechogenic foci either within the mass or within ducts. Calcifications should be classified as being in a mass, outside a mass, or as intraductal calcifications. When a US correlate is clearly present, the cluster can be subjected to US-guided biopsy. Fibroadenomas in older ages often present as masses with interior dystrophic calcifications. Those calcifications have usually been described as "pop-corn calcifications", but in the new edition of BIRADS lexicon the term "popcorn" is replaced with "coarse". Ultrasound can show dilated ducts filled with echoic content and can have correlates with mammographic finding of DCIS with suspicious clusters of microcalcifications, as well as with the "non-mass" enhancement of ductal cancer in situ on postcontrast subtraction sequences after contrast-enhanced MRI (11). The new BIRADS Lexicon introduces the term "non-mass" for corresponding ultrasound features as well. Non-mass lesions on ultrasound lack the three-dimensionality of the mass and are usually recognizable in two planes. If the lesion is malignant on histopathology, it is most likely ductal cancer in situ, and not an invasive carcinoma. It can be hypoechoic, isoechoic, hyperechoic or with mixed echogenicity. It can have regional, focal, segmental or linear distribution. Shape and margins cannot be assessed.

The ultrasound finding of ductal cancer in situ and correlate with non-mass enhancement on MRI is presented at Figures 13.12a. and 13.12b.

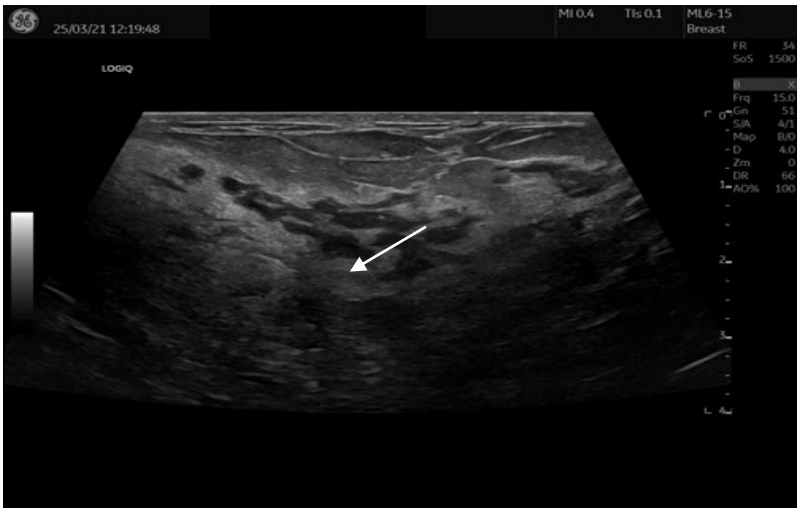

Figure 13.12a. Dilated ducts of lobar distribution- non-mass lesion according to the new edition of BIRADS lexicon

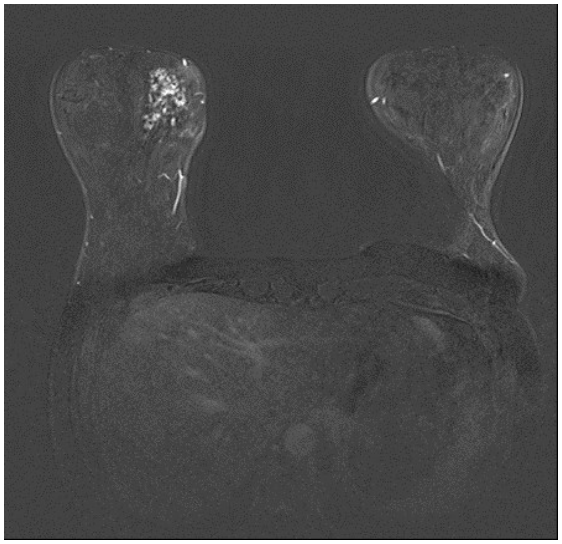

Figure 13.12b – MRI of the same patient with non-mass enhancemen on postcontrast subtraction image. Histopathologic diagnosis: Ductal cancer in situ, gr. 3

The fifth edition of ACR-BIRADS introduces associated features in ultrasound, like in mammography, as already mentioned: architectural distortion, duct changes, skin changes (thickening and retraction), edema, vascularity (absent, internal, vascularity in the rim), as well as elasticity assessment, using sonoelastography, both strain and shear-wave. The new element that is being introduced in the latest edition of BIRADS Lexicon among associated features is "echogenic rind". It is a thick ring/belt of echoic tissues that encircles the whole mass or part of the breast mass and disrupts the structure of the surrounding tissues. It is most likely the consequence of desmoplastic reaction/ peritumoral edema and has a high PPV for malignancy. When echogenic rind is seen around the mass on sonography, the core biopsy is indicated.

Multiparametric breast ultrasonography represents the pinnacle of breast sonographic evaluation, necessitating the assessment of all masses by a combination of B-mode imaging, color Doppler, and sonoelastography. Special cases refer to instances characterized by a distinctive sonographic diagnosis or results. These include simple cysts, clustered microcysts, complicated cysts, dermal or subdermal masses, foreign items such as implants, intramammary and axillary lymph nodes, vascular anomalies (arteriovenous malformations/pseudoaneurysms, Mondor disease), postsurgical fluid accumulations, and fat necrosis. Fat necrosis, recognized as a significant mimicker, frequently occurs post-surgery, particularly following reduction mammoplasty, and exhibits specific MRI characteristics. Postsurgical fluid collections, known as seromas, are more effectively visualized by ultrasonography and MRI compared to mammography.

Whenever possible, US should be correlated with mammographic and MRI findings and compared to previous imaging examinations. The knowledge of physical findings, family history, clinical symptoms (discharge, etc.), partial status and hormonal replacement therapy is important.

Hand-held ultrasound of the breast in most EU countries is performed by radiologists and enables direct communication with patients during the examination. Therefore, an integral part of the structured report should contain clinical data obtained during the examination, anamnestic data and correlation with previous imaging findings, as well as with mammography and MRI. If mammography and ultrasound are performed in a sequence, the composite finding of both is desirable. All findings should contain final assessment categories according to the BIRADS Lexicon, and management recommendations. When correlating US with mammography and MRI, one has to remember that the patient's position affects the location of the lesion, and it may differ considerably between ultrasound performed in supine or lateral oblique position and MRI performed in the prone position of the patient.

In Category 0 (incomplete assessment), the additional imaging evaluation is indicated, and this is almost always used in the screening situation. Category 1 is used for normal sonographic examinations, with no abnormalities. Category 2 includes typical benign findings, like simple cysts, intramammary lymph nodes, breast implants, stable postsurgical fluid collections and fibroadenomas unchanged for at least 2 or 3 years. Category 3 includes probably benign findings. A solid mass with circumscribed margins, oval shape and parallel orientation, most likely a fibroadenoma, should have less than 2% risk of malignancy, especially if it is soft on sonoelastography and demonstrates no distal acoustic phenomena or distal acoustic enhancement. However, some 3-4% of fibroadenomas are stiff on elastography. Clustered microcysts might also be placed in this category for short-interval (6-months) follow-up sonography. Suspicious lesions in the category BIRADS 4 are further subdivided into three additional groups, BIRADS 4a, 4b and 4c. The probability of cancer in this group is in a very wide range from 3% to 94%. Such lesions require tissue sampling and needle biopsy can provide histologic diagnosis. The BIRADS category 5 is highly suggestive of malignancy, with a very high probability of >95%. Category 6 is reserved for lesions with biopsy proof of malignancy prior to the commencement of therapy or known cancers that are reexamined during neoadjuvant chemotherapy. Postsurgical breasts with no pathological findings are assigned to category BIRADS 2.

Ultrasound features of benign breast lesions

The most prevalent benign breast lesions include cysts, fibroadenomas, duct ectasia, intraductal papillomas or papillomatosis, sclerosing adenosis, and epithelial hyperplasia affecting lobules or larger ducts. Infrequent benign disorders include fat necrosis, mastitis, lipomas, and sclerosing phlebitis (Mondor's Disease). Cysts are prevalent, occurring in around 50% of women aged 30 to 40 years; while mammography can reveal well-defined confined lesions, ultrasonography can effectively distinguish cysts from solid lesions. Ultrasound may accurately visualize microcysts of 1-2 mm in diameter, along with simple or multiloculated macrocysts, which do not need additional evaluation or tissue diagnosis via fine-needle aspiration or core biopsy. Galactoceles are retention cysts containing milk that arise during pregnancy, whereas oil cysts are filled with necrotic material, exhibit peripheral eggshell

calcifications, and are associated with trauma or breast surgery. Simple cysts manifest on ultrasound as round or oval, well-defined anechoic masses, with good vision of the posterior wall, a sharp interface with surrounding tissue, posterior acoustic enhancement, and lateral thin refraction shadows, with no interior color on sonoelastography. The ultrasound diagnosis of small cysts is highly reliable and comparatively straightforward. Fig. 13.13.

Complex cysts may possess septa, necessitating ultrasound-guided aspiration or tissue sampling to distinguish septa from solid intracystic formations indicative of malignancy when uncertainty arises. Complex cysts exhibit characteristic features on sonoelastography, such as a layering pattern of blue, red, and green. Fig. 13.14.

Sonographic presentation of epithelial hyperplasia, focal fibrosis, adenosis and pseudoangiomatous stromal hyperplasia is very diverse and inconsistent, with hypoechoic or irregular areas, solid and cystic lesions, and hyperechoic areas, and the diagnosis of these conditions is primarily histopathologic, when core-biopsy of irregular areas seen on ultrasound is performed under ultrasound guidance.

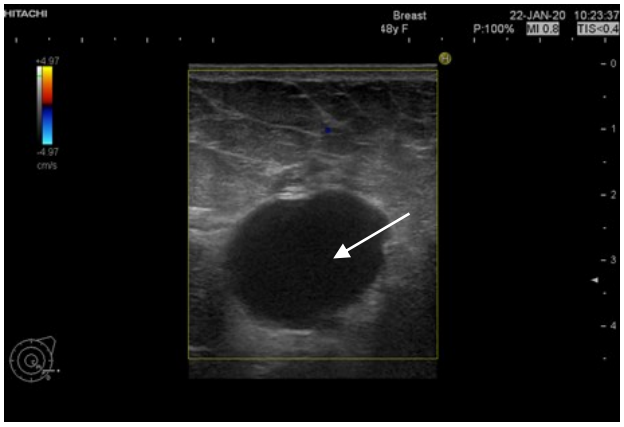

Fig. 13.13: Large simple cyst

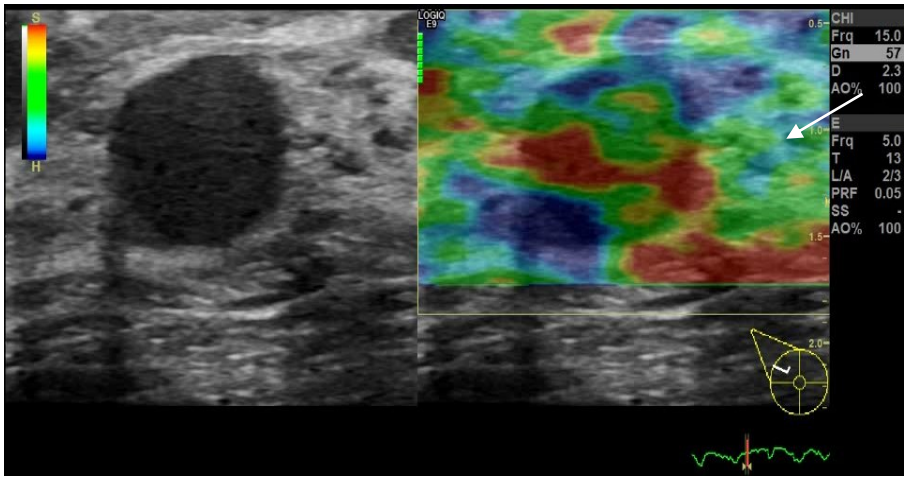

Fig. 13.14: Complicated cyst: a layering color pattern of blue, green and red (BGR artefact)

Radial scar is a lesion that resembles on US and mammography invasive cancer because of spiculated appearance and may be assigned BIRADS 5 category on both imaging modalities; it is a focal tubular proliferation around a fibrous elastoid center, and carcinoma can develop within the radial scar, so it should be excised

Focal fibrosis is a stromal proliferation occurring in younger women, that can resemble malignancy when it is manifesting with hypoechoic focal lesions with acoustic shadowing.

Fibroadenomas are most common benign breast tumors, typically occurring in young women, with the highest incidence between 25-35 years; they are mixed fibroepithelial hyperplastic tumors of the lobular connective tissue. They often have a quite typical palpatory finding. Typical sonographic features of fibroadenomas are round or oval masses with circumscribed borders, horizontal orientation, relatively homogeneous hypoechoic or slightly heterogeneous internal pattern, posterior enhancement, and soft appearance on sonoelastography. The incidence of fibroadenoma decreases after the age of 40 and all newly diagnosed solid lesions in women over 40 years of age should be suspected for cancer, even if they have regular borders. Fibroadenomas are solitary or multiple lesions and are observed in 10% of patients. They typically measure 1-2 cm and rarely more than 4 cm in diameter. In our practice, newly discovered lesions are further evaluated by tissue sampling, and when the diagnosis of fibroadenoma is confirmed, they are categorized as BIRADS 2 lesions. Gray scale features of some aggressive invasive breast cancers, like triple negative cancers may resemble those of fibroadenomas, since they can present as well-circumscribed, smoothly margined, horizontally oriented lesions, but they typically are not as soft as fibroadenomas on sonoelastography. Some 3-4% of fibroadenomas can be hard on sonoelastography, and it is a false-positive elastographic finding. The same situation may occur with fat necrosis.

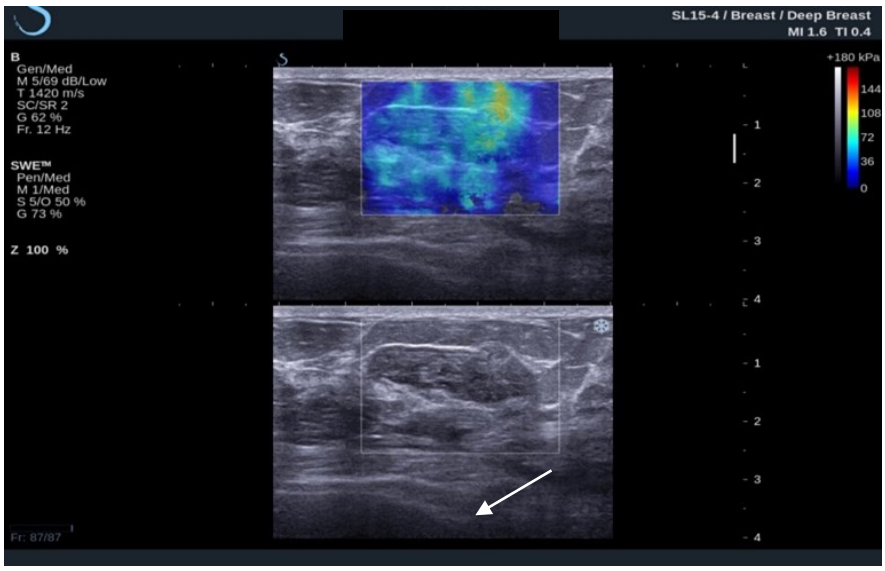

Fig. 13.15: Biopsy proven fibroadenoma of the breast, horizontally oriented, well circumscribed, smoothly marginated, with regular borders, without distal acoustic phenomena, soft on shear-wave elastography

Hamartomas are benign abnormal collections of tissues normally found in breast (fat, parenchyma and smooth muscle), surrounded by a pseudocapsule, that appear on ultrasound as well-defined, horizontally oriented lesions with smooth margins and the final diagnosis is established by excision biopsy.

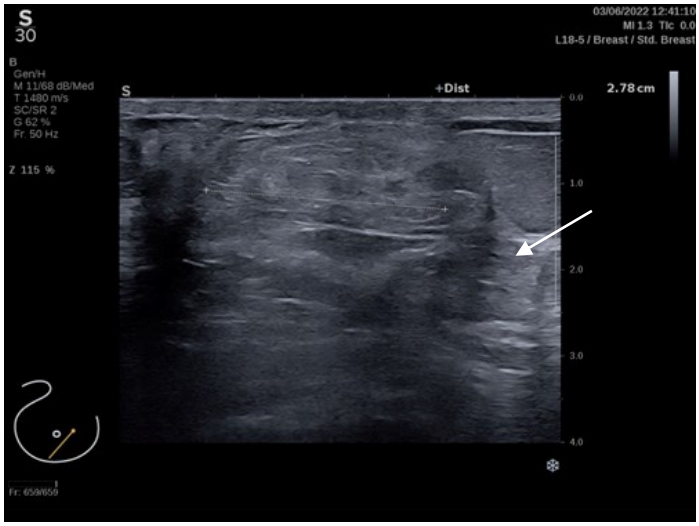

Fig. 13.16: Biopsy proven hamartoma, like breast in breast lesion, solid, inhomogeneous, oval, horizontal lines, well-defined

Papillomas are benign fibroepithelial tumors located within the milk ducts. They are relatively rare and can present on sonography as intraductal mass with or without ductal dilatation, intracystic mass and a predominantly solid pattern with the intraductal mass totally filling the duct and are typically highly vascularized. Reliable sonographic differentiation between benign papilloma and papillary carcinoma is not possible and yields further diagnostic evaluation. Inadequately treated acute mastitis may turn into subacute and chronic forms, with formation of abscesses.

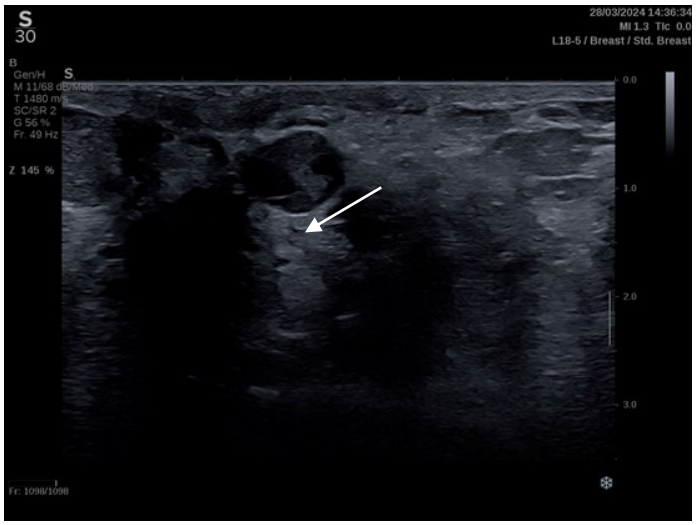

Fig. 13.17: Intraductal papilloma with small ductal ectasia

Ultrasound shows skin thickening, changes in echogenicity of parenchyma and subcutaneous tissue, dilated ducts, and in case of abscesses low-echogenicity lesions, irregularly circumscribed, with multiple internal echoes of pus, surrounded by a hyperechoic rim of edema. Tissue sampling is needed to distinguish them from cancer.

Ultrasound features of malignant breast lesions

The extensive implementation of mammographic screening has led to a significant rise in the diagnosis of ductal carcinoma in situ (DCIS), identified through mammographically detectable microcalcifications (12). Ultrasound and MRI are less effective than mammography in identifying suspicious microcalcifications; however, their significance in evaluating BIRADS 4 and 5 mammographic microcalcifications should not be overlooked. Carcinomas in situ are neoplasms that do not invade the basement epithelial membrane of the duct and pose a significant risk for the development of invasive malignancy. DCIS originates from the ductal epithelium of milk ducts and is frequently multifocal; various kinds of DCIS exhibit differing levels of differentiation and malignant potential. Comedo DCIS advances to invasive carcinoma in approximately 50% of instances, although certain well-differentiated variants proceed to invasive malignancy less frequently, in about 20-30% of cases (11). Sonographic features of DCIS include ductal abnormalities, predominantly ductal dilatation with intraductal content, usually with small echoic dots representing microcalcifications, architectural distortions and less commonly hypoechoic irregular areas or masses. In our experience, in more than 70% of DCIS, hyperechoic foci can be found on ultrasound, either within a mass or within a duct, representing microcalcification clusters visible on mammography. When such changes are visible on ultrasound, performing a biopsy under sonographic guidance is an option. Lobular cancer in situ (LCIS) is not recognizable on ultrasound, it arises in ductolobular units of parenchyma, it has much smaller malignant potential than DCIS and is considered as severe epithelial atypia and not a true carcinoma. DCIS on ultrasound is manifested as non-mass lesion with dilated ducts, as shown in Figure 12 a+b. It is also useful to perform color Doppler to detect hypervascularization in some cases of DCIS, as shown in Fig. 13.18.

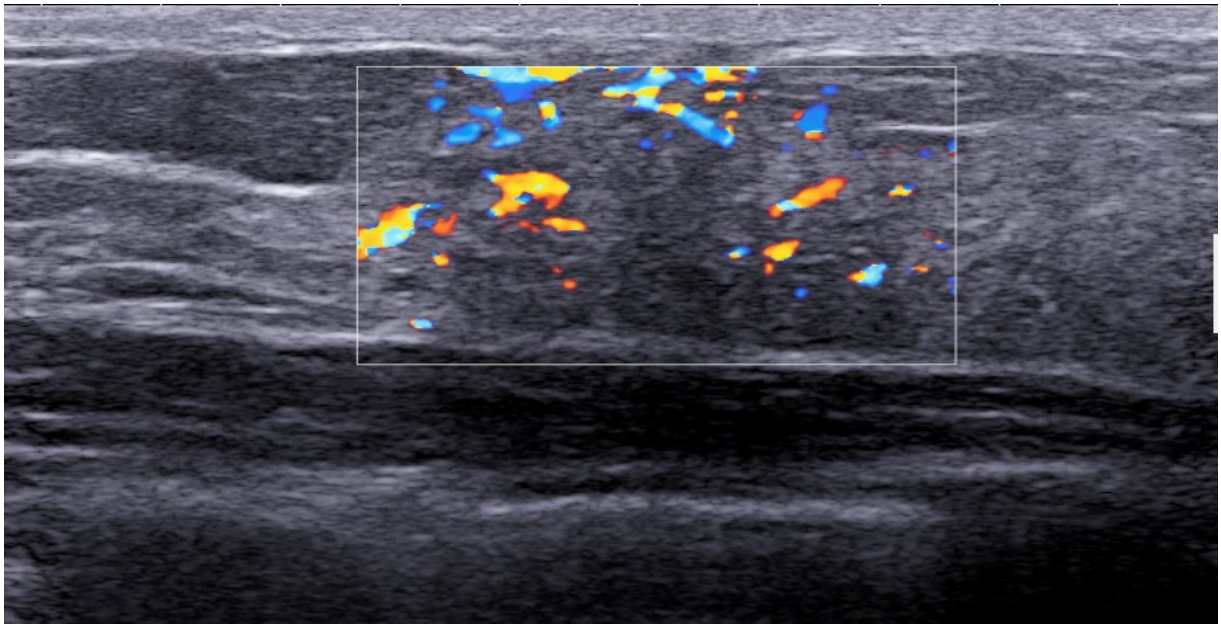

Fig. 13.18: Color Doppler image of hypervascularized large hypoechoic area, that contained pathological clusters of microcalcifications on mammography - core biopsy and final histopathologic diagnosis demonstrates hypersecretory DCIS

Invasive breast cancers are categorized into invasive ductal carcinoma (IDC), originating from ducts and comprising several subtypes, and invasive lobular carcinoma (ILC), originating from lobules. Invasive ductal carcinoma (IDC) is significantly more prevalent than invasive lobular carcinoma (ILC) and is more readily detected using ultrasound. Invasive lobular carcinoma constitutes 10-15% of invasive breast malignancies, frequently presenting as multicentric and bilateral, necessitating preoperative MRI imaging. Ultrasound is superior to mammography in assessing multifocality, multicentricity, and intraductal spread, however it is inferior to MRI. The existing criteria mandate an accurate pre-treatment diagnosis of the breast cancer kind. To obtain an accurate histopathologic diagnosis, it is necessary to do an ultrasound-guided core biopsy, which yields the histopathologic type and grade of cancer, hormonal receptor status (estrogen, progesterone), HER2 expression status, and proliferation index value (Ki-67). These criteria are essential for determining the appropriate treatment and its sequence. Magnetic Resonance Imaging offers the most accurate evaluation of the cancer extent. A US-guided core biopsy or fine needle aspiration of regional lymph nodes is also required. The classification of cancers into Luminal A and B, HER2 positive or negative, pure HER2, or triple negative, along with previously outlined parameters, facilitates the multidisciplinary team's decision regarding whether the primary treatment for breast cancer should be neoadjuvant chemotherapy followed by surgery or the reverse. The surgical approach is contingent upon the size, extent, and type of malignancy. Ultrasound and ultrasound-guided tissue sampling play a vital role in acquiring such data. The efficacy of neoadjuvant chemotherapy is often assessed with MRI, however ultrasound, particularly contrast-enhanced ultrasound, may also be employed. Thirty years ago, Stavros

described gray-scale sonographic features of malignant and benign breast lesions. Malignant features include vertical orientation (larger anteroposterior than latero-lateral diameter), spiculation, distortion of breast tissue architecture, marked hypoecogenicity, angular margins, posterior acoustic shadowing and microcalcifications, while benign features include gentle lobulations, ellipsoid shape, homogeneous echotexture, thin capsule, horizontal orientation (larger latero-lateral than anteroposterior diameter) (7,13) Fig. 13.19. Echogenic rind should be added to these gray-scale features.

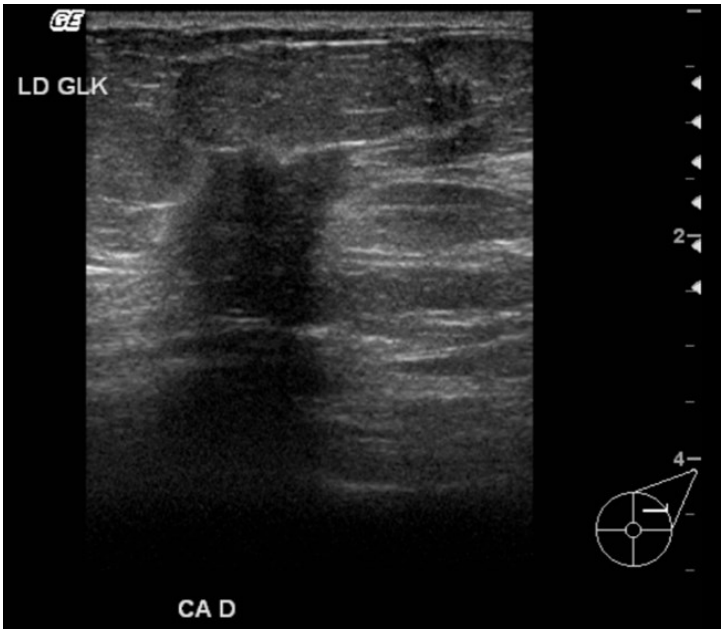

Fig. 13.19: Sonographic image of spiculated, hypoechoic mass – histopathologic diagnosis invasive ductal cancer, cribriform type, Luminal B

However, one needs to be very careful in differenting between invasive cancers and benign lesions, because the straightforward distinction on the basis of former categories is not completely accurate and there is a considerable overlap of sonographic features among benign lesions and invasive cancers. Some very aggressive cancers, like triple negative cancers, that are considered to be the most biologically aggressive cancers, may demonstrate benign morphologic sonographic features (horizontal orientation and well-circumscribed, regular masses) and the correlation with mammography and MRI is needed. Image-guided biopsy is the best way to establish an accurate diagnosis. Multiparametric ultrasound evaluation, combining gray-scale features with the assessment of vascularization with color Doppler and sonoelastographic examination is important. Most carcinomas are stiff on sonoelastography examinations, while most benign lesions are soft. Fig. 20 a-c is an example of multiparametric breast US examination combining the evaluation of a mass with gray-scale, color Doppler and shear-wave sonoelastography.

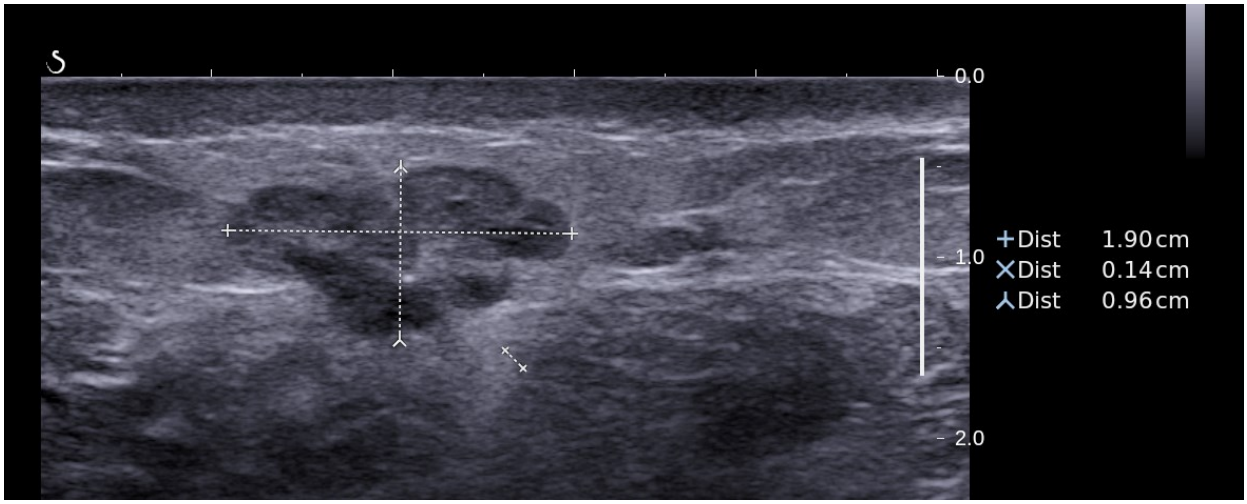

Fig. 13.20 a: Gray-scale image of hypoechoic, discretely heterogeneous horizontally oriented lesion, with lobular borders and no distal shadowing

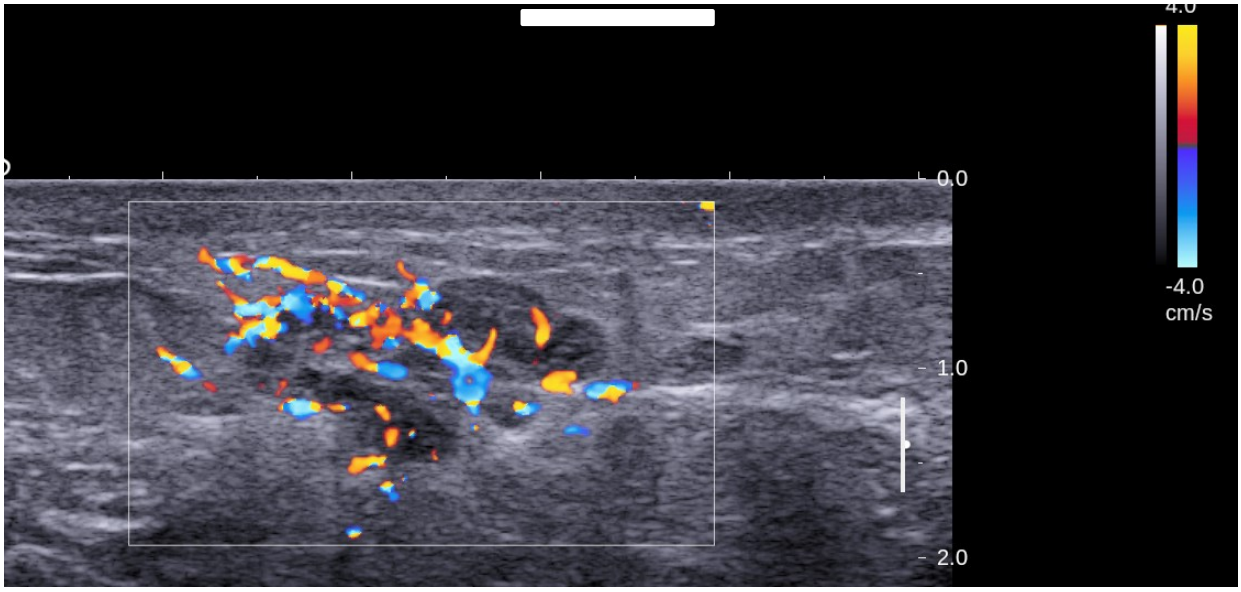

Fig. 13.20 b: Color Doppler image of the same lesion, with irregular, internal penetrating vessel – hypervascular tumor.

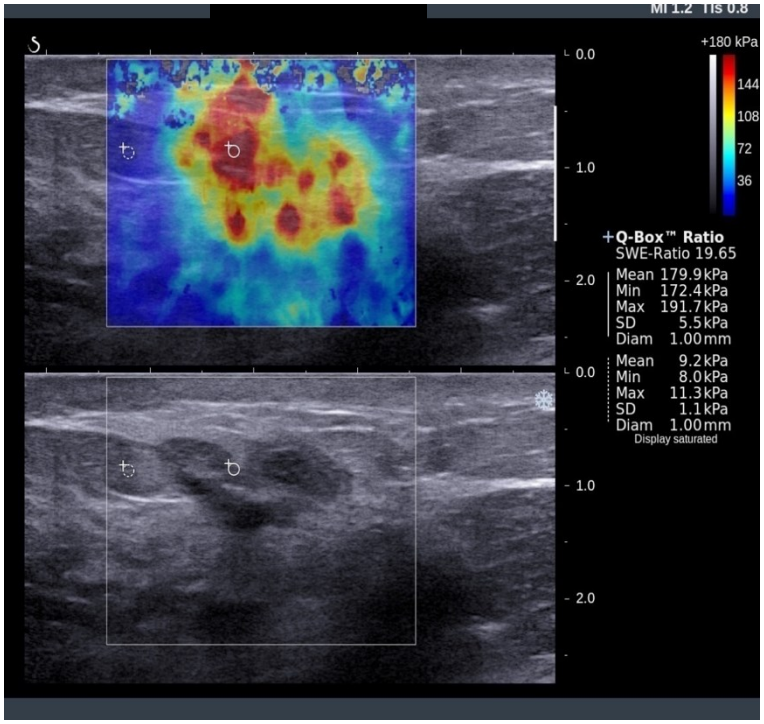

Fig. 13.20 c: Shear wave sonoelastography image of this patient demonstrates very stiff lesion. The diagnosis was triple negative invasive breast cancer.

The correlation of ultrasound with mammography is very important, since some invasive cancers invisible on mammography may be visualized on ultrasound, such as invasive lobular cancer that infiltrates breast like a spider web and can often not be well visualized at mammography, particularly in dense breasts. When small invasive cancers are not visible in mammographically dense breasts due to the superposition of the abundant fibroglandular tissue and mass, they might be visualized on ultrasound, since they are hypoeochoic, surrounded by echogenic parenchyma. Medullary and mucinous cancers may be circumscribed masses and may resemble dense cysts with some internal echoes on ultrasound. Posterior acoustic shadowing is more common in malignant tumors, but some carcinomas do not exhibit posterior shadowing, and may even rarely have posterior enhancement, like some medullary and mucinous carcinomas. Some benign lesions that are extensively fibrosed are reliably distinguished on mammography from malignant lesions, like calcified fibroadenomas because of typical coarse internal calcifications. Therefore, neither the absence of malignant sonographic features, nor the presence of benign features can be evaluated apart from mammographic findings, clinical examinations, and MR findings in selected cases.

Targeted, second-look ultrasound after MRI, i.e. focused evaluation of lesions detected on contrast-enhanced MRI, is very important for the further evaluation of such lesions and most of them are visible on ultrasound and can be biopsied under ultrasound guidance. The larger the lesion is on MRI the higher is the likelihood that it would be visible on ultrasound.

Use of ultrasound after surgery and in screening

Postoperative imaging after oncoplastic surgery and radio and chemotherapy is very common, and such patients need to be regularly examined for the rest of their lives to detect recurrences as early as possible. Postoperative scars after breast conserving surgery, as well as fat necrosis may resemble cancers, and appear hypoechoic and spiculated, irregularly marginated, with varying degrees of distal acoustic shadowing. Postoperative seromas are liquid collections that may undergo secondary inflammation. Thickening of the skin is usual found after radiation therapy, as well as edema and architectural distortion. Within one year after surgery most changes regress spontaneously. Mammography and ultrasound are not reliable to differentiate between the postoperative scar and the tumor recurrence in the area of the scar. Contrast enhanced MRI has the highest accuracy in distinguishing postoperative scars from cancer. CE-MRI is also the most accurate modality to detect residual tumors after surgery and recurrent tumors, and in such cases second-look US and US-guided biopsy a often performed. Recurrent tumors are also most commonly stiff on sonoelastography, like the primary cancers.

Regarding the use of ultrasound in screening, mammography is the primary modality, however, it has considerable limitations in women with dense breasts, and an additional 2.3-4.6 of mammographically occult breast cancers per 1000 women can be diagnosed if ultrasound is added to mammography in women with dense breasts. Some national mammographic screening programs in Europe, like the Austrian and Croatian ones, recommend breast ultrasound to all women with ACR C and D density categories, and breast ultrasound examinations can be performed free of charge for the patient, within the scope of the national healthcare systems. Automated whole-breast ultrasound has been recently developed as an alternative to hand-held ultrasound. However, the new guidelines from ECR and EUSOBI recommend the use of MRI once every two to four years in women who have very dense breasts for the screening, even if they do not have a high tumor risk. Women with high-risk should undergo annual contrast enhanced MRI examination followed six months after by breast ultrasound examinations.

Male Breast

The place of ultrasound in the diagnostic gynecomastia is under debate, placing ultrasound as the initial examination in young males, or in those refusing mammography, emerging as possible primary tool especially in clinical settings. Sonography is reported to enhance clinical management when mammography identifies additional findings alongside gynecomastia, and medical literature advocates for its use as the primary examination for patients under 30 years of age or for men who decline mammography (17). From the clinical point of view there are some clear questions to be answered in face of any male, regardless of age, with breast enlargement:

1. Is it true or false (gynecomasty versus pseudogynecomasty, or adipomasty)
2. Is it physiological or pathologic?
3. Is it acute (florid stage) or inactive (florid stage)?
4. Is there any risk of malignancy?

The rationale behind these questions is the clinical attitude determined by the result: weight loss with no follow up in pseudogynecomasty, rare follow up in the physiologic gynecomasty (GM), active identification caused by hormonal imbalance in pathological GM, with treatment in florid variants and morphological follow up in fibrotic variants, since the presence of GM has to be considered a oncological alert, as even inactive, remnant gynecomastia has to be considered a cancer precursor with 3 to 5 times higher breast cancer incidence than in normal male population.

In order to understand the male breast, it is important to understand the physiology of male breast development. Regardless of gender, breast development appears during intrauterine life, arising from a single epithelial ectodermal bud, and the development of a rudimentary mammary gland: growing downwards in the mesenchyme, enlargement, indentation appearance, with both epithelial and mesenchymal cells, differentiating to fibroblasts, smooth muscle cells, capillary endothelial cells, and adipocytes. In the second trimester of pregnancy, a lactiferous duct develop with a lineage of epithelial cells, with well-defined tubular architecture, with apparent breast tissue, both in boys and girls. In the third trimester, there is a continuation of the breast development, with additional branching of the secondary epithelial buds, and canalization with rudimentary lobular structures.

At birth, from the structural point of view, there is the basis for breast development, whenever the hormonal milieu is favorable to this process: roughly 15 to 20 lobes of glandular tissue have developed, each comprising a lactiferous duct that exits onto the breast surface via the mammary pit. The surrounding skin and the fibrous suspensory Cooper ligaments, which secure the breast to the pectoralis major fascia, offer support to the breast.

Decreasing maternal estrogen levels in neonates activate the neonatal pituitary gland to secrete prolactin, leading to unilateral or bilateral breast augmentation and/or transitory milk secretion in approximately 70% of term infants. It is hypothesized that the newborn breast experiences stimulation about 3 to 4 months postnatally due to a surge of the infant's reproductive hormones, particularly estradiol. This surge, also known as minipuberty, can associate positive breast symptoms like swelling or discharge (Fig. 13.21a), due to the glandular differentiation and functional maturation, with appearance of secretory activity. Since there is natural involution, no active treatment is needed. Fig. 13.21 b.

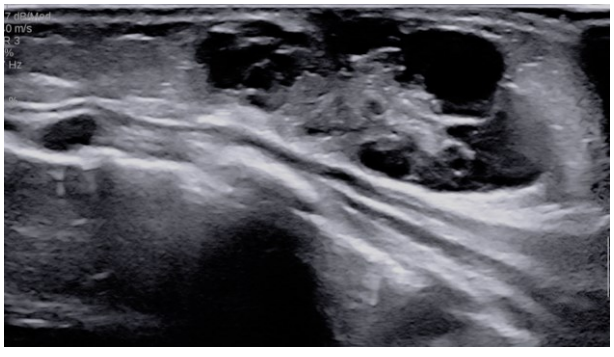

Fig. 13.21a: 2 months old infant, with breast bud, mastitis like changes

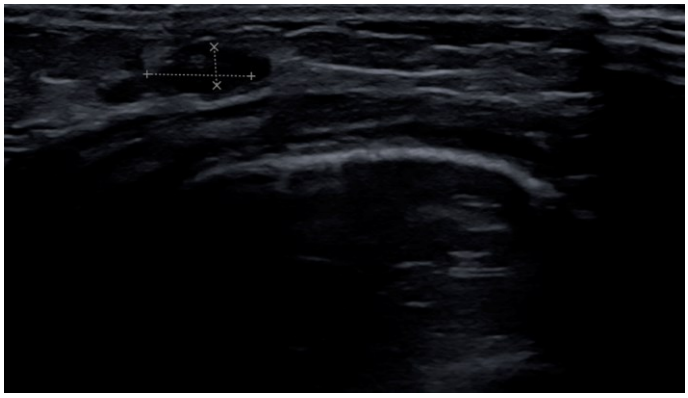

Fig. 13.21b: Same case after one month, with spontaneous involution of the breast tissue, remnant small hyperplastic retro mamelonary bud

In the first 2 years of life, the gland remains quiescent, up to the puberty onset. During puberty, male breast development ceases due to increased testosterone levels. During puberty, as many as 40% of males may experience transitory gynecomastia, likely attributable to relative estrogen dominance. Gynecomastia results from ductal and stromal enlargement, but not lobular hypertrophy. While mostly temporary, gynecomastia can be an unpleasant physical condition for a young boy. Infrequently, pubertal gynecomastia may endure, likely resulting from either end-organ idiosyncrasy or an atypical estrogen-androgen ratio at the outset of puberty. Morphologically, the breast budding looks similar in boys, Fig. 13.22, as in girls.

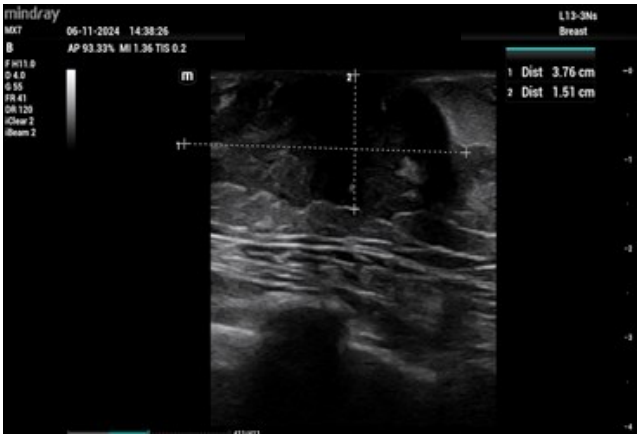

Fig. 13.22: 13 years old boy, Tanner 2 puberty stage, retromamelonary florid GM (active glandular hyperplasia*)*

The phenomenon is self-limited, with spontaneous remission in about 90% of cases within up to two years, and neither follow up nor treatment are needed. Normal male breast appears as a rudimentary structure consisting of remnant ductal tissue and a small nipple areola complex. Fig. 13.23.

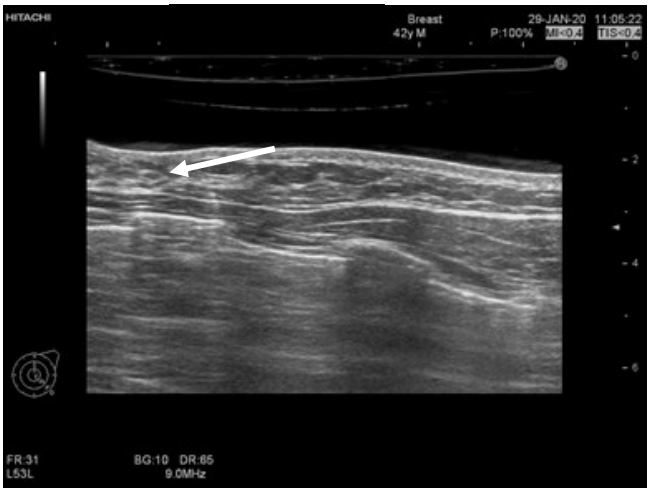

Fig. 13.23: Normal breast US in males (the arrow marks the nipple)

Ultrasound imaging of the adult male breast has characteristics analogous to those of the female breast. Isoechoic fat lobules corresponding to subcutaneous adipose tissue is a major finding of normal male breast seen in US. The breast structure can be observed, including the lobar structure, as seen in Fig.25a, but with minimum epithelial component, with fibrotic involuted ductal branching, however, even well-defined lobar structure can be observed in some cases, as shown in Fig. 13.24.

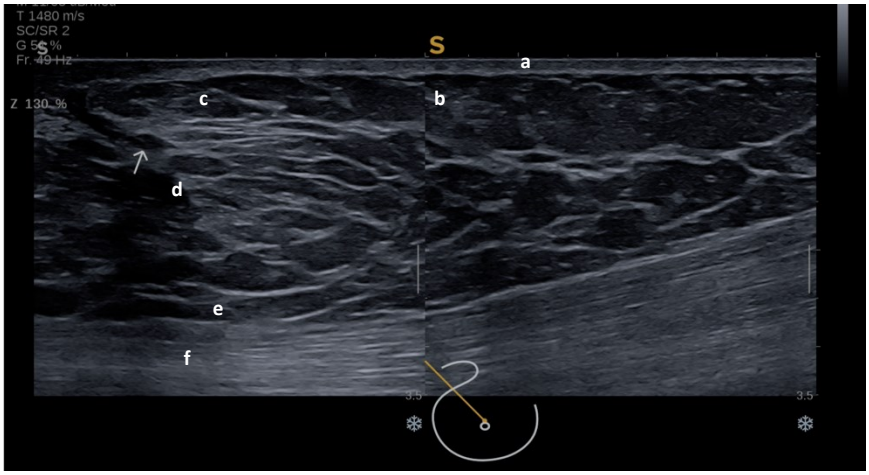

Fig. 13.24:73 y male, inactive fibrotic gynecomastia

a - skins; b - superficial fold of the fascia; c - Cooper ligaments;
d - glandular (predominant adipose variant); e - profound layer fascia; f - pectoralis layer

These particular examples are part of the 3rd life span period, when gynecomastia is frequently seen during older age (>60 years), with a reported prevalence that varies from 36 to

57%, increasing with age, secondary to increased peripheral aromatase activity, facilitated by increased total body fat, relatively elevated LH concentrations, and decreased serum testosterone concentrations associated to aging, but the identification of an underlying pathology and medications known to facilitate GM are mandatory, physiologic GM being an exclusion diagnosis.

Pseudo-gynecomastia refers to bilateral breast enlargement resulting from an accumulation of adipose tissue, not necessarily linked to general obesity or changes in the breast parenchyma, which remains of a normal volume. It is clinically characterized by broad, non-nodular, and symmetrical volumetric increases. The diagnosis relies on clinical observations. Ultrasonography indicates the existence of uniformly distributed lobular adipose tissue Fig. 13.25. In the presence of lipomasty, there is no need for any additional evaluation or morphological follow up.

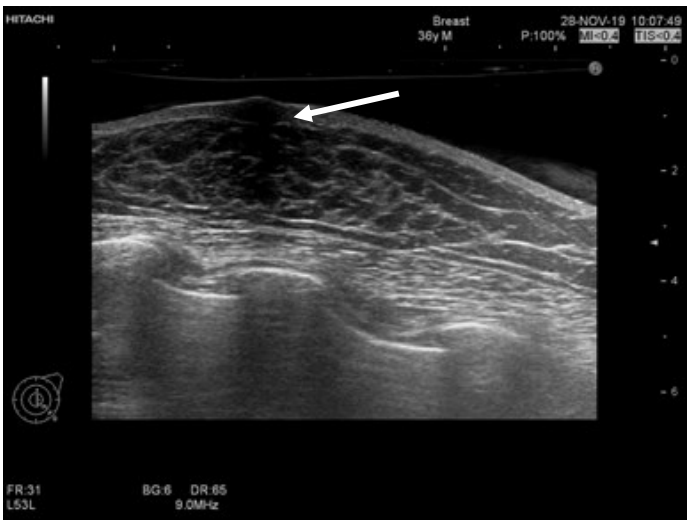

Fig. 13.25: Pseudo-gynecomasty – 32 years old male, strict adipose subcutaneous fat in between the superficial and the profound fascial layer (water bag device image)

Besides the above-mentioned situations, any case with real gynecomastia has to be considered pathologic and secondary causes have to be depicted. Pathologic reactive GM is due to an increase of systemic or local estradiol to testosterone ratio: sex steroid producing tumors (testicular or adrenal or extragonadal germ cell tumor such as lung, gastric, renal or hepatocellular carcinoma), increased aromatase activity (obesity), displacement of estrogens from Sex Hormone Binding Globulin (spironolactone, ethanol), testosterone decrease, both in primary and secondary hypogonadism forms, or additional end stage kidney disease, severe hepatic insufficiency, thyrotoxicosis, spinal cord disorders, or androgen resistance. Twenty percentage of GM is considered to be secondary to medication or exogenous chemicals , due to estrogen like properties (estrogen creams, delousing powder, digitalis, clomiphene, marihuana), estrogen production facilitation (gonadotropins, growth hormone) or estrogen precursors (exogenous androgens, androstenedione, DHEA) respectively altering testosterone levels by transient testosterone

decrease (chronic exposure to cocaine, heroin, methadone or amphetamines), direct testicular damage (busulfan, nitrosurea), testosterone synthesis block (ketoconazole, spironolactone), block androgen action (Flutamide, Bicalutamide). Primary proliferative breast disease has also to be considered in the differential diagnosis of GM, regardless of whether it is of stromal or ductolobular origin.

Mammography classifies true GM into nodular, dendritic, and diffuse forms, considering the nodular form as active, florid, reversible secondary to epithelial hyperplasia, the dendritic form as inactive, irreversible due to ductal hyperplasia and periductal stromal fibrosis, and the diffuse form as a combination among the previous forms, with both nodular and dendritic pattern.

From the clinical point of view, the only major aspect to be clarified is, besides ruling out malignancy, which actually is very rare, comprising 0.2% of all male cancers, with an overall prevalence of 0.11% invasive carcinomas and of 0.18% in situ carcinomas in male with GM, as accordingly the exception to the rule, to see if there is an acute/florid component of the GM or not. Florid component means active proliferation due to active ongoing estradiol to testosterone imbalance, target to treatment and more important reversibility of the pathology. Lastly, ultrasound can be highly beneficial for assessing the link between nipple masses and axillary lymph node involvement. For suspected lesions, vascularity examination may be conducted with the Doppler mode. Sonoelastography may serve as an adjunctive modality, however not routinely employed.

The dendritic form of GM is typically seen in ductal hyperplasia, whenever there is an acute breast growth process, regardless of the age of the patient. It starts as retromamelonary, as seen in Fig. 13.28, and in can evolve along the ductal remnants, if the process is active for a longer period of time, as seen in Fig. 13.26.

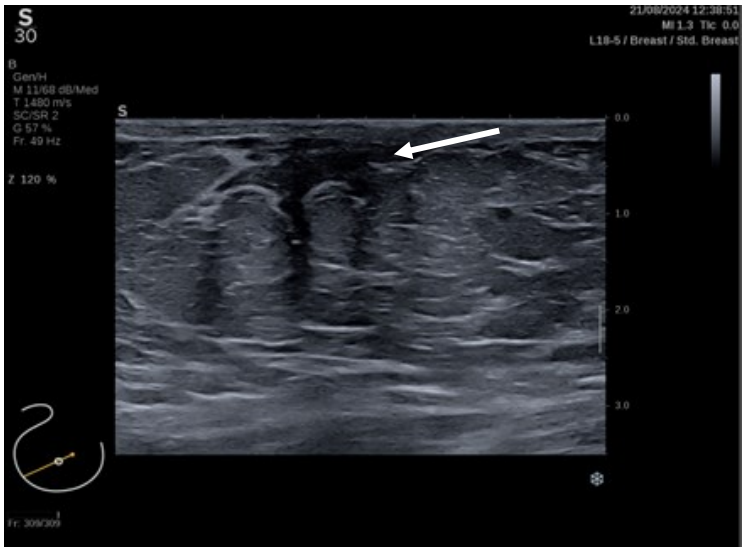

Fig. 13.26: Retro mamelonary dendritic growing pattern GM

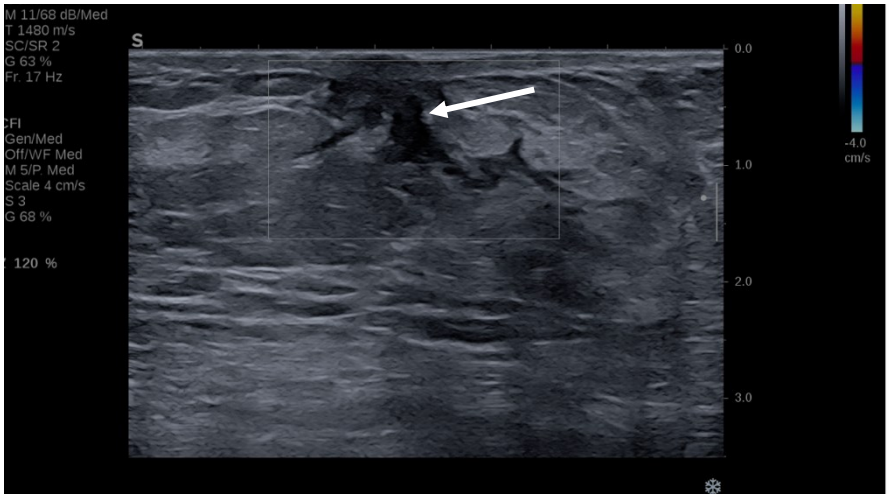

Fig. 13.27: Retro mamelonary dendritic growing pattern GM

Acute proliferation can also mimic an oval shape, the nodular variant of the GM, as shown in Fig. 13.28, usually presented like a unpainful deformation of the left breast, in a male 23 years old, with normal BMI, in the context of anabolic steroid use.

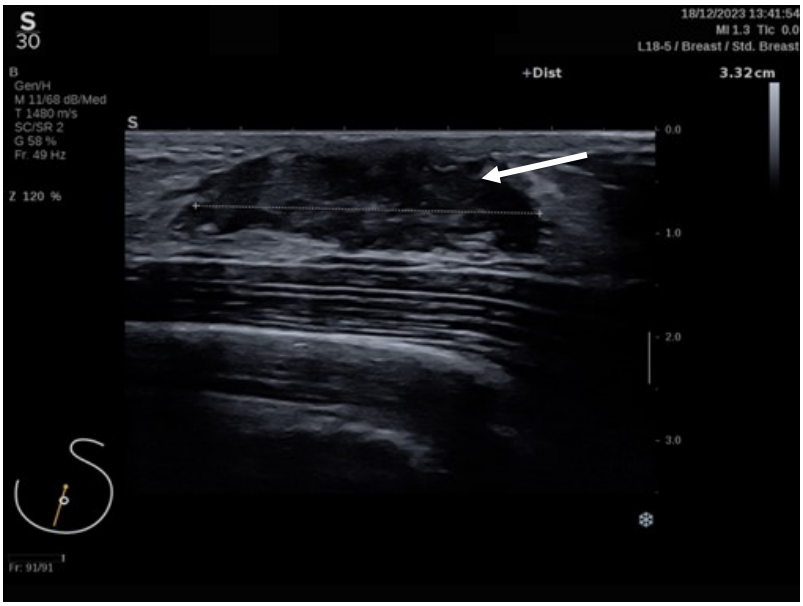

Fig. 13.28: Nodular homogenous, well defined solid lesion, no posterior phenomenon B-3

The diffuse, mixed pattern is shown in Fig. 13.29.a. On top of a well-defined diffuse inactive GM, acute dendritic hyperplasic phenomenon, highly suggestive for epithelial growth along the remnant ducts. Focused retromamelonary evaluation shows the active florid component

(Fig. 13.29.b) with low vascularization (Fig. 13.29.c) and low stiffness (Fig. 13.29.d), reemphasizing the benignity of the process.

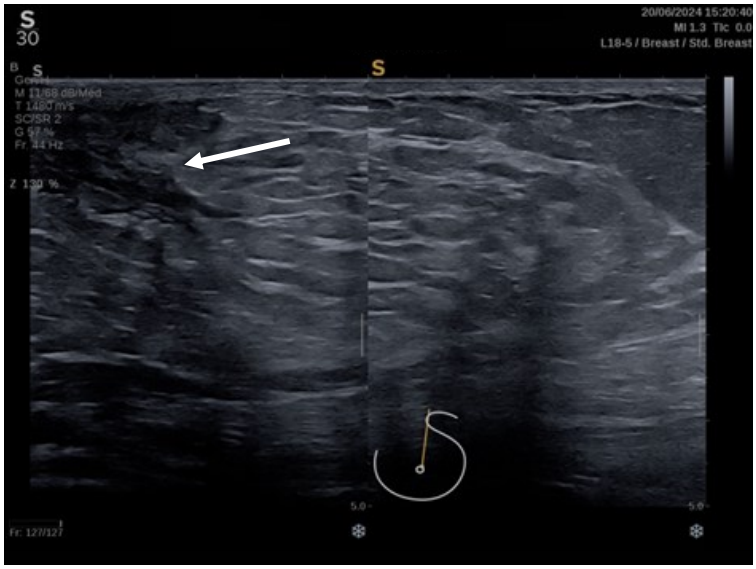

Fig. 13.29.a: Diffuse GM, florid component, 23 years old male with obesity

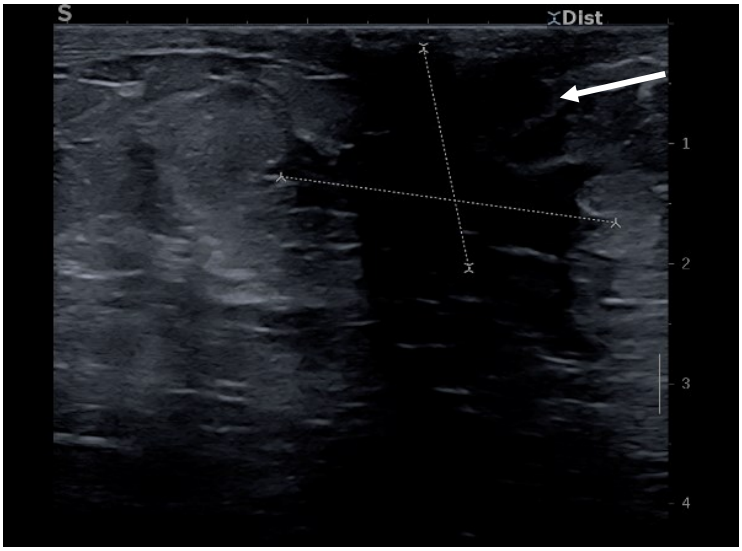

Fig. 13.29.b: Retro mamelonary focus 2b US- solid, spiculated, intense hypoechoic, posterior shadowing

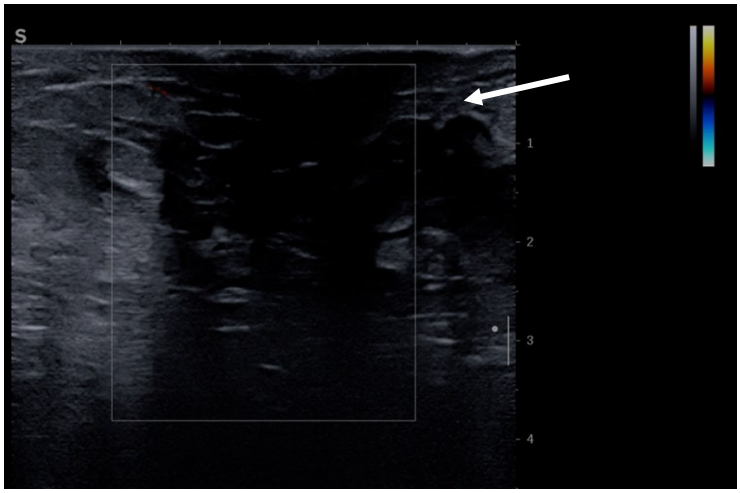

Fig. 13.29.c: Retro mamelonary CD US – no vascularity in the proliferation bud

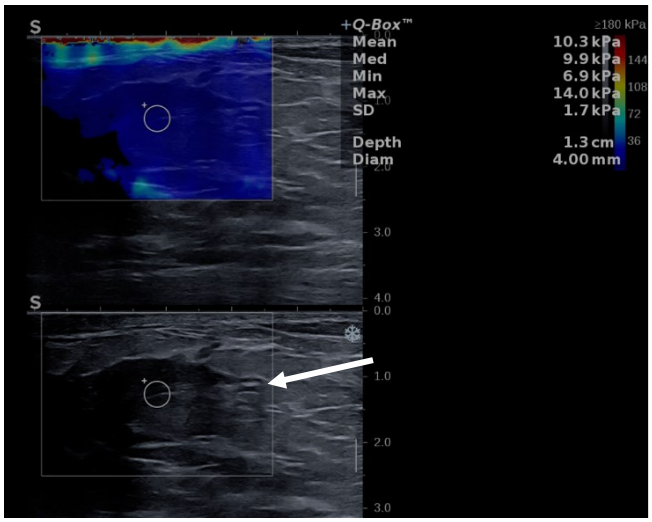

Fig. 13.29.d: Focused Shear wave elastography evaluation: high elasticity of the hyperplastic tissue (Emax = 14kPA)

Whenever GM is only inactive regardless of shape, looking for secondary causes, respectively thinking about systemic ones is useless since the treatment window opportunity is closed, and it has to be considered residual GM, eligible for surgical treatment (36). Fig. 13.32 shows such a residual GM in a 47 years old male, with no active secondary cause for the condition. Note the absence of any hyperplasia sign.

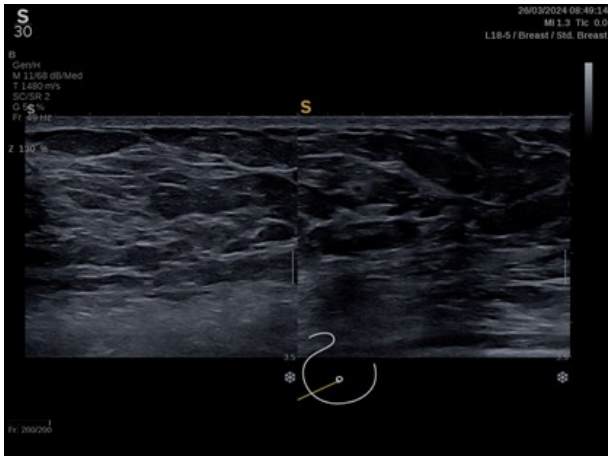

Fig. 13.30: Residual GM – with clear lobar structure, glandular component, adipose intralobar stroma

Besides this classification, extrapolated from the one in mammography, other classifications are proposed in the literature: focal versus diffuse, respectively nodular, flamed, shaped, poorly defined and non-mass.

The involution of the ductal system results in reduced ductal branching, making ductal malignancies infrequently observed in males, and when present, they are situated near the nipple-areolar complex. Furthermore, microcalcifications, which may indicate ductal involvement, are less frequently observed in male breast malignancies, possibly due to the involuted ductal architecture. Aside from that, fibroepithelial (biphasic, i.e., fibroadenoma, phyllodes tumor) and lobular (invasive lobular carcinoma (ILC), lobular carcinoma in situ (LCIS), fibrocystic alterations, adenosis) diseases are few due to the rare occurrence of terminal duct lobular units (TDLU).

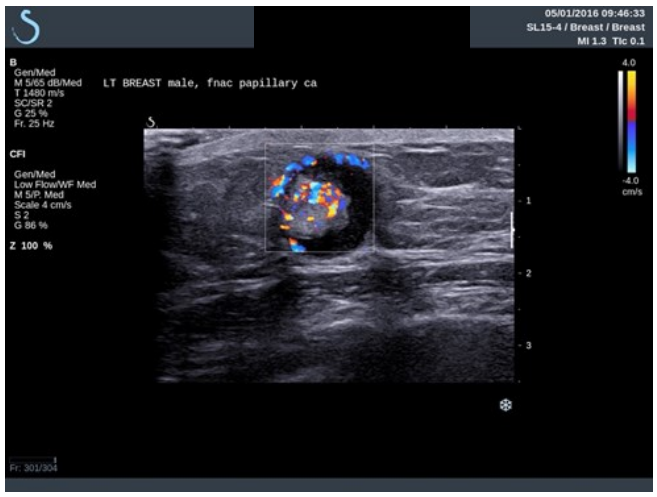

Fig. 13.31: Male cancer case – cytological proven papillary carcinoma

Last but not least ultrasound can be used for active follow up of the florid form of GM, when estrogen receptor modulator treatment can be used, in order to accelerate the involution of the active hyperplasic changes as presented in Fig. 13.34 *(36)* with florid, dendritic form of GM (Fig. 13.32.a), secondary to cocaine use, with decrease of the glandular hyperplasia following Tamoxifen treatment, three months after treatment (Fig. 13.32.b) with complete remission after another 6 months of treatment (Fig. 13.32.c).

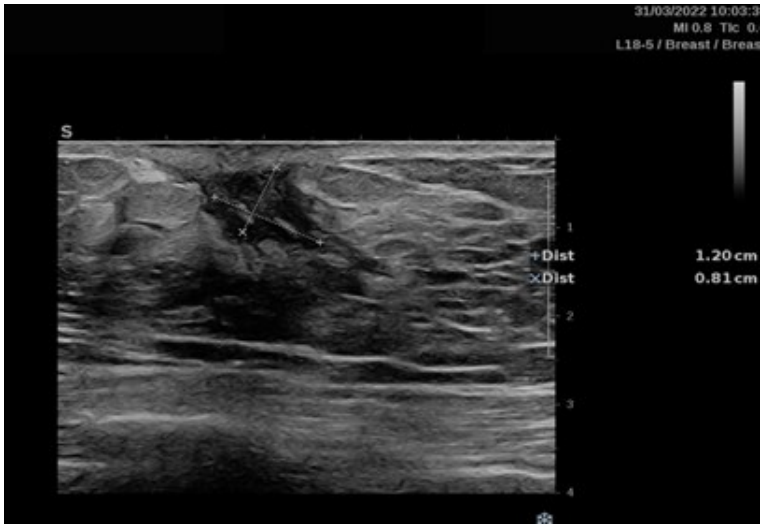

Fig. 13.32.a: Dendritic florid GM (at presentation)

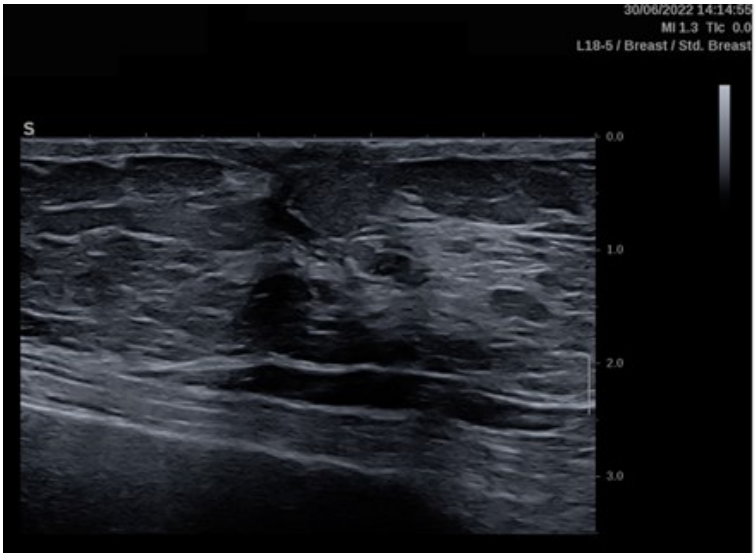

Fig. 13.32.b: Dendritic florid GM in involution – small remnant intraductal hypoechoic tissue (3 months after initial presentation)

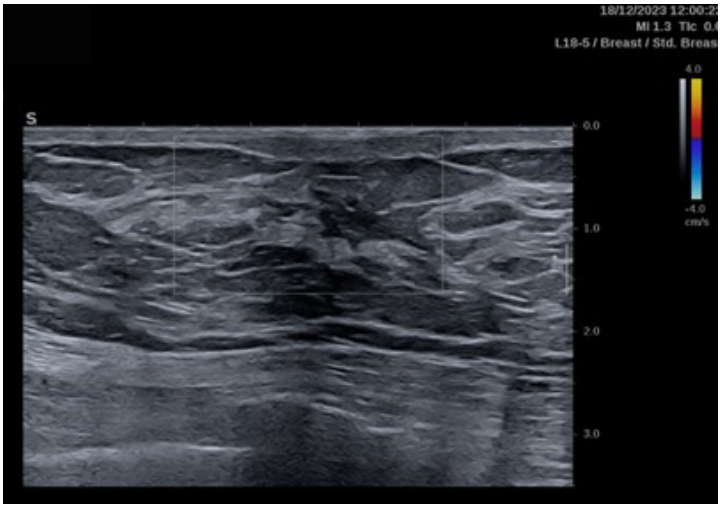

Fig. 13.32.c: Absent hypoechoic tissue in the retro mamelonary area (9 months after initial presentation)

In **conclusion**, ultrasound assessment plays a crucial role in the clinical evaluation of suspected gynecomastia, aiding in the differentiation between true and pseudogynecomasty, acute and residual forms, as well as physiological and pathological cases. This approach helps refine patient management and minimizes the need for additional imaging or invasive procedures.

Selective References

1. Fuchsjäger Michael, Morris Elizabeth, Helbich Thomas. Breast imaging : diagnosis and intervention. 2022;453.
2. Brkljačić B, Ivanac G. Ultrasonography of the breast. Ultrasound Clin . 2014 [cited 2025 Feb 3];9(3):391–427.
3. Brkljačić B, Ivanac G. Ultrasonography of the breast. Ultrasound Clin . 2014 [cited 2025 Feb 3];9(3):391–427.
4. Divjak E, Ivanac G, Radović N, Biondić Špoljar I, Sović S, Bahnik V, et al. Second-Look Ultrasound Using Shear-Wave Elastography in MRI-Suspected Locoregional Recurrence of Breast Carcinoma. Ultraschall Med [Internet]. 2022 Jun 1;43(3):274–9.
5. Pustahija AH, Ivanac G, Brkljacic B. US and MRI in the evaluation of mammographic BI-RADS 4 and 5 microcalcifications. Diagnostic and Interventional Radiology. 2018;24(4):187.
6. Pustahija AH, Ivanac G, Brkljacic B. US and MRI in the evaluation of mammographic BI-RADS 4 and 5 microcalcifications. Diagnostic and Interventional Radiology. 2018;24(4):187.
7. Turkey Sardanelli and. Position paper on screening for breast cancer by the European Society of Breast Imaging (EUSOBI) and 30 national breast radiology bodies from. Eur Radiol. 27(7):2737–43.
8. Stavros T. Normal Breast Ultrasound. 2004.785.

9. Sencha AN, Patrunov Y. Ultrasound imaging of male breast. Multiparametric Ultrasound Diagnosis Of Breast Diseases. 2018 Jan 1;223–63.
10. Russo J, Russo IH. Development of the human breast. Maturitas. 2004 Sep 24;49(1):2–15.

14. HOW CAN I USE US IN THE THYROID AND PARATHYROID PATHOLOGY?

Dana Stoian, Andreea Bena
WFUMB Center of Education Timișoara, Romania

High-resolution ultrasonography (US) remains the most accurate imaging technique for assessing the thyroid gland and identifying related morphological abnormalities. This method is non-invasive, widely accessible, cost-effective, and eliminates exposure to ionizing radiation, making it a fundamental tool in thyroid evaluation. Moreover, real-time ultrasound imaging is invaluable for guiding both diagnostic and therapeutic procedures, enhancing precision in thyroid disease management. Its capability to provide detailed structural and vascular information significantly improves the detection, characterization, and monitoring of thyroid conditions. Modern ultrasonographic techniques enable the real-time visualization of very small structures, as tiny as 2 mm in diameter, allowing for the detection of subtle abnormalities within the thyroid and parathyroid glands. However, despite its high-resolution capabilities, thyroid ultrasonography does not always correspond perfectly with histopathological findings. This limitation highlights the importance of a multiparametric ultrasound approach, which combines various imaging techniques—such as elastography, Doppler flow analysis, and contrast-enhanced ultrasound—to improve diagnostic precision and enhance differentiation between benign and malignant thyroid lesions.

This chapter will explore the clinical utility of thyroid ultrasonography, emphasizing its role in diagnosis, risk stratification, monitoring of treatment, and guiding interventional procedures.

1. Indications for Thyroid Ultrasonography

International guidelines provide recommendations on the appropriate use of thyroid ultrasound. The American Thyroid Association (ATA) advises its use primarily for evaluating thyroid nodules, assessing suspected thyroid abnormalities, and guiding FNA biopsies. The European Thyroid Association (ETA) and British Thyroid Association (BTA) further emphasize its role in preoperative cancer staging, postoperative surveillance, and risk stratification. There are currently no indications for performing ultrasound as a screening method in the general population.

Thyroid ultrasonography serves as an essential tool in the assessment and management of various thyroid conditions. Its primary indications include:

- Evaluation of thyroid anatomy in patients with compressive cervical symptoms or palpable anterior cervical masses: Assessing the size, shape, diffuse characteristics of the thyroid gland and the presence of thyroid nodules.

- Evaluation of thyroid incidentalomas: Assessing morphology details on nodules incidentally detected by other imaging modalities evaluating the neck.
- Monitoring thyroid nodules: Tracking changes in size or appearance over time to guide clinical decisions.
- Evaluating thyroid morphology in patients with thyroid dysfunction (hypo- or hyperthyroidism): Distinguishing between different causes of thyroid dysfunction and enlargement.
- Screening in high-risk individuals: Identifying thyroid cancer in populations with genetic predisposition (familial follicular cell–derived and medullary thyroid cancer), familial adenomatous polyposis (FAP), personal history of radiation exposure, or increased serum calcitonin.
- Assessment of fetal goiter or thyroid dysfunction: Evaluating thyroid abnormalities in prenatal imaging when maternal thyroid dysfunction is suspected.
- Preoperative planning for thyroid cancer: Mapping glandular and lymph node involvement to optimize surgical strategy.
- Postoperative surveillance: Detecting recurrence in patients with a history of thyroid malignancy.
- Guidance for fine-needle aspiration (FNA): Enhancing the accuracy of biopsies for thyroid nodules and suspicious cervical lymph nodes.
- Assisting in minimally invasive procedures: Ablation of selected thyroid nodules, such as ethanol or radiofrequency ablation.
- Support for epidemiologic studies: Contributing to population-based research on thyroid disease prevalence and risk factors.

The overuse of thyroid ultrasound in clinical settings has become a growing concern, with a significant proportion of these examinations being requested without adhering to established medical guidelines. This pattern of excessive imaging often arises from factors such as insufficient knowledge of proper indications among healthcare providers, pressure from patients seeking reassurance, and healthcare systems that incentivize testing. Such unwarranted imaging frequently results in the detection of incidental harmless nodules, leading to avoidable biopsies and even thyroidectomies, overtreatment, increased anxiety, and unnecessary healthcare costs.

2. Ultrasound Features of the Normal Thyroid

Echogenicity, Structure and Vascularity: The normal thyroid gland is characterized by its homogeneous echogenicity. This echogenicity is due to the gland's unique composition of follicular cells and colloid. Its somewhat greater echogenicity compared to surrounding tissues is due to its elevated iodine concentration. The sternocleidomastoid, sternohyoid, and sternothyroid strap muscles and longus colli behind the thyroid are useful US muscular landmarks. The muscle landmarks are hypoechoic compared to normal thyroid parenchyma. For better accuracy, the echogenicity of normal thyroid tissue can be compared to that of salivary glands (Figure 14.1), particularly the parotid glands, which serve as a useful reference standard in ultrasound evaluations.

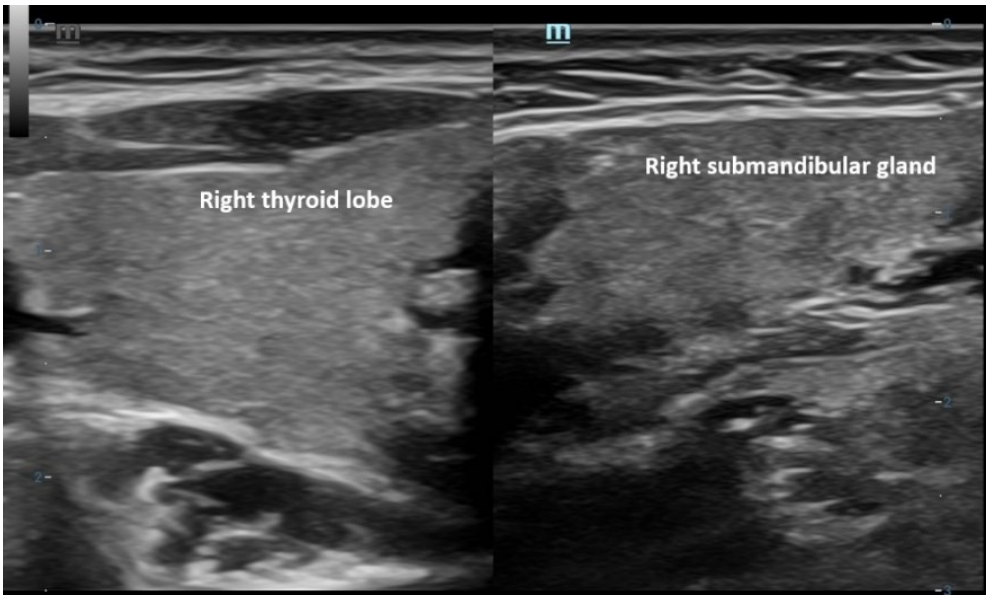

Fig. 14.1: Reference for normal thyroid echogenicity – same side salivary (submandibular gland) = isoechoic

The thyroid gland has an incomplete capsule - thin connective tissue around the thyroid, which is best observed anteriorly as an echogenic line orthogonal to the ultrasound beam. Each thyroid lobe is posterolateral to the carotid sheath, which has the common carotid artery medially and the internal jugular vein laterally. Thyroid extension anterior to the common carotid artery in a transverse plane shows gland enlargement. The left thyroid lobe exhibits the esophagus positioned posteriorly to it. A transverse scan shows its multilayered gut characteristic. Figure 14.2 displays normal transverse thyroid and its neighboring structures.

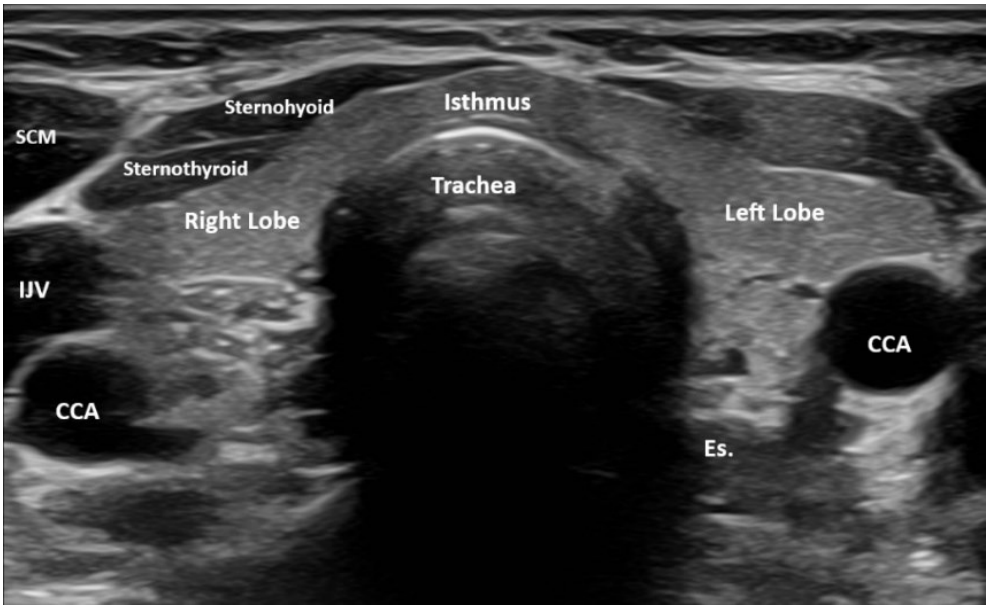

Fig. 14.2: Normal Thyroid Ultrasonography – transverse scan. CCA = Common carotid artery; IJV = internal jugular vein; SCM = sternocleidomastoid muscle; Es.= esophagus.

Besides echogenicity, evaluating vascularity is an important part of thyroid ultrasound. Normal thyroid tissue generally exhibits a specific vascular pattern, characterized by blood flow focused in the gland's periphery. This vascular pattern aids in distinguishing normal thyroid tissue from pathological alterations, such as thyroiditis or neoplasms, which may have modified vascularity.

Size and Volume: Typically, each lobe measures roughly 5x2x2 cm (sagittal, anteroposterior, transverse), with the isthmus up to 0.3 cm in the anteroposterior diameter. The size of the thyroid gland can vary significantly among individuals, but it is essential to establish reference ranges for normal thyroid volume based on ultrasound measurements. The average volume of the thyroid gland in healthy adults typically ranges from 10 to 20 mL, depending on factors such as age, sex, and body surface area.

Thyroid Elasticity: Elastography assesses thyroid stiffness, with healthy glandular tissue typically being soft. This is reflected by an Asteria score of 1 (completely soft image) on strain elastography (SE). Published data indicates that typical thyroid stiffness measurements using two-dimensional shear-wave elastography (2D SWE) techniques are approximately 9.0 ± 11.3 kPa or 13.5 ± 3.3 kPa, depending on the study and methodology applied.

2.1. Ultrasound Evaluation in Diffuse Thyroid Disease (DTD)

2.2. Ultrasound as a Diagnosis Tool - DTD versus Normal Thyroid Gland

Thyroid ultrasound has proven useful in identifying asymptomatic DTD by revealing significant differences compared to normal thyroid tissue. These include variations in echogenicity, texture, gland thickness, margins, and vascularity.

In B-mode, DTD often appears on ultrasound as a gland with uneven echotexture and reduced echogenicity, which is considered a reliable indicator of autoimmune thyroid disease. In autoimmune thyroiditis or Hashimoto's thyroiditis (HT), the gland may show a patchy hypoechoic pattern, echogenic streaks, micronodular texture, or a giraffe-skin aspect. Early stages can present with a normal or enlarged gland, while advanced cases may develop fibrosis, irregular margins, hyperechoic bands, and reduced volume. Some studies suggest that a single ultrasound feature can be highly accurate in detecting DTD. Other research suggests that the presence of at least three ultrasound abnormalities—such as hypoechogenicity, heterogeneous texture, increased vascularity, increased AP diameter, and irregular gland margins—strongly indicates DTD, frequently associated with Hashimoto's or chronic lymphocytic thyroiditis. This approach improves diagnostic confidence when assessing patients with suspected DTD. On Color Doppler ultrasound, autoimmune thyroiditis can display a spectrum of vascular modifications ranging from increased, normal, to reduced blood flow. These variations are influenced by factors such as serum TSH levels and the time elapsed since disease onset. Elevated intraglandular flow is often noted in the early, active phases, whereas vascularity tends to decrease in atrophic stages. Extensive research has shown that thyroid stiffness measured by elastography in individuals with HT is significantly elevated compared to healthy thyroid tissue, with average 2D-SWE values reported between 19.5 ± 6.8 kPa and 36.15 ± 18.7 kPa. Comparable results have been documented in pediatric populations as well. Fig.3 displays a multiparametric ultrasound evaluation of a DTD case.

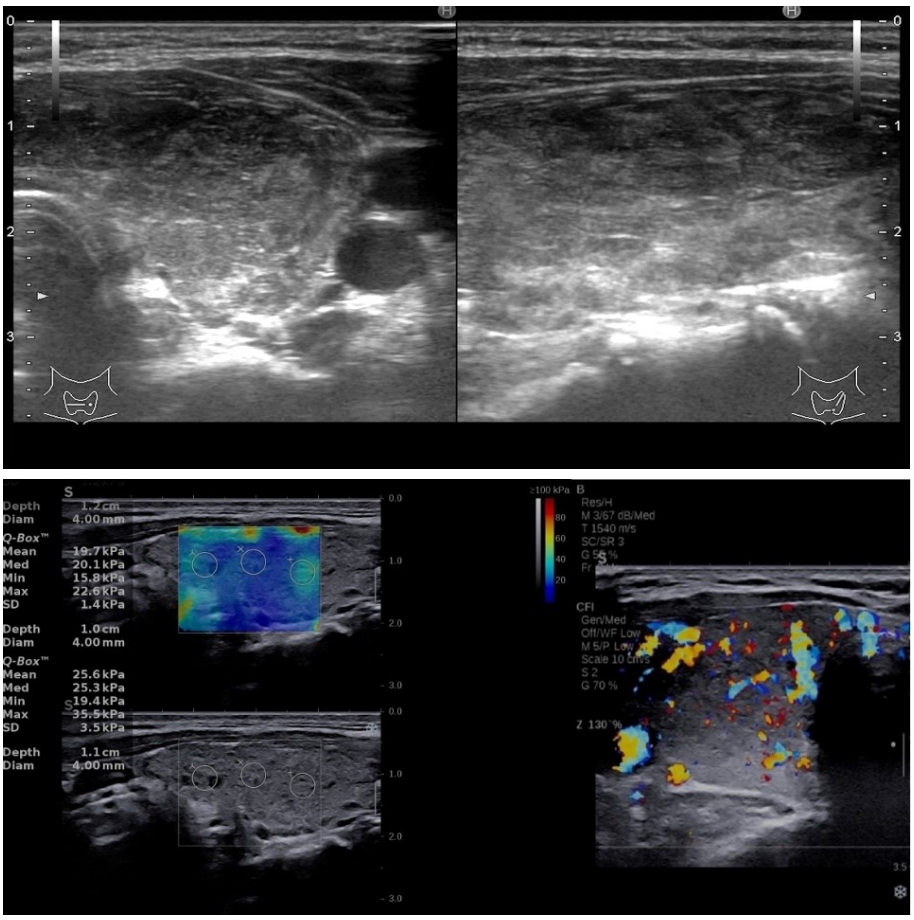

Fig. 14.3: Ultrasound assessment in a patient with Hashimoto's Disease. Upper left – transverse view of left thyroid lobe (LTL) and upper right – longitudinal view of LTL: inhomogeneous, hypoechoic appearance with lines of fibrosis; lower left: shea-wave elastography assessment of thyroid parenchyma: 19.7 kPa and 25.6 kPa mean elasticity; lower right: Color Doppler assessment showing diffusely increased vascularity.

Graves' disease typically shows uniform hypoechogenicity with increased vascularity and increased volume, while subacute thyroiditis reveals poorly defined hypoechoic zones with diminished blood flow resembling merging patches usually with normal volume.

Biochemical tests are key to distinguishing Graves' disease, Hashimoto's thyroiditis, and other thyroiditis types based on hormonal and antibody patterns. Graves' shows high thyroid stimulating antibodies (TSI) with hyperthyroidism, Hashimoto's presents anti-thyroperoxidase (ATPO) and antithyroglobulin (ATG) antibodies with variable thyroid function, while subacute or silent thyroiditis often lacks antibodies but shows transient hyperthyroidism. Overlapping clinical profiles can occur, requiring comprehensive evaluation.

Differentiating Hyperthyroidism: Hyperfunction versus Destructive Thyroiditis (Multiparametric US Approach)

Destructive thyroiditis includes subacute (SAT) or De Quervain's, silent, painless, postpartum, drug-induced, and radiation-induced forms, all causing follicular disruption and hormone leakage without increased production. Ultrasound can support diagnosis by helping distinguish destructive forms from hyperproduction - Graves' disease and other hyperthyroid states based on structural and vascular patterns.

On B-mode ultrasound, Graves' disease typically shows a diffusely enlarged, with smooth contours, uniformly hypoechoic texture due to increased vascularity and lymphocytic infiltration, while destructive thyroiditis often displays patchy, ill-defined hypoechoic regions with asymmetric or lobar involvement, the heterogeneous echogenicity being explained by the inflammatory changes (Fig. 14.4). Gland volume in Graves' is typically increased, but can also be normal, whereas destructive forms may present with normal or slightly increased size, later becoming smaller as inflammation subsides. Graves' tends to have more diffusely homogeneous changes, whereas destructive processes create a more irregular parenchyma.

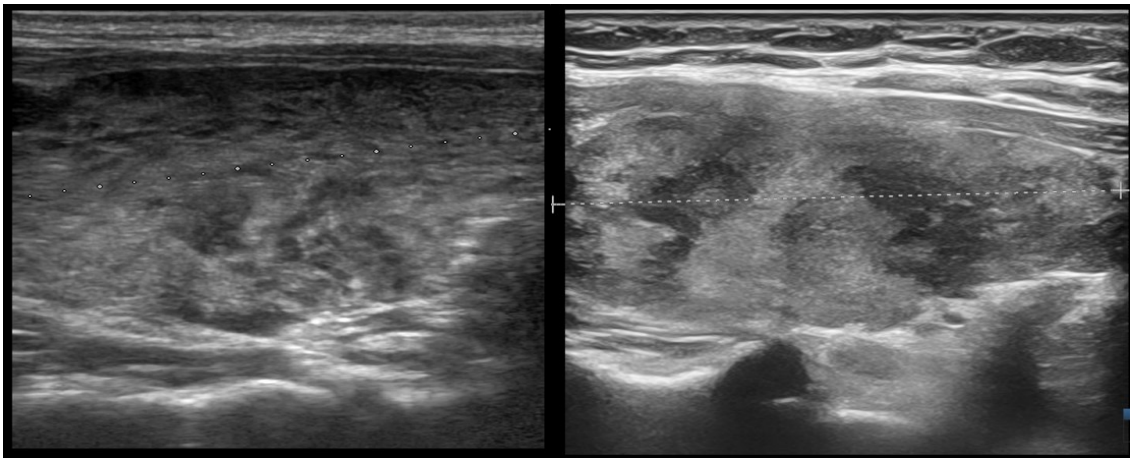

Fig. 14.4: B-mode Graves disease with diffuse hypoecogenicity (left),
subacute thyroiditis with patchy inhomogeneous appearance (right)

Graves' disease is distinctly characterized by diffusely enhanced intrathyroidal perfusion, a hallmark feature readily identified on Color Doppler imaging, Fig. 14.5. This pattern, often described as a "thyroid inferno," reflects the hyperdynamic state of the gland. Destructive thyroiditis presents a more dynamic vascular profile depending on the disease phase. During the acute inflammatory stage, Color Doppler might reveal increased perfusion. However, as the condition progresses, vascularity typically declines, correlating with hypoechoic, damaged areas seen on grayscale ultrasound. Upon recovery, a heterogeneous pattern may emerge, with both revascularized regions and zones of diminished flow.

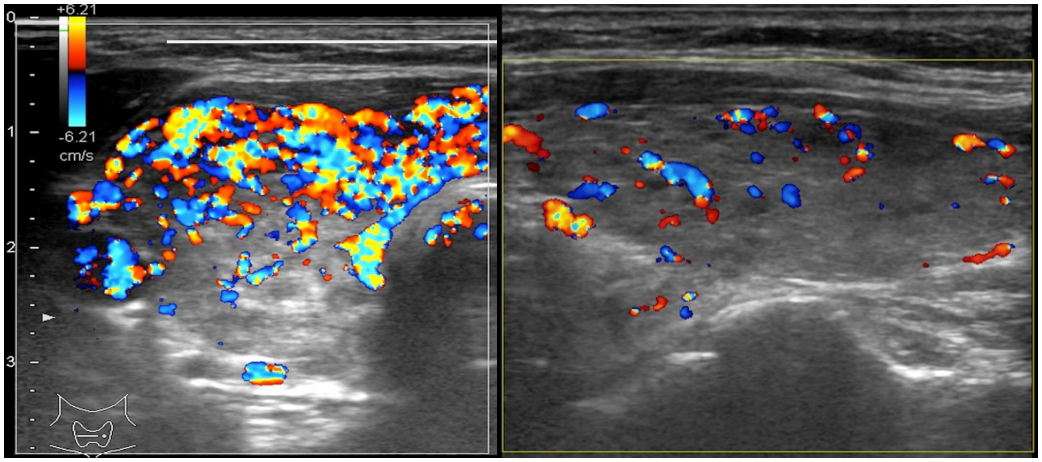

Fig. 14.5: Color Doppler ultrasound of the thyroid in a case with Graves Disease and markedly increased vascular pattern (right) and slightly increased vascular pattern (left).

Spectral Doppler ultrasound (SD) complements Color Doppler by offering a quantitative evaluation of blood flow velocities in thyroid arteries, proving especially valuable in differentiating Graves' disease from other types of thyroiditis. Measuring Peak Systolic Velocity (PSV) in the superior thyroid arteries bilaterally is a widely accepted approach. Proper technique involves maintaining the Doppler angle at or under 60° and ensuring the correction aligns with the blood flow direction. PSV values, expressed in cm/s, have demonstrated a strong correlation with radioactive iodine uptake on diagnostic thyroid scintigraphy at both 3-hour and 24-hour evaluations, reinforcing the reliability of this method. Research suggests a PSV threshold between 40-50 cm/s can effectively distinguish Graves' disease from other thyroid inflammatory disorders. In Graves' disease, thyroid tissue typically exhibits low stiffness, with elasticity values comparable to normal thyroid, averaging between 11.6–17.4 kPa. Elastography proves particularly useful in distinguishing SAT from other thyroid disorders, as SWE measurements in SAT often exceed 100 kPa, contrasting sharply with the values observed in autoimmune thyroid diseases, which generally remain below 25 kPa – figure 6. This marked difference is reflected in AUC values, with SWE achieving an AUC of 0.989 when differentiating SAT from Graves' disease, whereas its performance is more limited when distinguishing Graves' disease from Hashimoto's thyroiditis (HT) (AUC 0.549) or normal thyroid tissue. Nonetheless, elastography can assist in separating Graves' disease from SAT (AUC 0.953; mean elasticity in SAT < 24 kPa), though overlap may still occur in certain cases involving Graves’ disease and HT.

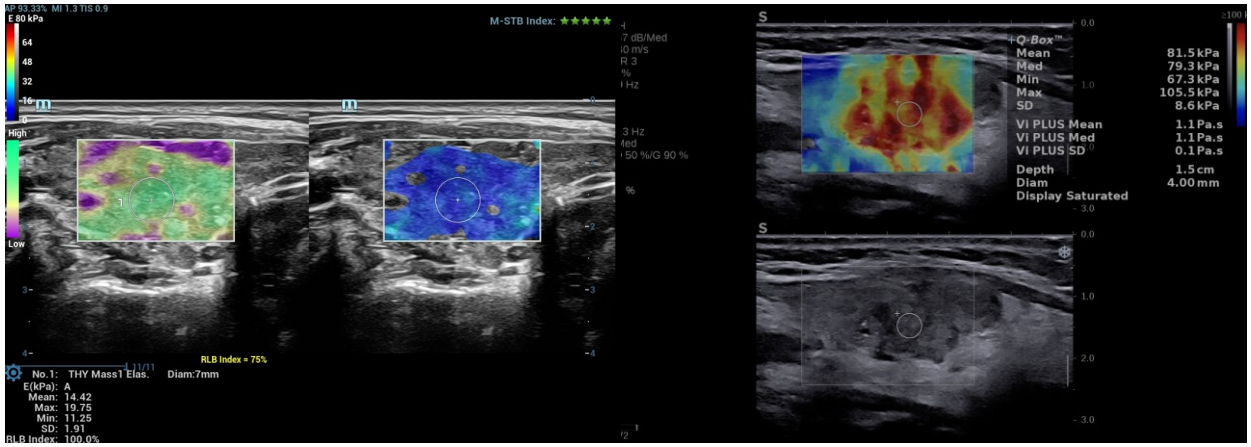

Fig. 14.6: 2D-shear wave elastography evaluation showing soft thyroid parenchyma, 14.42 kPa (left) - GD and markedly increased stiffness 81.5 kPa (right) – SAT

The MPUS approach enhances diagnostic precision and supports more individualized management of DTD. Combining various ultrasound techniques with laboratory findings allows for a detailed assessment, facilitating targeted treatment strategies. This integrated methodology shapes the future direction of thyroid diagnostics and patient care.

2.2.1. Ultrasound in Staging/Monitoring the Evolution of Disease

Evolution of Autoimmune thyroiditis: Autoimmune thyroiditis can show different ultrasound patterns over its course. In the early phase, inflammation but also an increased TSH may cause the thyroid to enlarge and exhibit increased vascularity. However, as the disease progresses, chronic inflammation leads to fibrosis, resulting in a smaller gland with reduced blood flow suggesting minimal thyroid function – Fig. 14.7.

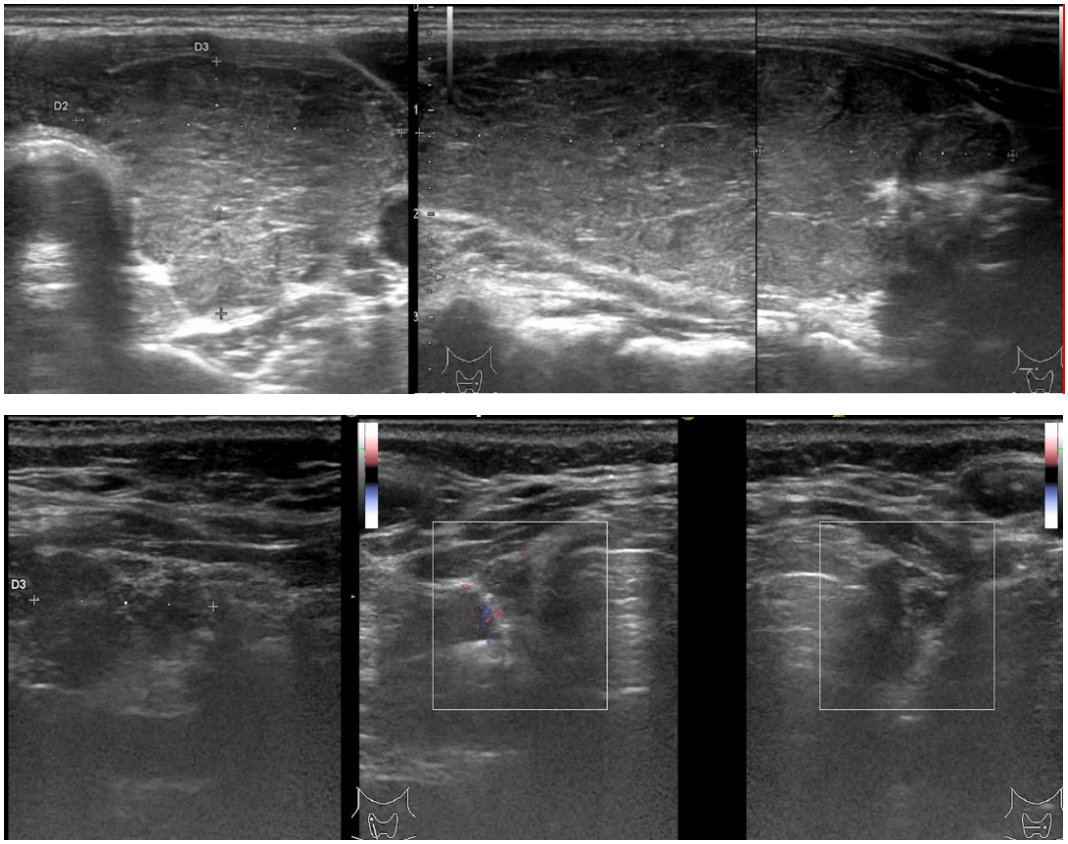

Fig. 14.7: CAT cases: upper left – tranverse and right dual longitudinal view side-by-side in a case with Hashimoto, thyroid volume 45 ml; lower left – longitudinal and right dual view tranverse side-by-side in a case with atrophic thyroiditis, thyroid volume 45 ml;

Evolution and Monitoring Graves Disease: Ultrasound is essential for monitoring Graves' disease during treatment. Serial thyroid volume measurements track gland shrinkage as hyperactivity subsides, and Doppler often shows a decrease in the characteristic "thyroid inferno" as blood flow normalizes. Even when hormone levels normalize with treatment, ultrasound markers—especially vascularity—often remain elevated. This persistent vascularity may signal an increased risk of relapse, suggesting that ultrasound can help predict recurrence even in biochemically controlled patients as seen in Fig. 14.8.

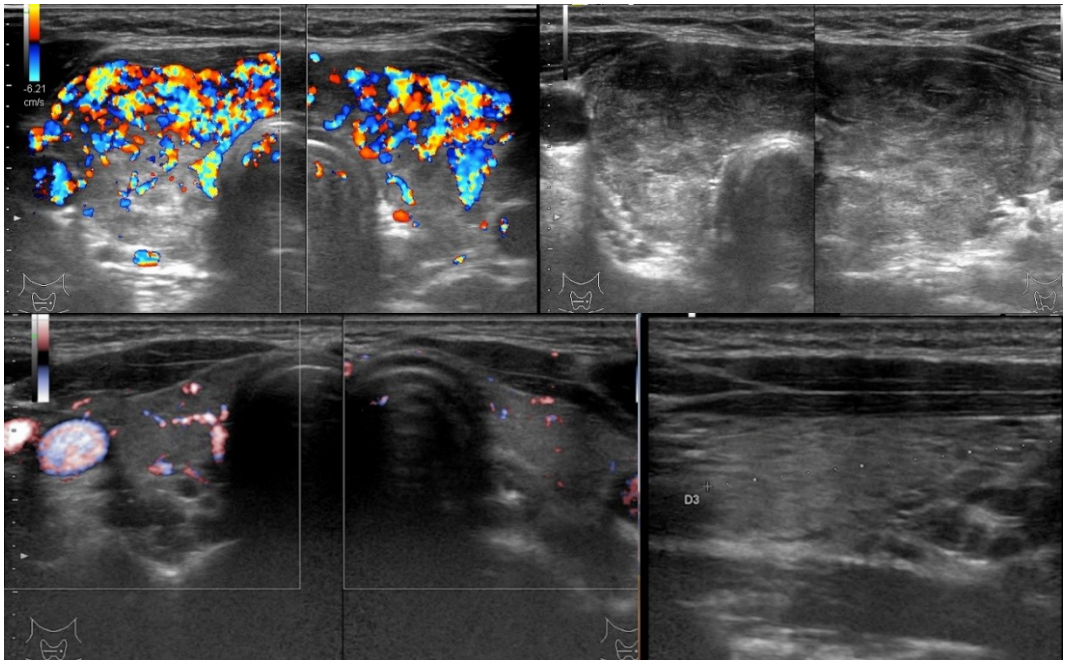

Fig. 14.8: Thyroid B-mode ultrasound (upper right) showing increased thyroid volume (40 ml) and thyroid inferno in Color Doppler (upper left) – active Graves' Disease; and normalized volume (15 ml) B-mode longitudinal view (lower right) and normal vascular pattern (lower left) – inactive Graves' disease.

Monitoring subacute thyroiditis: Ultrasound is an excellent tool for monitoring subacute thyroiditis. Beyond the typical diagnostic features, elastography adds valuable insights by assessing tissue elasticity. A normalization of elasticity, Fig. 14.9 - diffusely or in patches—suggests resolution of inflammation, while a renewed increase in elasticity following treatment discontinuation may serve as an early indicator of relapse.

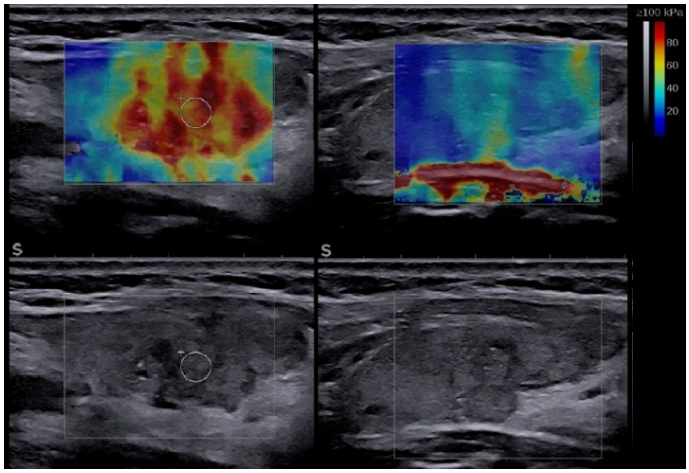

Fig. 14.9: Evolution of a case with subacute thyroiditis; initial assessment (left) showing very increased stiffness (mostly red on the color map) and evaluation after 90 days-resolution showing mostly blue-green color map (right)

2.3. Ultrasound evaluation of thyroid nodules

Thyroid nodular disease is frequently encountered in endocrine practice, with ultrasound revealing nodules in over half of the population, underscoring the ongoing challenge of accurately distinguishing benign from malignant lesions—an increasingly critical task given the rising incidence of thyroid cancer and the widespread use of imaging leading to earlier detection. The initial step is determining the presence or absence of nodules; if a nodule is identified, it must then be carefully characterized using a standardized approach.

Standardized Reporting in Thyroid Ultrasound: The Role of TI-RADS

Implementing a uniform reporting system in thyroid ultrasound is key to improving diagnostic precision and ensuring consistency across clinical settings. The Thyroid Imaging Reporting and Data System (TI-RADS) has become a fundamental tool in this regard, offering a structured terminology to describe sonographic nodule characteristics. This standardized approach aids in malignancy risk stratification and assists in determining the necessity for fine-needle aspiration (FNA). Studies have demonstrated that non-standardized descriptions often omit important nodule features, whereas adopting TI-RADS improves documentation and risk evaluation. Additionally, it reduces the frequency of unnecessary biopsies while preserving a high sensitivity for cancer detection. Beyond enhancing reporting uniformity, TI-RADS contributes to practitioner education by promoting an objective, feature-based evaluation process. This is particularly valuable in settings with limited specialized expertise. Research has consistently validated the system's accuracy, showing strong alignment with histopathological outcomes.

Thyroid ultrasound reports should consistently include details on the gland's overall appearance, volume, the presence or absence of nodules, their number and for each described lesion the dimensions, position, extracapsular relationships, and a thorough description of nodule features. These features include internal composition (solid, cystic, spongiform or mixed), shape (taller-than-wide or wider-than-tall), margins, echogenicity, echotexture (homogeneous or inhomogeneous), the presence of echogenic foci (comet-tail artefacts, micro or macrocalcifications) and vascular pattern on Doppler evaluation (absent, peripheral, mixed).

Certain ultrasound characteristics are strongly associated with malignancy, particularly in papillary thyroid carcinoma (PTC). These include a predominantly solid structure, microcalcifications, irregular or spiculated margins, marked hypoechogenicity, extrathyroidal extension, and a "taller-than-wide" shape (an anteroposterior diameter greater than the transverse). Follicular thyroid carcinomas (FTC) often resemble benign follicular adenomas on imaging. However, FTCs more frequently exhibit a solid composition, absent or irregular halo, hypoechogenicity, heterogeneous texture, and intranodular calcifications. There is no classic ultrasound pattern described for medullary thyroid carcinoma (MTC). Small studies have reported variable results, although some suggest that MTCs may occasionally share features with PTC, such as hypoechogenicity, a solid structure, and microcalcifications. Conversely, findings more suggestive of benignity include smooth margins, a homogeneous isoechoic appearance in a solid nodule, a spongiform appearance, and purely cystic composition. High-risk features suggestive of malignancy are represented in Fig. 14.10.

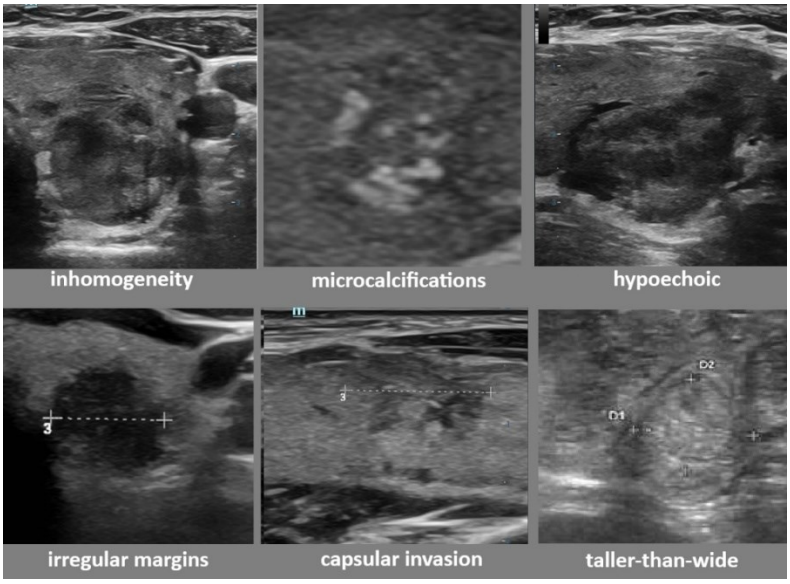

Fig. 14.10: High-risk features of malignancy: intranodular inhomogeneity, microcalcifications, intense hypoechogenicity, irregular or lobulated margins, thyroid capsule invasion, and taller-than-wide shape.

Selecting Nodules for Thyroid FNA

The latest 2023 European Thyroid Association (ETA) recommendations provide clear criteria for determining when fine-needle aspiration (FNA) is warranted, relying on nodule ultrasound appearance and size. Nodules classified as very low risk, such as pure cystic or entirely spongiform lesions, generally do not require FNA, unless intervention is considered for symptom relief or cosmetic reasons. Low-risk nodules, typically iso- or hyperechoic without suspicious features, should undergo FNA if >20 mm. Intermediate-risk nodules, usually mildly hypoechoic without other worrisome US features, require FNA if >15 mm, while high-risk nodules, displaying at least one suspicious characteristic (e.g., microcalcifications, irregular margins, marked hypoechogenicity, or taller-than-wide shape), warrant FNA if >10 mm. FNA is also recommended regardless of nodule size and risk category if pathological lymph nodes are detected or if extrathyroidal extension is suspected. For high-suspicion nodules between 5–10 mm, FNA should be considered if suspicious lymph nodes or signs of extrathyroidal spread are present. Compared to AACE (2016) and ATA (2015), the ETA approach is similar, though AACE allows FNA in 5–10 mm high-risk nodules more flexibly, and ATA also favors FNA in intermediate-risk nodules >10 mm. The Korean guidelines (2016) are more inclined to biopsy high-risk nodules <10 mm, aiming to reduce long-term surveillance.

Nodules considered benign based on ultrasound features may be monitored with follow-up ultrasound at intervals of 6 to 18 months, with subsequent evaluations potentially spaced further apart (e.g., every 3 to 5 years), depending on initial nodule size, patient risk factors, and stability over time.

Monitoring Thyroid Nodules Over Time

For nodules not requiring immediate intervention, follow-up ultrasound aims to detect significant growth and any changes suggesting increased malignancy risk. Growth is considered relevant if there is: a) ≥20% increase in at least two perpendicular diameters, with a minimum change of 2 mm, or b) volume increase exceeding 50% compared to the previous evaluation. During follow-up, any alterations in ultrasound characteristics that might change the malignancy risk stratification should prompt reassessment. Cervical lymph nodes, particularly in the lateral neck compartments, should also be reviewed periodically to detect any suspicious changes. Ultrasound features suggesting malignancy in cervical lymph nodes in patients with differentiated thyroid cancer include cystic changes, microcalcifications (hyperechoic punctuations), absence of hilum, round shape (long-to-short axis ratio <2), hypoechogenicity, and peripheral vascularity. Cystic appearance and microcalcifications are highly specific, while peripheral vascularization offers better sensitivity and specificity balance. Evaluation should consider multiple features for accurate malignancy detection. Additionally, re-evaluation is advised if the patient develops local compressive symptoms (e.g., dysphagia, neck tightness) or voice changes, which may indicate nodule enlargement or extrathyroidal extension.

Multiparametric US-Based Evaluation – Risk upgrade

Ongoing developments, such as the incorporation of elastography and contrast-enhanced ultrasound (CEUS) into risk assessment, hold great potential to enhance TI-RADS by improving diagnostic precision and reducing unnecessary biopsies; however, while these techniques are not yet standardized or guideline-integrated, growing evidence strongly supports their significant value when available in clinical practice.

Given their diagnostic utility but notable limitations, both elastography and CEUS are currently considered only for risk upgrade in clinical practice, without supporting evidence for downgrading nodules based on their findings.

Thyroid Elastography: Strain Elastography (SE) evaluates tissue stiffness by measuring deformation under compression, using qualitative scoring systems (e.g., Asteria, Rago) or semiquantitative strain ratio (SR) for more objective assessment. Meta-analyses report sensitivity of 84–89% and specificity of 80–90%, though cutoff values for SR (commonly >2–4) vary by equipment. Combining SE with grayscale ultrasound, meaning considering high stiffness as an additional high-risk ultrasound feature, has shown improved diagnostic accuracy in some studies. However, large nodules, micro-nodules, calcifications, and follicular carcinomas may reduce reliability. Operator dependency and technical variability limit SE's inclusion in risk stratification systems. Figure 11 shows the colormap on strain in nodules with no risk upgrade in the case of a soft nodule and with risk category upgrade in the case of a stiff nodule (SE).

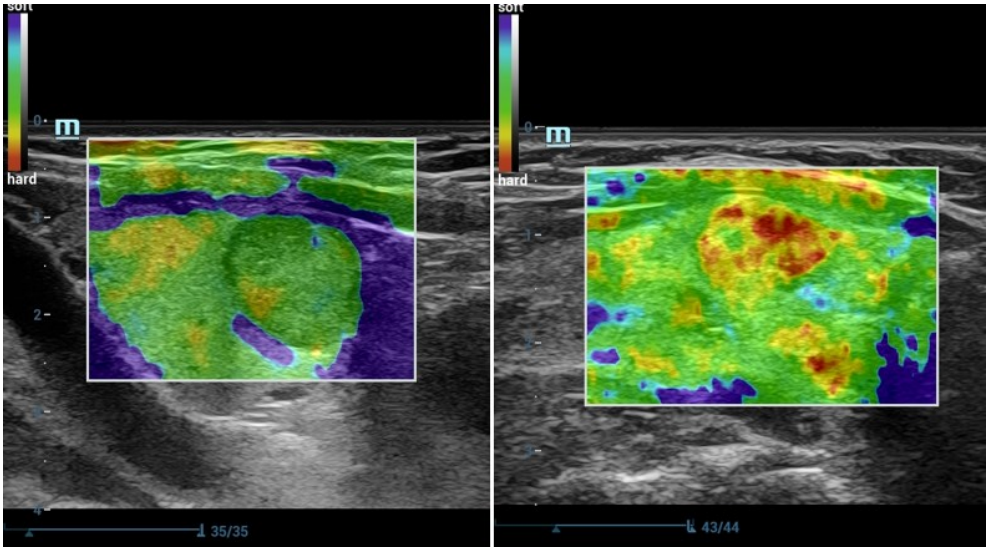

Fig. 14.11: Strain elastography map depicting a soft nodule Asteria score 1 in the left image, with no risk upgrade and a mostly stiff nodule Asteria score 3 in the right image with risk category upgrade.

2D-SWE offers quantitative stiffness assessment, making it less operator-dependent and more reproducible than SE. It uses acoustic impulses to induce shear waves, with tissue stiffness measured as shear wave velocity (m/s) or elasticity index (kPa). 2D-SWE provides color-coded elasticity maps with stiffness parameters as elasticity indices (EI): EI mean, EI max, EI min, while point SWE (pSWE) gives a single velocity reading in a region of interest. For evaluating nodule stiffness, EI mean is most reliable in 2D-SWE, though cutoff values vary (e.g., ≥34.5–42.1 kPa). High stiffness values or EI ratios comparing nodule to normal tissue may suggest malignancy – see figure 14.12.

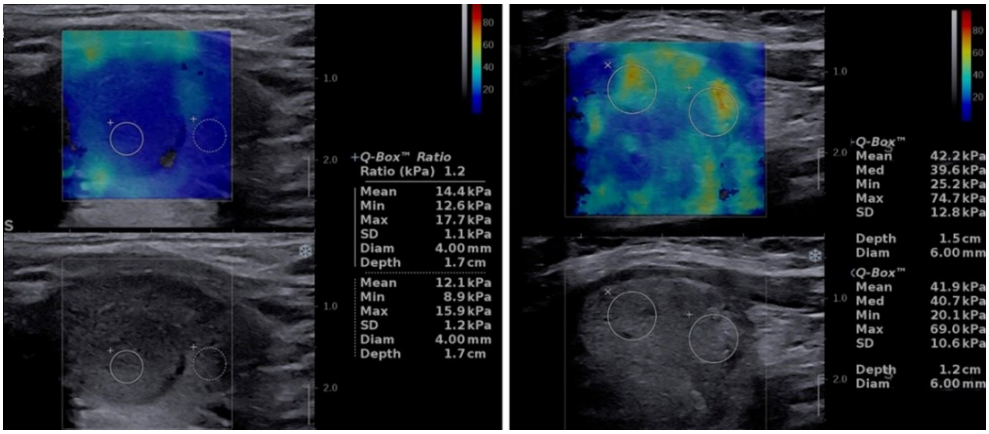

Fig. 14.12: Elasticity assessment in intermediate risk nodules: left image – low EI, no risk upgrade; right image increased EI, risk category upgrade; EI = elasticity index.

Thyroid CEUS: Microbubble contrast agents used in CEUS are well-tolerated and safer than CT or MRI contrast, with no risk of kidney damage and allergic reactions occurring in less than 0.01% of cases. For thyroid evaluation, a small dose of 1.0–2.0 mL of contrast agent is given intravenously, followed by 5–10 mL saline; repeated doses may be needed for multiple nodules.

In qualitative CEUS evaluation of thyroid nodules, malignant features include hypoenhancement, inhomogeneous enhancement, incomplete enhancement, absence or irregular peripheral ring, centrifugal or non-concentric wash-in, and early washout, with hypoenhancement and early washout being particularly important indicators of malignancy. Benign characteristics are isoenhancement or hyperenhancement, homogeneous enhancement, complete enhancement, a regular, intense peripheral ring, and centripetal wash-in, suggesting organized vascularity. While quantitative parameters can be obtained through post-processing software, most studies have shown little added value over qualitative assessment, making real-time visual interpretation the primary diagnostic approach. Figure 13 presents typical malignant and benign CEUS patterns.

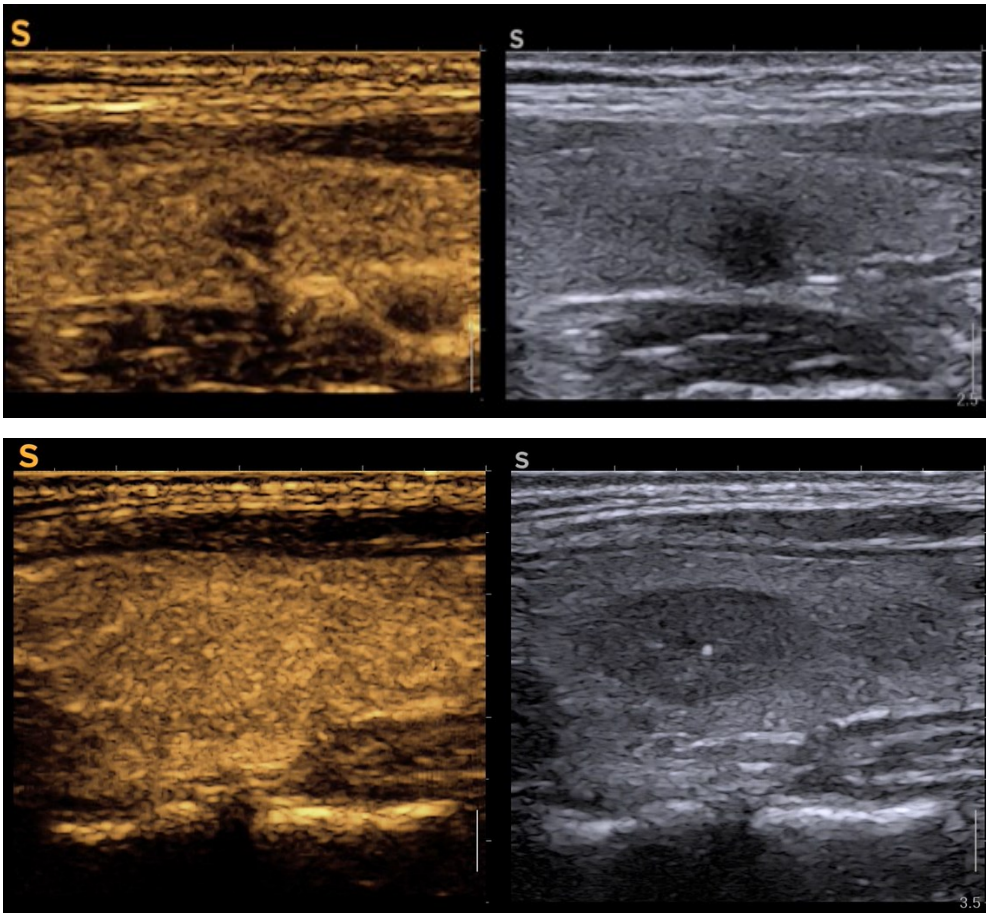

Fig. 14.13: CEUS patterns in a high-risk nodule (PTC) with no peripheral ring, blurred marginal enhancement, intense hypoechoic intramodular enhancement in the left upper image and corresponding B-mode image on the upper right; a low risk nodule (follicular adenoma) enhancement pattern on the lower right with heterogeneous enhancement, with a fine, peripheral hyperenhanced ring

CEUS can also help in evaluating thermal ablation treatments, such as laser, RFA, microwave, and HIFU, used for benign thyroid nodules, recurrent thyroid cancer, and metastatic lymph nodes, by distinguishing viable from nonviable tissue, improving assessment of the ablation zone and follow-up. CEUS is a promising tool for distinguishing malignant from benign thyroid nodules by visualizing microvascularity. However, its clinical use depends on standardizing protocols, addressing technical limitations and ensuring operator expertise.

3. Postoperative Follow-Up Using Ultrasound

US is the preferred imaging modality for the postoperative evaluation of the neck region following thyroidectomy; it is crucial for monitoring potential complications, assessing the surgical site, and detecting residual or recurrent disease.

US allows prompt detection of postoperative complications such as hematomas, seromas, abscesses, and surgical site infections. Fluid collections typically present as anechoic or hypoechoic areas, while abscesses may show internal debris and increased Doppler vascularity. Hematomas may appear hyperechoic in the acute phase and become more complex over time. Cervical lymph node assessment (figure 14.14) is critical for identifying metastases. Suspicious features include hypoechogenicity, loss of the fatty hilum, microcalcifications, cystic changes, and peripheral or chaotic vascularity on Doppler examination.

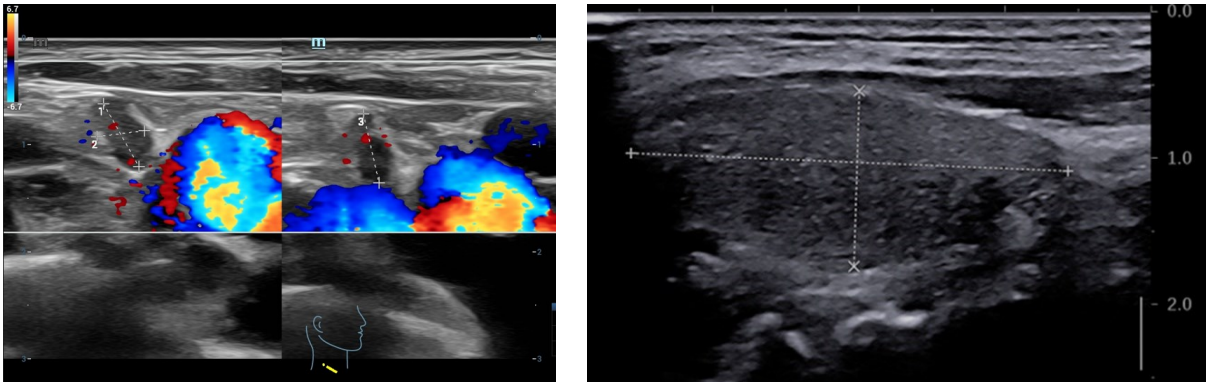

Fig. 14.14: Cervical lymph-node ultrasound in a patient with thyroidectomy after medullary thyroid cancer showing lymph node metastasis: vertical shape, hypoechoic, no hylum (left); lymph node metastasis of a PTC after total thyroidectomy in another patient with isoechoic, parenchymatous structure and microcalcifications (right).

Residual thyroid tissue may be detected in the thyroid bed as hypoechoic remnants (see figure 14.15), occasionally containing nodules. Recurrent disease may exhibit irregular margins, increased Doppler flow, and microcalcifications. Elastography can help distinguish recurrent malignancy (stiff) from benign residual tissue (soft), but also to detect lymph node metastasis.

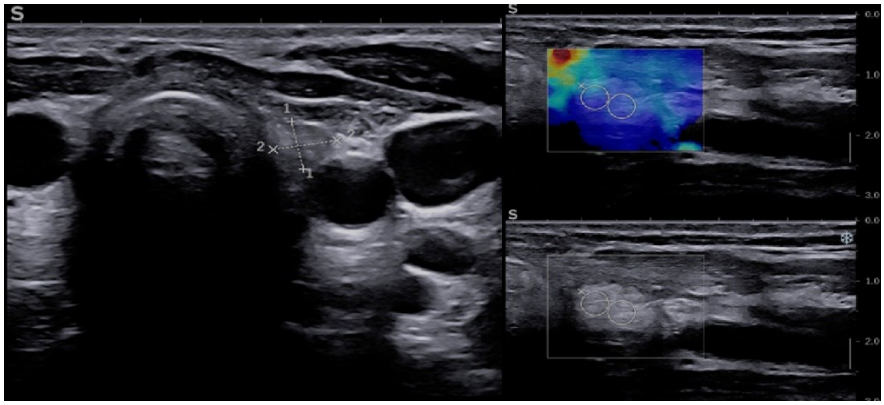

Fig. 14.15: cervical ultrasound showing residual thyroid tissue with involution, no nodules, soft appearance in SWE.

Ultrasound surveillance is typically performed every 6 to 12 months, depending on the patient's risk profile and clinical status. High-risk patients or those with biochemical evidence of disease (elevated thyroglobulin levels and history of differentiated cancers) may require more frequent evaluations.

4. Anatomical Anomalies of the Thyroid

Because of its embryological development and growth pathway, the thyroid is prone to various structural abnormalities. These variations may significantly impact clinical evaluation, management, and surgical approaches.

Complete agenesis is the absence of the entire thyroid gland, appearing as an empty thyroid fossa on ultrasound (figure 14.16), often detected in neonates with congenital hypothyroidism. Isthmus agenesis presents as separated thyroid lobes without a connecting bridge, while hemiagenesis shows the absence of one lobe, most often the left. In hemiagenesis, the remaining lobe is often hypertrophic with increased vascularity on Doppler due to compensatory function.

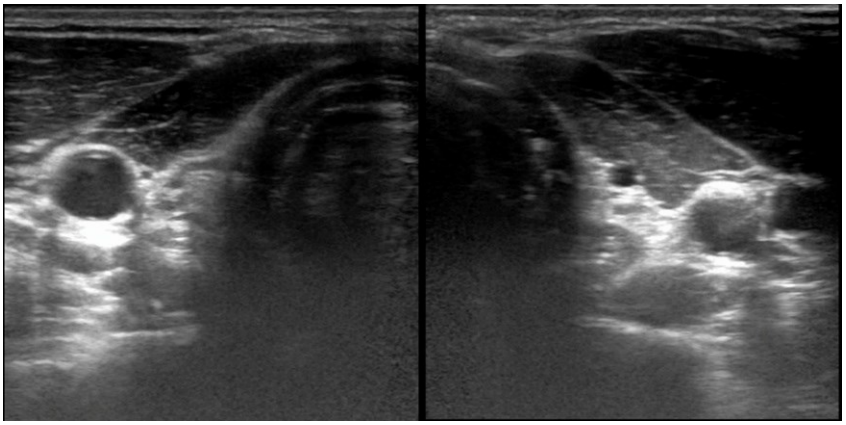

Fig. 14.16: Cervical ultrasound showing complete agenesis of the thyroid.

Ectopic thyroid tissue should be suspected in patients with a normal or absent thyroid gland in its usual position, particularly those with congenital hypothyroidism or a midline neck mass. Ultrasound reveals it as a homogenous, hypoechoic mass with echogenicity similar to normal thyroid tissue (figure 14.17). Common locations include the sublingual, submandibular, and pretracheal regions. Doppler imaging typically shows internal vascular flow, aiding in differentiation from cystic or lymphatic lesions.

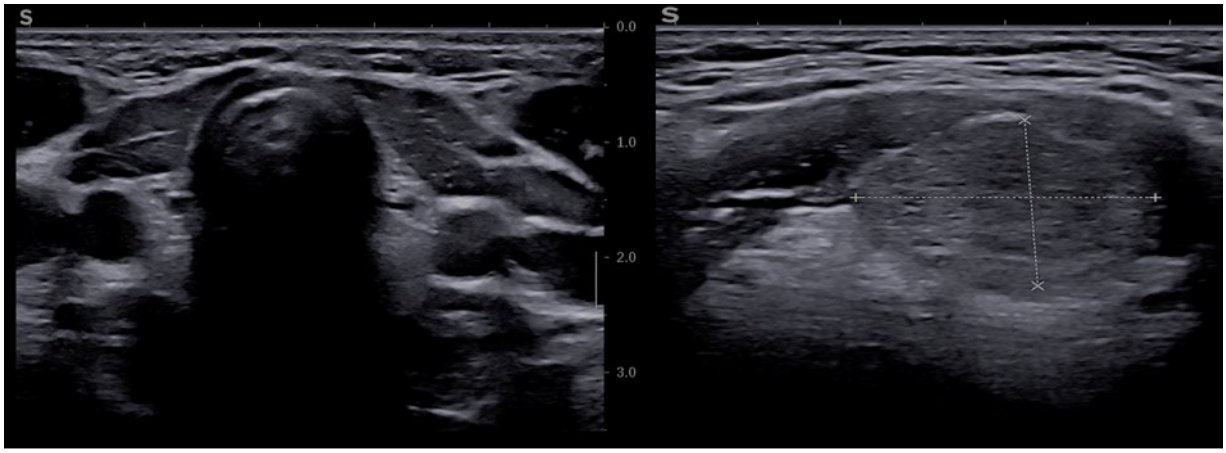

Fig. 14.17: Ultrasound showing no cervical thyroid tissue (left) and sublingual scan suggesting ectopy (right)

The pyramidal lobe is a common anatomical variant, seen in up to 50% of individuals, extending cranially from the isthmus toward the hyoid bone. On ultrasound (figure 14.18), it appears as a hypoechoic, tapering structure with vascular flow on Doppler. Clinically, it is important in thyroid surgery, as unrecognized pyramidal lobe tissue can lead to incomplete resection and disease recurrence, particularly in malignancy. It can also be involved in diffuse thyroid diseases like Graves' or Hashimoto's, requiring careful evaluation during imaging.

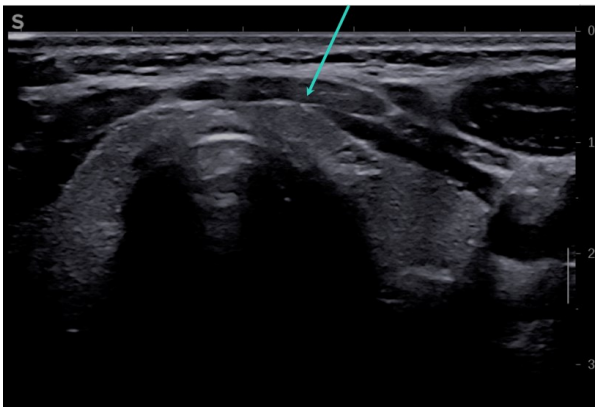

Fig. 14.18: Transverse thyroid scan showing anterior to the isthmus – the pyramidal lobe.

A thyroglossal duct cyst is a common congenital anomaly resulting from incomplete closure of the thyroglossal duct during thyroid descent. It typically presents as a painless, midline neck mass near the hyoid bone, which may move with swallowing or tongue protrusion. While generally benign, it can become infected, requiring drainage or surgical removal. On ultrasound, it appears as a well-defined, anechoic or hypoechoic cyst, sometimes with internal debris if infected. Differentiation from ectopic thyroid tissue or lymphadenopathy is essential for proper management.

Zuckerkandl's tubercle is a posterior thyroid projection, best seen on ultrasound (figure 14.19) as a focal bulge near the cricoid, adjacent to the recurrent laryngeal nerve. Its size varies, and an enlarged tubercle may suggest underlying pathology. Recognition is crucial in surgery to avoid nerve injury during thyroidectomy.

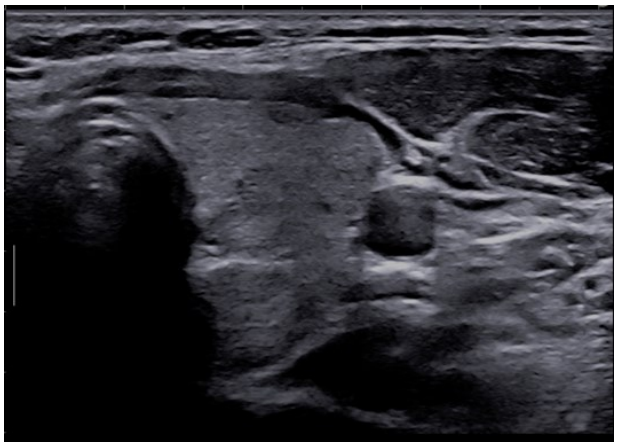

Fig. 14.19: Transverse thyroid scan of left thyroid lobe showing posterior to the lobe – the Zuckerkandl tubercle.

5. Parathyroid Ultrasound Aspects

Visualizing normal parathyroid tissue: High-resolution ultrasound enables real-time identification of normal parathyroid glands (figure 20), facilitating their preservation during thyroid surgery and reducing the risk of postoperative hypoparathyroidism. Normal parathyroid glands appear as well-defined, oval, hyperechoic or isoechoic nodules with minimal vascularization, while shear wave elastography showing very soft tissue further enhances differentiation from surrounding tissues. Beyond surgery, ultrasound is valuable in detecting residual normal parathyroid tissue postoperatively and, in some cases, excluding pathology, aiding in both surgical planning and long-term patient management.

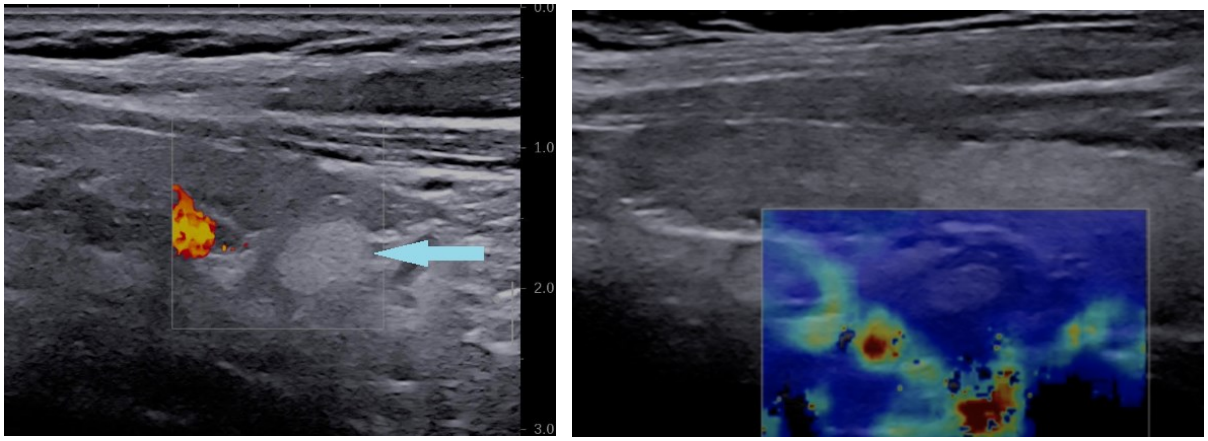

Fig. 14.20. Right inferior normal parathyroid gland: hyperechoic, oval, homogeneous on ultrasound (left); soft on elastography, completely blue color-map (right)

Detecting parathyroid pathology – adenomas and hyperplasia: Parathyroid adenomas typically appear as well-defined, hypoechoic, oval lesions, often located posterior to the thyroid gland. They may exhibit peripheral vascularization on color Doppler imaging and can be further characterized as very soft lesions using SWE to differentiate them from lymph nodes or thyroid nodules. Hyperplastic glands, often seen in secondary and tertiary hyperparathyroidism, tend to be smaller, multiple, and less well-defined. Ultrasound diagnostic accuracy is comparable to or even superior to second-line imaging techniques such as computed tomography or magnetic resonance imaging.

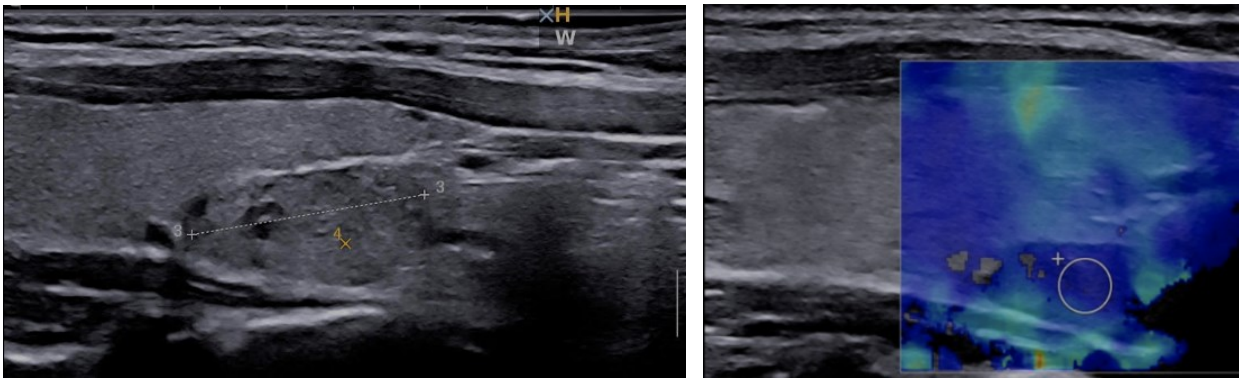

Fig. 14.21. Right inferior parathyroid adenoma, extracapsular hypoechoic, oval structure on ultrasound (left), soft on elastography (right)

Conclusion

Ultrasound remains the cornerstone of thyroid an parathyroid evaluation, offering unmatched real-time, high-resolution imaging of both normal anatomy and pathological changes. Understanding normal sonographic patterns and recognizing anatomical variants prevents misinterpretation and

guides clinical decisions. In diffuse thyroid disease, ultrasound is indispensable for assessing gland texture, vascularity, and volume, while nodular pathology relies on systematic evaluation using risk stratification systems. Elastography refines the assessment of nodule stiffness, aiding malignancy risk estimation, while CEUS enhances the detection of subtle vascular changes and treatment response, especially post-ablation. Mastering these techniques allows for a more accurate, patient-centered, and often non-invasive approach to thyroid diagnosis and management.

Selected references

1. Russ G, Bonnema SJ, Erdogan MF, Durante C, Ngu R, Leenhardt L. European Thyroid Association Guidelines for Ultrasound Malignancy Risk Stratification of Thyroid Nodules in Adults: The EU-TIRADS. Eur Thyroid J 2017;6:225–37.
2. Papini E, Monpeyssen H, Frasoldati A, Hegedüs L. 2020 European Thyroid Association Clinical Practice Guideline for the Use of Image-Guided Ablation in Benign Thyroid Nodules. Eur Thyroid J 2020;9:172–85.
3. Bible KC, Kebebew E, Brierley J, Brito JP, Cabanillas ME, Clark TJ, et al. 2021 American Thyroid Association Guidelines for Management of Patients with Anaplastic Thyroid Cancer American Thyroid Association Anaplastic Thyroid Cancer Guidelines Task Force
4. Haugen BR, Alexander EK, Bible KC, Doherty GM, Mandel SJ, Nikiforov YE, et al. 2015 American Thyroid Association Management Guidelines for Adult Patients with Thyroid Nodules and Differentiated Thyroid Cancer: The American Thyroid Association Guidelines Task Force on Thyroid Nodules and Differentiated Thyroid Cancer. Thyroid 2016;26:1–133.
5. Weller A, Sharif B, Qarib MH, St Leger D, De Silva HSL, Lingam RK. British Thyroid Association 2014 classification ultrasound scoring of thyroid nodules in predicting malignancy: Diagnostic performance and inter-observer agreement. Ultrasound: Journal of the British Medical Ultrasound Society 2019;28:4.
6. Solbiati L, Volterrani L, Rizzatto G, Bazzocchi M, Busilacci P, Candiani F, et al. The thyroid gland with low uptake lesions: evaluation by ultrasound. Https://DoiOrg/101148/Radiology15513883413 1985;155:187–91.
7. Stoian D, Borlea A, Moisa-Luca L, Paul C. Multiparametric ultrasound-based assessment of overt hyperthyroid diffuse thyroid disease. Front Endocrinol (Lausanne) 2023;14:1300447.
8. Durante C, Hegedüs L, Czarniecka A, Paschke R, Russ G, Schmitt F, et al. 2023 European Thyroid Association Clinical Practice Guidelines for thyroid nodule management. Eur Thyroid J 2023;12.
9. Sidhu PS, Cantisani V, Dietrich CF, Gilja OH, Saftoiu A, Bartels E, et al. The EFSUMB guidelines and recommendations for the clinical practice of contrast-enhanced ultrasound (CEUS) in Non-Hepatic Applications: Update 2017 (Long Version). Ultraschall in Der Medizin 2018;39:e2–44. https://doi.org/10.1055/A-0586-1107/ID/JR513-18/BIB.
10. Bena A, Luca LM, Stoian D, Bena A, Luca LM, Stoian D. Contrast-Enhanced Thyroid Ultrasound in Detecting Thyroid Cancer. Ultrasound . in Stoian D, The Next Step in Clinical Evaluation. Intech 2025.

15. US IN PEDIATRIC PATHOLOGY

Blerina Saraci Qirinxhi, Durim Cela, Denis Qirinxhi
WFUMB Center of Education Tirana, Albania

15.1 Introduction

Imaging is a real time, noninvasive, low cost and bedside examination, without ionizing radiation or sedation. Ultrasound is an ideal imaging modality in the pediatric and neonatal population even in premature one.

US is used in all areas of pediatric and neonatal medical diagnosis, such as brain, head, neck, spine, muscle-skeletal, chest/lung, abdomen, pelvis, scrotum, etc.

15.2 Head US

15.2.1 Head US (Trans/cranial access)

Is a method for scanning the human brain using US. We used it almost exclusively in babies because their characteristics like soft spot in infant head, which is called fontanelle, provides an "acoustic window". The maximum age with an open fontanelle is generally 12 months. We mainly use the anterior fontanelle, but the posterior one can be used too. This procedure requires little to no special preparation for the kid. An important limitation for this exam is if we have an active or crying baby which will slow or affect the process, because of the sensitivity to motion US has.

15.2.2 Position and special conditions when you perform Head US.

The kid should be quiet. We can perform the examination in supine position with the head facing up or in prone position with the head turned to either side.

If the kid is in oxygen therapy, it is recommended to keep it as much as possible.

15.2.3 Transducer and scanning technique in Head US.

We can use both linear and microconvex probe to perform the examination.

We use a 3.0 to 5.0 MHz for term and older infants with appropriate acoustic window and 7.5 MHz for preterm infants (less than 1500 g or less than 32 weeks gestation).

In US examination of the infant brain we can scan in coronal and sagittal survey.

Coronal survey starts with the probe perpendicular in anterior fontanelle and then slowly angle the probe anteriorly and then posteriorly, you can take several scan imagines. (recommended 7).

Sagittal survey starts with the probe perpendicular in anterior fontanelle and then slowly angle the probe laterally through the right ventricle and then left ventricle, you can take several scan imagines (recommended 5). Fig. 15.1 and 15.2

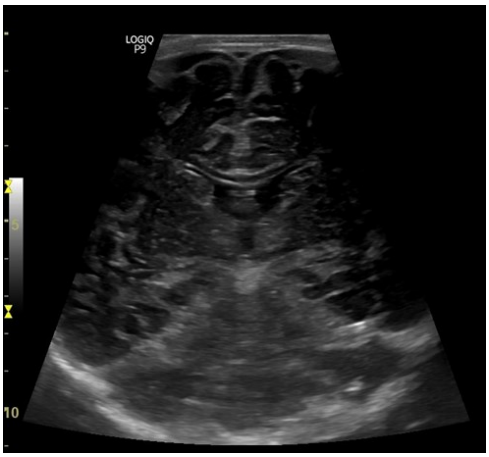

Fig. 15.1 Scan imagines of Lateral Ventricles and Basal Ganglion

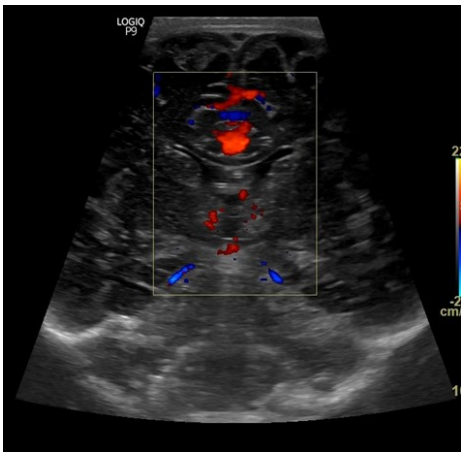

Fig. 15.2 Doppler Evaluation

15.2.4 The most frequent pathologies and ultrasound findings in pediatrics.

15.2.4.1 Peri Ventricular Leukomalacia (PVL) is graded based on periventricular echogenicity and cyst formation. PVL grades 1–3 are more common in preterm infants, while grade 4 is typically seen in full-term babies.

Until now ischemia was thought to be the only cause of PVL, also known as Hypoxic-Ischemic Encephalopathy, but now we know for sure that other causes like infection or vasculitis influence this situation. Early preterm newborn or low-weight premature babies are more at risk of developing PVL gr1, 2 and/or 3, PVL gr 4, seen mostly in full-term babies.

	PVL Gr I	PVL Gr II	PVL Gr III	PVL Gr IV	Flaring
Periventricular hyperechogenicity	+	+	+	+	+
Cyst formation, small one	_	+	_	_	_
Cyst formation Extensive one	_	_	+	_	_
Persisting more then7 day	+	+	+	+	
Preterm neonates	+	+	+		+, but not only
Cyst formation, Extensive one placed in deep white matter	_	_	_	+	_

15.2.4.2 Periventricular hemorrhage or preterm caudothalamic hemorrhage, also known as Germinal Matrix Hemorrhage (GMH Grade 1-4). It is classified into four grades based on severity, with higher grades associated with long-term neurological deficits and hydrocephalus.

Grade 1: US images shown from a Gr I subependymal hemorrhage which in the acute phase bleedings, are hyperechoic, and then change to iso- and/or hypo-echoic with time.

Grade 2: On the coronal image only the cavum septi pellucidi is seen. Bleeding in both lateral ventricles is found, but without ventricular dilatation at the beginning, which we can find later (the 3rd day) with clot formation too. Good prognosis is a characteristic of Gr I and II.

Grade 3: A small venous infarction in the lateral ventricular area can be found. Cyst formation within venous infarction is also found.

Grade 4: Venous hemorrhagic infarction is the result of a venous infarct, finally resulting into a porencephalic cyst.

Grade 3 and 4 have variable long-term deficits, Grade 3 has a better prognoses than the 4 one. Hydrocephalus require ventriculoperitoneal shunting.

15.2.4.3 Ultrasound finding in corpus callosum agenesis.

In corpus callosum agenesis (can be primary or secondary).

Structure	Finding
Ventricles	• Lateral ventricles look like small frontal horns and widely spaced parallel bodies. • Colpocephaly, which can give a "teardrop" configuration on axial scans. • Third ventricle is dilated, can be elevated or dorsally displaced, and also may communicate with the interhemispheric cistern. It may project superiorly as a dorsal cyst. Choroid may be seen as an echogenic structure in the roof of the cyst.
Interhemispheric fissures	• Interhemispheric fissures are widened.
Gyri	• May be seen in a "sunray appearance" on the sagittal plane.
Septum pellucidum	• Is absent
pericallosal arteries	• Color Doppler study may show an abnormal course of pericallosal arteries.

15.2.4.4 Cephalohematomas and Subgaleal Hematomas differentiated by their anatomical location and ability to cross cranial sutures.

	Fluid accumulate between the periosteum and the skull	Fluid accumulate in the virtual space between the periosteum and the galea aponeurotica	Can cross the sutures	US Finding
Cephalo hematomas	+	_	_	+
Subgaleal hematomas	_	+	+	+

Cephalohematomas is usually found in newborns who have been subjected to a difficult (traumatic) delivery, where the use of forceps, etc. may have been required. It is unusually found it in the parietal bone. A US examination frequent finding is fluid collection accompanied with the Mirror Sign.

In Subgaleal hematomas, a US examination demonstrated an extensive, simple fluid collection that extended across the suture line. This hematomas are associated with skull fractures in many cases.

15.3 Neck US

Neck masses are common in the pediatric population, more often benign. US has an important role as the first-line imaging modality for the evaluation of neck masses in the pediatric age group, as well as head masses when conditions permit. Without using radiation, iodinated contrast material and/or sedation, it provides a means of quickly and cost-effectively obtaining information like the location, size, internal contents, and vascularity context of the mass.

Specifically, covered entities include epidermoid, dermoid cysts, lymph nodes, fibromatosis colli, torticollis, thyroglossal duct cyst, thyroid bronchus cyst, thyroid gland carcinoma, different type of adenomas, lymphangioma, hemangioma, vein phlebectasia (jugulare one), parotitis, leukemia, lymphoma, lemierre syndrome, etc. Now that antibiotics are widely used, the last condition is rare, with the peak in young adults.

15.3.1 Torticollis

It is a relatively common finding in infants younger than 3 months (0 to 3 month baby). We still don't know the cause why some kids manifest it and others do not. It is believed that it might be caused by an inflammatory condition, traumas or it could also be congenital (called fibromatosis colli).

There is not a gender selection, but it was noticed that some of these babies manifest also a development of the hip dysplasia (condition determined by the fetal positioning and difficult birth).

Usually the US is a valid examination technique to confirm the diagnosis, for this purpose we use a linear high frequency probe. We scan sternocleidomastoid muscles in longitudinal and transversal surveys and the echogenicity of the muscle.

15.3.2 Lymphatic Malformations

Formerly termed lymphangiomas, these lesions are typically benign and appear as multilocular cystic masses with internal septa on US. They are most frequently located in the neck and axillary regions.

15.3.3 Diagnostic Approach

US is the first-line imaging modality for pediatric neck masses due to its safety and cost-effectiveness. For large, hyperechoic, or deep-seated lesions, cross-sectional imaging (CT/MRI) is recommended for further evaluation.

15.4 Lung Ultrasound

15.4.1 Principles and Applications

Lung US (LUS) relies on artifact-based imaging, such as A-lines and B-lines, to assess pulmonary conditions. Its use has expanded significantly, particularly during the COVID-19 pandemic, due to its rapid, bedside applicability. Lung US uses other principles of interpretation compared to ultrasound examinations that we encounter in other organs.

Many studies show that compared to Chest X-Ray, US may have higher sensitivity and specificity in the detection of pleural effusion etc.

One of the limitations of Lung US to chest X-ray is related to the dependence on the operator who performs the exam and his skills (is operator dependent). Technical skills advanced of him increase the diagnostic yield. Another limitation is the long time it takes to perform the examination. A complete US examination of the lungs may require up to 20 minutes, while a chest X-ray can be done in a few minutes. Lines A and/or B can be seen in some pathologies, so they do not have high specificity for special diagnoses; however, this problem does not exist only in the case of US and other chest examinations, such as x-rays, and to a lesser extent CT cope with these problems.

CT, X ray and ultrasound are not rival modalities but complementary to each other, which can be used together for the benefit of the patient.

How is acquisition of images made in Lung US?

We have to provide examination of the pulmonary areas. All pulmonary fields should be examined. The patient can be examined both in the supine position and in the orthostatic one. The probe should be held perpendicular to the skin, parallel to pleural line, in order to produce the necessary artifacts for interpretation. Different probes can be used depending on the age of the patient, for example Cnovex5-9MHz probes are well suited for lung examination, linear 7-12MHz

probe provide better resolution in the evaluation of superficial structures, especially useful in children (who have small chest diameters) and for assessment of pneumothorax.

In neonates, a linear probe with a high frequency of 10MHz or more is mainly used.

15.4.2 Normal findings

The first one finding in LUS to confirm that we are in the right position is to look for two shadows of the ribs (Batwing sign). This ensures that the probe is between the tworibs.

The next finding we should look for is lung sliding, a normal finding where the visceral pleura and the parietal one slide over each other as the patient inhales. This is a simple finding though extremely useful, as lung sliding means that the visceral and parietal pleura are next to each other, effectively excluding pathologies such as pneumothorax. If lung sliding is not immediately apparent, it can be further assessed using M-Mode. The purpose of M-Mode is to see if the patient has a normal coastline sign. This can help in confirming the presence or absence of pneumothorax.

When we place the probe perpendicular to the pleura, the ultrasound is reflected by the air from the pleura and surface of the probe, producing an image that looks like pleural lines, which are at a distance of equal to the true pleural line. These reverberation artifacts may persist reflect back and cause some A-lines to appear before disappearing.

These A-line artifacts are an important sign to confirm the presence of air in the pleura and can help identify conditions such as pneumothorax. Clinically, A-lines may indicate healthy alveolar ventilation. However, A lines may be seen in cases of pneumothorax too, as there will be a reflection of air in the parietal pleura. The difference is the lack of lung sliding. A lines, normal findings (Fig. 15.3).

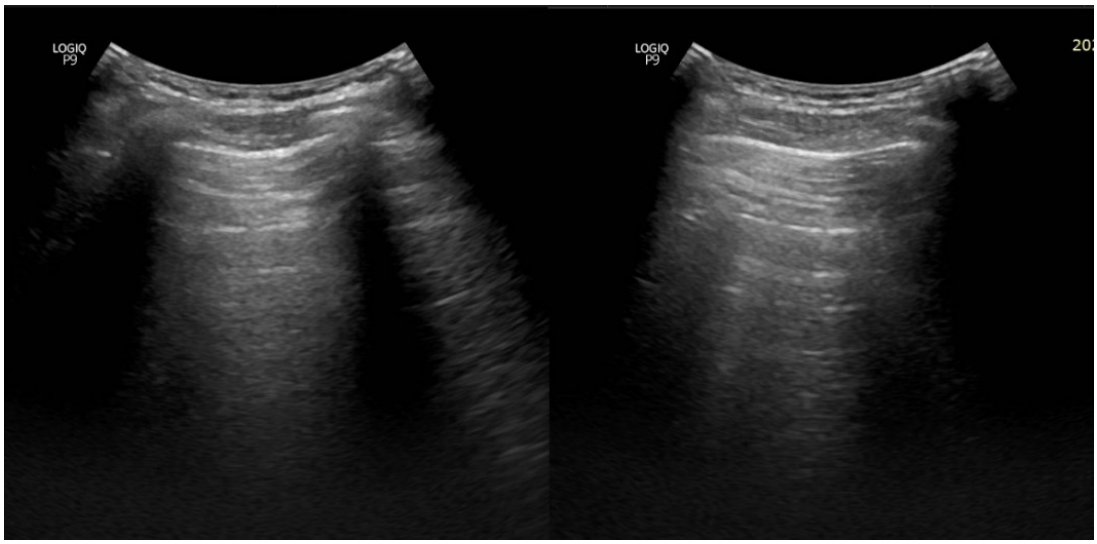

Fig. 15.3 Normal A Lines, convex probe

15.4.3 Pathological Findings

- **A-lines**: Horizontal artifacts indicating normal alveolar ventilation or pneumothorax also.

- **B-lines**: Vertical hyperechoic lines suggesting interstitial syndrome or pulmonary edema.

- **Pleural Effusion**: Detected as anechoic or complex fluid collections in pleural space.

- **Pneumothorax**: Diagnosed by the absence of lung sliding and the presence of a lung point.

- **Pneumonia**: Characterized by B-lines, consolidation, and air bronchograms.

B-lines are vertical, hyperechoic lines that extend from the pleura distally without fading. Those sweep the A lines and move synchronously with the pulmonic slide. Sometimes the B line can also be evident in normal lung, mainly in the bases. Fig. 15.4

Overall distribution of B lines, effect on pleural line and associated findings ultrasound can help differentiate these pathologies.

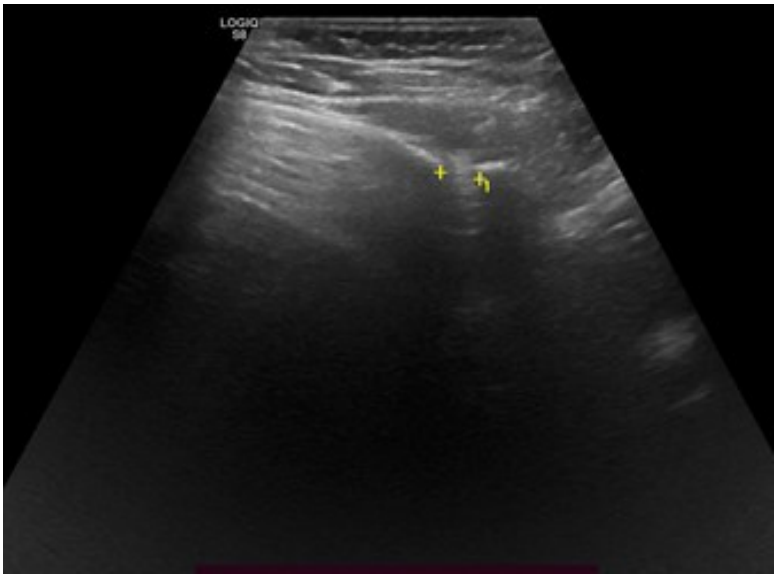

Fig. 15.4. A and B Lines

In pneumothorax, lung point identification in ultrasound increases up to 100% the specificity of pneumothorax diagnosis. Thoracic ultrasound has a higher sensitivity than radiography in the examination of pneumothorax.

Pneumonia

LUS is an excellent modality for the evaluation and monitoring of infections known or suspected pulmonary.

15.5 Soft tissues and joints US

15.5.1 US of Developmental dysplasia of the hip (DDH)

US to hip joints evaluation is recommended between the 6th and 12th weeks of life (for term newborn's), it represents an appropriate diagnostic tool classification of DDH. Screening (universal) US and diagnostic (selective) US have ameliorated the prognosis and lowered the number of open pelvic surgery. Selective screening is made in case of specific clinical conditions, like abnormal examination findings at neonatal evaluation, oligo-hydramnios, family history, and/or neuromuscular disorders. In these cases, US can be performed before the 6th week newborn's life. In case significant instability or dislocation is noted, we perform immediately an US examination. But in case, when it is not noted, screening ultrasound must be performed after 5th weeks of age (between the 6th and 12th weeks life), to diminish the risk of false-positive results, secondary to physiologic laxity of the joint. Hip joint US scanning protocol examination include coronal and transversal survey. The images in the coronal survey need to include the iliac wing parallel to the transducer, the triradiate cartilage and the ischium too. We have to check the possibility of instability using the transverse survey and perform the dynamic test.

Graph classification table provides further information on joint hip type examination findings. Fig. 15.5 and Fig. 15.6

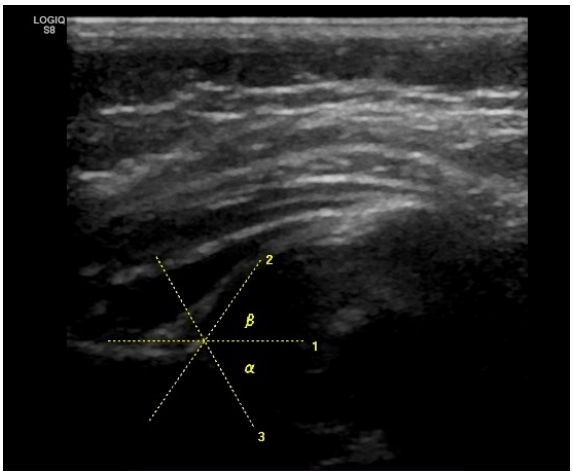

Fig. 15.5. Normal Right Hip US, Type I

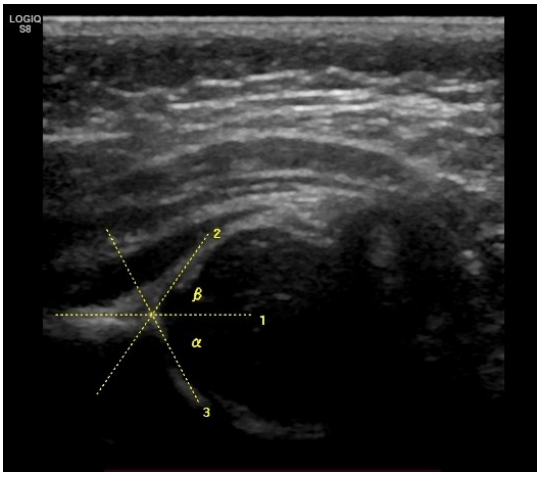

Fig. 15.6. Normal Left Hip US, Type I

Graf Classification, Short Version

Type	I	II a (>3 months)	II b	II c	IID	III	IV
α-Angle	≥ 60°	50-59°	50-59°	43-49°	43-49°	<43°	<43°
β-Angle	<55°	>55°	>55°	<77°	>77°	Eccentric hip	Inverted labrum

15.5.2 Inflammatory disorders, US appearance

US is effective in detecting joint effusions, synovial hypertrophy, and hypervascularity in conditions such as transient synovitis and juvenile idiopathic arthritis (JIA). Fig. 15.7

US can also be used in patients with the identified disease to perform invasive procedures like intra articular corticosteroid injections.

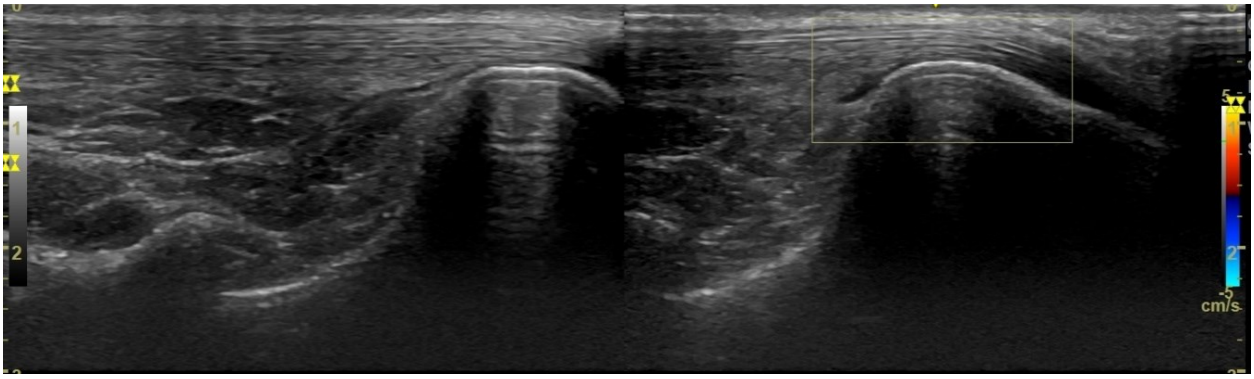

Fig. 15.7. Achilles tendon with minimal regional fluid

15.5.3Soft tissue tumor mass disorders in pediatrics, US appearance.

Infantile hemangioma (IH) is well known like the most common vascular tumor in the pediatric population and soft tissues (skin) is its most frequent location. It is more common in female than in male subjects. It can already be present in its birth, but sometime can also develop later, usually present in the first trimester of life. Infantile hemangioma shows a biphasic development: the proliferative phase (the first one), evident in the first months of life of the newborn, succeeded from the involuting phase (second one). The latter is slower and can last for several years. IH can be multiple in 20% of the cases. It can manifest themselves in all the parts of the body, but especially in cutaneous localization, which help to made the clinically diagnosis. In deeper lesions, US is helpful in making the diagnosis. The US appearance is hyperechoic.

Malignant soft-tissue neoplasms fortunately are not common findings in the pediatric population. An ill-defined margin and/or a heterogeneous and infiltrative lesion should raise suspicion for a possible neoplasm. In this case, MRI is the gold standard for better characterization.

15.6 Abdominal findings in pediatrics: their US appearance

Abdominal US is a known target exam, in acute and in congenital conditions pathologies of all the infant's age group. For a full exam protocol, we put the baby in different positions like supine, prone, and lateral decubitus. To perform the exam we can use both linear and convex probes. Usually the scanning technique is similar to adults, except special cases conditioned by age and/or pathologies that we encounter.

15.6.1 Hypertrophic Pyloric Stenosis, US appearance

Hypertrophic pyloric stenosis is a relatively common finding, even more common if the baby is a firstborn male infant. It is caused by the hypertrophy of the muscular layer of the pylorus. To find the pylorus in a US examination we need a linear probe and place the infant in a supine position. We need to scan the patient in a transverse position by showing first the gallbladder and then we have to found the pylorus located posteriorly. If a target sign appears we have to measure the muscular layer both in longitudinal and transverse views. If the layer is more than 3 millimeters thick, it could be hypertrophic. It is recommended to describe them as well the measures of the width and length of the pyloric channel.

15.6.2 Biliary atresia in pediatrics, US appearance

Biliary atresia is not a common finding among the diseases of the liver and biliary duct, but which still can be noticed in infants. US examination can show the absence of the gallbladder or if it is present we notice its abnormal length and contraction. To perform a correct examination, we need a fasting infant (infants are usually required to fast for a maximum of 3 hours). In 1996 Choi et al. reported a new US finding, where he describes the existence of a triangular or tubular fibrotic structure located to the portal vein bifurcation named “the triangular cord sign”. Then, they concluded that the detection of this sign is an important tool to perform the diagnosis of biliary atresia in sonographic examination.

15.6.3 Patent urachus duct

The so called urachus is a channel between the bellybutton and the bladder in the uterine life. Usually this channel closes before birth. Urachal duct abnormality is a rare finding with the prevalence 1:2 cases for 100,000 births. Even now US exam of abdominal pelvis is the first choice examination to diagnose this pathology, in which we can visualize a tubular structure localized in the median line, and which extends from the bellybutton to the bladder. To visualize this image we use a linear probe in a coronal and transversal survey.

15.6.4 Infant urinary tract sonography appearance

The infants’ urinary tract has some different details compared to an adults’ one. Kidney appearance specifics: the low distribution of fat in the medullary part of the kidney and the cortex appears more echogenic because the glomerulus has an increased density. For this reason, in the US image, the cortico-medullary index decreases compared to the adult kidney. Fig. 15.8 and Fig. 15.9

During the examination we have to determine the presence, the position, and the size of the kidneys. We also have to evaluate the urinary tract for congenital abnormalities. Using this technique, we can also find abnormalities related to the position, rotation, number and fusion malformation. Such findings can be seen, as the horseshoe kidney, the duplex kidney, the ectopic kidney, unilateral renal agenesis or hipoplasia. Other pathologies that can be evaluated through ultrasound are: ureteroceles, ureteropelvic junction obstruction and vesicoureteral reflux. The last one can’t be characterized properly with the conventional sonography technique. In fact it needs a

retrograde cystouretherography to be seen, now with the CEUS we have the possibility to make this diagnosis by US, saving radiation for the patient and reducing the costs of the equipment, but unfortunately, the contrast for CEUS is not available everywhere and even less in the pediatric community, but without a doubt, the bubbles are the future in pediatric patient too.

In case of urinary tract infections we have to look for the presence or the lack of presence of hydronephrosis, the thickness of the bladder and renal collecting system walls, which can suggest the presence of inflammation.

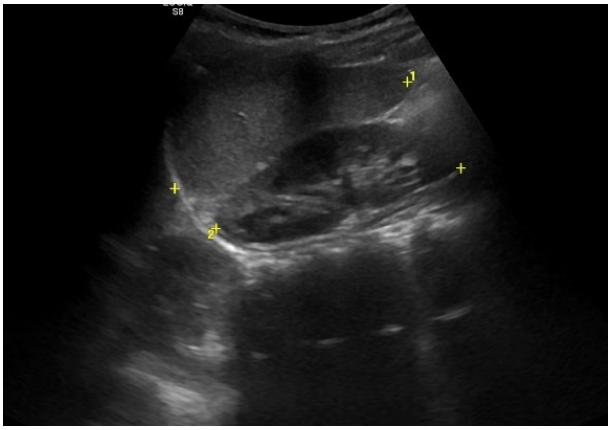

Fig. 15.8. Normal right Kidney

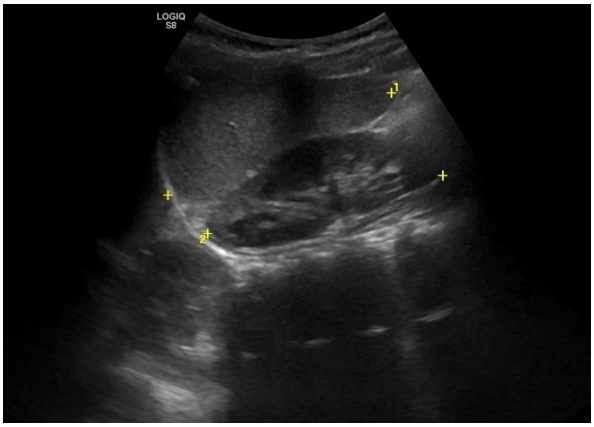

Fig. 15.9. Normal left Kidney

15.6.5 Intussusception

The majority of intussusceptions cases in children are idiopathic. The most common cause of intestinal obstruction in children under two years, characterized by a "target sign" on US and only about one fourth of cases have known certain epidemiology such as lymphoid hyperplasia, and/or benign or malignant tumors.

It can be variable and age dependent. The pain is the most common presenting symptom, but a non-specific sign may make it difficult to guide the clinical diagnosis in younger non-verbal children. Ileo-colic intussusception is the most common type, for this reason we find the target in the right iliac quadrant most commonly. Even though the most frequent location is in the ileo-colic portions, when seen in the small intestine, the difference in size is typical, they are usually thinner and often spontaneously reduced. If symptoms and US findings persist, X ray and computed tomography (CT) is recommended.

15.7 Conclusions

Ultrasound is a crucial tool in pediatric imaging, offering real-time, noninvasive diagnostics across multiple organ systems. Its applications in neonatal brain imaging, lung pathology, and

musculoskeletal disorders are particularly significant. While US has limitations, such as operator dependence and longer examination times, it complements other imaging modalities like CT and MRI, enhancing comprehensive patient care exams.

Selective references

https://radiopaedia.org/articles/lymphatic-malformations-1

https://radiopaedia.org/articles/lemierre-syndrome

https://radiologyassistant.nl/pediatrics/spine/neonatal-brain-us

https://radiopaedia.org/articles/dysgenesis-of-the-corpus-callosum

https://pubs.rsna.org/doi/full/10.1148/rg.2018170165

https://pmc.ncbi.nlm.nih.gov/articles/PMC8143819/

1. Marini TJ, Rubens DJ , Zhao YT , Justin Weis J, Timothy P O'Connor TP et al. Lung Ultrasound: The Essentials. Radiol Cardiothorac Imaging. 2021 Apr 29;3(2):e200564. doi: 10.1148/ryct.2021200564. e Collection 2021 Apr.
2. Saraci Qirinxhi B, Kosiak W, Basics in Pediatrics, Chap 22, WFUMB Ultrasound Book. Editors Dieter Nurnberg, M.Cristina Chammas, Odd Helge Gilja, Ioan Sporea and Roxana Sirli. Published by WFUB (World Federation for Ultrasound in Medicine and Biology), 1st Edition published 2021. ISBN: 979-1-8384990-0-6
3. Berkowitz, Tal. Pyloric Stenosis (Infant with Vomiting). Pyloric Stenosis (Infant with Vomiting) | Emory School of Medicine, med.emory.edu/departments/emergency-medicine/sections/ultrasound/image-of-the-fortnight/abdominal/pyloric-stenosis.html.
4. Hryhorczuk, Anastasia L., et al. Pediatric Musculoskeletal Ultrasound: Practical Imaging Approach: American Journal of Roentgenology : Vol. 206, No. 5 (AJR).” American Journal of Roentgenology, May 2016, www.ajronline.org/doi/10.2214/AJR.15.15858.
5. Paliwalla, M, Park K. “A Practical Guide to Urinary Tract Ultrasound in a Child: Pearls and Pitfalls.” Ultrasound (Leeds, England), SAGE Publications, Nov. 2014, www.ncbi.nlm.nih.gov/pmc/articles/PMC4760558/.
6. “Torticollis: Symptoms and Causes: Boston Children's Hospital.” Boston Children's Hospital, www.childrenshospital.org/conditions-and-treatments/conditions/t/torticollis/symptoms-and-causes.

16. NEW TECHNOLOGIES IN ULTRASOUND – BASIC INFORMATION (CEUS, ELASTOGRAPHY, HIFU, FUSION)

Felix Bende, Tudor Moga
WFUMB Center of Education Timișoara, Romania

Ultrasound technology has evolved significantly over the past decades, incorporating advanced techniques that enhance diagnostic accuracy and therapeutic applications. Among the most notable innovations are Contrast-Enhanced Ultrasound (CEUS), Elastography, High-Intensity Focused Ultrasound (HIFU), and Fusion Imaging. These modalities have revolutionized the way clinicians assess and treat various conditions, from liver disease to oncological applications.

This chapter provides an overview of these emerging ultrasound technologies, their principles, applications, and clinical benefits.

16.1 Contrast-Enhanced Ultrasound (CEUS)

Contrast-Enhanced Ultrasound (CEUS) represents a pivotal advancement in diagnostic imaging, leveraging microbubble-based contrast agents to enhance conventional ultrasonography. This technique provides superior delineation of vascular structures and tissue perfusion, significantly augmenting diagnostic accuracy across a wide array of clinical applications. Compared to alternative imaging modalities such as computed tomography (CT) and magnetic resonance imaging (MRI), CEUS offers real-time, dynamic visualization with a superior safety profile due to the absence of ionizing radiation and nephrotoxic contrast agents.

Beyond its diagnostic advantages, CEUS has also emerged as a valuable tool for procedural guidance and therapeutic monitoring. The ability to visualize microvascular perfusion in real-time allows for more precise interventions, such as targeted biopsies and ablation therapies. Additionally, research is ongoing into the use of CEUS for molecular imaging applications, where contrast microbubbles can be functionalized to bind specific cellular targets, paving the way for precision diagnostics and personalized medicine.

Fundamental Principles of CEUS

CEUS relies on the administration of ultrasound contrast agents (UCAs), which consist of gas-filled microbubbles encapsulated in a stabilizing phospholipid or protein shell. These microbubbles remain strictly intravascular due to their size, providing a high degree of contrast when insonated at specific frequencies. The strong acoustic backscatter from these microbubbles significantly enhances the visualization of blood flow, enabling the detection of microvascular perfusion patterns and pathophysiological alterations.

Mechanisms of Contrast Enhancement

The contrast enhancement observed in CEUS is attributed to the unique acoustic properties of microbubbles. When exposed to ultrasound waves, microbubbles undergo nonlinear oscillations, generating harmonic frequencies that differentiate them from surrounding tissues. This phenomenon, known as acoustic resonance, results in increased echogenicity, facilitating the visualization of even the smallest vascular structures.

Another important mechanism is the dynamic phase-specific enhancement pattern observed with CEUS. As the microbubbles circulate through different vascular compartments, characteristic enhancement patterns emerge, allowing for differentiation between benign and malignant lesions. For example, arterial-phase hyperenhancement followed by late washout is highly suggestive of hepatocellular carcinoma (HCC).

Imaging Protocol

The CEUS procedure follows a structured protocol to optimize image acquisition and interpretation:

1. Baseline Ultrasound Assessment – A conventional ultrasound scan is initially performed to obtain anatomic and functional reference images.
2. Administration of Contrast Agent – A bolus injection of a CEUS contrast agent (e.g., sulfur hexafluoride microbubbles) is administered intravenously, followed by a saline flush.
3. Dynamic Imaging in Real-Time – Continuous ultrasound monitoring is employed to evaluate contrast enhancement patterns in arterial, portal venous, and late phases.
4. Quantitative and Qualitative Analysis – The acquired images are analyzed for enhancement characteristics, kinetics, and perfusion heterogeneity to facilitate precise diagnosis.

Table 16.1. Vascular phases in contrast-enhanced ultrasound (CEUS) of the liver

Phase	Start (sec.)	End (sec.)
Arterial	10-20	30-45
Portal venous	30-45	120
Late venous	>120	240-360

Advantages of CEUS in Clinical Practice

- Radiation-Free Modality: Unlike CT and nuclear medicine techniques, CEUS does not involve ionizing radiation, making it ideal for repeated imaging studies.
- Dynamic Perfusion Assessment: Enables real-time observation of vascular perfusion and microcirculation, particularly in oncology and vascular pathology.

- Enhanced Sensitivity to Microvascular Flow: Provides superior detection of slow-flow capillary perfusion, often undetectable by color Doppler ultrasound.
- Minimal Nephrotoxicity Risk: CEUS contrast agents do not contain iodine or gadolinium, rendering them safe for patients with renal impairment or contrast allergies.
- Portable and Bedside Utility: CEUS can be performed in intensive care and emergency settings, reducing the need for patient transport to radiology suites.
- Improved Characterization of Lesions: CEUS enhances the differentiation of solid versus cystic masses, aiding in the early detection of malignancies.

Clinical Applications of CEUS

CEUS has been extensively validated for multiple clinical indications, spanning hepatic, renal, cardiovascular, and vascular imaging.

Table 16.2. Clinical applications of CEUS

Medical Specialisation	**Key Applications**
Hepatic Imaging	Differentiation between benign and malignant hepatic lesions Surveillance and follow-up of hepatocellular carcinoma (HCC) Assessment of liver transplant graft perfusion Detection of hepatic metastases and intrahepatic cholangiocarcinoma
Renal Imaging	Characterization of indeterminate renal masses Evaluation of renal perfusion in acute kidney injury and transplant monitoring Differentiation of complex renal cysts from solid tumors
Cardiovascular Imaging	Myocardial perfusion assessment in ischemic heart disease Detection of left ventricular thrombi and endocardial lesions Visualization of intracardiac shunts and structural abnormalities
Vascular Imaging	Characterization of carotid atherosclerotic plaques Identification of endoleaks in post-endovascular aneurysm repair (EVAR) patients Evaluation of deep vein thrombosis and peripheral vascular disease
Miscellaneous Applications	Evaluation of pancreatic and splenic lesions Testicular and ovarian torsion diagnostics Trauma assessment, particularly in blunt abdominal injury Assessment of tumor vascularity in oncology imaging

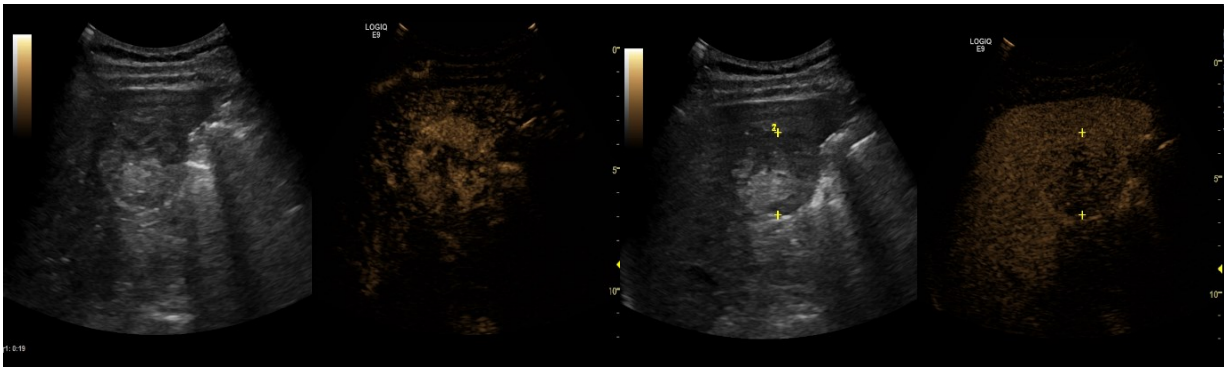

Figure 16.1. Contrast-Enhanced Ultrasound (CEUS) for Hepatocellular Carcinoma (HCC).
The left image illustrates the arterial phase, showing a nodule with intense arterial hyperenhancement. The right image corresponds to the late phase, where the lesion demonstrates contrast washout, a characteristic feature of malignancy. These findings are consistent with HCC, classified as CEUS LR-5 according to LI-RADS criteria.

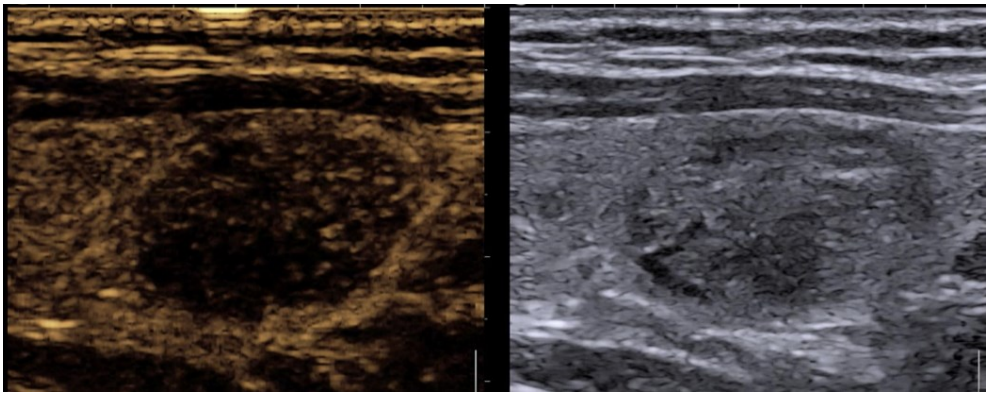

Figure 16.2. Contrast-Enhanced Ultrasound (CEUS) for thyroid cancer. A solid, well-defined, isoechoic with some areas of hypoechogenicity which includes the nodule in EU TIRADS 4, CEUS high risk due to diffuse hypoechancement (upgraded to modified-TIRADS 5) = medullary thyroid cancer. TIRADS 4 represents nodules with moderate suspicion of malignancy, whereas TIRADS 5 includes those with high suspicion, often requiring biopsy confirmation.

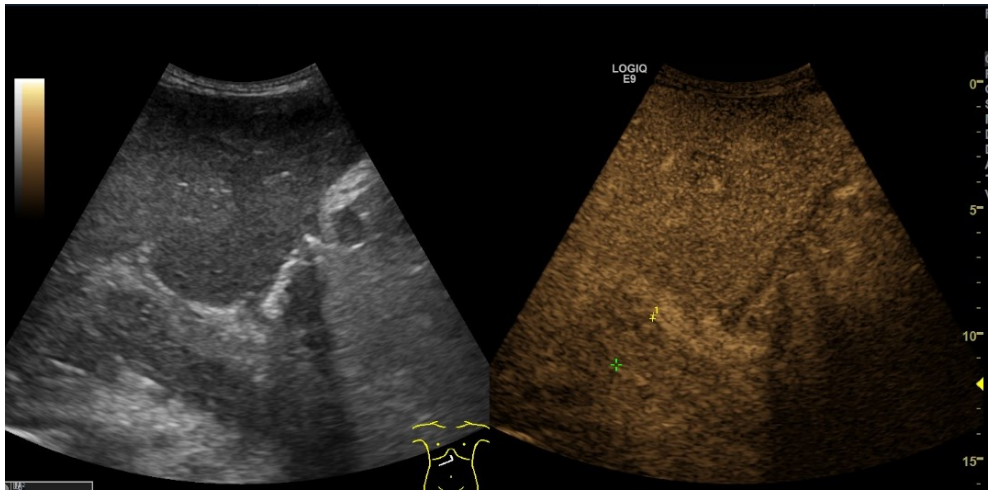

Figure 16.3. Contrast-Enhanced Ultrasound (CEUS) for Portal Vein Thrombosis. CEUS examination demonstrates contrast enhancement within the portal vein thrombus, a characteristic feature of malignant portal vein thrombosis (tumor invasion of the vein). These findings support the diagnosis of tumor thrombus rather than bland thrombosis.

Safety Considerations and Technical Limitations

Safety Profile

CEUS contrast agents demonstrate an excellent safety profile, with a significantly lower risk of hypersensitivity reactions, compared to iodinated or gadolinium-based agents. Reported adverse effects, such as transient headache, nausea, and injection site discomfort, are typically mild and self-limiting. Severe anaphylactoid reactions are exceedingly rare.

Technical Constraints

- Operator Dependency: The diagnostic accuracy of CEUS is highly reliant on the skill and experience of the sonographer.
- Attenuation in Obese Patients: Ultrasound signal penetration is diminished in individuals with increased adiposity, potentially compromising image quality.
- Short Imaging Window: The rapid clearance of microbubbles necessitates precise timing of imaging acquisition to capture arterial, venous, and delayed enhancement phases.
- Limited Standardization: Unlike CT and MRI contrast imaging, CEUS protocols vary between institutions, which can affect interobserver reproducibility.

Future Perspectives in CEUS

The field of CEUS continues to evolve, with emerging applications that extend beyond conventional diagnostics. Innovations such as targeted microbubble contrast agents are being investigated for their potential in molecular imaging, where they could selectively bind to biomarkers of disease, enabling earlier and more specific diagnoses.

Additionally, quantitative CEUS techniques are gaining traction, allowing for objective perfusion assessment through time-intensity curve analysis. These advancements hold promise for improved lesion characterization, treatment response evaluation, and individualized therapeutic strategies.

Conclusion

CEUS has emerged as an indispensable tool in modern diagnostic imaging, offering unparalleled real-time assessment of microvascular perfusion while maintaining an excellent safety profile. Its applications continue to expand, particularly in hepatology, nephrology, cardiology, and vascular medicine. With ongoing technological advancements, CEUS is poised to play an increasingly significant role in precision medicine and personalized diagnostic approaches, solidifying its place as a cornerstone of modern ultrasound imaging.

16.2 Elastography

Elastography represents a sophisticated imaging modality designed to quantitatively assess tissue mechanical properties, primarily stiffness and elasticity. This technique has emerged as an indispensable tool in the diagnostic evaluation of hepatic fibrosis, oncological lesions, and musculoskeletal pathologies. By utilizing mechanical wave propagation and deformation analysis, elastography extends the diagnostic potential of conventional imaging techniques such as ultrasonography (US) and magnetic resonance imaging (MRI), offering a non-invasive alternative to histopathological tissue characterization.

The evolution of elastography has been driven by the necessity for precise and reproducible tissue stiffness measurements, especially in the context of chronic disease management. Traditional imaging modalities provide structural information but lack insight into tissue biomechanics, which can be crucial in early disease detection. Elastography addresses this limitation by mapping stiffness variations that often precede morphological changes.

Fundamental Principles of Elastography

The foundational principle of elastography is predicated on the mechanical heterogeneity of biological tissues, where pathological processes often induce alterations in viscoelastic properties. Softer tissues exhibit higher deformability under external or intrinsic stress, whereas stiffer tissues display greater resistance to deformation. Elastography exploits these biomechanical disparities to construct elastograms—spatially resolved maps depicting tissue stiffness distributions.

Tissue elasticity is influenced by several intrinsic and extrinsic factors, including collagen content, vascularity, and cellular composition. Understanding these factors is essential for accurate interpretation of elastographic findings. Furthermore, different pathophysiological processes—such as fibrosis, malignancy, and inflammation—affect tissue stiffness in distinct ways, necessitating the integration of elastographic data with conventional imaging and clinical parameters.

Elastographic modalities can be categorized into two primary classifications:

1. Ultrasound Elastography (USE): Utilizes high-frequency acoustic waves to interrogate tissue stiffness, providing real-time, dynamic assessment. This approach benefits from widespread availability, making it an accessible tool in various clinical settings.
2. Magnetic Resonance Elastography (MRE): Employs phase-contrast MRI sequences to visualize the propagation of externally induced mechanical waves within tissue matrices, yielding quantitative stiffness metrics. MRE is particularly advantageous in assessing deep-seated structures and minimizing operator dependence.

Ultrasound-Based Elastography Techniques

Ultrasound elastography is broadly classified into Strain Elastography (SE) and Shear Wave Elastography (SWE). Strain elastography evaluates tissue deformation in response to externally applied pressure or physiological motion and provides qualitative stiffness assessments.

Shear Wave Elastography (SWE) is further divided into multiple subtypes. One notable technique is Vibration-Controlled Transient Elastography (VCTE) implemented on the Fibroscan® device, which utilizes controlled mechanical impulses to generate shear waves, facilitating non-invasive liver stiffness estimation—an essential tool in hepatology for fibrosis staging.

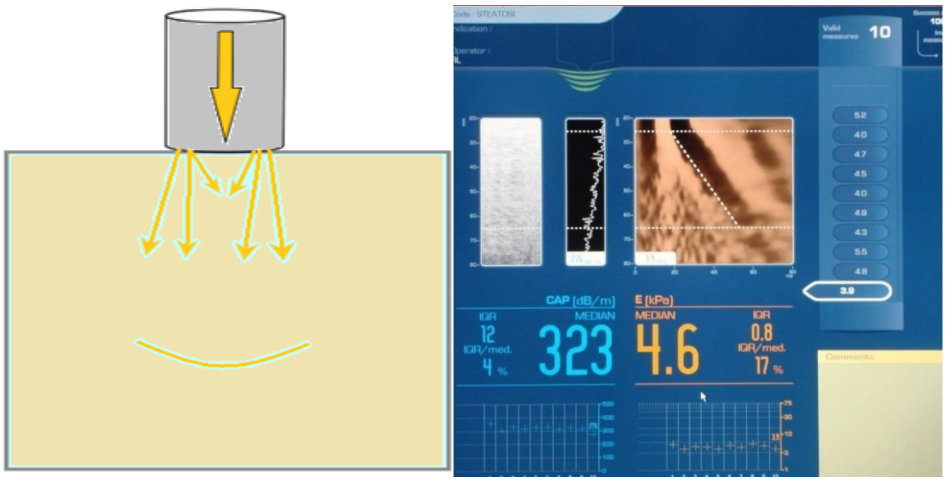

Figure 16.4. The left image illustrates the schematic representation of the VCTE principle, where a mechanically induced impulse at the tissue surface generates shear waves that propagate outward from the point of application. The right image displays the FibroScan® device interface, where numerical values for the Controlled Attenuation Parameter (CAP) are shown on the left in blue (dB/m), while liver stiffness measurements (VCTE values) are displayed on the right in yellow (kPa).

Another key approach under SWE is Acoustic Radiation Force Impulse (ARFI) Technology, which generates localized tissue displacement through focused ultrasound pulses. This category includes Point SWE (pSWE), which provides localized stiffness measurements at a

specific point, and 2D-SWE, which produces real-time, two-dimensional stiffness maps for more comprehensive tissue characterization.

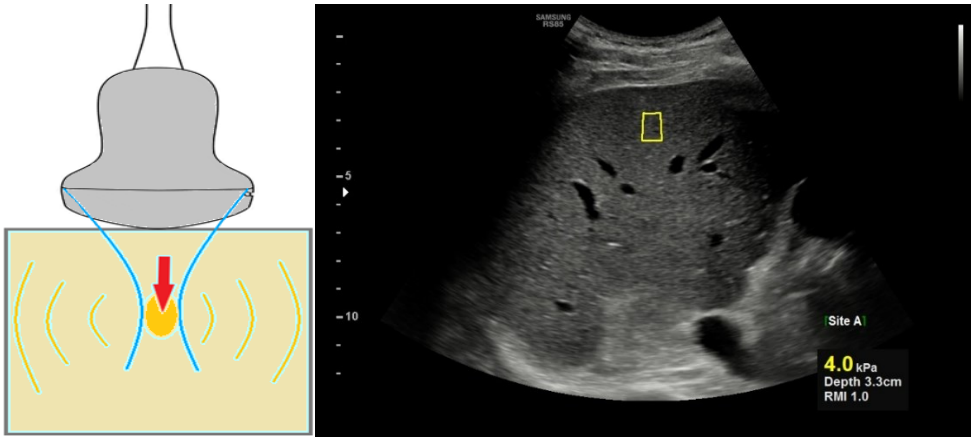

Figure 16.5. The left image illustrates a schematic representation of the pSWE principle, where an ARFI impulse is generated at a controlled depth, inducing a lateral shear wave within a region of interest (ROI). The velocity of the shear wave is measured to assess tissue stiffness. The right image showcases pSWE elastography implemented on the Samsung system, where a ROI is positioned 1–2 cm below the liver capsule. The resulting liver stiffness measurement is displayed in kPa.

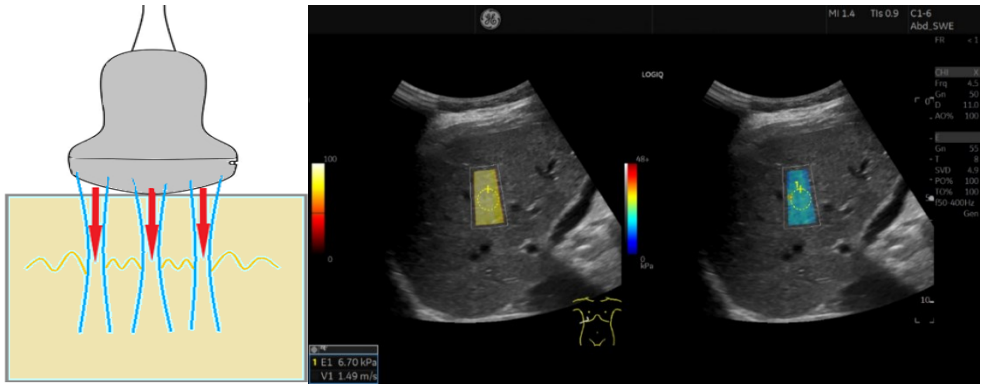

Figure 16.6. The left image illustrates a schematic representation of the 2D-SWE elastography principle, where multiple ARFI impulses generate transverse shear waves for tissue stiffness assessment. The right image demonstrates 2D-SWE elastography implemented on the General Electric system. The elastogram, overlaid on the B-mode image, is positioned 1–2 cm below the liver capsule. A circular region of interest (ROI) is placed within the elastogram to measure liver stiffness. Additionally, a color-coded quality map (left image) is available to assist in ROI placement within the most homogeneous area. Results are expressed in kPa and m/s. This technique is supported by multiple ultrasound systems from various manufacturers, including SuperSonic Imagine/Hologic, GE Healthcare, Canon, Philips, Siemens, Mindray, and others.

Clinical Applications of Elastography

- Hepatic Pathology: Widely implemented in chronic liver disease management for the non-invasive staging of fibrosis and cirrhosis, often reducing the necessity for liver biopsy. Elastography plays a crucial role in the longitudinal monitoring of hepatic stiffness, aiding in therapeutic decision-making and prognostication.
- Breast Imaging: Differentiates benign from malignant breast lesions based on stiffness characteristics, improving the specificity of breast ultrasound. Integrating elastography with Doppler studies and contrast-enhanced imaging enhances lesion characterization.
- Thyroid Evaluation: Assists in risk stratification of thyroid nodules, refining clinical decision-making regarding fine-needle aspiration biopsy. The ability to distinguish between indeterminate and suspicious nodules reduces unnecessary interventions.
- Musculoskeletal Diagnostics: Evaluates tendinopathies, muscular dystrophies, and ligamentous injuries by assessing biomechanical integrity. Elastography provides a novel approach to diagnosing conditions such as Achilles tendinopathy and rotator cuff tears, supplementing conventional ultrasound findings.
- Prostate Oncology: Provides supplementary data for prostate cancer detection and risk assessment, enhancing multiparametric imaging protocols. Combining elastography with multiparametric MRI has demonstrated improved sensitivity in prostate cancer localization.
- Pancreatic and Gastrointestinal Applications: Emerging applications in pancreatic fibrosis assessment and inflammatory bowel disease monitoring highlight elastography's expanding role in gastroenterology.
- Cardiovascular Imaging: Recent advancements explore the use of elastography in evaluating arterial stiffness and myocardial elasticity, potentially contributing to early cardiovascular risk stratification.

Advantages and Constraints

One of the primary advantages of elastography is its non-invasive nature, allowing for real-time and radiation-free imaging that can be seamlessly integrated into routine clinical workflows. By providing quantitative metrics, elastography complements conventional imaging techniques, offering additional diagnostic insights that enhance accuracy, particularly in fibrosis staging and tumor characterization. Another significant benefit is its ability to reduce the reliance on invasive procedures, such as biopsies, which in turn minimizes patient morbidity and procedural risks. Additionally, elastography facilitates disease monitoring over time, enabling more personalized and tailored therapeutic approaches.

Despite these advantages, elastography presents certain limitations. Technique-dependent variability, particularly in strain elastography, underscores the necessity for operator proficiency to ensure reproducibility and accuracy. Additionally, in obese patients, attenuation effects may compromise imaging depth and resolution, potentially limiting its diagnostic effectiveness. Another

constraint is the requirement for specialized training and equipment, which can hinder widespread accessibility and adoption in some clinical settings. Furthermore, the standardization of cutoff values for disease staging remains a challenge, necessitating ongoing research and validation efforts to establish universally accepted thresholds. Motion artifacts and physiological variations, such as respiratory or cardiac motion, may also impact image quality and interpretation, further emphasizing the need for careful acquisition protocols and advanced post-processing techniques.

Future Directions and Emerging Trends

As elastographic techniques continue to evolve, several advancements are shaping the future of this modality:

- Artificial Intelligence Integration: AI-driven algorithms are being developed to enhance the accuracy, reproducibility, and automation of elastographic measurements, reducing operator dependence.
- Multiparametric Imaging: Combining elastography with contrast-enhanced imaging, Doppler ultrasound, and functional MRI parameters may improve diagnostic performance.
- Portable and Handheld Elastography Devices: The development of compact, cost-effective elastography solutions has the potential to increase accessibility in resource-limited settings.
- Biomechanical Modeling: Advanced computational models are being explored to refine stiffness quantification and improve correlation with histopathological findings.

Conclusion

Elastography has revolutionized the field of non-invasive tissue characterization, bridging the gap between conventional imaging and histopathological assessment. Its applications in hepatology, oncology, musculoskeletal diagnostics, and emerging fields such as cardiovascular and pancreatic imaging underscore its clinical significance. Ongoing advancements in elastographic methodologies, including artificial intelligence-driven analysis and multiparametric integration, are poised to further enhance its diagnostic precision and prognostic utility in personalized medicine. As research continues, the optimization and standardization of elastographic techniques will be critical in maximizing their clinical impact and broadening their applicability across diverse medical disciplines.

16.3 High-Intensity Focused Ultrasound (HIFU)

High-Intensity Focused Ultrasound (HIFU) is an advanced non-invasive therapeutic modality that utilizes highly focused acoustic energy to induce thermal ablation of pathological tissues. The technique has demonstrated significant efficacy in oncological, neurological, and aesthetic applications, owing to its precision and minimal invasiveness. By exploiting the physics of ultrasound wave propagation and bioheat transfer, HIFU enables selective tissue necrosis while

sparing adjacent structures, positioning it as a viable alternative or adjunct to conventional surgical and radiotherapeutic interventions.

HIFU has been developed over several decades, with significant improvements in transducer technology, imaging guidance, and computational modeling. Modern HIFU systems integrate real-time imaging for enhanced targeting accuracy and treatment monitoring, significantly reducing risks and improving clinical outcomes. Research continues to optimize parameters such as frequency, intensity, and exposure duration to maximize therapeutic efficacy while minimizing adverse effects.

Principles of HIFU

HIFU operates by converging high-frequency ultrasound waves at a predetermined focal zone, thereby generating localized hyperthermia and subsequent coagulative necrosis. The underlying mechanisms of HIFU-induced tissue destruction include:

- Ultrasonic Energy Convergence: Focused transducers direct high-intensity ultrasound waves toward a specific target, concentrating acoustic energy within a confined focal volume. This allows for the precise delivery of energy without affecting the overlying or surrounding tissues.
- Thermal and Mechanical Interactions: Localized temperatures exceeding 56°C induce protein denaturation, cellular apoptosis, and necrosis. Additionally, the mechanical effects of acoustic cavitation—characterized by microbubble formation and implosion—contribute to enhanced tissue fragmentation. In some cases, inertial cavitation can amplify tissue destruction, making it useful in cases where thermal ablation alone may be insufficient.
- Real-Time Imaging Integration: Contemporary HIFU systems are coupled with diagnostic ultrasound or magnetic resonance imaging (MRI) to facilitate real-time treatment planning, targeting, and monitoring. MRI-guided HIFU allows for thermal dose mapping, enabling clinicians to assess the extent of tissue damage and adjust parameters dynamically.

Clinical Applications of HIFU

HIFU is an established therapeutic strategy across multiple medical disciplines, with ongoing research further expanding its clinical utility.

Oncological Applications

- Prostate Cancer: HIFU serves as a focal therapy option and has shown efficacy comparable to radical prostatectomy while preserving genitourinary function. It is particularly valuable for patients with localized prostate cancer who seek a minimally invasive treatment alternative.
- Hepatic and Pancreatic Tumors: The modality is particularly advantageous in patients deemed ineligible for surgical resection, offering a non-invasive approach to localized

tumor ablation. HIFU has been explored as a palliative option for hepatocellular carcinoma and pancreatic adenocarcinoma, where conventional surgical interventions may not be viable.

- Breast and Uterine Fibroids: HIFU has gained approval for treating benign and malignant tumors, providing symptom relief and improving patient quality of life. In fibroid treatment, it offers a uterus-preserving alternative to hysterectomy, significantly improving patient outcomes in reproductive-age individuals.

Neurological Applications

- Essential Tremor and Parkinson's Disease: MRI-guided HIFU is emerging as a non-invasive neurosurgical tool for ablating deep brain structures implicated in movement disorders. Focused ultrasound thalamotomy has shown promise in improving tremor severity and patient quality of life, making it a viable alternative to deep brain stimulation for select patients.
- Glioblastoma Therapy: Research is exploring the potential of HIFU in treating glioblastomas by disrupting the blood-brain barrier, enhancing drug delivery, and selectively ablating tumor tissues.

Dermatological and Aesthetic Interventions

- Skin Rejuvenation and Lipolysis: HIFU-based dermatologic treatments leverage its ability to induce neocollagenesis and selective adipocyte destruction, making it a preferred technique for non-surgical lifting and body contouring. Its application in non-invasive skin tightening has gained widespread adoption in aesthetic medicine.
- Scar and Acne Treatment: Emerging evidence suggests that HIFU may play a role in improving skin texture and reducing scarring by stimulating dermal remodeling and collagen synthesis.

Advantages of HIFU

- Minimally Invasive Nature: Eliminates the need for surgical incisions, reducing procedural morbidity and infection risks.
- Accelerated Recovery: Patients typically experience rapid post-procedural recuperation, allowing them to resume normal activities within a short period.
- Selective Cytotoxicity: Precisely targets pathological tissues while preserving surrounding structures, reducing collateral damage compared to radiation therapy.
- Outpatient Feasibility: Many indications permit ambulatory treatment with no requirement for hospitalization, reducing healthcare costs and improving patient convenience.
- Reduced Anesthesia Requirements: HIFU procedures often require only local or mild sedation, making it a viable option for patients who cannot tolerate general anesthesia.

Limitations and Considerations

Despite its numerous benefits, HIFU is subject to certain constraints:

- Restricted Depth Penetration: The therapeutic efficacy is contingent upon tissue depth and acoustic window accessibility. Deep-seated tumors or those located behind air-filled structures may pose challenges.
- Thermal Spread: Unintended heat diffusion may pose risks to adjacent anatomical structures. Advanced targeting strategies and cooling techniques are being investigated to mitigate this issue.
- Technological and Financial Barriers: High capital costs and specialized operator expertise restrict its widespread adoption. Many hospitals lack the infrastructure to integrate HIFU into routine clinical practice.
- Patient-Specific Factors: Eligibility for HIFU treatment depends on lesion size, location, and individual patient characteristics. Personalized treatment planning is crucial to optimizing outcomes.
- Limited Long-Term Data: Although HIFU has demonstrated promising short-term results, further longitudinal studies are necessary to establish long-term efficacy and safety profiles.

Prospects for Future Development

The evolution of HIFU is closely tied to advancements in imaging modalities, transducer technology, and treatment protocols. Current research efforts focus on expanding its application to novel oncological targets, neurostimulation, and regenerative medicine. Enhanced energy delivery mechanisms and integration with artificial intelligence hold promise for refining HIFU's precision, efficacy, and accessibility in clinical practice.

- Artificial Intelligence in HIFU Planning: AI-driven models can optimize energy delivery, predict treatment outcomes, and reduce operator variability, enhancing overall success rates.
- Personalized Treatment Approaches: Combining HIFU with genetic and molecular profiling may enable tailored therapy for individual patients, improving efficacy and minimizing side effects.
- Combination Therapies: Researchers are investigating synergistic approaches combining HIFU with immunotherapy, chemotherapy, and targeted drug delivery to enhance therapeutic effects.

Conclusion

High-Intensity Focused Ultrasound (HIFU) represents a paradigm shift in non-invasive therapeutic interventions, offering a compelling alternative to conventional surgical and radiotherapeutic modalities. Although challenges persist, ongoing innovations in bioengineering and imaging technologies are poised to further optimize its clinical applicability and therapeutic

outcomes. With advancements in precision medicine and integration with emerging technologies, HIFU has the potential to redefine the landscape of non-invasive treatment across multiple disciplines.

16.4 Image fusion ultrasonography

Image fusion ultrasonography represents a cutting-edge integration of real-time ultrasound (US) with computed tomography (CT), magnetic resonance imaging (MRI), and positron emission tomography (PET). This multimodal approach enhances spatial accuracy, procedural guidance, and diagnostic efficacy, thereby optimizing clinical decision-making in hepatology, oncology, and interventional radiology. By leveraging the strengths of each imaging modality, image fusion mitigates the limitations of individual techniques, such as ultrasound's operator dependence and limited tissue penetration, while reducing reliance on ionizing radiation inherent to CT-guided interventions.

The rapid evolution of imaging technologies, particularly in artificial intelligence (AI), computational modeling, and high-resolution imaging, has significantly improved multimodal image registration and real-time anatomical correlation. These advancements are paving the way for more precise interventional procedures, improved lesion characterization, and enhanced therapeutic monitoring, making image fusion an indispensable tool in modern radiological and interventional practice.

Principles of Image Fusion

Image fusion ultrasonography relies on the accurate co-registration and superimposition of datasets acquired from distinct imaging modalities. The primary objectives are to improve lesion localization, procedural precision, and diagnostic confidence. The core principles include:

1. Spatial Registration: Precise alignment of multimodal images using anatomical landmarks, electromagnetic tracking, or automated deep-learning algorithms to minimize spatial discrepancies.
2. Real-Time Ultrasound Integration: Overlaying static pre-acquired cross-sectional images with real-time ultrasound to enhance visualization and facilitate intra-procedural adjustments.
3. Multimodal Data Synthesis: Combining the high-resolution anatomic details of CT/MRI with the dynamic, real-time imaging capabilities of ultrasound for improved lesion detection and characterization.
4. Contrast-Enhanced Ultrasound (CEUS): Augmenting lesion conspicuity and vascular assessment by integrating CEUS with fusion imaging, thereby refining the differentiation of benign and malignant pathologies.

5. AI-Enhanced Image Fusion: Employing machine learning algorithms for automated segmentation, motion tracking, and adaptive spatial registration to reduce operator variability and improve reproducibility.

Clinical Advantages and Implications

The integration of image fusion ultrasonography offers numerous advantages over conventional imaging techniques:

- Superior Lesion Detection and Characterization: Enhanced visualization of hepatic, pancreatic, renal, and prostate lesions, particularly in cases where ultrasound alone is suboptimal.
- Optimized Procedural Guidance: Increased accuracy in percutaneous biopsies, tumor ablations, and vascular interventions, minimizing complications and improving clinical outcomes.
- Reduced Ionizing Radiation Exposure: Decreased reliance on fluoroscopic and CT-guided interventions, mitigating radiation risks to both patients and healthcare providers.
- Enhanced Soft Tissue Contrast and Functional Assessment: Leveraging MRI's superior soft tissue differentiation with real-time ultrasound imaging enhances diagnostic specificity and procedural success.
- Cost-Effectiveness and Minimally Invasive Implementation: Reduced need for repeat imaging and unnecessary invasive procedures, leading to improved healthcare efficiency.
- Real-Time Vascular and Tissue Elasticity Analysis: Facilitates improved characterization of lesions by correlating perfusion dynamics and elasticity mapping in real time.

Key Clinical Applications

Image fusion ultrasonography is widely employed across multiple medical disciplines, with its primary applications including:

- Hepatic Imaging and Interventions: Improved detection and monitoring of hepatocellular carcinoma (HCC), with enhanced targeting precision in radiofrequency and microwave ablation.
- Oncology: Facilitates precise image-guided biopsy and localized ablation of solid organ tumors, improving diagnostic yield and treatment efficacy.
- Interventional Radiology: Enhances guidance for percutaneous vascular access, catheter placements, and embolization procedures, reducing complication rates.
- Urological Applications: MRI-US fusion biopsy has significantly improved the diagnostic accuracy of prostate cancer detection, allowing for more targeted sampling of lesions.

- Obstetrics and Gynecology: Aids in the assessment of placental abnormalities, fetal anomalies, and uterine pathologies by integrating MRI and ultrasound data.
- Musculoskeletal Imaging: Provides enhanced precision for image-guided musculoskeletal interventions, including joint injections and soft tissue biopsies.

Challenges and Technical Considerations

Despite its numerous advantages, image fusion ultrasonography presents certain limitations:

- Registration Errors and Motion Artifacts: Variability in patient positioning, respiratory motion, and organ deformation can compromise spatial alignment, necessitating advanced compensation techniques.
- Operator Dependency and Learning Curve: Effective implementation requires proficiency in both ultrasound acquisition and multimodal image interpretation, which may present a barrier to widespread adoption.
- Hardware and Software Constraints: The availability of high-end imaging systems with robust computational capabilities is essential for seamless image fusion, yet accessibility and cost remain challenges.
- Standardization Issues: Variability in software algorithms and proprietary fusion techniques across different vendors leads to inconsistencies in image quality and diagnostic reproducibility.

Future Perspectives and Technological Advancements

The future of image fusion ultrasonography is closely tied to the continued evolution of AI, automation, and real-time imaging technologies. Potential advancements include:

- AI-Driven Automated Image Registration: Reducing reliance on operator expertise by implementing deep-learning models for real-time spatial alignment and motion correction.
- Enhanced Motion Compensation Techniques: Integration of real-time tracking algorithms to minimize the impact of physiological motion on image fusion accuracy.
- Robotic-Assisted Fusion Imaging: Combining image fusion with robotic-assisted procedures to improve precision in interventional and surgical applications.
- Advanced 3D Reconstruction Methods: Implementing volumetric ultrasound with multimodal fusion for improved anatomical visualization and procedural planning.
- Real-Time Cloud-Based Image Processing: Enabling remote access and AI-driven analytics for improved diagnostic workflow and interdisciplinary collaboration.

Conclusion

Image fusion ultrasonography represents a transformative advancement in medical imaging, seamlessly integrating real-time ultrasound with high-resolution cross-sectional

modalities to enhance diagnostic accuracy and procedural precision. By leveraging AI-driven automation, motion-tracking algorithms, and multimodal image synthesis, this technology is poised to play an increasingly pivotal role in precision medicine. As research and development continue to refine fusion imaging capabilities, its adoption is expected to expand across a broader range of clinical applications, reinforcing its status as a cornerstone of modern interventional radiology and diagnostic imaging.

Selective references

1. Pang, E. H. T., Chan, A., Ho, S. G., & Harris, A. C. (2018). Contrast-Enhanced Ultrasound of the Liver: Optimizing Technique and Clinical Applications. American Journal of Roentgenology, 210(2), 320-332.
2. Sidhu, P. S., Cantisani, V., Dietrich, C. F., Gilja, O. H., Saftoiu, A., Bartels, E., ... & Wijkstra, H. (2018). The EFSUMB Guidelines and Recommendations for the Clinical Practice of Contrast-Enhanced Ultrasound (CEUS) in Non-Hepatic Applications: Update 2017 (Short Version). Ultraschall in der Medizin (European Journal of Ultrasound), 39(2), 154-180.
3. Barr, R. G., Ferraioli, G., Palmeri, M. L., Goodman, Z. D., Wilson, S. R., Rubens, D., & Garra, B. (2015). Elastography Assessment of Liver Fibrosis: Society of Radiologists in Ultrasound Consensus Conference Statement. Radiology, 276(3), 845-861.
4. Dietrich, C. F., Bamber, J., Berzigotti, A., Bota, S., Cantisani, V., Castera, L., ... & Ferraioli, G. (2017). EFSUMB Guidelines and Recommendations on the Clinical Use of Liver Ultrasound Elastography, Update 2017 (Short Version). Ultraschall in der Medizin (European Journal of Ultrasound), 38(4), 377-394.
5. Coussios, C. C., Farny, C. H., Haar, G. T., & Roy, R. A. (2007). Role of Acoustic Cavitation in the Delivery and Monitoring of Cancer Treatment by High-Intensity Focused Ultrasound (HIFU). International Journal of Hyperthermia, 23(2), 105-120.
6. Zhang, L., Chen, W., Liu, Y., Hu, X., Ge, W., & Zheng, Y. (2015). Feasibility of High-Intensity Focused Ultrasound Treatment for Patients with Localized Breast Cancer Followed by Delayed Surgical Resection: A Preliminary Report. Ultrasound in Medicine & Biology, 41(4), 927-934.
7. Xu, E. J., Luo, W., Zhou, X. H., & Zheng, R. Q. (2016). Fusion Imaging of Contrast-Enhanced Ultrasound and Contrast-Enhanced CT/MRI Improves Radiofrequency Ablation Treatment Outcome in Patients with Hepatocellular Carcinoma. British Journal of Radiology, 89(1060), 20160397.
8. Noble, J. A., & Boukerroui, D. (2006). Ultrasound Image Segmentation: A Survey. IEEE Transactions on Medical Imaging, 25(8), 987-1010.
9. Cosgrove, D., Piscaglia, F., Bamber, J., Bojunga, J., Correas, J. M., Gilja, O. H., ... & Dietrich, C. F. (2013). EFSUMB Guidelines and Recommendations on the Clinical Use of Ultrasound Elastography. Part 2: Clinical Applications. Ultraschall in der Medizin (European Journal of Ultrasound), 34(3), 238-253.
10. Wilson, S. R., & Burns, P. N. (2010). Microbubble-Enhanced US in Body Imaging: What Role? Radiology, 257(1), 24-39.

17. NEW TRENDS IN ULTRASOUND PRACTICE

Dieter Nürnberg, Ioan Sporea
Chairs WFUMB COE Task Force

1. Handheld Ultrasound (HHUS)

The further development and miniaturization of ultrasound technology paves the way for the complete integration of ultrasound diagnostics into clinical examinations (echoscopy, sonoscopy). The first battery-powered handheld ultrasound device (MiniVisor, 1978) weighed 1.5 kilograms and had a display the size of a postage stamp. The technology then developed rapidly from the mid-2010's onwards on the basis of app-based hybrid solutions between ultrasound beamformers and probes with laptops, tablets and smartphones. Modern handheld ultrasound devices (HHUS) are now the size (and shape) of an electric razor, are equipped with one or two different transducers and mostly with Doppler technology, for vascular diagnostics. They have an operating time of 1 - 3 hours. The mobile smart devices are connected via cable or increasingly wirelessly with WiFi or Bluetooth. Today, HHUS are the fastest growing segment of the global ultrasound market. Numerous studies have now shown for various areas of application that the quality of these systems is sufficient to answer most clinical questions in Point-of-Care diagnostics (PoCUS).

Due to this unmatched mobility, ultrasound (US) has gained a unique position in imaging: the method is the only imaging technique that can be used in point-of-care diagnostics. Point-of-Care ultrasound (PoCUS) refers to US that is performed and interpreted directly at the bedside by the clinically supervising physician, i.e. the US is used in a symptom- and problem-based manner ("focused"), similar to a stethoscope. In the literature, the quick, clinically oriented overview with functionally limited mobile ultrasound technology was therefore referred to early on as "echoscopy". In addition to the imaging clarification of acute symptoms or time-critical questions, often with binary questions, PoCUS is also used for monitoring during therapy and for imaging guidance of bedside interventional measures. US systems in doctor's bag or lab coat pocket format have the potential to bring about a paradigm shift in imaging diagnostics in several respects: their use is no longer tied to hospitals or practices, but can take place wherever the patient is in their acute or chronic illness situation - at home, in an ambulance, on the street, on the sports field, in a nursing home, in a hospice, on a moving train or in an airplane.

Areas of application for HHUS today are:

- Emergency sonography outdoors (doctors on duty with emergency patients: at the scene of the accident, outside, at home):
  - Resuscitation (wherever).
- Emergency sonography indoors (emergency ward):
  - Resuscitation (wherever).
- Sonography indoors ("sono-visit", patients on the ward, in the doctor's office).
- General practitioner ultrasound during home visits (home care).
- Palliative care (nursing home, hospice, at home with specialized palliative care programs).
- Use by the armed forces (disaster and military deployment).

HHUS allow the examination to be repeated immediately whenever necessary. They are operated intuitively via apps on smart devices, they can be purchased even with limited financial resources, and, thanks to their web-based interconnectivity, they enable the transmission of image and video files and integration into a "swarm intelligence" in parallel with the telephone or messenger-based exchange of clinical information.

Fig. 17.1. Selection of HHUSD (Clarius, Viamo from Canon, Lumify from Philips, Vscan Air from GE, Butterfly).

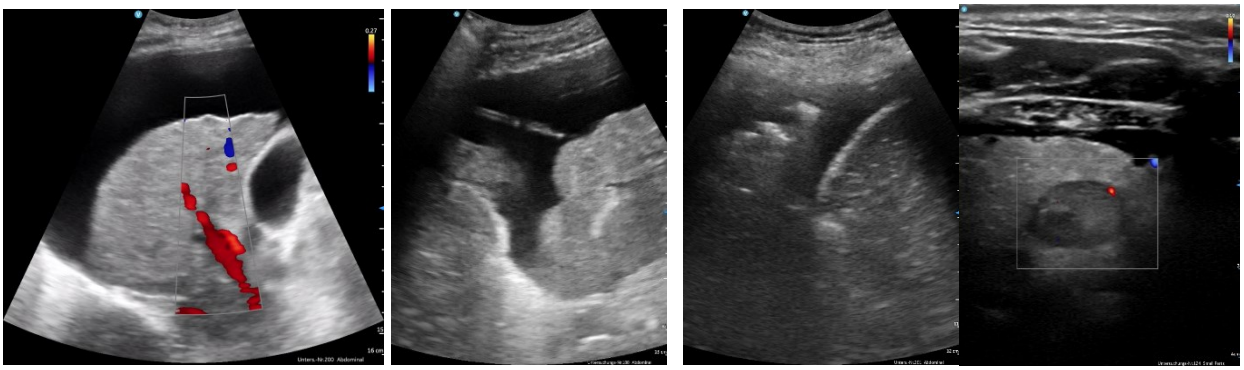

Fig. 17.2-17.5. Vscan air images of cirrhosis, ascites puncture, pleura effusion, thyroid nodule

Today, there are already more than 100 HHUS systems on the market. But despite all the great developments, there are strengths and weaknesses in the methodology. The latter are certainly hindering its widespread use.

Strengths (according to Nielsen and Dietrich)

▪ Small, light, portable, can be carried in a lab coat pocket, doctor's bag, emergency backpack;

▪ Wireless (power supply, data transfer, sometimes also transducer connection);

▪ Low-voltage supply;

▪ Some modern wireless charging technologies (Qi);

▪ Cost-effective purchase;

▪ Can be operated with one hand (second hand guides the transducer);

▪ Flexible and versatile for diagnostic and interventional use;

▪ Supplements clinical examinations with little additional effort;

▪ Outpatient and pre-clinical use;

▪ Use under difficult conditions (e.g. high infectious disease effort, accident situations, confined spaces, on board aircraft or ships, inaccessible regions, etc.);

▪ Use of apps (intuitive operation, unproblematic updates).

Weaknesses (according to Nielsen and Dietrich)

▪ Limited screen size;
▪ Transducer-screen conformity;
▪ Different image quality, not always sufficient for detailed diagnoses and examinations;
▪ Screen not always easy to position during the examination;
▪ Limited fine tuning of image settings;

▪ Limited availability of imaging modalities;
▪ Partially limited documentation options;
▪ Limited battery life;
▪ Possible additional costs due to subscription fees;
▪ Resistance to innovation;
▪ Professional reservations;
▪ Currently no remuneration;
▪ Course systems and defined quality requirements not yet established in all professional societies.

2. Artificial intelligence algorithms and **telemedical supervision** ***(tele-guidance, tele-mentoring, tele-consultation)*** are increasingly being used in HHUS to support even less experienced examiners in their use.

This opens up the potential for increasing "democratization" of ultrasound, by making it available to any sufficiently trained and/or supervised medical professional anywhere, any time and for almost any indication. This may be one of the most groundbreaking developments in modern medicine, as ultrasound is evolving from a classic imaging method in the hands of radiologists and clinical specialists, casually, almost regardless of location and with limited financial and time expenditure, to the "fifth pillar" of clinical examination in the hands of every user.

3. Artificial Intelligence (AI)

One of the future developments in ultrasound (as with all other imaging methods) is the use of ***Artificial Intelligence (AI)*** for diagnosis and images interpretation. In recent years, there has been a dramatic increase in research and publications in this emerging field.

AI in ultrasound can be utilized for the automated detection and diagnosis of various pathological conditions. In abdominal ultrasound, AI is used for diagnosing gallbladder pathologies, quantifying fatty liver, assessing patients with MASLD (Metabolic Dysfunction-Associated Steatotic Liver Disease), and detecting liver fibrosis. It can also enhance the reliability of liver elastography assessments. Tumor detection and characterization, as well as the development of software for Contrast-Enhanced Ultrasound (CEUS) interpretation, remain more challenging. AI has been proposed for hepatocellular carcinoma diagnosis, significantly increasing the accuracy of ultrasound-based methods.

In obstetrics, AI is employed for automated fetal biometry and anomaly detection. Substantial progress has also been made in thyroid and breast ultrasound, where AI aids in lesion detection and subsequent differentiation between benign and malignant formations. For example, the "Breast Assistant" software proposes a BIRADS classification for breast lesions. In cardiological ultrasound, AI is applied for detecting valvular abnormalities and ventricular

dysfunction. In urology, it is used in Shear Wave Elastography for predicting prostate cancer. Across all fields of ultrasound, AI applications are rapidly expanding.

To enhance workflow efficiency in ultrasound, AI can facilitate automated report generation. It can also contribute to ultrasound training and the development of training programs. Looking ahead, AI-powered robotic ultrasound systems are an area of growing interest in clinical practice.

All these developments are in this moment subject to regulatory and ethical considerations. At present, these aspects are actively being studied and refined at all levels.

Finally we like to present a painting of ultrasound made with AI, in van Gogh style.

Selective references

1. EFSUMB. Birth of "Echoscopy"-The EFSUMB Point of View. Ultraschall in Medizin 2013; 34: 92

2. Nielsen MB, Cantisani V, Sidhu PS et al. The Use of Handheld Ultrasound Devices – An EFSUMB Position Paper. Ultraschall Med 2019; 40: 30–39. doi:10.1055/a-0783-2303

3.Dietrich CF, Bulla P, Dudwiesus H, Lo H, Hocke M, Hoffmann B, et al. [Perspectives and Challenges of hand-held Ultrasound]. Z Gastroenterol. 2023;61(7):836-51.

4. Merkel D, Zullich TF, Schneider C, Yousefzada M, Beer D, Ludwig M, et al. Prospective Comparison of Handheld Ultrasound Devices from Different Manufacturers with Respect to B-Scan Quality and Clinical Significance for Various Abdominal Sonography Questions. Diagnostics (Basel). 2023;13(24).

5. Weimer JM, Beer D, Schneider C, Yousefzada M, Gottwald M, Zullich TF, et al. Inter-System Variability of Eight Different Handheld Ultrasound (HHUS) Devices-A Prospective Comparison of B-Scan Quality and Clinical Significance in Intensive Care. Diagnostics (Basel). 2023;14(1).

6. Kim S, Fischetti C, Guy M, Hsu E, Fox J, Young SD. Artificial Intelligence (AI) Applications for Point of Care Ultrasound (POCUS) in Low-Resource Settings: A Scoping Review. Diagnostics (Basel). 2024;14(15).

7. Alhussein M. Use of Real-Time Remote Tele-mentored Ultrasound Echocardiography for Cardiovascular Disease Diagnosis in Adults: A Systematic Review. Ultrasound Med Biol. 2024;50(6):779-87.

8. Cal EM, Gunnell E, Olinger K, Benefield T, Nelson J, Maggioncalda E, et al. Utility of tele-guidance for point-of-care ultrasound: a single center prospective diagnostic study. J Ultrasound. 2024.

9. Kim K, Cho K, Jang R, Kyung S, Lee S, Ham S, Choi E, Hong GS, Kim N. Updated Primer on Generative Artificial Intelligence and Large Language Models in Medical Imaging for Medical Professionals. Korean J Radiol. 2024 Mar;25(3):224-242.

10. Waldner MJ, Strobel D. Ultrasound Diagnosis of Hepatocellular Carcinoma: Is the Future Defined by Artificial Intelligence? Ultraschall Med. 2024 Feb;45(1):8-12

This book was written for “ultrasound lovers” by a large team of people with extensive experience in the field of ultrasound. Each chapter starts with: “How can I use Ultrasound in…?” and then attempts to solve a clinical problem in different organs. Numerous interesting images help readers enhance their ultrasound expertise.

Enjoy this book in your daily practice!

"Victor Babeş" Publishing House
Timişoara, 2025

ISBN 978-606-786-416-8 E-Book